



Dokuz Eylül University
Faculty of Engineering
Department of Textile Engineering

3rd INTERNATIONAL
TECHNICAL TEXTILES CONGRESS

3rd INTERNATIONAL TECHNICAL TEXTILES CONGRESS

1 - 2 December 2007

Istanbul EXPO Center

Istanbul / TURKEY

3rd INTERNATIONAL
TECHNICAL TEXTILES CONGRESS

A METHODOLOGY TO SELECT THE ADEQUATE GARMENT FOR SPORT PRACTICE

N. MARTÍNEZ, J.C. GONZÁLEZ, D. ROSA, E. ALCÁNTARA

Institute of Biomechanics of Valencia

ABSTRACT

Choosing the adequate garment for sports practice in adverse weather conditions, either cold or hot, is an aspect of great influence on activity performance. The Institute of Biomechanics of Valencia has developed a methodology which allows assessing the fit of the garment to the real situation of use by evaluating its influence in the thermoregulatory response of the human body. Under controlled environmental conditions and at fixed activity levels, two shirts were tested in the laboratory. Eight subjects performed a test which consisted of six phases of different activity level in two conditions (25°C/50% RH and 10°C/60% RH). Throughout the test, physiological parameters of the thermal response as well as work load indicators were registered. Skin temperature at three different locations (chest, arm and thigh), microclimate variables in some areas of subject-garment interface (in armpit and upperback) and heart rate were measured continuously. Six samples of sweat were also collected regularly from dorsal region during the test to estimate the sweating rate and the loss of salts. Weight loss was also checked before and after performing the test to estimate the dehydration level. Subjects were asked during the test about humidity and temperature perception on the body as a whole or by different zones. The results allowed measuring a significant influence of the shirt in skin temperature. Therefore, the methodology developed for studying of the user-product interaction through the assessment of the thermophysiological response and the subjective perception allows recommending the comfort ranges for each piece of garment as well as indicating those work load and environmental conditions for which the influence of garment on user's performance is optimal.

Key Words: Thermophysiology, Thermal Comfort, Garment Selection.

1. INTRODUCTION

High performance is a desirable objective for all professionals, especially at sport competitions. At the same time, comfort is well-known as an important item to improve the quality and efficiency of an activity. Many people daily perform their tasks in adverse thermal conditions (for example at work like fire-fighters or people working in foundry workshops or cold-storage rooms) which increase demands on the thermoregulatory system. This in the end can reduce human abilities and performance with a negative effect upon comfort and even putting health and safety at risk. In this sense, thermal requirements are determined for each person by a great number of factors such as environmental conditions or the physical activity level and also intrinsic human factors but clothing can have a determinant role and therefore, exposition to cold or heat environments should be done with proper thermal protective equipment. With this respect, the textile industry's current development has flooded various sectors (such as fashion, sports

clothing, protection equipment, etc.) with a wide variety of technical textiles offering sufficiently diversified properties to be capable of satisfying the user's needs in many situations. This has not, however, been accompanied by a development in accordance both with assignation criteria and methods for evaluating their performance. For these reasons, an appropriate clothing selection is not usually easy to be carried out as far as a correct information management does not exit at present. To select the clothing according to end-users requirements, information about thermal properties of the products and the thermal interaction between users and products in the different environments and situations must be characterised and related to users' necessities. This paper focuses on the development of a clothing selection methodology according to thermal requirements.

2. MATERIAL AND METHODS

Two commercial shirts were tested at different situations of use in the laboratory. Both commercial shirts were made of the same textile (100% polyester) but with different thickness and consequently different thermal properties. Both were thermally characterised (thermal resistance R_{ct} and evaporation resistance R_{et}) according to Skin Model test described in ISO 31092 standard.

Thermal properties are shown in the next table:

Table 1. Thermal properties of the shirts participating in the study

Shirt	Thermal resistance R_{ct} ($m^2 \cdot K/W$)	Evaporation resistance R_{et} ($m^2 \cdot Pa/W$)
1 Low resistance	0.0342±0.0002	3.56±0.03
2 High resistance	0.0512±0.0005	4.89±0.01

Eight trained male subjects (Average age: 25,25 years (Std dev:1,38) ;average height: 1,76m (Std dev: 0,068) ; average weight: 72,45 Kg (Std dev:0,67)) performed a test on a tread-mill which consisted of six phases at different activity level in two environmental conditions (25°C/50% RH and 10°C/60% RH) .The activity test designed lasted for 60 minutes and included different phases of activity and rest in order to cover the wide range of activity possibilities for the use of the shirts. The test is described below:

1. **Acclimatization** (10 minutes). This step includes a first phase of walking at a speed of 2-3 Mph during 5 minutes followed by a second phase of jogging at 5 Mph.
2. **Rest** (5 minutes). The subject rested but he was not allowed to seat at any moment.
3. **Low intensity activity** (15 minutes). This step includes three phases of running at different speeds (5 minutes of duration each): 6, 7 and 8 Mph.

4. **Rest** (5 minutes). The subject rested but he was not allowed to seat at any moment.
5. **High intensity activity** (15 minutes). This step includes threephases of running at different speeds (5 minutes of duration each): 8, 9 and 10 Mph.
6. **Rest** (10 minutes). The subject rested but he was not allowed to seat at any moment.

The methodology proposed consists of measuring different kinds of variables regarded to the thermal state throughout the test described above. Objective measurements as thermal comfort variables (skin temperature and microclimate variables) or physiological (heart rate, fluid loss and sweat composition) were done together with subjective variables (thermal perception and comfort degree). Combined analysis of both allowed to assess the garment fitness to user thermal needs.

2.1. Thermal Comfort Variables and Heart Rate

Skin temperature at three different locations (chest, arm and thigh) and microclimate variables in subject-garment interface (at the armpit and upperbacks) were measured each 2 seconds during the whole test by means of digital sensors (developed by the IBV). Heart rate was measured as well using a POLAR™ heart rate monitor. Figure 2 shows the exact locations of the sensors. After checking the existence of a pattern in chest, arm and thigh temperature registers; average skin emperature has been calculated according to equation (Daannen ,1997).

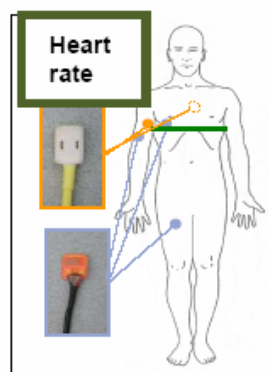


Figure 1. Instrumentation

$$T_{\text{Average Skin Temperature}} = 0,36.T_{\text{Arm}} + 0,25.T_{\text{Chest}} + 0,34.T_{\text{Thigh}} + 1,19$$

From the curve of average skin temperature, 13 variables were obtained by parameterization of the calculated registered. The selected values corresponded with the phase changes of the activity test.

2.2. Sweat Samples

Six samples of sweat were also collected regularly from dorsal region during the test in order to estimate the sweating rate and the loss of salts. The location of the patches can be observed in the Figure 3. The patches were removed at the beginning and at the end of the resting steps for monitoring the increment in sweating due to activity bouts and rest periods. After having been retired, each patch was immediately encapsulated in a tube and placed in a freezer at -20°C to avoid evaporation. The sweat samples were removed from the patches by centrifugation in order to be analysed for sodium and potassium by means of a mass spectrometer.

The methodology for collecting the sweat samples has been developed according to literature (*Alvear et al.,2004*).

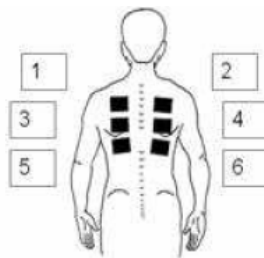


Figure 2. Sweat patches distribution

2.3. Fluid Loss

Fluid loss was registered by means of weighting the subject in nude conditions before and after performing the test to estimate the dehydration level. To estimate the absorption capacity of each piece of garment, all of them were also weighed separately before and after the test. The parameters obtained from the collected information correspond to the loss of weight of the subject and the increment of weight of each piece of clothing and measurement equipment worn by the subject.

2.4. Thermal Perception

The aim of the subjective test was to gather the thermal perception of users and about the sensations of general comfort or the incidence of discomfort associated with a certain thermal state. In this way, the subject's opinion was recorded at the same time as the temperature and humidity data during the different stages of the study. The survey was divided into a preliminary survey and another while the activity test was being carried out. Different questions were asked before and after the subject did the test, to assess their tendencies in relation to the thermal perception of a situation. Subjects were asked during the test about humidity and temperature perception on the body as a whole or by different zones. Global comfort degree was also

registered in each case. The survey was based in a 5-points scale as it follows: *Very warm (Dry)* - *Warm(Dry)*- *Neither warm(Dry) nor cold (Wet)*- *Cold(Wet)*- *Very cold (Wet)* for thermal perception and *Extremely uncomfortable*- *Very uncomfortable*- *Uncomfortable*- *Uncomfortable*- *Slightly uncomfortable*- *Comfortable* for comfort degree.

Data analysis

For each parameter of the study obtained from the collected information an statistical analysis was done using SPSS 14.0 software. The analysis consists firstly of a descriptive analysis, followed by an analysis of the variance (ANOVA for parametric variables and Kruskal-Wallis analysis for non-parametric ones) to check the influence the shirt for each environmental condition on each thermophysiological variable of the body response.

3. RESULTS

3.1. Thermal Comfort Variables and Heart Rate

Descriptive analysis: Next graphs show the evolution of the parameters obtained from the average temperature of the skin for all the subjects at each condition for both shirts in cold and heat conditions.

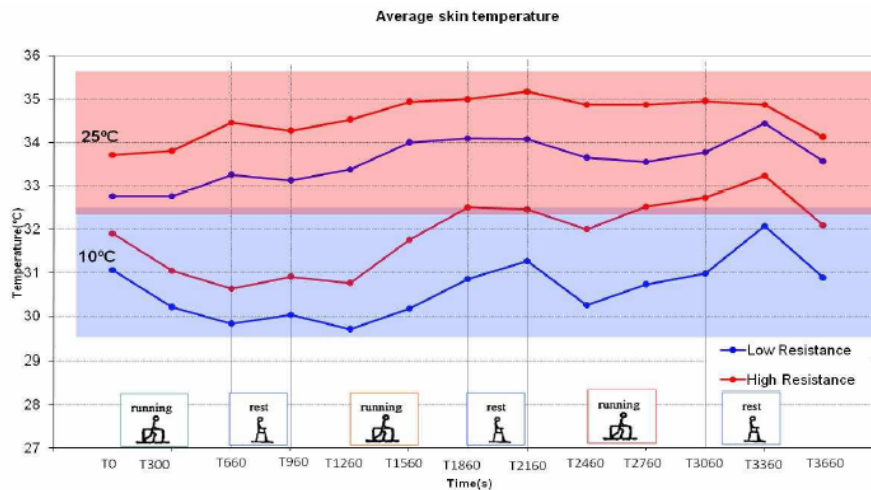


Figure 3. Evolution of the average skin temperature in each case of the study.

Analysis of the variance (ANOVA) results showed that the shirt with higher thermal resistance produces higher average skin temperature significantly ($p=0.05$) during the test with the exception for high level of activity (end of the test) independently from the environmental conditions. Regarding the heart rate and after the parameterization of the curves, a descriptive analysis was done for estimating the average heart rate values for each test configuration. After the descriptive and having checked that the ANOVA did not show significant differences for any heart rate parameter due to the shirt or the environmental

conditions (in this case, heart rate for 25°C/50%RH was systematically higher but not significantly), individual differences were considered. The data shows a great variability in heart rate between subjects. It is discussed to be a possible reason for not detecting significant differences due to study factors.

3.2. Sweat Samples

Having collected a sample at each phase activity change in case of both shirts has shown in a first place how for shirt with higher thermal resistance sweat amount has been systematically higher at every instant collection. Besides, sodium and potassium concentration were found to be also higher in this case. Regarding to the sodium and potassium contents it can be observed that the concentration modifies during the test: after having sweat for some time during the test, the salts concentration found in sweat slightly decreases (see Figure 4).

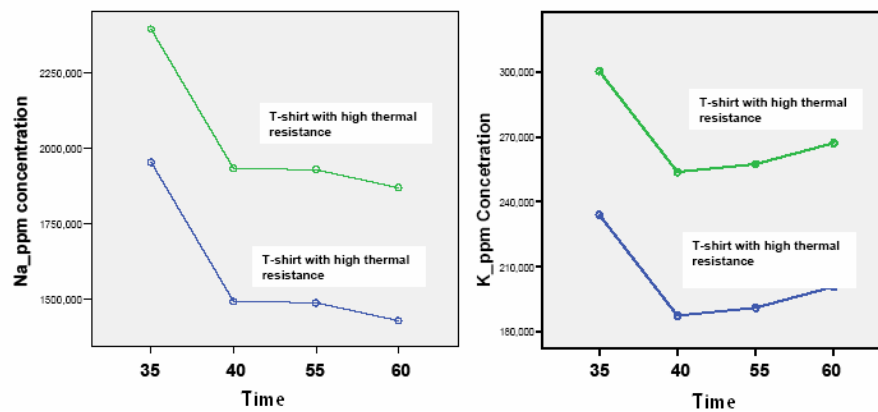


Figure 4. Evolution of sodium and potassium concentration in sweat during the test for each shirt.

3.3. Fluid Loss

Descriptive analysis gave an estimation of the weight loss. Differences in weight loss have been found due to the environmental conditions by means of ANOVA ($p < 0.05$) but not due to the shirts. Exercising in warm conditions (25°C/50%HR) results in a bigger weight loss than exercising in cool conditions (10°C/60%) regardless of the garment.

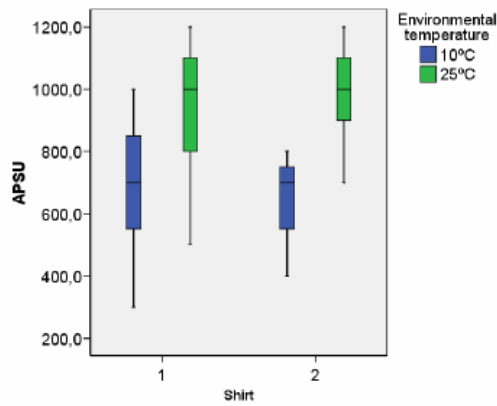


Figure 5. Box and whiskers diagram for weight loss for each condition and shirt.

3.4. Thermal Perception

Data representation for 'Perception of temperature' and 'Thermal comfort degree' was carried out by means of histograms done separately for each test condition (environmental condition and shirt) and for the survey at the end of each activity step. 'Perception of temperature' was systematically found 'Warmer' at 25°C than at 10°C regardless of the shirt and the instant of the test. In the next figures a histogram for the 'Perception of temperature' and another one for the associated 'Comfort degree' are presented. The relationships between both allowed to know which sensation was pleasant for the user. Furthermore, adding the objective thermal comfort variables is possible to decide which level of thermophysiological variables as skin temperature are found satisfactory and give comfort sensation to the user.

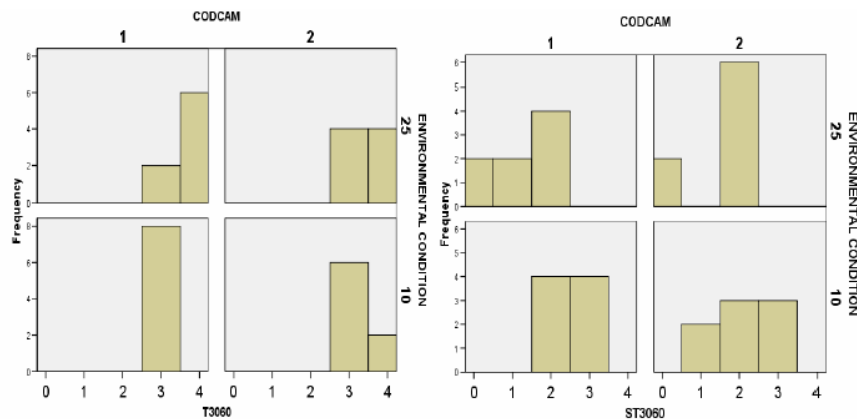


Figure 6. Histograms of the thermal perception (left) and the degree of comfort (right) at the end of the last phase of activity for each condition and garment.

Analysis of the variance (Kruskal-Wallis) showed that, only the environmental conditions caused significant differences ($p < 0.05$) at any activity level.

4. DISCUSSION AND CONCLUSION

After this study, it has been concluded that it is possible to estimate the adaptation of the garment for a particular situation of use defined by the user, the environmental conditions and the activity performed with different degrees of accuracy. The proposed methodology consists of different steps with an increasing degree of complexity.

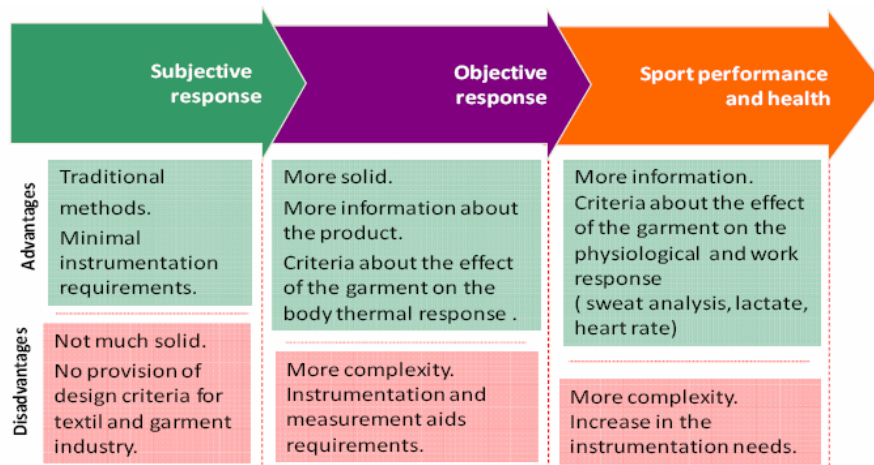


Figure 7. Levels of complexity in thermal comfort studies

It starts by gathering subjective opinion of users. This level of the methodology in its own is capable of giving enough information about the product in order to know the adequation or not of the product by means of a simple survey to the user. The results of the thermal perception study have allowed us to find differences between tested garments and between the performances of a garment under different thermal requirements. However and in spite of that this type of information is determinant in the purchase decision, information presented in this form do not provide designers and manufactures with designs criteria for products development. Second step consist of combining this with objective measurement of thermoregulatory response. In the test, we measured skin temperature and microclimate what provides more useful information to include in the product development process. Thermal comfort variables analysis has shown that indeed skin temperatures are different due to the garment and the environments and has also shown that the influence of the garment on them is presented as a function of the activity level.

By means of this values and their relationship with the user perception enough information is available to know what objeive values of thermal comfort variables are perceived as comfortable by the users. In fact, the point of measuring both simultaneously is having a translation of the user

perception into quantified variables. Third level of complexity consider measuring variables related to user health that includes heart rate and sweat composition. Our results did not show differences in heart rate due to the garment. In this case, a high individual variability was detected and it was discussed it may conceal any possible difference due to the shirt. However, the effect of the environmental condition had enough size to be independent of the individual variability (anyway it was not in a significant way). Regarding sweat composition (sodium and potassium contents), with the methodology proposed we could measure both parameters on the sweat at different moments throughout the test, getting information about the dynamical behavior of the sweating mechanism. In our study it were found the same trends for the evolution of sodium and potassium concentrations. Besides, levels of both parameters differ between garments possibly due to the sweat rate. In this sense, it has been reported in many occasions in the literature that lower sweat rate let the re-absorption of sodium in the duct of the gland (*Sato, 1993*).

The decrease seen in the Figure 4 is supported by numerous studies in the literature, and reveals the adaptive nature of the perspiration mechanism. During prolonged physical exercise, the reduction in volemia and the loss of salts stimulates the secretion of aldosterone, which is responsible for keeping sodium at adequate levels (*Willmore and Costill, 2000*). The sodium retention induced by the rise in aldosterone levels has been extensively documented for prolonged periods of exercise (over 6 hours) (*Pattersson, 2004*), though the effect does not appear so well documented for intermediate periods of activity. The research team postulates the existence of a lesser effect of this hormone (aldosterone), which in combination with the effect of training upon the sweat glands in subjects adapted to situations of thermal stress (*Ahlman and Karvonen, 1961; Pattersson, 2004*), could explain why beyond a given moment during perspiration the secreted sweat becomes more hypotonic as a defence measure against salt depletion - though the evidence in this sense is still inconclusive. By improving and implementing this methodology, people involved in sports world and other professionals as safety managers of the enterprises, would be able to choose the most suitable gear for each person, according to the kind and duration of the activity which is performing and the environmental conditions in which it is developed. Choosing the right equipment enhance the efficiency and performance by means of a higher user's comfort and satisfaction.

ACKNOWLEDGEMENTS

Collaborations of the Physiology Department of the University of León (Spain) and the Research Unit for Physical and Sports Performance of the University of Valencia (Spain) have been much appreciated in this work.

REFERENCES

- AHLMAN, K., H., KARVONEN, M.J.: *Stimulation Of Sweating By Exercise After Heat Induced "Fatigue" Of Sweating Mechanism*. Acta physiol. Scand. 1961. 53:381-386
- ALVEAR-ORDENES, I. (1998). *Índice De Excreção De Amoníaco No Suor Em Atletas De Fundo Durante Exercício Até Exaustão*. (tesis de máster em ciências). Universidade federal do rio de janeiro.
- ALVEAR-ORDENES, I., FLEGNER, A.J., GONZÁLEZ-GALLEGO, J. (2001). *Índice De Excreción De Amoníaco En El Sudor De Atletas De Fondo Durante Ejercicio Hasta La Fatiga*. Arch med dep. Xviii(86):593-599.
- ALVEAR-ORDENES, I. (2003). *Efectos Del Ejercicio Físico Sobre Los Niveles De Amoníaco Y Urea En El Sudor Y En La Sangre: Relación Con El Daño Muscular*. (tesis de doctorado). Universidad de león.
- ALVEAR-ORDENES, I., GARCÍA-LÓPEZ, D., DE PAZ, J.A., GONZÁLEZGALLEGO, J. (2005). *Sweat Lactate, Ammonia, And Urea In Rugby Players*. Int j sports med. 26(1):632-137.
- ALVEAR ORDENES, I. (1998). *Índice De Excreción De Amoníaco En El Sudor De Atletas De Fondo Durante Ejercicio Hasta La Fatiga*. (tesis de maestria). Universidad federal de rio de janeiro.
- ALVEAR ORDENES, I. (2003). *Efectos Del Ejercicio Físico Sobre Los Niveles De Amoníaco Y Urea En El Sudor Y En La Sangre: Relación Con El Daño Muscular*. (tesis de doctorado) departamento de fisiología, universidad de león.
- ALVEAR-ORDENES, I., GARCÍA-LÓPEZ, D., DE PAZ, J.A., GONZÁLEZGALLEGO, J. (2005). *Sweat Lactate, Ammonia, And Urea In Rugby Players*. Int j sports med. 26:1-6.
- DAANEN, H. (1997). *Central and peripheral control of finger blood flow in the cold*. Thesis. Vrije Universiteit.
- MORGAN R.M., PATTERSON M.J., NIMMO, M.A.: *Acute Effects Of Dehydration On Sweat Composition In Men During Prolonged Exercise In The Heat*. Acta physiol scand 2004,182:37-43
- PATTERSON M.J., S.D. GALLOWAY, AND M.A. NIMMO. *Variations In Regional Sweat Composition In Normal Human Males*. Exp. Physiol. Nov. 85(6): 869-875. 2000.
- RAV-ACHA M, HADAD E., EPSTEIN Y et al: *Fatal Exertional Heat Stroke: A Case Series*. Am j med sci 2004, 328:84-87.
- SATO, K., DOBSON, R.L. (1970) *The Effect Of Intracutaneous Aldosterone And Hydrocortisone On Human Eccrine Sweat Gland Function*. J. Invest. Dermatol. 54:450-462
- WILLMORE J, COSTILL D.1994 *Physiology Of Sport And Exercise*. Ed: human kinetics. Canada.

A STUDY ABOUT PHYSICAL PERFORMANCE OF KNIT FABRIC LAMINATED STRUCTURE

O.G. ARMAĞAN, H. KARAKAŞ

Istanbul Technical University, Textile Technologies and Design Faculty

ABSTRACT

Lamination techniques are frequently used with the woven and nonwoven fabrics. However, there is not much study carried out on knit fabric laminations. In this investigation, we aimed to find some evidence that knit fabric structure is also appropriate for lamination from the point of view about physical performance. One side of single jersey knitted fabrics made by viscose, polyester, cotton and bamboo yarns are laminated with the polyether polyurethane and polyester polyurethane membranes by the help of reactive polyurethane adhesives. Experiments show that lamination improves bursting strength, abrasion resistance and spirality of the knit fabric. However, pilling resistance is getting worse. Widthwise dimensional change is also improved while lengthwise dimensional change increased. Besides, while weight of the samples naturally increases, thickness of samples decreases by lamination. The physical performances of the samples have also been tested after washing process. The results are compared and analyzed.

Key words: Knit fabric, lamination, physical performance.

1. INTRODUCTION

Different from the classic textile structure such as woven and knitting, laminated fabrics become widespread in textile applications. Laminated fabrics are also called layered fabrics. Laminations are generally made with the application of membranes or films over the textile fabrics by the help of adhesives. Some membranes give breathability properties to the fabrics and some provide UV protection, flame retardancy, waterproofness, filtration, etc., while more than one property may also be achieved. Some researches [1-5] are carried out related with the water vapor transfer of layered fabrics and some are [6,7,8] related with water and heat transfer properties of layered fabrics. Waterproof and breathable fabrics form an important area of study related with the layered fabrics done by researchers. Ruckman made series of researches about waterproof and breathable laminated fabrics [9,10,11,12,13]. Ruckman [14] also studied about outdoor clothing application of layered system. Knitting layered fabrics which used membranes are studied by some researchers [4,7]. However, there are not enough experiments carried on physical properties such as bursting strength, abrasion resistance, spirality, dimensional change of the membrane laminated knitting. In this investigation, we aimed to study the physical properties of membrane laminated knitting fabrics.

2. EXPERIMENTAL

2.1. Materials

Firstly, fibers used with the knitted fabrics were selected; these are 100% viscose, polyester, cotton, bamboo. Ne 30/1 yarns are composed with these fibers and then single jersey knitted fabrics were produced in the same knitting machine (Mayer CIE Relanit II, 32 pus 28 fine single plate circular knitting machine) in order to compare the effects of fiber type over the laminated knitting fabrics. After production of fabrics, fixation of fabric width takes place. Finally, one side of the fabrics is laminated with polyester-polyurethane and polyether-polyurethane membranes by the help of reactive polyurethane adhesive. The lamination machine is hot-melt gravure roller dot printing system. As an adhesive; reactive polyurethane has 70-110°C application temperature, density is 1,1 g/cm³, weights is 10-40 g/m² and viscosity is 3300 mPa.s.

Yarn, fabric and membrane parameters are given in the Table 1, Table 2 and Table 3. Samples are coded on Table 4, Ex. "VL1.Aw" means; Viscose (V) and 1st type membrane laminated fabrics (L1), which are subjected to 5 times washing and flat drying cycles (Aw).

Table 1. Yarn Properties

Fiber	Yarn Blend	Yarn Number	Yarn Type	Twist
Viscose	100%	Ne 30/1 (Ne 29,59)	Ring	816 (T/m)
Polyester	100 %	Ne 30/1 (Ne 30,57)	Ring	650 (T/m)
Cotton	100%	Ne 30/1 (Ne 30,46)	Ring	719 (T/m)
Bamboo	100 %	Ne 30/1 (Ne 29,50)	Ring	707 (T/m)

Table 2. Greige Fabric Properties

Fabric	Knitting Type	Stitch Density (1/cm ²)	Fabric Thickness (mm)	Weights (g/m ²)	Yarn Stitch Density (mm)
Viscose	Single-jersey	315	0,583	160,65	2,60
Polyester	Single-jersey	315	0,592	162,35	2,69
Cotton	Single-jersey	315	0,667	161,95	2,65
Bamboo	Single-jersey	315	0,570	162,75	2,61

Table 3. Membrane Properties

Code	Membrane	Thickness	Color	Density (g/cm ³)
1	Polyester-based Polyurethane	20µm	White, translucent	1,17
2	Polyether-based Polyurethane	20µm	White, opaque	1,23

Table 4. Sample Codes

Sample Code	Sample
V	Viscose
P	Polyester
C	Cotton
B	Bamboo
G	Greige
L	Laminated
Aw	After 5 Wash and Flat Dry

2.2. Method

Physical performances of laminated sample fabrics have been tested. Bursting strength was performed according to TS 393, abrasion resistance according to ISO 12947-2, pilling tendency according to ISO 12945-1, spirality according to AATCC 179, dimensional changes according to TS 392, weight of the samples according to TS 251 and thickness according to BS 2544. The results are analyzed and compared with the pre-lamination values and after washing values.

3. RESULTS AND DISCUSSION

3.1. Bursting Strength

As we look at Table 5 and Table 6, it is seen that lamination improves bursting strength. Besides, 2nd type membranes have higher strength than the 1st type. Successively, viscose improves 8-9 %, cotton improves 6-8 %, meanwhile polyester decline 2-3 % and bamboo decline 1-2 % after the lamination. After washing, bursting strength of polyester and cotton improves while bursting strength of viscose and bamboo decreases. Successively, polyester improves by 11 %, cotton improves by 10 %, and meanwhile viscose decreases by 10 % and bamboo decreases by 8 %. Samples which have greater dimensional changes have lower strength because the membrane does not shrink against the fabric and effective binding does not take place between fabric and membrane. Consequently, strength decreases.

Table 5. Bursting Strength of Greige Fabrics

GREIGE	Bursting Strength (kg/cm ²)
Viscose	3,140
Polyester	9,091
Cotton	5,481
Bamboo	4,037

Table 6. Bursting Strength of Fabrics

	Bursting Strength (kg/cm ²)		
VL1	3,406	VL2	3,425
PL1	9,220	PL2	9,418
CL1	5,866	CL2	5,906
BL1	4,052	BL2	4,113
VL1.Aw	3,037	VL2.Aw	2,983
PL1.Aw	10,343	PL2.Aw	10,517
CL1.Aw	6,690	CL2.Aw	6,433
BL1.Aw	3,717	BL2.Aw	3,770

3.2. Abrasion Resistance

Weight loss of the samples related with the abrasion resistance is given in Table 7 to 9. According to the abrasion resistance of fabric faces; it is seen that lamination improves the abrasion resistance of samples especially viscose and cotton samples. However, abrasion resistance of samples decline after washing. 1st membrane type has better effect on viscose and cotton samples. Polyester and bamboo samples are not influenced from membrane types.

Table 7. % Weight Loss of Grieger Fabrics

%	VG	PG	CG	BG
Wiegth Loss	5,641	0,505	4,390	2,752

Table 8. % Weight Loss of Fabric Faces

%	VL	PL	CL	BL	VL.Aw	PL.Aw	CL.Aw	BL.Aw
1	1,119	0,457	1,594	2,358	3,478	0,957	2,791	3,540
2	1,923	0,439	2,463	2,273	4,706	0,897	2,905	3,571

According to the abrasion resistance of membrane faces; there is almost no weight loss in the fabrics. Washing cycles had no effect on abrasion of polyester and cotton samples while viscose and bamboo samples lost their weights. As we compare the membrane type, 2nd type is slightly better than the 1st type with regard to abrasion resistance.

Table 9. % Weight Loss of Membrane Faces

%	VL	PL	CL	BL	VL.Aw	PL.Aw	CL.Aw	BL.Aw
1	0,576	0	0,483	0	1,024	0	0,424	0,791
2	0,442	0	0,469	0	0,813	0	0,386	0,760

3.3. Pilling Resistance

Pilling Resistance of samples is given in Table 10 and 11. As we look at the results, pilling increases in laminated fabrics except for polyester. Washing cycles also increased pilling tendency. As a result, lamination does not affect the pilling performance in a positive way.

Table 10. ICI Pilling Values of Greige Fabrics

Pilling	VG	PG	CG	BG
ICI Pilling Box	3	3-4	4	4

Table 11. ICI Pilling Values of Fabrics

	VL	PL	CL	BL	VL.Aw	PL.Aw	CL.Aw	BL.Aw
1	3	3-4	3	3	2	2-3	2	2-3
2	2-3	3-4	3	3	2	2-3	2	2

3.4. Spirality

Spirality values are found after 5 washing cycles and they are given in Table 12. As we see in the table, spirality of fabric samples from great to low is bamboo, viscose, cotton and polyester in an order. Spirality is decreased by the lamination because membrane tightly sticks to the fabrics and it does not permit them to turn easily. In terms of membrane, 2nd type is more efficient than the 1st type.

Table 12. % Spirality Values of Fabric Samples

Sample	Spirality (%)	Sample	Spirality (%)	Sample	Spirality (%)
VG.Aw	5,25	VL1.Aw	3,75	VL2.Aw	1,25
PG.Aw	1,25	PL1.Aw	1,00	PL2.Aw	0,75
CG.Aw	3,00	CL1.Aw	1,75	CL2.Aw	0,50
BG.Aw	8,25	BL1.Aw	6,00	BL2.Aw	4,50

3.5. Dimensional Changes

Dimensional changes of samples after 5 washing cycles are given in Table 13. Generally, widthwise dimensional changes were decreased whereas lengthwise dimensional change increased by membrane lamination. Greige viscose fabric makes great shrinking in width and makes relatively elongation in length, but widthwise changes considerably reduced and lengthwise changes considerably increased after lamination. Dimensional changes of polyester fabric have lowest value amongst them, even after lamination, due to its structure. Observed behaviour of samples are nearly the same according to the membrane types.

Table 13. % Dimensional Changes of Fabric Samples

Sample	Width (%)	Length (%)			
VG.Aw	-15,0	6,0			
PG.Aw	-1,0	-1,0			
CG.Aw	-3,5	-2,5			
BG.Aw	-7,5	-7,5			
Sample	Width (%)	Length (%)	Sample	Width (%)	Length (%)
VL1.Aw	-1,0	-18,0	VL2.Aw	-1,0	-19,0
PL1.Aw	0,5	-2,0	PL2.Aw	1,0	-3,0
CL1.Aw	1,0	-7,5	CL2.Aw	-1,0	-7,0
BL1.Aw	-3,5	-16,0	BL2.Aw	-2,5	-18,5

3.6. Weight in Grams

Weight in grams of membrane 2 is 5% heavier than membrane 1 and so this difference shows itself in the samples weights on Table 14. The samples used with membrane 2 are heavier than membrane 1. After washing cycles, weights in grams of samples are parallel with dimensional changes. For instance, weights in gram of polyester laminated fabric show little difference after washing cycles because of low dimensional changes. On the other hand, viscose and bamboo laminated fabrics have great weight in grams because these fabrics shrink too much especially in lengthwise direction and its loop density increases. Viscose rises by 25%, bamboo rises by 20%, cotton rises by 10% and polyester rises by 1% for laminated fabrics after washing cycles.

Table 14. Weight in Grams of Fabric Samples

Weights (g/m ²)	Greige	L1	L1.Aw	L2	L2.Aw
Viscose	160,65	174,4	215,6	178,7	223,6
Polyester	162,35	186,8	189,3	190,3	192,8
Cotton	161,95	179,4	194,6	186,8	202,5
Bamboo	162,75	185,6	220,3	190,1	227,3

3.7. Thickness

Thickness values are given in Table 15. Thicknesses of fabrics are decreased amazingly by the lamination. Thicknesses of membranes are only 20 µm. Greige fabrics have not uniform strength, and it is thought that pressure and tension come into being while membranes are applied with fabrics by lamination. Fabrics are getting thinner by these effects while membranes being applied. After washing cycles, fabrics are shrunked contrary to membrane because membrane is a hydrophobic structure and it swirls over the fabric, and thus thickness is increasing accordingly. Ascending thicknesses in the order; viscose and bamboo are 50%, cotton is 35% and polyester is 15%. Moreover, it is found that fabrics with membrane 2 are 2% thicker than fabrics with membrane 1.

Table 15. Thickness of Fabric Samples

Thickness (mm)	Greige	L1	L1.Aw	L2	L2.Aw
Viscose	0,583	0,500	0,785	0,523	0,802
Polyester	0,592	0,513	0,597	0,553	0,622
Cotton	0,667	0,553	0,762	0,583	0,758
Bamboo	0,570	0,507	0,763	0,517	0,769

4. CONCLUSION

When all the results are considered, it is seen that physical performance of knitting fabrics, except pilling resistance, improved by the lamination.

Bursting strength and abrasion resistance increased while thicknesses decreased by lamination. On the other hand, pilling resistance is worsened.

Knitting laminated fabrics are also affected by 5 washing cycles. Abrasion and pilling resistance decreased, strength of cotton and polyester increased while viscose and bamboo decreased after washing cycles. Widthwise dimensional changes of samples decreased, so this performance improved but lengthwise dimensional changes unexpectedly increased comparing to samples that are not subjected to washing. Spirality values also decreased expectedly.

ACKNOWLEDGEMENTS:

This study is supported by I.T.U. Scientific Research Projects Unit. The authors would like to express their thanks to Atateks Company and Dima Lamination Company for production of samples.

REFERENCES

1. Wilbik-Halgas, B., Danyinch, R., Wiecek, B., Kowalski, K., 2006. Air and Water Vapour Permeability in Double-Layered Knitted fabrics with Different Raw Materials. *Fibres and Textiles in Eastern Europe*, Vol. 14, No. 3(57), p. 77-80

2. Suprun, N., 2003. Dynamics of moisture vapour and liquid water transfer through composite textile structures. *International Journal of Clothing Science and Technology*, Vol. 15, No. 4, p. 218-223.
3. Barnes, J.C. and Holcombe, B.V., 1996. Moisture Sorption and Transport in Clothing During Wear. *Textile Research Journal*, Vol. 65, No. 12, p. 777-786.
4. Oh, A. and Cho, H., 2005. Evaluation of the Water Vapour Transfer Rates of Performance Fabrics. *SEN'I GAKKAISHI*, Vol. 61, No. 6, p. 56-60.
5. Long, H., 1999. Water transfer properties of two-layer weft knitted fabrics. *International Journal of Clothing Science and Technology*, Vol. 11, No. 4, p. 198-205.
6. Wang, J.H. and Yasuda, H., 1991. Dynamic Water vapor and Heat transport Through Layered Fabrics Part 1: Effect of Surface Modification. *Textile Research Journal*, Vol. 61, No. 1, p. 10-20.
7. Yasuda, H., Miyama, M. and Yasuda, H. 1992. Dynamic Water vapor and Heat transport Through Layered Fabrics Part 2: Effect of the Chemical Nature of Fibers. Vol. 62, No. 4, p. 227-235.
8. Fohr, J.P., Couton, D. and Treguier, G., 2002. Dynamic Heat and Water Transfer Through Layered Fabrics. *Textile Research Journal*, Vol. 72, No. 1, p. 1-12.
9. Ruckman, J.E., 1997. Water vapour transfer in waterproof breathable fabrics, Part 1: Under steady-state conditions, *International Journal of Clothing Science and Technology*, Vol. 9, No. 1, p. 10-22.
10. Ruckman, J.E., 1997. Water vapour transfer in waterproof breathable fabrics, Part 2: Under windy conditions. *International Journal of Clothing Science and Technology*, Vol. 9, No 1, p. 23-33.
11. Ruckman, J.E., 1997. Water vapour transfer in waterproof breathable fabrics, Part 3: Under rainy and windy conditions, *International Journal of Clothing Science and Technology*, Vol. 9, No. 2, p. 141-153.
12. Ruckman, J.E., 2003. Water Vapour Transfer in Wet Waterproof Breathable Fabrics. *Journal of Industrial Textiles*, Vol. 32, No. 3, p. 165-175.
13. Ren, Y.J. and Ruckman, J.E., 2004. Condensation in three-layer waterproof breathable fabrics for clothing. *International Journal of Clothing Science and Technology*, Vol. 16, No 13, p. 335-347.
14. Ruckman, J.E., 2005. The application of a layered system to the marketing of outdoor clothing. *Journal of Fashion Marketing and Management*. Vol. 9, No. 1, p. 122-129.

REDUCED FRICTION TO IMPROVE RUNNER'S COMFORT

E. BERTAUX

Empa, Swiss Materials Science & Technology

Clothing comfort is one of the major current concerns of textile manufacturers. Indeed, customers require more and more comfort and wellbeing especially in sport activity fields. For fabrics that come in direct contact with human skin, some friction between skin and clothes can appear due to the cyclic dynamic movement. Recently, we investigated the friction behaviour of socks in contact with feet. Furthermore, friction plays an important role for runners, for instance friction can cause bleeding nipples, named jogger's nipples. In the worst case, the sensation of pain and discomfort provoked by this skin irritation can make men runners to stop their sport activity.

The aims of this study were to understand skin friction during running and to minimize it. At first, some measurements were carried out to characterize the relative movement of the T Shirt and the pressure applied on the skin during running using fast adapting cameras and pressure sensors. The second step of this study was to further develop the Textile Friction Analyzer at Empa using the re-sults obtained. These new testing conditions permit to generate simulations of friction between T Shirts and skin that are very close to real running condition. Finally, the coefficient of friction between the skin model and different T Shirts has been investigated using the Textile Friction Analyzer.

It has been shown from the initial results that the influence of fibre type and structure of knitting on friction are significant. A suitable association between fibres and structure can be identified from these results, permitting the reduction of friction and the increase of comfort in the same time.

Keywords: Friction, skin irritation, textile structure, sport activity.

PRACTICAL ANALYSIS AND DESIGN OF STABILIZED RETAINING WALL STRENGTHENED WITH GEOTEXTILES

K.A. KORKMAZ

Department of Civil Engineering, Pennsylvania State University

ABSTRACT

Geotextile materials are used for strengthening and repair purposes in civil engineering. Design procedure for a structure with geotextile material for repair or strength becomes important throughout practical engineers in industry. Especially for structural designer, easy procedures for application are very crucial. Increase of geotextile material usage in engineering application is directly related with easy applied formulation and design procedures. From this point of view, In the present study, a practical analysis method with design and construction considerations for structural system with geotextile materials is investigated. A mechanically stabilized retaining wall strengthened with geotextile materials is considered. Analysis and design procedure is discussed in detail.

Keywords: Geotextile material, Stabilized Retaining Wall, Strengthening with Geotextile

1. INTRODUCTION

Geotextiles are used for retaining structures in the field of geotechnical and structural engineering. In the applications, geotextile compensates for the obvious weakness of structure in withstanding forces through the geotextile's strength and structure/geotextile interaction. For structural design, easy procedures for application are important. Increase of geotextile material usage in engineering application is directly related with easy applied formulation and design procedures. In this study, an easy methodology for application of geotextiles is given. The objective is to obtain information about the deformation, stress and strain distribution, and the influences on constituent fiber properties and structure-related parameters of geotextiles (1). In the present study, a practical analysis method for structural system with geotextile materials is investigated. In the analyses, a mechanically stabilized retaining wall strengthened with geotextile materials is considered. Analysis and design procedure is discussed in detail.

2. STABILIZED RETAINING WALLS

Stabilized retaining walls are built to accomplish exactly retain earth, reinforce a mass of soil, rock, or other material. Many different types of retaining walls exist, and include gravity and cantilever concrete retaining walls, and mechanically stabilized retaining structures constructed using geotextiles (Figure 1). The geotextile wall has layers of geotextile fabric

anchored by placing select fill retained at the face by extending the fabric over a removable form brace and re-embedding the remaining fabric back into the select fill. The materials and construction methods comply with provisions and the requirements specified by the geotextile engineer.

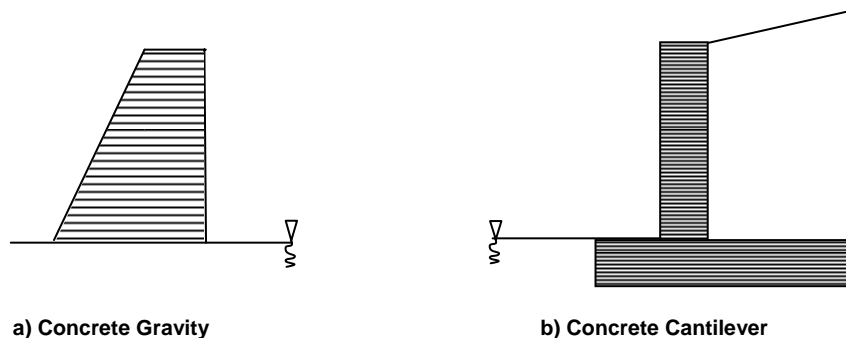


Figure 1. Retaining Wall Sections

Lateral loads due to the adjacent backfill soil are resisted by virtue of the walls' large mass, or externally stabilized (2). Cantilever retaining structures (Figure 1) are a refinement of the massive gravity wall concept. These walls have a much thinner stem, and utilize the weight of the backfill soil to provide most of the resistance to sliding and overturning (2).

Retaining walls are considered as proprietary systems. Their analysis or design has been relied on the limited past experience. Current US practice on stabilized retaining walls employs either the allowable stress design (ASD) method or the load factor design (LFD) method (3). In 1994, American Association of State Highway and Transportation Officials (AASHTO) introduced the load and resistance factor design (LRFD) method (4), which is generally known as the limit states design in Europe and the rest of the world. (5)

3. GEOTEXTILE MATERIALS

Geotextile materials are made from polypropylene, polyester, polyethylene, polyamide (nylon), polyvinylidene chloride, and fiberglass. Polypropylene and polyester are the most used. Sewing thread for geotextiles is made from Kevlar¹ or any of the above polymers. The physical properties of these materials can be varied by the use of additives in the composition and by changing the processing methods used to form the molten material into filaments. Yarns are formed from fibers which have been bundled and twisted together, a process also referred to as spinning. (This reference is different from the term spinning as used to denote the process of extruding filaments from a molten material.) Yarns may be composed of very long fibers (filaments) or relatively short pieces cut from filaments (staple fibers) (6, 7). Exposure to sunlight degrades the physical properties of polymers.

The rate of degradation is reduced by the addition of carbon black but not eliminated. Hot asphalt can approach the melting point of some polymers. Polymer materials become brittle in very cold temperatures. Chemicals in the groundwater can react with polymers. All polymers gain water with time if water is present. High pH water can be harsh on polyesters while low pH water can be harsh on polyamides. Where a chemically unusual environment exists, laboratory test data on effects of exposure of the geotextile to this environment should be sought. Experience with geotextiles in place spans only about 30 years. All of these factors should be considered in selecting or specifying acceptable geotextile materials (6, 7).

4. DESIGN METHODOLOGY

In general, retaining walls shall be analysed considering these limit states:

- (1) sliding resistance of the reinforced soil zone;
- (2) bearing resistance of soil upon which the reinforced soil zone resides;
- (3) overturning of the reinforced soil zone;
- (4) overall stability of foundation materials below the structure;
- (5) structural capacity of wall facing and connections;
- (6) rupture and pullout resistance of reinforcing elements;
- (7) vertical and differential settlement of foundation.

In Figure 2, detailed flow chart is given the steps and the formulation for each steps are given in this section from 4.1 to 4.6 and In Figure 3 to Figure 5 to explain the steps.

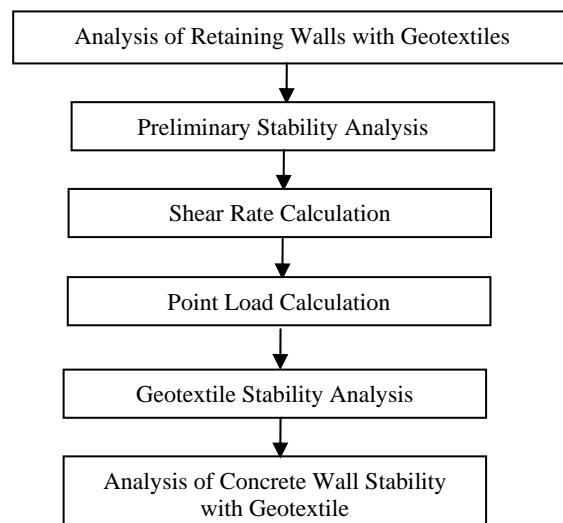


Figure 2. Analysis Steps

4.1. Preliminary Stability Analysis

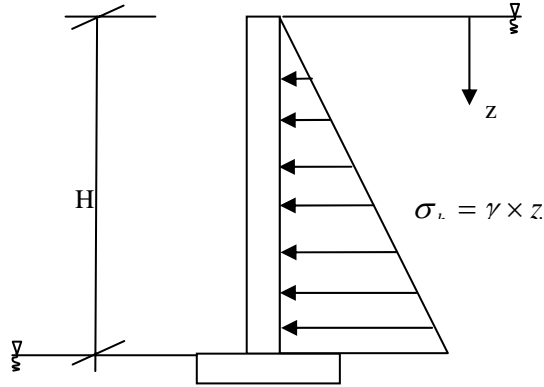


Figure 3. Preliminary Analysis Model

$$\text{Weight Stem: } W_{ts} = H \cdot W \cdot 1 \cdot \gamma_{\text{conc}} \quad (1)$$

$$\text{Weight Footing: } W_{tf} = B \cdot D_f \cdot 1 \cdot \gamma_{\text{conc}} \quad (2)$$

$$P_A = \int_0^H \sigma_n dz = \int_0^H \gamma_z dz = \frac{1}{2} \gamma \cdot z^2 \Big|_0^H = \frac{1}{2} \gamma H^2 \quad (3)$$

$$FS_{OT} = \frac{\sum M_{\text{resisting}}}{\sum M_{\text{drinning}}} \quad (4)$$

$$FS_{LL} = \frac{\sum F_{\text{resisting}}}{\sum F_{\text{drinning}}} \quad (5)$$

$$FS_{BC} = \frac{q_{ult}}{q_{act}} \quad q_{ult} = cN_c + qN_q + \frac{1}{2} \gamma_B N_\gamma \quad (6)$$

4.2. Shear Rate Calculation

$$\text{Shear Rate: } R = \frac{d_f}{50} \cdot t_{50} \times O \quad (7)$$

Where, R: Rate of the horizontal displacement; D_f : Rate of Horizontal Displacement; t_{50} : time required to reach 50% consolidation (min); O: Factor of account for drainage conditions on the shear plane

4.3. External Stability Analysis

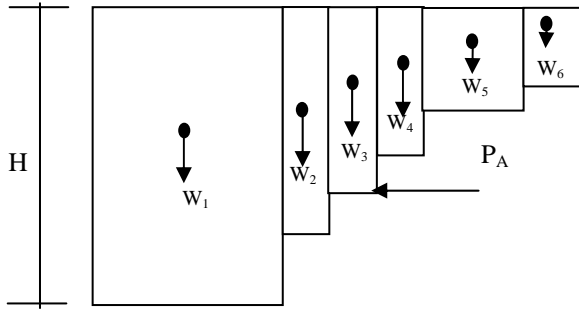


Figure 4. External Stability Analysis Model

$$P_A = \frac{1}{2} \gamma H^2 K \quad (8)$$

By using Eq. 4 and Eq. 5. , Eq. 9 is defined:

$$FS_{SL} = \frac{C_a + \sigma \tan \delta}{P_a} \quad (9)$$

$FS_{\text{Bearing Capacity}}$: Shallow Foundation Bearing Capacity

$$q_{ult} = cN_c + qN_q + \frac{1}{2} \gamma B N_\gamma \quad (10)$$

4.4. Point Load Calculation

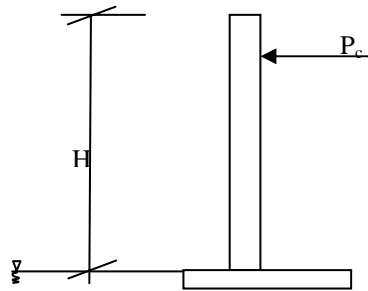


Figure 5. Point Load Analysis Model

Total Weight = Weight Stem + Weight Footing as given in Eq 1 and Eq. 2.

Eq. 4. is also valid for point load calculation

4.5. Geotextile Stability Analysis

Eq. 4 and Eq. 5 is valid also, Eq. 8. is valid for geotextile stability analysis.

$$FS_{SL} = \frac{C_a + \sigma \tan \delta}{P_a} \quad (11)$$

4.6. Analysis of Concrete Wall Stability with Geotextile

Eq. 4 and Eq. 5 is valid also, Eq. 8. is valid for concrete wall stability with geotextile.

5. CONCLUSION

In the present study, geotextile materials are taken into consideration in the aspect of civil engineering applications. Especially stabilized retaining walls are considered and practical formulations and design frame work is given. Easy procedures for application are very important. Increase of geotextile material usage in engineering application is directly related with easy applied formulation and design procedures. From this point of view, a practical analysis method with design for structural system with geotextile materials is investigated. Analysis and design procedure is discussed in detail. In figure 2, design process steps are given. Following this flow will lead the engineer for design of retaining wall strengthened by geotextile material.

REFERENCES

1. Adanur, S. (1997) Design and Characterization of Geotextiles for High Performance Applications - Textile Engineering, Auburn University David Elton - Civil Engineering, Auburn University, National Textile Center Annual Report: November.
2. Coduto (2001), Foundation Design: Principles and Practices. Prentice Hall 2001.
3. AASHTO, (1996) Standard specifications for highway bridges, 16th edn. Washington, DC: American Association of State Highway and Transport Officers.
4. AASHTO, (1994) LRFD bridge design specifications, 1st edn. Washington, DC: American Association of State Highway and Transport Officers.
5. Yohchia C. (2000), Practical analysis and design of mechanically-stabilized earth walls—I. Design philosophies and procedures Engineering Structures 22 793–808.
6. Departments of The Army And The Air Force, (1995), Engineering Use of Geotextiles Technical Report, 20.
7. Brandon R. Parrish (2006), Geotextile Wrap-Face Wall Using Marginal Backfill Master Of Science Civil And Environmental Engineering University Of Missouri-Columbia.

CONDUCTIVITY AND MAGNETIC PROPERTIES OF COATED FABRICS WITH BARIUM FERRITE DOPED ANILINE SOLUTION

N. ONAR¹, A. CİRELİ AKŞİT¹,

M. F. EBEÖĞLÜĞİL², İ. BİRLİK², E. ÇELİK², İ. ÖZDEMİR²

¹Dokuz Eylül University, Textile Engineering Department

²Dokuz Eylül University, Material and Metallurgy Engineering Department

ABSTRACT

In this study, we aimed the development of the multifunctional and intelligent fabric with magnetic and electroconductive properties. As to this aim, cotton fabrics were coated with barium ferrite ($\text{BaFe}_{12}\text{O}_{19}$) doped aniline solution. Barium ferrite nanopowders were produced with co-precipitation calcination process and the polymerization of aniline was carried out by chemical oxidative polymerization process. The structural properties of the prepared barium ferrite nanopowders were investigated by using X-ray diffractogram. The magnetic properties of ferrite powders and coated fabrics were measured with the use of vibrating sample magnetometer (VSM). The microstructures of produced ferrite powders and the coated fabrics were analyzed with scanning electron microscopy (SEM). Furthermore, the effects of the amounts of the doped barium ferrite powders in polyaniline film on the fabric to the conductivity properties of the coated fabrics were investigated. The composite fabric with good conductivity and magnetic properties was successfully produced during the current process.

Key Words: ferrite, cotton fabric, magnetic properties, electrical properties, polyaniline

1. INTRODUCTION

Ferrites are widely used in many industrial applications because of their spontaneous magnetization. Therefore, the development of new and cost-effective techniques for fabricating nanostructures based on ferrites is of great commercial and scientific interest [1].

Conducting polymers have attracted also a lot of interest for both academic and industrial applications such as conductive coatings, rechargeable batteries, light emitting diodes, gas sensors and antistatic materials. Among these polymers, polyaniline (PAn) has been widely investigated due to low cost, easy synthesis, high conductivity depending upon the level of doping, environmental stability and interesting redox properties. It was reported that it was possible to prepare a conductive composite fabric with chemical polymerization of aniline upon Nylon 6, the chemical coating of polypyrrole upon acrylic as well as nonwoven fabrics, and the chemical polymerization of pyrrole upon synthetic fabrics. Cotton is one of the most popular materials used as fiber and fabric in textile. The conductive composites of cotton

fabrics are used as protective materials against electromagnetic interference, antistatic materials, anti dust and antibacterial cloths, deelectrifying and camouflaging compounds [2].

C. Forder et. al. (1993) described the preparation of superparamagnetic–conductive textile composites by a facile, two-step solution deposition process. First, colloidal magnetite particles (5–20 nm in diameter) are adsorbed spontaneously onto the textile fibres (polyester, nylon, cotton etc.) from an aqueous dispersion utilising a simple dip-coat procedure. Secondly, these treated fibres are then further coated with a conducting polymer overlayer (polypyrrole) [3].

By definition, ferrogel contains ferromagnetic fluid or finely distributed ferromagnetic particles, which are attached to the flexible network chains by adhesive forces giving rise to direct coupling between the magnetic and mechanical properties of both materials. Colloidal dispersion of monosized magnetic particles with a typical size of below 10 nm or a ferrofluid within a crosslinked polymer network endow superparamagnetic behavior, the same as ferromagnetic fluids. On the other hand, particles with diameters of about 100 nm or larger correspond to ferromagnetism [4].

M. Rubacha and J. Ziêba (2006) used a hard magnetic material, $\text{BaFe}_{12}\text{O}_{19}$, and soft magnetic materials, nano-crystalline alloy, as magnetic filler in obtaining fibers from concentrated cellulose solutions by using Lyocell process. Both the magnetic filler used were introduced into the spinning solution in the form of powders with an average grain diameter of 8 μm . They found that the magnetic properties depend on the kind of the implemented magnetic filler and its percentage content by volume in the fibre matter [5].

P. Gupta et. al., (2006) incorporated nanoparticles (~14 nm) of a mixed ferrite of Mn–Zn–Ni in submicron (200– 500 nm) fibers of an elastomeric polymer via electro-spinning. The back-scattered electron Field emission scanning electron microscopy (FESEM) images indicated agglomeration of the nanoparticles at higher wt % (ca. 17–26 wt %) loading in the electrospun fibers. The induced specific magnetic saturation and the relative permeability were found to increase linearly with increasing wt % loading of the ferrite nanoparticles on the submicron electrospun fibers. A specific magnetic saturation of 1.7–6.3 emu/g at ambient conditions indicated superparamagnetic behavior of these composite electrospun substrates [1]. A similar approach was used by M. Wang et al., where superparamagnetic composite polymer/magnetite nanofibers based on water-soluble poly(ethylene oxide) (PEO) and poly(vinyl alcohol) (PVA) were produced [6].

In this study, the diamagnetic cotton fabric was coated by barium ferrite ($\text{BaFe}_{12}\text{O}_{19}$) doped polyaniline film in order to improve the multifunctional and intelligent fabric with magnetic and electroconductive properties. Barium ferrite nanopowders as a hard magnetic material were prepared with co-

precipitation calcination process. Aniline polymerized with *in situ* polymerization method on the fabric surface composed of conductive polyaniline film layer on the fabric. The structural properties of the prepared barium ferrite nanopowders were determined by using X-ray diffractogram. The magnetic properties of barium ferrites and the coated textiles were measured with the use of VSM magnetometer. The microstructures of produced ferrite powders and the coated fabrics were analyzed with scanning electron microscopy. The composite fabric with good conductivity and magnetic properties was successfully produced during the current process.

2. MATERIAL AND METHODS

2.1 Fabrication

The synthesis of nanocrystalline barium ferrite powders was achieved through co-precipitation-calcination route. Guaranteed chemically grade ferric chloride ($\text{FeCl}_3 \cdot 6\text{H}_2\text{O}$, Horasan Chemistry) and barium chloride ($\text{BaCl}_2 \cdot 2\text{H}_2\text{O}$, Horasan Chemistry) were used as starting materials. Ferric and barium chlorides solutions in distilled water (Fe:Ba molar ratio 8) were prepared. The ferrite precursors were precipitated from the mixture by adding gradually sodium hydroxide (5 M NaOH, Merck) solution at room temperature to pH 12. The aqueous suspensions were stirred at constant 500 rpm for 15 min to achieve homogeneity and attain a stable pH condition. The (brownish) co-precipitate were filtered off, washed with distilled water and dried in an oven at 100°C for overnight. In order to form the hexaferrite phase, the dry precursors (brownish solids) were heated (calcined) at a rate of $15^\circ\text{C}/\text{min}$ in static air atmosphere up to 1200°C where it was maintained for 2 h [7].

A 10×10 cm dimensioned cotton fabrics, which desized, scoured and bleached (weft density of 20 yarn/cm, warp density of 24 yarn/cm, a weight density of 138 g/m^2), were used in this research. All chemicals used were reagent grade.

Distilled aniline (0.02 mol/L) and oxidizing agent ($\text{K}_2\text{Cr}_2\text{O}_7$, 0.008 mol/L) were dissolved in aqueous solution of 0.5 N HCl, and then available barium ferrite nanopowders ($<100 \text{ nm}$ particle size (BET), 99.5%, Aldrich) with different ratios as 0, 5%, 10%, 20% and 30 wt.% were added in the solution. The cotton fabrics were placed into beaker and the solution was added. Bath ratio was 1/100 (w/w) and the polymerization was conducted at 25°C for 4 hours. After the polymerization, the textiles were removed from the beaker and rinsed with distilled water. Then they were immersed in 0.5 N HCl for 15 min and dried in a hot air dryer at 50°C [8].

2.2 Characterization

The calcined powders were ground gently by agate mortar prior to their characterization. XRD patterns of prepared barium ferrite powders by co-precipitation-calcination route were determined to identify phase structure

by means of a Rigaku (D/MAX-2200/PC) diffractometer with a $\text{CuK}\alpha$ irradiation (wavelength, $\lambda=0.15418$ nm) by both θ - 2θ mode and 2θ scan mode with a scan speed of $8^\circ/\text{min}$. Thin-film XRD geometry where incident angle was fixed at 1° was used to collect data from only thin films. The diffracted X-ray beam was collected by scanning the detector between $2\theta = 3^\circ$ and 90° .

The surface topographies and qualities of prepared barium ferrite powder by co-precipitation-calcination route, bare fabric and coated fabrics with 5%, 10%, 20% and 30 wt.% barium ferrite doped polyaniline film were comparatively observed by using SEM (JEOL JSM 6060) with attached Energy Dispersive X-ray Spectroscopy (EDS) unit.

The magnetic properties of coated fabrics and barium ferrite powders were measured at room temperature on a vibrating sample magnetometer (VSM, Lakeshore 736, 7400 Series) in a maximum applied field of 15000 Gauss. From the obtained hysteresis curves, the saturation magnetization (M_s), the remanence magnetization and coercivity (H_c) were determined. Room temperature conductivity measurements of bare fabric and coated fabrics were performed by Novocontrol Alpha-N high resolution dielectric analyzer under alternative current (AC) as 3 Volt.

3. RESULTS AND DISCUSSION

3.1 Structural analysis of barium ferrite powders

Fig. 1 displays X-ray pattern of the barium ferrite powders produced by co-precipitation process. The diffractogram shows the presence of hexagonal form of $\text{BaFe}_{12}\text{O}_{19}$ with $a=b= 5.892$, $c=23.183$ Å of lattice parameters and 00-043-0002 PDF card number.

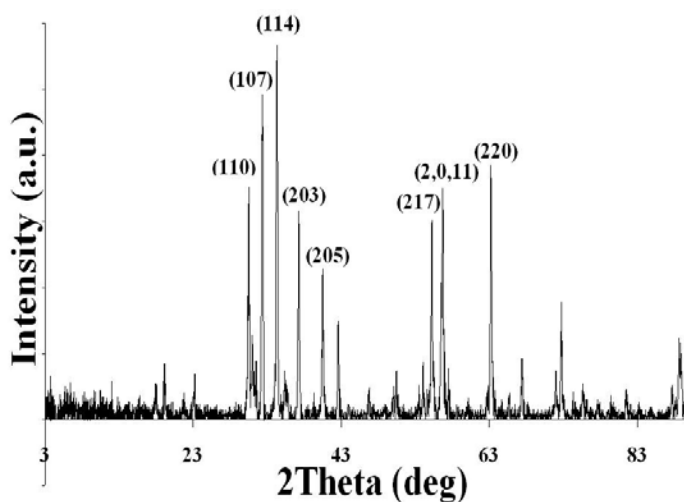


Figure 1. X-ray pattern of the barium ferrite powders produced by co-precipitation process.

3.2 Surface morphologies

Fig. 2 demonstrates SEM micrographs of the produced barium ferrite powder by co-precipitation process, bare fabric, the coated fabrics with 5, 10, 20, 30 wt.% barium ferrite doped polyaniline film. SEM micrographs of the produced barium ferrite powder by co-precipitation process show that the dimensions of granules were below micrometers and essentially fairly large as approximately 400-500 nm but the dimensions of granules were significantly different from each other. That's why, agglomeration of fine granules could have been carried out during the heat process and the grinding process was carried out after heat process at 1200 °C for 2 h but not after drying at 100 °C for overnight.

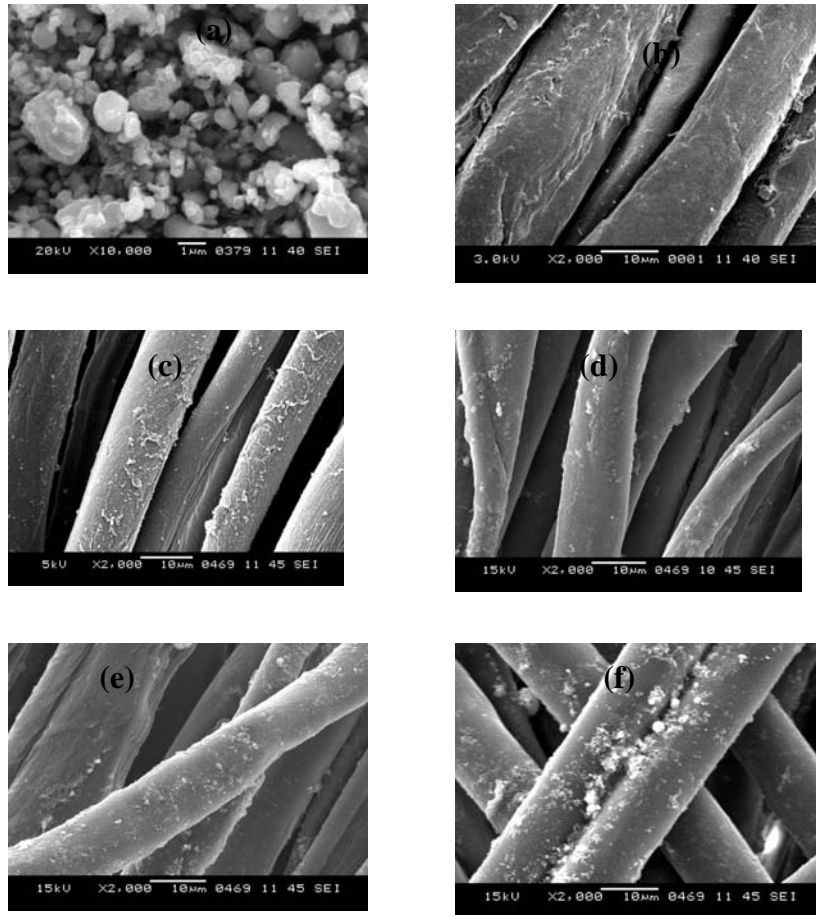


Figure 3. SEM micrographs of (a) the produced barium ferrite powder by co-precipitation process, (b) bare fabric, (c) the coated fabrics with 5 wt.%, (d) 10 wt.%, (e) 20 wt.%, (f) 30 wt.% barium ferrite doped polyaniline film

As shown in Fig. 3, barium ferrite powders were also unhomogeneously distributed on the fabric. While the amount of doped barium ferrite in polyaniline film was increasing, the particle size of doped barium ferrite powders in polyaniline film increased. Especially, SEM image of coated fabric with 30 wt.% barium ferrite doped polyaniline film displayed agglomerated particles on the fibre. The effect of some surfactants will be investigated to prevent the agglomeration of ferrite particles on the fiber in our further studies. The mean fibre thickness of bare fabric and coated fabrics was determined as 12.7 μm by using SEM. What is the increasing amount of the thickness of fiber of coating was not determined so that the thickness of fiber has quite variations in fabric.

Energy dispersive spectrometer (EDS) analysis of the produced barium ferrite powder by co-precipitation process proved the presence of 62.103 wt.% iron, 8.668 wt.% barium and 29.229 wt.% oxygen. Furthermore, EDS analysis of the coated fabrics with 5, 10, 20, 30 wt.% barium ferrite doped polyaniline film showed that the content of barium and iron in the coated fabrics increased while the amount of doped barium ferrite to polyaniline film was increasing (Table 1).

Table 1. The percentage of weight of Ba, Fe and O elements versus the amount of doped ferrite in polyaniline film coated on the fabric as EDS analysis.

Rating components	of 5wt.%barium ferrite	10wt.%barium ferrite	20wt.%barium ferrite	30wt.%barium ferrite
Fe(wt.%)	1.378	5.984	8.438	8.971
Ba(wt.%)	1.172	1.529	3.206	3.32
O(wt.%)	81.433	84.923	81.865	82.892

3.3 Conductivity properties of textile composites

Fig. 4 shows the conductivity values of the bare fabric and coated fabrics with different ratio of barium ferrite doped polyaniline film on the range of 10^{-10} to 10^7 hertz of frequency. The conductivity values of the fabrics increased in order of 10^{-8} to 10^{-3} S/cm at 10 Hertz by means of coating with the polyaniline film. The highest conductivity was obtained at the coated fabric with 5wt.% barium ferrite powder doped polyaniline film on the range of 10^{-10} to 10^7 hertz of frequency. Especially, the conductivity was higher than the conductivity of the coated fabric with polyaniline film without doping of barium ferrite powder. However, the further inclusion of barium ferrite powder in polyaniline film on the fabric decreased the conductivity of the coated fabrics compared with that of the coated fabrics with 5wt.% barium ferrite powder doped polianiline film and polyaniline film without barium ferrite powder.

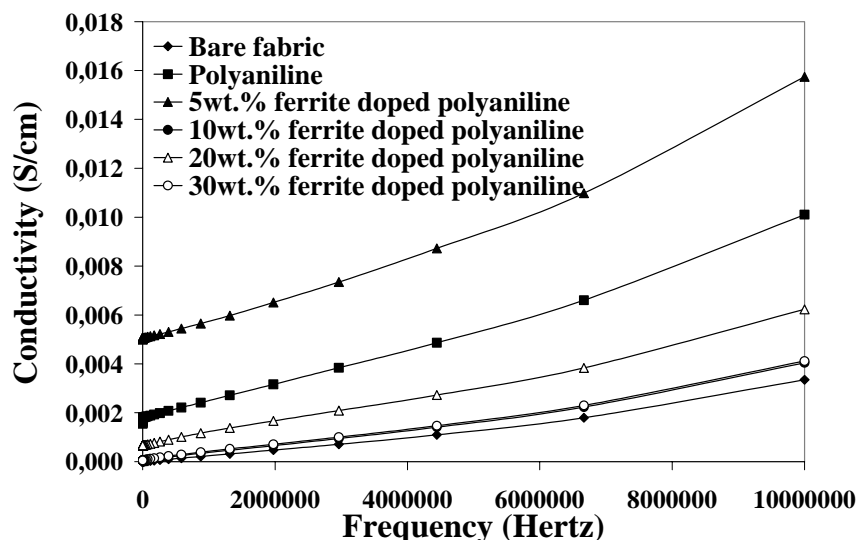


Figure 4. The conductivity values of the bare fabric and the coated fabrics on the range of 10^7 hertz of frequency.

3.4 Magnetic properties of textile composites and powders

Introducing ferromagnetic powder into coating on the diamagnetic cotton fabric resulted in obtaining a composite of new magnetic properties. Fig. 5 shows the hysteresis curves of the produced and available barium ferrite powder (Aldrich) and the coated fabric with 30wt.% barium ferrite (Aldrich) doped polyaniline film. Coercivity value of produced barium ferrite powders with co-precipitation process decreased from 3700 G to 2700 G compared with that of available barium ferrite powders while the coercivity value of the coated fabric was 4700 G. Magnetic saturation values were determined as 55.64 emu/g for produced barium ferrite powders by co-precipitation process, 34.38 emu/g for available barium ferrite powders and 0.95 emu/g for the coated fabric. The remanence magnetization values of produced and available barium ferrite powders and the coated fabrics were 28.4, 17.89 and 0.54 emu/g, respectively. The remanence magnetization as 0.54 emu/g and coercivity value as 4700 G of the coated fabrics at ambient conditions indicated ferromagnetic behavior of these composite fabrics. As a result, ferromagnetic fabrics can be prepared by coating with barium ferrite nanoparticles (<100 nm particle size) doped polyaniline film.

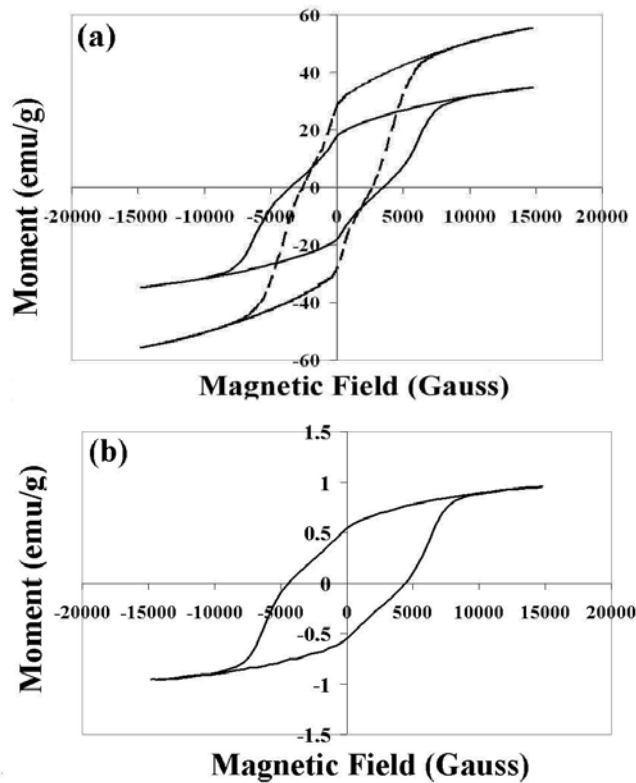


Figure 6. The hysteresis curves of (a) the produced (dashed line) and available barium ferrite powder (straight line) and (b) the coated fabric with 30wt.% barium ferrite doped polyaniline.

4. CONCLUSION

In conclusion, introducing ferromagnetic powder into coating on the diamagnetic cotton fabric resulted in obtaining a composite of new magnetic properties. The remanence magnetization as 0.54 emu/g and coercivity value as 4700 G for the coated fabrics at ambient conditions indicated ferromagnetic behavior of these composite fabrics. On the other hand, the conductivity values of the fabrics increased in order of 10^{-8} to 10^{-3} S/cm at 10 Hertz by means of coating with polyaniline film. It was deduced that the multifunctional and intelligent fabrics with electroconductive and magnetic properties can be successfully produced during the current process.

ACKNOWLEDGEMENT

The authors would like to acknowledge to Dr. Suleyman Tari in Dept. of Physics of Izmir Institute of Technology, for supporting of the magnetic characterization studies. This work has been supported by The Scientific

and technological Research Council of Turkey (TUBITAK) with 106M391 of project number.

REFERENCES

1. P. Gupta, R. Asmatulu, R. Claus, G. Wilkes: Superparamagnetic Flexible Substrates Based on Submicron Electrospun Estane® Fibers Containing MnZnFe–Ni Nanoparticles, *Journal of Applied Polymer Science* 100 (2006), 4935–4942.
2. S. Kutanis, M. Karakısla, U. Akbulut, M. Sacak: The conductive polyaniline/poly(ethylene terephthalate) composite fabrics, *Composites: Part A* 38 (2007), 609–614.
3. C. Forder, S. P. Armes, A. W. Simpson, C. Maggiore, M. Hawley: Preparation and characterisation of superparamagnetic conductive polyester textile composites, *J. Mater. Chem.* 3 (1993), 563 – 569.
4. N. Sahiner: Colloidal nanocomposite hydrogel particles, *Colloid. Polym. Sci.* 285 (2007), 413–421.
5. M. Rubacha, J. Ziêba: Magnetic Textile Elements, *FIBRES & TEXTILES in Eastern Europe* 14 (2006), 49-53.
6. M. Wang, H. Singh, T.A. Hatton, G.C. Rutledge: *Polymer* 45 (2004), 5505.
7. M. Radwan, M.M. Rashad, M.M. Hessien: Synthesis and characterization of barium hexaferrite nanoparticles, *Journal of Materials Processing Technology* 181 (2007), 106-109.
8. R. Hirase, T. Shikata, M. Shirai: Selective formation of polyaniline on wool by chemical polymerization using potassium iodate, *Synthetic Metals* 146 (2004), 73–77.

EFFECT OF SYSTEM PARAMETERS ON NANOFIBER MORPHOLOGY IN ELECTROSPINNING METHOD

A. DEMİR¹, M. DASDEMİR², M. TOPALBEKİROĞLU², G. S. KOZANOĞLU³

¹Istanbul Technical University, Department of Textile Engineering

²Gaziantep University, Department of Textile Engineering

³TSE Quality Campus, Gebze

ABSTRACT

Fibers are the main building blocks of all textile structures. Fabrics, yarns, and other textiles are constructed by fibers which directly affect the finished products in functionality and performance. Fine fibers have increasingly been used in textile products due to the fact that the handling and performance of yarns and fabrics. In terms of fibers, “*nano*” refers to the diameter of the fiber. Nanofibers have diameters less than one micron and cannot be seen without visual amplification. In the nanometer range, electrospinning technique has been proved to be convenient, effective and has been used for processing various polymers.

In electrospinning process, electrostatic forces are used instead of mechanical forces. Simply stated, applied potential voltage difference between a charged polymer and a grounded or oppositely charged collector causes to begin the process. The applied voltage leads to formation of the electrical force at the surface of a polymer solution or melt, which overcomes the surface tension. Then a charged jet is ejected from polymer drop. The jet extends in a straight line for a short distance (stability region), and then bends and follows a spiraling path (instability region). When the electrical forces elongate the jet thousands or even millions of times and the jet becomes very thin, the solvent evaporates, or the melt solidifies. Finally, very long nanofibers are collected on an electrically grounded collector

In order to investigate working of electrospinning system and determine optimum process parameters by using thermoplastic polyurethane (TPU), fiber morphology and method were examined and effect of system parameters on nanofiber morphology in electrospinning method were studied. The applied voltage, the variations in collector and feeding units, the distance between collectors and feeding units were chosen as variables in the system. In addition to these parameters, the effect of concentration on system and fiber morphology was studied.

In conclusion, increasing voltage causes irregular flow rates so roughness and high diameter ranges were observed on nanofibers. A decrease in fiber diameter was obtained by increasing the distance between collector and feeding unit. Also it has been found that polymer concentration affects the fiber diameter and the formation of beads. As the polymer concentration increase the fiber diameter increases and bead formation decreases.

Keywords: Electrospinning, Nanofiber, Thermoplastic Polyurethane(TPU)

1. INTRODUCTION

Within the past decade, the industry has rediscovered and continued to develop technologies that enable production of extremely small fibers “*nanofibers*” using a process called “*electrospinning*” [1].

Nanofibers are able to form a highly porous mesh and their large surface-to-volume ratio improves performance for many applications. Electrospinning

has the unique ability to produce nanofibers of different materials in various fibrous assemblies. The relatively high production rate and simplicity of the setup makes electrospinning highly attractive to both academia and industry. A variety of nanofibers can be made for applications in energy storage, healthcare, biotechnology, environmental engineering, defense and security [2].

In electrospinning, electrostatic forces are used in addition to mechanical forces to drive the fiber forming process [3]. Simply stated, electrospinning is a process that uses the electrostatic attraction between a charged polymer and a grounded or oppositely charged collection plate to produce extremely fine fibers ranging in diameter from less than 10 nanometers (nm) to several micrometers. Recent developments have shown it can be performed on polymers both in the molten state and in solution [1].

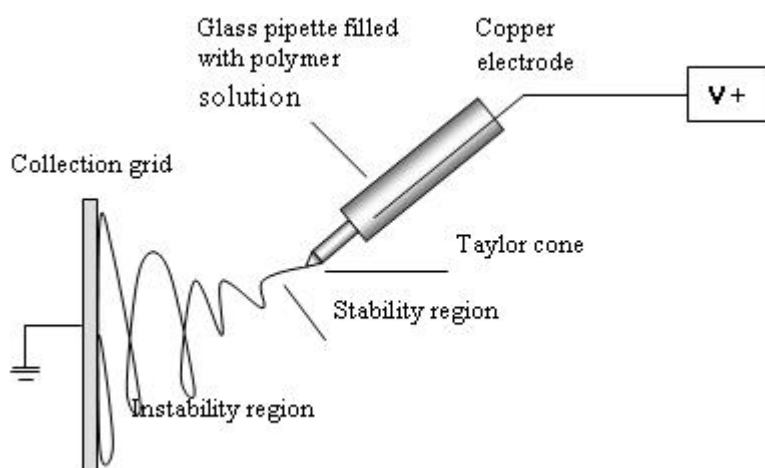


Figure 1. Electrospinning station

2. EXPERIMENTAL

2.1. Materials

All reagents were used without further purification. Thermoplastic polyurethanes (TPU) with the trademark name of Elastollan® in granule form was obtained from Renko Tekstil Sanayi ve Ticaret Ltd. Sti [Istanbul-Turkey].

Elastollan® TPU is produced by Elastogran GmbH and is an exceptionally versatile polymer. It is elastic with good dimensional stability and is stable at temperatures from -40° to $+125^{\circ}$ C. Together with good resilience, it has resistant to abrasion, microorganisms, oils, fuels, UV radiation and hydrolysis, thereby giving it an optimum fit in a very broad span of

applications and industries. Many commercially available TPU's can be used to make good electrospinning solutions [4,5].

N,N-Dimethylformamide (HCON(CH₃)₂) (DMF) that is the product of MERCK was used as a solvent for TPU.

Three different solutions from TPU were prepared. The concentrations of solutions were wt. 5 %, wt. 7.5 %, and wt. 10 %. For example, wt. 5 % solution has 5 gr TPU granules and 95 gr dimethylformamide.

The solutions were prepared the same days of electrospinning at room temperature and stirred gently. Special care was taken to avoid any contact with humidity since TPU solution coagulates easily in aqueous media [6].

2.2. Electrospinning System

2.2.1. Apparatus for Electrospinning

Electrospinning system needs three main parts to realize the process. They are feeding unit, collector, and high voltage power supply. In addition, some other auxiliary apparatus and devices were used to make the process easy.

A medical serum set was utilized as a feeding unit in the process of solution electrospinning.

The medical serum set used in experiments had a capacity of taking 100 ml liquid and ability of adjusting liquid flow. One drop of liquid which drips from the serum set is 0.05 ml. The serum set was firstly cleaned with distilled water and then dried. After that, polymer solution was filled in it by the help of syringes. The flow was adjusted manually with the flow adjuster. Finally, desired flow could be provided.

There are several collector types used in the electrospinning process. Their main functions are to provide grounding and to collect fibers. In this study, a circular shaped galvanized thin metal plate coated with aluminum foil was used as collector. Its diameter and thickness of the plate were 150 mm and 1.5 mm respectively.

Gamma ES 100 type DC power supply that is able to apply voltage up to 100 kV, was used in all experiments.

2.2.2. Solution Electrospinning Process

Prepared solutions were injected into the serum set with the help of suitable syringes. The polymer solution flow rate was manually adjusted. The thin plate collector was coated with aluminum foil and weighed together. So, the collector was made ready. It was then placed on to tripod. After that, the needle which is a part of the serum set was fixed at a desired distance from collector. The mini alligator clip of the high voltage power supply was mounted on to the needle. This was anode (+). The other electrode, cathode (-), which was connected with grounding electric cable was clipped on to collector. Then the desired voltage

was adjusted on high voltage power supply. Finally, power supply was switched on and system started to run as seen in the Figure 2.

Electrospun fibers were produced by using solution electrospinning system in an average temperature of 33 °C and relative humidity of 30 %.

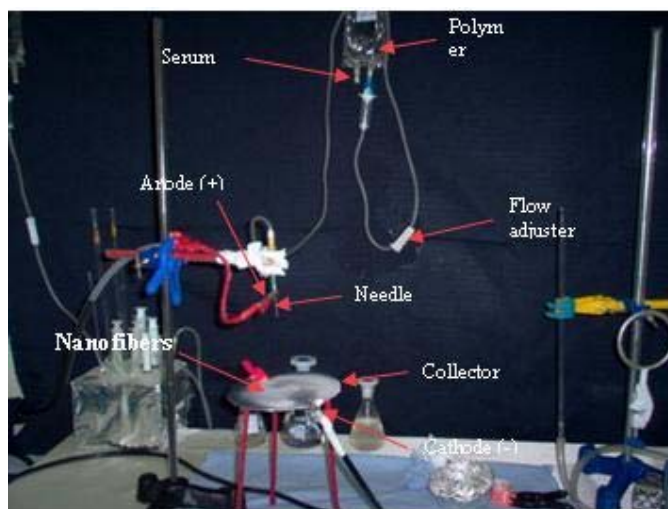


Figure 2. Solution Electrospinning Set-Up

2.3. Experimental Parameters

Table 1. summarizes the experimental parameters used in obtaining nanofibers from TPU polymer solutions.

Table 1. List of experimental variables in solution electrospinning

Material	Solution of TPU with dimethylformamide
Solution Concentrations	wt. 5 %, wt. 7.5 %, wt. 10 %
Applied Voltages	2 kV/cm, 3 kV/cm, 4 kV/cm
Distances	6 cm, 8 cm, 10 cm
Time	2 min, 4 min, 8 min
Flow Rate	0.05 ml/min

2.3. Measurements and Characterization

The JEOL JSM-6335F which is a cold cathode field emission scanning electron microscope (FESEM) was used to characterize nanofibers. It has a resolution of 1.5 nm at 15kV and 5 nm at 1kV. Scanning electron micrographs were taken for characterization and measurements by using FESEM.

Electrospun fiber diameters were measured to proportionate between electrospun fiber diameter and ratio scale which is stated on the bottom right of the FESEM images. Totally 60 diameter measurements were done for each FESEM images. These measurements were performed by determining 20 fibers chosen from each FESEM images and 3 diameter measurement for each of these fibers.

3. RESULTS AND DISCUSSION

3.1. Process Observations

The electrospinning process was initialized with an early adjusted voltage value. However, voltage value was gradually increased in order to determine critic voltage value (V_c) while the process was taking place. Thus, V_c was found as 5 kV at wt. 5 % TPU concentration and 6 cm distance from tip of the needle to collector. The first polymer jet formed at this voltage value. Because of higher voltage values used in experiments, it was observed that more than one jet could be formed from the handled drop that stayed at the tip of needle during the electrospinning process.

3.2. Electrospun Fiber Collection

Electrospun fibers that were carried by jets were collected homogeneously onto the collector. After a while, electrospun fibers which collected onto a certain part of the collector moved to another part of the collector (seen in Figure 3.). The reason of this is that the first collection part of the electrospun fibers is isolated in the course of time. Also, it was observed that at the beginning of the process and during the exchanging of jet or jets, very little solution drops dripped onto collector.

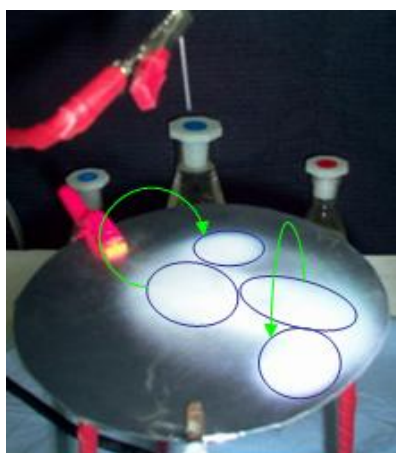


Figure 3. Electrospun TPU fibers collection as a result of jet movement Another observed result is that when applied voltage is increased, electrospun fibers are positioned as covering more surface area onto the collector.

3.3. Electrospun Fiber Weight

The weights of the electrospun fibers were measured with subtracting the weight of the collector weighed before the process from weight of the collector weighed after the process by using a sensitive weigh balance. The graphs given in Figure 4. show that, an increase on the applied voltage causes an increase on fiber weight. Furthermore, according to the comparison of graphs, increase of weight ratio of the electrospun fibers which were produced at 10 cm distance from tip of the needle to collector (seen in Figure 4. b) is higher than that of 6 cm (seen in Figure 4. a).

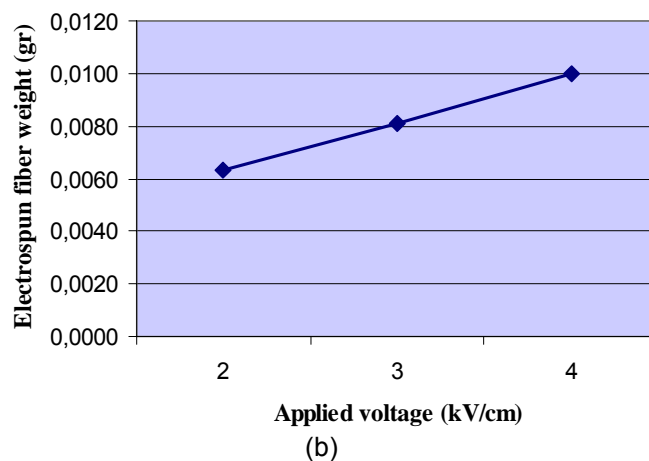
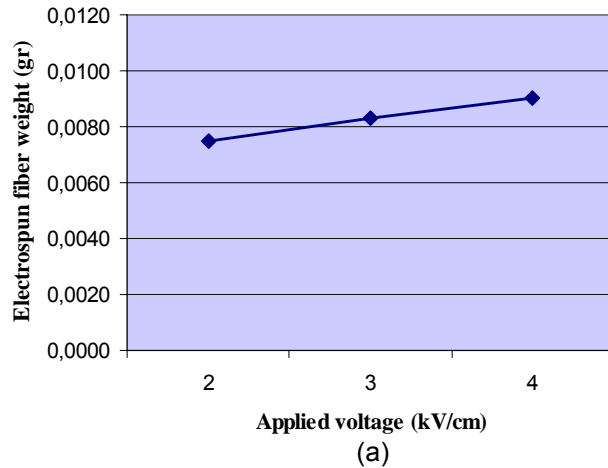


Figure 4. Effect of applied voltage on electrospun fiber production weight at 4 min with distances of (a) 6 cm, (b) 10 cm

3.4. Effect of Solution Concentration on Final Product

Of the solutions containing TPU at percentages of wt. 5 %, wt. 7.5 %, and wt. 10 %, fibers could only be produced from the solution of wt. 5 %. Nanofibers made from this concentration have great morphological surface structures (shown in Figure 5.8). However, after analyzing FESEM images shown in Figure 5.9 and Figure 5.10, it was observed that the products of other solutions, wt. 7.5 % and wt. 10 %, are in the shape of small particles that resemble polymer drop rather than fibers on the collector.

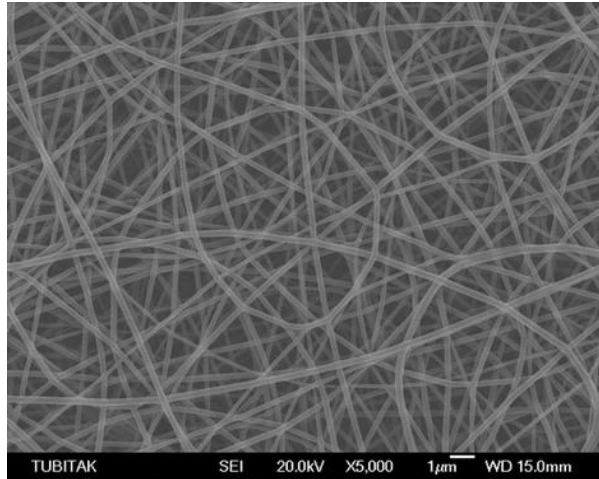


Figure 5. Scanning electron micrograph of solution electrospun TPU nanofibers produced at wt 5 % TPU concentration, 4 kV/cm applied voltage, and 10 cm distance

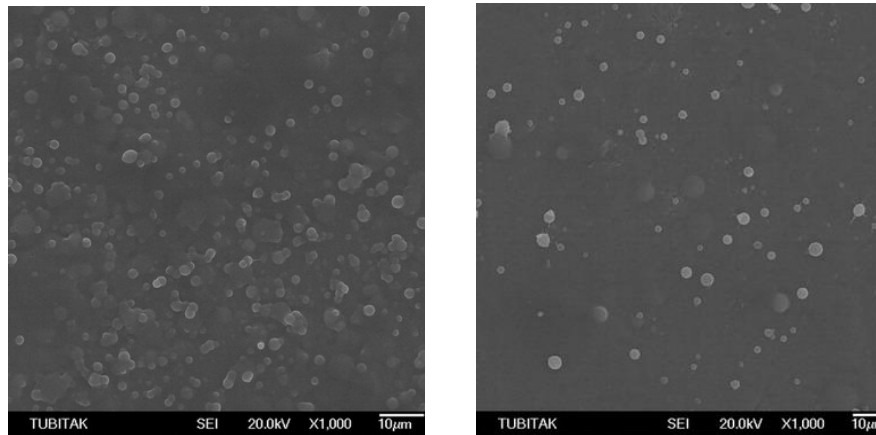


Figure 6. Scanning electron micrograph of solution electrospun TPU polymer drops produced at wt. (a) wt. 7.5 % and (b) wt. 10 %, 4 kV/cm applied voltage, and 10 cm distance

3.5. Effect of Applied Voltage on Fiber Diameter

As soon as the effect of voltage values on average fiber diameter is determined, the factors of distance and concentration are fixed. Afterwards, it was observed that when applied voltage value on each cm increased, average fiber diameter decreased (seen in Figure 7.).

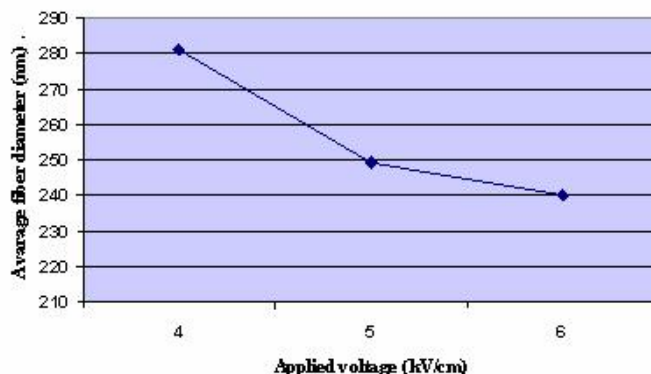


Figure 7. Effect of applied voltage on fiber diameter

3.6. Effect of Distance from Needle to Collector on Fiber Formation

When the effect of distance from tip of the needle to collector is examined, the factors of concentration and applied voltage value on each cm are fixed. In conclusion, when the distance value is increased, it was observed that the formed web was smoother. After FESEM images were examined, with increase of distance value, fibers tended to stick to together (seen in Figure 8.). It was observed that the most correct fiber forms were obtained at distance of 10 cm.

3.7. Effect of Processing Time on Fiber Diameter

With the aim of observing the effect of processing time on fiber diameter, two samples that were produced at factors of 2 kV/cm applied voltage and 8 cm distance from tip of the needle to collector from wt. 5 % TPU were evaluated. While the first sample was obtained by the electrospinning process done in 4 min, second sample was obtained in 8 min. According to the statistical analysis taken from diameter measurement values, average diameter value of the first and second experiments are 281 nm and 279 nm respectively. These values are very close to each other and it is concluded that process can be repeated in a reliable way. Another important conclusion of these samples is standard deviation on the diameter value of electrospun nanofibers produced in that two different time intervals. When the upper layer of electrospun webs were closely examined, nanofibers formed after the process time of 8 min showed a standard deviation value of 9 %. Nevertheless, nanofibers which were formed after the process in 4 min had a standard deviation value of 15 %. After this, it is proven that variation on the average diameter is less with the increase of process time.

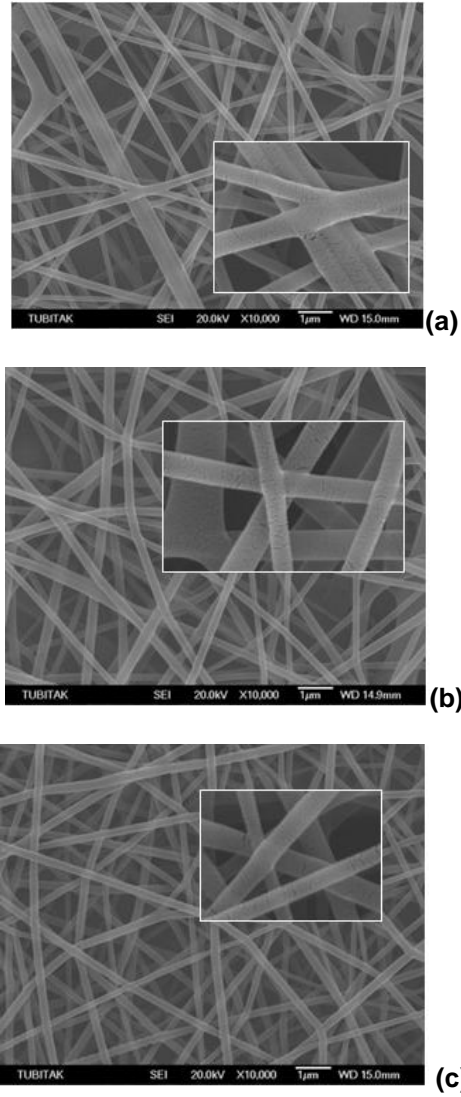


Figure 8. Scanning electron micrograph of solution electrospun TPU nanofibers produced at wt. 5 % TPU concentration, 4 kV/cm applied voltage, (a) 6 cm, (b) 8 cm and (c) 10 cm distance.

4. CONCLUSIONS

In solution electrospinning, the reason why nanofibers can not be formed from solution of wt. 7.5 % and wt. 10 % that contain high amount of TPU is to have these solutions more viscosity than the solution of wt. 5 % TPU concentration. The more concentration of the solution increases, the more its viscosity value increases. Thus, voltage needed to create a jet also increases.

As the voltage value increases, so does the quantity of fibers collected on collector surface. At the same time, the quantity of area surrounding on collector surface increases, too. Therefore, more fiber could be produced at high voltage values. Another crucial result is that the mean electrospun fiber diameter decreases with the increasing voltage in solution electrospinning of TPU.

It was observed that, the electrospun nanofibers were collected more homogenously by spreading on a wide area in solution electrospinning. Also, it was observed that while process continued, with increasing fiber quantity that was collected on certain areas on the collector surface, jets, by changing their paths, turned towards empty surfaces on collector in the course of time. In the end of this observation, an active carrier band can be used as a collector in future experiments.

Electrospun nanofibers that were formed with the increase of distance from tip of the needle to the collector in solution electrospinning system were observed to be smoother, although in low distance values electrospun nanofibers tended to stick together.

The results obtained from the average fiber diameter statistics showed that the standard deviation decreases with an increase in process time. Besides, it was observed that there was only a difference of less than 1 % in average fiber diameter value. The fact is that the process is reliable and the repeatability is ensured.

When the results obtained this study are compared with former studies [6], there is direct relation at effect of applied voltage in solution spinning. Also, in this study some improvements achieved such as low standard deviation in solution electrospinning.

ACKNOWLEDGEMENTS

The authors wish to acknowledge the support of this research by the TUBITAK, the Scientific & Technological Research Council of Turkey, Grants No. 104M414

REFERENCES

- [1] Lyons, J. and Kaufmann, J. (2004, August). Electrospinning: Past, Present & Future. *Textile World*.
- [2] Ramakrishna, S., Fujihara, K., Teo, W.E., Yong, T., Ma, Z., and Ramaseshan, R. (2006). Electrospun Nanofibers: Solving Global Issues, *Materials Today*, 9, 3, 40-50.
- [3] Mohan, A.(2002). *Formation and Characterization of Electrospun Nonwoven Webs*. M. Sc. Thesis, The Graduate Faculty of North Carolina State University.
- [4] Pedicini, A. and Farris, R.J. (2003, August 28). Mechanical Behaviour Of Electrospun Polyurethane. *Polymer*, 44, 6857-6862.
- [5] <http://www.newmaterials.com/news/164.asp>
- [6] Demir, M.M., Yilgor, I., Yilgor, E. and Erman, B. (2002). Electrospinning of polyurethane fibers, *Polymer*, 43, 3303-3309.

DEFINITION OF STRUCTURAL CHARACTERISTICS OF NANO FILTER MEMBRANE BY IMAGE PROCESSING

M. MALEKI, M. LATIFI, M. AMANI TEHRAN

Department of Textile Engineering, Amirkabir University of Technology

ABSTRACT

The extensive application in future of nano webs is in filtration. Filtration is necessary in many engineering fields. It is very important to know structural characteristics of nano webs for controlling the performance of filtration. Conventional techniques introduced for nonwoven layers are not completely applicable to measure nano web properties due to smaller fiber size and thinner structure. Image processing techniques can be utilized for extracting pore size & shape, fiber bonding and uniformity of nano webs from their images. The pore structure of filters is quite complex and their shapes are characterized by different indexes. Fiber bonding is also determined since it has an important role in mechanical and physical properties of nano webs. In order to define uniformity of nano webs, web images are broken up into number of windows. For each window area density is recorded and uniformity index is measured.

In the present work, structure and morphology of nano webs related to filtering use is studied by processing scanned electron microscopy (SEM) and simulated images. Having good images and proper image processing algorithms, the method can be proposed and applied for industry to determine and optimize product properties easily and shortly. This paper will discuss the development of image analysis algorithms to measure and evaluate structural and morphological characteristics of simulated and real nano web images.

Key Words: Structural Property, Nano Web, Image Processing, Pore Size & Shape, Mass Uniformity

1. INTRODUCTION

Nanotechnologies focus on the design, characterization, production, and application of nano scale systems and components [1]. The nonwoven industry generally considers nanofibers as having a diameter of less than one micron, although the National Science Foundation (NSF) defines nanofibers as having at least one dimension of 100 nanometer (nm) or less [2].

Filtration is necessary in many engineering fields. One direct way of developing high efficient and effective filter media is by applying nanometer sized fibers in filter structures [3]. Nanofiber membranes which are provided with electro-spinning have low basis weight, high permeability, very high surface area-to-volume ratio and small pore size that make them appropriate for a wide range of filtration applications [3,4]. In addition, nanofiber webs offers unique properties such as high specific surface area, good interconnectivity of pores and potential to incorporate active chemistry or functionality on nano scale. Therefore, nanofibers membranes are extensively being studied for air and liquid filtration [4]. Nano fibrous

materials used for filter media provide advantages of high filtration efficiency and low air resistance [3]. A few prototype applications of nanofiber filtering materials are included air filtering media for engine air filtration and cabin air, filter media for pulse clean cartridges in dust collection, penetrating aerosol particulate filtering media, high efficiency air filtering media, cigarette filter for filtration of smoke, adsorptive catalytic gas filter for respirators, filter media for wound dressing, biocatalyst filtering, ion-exchange filtering media, virus removal, metal recovery from wastewater and etc [4,5,6].

Electro-spinning is a fiber spinning technique driven by a high-voltage electrostatic field using a polymeric solution or liquid that produces polymer fibers with nanometer scale diameters [7]. The extremely small fiber size and low mass of nanofibers makes quality control measurement very difficult. For determining and controlling mechanical and physical properties of nano membranes filters, the structural properties of them are needed to determine. Most commercially available contact measurement equipment cannot work with the nanofiber without altering its characteristics. Generally, non contacting optical methods are not effective because the wavelength of the light used is greater than the diameter of the nanofibers [8]. Therefore, conventional techniques introduced for nonwoven layers are not completely applicable to measure nano membranes and these limitations of available test methods have directed users to the methods based on Imaging of nano filter membranes. The morphology of the nano webs are examined by scanning electron microscopy (SEM).

The present work describes the application of image processing techniques for extracting structural characteristics of nano filter membranes.

2. PORE FEATURES

The filtration performance of nano webs depends on their pore structure parameters. A pore can not be characterized by a single measurement. Several indexes have to be defined and considered for specific pore characteristics. Geometric descriptors are direct representatives of pore geometry. In this study, different descriptors are used to characterize and quantify shape features of pores.

2.1 Pore Numbers and Pore Density

Counting number of features represented in an image is one of the most common procedures in image analysis techniques. But, it is not proper to count all pores that can be seen in a nano filter web image. It is because the size, shape and position information of pores which intersect the edge of the image are unknown. The solution is to ignore pores which touch any edge of the image. Therefore, pore number is calculated as shown in equation (1) [9]:

$$Pore\ number = M \cdot \frac{d1 \cdot d2}{(d1 - o1) \cdot (d2 - o2)} \quad (1)$$

Where $d1$, $d2$ are dimensions of the image, and $o1$, $o2$ are dimensions of maximum boundary box of counted pores and $N1$ is the number of pores without considering edge pores. Figure (1.a) shows a simulated nano web in which fibers and pores are displayed in black and white respectively. Figure (2.b) shows boundary pores in black. The area of the pores to the entire area of image provides the *Pore Density* for each nano filter membranes.

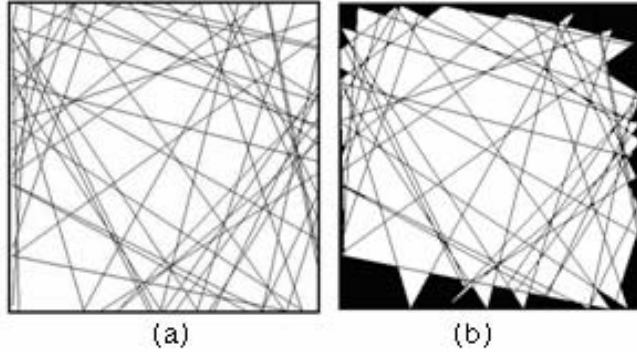


Figure 1. Simulated nano filter web
(a) fibers in black and pores in white (b) removed boundary pores

2.2 Pore Area and Perimeter

If $(\Delta x_i, \Delta y_i)$ are in pore area, (x_{k-1}, y_{k-1}) and (x_k, y_k) are consecutive pixels on the enclosed boundary. Area (A) and perimeter (P) of every pore are calculated as shown in equations (2) [10].

$$A = \sum \sum \Delta x_i \cdot \Delta y_j \quad (2)$$

$$P = \sum \sqrt{(x_k - x_{k-1})^2 + (y_k - y_{k-1})^2}$$

In the present work, pixels number of every pore and its boundary pixels number are reported as the pore area and perimeter respectively.

2.3 Pore Orientation

The moment axis of a feature is the axis which best fits all of the pixels in the sense that the sum of the square of their individual distances from the axis is minimized. Orientation is the angle (in degree) between the x-axis and the major axis of this ellipse which has the best fit of all pixels. This index shows the direction in which the pore is elongated [9].

2.4 Shape Factor

Shape factor or roundness is the index of similarity of a given shape to a circle. The ratio of a pore area to the area of a circle, whose perimeter is equal to the pore, is shape factor (R) which is defined as equation (3) [10].

$$R = \frac{4 \times \pi \times A}{P^2} \quad (3)$$

Where, A is area and P is perimeter of every pore which are already calculated. This parameter has no dimension. (R) ranges from 0 to 1. It is equal to 1 for a circle.

2.5 Ellipticity of Best Fit Ellipse

Recognizing that not all pores are round, there are many elliptical descriptors to describe the feature. The second moment of a best fit ellipse to a pore shape is one of them. The major and minor axes of this ellipse are determined in several ways. Ellipticity (E) is calculated by equation (4) in which A_1, A_s are the length of the semi-major and semi-minor axis, respectively [9].

$$E = \frac{A_1}{A_s} \quad (4)$$

2.6 Eccentricity of Best Fit Ellipse

The shape of an ellipse is described by its eccentricity. The eccentricity (e) is defined as:

$$e = \frac{c}{a} \times 100 \quad (5)$$

Where $2c$ is distance between two foci and a is semi-major axis.

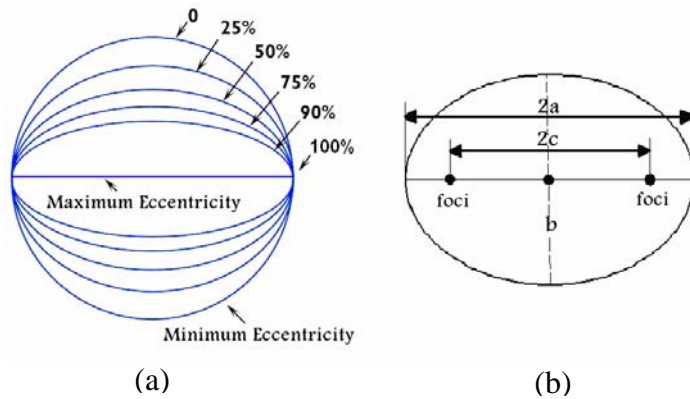


Figure 2. Eccentricity

(a) different values of eccentricity (b) different parameter in a ellipse

2.7 Aspect Ratio

The boundary rectangle of a pore is the smallest rectangle containing the pore. Its height and width are denoted as H and W . It should be noted that these are not the vertical and horizontal projection of the shape. It is because a pore may be oriented in any direction which should be considered to have the boundary box dimensions. Therefore, aspect ratio (AR) is defined by equation (6) [10]:

$$AR = \frac{H}{W} \quad (6)$$

2.8 Convex Hull

The convex hull of a set of points is the smallest convex boundary which contains those points. In some cases, a combination of dilation and erosion operations can be used to construct a convex hull for the shape and fill any boundary irregularities. Therefore, solidity would be derived from the area of the convex hull by equation (7) [9]:

$$Solidity = \frac{A(x)}{A_c(x)} \times 100 \quad (7)$$

For a pore, $A(x)$ is its area and $A_c(x)$, is the area of its convex hull.

3. WEB UNIFORMITY

Mass uniformity in fibrous structures such as nano filter membranes, plays an important role in their physical appearance, performance, and process ability. In filtration processes, membranes performance highly depends on the uniformity of the web. Thin spots in the fibrous sheet affect filtration performance by allowing large particles to pass through. The uniformity of nano membranes is determined by the way based on fractal theory and by Pourdeyhimi's method [11] which is a statistical technique.

3.1 Statistical Technique

Image is broken up into a number of windows. For each window, the area density of fibers (%black in windowed image) is reported. If randomness prevails, the Poisson distribution is the appropriate statistical descriptor of data. A commonly employed goodness-of-fit test for Poisson data is the index of I as defined in equation (8) [11]:

$$I = \frac{\text{observed variance}}{\text{observed mean}} \quad (8)$$

The simplest statistics test for the index of dispersion is the χ^2 [11]:

$$\chi^2 = I(n-1) \quad (9)$$

To determine an index describing the χ^2 data, data are divided by the total sum of the window numbers as defined in equation (10) [11]:

$$\text{Uniformity index} = \left(1 - \frac{\sum_{i=2}^{i=n} \chi_i^2}{\sum_{i=2}^{i=n} (n_i - 1)}\right) \times 100 \quad (10)$$

This normalization results in an index between 0 and 100, where 0 represents the least uniform and 100 the most uniform [11].

3.2 Fractal Analysis

Fractal concepts introduced by Benoit Mandelbrot (1983) have had major impression on understanding the structural disorder and its formation. Fractals are generally self-similar and independent of scale and they are not regular and may have an integer or non-integer dimension. Fractal geometry has provided a new approach for quantifying the geometry of complex shapes and irregular patterns [12]. Fractal behaviour has many applications in science and textile industry too. Since the nano membrane structures have complex geometric forms, fractal analysis can provide a quantitative value for determining the non uniformity of a web. One of the procedures of fractal dimension estimation based on measurement is the box-counting method. In this method, each image is covered by a virtual mesh whose cells' sizes can be varied. Two values are recorded for each cell: the number of cells intersected by the image ($N(s)$) and the side length of each cell (s). The regression slope (D) of the straight line formed by plotting $\log(N(s))$ against $\log(1/s)$ indicates the fractal dimension which ranges between 1 and 2. In this work, the box-counting method is used to evaluate the degree of non-uniformity of a nano web. The presence of fibers in each cell is considered to count the number of boxes as $N(s)$.

4. RESULTS

4.1 Simulated Nano Webs

Simulated nano web images are utilized to verify analysis algorithms. These simulated webs are different in fiber orientation distribution, web density, number of fibers per unit area of web, fiber diameter distribution and mean length of fibers. The measured pore features of simulated nano web images (figure 3) are listed in table 1.

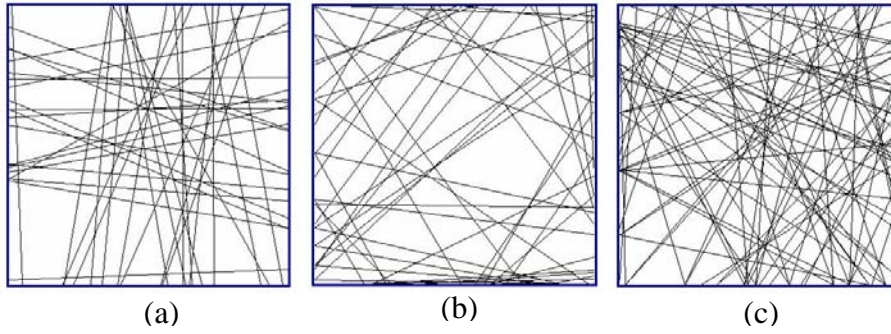


Figure 3. Simulated nano webs (a,b,c)

Table 1. Measured pore features of the simulated nano webs

	(a)		(b)		(c)	
	mean	std	mean	std	mean	std
area (pixel)	218.43	504.29	316.76	635.62	89.05	143.43
perimeter (pixel)	61.65	51.79	82.14	68.85	42.56	30.68
orientation(degree)	97.93	54.95	77.22	62.40	100.14	47.09
shape factor	0.52	0.17	0.42	0.17	0.51	0.18
ellipticity	3.04	2.11	3.36	2.58	2.75	1.64
eccentricity	86.43%	13.32	86.85%	14.23	86.03%	12.61
aspect ratio	0.54	0.41	0.28	0.26	0.53	0.39
solidity	89.37%	5.66	91.20%	5.97	89.17%	5.53

The uniformity of other three web images (figure 4), measured by fractal and statistical method, is presented in table (2).

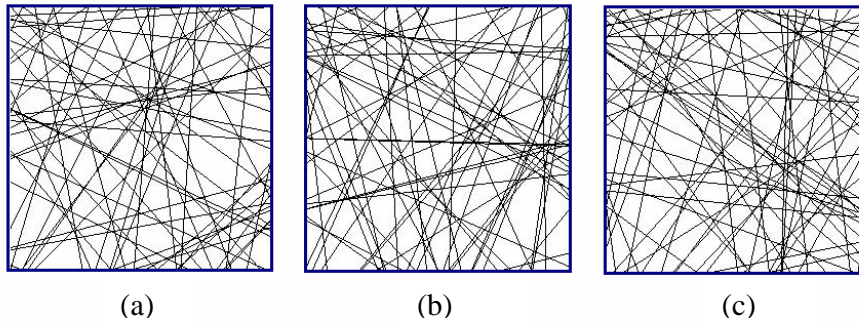


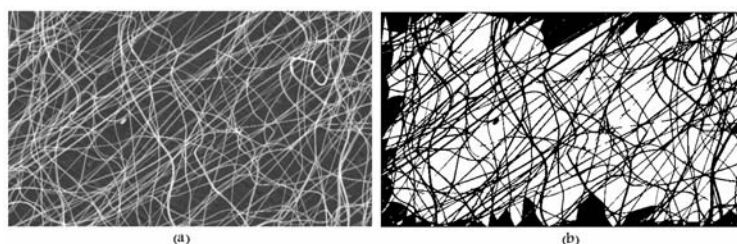
Figure 4. Simulated nano webs

Table 2. Uniformity of simulated nano webs

		Image		
		(a)	(b)	(c)
Method	Statistical technique	83.858	83.860	84.269
	Fractal dimension	1.832	1.840	1.850

4.2 Real Nano Webs

Analysis of real nano web images requires more process. The SEM images are first cropped to a desired size (figure 5.a). The images are converted to binary. Noise and undesirable pixels are eliminated by suitable filters and morphological processing (figure 5.b).

**Figure 5.** Real nano web**Table 3.** Measured pore features of the real nano web

	area (pixel)	perimeter (pixel)	orientation (degree)	Shape factor	ellipticity	eccentricity	Aspect ratio	solidity
mean	163.717	63.142	64.590	0.454	2.884	87.436	0.488	89.149
std	264.256	56.683	35.581	0.195	1.575	11.884	0.354	6.209

5. CONCLUSIONS

The present work shows that image processing technique can be applied on SEM images of nano webs to characterize and quantify pores features by geometric descriptors.

Variation of mass in webs has historically been used as an index of uniformity. This study was also devoted to characterize the variation of mass in nano webs with the aid of image analysis method.

The results from simulated nano webs confirm the application of used algorithms for characterizing real nano membranes.

REFERENCES

1. Uskokovic, V. (2007), "Nanotechnologies: What We do not Know", *Technology in Society*, vol. 29, pp. 43–61.
2. Grafe, T., Graham, K. (2002), "Polymeric Nanofibers and Nanofiber Webs: A New Class of Nonwovens", *International Nonwovens Technical Conference, INTC*, pp.1-13.
3. Qin, X. and Wang, S. (2006), "Filtration Properties of Electrospinning Nanofibers", *Journal of Applied Polymer Science*, vol. 102, pp. 1285–1290.
4. Barhate, R. and Ramakrishna, S. (2007), "Nanofibrous Filtering Media: Filtration Problems and Solutions from Tiny Materials", *Journal of Membrane Science*, vol. 296, pp.1–8.
5. Ahn, Y., Park, S., Kim, J., Hwang, Y. (2006), "Development of High Efficiency Nanofilters Made of Nanofibers", *Current Applied Physics*, vol. 6, pp. 1030–1035.
6. Bowen, W., Welfoot, J. and Williams, P. (2002), "Linearized Transport Model for Nanofiltration: Development and Assessment", *AIChE Journal*, vol. 48, No. 4, pp. 760-773.
7. Kwon, K., Kidoaki, S. and Matsuda, T. (2005), "Electrospun Nano- to Microfiber Fabrics Made of Biodegradable Copolyesters: Structural Characteristics, Mechanical Properties and Cell Adhesion Potential", *Biomaterials*, vol. 26, pp. 3929–3939.
8. Luzhansky, D. (2003), "Quality Control in Manufacturing of Electrospun Nanofiber Composites", *International Nonwovens Technical Conference*, Baltimore, Maryland.
9. Gonzalez, R. Woods, R. (2002), "Digital Image Processing", second edition, New Jersey, Prentice-Hall.
10. Xu, B., Pourdeyhimi, B. and Sobus, J. (1993), "Fiber Cross-Sectional Shape Analysis Using Image Processing Techniques", *Textile Research Journal*, vol. 63, no. 12, pp. 717-730.
11. Pourdeyhimi, B. and Kohel, L. (2002), "Area-Based Strategy for Determining Web Uniformity", *Textile Research Journal*, vol. 72, no.12, pp. 1065-1072.
12. Jelinek, H., Jones, C., Warfel, M., Lucas, C. (2006), "Understanding Fractal Analysis? The Case of Fractal Linguistics", *Complexus*, vol. 3, pp. 66–73.

NOVEL MICRO-CHANNEL MEMBRANES FOR CONTROLLED DELIVERY OF BIOPHARMACEUTICALS

G. K. STYLIOS, T. WAN

Research Institute for Flexible Materials, Heriot-Watt University

ABSTRACT

As medical practice enters a new era with the exciting new applications of nanoscience and technology, the paper introduces the philosophy and the principles of precisely controlled drug delivery. The paper concentrates in two materials; the first one is an optimal textile membrane for bone tissue engineering which has interconnected networks of pores, micro and nanoscale in size to allow extensive body fluid transportation through the pores and hence triggering bone in-growth, cell migration, tissue in-growth, and eventually vascularization. The second one is a super gel membrane which is used as a payload vehicle for controlled release of growth bone hormone and it is capable of controlling release of up to 50 days, using harmless magnetic field. The paper goes on to highlight the process of those new materials for medical applications citing particularly a successful process for coating them onto flexible materials such as fabrics.

Key Words: Nanoscience, nanotechnology, drug delivery, nanoporous polymer, membranes, phase separation, polymer coating, cell biology, tissue engineering.

1. INTRODUCTION

Controlled release formulations can be used to reduce the amount of drug necessary to cause the same therapeutic effect in patients. The convenience of fewer and more effective doses also increases patient compliance. The inductive approach to controlled delivery of biopharmaceuticals seeks to combine the fabrication of micro-channeled polymeric scaffolds, smart functional materials with drug delivery technology, which has the potential to guide bone healing and other medical application with antibacterial function through a controlled release of bioactive factors directly into the patient's wound. Scaffolds designed to the micro-channel membranes for controlled delivery of biopharmaceuticals must have several basic requirements, which include being biodegradable and biocompatible, and having a high surface area/volume ratio with sufficient mechanical integrity [1].

An overview of the current state of the porous scaffolds systems based on the application of guiding bone healing reported in literature is reviewed [2]. Metals, polymers, ceramics and composites are used in the design of different components of bone graft substitutes and drug delivery systems [3-7]. A variety of fabrication processes have been developed, resulting in porous implant substrates and delivery system that can address unresolved

clinical problems. The merits of these biomaterial systems are evaluated in the context of mechanical properties and biomedical performances most suitable for bone healing and other biomedical applications. An optimal scaffold for guided bone healing should be biocompatible for in vitro and in vivo bone growth, with degradation products that are non-toxic that can be easily excreted by the body. To achieve this it must consist of an interconnected porous network of micro- and nano in scale to allow extensive body fluid and drug transport through the porous scaffold matrix, which can trigger bone in-growth, cell migration, tissue in growth and eventually vascularisation. The advantages of organic and ceramic nanocomposites exhibiting surface or bulk porosity have led researchers to conduct systematic research aimed at clarifying the fundamental aspects of interactions between porous materials and applied objects.

Hydrogels are polymeric networks that absorb large quantities of water while remaining insoluble in aqueous solutions due to chemical or physical cross linking of individual polymer chains. Due to their good biocompatibility and mechanical properties, mechanical strength and high elasticity and swelling upon immersion in water, polyvinyl alcohol (PVA) hydro gels have been used in numerous biomedical applications, for example as implants, artificial organs, contact lenses, drug delivery devices, and also wound dressings in wounds management [7-11].

The paper is aimed to develop a set of novel intelligent drug delivery system in the form of coat layer for recovery and cure after bone breaking, based on a novel micro-channel membrane for the controlled drug delivery of encapsulated pharmaceuticals, combined with a large surface area of a biocompatible polymer nanostructure and stimuli response hydro gels as drug carriers within the matrix. In order to achieve these requirements, several novel approaches will be studied to control the pore size, shape, distribution and surface functionality. It is expected that the size of the cavities generated can be reduced down to a nano-level in controllable morphology, distribution and surface functionality with good accuracy by using micro phase separation, inter-particular cross-linking and polymerization of micro emulsion. The novel micro-channel matrix will be developed with a higher degree of control over such properties as pore size, pore size distribution, pore volume, surface area, and material density, using various porous scaffold development techniques, covering the development of micro and nano-porous structures in the membranes. Drugs will be loaded into the system during the process or after the process. Initially for the application in recovery and cure after bone breaking, the controlled drug delivery system will provide more potential in biopharmaceutical bioprocessing, including minimization of medical crises and side effects. We studied varied kinds of polymer scaffolds, including 3D porous polyurethane polymer scaffolds, poly(vinyl alcohol) hydro gels and hybrid composites, by the assembly and immersion of drug loading using a micro emulsion and freeze-thawing process. The incorporation of encapsulated pharmaceuticals with stimuli response hydro gels and polymers in the porous scaffolds matrix will provide a

novel process to develop a new intelligent drug delivery system in the form of the membranes for medical treatments. Our work focuses on the development of the technology for use as a controlled slow-delivery means for biopharmaceuticals to provide 'active' cure while minimize medical crises and side effects.

2. THE PHILOSOPHY AND THE PRINCIPLES OF PRECISELY CONTROLLED DRUG DELIVERY

There is convincing evidence that constant drug delivery is not always effective from a pharmacological point of view. Nearly all functions of the body show significant daily variations or patterns, coordinating biological rhythms with medical treatment. If we can deliver the right biopharmaceuticals at the controlled and prolonged delivery rate, we can minimize medical crises and side effects, and eventually lower the cost and improve compliance.

Incorporation of a drug within a biodegradable, biocompatible polymer nanostructure within micro/nano porous polymer matrix will be a promising approach, by the combination of in-situ formation of the stimuli responsive hydro gels on porous hydrophobic polymer matrix. It is expected to swell or shrink in response to small changes in environmental conditions in which they are placed. In this case, the use of environmentally-sensitive hydro gels as carriers will cause the release of an active agent at predetermined intervals associated with the circadian rhythm. Such a novel drug delivery system is being prepared by the combination of the following two materials:

- Biodegradable porous polymer matrices for supporting stimuli-sensitive hydro gels formation with entrapped enzymes and drugs. It is expected that this size of the pores could be reduced to a nano-level by micro phase separation, interparticle cross linking and micro emulsion.
- Super porous PVA hydro gels of polymeric networks with controlled and prolonged delivery of biopharmaceuticals that absorb large quantities of water while remaining insoluble in aqueous solutions due to chemical or physical cross linking of individual polymer chains. This intelligent hydro gel is developed to undergo reversible swelling changes in response to small changes in solvent composition, pH, temperature, intensity of light as well as magnetic and electric fields.

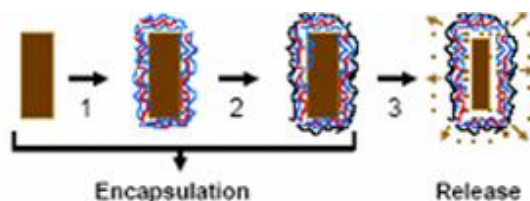


Figure 1. The conception of intelligent drug delivery system

Drug delivery control can also be created by filling gel-like liquid crystals with magnetic components into the porous matrix, as seen in Figure 1. When this drug delivery system is exposed to an alternating magnetic field frequency, magnetic particles are made to vibrate and the drug is squashed out. Generated heat of the hydro gel can also aid in rapidly releasing the encapsulated drugs.

3. THE POLYURETHANE MEMBRANE

The majority of porous membranes are prepared by controlled phase separation of polymer solutions onto two phases: one with a high polymer concentration, and one with a low polymer concentration. Phase separation mechanisms can generally be subdivided in three main categories depending on the parameters that induce de-mixing. If the phase separation is induced by exchange of a non-solvent for the solvent used to prepare the solution, the process is referred to as diffusion induced phase separation (DIPS) or phase inversion. In the above mentioned phase separation techniques the most widely used ones are the thermally induced phase separation (TIPS), immersion precipitation, and phase inversion method. By changing the temperature at the interface of the polymer solution, heat exchange can take place and consequently we have de-mixing induced TIPS.

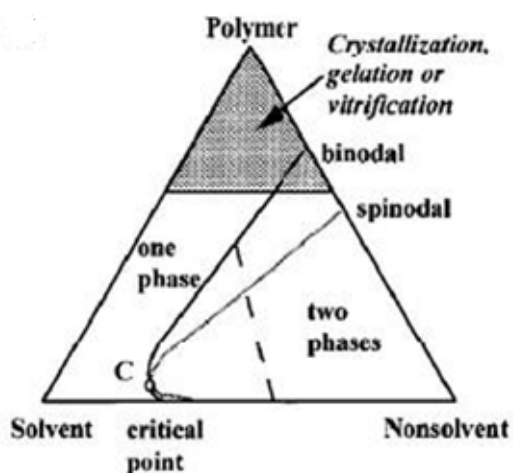


Figure 2. Phase diagram of ternary polymer solution [12]

Liquid-liquid demixing processes play an important role in most of the TIPS processes. The combinations of liquid-liquid demixing with crystallization of the polymer, nitrifications, association, and also crystallization of the solvent are of special importance for the generation of porous structures. Figure 2 shows a typical ternary polymer solution phase diagram, showing the binodal and spinodal points, as well as the solidification region.

Figure 3 illustrates schematically a phase diagram for a binary polymer solvent system. In this figure the temperature is plotted as a function of the polymer concentration of the polymer solution. At high temperatures the solution is still homogeneous. At lower temperatures liquid-liquid phase separation of a polymer poor and rich phases take place. The boundary of the liquid-liquid de-mixing gap is usually called the binodal, but for poly-disperse polymers, the term "cloud point curve" is more appropriate. Usually the liquid-liquid de-mixing gap is subdivided into a region of spinodal de-mixing, bounded by the spinodal, and two regions of nucleation and growth between the binodal and the spinodal. Compositions that are in equilibrium are located on the binodal, and are connected by horizontal tie lines. It is important to note that the transition between binodal decomposition and spinodal decomposition should not be regarded as a sudden change in decomposition mechanism but as a gradual one.

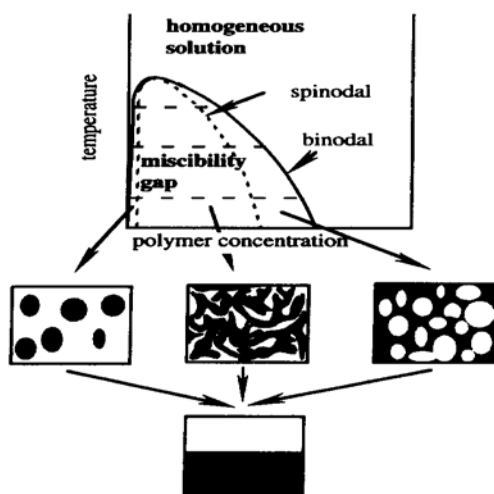


Figure 3. Schematic representation of binary phase diagram of a polymer solution, showing the liquid-liquid de-mixing gap. In addition, the possible structure formation in the different parts of the liquid-liquid de-mixing gap is indicated: nucleation and growth of the polymer rich phase (left picture), bi-continuous morphology due to spinodal decomposition (middle picture) and nucleation and growth of a polymer poor phase (right picture). [13]

More recently, we have presented a novel emulsion-coating method to generate a special porous microstructure, by casting the membrane from a solution comprising a mixture of surfactant, pore-forming polymer and film-forming polymer, viscosity control polymer, a solvent for the mixture of polymers, and a non solvent wherein an emulsion process occurs at different temperatures. It relates to a new coating process for coating frozen and gelled coating solution in the form of a water-in-oil emulsion. In this new process, a water-in-oil emulsion, from an aqueous solution and a polymer solution, is frozen partially according to

the requirement of viscosity and then forced into a coating layer on a matrix fabric by a coating process.

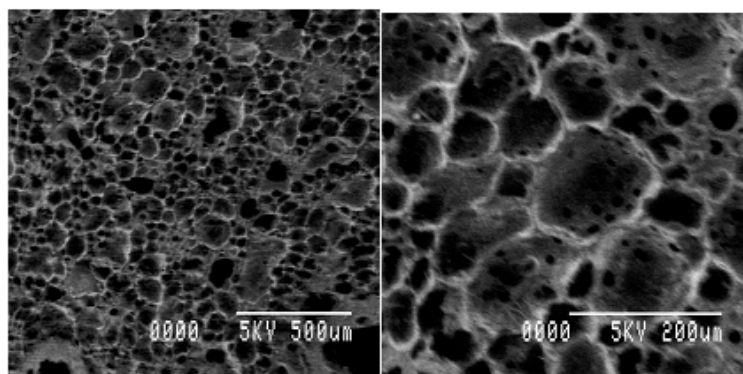


Figure 4. Porous structure of polyurethane film from emulsion coating.

When the temperature is low enough to allow freezing of the solution, the emulsion solution would be at the solid–liquid demixing stage, which forms frozen solvent and concentrated polymer phases. Then, the coating solution of these matrices, partly in solidification, is passed through a freeze box. After the removal of the frozen solvent, the remained space would become porous. Macro-micro/nano double scale porous scaffolds, with a porosity of 65 vol % were prepared by this process, as illustrated in the example, Figure 4.

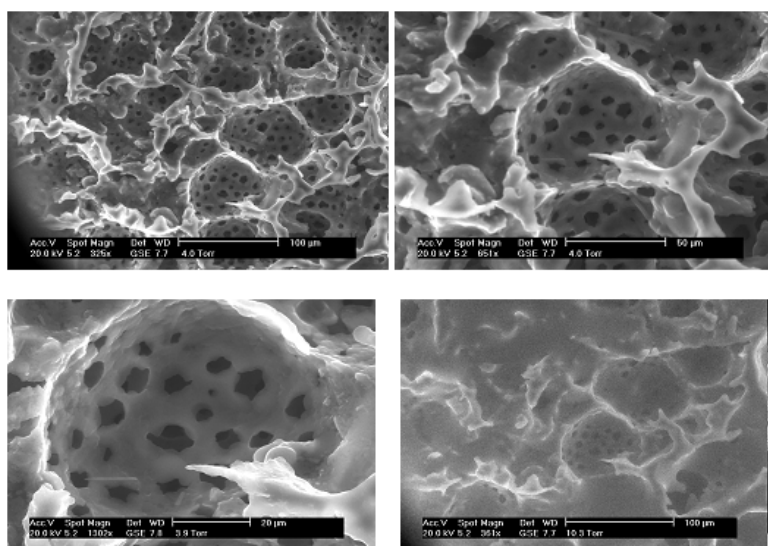


Figure 5. Porous structure of polymer membrane by emulsion freezing–drying process



Figure 6. Samples of smooth coated PU membrane on fabrics using continuous coating knife over roller method.

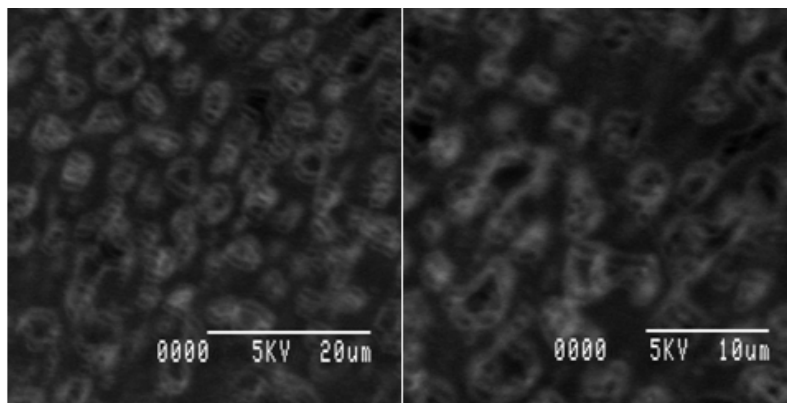


Figure 7. Micro/ Nano scale Porous structure of the polymer membrane.

The microstructure observation of the membrane examined using an Environmental Scanning Electron Microscope (ESEM) has indicated that the microstructure assimilates body tissue: vis a vis., a lot of micro cavities containing nano pore inside them, Figure 5. Membranes used for scaffolds, with a porosity of 20-50 vol% and pores of approximately 10-20 μm containing within them pore sizes of 200–400 nm were developed by this process. In addition, in-situ observation of water absorption by ESEM has shown that such a pore structure can quickly absorb water, several magnitudes higher than conventional artificial film cotton or wool fabrics with similar thickness. This makes these materials

particularly important as payload carriers, with many applications as delivery systems, due to the large volume to size ratio. Products that are super absorbers can be made, products acting as insulators, even flexible cooling systems by trapping water inside their structure. This new method appears to be promising also for tissue engineering applications. In this process, a water-in-oil emulsion, from an aqueous protein solution and a polymer solution, is coated on a fabric matrix as shown in Figure 6. The size of the cavities generated are controllable and the distribution and surface functionality of the material can also be engineered with good accuracy by using micro phase separation, as shown in Figure.7.

4. POLYVINYL ALCOHOL HYDROGEL

To avoid chemical cross linking of PVA ensuing toxicity and leaching problems, a novel method of PVA solidification has been developed by freezing and thawing of aqueous PVA solutions are described in the following section. The new material in an ultra pure three dimensional network held together by crystallites acting as physical cross links forming a physical network, as shown in Figure 8. It can provide a relatively mild network fabrication and drug encapsulation conditions that make them suitable for protein delivery. As a consequence, a new hydro gel of high mechanical strength and high water content if formed without the help of any chemical cross-linking agent.

Figure 9 illustrates an example of PVA hydro gels. The freezing/thawing method involves casting aqueous PVA solutions in molds, freezing them in a freezer for 2h-24 h at - 20°C -60 °C and then allowing them to thaw at 4°C - 25°C for 2-6 h. This process may be repeated for up to several cycles. It was found that several parameters significantly alter the overall structure, morphology, and stability of the resulting materials. In particular, the number of freezing and thawing cycles, concentration of aqueous solution, and molecular weight of PVA can be manipulated to control properties such as the overall water content, the mechanical strength, the adhesive characteristics, and its diffusive properties.

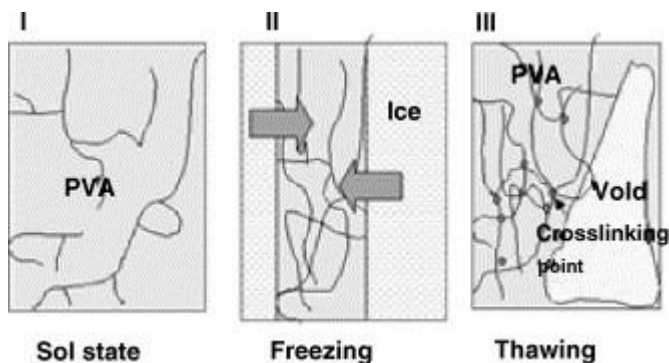


Figure 8. Schematic illustration of gel formation by freezing and thawing.

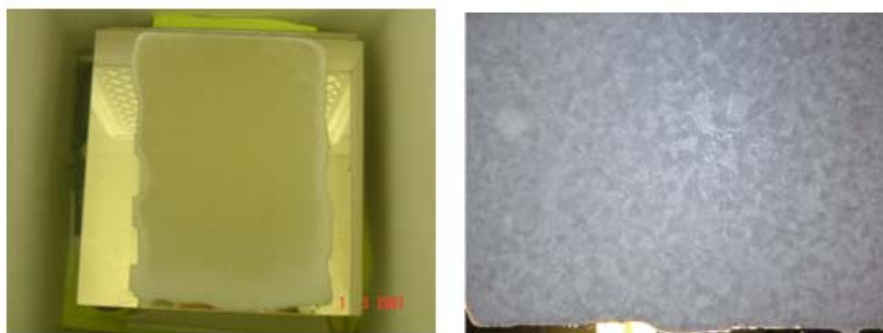


Figure 9. PVA hydro gels formation example

Figure.10 illustrated several examples of PVA hydro gels from a poly(vinyl alcohol) solution in a mixed solvent, consisting of water and water-miscible organic solvent. In previous work, no organic solvent is employed for gel preparation; the aqueous solution is frozen to induce phase separation into an ice phase and polymer phase, which result in a larger pore size. In new work, a porous and transparent hydro gel is prepared from a poly(vinyl alcohol) solution in a mixed solvent consisting of water and a water-miscible organic solvent, such as acetone, ethyl alcohol, tetrahydrofuran, dimethyl formamide, ethylene glycol, glycerol, triethylene glycol, and dimethyl sulfoxide. Upon cooling the (vinyl alcohol) solution below room temperature, a gel is formed as a consequence of crystallization of poly(vinyl alcohol) molecules. The mixed solvent hinder the PVA solution from freezing at lower temperature and hence the PVA crystallization takes place without accompanying a significant volume expansion, i.e., pores of smaller size. Consequently, the resulting porous gel carries pores of small size, which result in an insignificant difference in refractive index, therefore, in formation of a transparent gel.



Figure 10. PVA hydro gel from a poly(vinyl alcohol) solution in a mixed solvent consisting of water and a water-miscible organic solvent

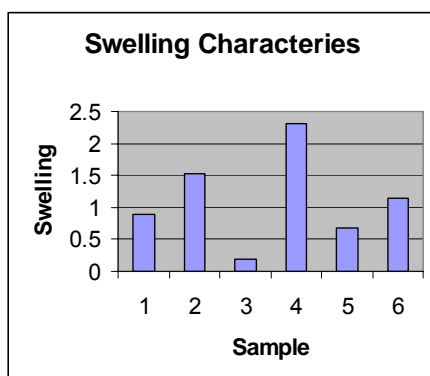
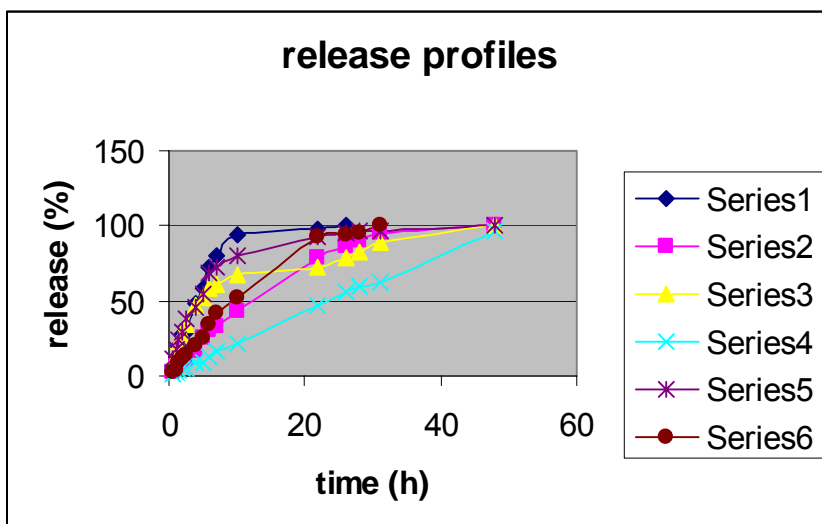
In addition, membrane structure and performances may be regulated by the addition of the plasticizer or other chemicals, such as PEG (MW 67, 1000, 6000), PVP, sodium hydroxide, calcium chloride and clay of different amounts separately. Polyvinyl alcohol films plasticized with these humecatan-type materials, will absorb moisture when exposed to high humidity conditions.

To assess whether a controlled release can also be obtained using porous polyurethane and PVA hydrogel with different microstructure, the film was immersed in water for 10 hours, then exposed in the air. Swelling characteristics of samples in water were measured by weighing their water content rise. The dry hydro gels were weighed, transferred into water, and reweighed at room temperature. The following equation was used to calculate the percent of swelling:

$$\text{Swelling\%} = \frac{w_t - w_0}{w_0} \times 100\%$$

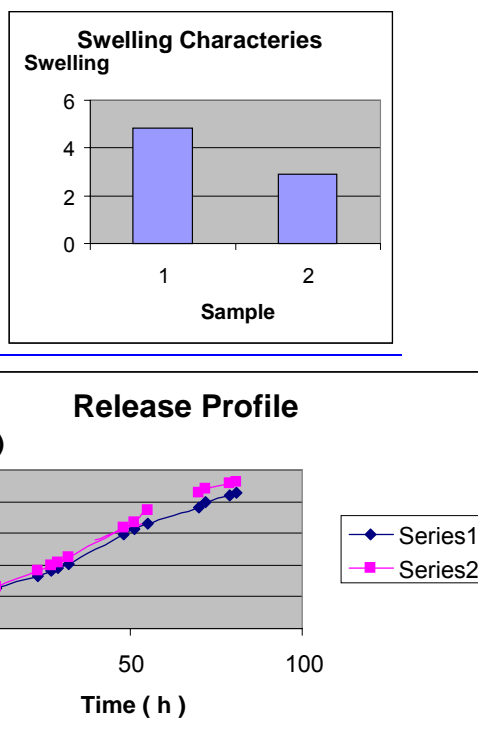
Here w_0 is the mass of the dry gel before swelling and w_t is the mass after swelling to time t .

Simulated drug release profiles are illustrated in Figures 11 and 12. As seen the porous polyurethane film exhibited rapid release behaviour, whereas with PVA hydro gel film as shown, a much prolonged release was observed, figure 11. After 4 days a total of about 85% was released. The newly developed PVA hydro gel film, mixed with miscible solvent and suitable humectants, has shown prolonged release more than 20 days of only about 65 % of the drug, shown in Figure. 12. The remaining 35% is released after 30 days, making the total release of the drug to be over 50 days. There is initial large bolus of drug is released before the release rate reaches a stable profile. Burst release leads to higher initial drug delivery and also reduces the effective lifetime of the device.



(a)

Figure 11 (a) Water released from: porous polyurethane film.



(b)

Figure 11 (b) Water released from:PVA hydro gels without organic solvent as a function of time.

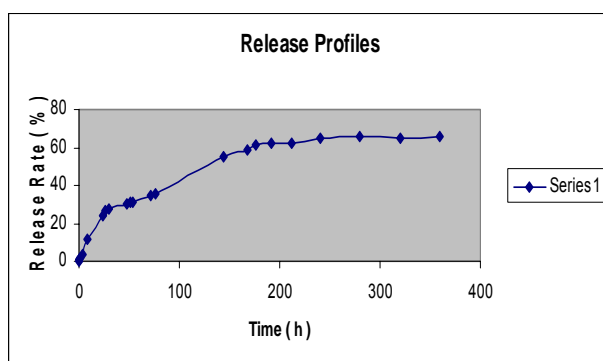
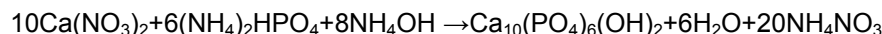


Figure 12 Water released from porous PVA hydro gels made from mixture water and non solvent.

The differences in the performance of hydro gels and polyurethane were considered as important parameters determining the release profiles performance needed for different end uses. Achieving prolonged release with PVA hydro gels indicated that other factors, such as interactions between water–hydrophilic PVA molecules, and solubility, and swelling characteristics of the water in the hydro gels, also play a major role.

5. PVA HYDROGELS WITH THE ENTRAPMENT OF NANOPARTICLES SECOND PHASE

Hydroxyapatite shows a strong interaction with bio-molecules such as collagen, chitosan, glycoprotein, etc. As a consequence, in this part, we further studied the synthesis of nano-HA/PVA-H composite to improve the cell adhesion ability of the PVA due to a role in bio-adhesion between soft tissue and hard tissue, and other biomaterials. The hydroxyapatite nanoparticles were prepared, by in-situ a chemical precipitation process:



Calcium nitrate and ammonium phosphate were separately dissolved in aqueous solution. Calcium nitrate solution was dropped slowly into the ammonium phosphate solution at a rate of 1.5 ml/min under constant stirring. The pH value of solution was kept between 10 and 12 by adding ammonium hydroxide. The white precipitates were aged for 100 h to form HA nanofibers.

Figure.13.shows the result from PVA/HAp composite gel. Hydrogels based on blends of poly(vinyl alcohol) with glycerol were prepared by a freeze/thawing procedure and used as matrices for the entrapment of HA nanoparticles that can be loaded up with drugs. Dispersion of PVAc nanoparticles about 30-50 nm within our hydro gel based delivery mechanism, expected to offers a further tools in controlling the amount of drug release and initial rate of release, for prolonging and controlling drug delivery time.



Figure 13. Samples of PVA-HAp composite gel

It is found that the concentration of the PVA solution and the casting process temperature has a great influence on the preparation of PVA-HAp composite. When the solution temperature is higher than 95 °C, sedimentation of the HAp particles becomes too fast and consequently the phase separation of the HAp from the PVA solution occurs while the process temperature is lower than 60 °C, the casting process become increasingly harder. Optimal temperature of the casting process is at 80 °C.

6. PREPARATION OF MAGNETIC PVA HYDROGELS

Figure.14 shows several examples of preparation of magnetic PVA hydro gels by in-situ synthesis of magnetite within the PVA matrix. Magnetic hydro gels were fabricated by in-situ co-precipitation process, and iron oxide nanoparticles were deposited directly in the PVA hydro gel containing surfactants with a base or a concentrated alkaline solution. The traditional method of preparing iron oxide nanoparticles usually used the chemical co-precipitation of iron salts in the alkaline medium [14]:

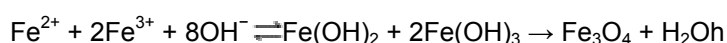


Figure 14.Preparation of Magnetic PVA hydro gels

However, the iron oxide nanoparticles formed by using this traditional method aggregated easily. To prevent aggregation, the PVA and iron salts were mixed in advance to become a homogeneous mixture in which iron and the carboxylic acid groups of polymer allow forming a homogeneous complex structure in the solution [15]. In the first step, PVA adsorbed iron ions homogeneously because of high chelating capacities of the hydroxyl group to obtain metal ions. In the second step, NaOH oxidized Fe(II) and Fe(III) ions to magnetite. The oxidization reactions resulted in slow color changes from orange-red through brown and black.

7. INDUSTRIAL APPLICATIONS

Coating of the porous foams with polyvinyl alcohol (PVA) on fabrics considerably improved the wet ability of the foams and allowed the cells to culture. Microscopic observations of the cells seeded onto the polymer foams showed that the interconnected pore networks were more favorable to cell attachment than the anisotropic pore structures.



Figure 15. The manufacture of PVA hydro gels on the fabrics.

Figure.15 illustrated an example of PVA hydro gels formed on the fabrics. The transparent hydro gel on the fabric was prepared from a poly(vinyl alcohol) solution in a mixed solvent consisting of water and a water-miscible organic solvent. After being kept at room temperature for 0.5-6 hours, the coated fabric is subjected below room temperature, and a gel is formed as a consequence of crystallization of poly(vinyl alcohol) molecules.



Figure 16. The manufacture of anti-Antibacterial PVA hydro gels with TiO_2 on the fabrics.

Figure 16. Illustrates the manufacture of anti-Antibacterial PVA hydro gels with TiO_2 fabrics Titanium dioxide *nano*-coatings with PVA may be applied to fabric surface materials as a photo catalytic *coating* on ordinary glass providing anti-fouling benefits. These photo catalytic surfaces are particularly useful in public areas such as rest rooms and hospitals for reducing bacterial contamination. Once exposed to daylight, the surface reacts chemically in two ways. Firstly, it breaks down any organic dirt deposits and secondly, rain water 'sheets' down the fabric surface to wash the loosened dirt away. TiO_2 nanocoatings on textiles may provide self-cleaning and antibacterial properties.

8. CONCLUSION

As medical practice enters a new era with the exciting new applications of nanoscience and technology, the paper provides interesting progress in the development, manufacture and end-use of novel micro-channel membranes for controlled delivery of biopharmaceuticals. It is demonstrated in the present work that porous Polyurethane scaffolds with delivery performance can be successfully prepared by the proposed emulsion freezing coating process. The prepared scaffolds are highly porous and have interconnected micro cavities containing nano pore inside them to allow extensive body fluid transportation through the pores and hence triggering bone in growth, cell migration, tissue in growth, and eventually vascularization.

Novel developing of a super gel membrane, including the entrapment of nanoparticles, such as HA, magnetic Fe_3O_4 and TiO_2 , both self-supported and coated on fabric, is presented as a payload vehicle for controlled release of growth bone hormone and other bio chemicals, and it is capable of controlling release of up to 50 days, using harmless magnetic field. Potential applications to tissue engineering of these membranes are also discussed.

REFERENCES

1. G. K. Stylios and T. Wan (2005), "Novel Micro-Channel Membranes for the Controlled Delivery of Encapsulated pharmaceuticals", project application report, June 2005.
2. G. K. Stylios, T. Wan, P. Giannoudis, (2006) "Present status and future potential of enhancing bone healing using nanotechnology". *Injury*, Vol. 38, 1, pp. S63-S74 G.
3. M. Karagienes, (1973) Porous metals as a hard tissue substitute. I. Biomedical aspects, *Biomater Med Dev Artif Organs*, pp. 171–181.
4. E. Piskin, (1997) Biomaterials in different forms for tissue engineering: an overview. *Mater Sci Forum* 250, pp. 1–14.
5. Y. Zhang and M. Zhang, (2001) Synthesis and characterization of macroporous chitosan/calcium phosphate composite scaffolds for tissue engineering. *J Biomed Mater Res* 55, pp. 304–312.
6. C. Du, F.Z. Cui, X.D. Zhu and K.D. de Groot, (1999), Three-dimensional nano-HAP/collagen matrixloading with osteogenic cells in organ culture, *J. Biomed. Mater. Res.* 44, pp. 407–415.

7. H. Schliephake, F.W. Neukam, D. Hutmacher and J. Becker, (1994) Enhancement of bone in-growth into a porous HA-matrix using a resorbable polylactice membrane. *J Oral Maxillofac Surg* 52 (1994), pp. 57–63;
8. Masanori Kobayashi, Yong-Shun Chang and Masanori Oka, (2005), A two year in vivo study of polyvinyl alcohol-hydrogel (PVA-H) artificial meniscus, *Biomaterials*, Vol. 26, 16, June 2005, pp. 3243-3248;
9. Yali Li, K.G. Neoh and E.T. Kang, (2005), Poly(vinyl alcohol) hydrogel fixation on poly(ethylene terephthalate) surface for biomedical application, *Biomaterials* Vol. 26, 16, June 2005, pp. 3243-3248
10. Tatsuko Hatakeyema, Junko Uno, Chika Yamada, Akira Kishi and Hyoe Hatakeyama , (2005), Gel–sol transition of poly(vinyl alcohol) hydrogels formed by freezing and thawing, *Thermochimica Acta*, Vol. 431, 1-2, 15 June 2005, pp. 144-148
11. Alejandro Sosnik and Daniel Cohn, (2005), Reverse thermo-responsive poly(ethylene oxide) and poly(propylene oxide) multiblock copolymers, *Biomaterials* Vol. 26, 4, February 2005, pp. 349-357
12. Masanori Kikuchi, Yoshihisa Koyama, Takeki Yamada, Yukari Imamura, Takao Okada, Noriaki Shirahama, Kazumi Akita, Kazuo Takakuda and Junzo Tanaka, (2004), Development of guided bone regeneration membrane composed of β -tricalcium phosphate and poly (L-lactide-co-glycolide-co- ϵ -caprolactone) composites, *Biomaterials* Vol. 25, 28 , December 2004, pp. 5979-5986,
13. ter verkrijging van de graad van doctor aan de Universiteit Twente op gezag van de rector magnificus, prof. dr. F.A. van Vught, membrane formation by phase inversion in multicomponent polymer systems Mechanisms and morphologies, <http://doc.utwente.nl/9375/1/t0000005.pdf>
14. Sauzedde F, Elaissari A, Pichot C, (1999), Hydrophilic magnetic polymer latexes. 1. Adsorption of magnetic iron oxide nanoparticles onto various cationic latexes. *Coll Polym Sci* 1999, 277:846-855
15. C.L. Lin, C.F. Lee and W.Y. Chiu, (2005), Preparation and properties of poly(acrylic acid) oligomer stabilized superparamagnetic ferrofluid, *Journal of Colloid and Interface Science* 291 (2005), pp. 411–420.

NEW BIOACTIVE TEXTILE DRESSING MATERIALS FROM DIBUTYRYLCHITIN STIMULATING WOUND HEALING

G. SCHOUKENS¹, P. KIEKENS¹, I. KRUCINSKA²

¹ Ghent University, Department of Textiles, Technologiepark

² Technical University of Lodz, Department of Textile Metrology

ABSTRACT

Dibutrylchitin (DBC) is an ester derivative of a natural polysaccharide – chitin. DBC is obtained by reaction of chitin with butyric anhydride in the presence of a catalyst. The production methods of DBC were elaborated and optimized. DBC is easily soluble in common organic solvents and has film- and fibre forming properties. Such characteristic allows obtaining classical fibres from the polymer solutions. DBC is also a raw material for manufacturing yarn and for a broad range of textile dressing materials. Fibres with good mechanical properties were obtained by an optimized spinning process from the DBC solutions.

The excellent biomedical properties of the DBC were confirmed by different experimental results which proved that DBC is a biocompatible and biodegradable polymer and stimulates regeneration of damaged tissues.

Tests of these DBC dressing materials under clinical conditions were done and proved the excellent results of DBC-based dressing materials for the ordered healing of tissues and wounds. The DBC dressing materials accelerate the healing of the wound and are biodegraded during the healing process. From the clinical tests, it was clearly observed that the DBC dressing materials were absorbed into the fresh tissue formed during the healing process of the wounds.

DBC and DBC-based dressing materials are good bioactive textile materials for wound healing and for understanding the biological properties of chitin derivatives. The obtained results proved the importance of the O-substitution of the hydroxyl groups present in chitin, not only for the solubility of the derivatives and the mechanical properties of the produced fibres, but still more important for the biological properties of these ester derivatives of chitin containing butyric acid. This development creates a link between textile products, based on material properties, and human health, based on the biological properties of the basic material.

The mechanical properties of DBC were further optimized by blending it with poly(ϵ -caprolactone). Good transparent and flexible products, such as films, with a high elongation to break were obtained by blending 10 to 20wt% of poly(ϵ -caprolactone) with DBC. This creates new possible bioactive applications for DBC or poly(ϵ -caprolactone).

Key Words: chitin, biomedical properties, mechanical properties, blends

1. INTRODUCTION

Chitin, the natural most abundant polysaccharide containing nitrogen, undergoes degradation by enzymes, induces human cells to promote the restoration of wounds, enhance and enhances the healing process of wounds and has high permeability for substances of medium molar masses in serum [1-3]. Chitin might be an ideal raw material for bioactive dressing materials, but due to its low solubility can be only hardly converted into useful forms like films, fibre or non-woven matrices.

An original method of synthesis of di-O-butyrylchitin (DBC), the soluble derivative of chitin, was worked out at the Technical University of Łódź, Poland [4]. The proposed method applied to chitin of different origin (crab, shrimp & krill shells, and insect chitin) gave the products of definite chemical structure with a degree of esterification very close to two. DBC is easily soluble in common organic solvents and has both film and fibre-forming properties [5]. Such properties of DBC created the possibility of manufacturing a wide assortment of DBC materials suitable for medical applications in the form of films, fibres, non-woven, knitted materials, and woven fabrics. Thus, O-butyrylation of chitin gives the possibility of practically unlimited manufacturing of DBC dressing materials comfortable and easy in use. The first investigations of biological properties of DBC materials, carried out *in vitro* and *in vivo* in accordance with the European standards EN ISO 10993 ("Biological evaluation of medical devices"), showed good biocompatibility of DBC [6, 7] and his ability to accelerate wound healing [6, 8]. The recent investigations published by Muzzarelli et. al. [9] confirms the biocompatibility of DBC. The presented results indicated that DBC is not cytotoxic for fibroblasts and keratinocytes.

The first clinical investigations into medical properties of DBC have been carried out at the Polish Mother's Health Institute in Łódź, Poland. DBC samples under investigation have been used in the form of non-woven materials. Results of their clinical investigations were presented on the 6th International Conference of the European Chitin Society and published [10].

2. MANUFACTURING OF WOUND DRESSINGS

2.1. Preparation of Dibutyrylchitin (DBC) and DBC Characteristics

DBC as a raw material used for manufacturing of non-woven dressing materials was prepared from shrimp chitin. Shrimp shell chitin powder with particle size of 200 mesh and viscosity average molar mass $M_v = 454,6 \times 10^3$ g/mol was delivered by FRANCE CHITIN, Marseille, France.

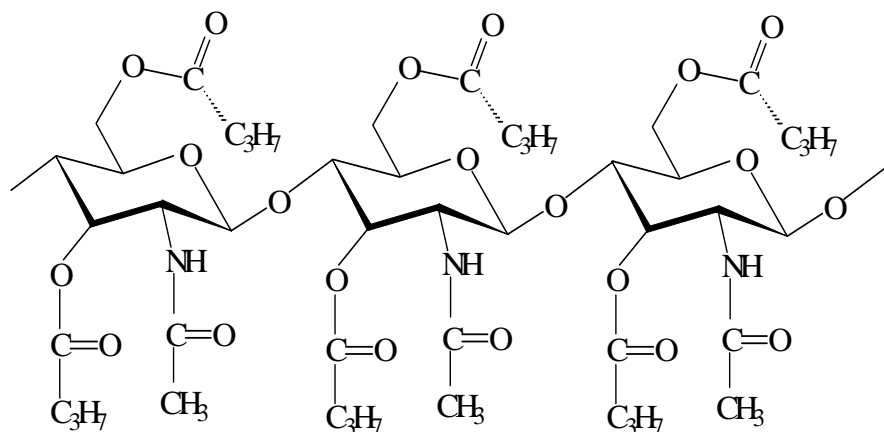


Figure 1. Dibutylchitin (DBC): chemical structure after complete o-butyrylation (degree of substitution = 2)

The synthesis of DBC was carried out under heterogeneous conditions using chitin, butyric anhydride, and 72% perchloric acid in approximate proportion equal to 10: 50: 6.8 (g/g). The intrinsic viscosity value of DBC determined in DMAc solutions at 25°C was 1.70 dL/g, the weight average molar mass, determined by SEC method coupled with light scattering and viscometry, was $M_w = 132 \times 10^3$ g/mol.

Another possible reaction to produce DBC is the so-called homogeneous reaction in methanesulphonic acid. Intrinsic viscosity value of the obtained DBC by the homogeneous reaction determined in DMAc solutions with DBC was 5.70 dL/g, the corresponding weight average molar mass was 456×10^3 g/mol.

A DBC with a higher molecular weight was obtained by the homogeneous reaction in methanesulphonic acid. The starting chitin has a mean amount of 2800 monomers in the polymer chain. The mean amount of monomers for the DBC obtained by the homogeneous reaction is 1340 and for the DBC obtained from the heterogeneous reaction is 450. There is less degradation of the polymer chains for the homogeneous reaction than for the heterogeneous reaction.

2.2 Mechanical Properties

The mechanical properties were measured on films cast from an acetone solution. The elasticity modulus, elongation and maximum stress were obtained from the tensile stress-strain data on the films using an Instron 3369 tensile tester. The product TUL-DBC was the DBC with an average molecular weight M_w of 153×10^3 g/mol and UGT-DBC the DBC with an average molecular weight M_w of 456×10^3 g/mol. The films were conditioned at room temperature and a relative humidity of 65%. The measured stress-strain curves are reproduced in figure 2.

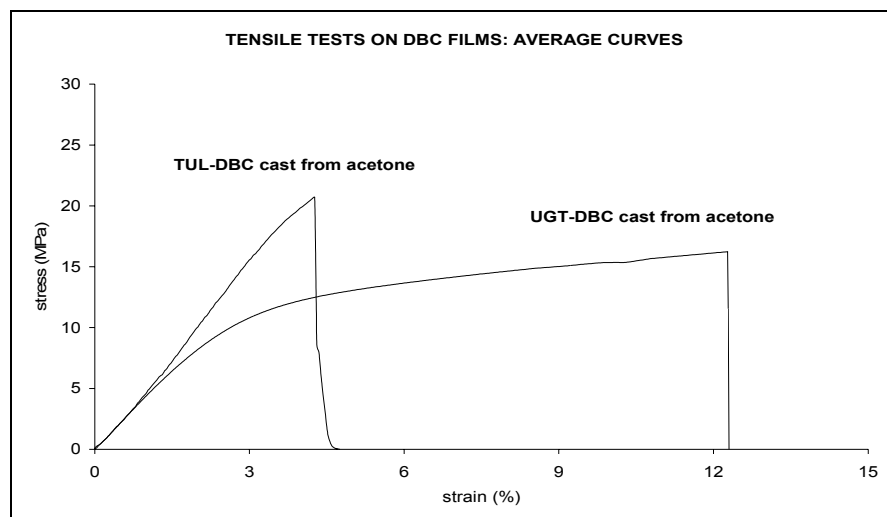


Figure 2. Stress-strain data for two different DBCs at room temperature.

The elasticity modulus, equal to 1025 MPa, was the same for the two samples, independent of the molecular weight, but the maximum elongation is increasing with increasing molecular weight. The maximum elongation is increasing from 4.3% for the lower molecular weight to 12.5% for the higher molecular weight. This resulted in better strength characteristics of the films, due to the more plastic behaviour of the DBC with the highest molecular weight.

2.3. Preparation Of Dibutylchitin Fibres

Wet spinning of DBC fibres was made at the Institute of Chemical Fibres, Łódź, Poland, on an apparatus commonly used for preparation of rayon fibres [5]. Dopes containing 15 % of DBC from krill chitin in dimethylformamide or 12 % of DBC from shrimp chitin in dimethylsulphoxide were added to the reservoir of the spinning system and extruded through a spinneret (300 holes, 80 μ m diameter of the hole) to a coagulation bath. The filaments were coagulated in water, drawn in hot water, collected on rollers with a rate of 40 m/min and dried.

DIBUTYRYLCHITIN FIBRE						
Fibre's symbol	dtex	Solvent	Tenacity (cN/tex)	Loop (cN/tex)	Elongation at break (%)	Max. Elongation (loop; %)
8 E/1	3.3	Ethanol	6.5	2.9	4.8	2.1
22/3	2.1	DMF	15.7	3.1	6.2	2.3
35/1	2.8	N-MP	13.0	2.2	9.4	3.4
68	2.9	DMSO	11.2	3.5	12.6	2.6

Low susceptibility to deformation during the drawing stage at about 70°C is linked to the rigid structure of the DBC macromolecules. The results of this are rather poor strength properties in the fibres, especially the maximum elongation for bending. By using ethanol as the solvent for DBC, porous fibres were obtained.

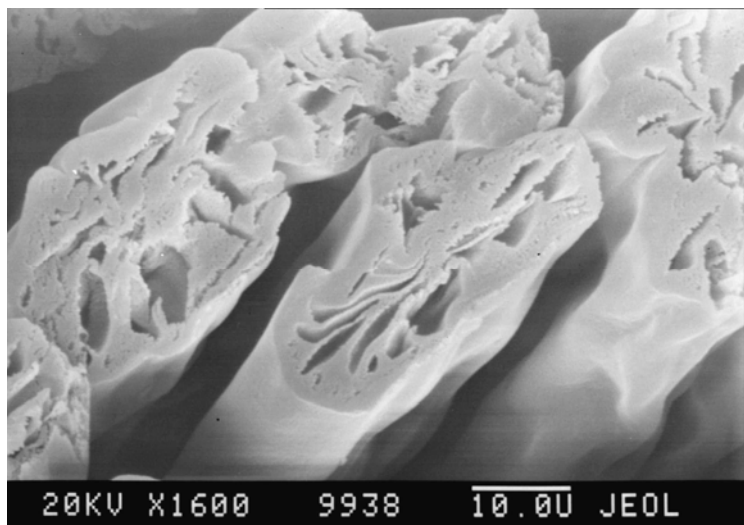


Figure 3. SEM photos of DBC Fibres (solvent-ethanol); cross-section

The presence of very large pores in the cross-section view is visible in the SEM micrograph (figure 3). The DBC fibres from DMSO-solution were round without visible pores. These tests confirmed that the supramolecular structure of fibre-forming polymers depends upon the solvent and the character of the solvent-polymer interactions.

2.4 Blends of DBC and Poly (E-Caprolactone)

Blending natural polymers with chemosynthetic polymers is a very interesting methodology by which to modify the properties of natural polymers and to develop novel composite materials based on natural polymers. Blending may be used effectively to modify physical and mechanical properties that each individual polymer does not have. The extent and rate of biodegradation of polymer blends are determined not only by the intrinsic degradability of the blend compositions themselves, but also by the blend composition, phase structure (miscibility, crystallinity of the components) and surface blend composition. In particular, hydration plays an important role in determining polymer degradation via hydrolysis of ester or β -glycosidic bonds [11]. Thus, the blending strategy is an important technique for biodegradable polymers, such as chitin, chitosan and DBC, not only to improve the properties of the components, but also to control the biodegradation profile.

In the last two decades, numerous biodegradable polyesters have been developed chemosynthetically. Among them, aliphatic polyesters including poly(ϵ -caprolactone) (PCL), poly(glycolic acid), poly(lactic acid) and their copolyesters, have considerable importance in several medical applications. Recently, blends of PCL and chitin or chitosan were studied. DSC thermal analysis revealed that the crystallization of PCL was suppressed by blending with chitin and chitosan [12].

All film samples were prepared by the solution-casting technique, using methylene chloride as the common solvent. PCL and DBC were dissolved separately in CH_2Cl_2 before blending. After the solutions had been homogenized, there were mixed. The blend films were prepared by casting the mixture on an aluminium dish, and then dried at room temperature for 2 days. Throughout this paper blend compositions are given in wt% of PCL. Weight ratios of PCL to DBC were fixed at 100/0, 80/20, 60/40, 50/50, 40/60, 20/80 and 0/100.

The mechanical properties were measured on films. The elasticity modulus, elongation and maximum stress were obtained from the tensile stress-strain data on the films using an Instron 3369 tensile tester.

The results of the elasticity modulus and elongation at break as function of the compositions of the blends are reproduced on the following two figures.

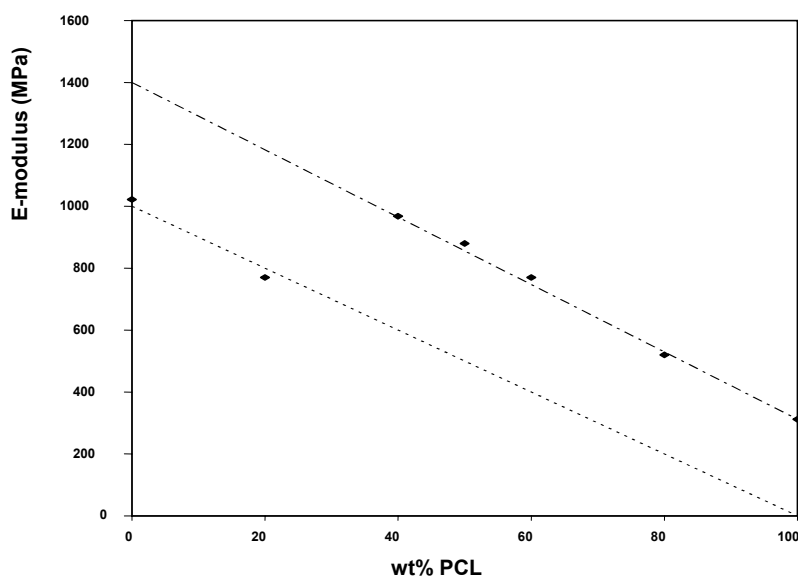


Figure 4 . The elasticity modulus of the blends DBC-PCL as function of the composition of the blends

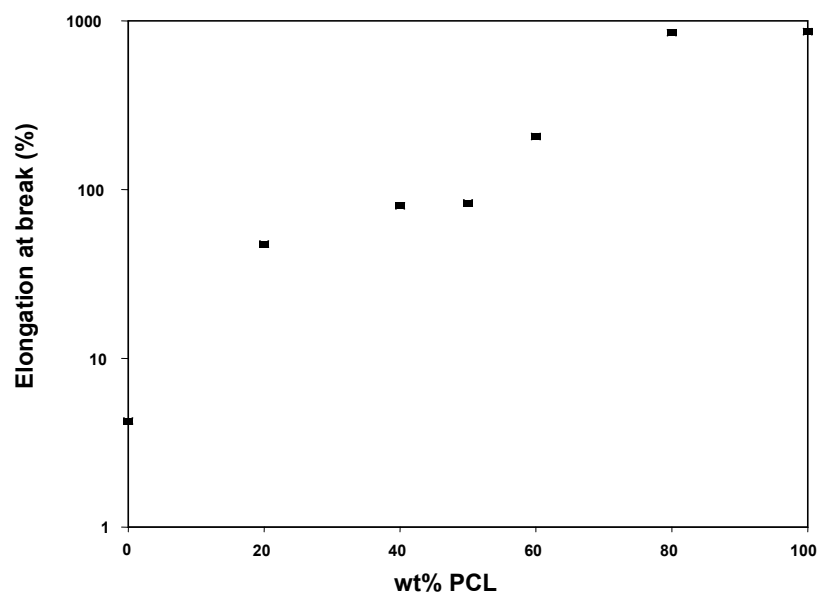


Figure 5. The elongation at break of the DBC-PCL blends as function of the composition

The elasticity modulus of the blend containing 20wt% PCL decreases from 1025 MPa to 770MPa and the elongation to break increases from 4.3% to 47.6%. In the DSC-measurements, no crystallinity of PCL is observed. This is an indication that the PCL is good miscible with DBC and behaves as a plasticizer in those blends. The blends containing between 10 and 20wt% PCL are plasticized by PCL, transparent and characterized by a high elongation to break. A good flexibility of the DBC-derived films and fibres can be obtained by adding 10 to 20wt% of PCL to DBC.

3. CLINICAL INVESTIGATIONS OF DBC NON-WOVEN DRESSING MATERIALS

3.1 Rationale for the Possible Provision of Butyrate

Short chain fatty acids, especially butyrate, play central metabolic roles in maintaining the mucosal barrier in the gut. A lack of butyrate, leading to endogenous starvation of enterocytes, may be the cause of ulcerative colitis and other inflammatory conditions. The main source of butyrate is dietary fibre, but they can also be derived from structured biopolymers like DBC. Butyrate has been shown to increase wound healing and to reduce inflammation in the small intestine (13). In the colon, butyrate is the dominant energy source for epithelial cells and affects cellular proliferation and differentiation by yet unknown mechanisms. Recent data suggest that the luminal provision of butyrate may be an appropriate means to improve wound healing in intestinal surgery and to ameliorate symptoms of inflammatory diseases. It was also suggested that

butyrate may inhibit the development of colon cancer (14, 15). Butyrate has a relatively short metabolic half life. The half-life of butyrate in plasma is extremely short, as peak plasma butyrate concentrations occurred between 0.25 and 3 h after application and disappeared from plasma by 5 h after the application.

3.3 Results of Clinical Investigations

The surgical staff of the Department of Pediatric Surgery was provided with a number of DBC petals for medical application (Fig.6).

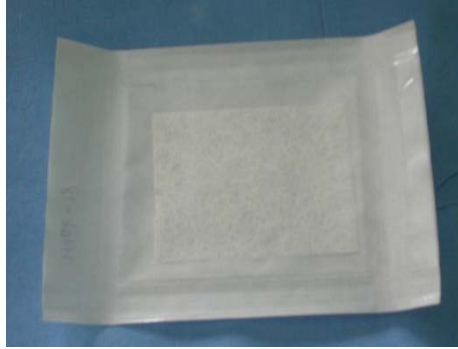


Figure 6: The flake of DBC

The first group of patients, composed of 10 persons, suffered from burns. The total area of thermal burns of patients changed within the range of 5-20%. The depth of burns was classified in each case as 2a. All the burns healed up within 1 – 2 weeks after DBC petal application. The healing processes are documented in Figure 7. The result of the healing process was very good.



Figure 7. Burn of right lower limb (left) and healing nearly completed (right)

4. CONCLUSIONS

As far as thermal burn patients are concerned, in all cases DBC dressings have been applied to the clean wound and not removed till the end of the healing process, while DBC has been disintegrated in the area of the wound. No other medical products have been applied for the wound healing. The presented observations are preliminary and further evaluation is necessary.

Summarising, it is possible to conclude from the preliminary results of DBC application that DBC seems to promote wounds' healing. Further randomised trials with referential groups should be completed to obtain evidence-based proofs of beneficial effects of DBC wound dressings.

Blending DBC with PCL gave very good flexible products, with a good value of elasticity modulus, a high elongation to break and a good transparency for films containing between 10 and 20wt% PCL.

ACKNOWLEDGMENTS

This work has been partly supported by the European Commission in frame of the Project CHITOMED, QLK5-CT-2002-01330.

REFERENCES

1. Oshimoma Y, Nishino K, Yonekura Y., Kishimoto S., Wakabayashi S.: Clinical application of chitin non-woven fabric as wound dressings. 1987. *Eur J Plast Surg* v. 10, 66-69.
2. Muzzarelli R.A.A.: In vivo biochemical significance of chitin-based medical items in Polymeric Biomaterials, 1993. S. Dimitriu (ed.), Marcel Dekker, Inc., N.Y., 179-197.
3. Muzzarelli R.A.A: Chitin in Polymeric Materials Encyclopedia. 1996. Salamone J.C. (ed.), CRC Press, Boca Raton, USA.
4. Szosland L.: Synthesis of highly substituted butyrylchitin in the presence of perchloric acid. 1996. *J. Bioactive and Compatible Polymer*, v. 11, 61-71.
5. Szosland L., Stęplewski W.: Rheological characteristic of dibutyrylchitin semi-concentrated solutions and wet spinning of dibutyrylchitin fibre. 1998. *Advances in Chitin Science*, Domard A., Roberts G.A.F, Varum K.M. (eds.), v. II, 531-536.
6. Szosland L., Cisko R., Krucińska I., Paluch D., Staniszevska-Kuś J., Pielka S., Soliski L., Żywicka B. : Dressings made from dibutyrylchitin and chitin accelerating wound healing. 2002. *Proceedings of International Conference MEDTEX'2002*, Łódź, Poland.
7. Szosland L., Krucińska I., Cisko R., Paluch D., Staniszevska-Kuś J., Soliski L., Szymonowicz M.: Synthesis of dibutyrylchitin and preparation of new textiles made from dibutyrylchitin and chitin for medical applications. 2001. *Fibres & Textiles in Eastern Europe*, v.9, (34), 54-57.
8. Pelka S., Paluch D., Staniszevska-Kuś J., Żywicka B., Soliski L., Szosland L., Czarny A., Zaczęńska E.: Wound healing accelerating by a textile dressing containing dibutyrylchitin and chitin. 2003. *Fibres & Textiles in Eastern Europe*, v.11, 79-84.
9. Muzzarelli R.A.A., Guerrieri M., Goteri G., Muzzarelli C., Armeni T., Ghiselli R., Cornellisen M.: The biocompatibility of dibutyryl chitin in the context of wound dressings. 2005. *Biomaterials*, v. 26, 5844-5854.
10. Chilarski A., Szosland L., Krucinska I., Błasinska A., Cisko R.: The application of chitin derivatives as biological dressing in treatment of thermal and mechanical skin injuries.

2004. The Annual of Pediatric Traumatic Surgery, The Devision of Pediatric Traumatic Surgery , v. 8 (XXXII), 58-61.
11. Park T. G., Cohen S., Langer R.: Poly(L-lactic acid)/Pluronic Blends, 1992, *Macromolecules*, v. 25, 116-122
 12. Wu C.:A comparison of the structure, thermal properties, and biodegradability of polycaprolactone/chitosan and acrylic acid grafted polycaprolactone/chitosan; 2005, *Polymer*, 147-155
 13. Wächtershäuser A., Stein J.: Rationale for the luminal provision of butyrate in intestinal diseases, 2000, *Eur. J. Nutr.* , v. 39, 164-171
 14. Hinnebusch B.F., Meng S., Wu J.T., Archer S.Y., Hodin R.A.: The effects of short-chain fatty acids on human colon cancer phenotype are associated with histone hyperacetylation, 2002, *J. Nutr.*, v. 132, 1012-1017
 15. . Emenaker N.J., Calaf G.M., Cox D., Basson M.D., Qureshi N. : Short-chain fatty acids inhibit invasive human colon cancer by modulating uPA, TIMP-1, TIMP-2, Bcl-2, Bax, p21 and PCNa protein expression in an in vitro cell culture model, 2001, *J. Nutr.* , v. 131 (suppl. 11), 3041S-3046S

ANTIMICROBIAL PERFORMANS OF CELLULOSE BASED WOUND DRESSING MATERIALS

B. BEYHAN¹, A. CİRELİ², M. MUTLU¹

¹Hacettepe University, Engineering Faculty, Plasma Aided Biotechnology and
Bioengineering Research Group (PABB)

²Dokuz Eylül University, Engineering Faculty, Textile Engineering Department

ABSTRACT

The novel approach in technological development is focused on the principles of "mimicing the nature". Due to this fact our recent approach on wound dressing materials has shifted from synthetic polymers into natural materials. For this purpose glow discharge modified and antibiotic loaded cellulosic fibers has been prepared and characterized as wound dressing materials and were introduced in our previous studies.

In the present study two different type of penicilin [Benzylpenicillin (penicillin G), Procaine benzylpenicillin (procaine penicillin)] were loaded as a model system in wound dressing materials (fabrics) and glow discharge plasma polimerisation treatments were carried out on to the wound dressing materials (fabric) for creating hidrophobic surfaces. Following the antibiotic release test, the inhibition zone tests was implemented to ascertain antimicrobial activity.

1. INTRODUCTION

The recognition, in the 1960s, that gauze and other absorbent materials (eg, cotton and gamgee) were passive products that "plugged and concealed" the wound but did little to encourage wound healing resulted in the creation of a minimal set of criteria for an "ideal dressing" [1]. Medical textiles are generally combined with materials other than textiles and used almost in every area of medicine and surgery. Wound dressings have been broadly classified as either adherent or nonadherent and absorbent or nonabsorbent.[1,2,3]. Surgeons wear, wound dressings, bandages, artificial ligaments, sutures, artificial liver/kidney/lungs, nappies, sanitary towels, vascular grafts/heart valves, artificial joints/bones, eye contact lenses and artificial cornea and the like are some of the examples of medical textiles [4]

The development in the medical textile and hygiene industry is related to the growth and innovations both in textile and medical methods. Textile materials and products that were produced for certain need are suitable for medical and surgical applications because of their resistance, elasticity and sometimes permeability of air and humidity. Also they are advantageous

because of wide variety, multifunctional character, and especially biocompatible with nature and the tissue. Materials used are monofilament or multifilament fibers, fabrics, nonwoven and composite materials.

Beside surgical and traumatic injuries, thermal burns still consists a large amount of death in the world [17]. Burn patients are susceptible to infections. In addition to loss of skin integrity, both the necrotic tissue in the burn eschar and serum proteins provide a rich culture medium for colonization and multiply of microorganisms. After burns, presenting microorganisms on the skin and gastrointestinal flora of the individual patients and microorganisms from the environment of the burn care facility colonize on burn wound. If microorganisms reach a marked concentration on the burn wound, they may spread to subcutaneous tissue first and then perivascular compartment. Invasion of the eschar tissue through the viable subcutaneous tissue results burn infection or burn sepsis. Burn patients especially who have a long hospitalization period, a large size of the burn wound, more frequent blood transfusion, and burn wound colonization with resistant microorganisms against topical and systemic antimicrobial drugs are at a higher risk of burn infections [18].

There are some series of textile materials which are very effective and suitable for external application are present for the prevention of the infection in the wounds caused by surgery or trauma [5, 6-7]. With clearer understanding of the cellular and molecular biology of healing, some other specifications such as antimicrobial agent content or healing agents were added to the novel medical textile materials for directing towards the functional characteristic of the material and the microenvironment, to minimize the need of oral or topical antibiotics therefore to optimize wound healing. Currently there are a variety of interactive products that control the microenvironment on the wound surface and some bioactive products that stimulate some part of the healing cascade.

Because of this it would appear that the future of wound treatment will be dictated by the condition of patient and wound, the phase of wound healing and most certainly will incorporate the concept of moist wound healing [21]. Many of the newer dressings are designed to create a moist wound healing environment which allows the wound fluids to remain in contact with wound [21]. The concept of moist wound healing has been around since the 1960s, [8] but only recently has become a more accepted treatment approach in the veterinary community [9]. A moist wound free of infection provides an environment rich in white blood cells, enzymes, cytokines and growth factors beneficial to wound healing [10]. The enzymes released primarily from the white blood cells cause autolytic debridement of the wound which appears to be selective for necrotic tissue [11]. Under these dressings autolytic debridement usually occurs 72 to 96 hours after wounding; thus cleaning the wound in preparation for the repair phase [9]. Fibroplasia (fibroblast migration, proliferation and secretion of ground substance) and

epithelialization are stimulated by growth factors present in the moist wound [12]. Cytokines which are signaling peptides also act locally to stimulate the migration and activation of macrophages and neutrophils within the wound [13]. Proposed benefits to moist wound healing include: (1) prevention of the formation of a scab which can trap white blood cells which prevents them from participating in their Department of Clinical Sciences, Colorado State University, Fort Collins, CO important wound healing functions, (2) the pH of the environment is reduced, thus adversely affecting bacteria, (3) prevention of bacterial strike through from outside the wound to the wound surface, (4) more rapid epithelialization, and (5) the moist environment favors colonization of bacteria but not infection. There appears to be no shortage in the numbers of advanced wound dressings available that provide a moist healing environment. Reportedly there are over 30 different companies offering more than 300 of these advanced wound dressings (Table 1) [0]. The consumption of Medical Textiles worldwide was 1.5 million tons in 2000 and is growing at an annual rate of 4.6%. The Indian market size of medical textiles was estimated to be INR 14.8 billion in 2003-04 and is expected to grow to INR 23.3 billion by 2007-08. Market is expected to grow by 8% p.a. [14]

Calcium alginate dressings are classified as a fibrous dextranomer. They are available from a variety of sources (Curasorb® Ken Vet, Greeley, CO; C-Stat® R S. Jackson Inc., Alexandria, VA, Nu-Derm® Johnson & Johnson Products Inc, New Brunswick, NJ) [21]. Since the dressing is hydrophilic it can absorb up to 20 to 30 times its weight in wound fluid [21]. This process converts the initial dry felt like material into a hydrophilic gel on the wound surface that is easily removed [21]. The hydrophilic alginate gel forms via a calcium and sodium ion exchange, providing a moist environment conducive to wound healing [15]. The presence of calcium modifies cell response [21]. All concentrations of calcium produce an initial fall in cell replication, however the intermediate concentrations subsequently stimulate cell division [21]. Other attributes that may be beneficial are that the dressing improves clotting [21]. The calcium ion released from the dressing is known to promote the activation of prothrombin in the clotting cascade.[1]

In this study, for the preparation of wound covering materials, following the arrestment of antibiotic inside the textile material via calcium alginate, plasma polymerization technique was applied at different power and duration parameters and the performance of the new composite material was evaluated according to the oxygen permeability, hydrophobicity, antibiotic release and antibiotic zone inhibition tests.

Table 1. Dressings Types and Numbers of Brands (Ostomy/Wound Management 2000 Buyers guide) [21]

Dressing Types	Numbers of Brands
Alginates	27
Antimicrobial	4
Biosynthetics and skin substitutes	11
Collagen	5
Composites	19
Contact layers	8
Foams	33
Films	19
Gauzes, all purpose	48
Impregnated	26
Nonadherent	12
Packing/debriding	33
Hydrocolloids	39
Hydrogels amorphous	27
Hydrogel sheets	21
Hydrogel gauzes	16
Silicone dressings	1
Specialty absorptives	18

2. MATERIALS AND METHODS

2.1. Materials

2.1.1. Fabrics

The fabrics used in this study were 100% cotton. The properties of the fabric were given in Table 2.

Table 2. The Properties of 100% Cotton Fabric

Fabric	Area Mass (g/m ²)	Setting (cm ⁻¹)		Linear Density	
		Warp	Weft	Warp	Weft
Cotton	120	35	25	53	52

2.2. Methods

2.2.1. Oxygen Permeability

Plain and modified wound dressing materials were separately placed between two compartments of a diffusion chamber, and 160 ml conditioned water was filled in both chambers. One side of the chamber was continuously fed with oxygen gas and the dissolved oxygen was monitored in the other side by an amperometric electrode polarized at 650 mV. A time course data was collected to observe the oxygen permeability of the wound dressing materials.

2.2.2. Antibiotic Immobilization

The fabrics were prepared firstly by the gelation of sodium alginate which was followed by antibiotic loading and crosslinking with calcium chloride.

At the first step sodium alginate was used as an encapsulation agent. 3% sodium alginate solution was prepared with stirring and 1,96% Penicillin G (*IECILLINE® 800 falcon*) as a model system was added to the medium. Fabrics (100% cotton) with 8x14 m² area were immersed in to the medium with antibiotic and sodium alginate and were shaken for 20 minutes. For crosslinking, 150mM calcium chloride was used.

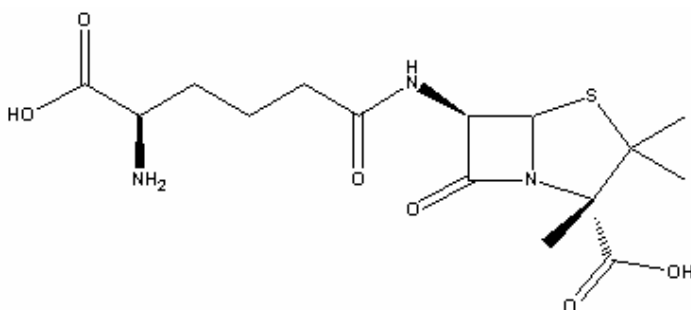


Figure 1. Benzylpenicillin (penicillin G) [16]

2.2.3. Plasma Treatment

Plasma polymerization treatments were carried out in PICO RF (radio frequency-13,56 MHz) Plasma Polymerization System (Diener electronic GmbH + Co. KG, Germany). At first, the reactor was evacuated to 22 Pa and then monomer inlet was opened and monomer (hexamethyldisilane-HMDS) (Figure 2) vapor was allowed to flow through the reactor for 10 minutes to remove impurities. Monomer flow rate was kept constant at 200 cm³/min. Then power was adjusted to 20-120 watt and the fabrics were exposed to glow discharge for 15 or 20 minutes. At the end of the process, the generator was turned off and argon gas was flowed through the chamber for 10 minutes to deactivate free radicals. Antibiotic immobilized fabrics were modified by five various HMDS plasma processes:

20W-5 min	20W-20 min	20W-60 min
-	45W-20 min	45W-60 min

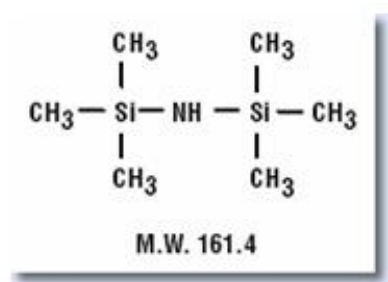


Figure 2. Hexamethyldisilane [20]

2.2.4. Contact Angle Test

A special microscope (QX3 computer microscope, 60X, Intel) and a computer system were used to measure contact angles. The volume of these bubbles did not exceed 5 μl . A computer screen provided an image of the captive bubble. The supporting computer software (Wettability Pro Classic, version 2.0.0 from Czech Republic) used these data to calculate the contact angles [19].

2.2.5. Antibiotic Release Tests

The matrices, in size of $4 \times 4 \text{ cm}^2$ were immersed in 200 ml water and the release of antibiotic with respect to time was followed by spectrometer.

2.2.6. Antimicrobial Tests

S. epidermidis which is the one of the causes infection in burn cases was used for the antimicrobial tests. The inhibition zones were determined on the 0,8mm diameter antibiotic loaded fabrics. In this study minimum and maximum zone diameters were measured as 0-30mm and the average zone diameter was found as 17,7mm

3. RESULTS AND DISCUSSION

Contact angle is shown in Table 3, release time is shown in Figure 2, oxygen permeability is shown in Figure 3, respectively.

Table 3. Contact angles.

Contact Angle				
Time Power	5min	20min	30min	60min
20W	106.3 ⁰ (max:123.7- min 84.1)	119.14 ⁰ (max:147.9- min:96.1)	—	140.7333 ⁰ (max:143.4- min:139.2)
45W	—	140.1125 ⁰ (max:147.5- min:125.5)	—	143.925 ⁰ (max:15.8- min:139)

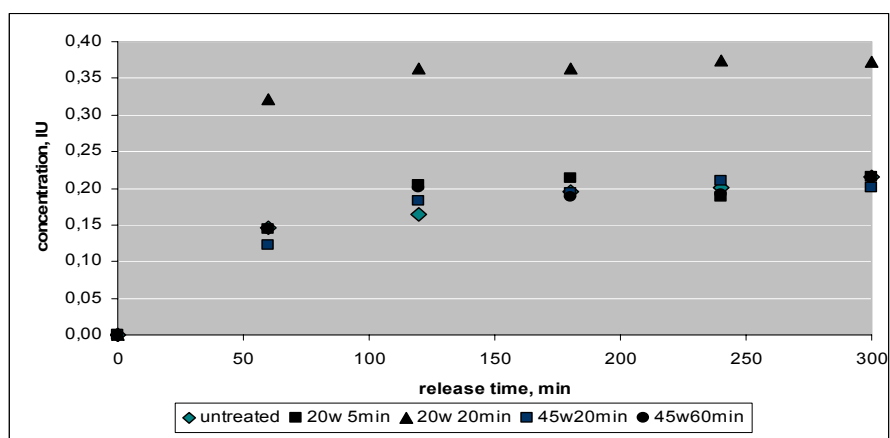


Figure 3. Release time

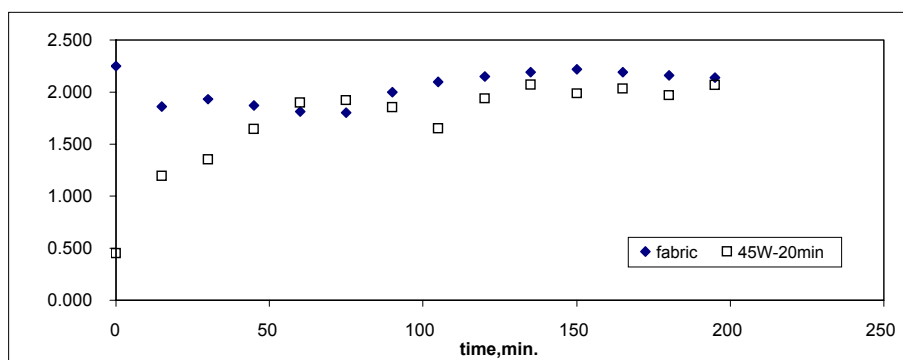


Figure 4. Oxygen permeability

The results of antimicrobial tests can be summarized as follows: The inhibition zones were determined on the 0,5mm diameter antibiotic loaded fabrics. In this study minimum and maximum zone diameters were measured as 0 and 30mm and the average zone diameter was found as 17,7mm.

4. CONCLUSION

By the collaboration of Hacettepe University, Plasma Aided Bioengineering and Biotechnology Research Group and 9 Eylül University, Textile Engineering Department, with this improved natural based wound cover material, fast and healthy recovery of the wound was aimed. In order to have a final product of this wound cover material, steps to be got over are planned and will be reported in the following time period.

The two results for the antibiotic release and antimicrobial activity shows that, in in-vitro conditions the performance of the prepared matrix as wound dressing can be successfully applied to wounds and burned areas without causing an problem on the basis of water loss (dehydration), oxygen transfer, antibiotic release and stable antimicrobial activity.

The actual results will be delivered after in-vivo tests on animals.

REFERENCES

1. Turner TD: The development of wound management products, in Krasner DL, Rodeheaver GT, Sibbald RG (eds): Chronic Wound Care: A Clinical Source Book for Healthcare Professionals (ed 3). Wayne, PA, HMP Communications, 2001, pp 293-310
2. Liptak JM (1977) An overview of the topical management of wounds. Aust Vet J 75:408-413.
3. Stashak TS: Equine Wound Management. Philadelphia, PA, Lea & Febiger, 1991, pp 19-51
4. Introduction to Medical Textile: An Indian Perspective, November 2006, Yarns and Fibers, p. 55 (http://www.reportbuyer.com/industry_manufacturing/textiles/introduction_medical_textile.html)

5. Leyden JJ, Kligman AM (1978). Rationale for topical antibiotics. *Cutis*. 22: 515-28.
6. Moylan JA (1980) The proper use of local antimicrobial agents in wounds. *World J. Surg.* 4: 433-37.
7. Pitt HA, Postier RG, Macgowan WAL, Frank LW, Surmak AJ, Sitzman JV, Bouchier Hayes D (1980) Prophylactic antibiotics in vascular surgery. Topical, systemic, or both?. *Ann. Surg.* 192: 356-64.
8. Winter GD (1962) Formation of scab and the rate of epithelialization of superficial wounds in the skin of the domestic pig. *Nature* 193:293-294.
9. Campbell BG (2004) Current concepts and materials in wound bandaging. *Proc North Am Vet Conf Orlando FL* 18:1217-1219.
10. Jones V, Harding K: Moist wound healing, in Krasner DL, Rodeheaver GT, Sibbald RG (eds): *Chronic Wound Care: A Clinical Source Book for Healthcare Professionals* (3rd ed). Wayne, PA, HMP Communications, 2001, pp 245-252
11. Dolynchuk KN: Debridement, in Krasner DL, Rodeheaver GT, Sibbald RG (eds): *Chronic Wound Care: A Clinical Source Book for Healthcare Professionals* (3rd ed). Wayne, PA, HMP Communications, 2001, pp 385-391
12. Katz MH, Alvarez AF, Kirsner RS (1991) Human wound fluid from acute wounds stimulates fibroblast and endothelial cell growth. *J Am Acad Dermatol* 25:1054-1058.
13. Kunimoto BT: Growth factors in wound healing, in Krasner DL, Rodeheaver GT, Sibbald RG (eds): *Chronic Wound Care: A Clinical Source Book for Healthcare Professionals* (3rd ed). Wayne, PA, HMP Communications, 2001, pp 391-397
14. http://www.reportbuyer.com/industry_manufacturing/textiles/introduction_medical_textile.html (28.08.2007)
15. Swaim SF, Gillette RL: An update on wound medications and dressings. *Comp Contin* (ed) 20:1133-1143, 1998
16. Kennesaw State University web page (www.chemcases.com/pheno/images/pen.gif)
17. Warden GD, Heimbach DM. Burns. In Schwartz SI, Shires GT, Spencer FC, Daly JM, Fischer JE, Galloway AC (eds): *Principles of Surgery*. 2nd Ed., McGraw-Hill, New York, s: 223-62, 1999.
18. Burn Infections: Current Status, Elaldı N, Bakır M (2003) *C. Ü. Tıp Fakültesi Dergisi* 25 (2): 79 – 88.
19. Gulec HA, Saroglu K, Mutlu M (2006) Modification of food contacting surfaces by plasma polymerisation technique. Part I: Determination of hydrophilicity, hydrophobicity and surface free energy by contact angle method. *Journal of Food Engineering* 75, 187–195.
20. www.piercenet.com/media/Hexamethyldisilazane (28.08.2007)
21. Stashak TS, Farsvedt E and Othic A (2004) Update on Wound Dressings: Indications and Best Use, *Clin Tech Equine Pract* 3:148-163

DO WE REALLY CARE FOR THE HEALTHCARE OF THE ELDERLY?

S.RAJENDRAN, S.C.ANAND

Centre for Materials Research and Innovation, The University of Bolton

ABSTRACT

The paper discusses in depth into the development of a novel single-layer compression bandage system which imparts correct and desirable level of compression starting from the ankle to just below the knee. 3D spacer fabrics have been used to design and develop a single-layer compression bandage. The paper also highlights the venous leg ulcer management, problems with the existing bandages and the need for developing novel bandages.

Key Words: Venous leg ulcers, compression bandages, 3D spacer fabrics

1. INTRODUCTION

Quality of life for the ageing population is a key issue in healthcare and healthcare research. It has been recognised that varicose veins, DVT and venous leg ulcers are growing problems for the elderly and in the UK alone about 1% of the adult population suffers from active ulceration during their lifetime. The prevalence of venous leg ulcers increases with age, from 10 per 1000 within the adult population to 36 per 1000 in the over 65 age group particularly in women. Whilst national statistics for the incidence of leg ulcers vary from country to country, obviously the chronic nature of venous ulcers creates considerable demands upon all healthcare authorities in terms of treatment costs and nursing resources. The total cost to the National Health Service in the UK for venous leg ulcers treatment is about £650 million per annum, which is 1-2% of the total healthcare expenditure. The estimated annual cost in the US is between \$1.9 - 2.5 billion and \$25 million in Sweden. In the EU, the cost for treating patients with VLU accounts for 1-2% of the overall healthcare expenditure. In Australia around 1% of the adult population suffers from venous ulceration.

Compression bandaging is considered as the “gold standard” for managing venous leg ulcers and treating the underlying venous insufficiency. In the UK four layer bandaging system is widely used. A typical four layer compression bandage system comprises of padding bandage, crepe bandage, high compression bandage and cohesive bandage. During the past few years there have been increasing concerns relating to the performance of

bandages for the treatment of venous leg ulcers. This is because the compression therapy is a complex system and requires multilayer bandages, and the performance properties of each layer differ from other layers. Because of the problems associated with the current practice of treating venous leg ulcers using four layer bandage system, it is very crucial and timely to research and develop alternative bandaging systems that meet all the requirements of an ideal compression bandage. Engineering and Physical Sciences Research Council (EPSRC) of the UK recognised the above problems and awarded the University of Bolton's innovative research programme for developing a single-layer compression bandaging system for the treatment of venous leg ulcers. This single layer approach is novel and revolutionary because no such system is available globally for the leg ulcers treatment. There is no doubt that there would be substantial savings for the hospitals because the research programme replaces the current multilayer bandages (up to 4) with a single layer integrated system, which will save the nursing time as well as the cost of the treatment.

2. VENOUS LEG ULCERS

It is important that the arterial and venous systems should work properly without causing problems to blood circulation around the body. Pure blood flows from the heart to the legs through arteries taking oxygen and food to the muscles, skin and other tissues. Blood then flows back to the heart carrying away waste products through veins. The valves in the veins are unidirectional which means that they allow the venous blood to flow in upward direction only (Figure 1). If the valves do not work properly or there is not enough pressure in the veins to push back the venous blood towards the heart, the pooling of blood in the veins takes place and this leads to higher pressure to the skin. Because of high pressure and lack of availability of oxygen and food, the skin deteriorates and eventually the ulcer occurs. The initial indications of venous leg ulcers are the swollen veins (varicose veins) and blood clots in veins (Deep Vein Thrombosis - DVT), a growing problem for long-haul flights.

2.1 Venous Leg Ulcer Management

The management of venous leg ulceration lies with '**CORE**' principles: **C**ompression, **O**ptimise the wound environment, **R**eview contributing factors and **E**stablish a maintenance plan. It will be mentioned that venous leg ulcers are chronic and there is no medication or surgery to cure the disease other than the compression therapy. A sustained graduated compression mainly enhances the flow of blood back to the heart, improves the functioning of valves and calf muscle pumps, reduces oedema and prevents the swelling of veins. Mostly elderly people are prone to develop DVT, varicose veins and venous leg ulcers. Venous leg ulcers are the most frequently occurring type of chronic wound accounting for 80% to 90% of all lower extremity ulceration.

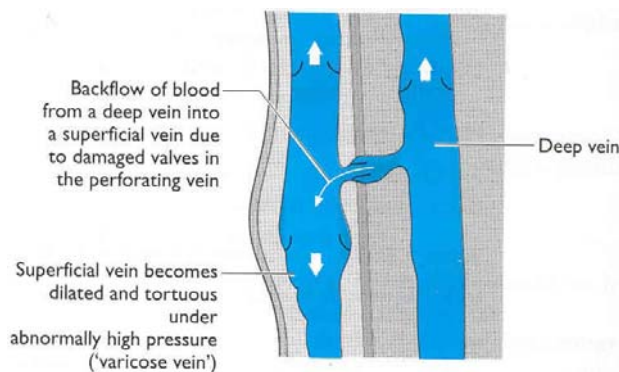


Figure 1. Illustration of backflow of venous blood

3. COMPRESSION BANDAGES

Compression bandages are mainly classified as elastic and non-elastic. Elastic compression bandages are categorised according to the level of pressure generated on the angle of an average leg. Class 3a bandages provide light compression of 14-17mmHg, moderate compression (18-24mmHg) is imparted by class 3b bandages and 3c type bandages impart high compression between 25 and 35mmHg [1]. The 3d type extra high compression bandages (up to 60mmHg) are not often used because the very high pressure generated will reduce the blood supply to the skin. It must be stated that approximately 30-40mmHg at the ankle which reduces to 15-20mmHg at the calf is generally adequate for healing most types of venous leg ulcers [2]. Compression stockings provide support to treat DVT and varicose veins, and to prevent venous leg ulcers. They are classified as light support (Class 1), medium support (Class 2) and strong support (Class 3) [1].

3.1 Ideal Compression Bandages

It should be noted that compression bandages may be harmful if not applied properly. They provide high tension as well as high pressure. A thorough assessment involving several criteria is therefore essential before applying a compression bandage on a limb. For example, it is important to consider the magnitude of the pressure, the distribution of the pressure, the duration of the pressure, the radius of the limb and the number of bandage layers. The ability of a bandage to provide compression is determined by its construction and the tensile force generated in the elastomeric fibres when extended. Compression can be calculated by Laplace's Law, which states that the pressure is directly proportional to the bandage tension during application and the number of layers applied but inversely proportional to limb radius [3]. The structure of a compression bandage is, therefore, regarded as an important factor in producing a uniform pressure distribution.

3.2 Compression System

Compression can be exerted to the leg either by a single layer bandage or multilayer bandages. In the UK four layer bandaging system is widely used whilst in Europe and Australia the non-elastic two layer short stretch bandage regime is the standard treatment. A typical four layer compression bandage system comprises of padding bandage, crepe bandage, high compression bandage and cohesive bandage. Both the two layer and four layer systems require padding bandage (wadding or orthopaedic wool) that is applied next to the skin and underneath the short stretch or compression bandages.

A plaster type non-elastic bandage, Unna's boot is favoured in the USA. However, compression would be achieved by three-layer dressing that consists of Unna's boot, continuous gauze dressing followed by an outer layer of elastic wrap. It should be realised that Unna's boot, being rigid, is uncomfortable to wear and medical professionals are unable to monitor the ulcer after the boot is applied.

A variety of padding bandages are used beneath compression bandages as padding layers in order to evenly distribute pressure and give protection. They absorb high pressure created at the tibia and fibula regions. It will be noticed that the structure of a padding bandage is regarded as an important factor in producing a uniform pressure distribution. Research has shown that the majority of the commercially available bandages do not provide uniform pressure distribution [4, 5].

4. PRESENT PROBLEM AND NOVEL BANDAGES

During the past few years there have been increasing concerns relating to the performance of bandages especially pressure distribution properties for the treatment of venous leg ulcers. This is because the compression therapy is a complex system and requires two or multilayer bandages, and the performance properties of each layer differ from other layers. The widely accepted sustained graduated compression mainly depends on the uniform pressure distribution of different layers of bandages in which textile fibres and bandage structure play a major role. The padding bandages commercially available are nonwovens that are mainly used to distribute the pressure, exerted by the short stretch or compression bandages, evenly around the leg otherwise higher pressure at any one point not only damages the venous system but also promotes arterial disease. Therefore there is a need to distribute the pressure equally and uniformly at all points of the lower limb and this can be achieved by applying an effective padding layer around the leg beneath the compression bandage. In addition, the padding bandages should have the capability to absorb high pressure created at the tibia and fibula regions. Wadding also helps to protect the vulnerable areas of the leg from generating extremely high pressure levels as compared to those required along the rest of the leg. The research carried out at the

University of Bolton involving 10 most commonly used commercial padding bandages produced by major medical companies showed that there are significant variations in properties of commercial padding bandages [5, 6], more importantly the commercial bandages do not distribute the pressure evenly at the ankle as well as the calf region. The integrity of the nonwoven bandages is also of great concern. When pressure is applied using compression bandages, the structure of the nonwoven bandages may collapse and the bandage would not impart cushioning effect to the limb. The comfort and cushioning effect are considered to be essential properties for padding bandages because they stay on the limb for several days. In order to address the problems, 12 nonwoven padding bandages which consisted of single component fibres, binary blends and tertiary blends incorporating polyester, bicomponent fibres and natural fibres such as cotton and viscose have been designed and developed at the University of Bolton and reported elsewhere [5, 6].

In the UK, multilayer compression systems are recommended for the treatment of venous leg ulcers [1]. Although multilayer compression bandages are more effective than single layer bandage in healing venous leg ulcers [1], it is generally agreed by the clinicians that multilayer bandages are too bulky for patients and the cost involved is high. A wide range of compression bandages is available for the treatment of leg ulcers but each of them having different structure and properties and this influences the variation in performance properties of bandages. In addition long stretch compression bandages tend to expand when the calf muscle pump is exercised, and the beneficial effect of the calf muscle pump is dissipated. It is a well established practice that elastic compression bandages that have the extension of up to 200% are applied at 50% extension and at 50% overlap to achieve the desired pressure on the limb. It has always been a problem for nurses to exactly stretch the bandages at 50% and apply without losing the stretch from ankle to calf, although there are indicators for the desired stretch (rectangles become squares) in the bandages. The elastic compression bandages are classified into four groups (3a, 3b, 3c and 3d) according to their ability to produce predetermined levels of compression and this has always been a problem to select the right compression bandage for the treatment. The inelastic short stretch bandage (Type 2) system, which has started to appear in the UK market, has the advantage of applying at full stretch (up to 90% extension) around the limb. The short stretch bandages do not expand when the calf muscle pump is exercised and the force of the muscle is directed back into the leg which promotes venous return. The limitations of short stretch bandages are that a small increase in the volume of the leg will result in a large increase in compression and this means the bandage provides high compression in the upright position and little or no compression in the recumbent position when it is not required. During walking and other exercises the sub-bandage pressure rises steeply and while at rest the pressure comparatively drops. Therefore patients must

be mobile to achieve effective compression and exercise is a vital part of this form of compression. Moreover the compression is not in tact with skin when reduction in limb swelling because the short stretch bandage is inelastic, and it has already been stretched to its full. To address the above problems, a novel Nonwoven Vari-stretch Compression Bandages (NVCB) has been designed and developed at the University of Bolton [7].

5. 3D COMPRESSION BANDAGES

Three-dimensional spacer fabrics are becoming increasingly important for developing novel medical textile products. In comparison to traditional woven or knitted fabrics, the range of physical and thermophysiological properties which can be achieved is considerably wider. These novel structures consist of two independent faces with interconnecting threads joining them. They can be exceptionally soft, incorporate large volumes of air, and provide good resilience to compression, temperature control, and moisture management. The layer of air that lies between the two independent textile faces creates a comforting, climate-controlling effect which prevents sweating and overheating of the skin. Spacer fabrics also provide an excellent cushioning effect which means that there is no need to use multiple layers of padding and compression bandages. When elasticated yarns are incorporated into the spacer fabric structure it is also possible to produce similar pressure-generating characteristics to those of traditional compression bandages.

6. MATERIALS AND METHODS

Four spacer fabrics identified as Black (1), White (2), White (3) and Blue (4) were used to study the pressure transference at various pressure ranges. Four padding bandages (PB1a to PB4a) recently available at Drug Tariff were also used for comparison.

6.1 Pressure Mapping Apparatus

The electronic pressure transference apparatus (Figure 2) developed at The University of Bolton was used. The apparatus consists of a wooden platform for presentation of test specimens, a strain gauge device and an electronic circuit board. A pressure pin (9mm diameter) is attached on to the load beam of the strain gauge and a corresponding hole drilled through the wooden platform. The height of the pressure pin is adjusted so that it protrudes through the hole of the platform by 1mm.

The specimen is placed onto the wooden platform over the pressure pin and a series of known metal block weights are placed onto its surface. The strain gauge device detects the pressure transmitted through the specimen at each known pressure in increments created by the metal blocks. The amount of pressure absorbed and dissipated within the textile structure and the actual pressure felt immediately below the specimen ie the patient's leg is determined. The transmitted pressure through the thickness of the specimen is the absolute pressure exerted on the patient's leg.



Figure 2. Pressure transference apparatus

A fabric extension device (Figure 3) has also been developed at the University of Bolton which facilitates the extension of spacer fabrics at the required length. The pressure transference of spacer fabrics at various extensions was measured utilising this device.

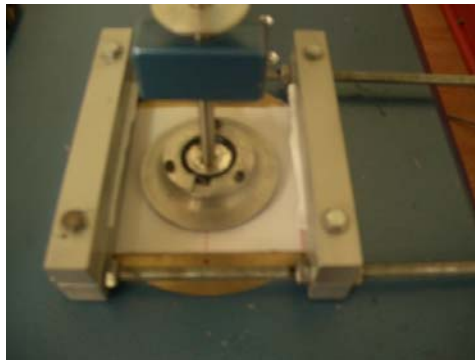


Figure 3. Pressure transference extension test rig

A prototype electronic mannequin leg developed at the University of Bolton was used to investigate the pressure mapping of bandages. The mannequin leg (Figure 4) simulates a lower limb and has definable tibia, calf and ankle regions. It has 8 pressure-measuring sensors of which 2 are positioned at ankle, 3 at calf and 3 at below knee. The sensors are connected with an electronic board display unit via strain gauges.

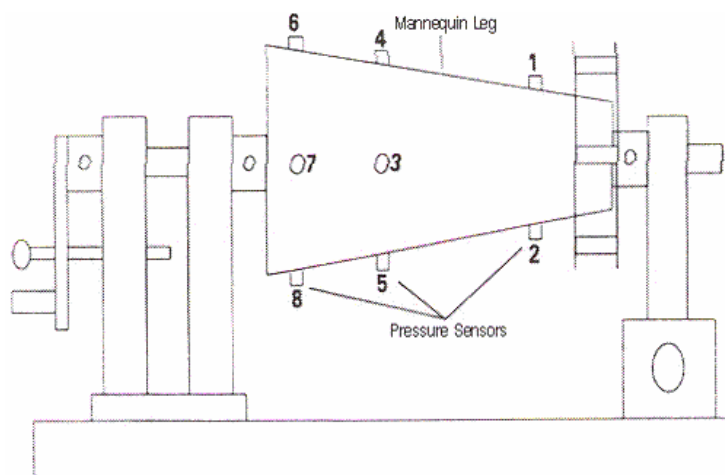


Figure 4. Schematic diagram of pressure profiling instrument

7. RESULTS AND DISCUSSION

7.1 Effect of Bulk Density

The basic properties of padding bandages and spacer fabrics used in this study are given in Table 1. The bulk density determines the bulkiness of fabrics, higher the bulk density lower is the bulkiness. It is one of the important parameters for treating venous leg ulcers because the padding bandage is applied next to the skin around the leg, and it must be capable of protecting bony prominence and imparting comfort and cushioning effect to the patient. An appropriate bulkiness would be required to protect the bony prominences in the leg.

Table 1. Basic properties of padding bandages (PB) and spacer fabrics

Sample	Thickness (mm)	Area Density (gm ⁻²)	Bulk Density (gcm ⁻³)
PB1a Padding	1.2	90	0.07
PB2a Padding	1.4	93	0.07
PB3a Padding	1.5	79	0.05
PB4a Padding	1.4	72	0.05
Black (1) Spacer	3.24	475	0.15
White (2) Spacer	2.37	295	0.12
White (3) Spacer	2.41	426	0.18
Blue (4) Spacer	1.87	279	0.15

It is observed in Table 1 that all the commercial padding bandages (PB1a – PB4a) possess essential bulkiness and the spacer fabrics registered significant higher bulk densities. It should be stated that spacer fabric is a three-dimensional structure and in 3D spacer fabrics, two separate fabric layers are connected at a distance with an inner spacer yarn or yarns using either warp knitting or weft knitting route. The two layers can be produced from different fibre types such as polyester, polyamide, polypropylene, cotton, viscose, lyocell, wool etc and can have completely different structures [8]. The three-dimensional nature of spacer fabrics makes them an ideal device for application next to the skin because they have desirable properties that are ideal for the human body [9]. 3D fabrics are soft, have good resilience that provides cushioning effect to the body and protects bony prominence, they are breathable and hence the ability to manage both heat and moisture generated by the body [8]. For venous leg ulcer applications, such attributes together with improved elasticity and recovery promote faster healing.

7.2 Effect of Pressure Transference of Commercial Bandages

Padding bandage is applied beneath the compression bandage. The degree of pressure that is induced into the leg by the compression bandage is of major importance. It has been demonstrated that too high a pressure on the leg not only leads to further complications of venous system but also promotes arterial disease. In contrast, inadequate pressure cannot help to heal the venous ulcers. Even if the compression bandage is applied at the correct tension it is probable that excessive pressure will be generated over the bony prominences of the leg. Therefore there is a need to distribute the pressure equally and uniformly at all points of the lower limb and this can be achieved by applying an effective padding layer around the leg below the compression bandage.

The pressure distribution characteristics of commercial bandages are shown in Figure 5. Obviously, none of the bandages provides uniform pressure distribution. It is vital that an ideal padding bandage should dissipate the pressure between 30 and 40mmHg, exerted by a high compression bandage (Type 3c), uniformly around the limb. Earlier studies also indicated the poor pressure distribution of commercial bandages [5,10]. However, a significant improvement in distributing the applied pressure of the novel padding bandages developed at the University of Bolton is reported elsewhere [5,10].

In order to ascertain the pressure transference of padding bandages exerted by high compression bandage (Type 3C), a prototype electronic instrument (mannequin leg) was used. The padding bandage was wrapped around the mannequin leg at 50% overlap (two complete layers) without stretching and high compression bandage (SurePress) was wrapped over the padding bandage at 50% overlap by rotating the leg. The compression bandage was stretched at 50% extension by applying 1 kgf load when wrapping around the leg. It should be stressed that nurses normally apply the bandages at 50% overlap, and at 50% extension for treating the venous leg ulcers.

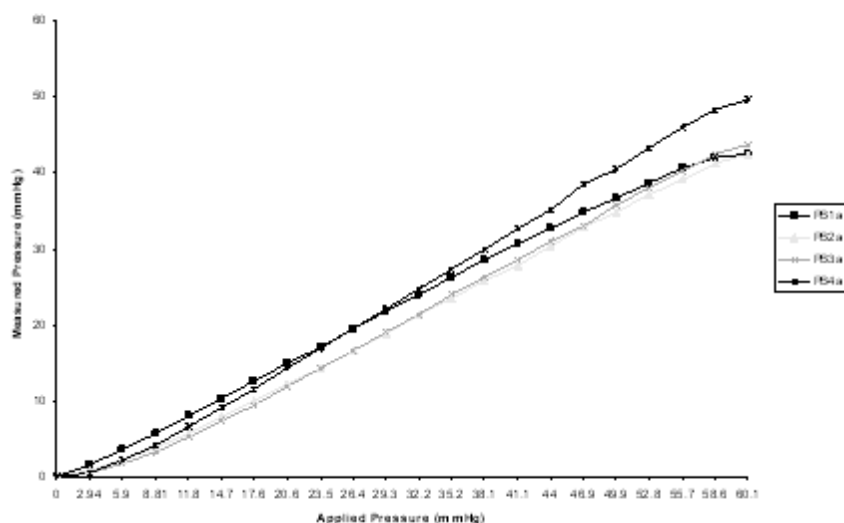


Figure 5. Pressure transference of commercial padding bandages

The pressure developed at ankle, calf and below knee positions in the mannequin leg was determined from the display unit and the values were corrected using the regression equations. Prior to the measurement, the pressure sensors in the leg were calibrated to the known pressure range of 0 to 300 mmHg by making use of a sphygmomanometer. The pressure mapping is depicted in Figure 6.

The interpretation of the results is summarised based on the following two major phenomena.

1. A sustained graduated compression, higher pressure at the ankle which gradually reduces to calf and upper calf according to Laplace's Law [11], aids the treatment of venous leg ulcers [12]. The graduated compression mainly enhances the flow of blood back to the heart, improves the functioning of valves and calf muscle pumps, reduces oedema and prevents the swelling of veins [13].
2. Approximately 30-40 mmHg at the ankle that reduces to 15-20 mmHg (50%) at the calf is generally adequate for healing most types of venous leg ulcers [14]. The ideal pressure just below the knee is around 17 mmHg [15].

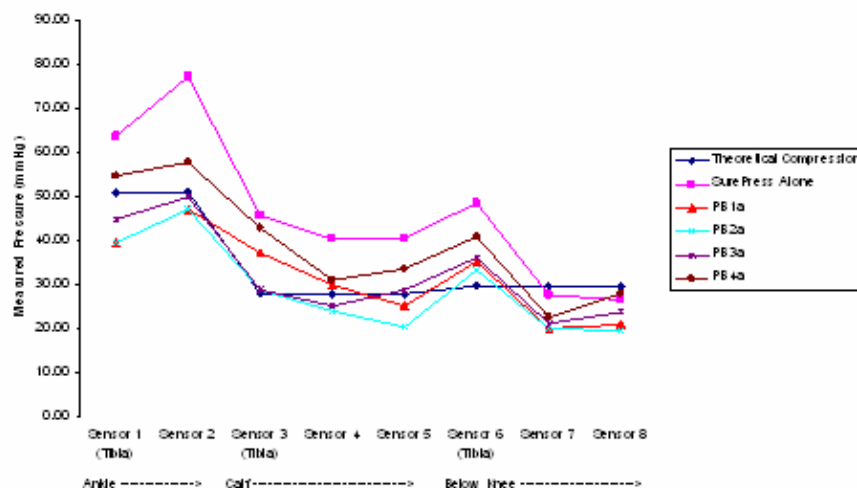


Figure 6. Pressure mapping of commercial bandages on mannequin leg

It is obvious from Figure 6 that the bandages do not fulfil the requirements of a sustained graduated compression of an ideal bandage system. The pressure measured by sensor 2 at the ankle is very high although the pressure is graduating down to the knee. It is obvious, however, that all padding bandages exhibited relatively lower compression values than the type 3C high compression bandage when applied on its own without orthopaedic wadding below it.

7.3 Effect of Pressure Transference of Space Bandages

Pressure transference apparatus and extension test rig were used to study the pressure transference of spacer bandages both at unrestrained and stretch conditions. It will be observed in Figure 7 that the pressure transference of different spacer bandages at any one point varies, and it mainly depends on the structure and fibre content of the material. It is interesting to note that spacer bandages distributed the applied pressure uniformly around the leg than that of commercial padding bandages. For instance, the White (2) spacer bandage absorbed the applied pressure of 43.9 mmHg and transfer 2 mmHg at one point. In other words the absorbed pressure of 41.9 mmHg is uniformly distributed inside the fabric structure which is one of the essential requirements for venous leg ulcer treatment. On the other hand, the commercial padding bandage (PB4a) absorbed 43.9 mmHg and transferred 35 mmHg at one point (Figure 5) and this means the bandage distributed only 8.9 mmHg uniformly inside the structure. The higher out put pressure from the bandage at one point is undesirable and may slow down and/or block the blood flow in arteries.

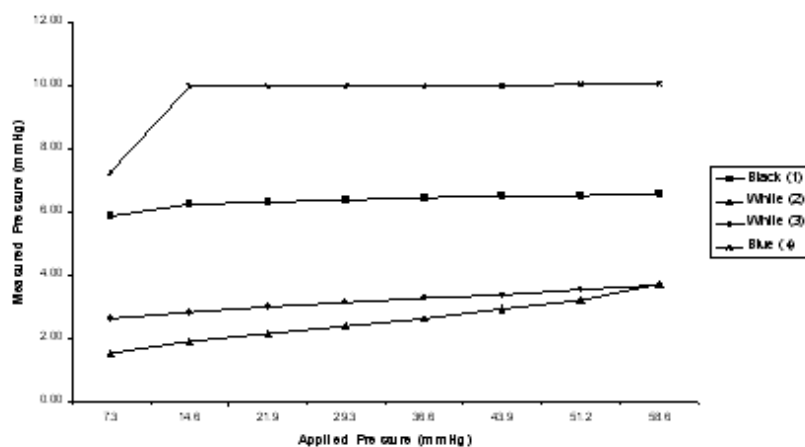


Figure 7. Pressure transference of spacer bandages (relaxed)

Figures 8 to 11 represent the pressure transference of spacer bandages at known pressures under extension up to 120%.

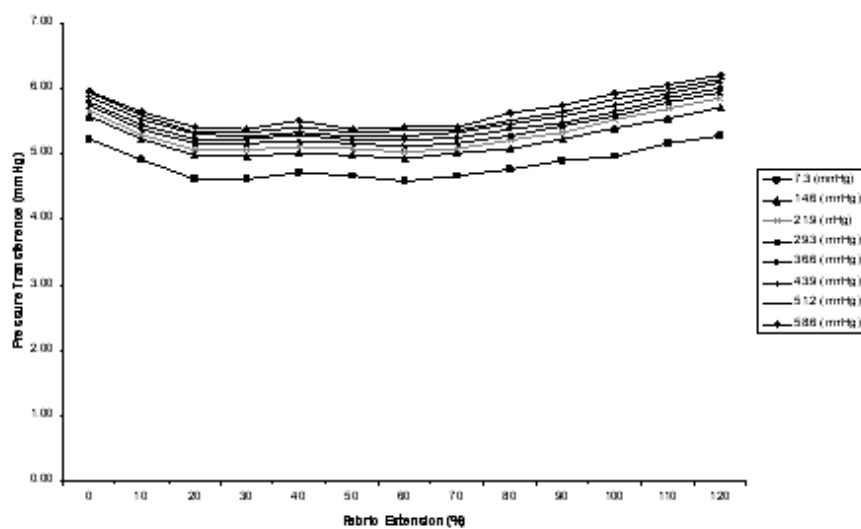


Figure 8. Effect of extension on pressure transference of spacer bandages - black (1)

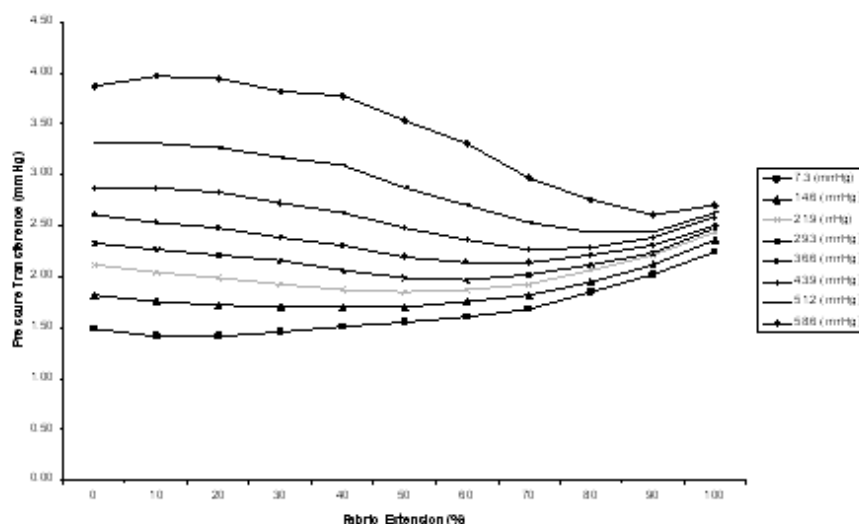


Figure 9. Effect of extension on pressure transference of spacer bandages - white (2)

It will be noticed that increase in applied pressure does not influence the pressure transference at any one point and the variation is marginal in all the samples. This affirms that these spacer fabrics can be used as ideal padding bandages, and by controlling the tension it will be possible to generate the required pressure for the treatment of venous leg ulcers.

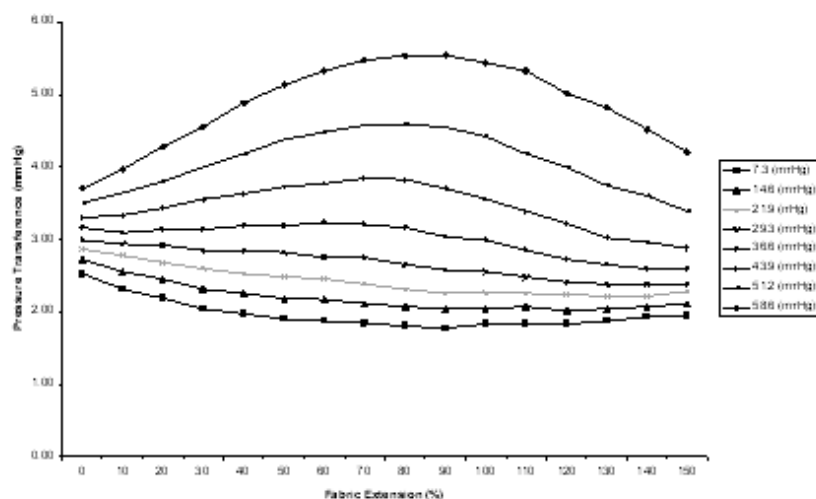


Figure 10. Effect of extension on pressure transference of spacer bandages - white (3)

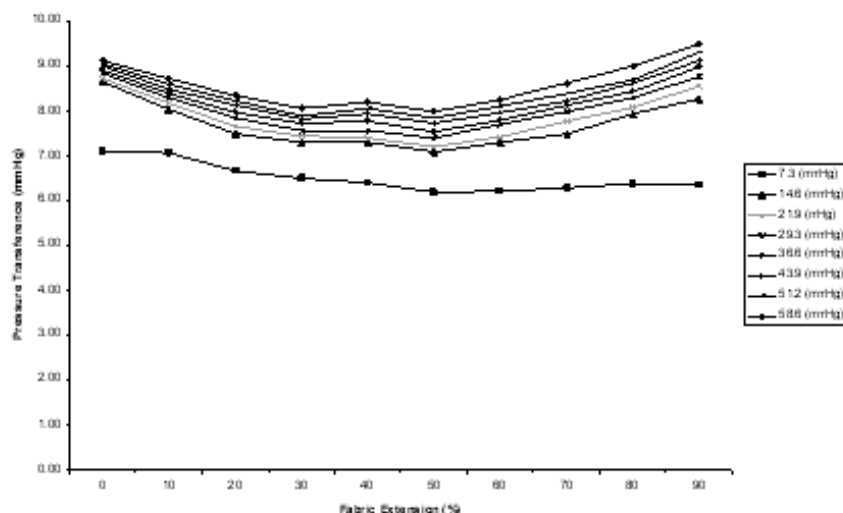


Figure 11. Effect of extension on pressure transference of spacer bandages - blue (4)

It should also be stated that according to Laplace equation the pressure generated on to the limb by a bandage is directly proportional to the tension of the bandage and the number of layers but inversely proportional to the width of the bandage and the circumference of the limb. Utilizing this concept, the research and development programme into the mathematical modeling of spacer fabrics to achieve the required pressure mapping for the treatment of venous leg ulcer is in progress at the University of Bolton.

6. SUMMARY

The effective management of venous leg ulcer involves careful selection of bandages to reverse the venous blood flow back to the heart. The paper has discussed the significant contribution of padding as well as compression bandages in healing the ulcer. The advantages and limitations of the existing two-layer and four-layer bandaging regimens are discussed in this paper. It is obvious that the pressure transference of commercial padding bandages varied and none of the padding bandages investigated satisfied the requirements of an ideal padding bandage. The study also demonstrated the need for developing a single-layer bandaging regimen for the benefit of elderly and cutting the cost of treatment. 3D spacer technology has been investigated and the results affirmed that spacer bandages would be utilised to design and develop a single-layer system that could replace the currently used cumbersome four-layer system. A suitable spacer structure can combine the desirable attributes of both the padding and 2-dimensional compression bandages into one composite 3-dimensional structure.

ACKNOWLEDGEMENTS

The research and development programme is funded by Engineering and Physical Sciences Research Council (EPSRC), UK. The authors are grateful to EPSRC for funding and supporting the research programme.

REFERENCES

1. N Cullum, '*Compression for venous Leg Ulcers* Cochrane Review', The Cochrane Library, Oxford, 2002.
2. D Simon, *Ostomy Wound Management*, 1996, 42, 34.
3. A A Ramelet, *Dermato Surg*, 2002, 28, 6.
4. S C Anand and S Rajendran, '*Effect of Fibre Type and Structure in Designing Orthopaedic Wadding for the Treatment of Venous Leg Ulcers*': In S C Anand, J F Kennedy, M Mirafab and S Rajendran (Ed), *Medical Textiles and Biomaterials for Healthcare*, Woodhead Publishing, Cambridge, 2006, p243.
5. S Rajendran and S C Anand, *Br J Nurs*, 2003, 11, 1300.
6. S Rajendran and S C Anand, '*Development of Novel Bandages for Compression Therapy*', Wounds UK 2002, Harrogate, 19-20 November 2002.
7. S.Rajendran and S.C.Anand, '*Challenges into Development of Woundcare Medical Devices*', FiberMed 06, 7-9 June 2006, Tampere, Finland.
8. S C Anand, '*Spacers – At the Technical Frontier*', *Knit International*, 2003, 110, 38-41.
9. Anon, '*Spacer Fabric Focus*', *Knit International*, 2002, 109, 20-22.
10. S Rajendran and S C Anand, '*The Contribution of Textiles to Medical and Healthcare Products and Developing Innovative Medical Devices*' *Indian J Fibre & Text Res*, 2006, 31, 215-229.
11. C Moffat and P Harper, *Leg Ulcers*, Churchill Livingstone, Edinburgh, 1997.
12. RCN, *Clinical Practice Guidelines. The Management of Patients with Venous Leg Ulcers*. RCN Institute, London, 1998.
13. M Collier, *Venous Leg Ulceration: In Wound Management: Theory and Practice*, Edited by M Miller and D Glover, London. Nursing Times Books, 1999.
14. D Simon, '*Approaches to Venous Leg Ulcer Care within the Community: Compression, pinch Skin Grafts and Simple Venous Surgery*', *Ostomy Wound Management*, 1996, 42, 2, 34-40.
15. R Stemmer et al, '*Compression Treatment for the lower extremities particularly with compression stockings*', *The Dermatologist*, 1980, 31, 355-365.

ELECTRO-CONDUCTIVE SENSORS AND HEATING TEXTILE ELEMENTS BASED ON A CARBON BLACK CONDUCTIVE POLYMER COMPOSITE

**F. BOUSSU¹, C. COCHRANE¹, M. LEWANDOWSKI¹,
C. DUFOUR², V. KONCAR¹**

¹GEMTEX Laboratory, ENSAIT

²IEMN, University of Lille

ABSTRACT

The need for sensors & actuators has been since a long time an important issue in many fields, such as in automotive and sports, and more generally, in all applications where there is a need for thermal comfort or warmth. On the other side, sensors truly flexible and adapted to textiles structures are necessary for applications in the field of smart textiles & communicative clothes. Important developments in sensing and heating textile elements consist in using for example non-metallic yarns, for instance carbon containing fibres, directly in the textile fabric. Another solution is to use electro-conductive materials based on conductive polymer composites containing carbon or metallic particles. Moreover, these solutions are generally designed so as to work with a low voltage supply. Our research is based on the use of a carbon black composite to design sensors and a textile heating element. The composite is applied as a coating, so that the heat distribution is more evenly distributed, and the integration of the electrical wires for the voltage supply or signal recording is as discreet as possible to ensure a good flexibility of the final structure.

Key Words: Actuators, conductive composites, intelligent textiles, sensors

1. INTRODUCTION

The term 'smart textile' describes a class of apparel that has active functions in addition to the traditional properties of clothing. These innovative functions or properties are obtained by utilizing special textiles or electronic devices, or a combination of the two. Thus, a sweater that changes colour under the effect of heat could be regarded as smart textile.

Amongst other technical elements or building blocks for integration in smart textile structures, sensors & actuators are very important. Clothes could be used to detect different actions, in particular the recognition of posture of the driver and passengers and their gestures in order to facilitate certain commands that are intuitive. Moreover, when these sensors and actuators are associated with computing and with the control unit, they may allow the recognition of situation and context for a better interpretation of reality. Sensors integrated in textile structures could also be used as psychological sensors for various parameters.

This term refers to the sensors used to record health or personal parameters in a broad sense and to alert if necessary. The applications rising from the use of these sensors are numerous. We can, for example, use sensors to provide a physical performance analysis of a driver or even a car racer pilot or to conduct elder people's medical follow-up in real time.

2. TEXTILE SENSORS

2.1 Conductive Composite

A sensor based on a thermoplastic elastomer (Evoprene)/carbon black nanoparticle composite has been developed in this work. This sensor presents general mechanical properties that are strongly compatible with any flexible and soft material such as a textile structure. It offers a great potential for use in clothing or home textiles. To improve the precision and reliability of these sensors, it is important to know the influence of external parameters such as rate of strain deformation, temperature or humidity on the sensor response and on its mechanical behaviour. The design and calibration of the sensor on a Nylon fabric have been demonstrated in previous papers [1,2,3]. The fully detailed sensor fabrication and optimization can be found in our previous work⁶. The conductive polymer composite of which is made the sensor material is prepared via a solvent process. Carbon black particles (Printex L6, from Degussa) are dispersed with a thermoplastic elastomer, Evoprene 007 from Alpha Gary, which is a Styrene-Butadiene-Styrene (SBS) co-polymer, in chloroform (Aldrich). After a certain time of mixing at 55°C, the blend obtained is applied as a coating on the textile substrate and left to dry at room temperature. The final concentration of carbon black filler particles is 27.6 vol. % in the Evoprene polymer matrix, after total evaporation of the chloroform solvent. This concentration is greater than the percolation threshold so that there is a good conducting network throughout the composite. Finally, a protective latex film is applied on the sensor. Fig. 1 shows schematically the dimensions of the sensor on the fabric which is a light Nylon fabric with a mass per unit area of 42 g/m². The linear density of the weft and warp yarns is equal to 3.3 tex.

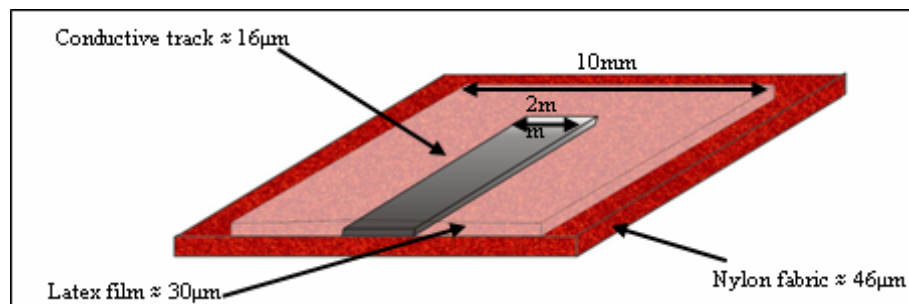


Figure 1. Schematic representation of the structure and dimensions of the sensor integrated on the fabric

The final sensor system (conductive polymer composite + latex film) has the following dimensions: 10 mm wide, 110 mm long and only 46 µm thick. The sensor track is parallel to the weft direction of the fabric (sample dimensions: 50 mm × 300 mm). Stainless steel yarns used as electrical connections are added at the ends of the sensor track in order to measure its electrical response (Fig. 2).



Figure 2. Set-up of sensor on fabric, with electrical connections

2.2 Experimental Results

The sample is set up on a tensile testing machine (MTS 2/M), with the sensor track positioned parallel to the direction of fabric extension, and at the centre of the test specimen (fabric test length = 200 mm). Different rates of extension, 16, 200 and 500 mm/min, were applied to different samples, and the electrical resistance of the sensor was recorded during elongation until the sample breaks. Since the different sensor specimens will necessarily present slight variations in their intrinsic resistance values, a normalized relative electrical resistivity is defined to characterize the sensor's electrical property (with $R_r = \Delta R / R$):

$$R_r = \frac{(R - R_i)}{R_i} \quad (1)$$

where R_i is the initial resistance of the sensor measured before extension, and R the resistance at a certain length l of the sample. The sample is left at rest for about 1 minute before beginning the test, and R_i represents the mean value of resistance measured during this lapse of time. The electrical resistance was measured until the breaking up of the fabric which occurs at around 45% elongation. In general textile applications such as weaving, the elongation zone of interest is within the 0 to 10% range. An example of the electrical behaviour of the sensor in this zone is given on Fig. 3.

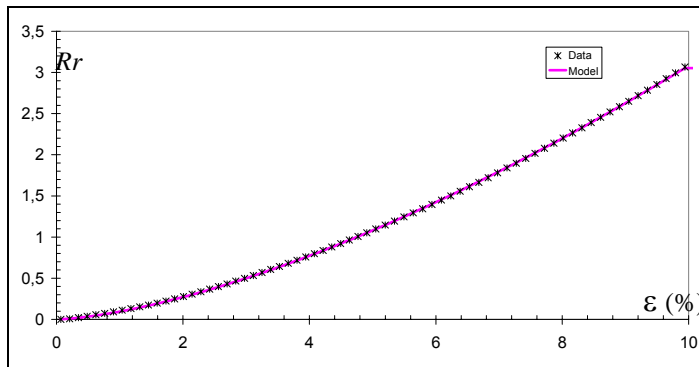


Figure 3. Dependence of relative electrical resistivity of sensor on elongation ϵ , at an extension rate of 16 mm/min

To be able to compare our gauge sensitivity to existing strain gauges, a first assumption of a linear variation was made. In this case, the gauge factor (K) is defined as follows:

$$K = (\Delta R / R) / \epsilon \quad (2)$$

In the elongation range [0-10%], K is greater than 30. In comparison, the K coefficient of a classic metal gauge (copper - nickel) is 2.1. Moreover, a classic metal gauge has a range of elongation between 0.1 and 0.5 %.

The linear relationship (Eq. 2) applied to our sensor is however not very satisfying. In fact, the electro-mechanical behaviour of the sensor can be better modelled by the following equation:

$$\Delta R / R = a \epsilon^b \quad (3)$$

a represents the sensitivity of the sensor, while b relates to the deviation from the linear model, in which ideal case $b = 1$ and $a = K$. The good fitting of this model is illustrated on Fig. 3 by the solid line. In this case, $a = 99.9$ and $b = 1.51$. The two parameters depend on the intrinsic characteristics of the sensor (initial resistance, length to width ratio, composite quality ...), but also on the elongation rate. Table 1. gives the values of a and b obtained at other rates of deformation. In all cases, there is good accordance between the experimental data and the model (Eq. 3).

Table 1. Elongation rates

Elongation rate (mm/min)			
	16	200	500
a	99,9	200,8	264,2
b	1,51	1,69	1,79

This investigation concerning the influence of climatic conditions is carried out with a climatic chamber (Excal 2221-HA, Climats®). The samples mounted on a metallic grid are placed at the centre of the chamber (Fig. 4). The electrical resistance R of each sensor is recorded by an ohmmeter during the experiment.

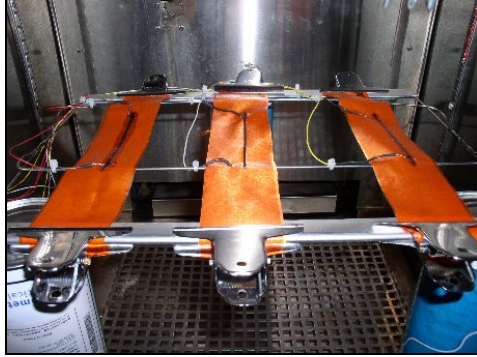


Figure 4. Set-up of samples in climatic chamber

In the aim of studying the separately the two parameters, temperature T and relative humidity RH , two types of tests have been performed in which one of the parameter is kept constant while the other one undergoes an cycle. In the iso-humidity cycle, RH is kept constant, and T is increased from 10 to 50°C and decreased back to 50°C, in successive 10°C steps. At each step, the temperature is maintained constant during 150 minutes, time during which the resistance of the sensor was recorded. In the isothermal cycles, T is kept constant while RH undergoes a cycle from 20 to 90% in increment steps of 10%, and again with a 150 min equilibrium time at each step. At the beginning of each cycle, a reference value of electrical resistance R_0 is measured at 20°C / 40% RH . As in the electromechanical characterization (Eq. 1), the resistance is expressed as a normalized relative resistance Rrc :

$$Rrc = \frac{(R - R_0)}{R_0} \quad (4)$$

For each cycle experiment, two values of Rrc are measured for each T/RH couple, one during the upward direction, and the second during the downward direction of the cycle. The main conclusion of these experiments is given below. Despite the fact that the carbon conducts electricity following a “metallic” behaviour, in the sensor, the carbon particles are surrounded by a polymer matrix, an insulator. RH and T probably have an impact on the molecular arrangement in the polymer, leading to a modification in the arrangement of the conductive carbon particles. The same behaviour is obtained at all temperatures. Rrc increases with RH , with somewhat a

sharper dependence for RH lower than 35% (sensitivity around 0.5% / % RH) and higher than 55% (sensitivity around 1.2 % / % RH). In between these two values, the resistance does not change a lot, and the sensor sensitivity amounts to only 0.2% / % RH . There are very few studies found in literature on the influence of humidity on conductive polymer resistance. The only study is about sensors used to measure hygrometry and in this particular application, the electrical resistance varies linearly with RH [4,5].

3. TEXTILE ACTUATORS

Heating textiles can find an application in numerous and varied fields such as sports and leisure, medical, or automotive [6,7,8]. The situation is quite complex with actuators because they need important power supplies that are rarely flexible and lightweight. The heating element developed and presented in this work is designed to be specifically adapted to flexible structures. It comprises a plane woven textile element in which are integrated electrodes composed of metallic yarns woven or stranded directly in the fabric in a comb architecture arrangement. These electrodes are connected to a power supply. In order to ensure a uniform heat distribution, a thin conductive coating is applied on the fabric surface and electrode arrangement. The coating is based on a conductive polymer composite consisting of a synthetic rubber and conductive Carbon Black nanoparticles. The heating element can thus be shaped in a desired pattern, by choosing specific dimensions of electrode structure and area of coating layer. Moreover, the whole assembly can be placed in selected areas depending on the application. The electrical resistance of the heating element (electrodes and conductive coating, Fig. 7) can be calculated. The two stainless steel yarns parallel to the warp direction are used to supply the power that is necessary to heat the fabric and also create - together with the stainless steel yarns on the weft direction - a comb structure. This comb structure electrode design is made to create a parallel resistance (decreases the resistance). Considering that the element is composed of a number of parallel resistances, the distance between the comb teeth being constant:

Number of parallel resistances = L/lp , with L : conductive coating width, lp : distance between 2 adjacent teeth.

The total resistance is thus:
$$R_{tot} = \frac{R}{L/lp} = \frac{\rho \times lp/S}{L/lp} = \frac{\rho \times lp^2}{LS}$$

where l : comb teeth superposition width, S : coating cross-section area, e is the coating thickness ρ : coating resistivity. The coating resistivity depends on the amount of carbon black loading in the composite. It can be predicted by the following relation:

$$\rho = \rho_0 (V - C_p)^{-t}$$

where ρ_0 : constant, V : %-vol of carbon black, t : critical index, C_p : concentration of carbon black (vol-%) at percolation threshold.

The textile fabric has been made on a hand weaving machine (ARM, electronic control Selectron). A plain weave has been chosen, and the warp and weft are made of cotton yarns with warp and weft densities of respectively 27 yarns/cm and 10 yarns/cm. For the electrodes, stainless steel 2-ply yarns (Créafibres, France) are used, each ply consisting of 275 filaments. The overall yarn count is 500 Tex, with a resistivity of 14 ohms/m. The distance between the teeth of the comb (lp, Fig. 3.1) is 0.7 cm, while the distance between the 2 parallel steel yarns in the warp direction is around 7 cm. The steel yarns are introduced manually during the weaving process according to the pattern on Fig. 7.

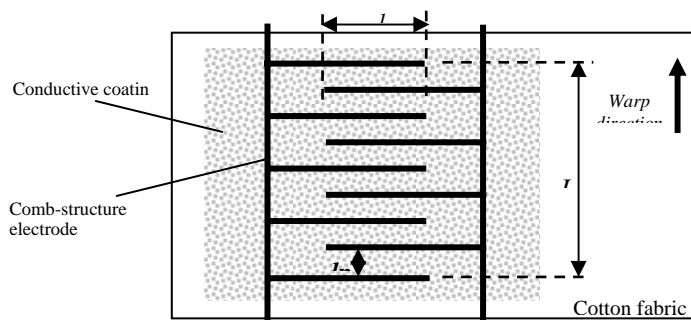


Figure 7. Pattern of heating element

The conductive carbon black coating composite was made with the following ingredients:

- a synthetic rubber latex solution, Kraton IR-401 (Kraton Polymers), an anionic dispersion of polyisoprene;
- a dispersing agent, Disperbyk-2010 (from SPCI)
- carbon black (CB) particles, Printex L6, from Degussa

The preparation procedure is as follows: the dispersing agent is put into water and the CB particles are gradually added while mixing continuously. A paste is obtained and left to rest for some time. The polymer is finally added while mixing gently in order to avoid too strong shearing. The coating was then applied on the fabric with a magnetic coating table equipped with a magnetic bar as scraper. The thickness of the coating was however hard to adjust with this technique. Moreover, the quantity of coating deposited depends on the viscosity of the solution, which itself depends on the amount of water in the coating solution. If the viscosity is different, even if the same thickness is deposited on the fabric, the final quantity of composite will differ since the absorption of the coating will be different. Hence, the final resistance will also be different. After drying at room temperature, the resistance of the actuator was measured with an ohmmeter, and was found to be equal to 12 ohm. The fabric with the electrodes

is shown on Fig. 8, before and after application of conductive coating. The final coated surface is approximately 5 cm x 7 cm.

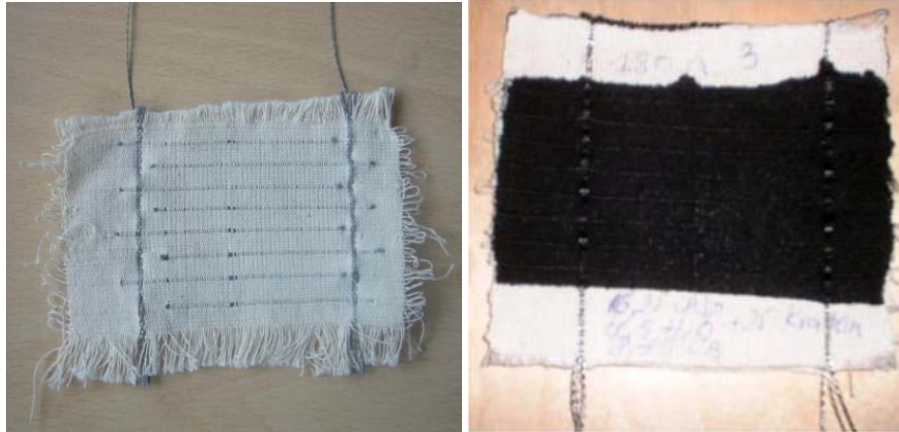


Figure 8. Fabric with heating element: before and after coating

The electrical and heating properties of the element were studied. The electrical resistance of 3 cm x 3 cm coated samples with various carbon black contents was measured (Fig. 3.3). It was found to depend of course on the CB loading level: the higher the amount of CB, the lower the resistance. The optimum CB loading is thus around 35 to 45 % in weight. A coating containing 37.5%-wt was used for the heating property study. The coated fabric was connected to an ammeter and a power supply according to Fig.9. It is important to note that the sample temperature may change in function of the time even when applying the same voltage. Because of this, the temperature of each sample was measured for 60-80 min for a given voltage. The temperature of the sample surface was recorded every five minutes with a temperature sensor (Testo® 925). The temperature was not the same in every point of the heating element, and the highest temperature was obtained at the centre of the sample, but the variation was not very important. The results are presented graphically on Fig.10. The measurement was made at room temperature (22°C).

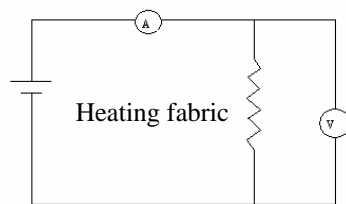


Figure 9. Power circuit with fabric heating element, and temperature sensor

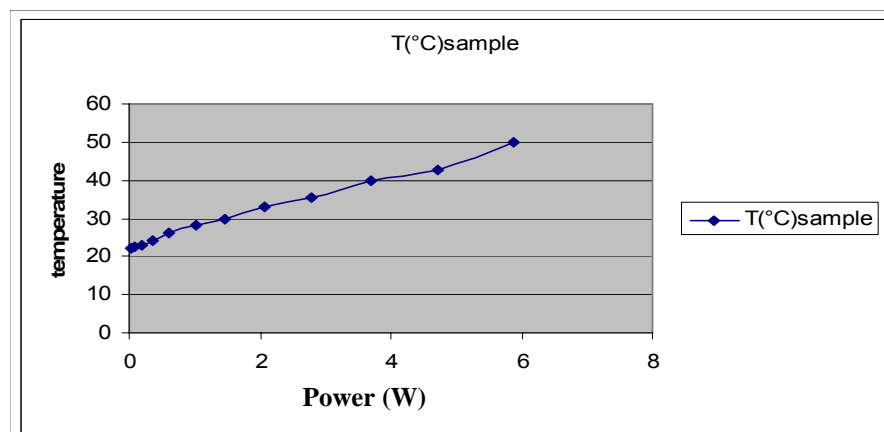


Figure 10. Temperature of heating fabric as a function of power supply.

The increase in temperature is important, about 30°C, from an initial temperature of 22°C, for the highest power supply (6 W). The heating process was found to be quite rapid; the time to reach the highest temperature was about 10 minutes. The increase of heating efficiency requires a quite important percentage of carbon black, more than 35%-wt. It was found that the temperature was not homogeneous over the whole coated surface, the sample being hotter at the centre than at the corners. So this point has to be improved, maybe by modifying the pattern design of the electrodes. The heating is moreover limited to the coated area; another possibility using intelligent design can result in the dissipation of the excess heat generated to other parts of the fabric. After coating with the CB solution, the woven samples became quite rigid. Other studies have therefore to be done to obtain a more flexible final structure, and our next work will be on knitted structures [9]. The steel yarns will be integrated inside the knitted fabric, and this type of textile structure being intrinsically more deformable than woven structures, the final heating element will be normally more flexible.

4. CONCLUSION

Different building blocks (sensors and actuators) have been presented in order to show development and integration possibilities of smart textile structures designed for car interior. Sensors based on conductive composites may be used to detect fabric lengthening, passenger presence or to evaluate safety belts ageing. They also may be used to control air bags deployments as shown in the Mr. Jayaraman patent [10]. On the other side heating fabrics are suitable for car seats or winter clothes. The advantage of our solution is that it is low cost, but with a long life time and particularly reliable. The other advantage is that the same actuator may be used as a sensor helping the temperature control and regulation.

REFERENCES

1. Cochrane C., Koncar V., Lewandowski M., Dufour C., "Design and development of a flexible strain sensor for textile structures based on a conductive polymer composite", *Sensors*, 7, 473-492, 2007
2. Cochrane C., Koncar V., Dufour C., "Création d'un capteur d'allongement souple, compatible textile", *Matériaux 2006 Conference*, November 13-17, Dijon, France, 2006
3. Cochrane C., Koncar V., Dufour C., "Nanocomposite material sensors for textiles", *AUTEX 2006 World Textile Conference*, June 11-14, Raleigh, NC, USA, 2006
4. Barkauskas J., "Investigation of conductometric humidity sensors", *Talanta*, 44, 1107-1112, 1997
5. Barkauskas J., Vinslovaite A., "Investigation of electroconductive films composed of polyvinyl alcohol and graphitized carbon black", *Materials Research Bulletin*, 38, 1437-1447, 2003
6. Droval G., Glouannec P., Feller JF., Salagnac P., Simulation of electrical and thermal behaviour of conductive polymer composites heating elements. *J. of thermophysics and heat transfert*, Vol. 19, N°3, 375-381, 2005.
7. El-Trantawy F., Kamada K., Ohnabe H. In situ network structure, electrical and thermal properties of conductive epoxy resin-carbon black composites for electrical heater applications. *Materials Letters*, Vol. 56, 112-126, 2002.
8. Kirkpatrick S., Percolation and conduction. *Reviews of Modern Physics*, Vol. 45, n°4, 574-588, 1973.
9. Lewandowski M., Koncar V., Cochrane C., Giraud S., Electro-conductive heating textile elements based on a carbon black conductive polymer composite. *Intelligent Textiles & Mass Customisation International Conference*, Casablanca, Morocco, Nov. 2007.
10. Jayaraman et al., Method and apparatus for controlling air bag deployment, Patent No. US 6,254,130 B1, Jul. 3, 2001.

HEATING BEHAVIORS OF METALLIC TEXTILE STRUCTURES

O. KAYACAN, E. BULGUN

Dokuz Eylul University Textile Engineering Department

ABSTRACT

The integration of electronic components with textiles to create very smart structures is getting more and more attention in recent years. Most of the textile materials are electrical insulators. Hence, there is an urgent need to develop various types of fibers and fabrics with electrical conducting properties. With this point of view, the electrical characteristics of textile-based products are one of the major topics of technical textiles. Various products having reasonably good electrical conductivity are required especially for electronically functional apparel products. This can be obtained by incorporating metallic fibers or coating with some agents. The textile materials being flexible and easily workable are the most preferred one in such cases. In this study, the concept of “electrically conductive fabrics” is investigated. The primer applications that impart electrical conductivity properties to textiles are summarized. Also the heated fabric panels produced by steel yarns are evaluated. Single and multi-ply steel fabrics are applied to electrical current and their heating behaviors are observed and compared.

Key words: Conductivity, steel yarns, textile based electronics, heating panels

1. INTRODUCTION

Since the 19th century, revolutionary changes have been occurring at an unprecedented rate in science and technology with a profound impact on our lives. Inventions in science and technology have transformed the entire world. As technology has progressed, it has been applied rapidly. Technological improvements in the field of smart and interactive materials have attracted more and more attention in recent years. There will be a boom in the use of these new ideas and components in the next few years. These new achievements of the textile industry enable electronic devices to be directly integrated into the structure of textile, therefore modifying the functionality of the apparel.

The worldwide smart materials market is estimated at \$8.1 billion in 2005 and is expected to rise at an average annual growth rate (AAGR) of 8.6% to \$12.3 billion in 2010. On the other hand, the global market for smart/interactive textiles reached \$304.0 million in 2005 and is expected to grow to \$642.1 million by 2008 a compound annual growth rate of 28,3%.

The materials of our surroundings are being “intellectualized”. Whereas, in the past, we needed several components to satisfy a certain function. Today, technology has allowed us to satisfy the same function with less components. The concept of “miniaturization” not only means the production of smaller components, but the elimination of components. Intelligent textile systems, integrated to electronics, have the capacity of improving the user’s performance by sensing, adopting itself and responding to a situational need.

The smart/interactive textile structures that integrate electronics and textile materials and the materials that react to the external stimuli physically and chemically have been developed. These products, which are called 'the garments of the future', involve different functions such as protection, actuation, communication etc. The garments, which can heat the body, will possibly be one of the most widely used products for future use in daily life. Beside the medical usage, these products are developed especially for the use of the people who work outside during their day such as military applications, security services, and country duties. The heating functions of the garments occur in the thermal panels.

The thermal panels can be produced by using electrically conductive textile based materials by weaving or knitting. Stitching is another method for placing the conductive yarns into the fabric surface. There are different textile based materials that can be used as a heating material such as silver coated, copper plated yarns, carbon-based fibers, tiny inox cables etc. In this study, conductive stainless steel yarns are chosen as a sample for metallic textile structure. The heated fabric panels produced by steel yarns are evaluated. Single and multi-ply steel fabrics are applied to electrical current and their heating behaviors are observed and compared. For this purpose, an electronic circuit that contains textile based warming panels connected to a power supply, has been developed.

2. CONDUCTIVE YARNS FOR SMART TEXTILE APPLICATIONS

Natural fibers have insulative characters. The integration of electronic functions in textiles can be realized in two extreme ways. One way is to produce the apparel or technical textile and then integrate electronic components. The other way is to process conductive yarns when producing textiles and create textile structures with electronic functions. There is a lot of research and development activity regarding the needs of conductive textile materials. The studies about transformation of the natural materials into conductive structures by different chemical processes such as coating, lamination and modification are progressing. One of the major electrically conductive textile-based materials is carbon fiber. In a similar way, metallic fibers and steel based yarns are also used for the same purpose. If examined by production types, there are different types of materials: Knitted fabric, Woven fabric, Non-woven structure.

Electrically conductive yarns can be used for;

- Transfer of power
- Transmission of signals between;
 - Sensors
 - Transmitters
 - Microcontrollers etc.
- Traditional use in;
 - Heating
 - Electromagnetic protection.

High conductive yarns are made from different materials and exist in a lot of different forms. Materials are metals like copper or stainless steel or alloys such as Nitinol, coated metals, carbon fibres and polymers. Insulating polymers can be coated or doped.

There are several criteria for selecting a conductive yarn for a certain application. The criteria can be based on the product and the processing. Costs, conductivity, chemical resistance (e.g. against moisture, wash ability), mechanical properties and contact ability (e.g. thermal resistance) of the product is the main factors regarding to selecting a conductive yarn.

The electrical resistance of the yarns is described in Ω/m , a value which in one case is a material parameter, the resistance depends on length and diameter, and in other case a yarn parameter, the resistance depends only on the length.

The metallic wires and tapes are the most typical materials that can be applied to textiles for their conductivity properties. They can be interlaced into the fabric structure. However there are some disadvantages about the material characteristics such as limited flexibility, increased weight and cutting problems.

Owing to the isolating characteristics of textile polymers, electrical conductivity is reached by modification of the polymer structure and/or addition of conductive materials. The modification of the fabric structure can be performed in two ways: Impregnation using antistatic agents and coating using conductive substances. Moreover, electrically conductive fibers were produced by wet spinning, melt spinning from conductive polymers; or coating fibers with electrically conductive materials such as metal powders and carbon black or intrinsically conductive polymers. Polyaniline, polyamide-11, polyvinilalcohol are the most common conductive polymers using such processes. However the major drawbacks are 'limited flexibility' and 'use only in blends with conventional fibers'. Modification of polymers can be carry out by filling with electro-conductive powder, vacuuming spread metal, galvanic coating and chemical coating

Among the manufacturing processes, various coating techniques have been attractive due to simple in process and easy to handle. The textiles produced not only gain controllable electrical properties, but also maintain their excellent physical properties of the textiles such as mechanical strength and flexibility.

3. MATERIAL AND METHOD

3.1. Heated Fabric

In previous studies, it's been indicated that, the resistance of heating panels produced by weaving techniques is lower than the knitted structures with the same dimensions because of the structural characteristics. When compared to knitted fabric, woven fabrics have less surface characters and quality properties. So they are more appropriate for implications, as a heating panel.

The heating panels used in this study were produced by using industrial narrow weft knitting machine. Two different types of stainless steel were placed into the fabric construction but owing to the inadequate electrical characteristics, the appropriate one was chosen to use as a heating panel. In the panel construction, the conductive yarns were placed in coarse direction while polyester yarns were placed in wale direction.

As seen on Figure 1., the conductive yarns were placed in a parallel form. After laying process, the yarns leave the fabric without any cut, brake or any interruption

In a regular heating element the electrical wires have a similar structure. So, this is the most suitable fabric formation for heating pad production.

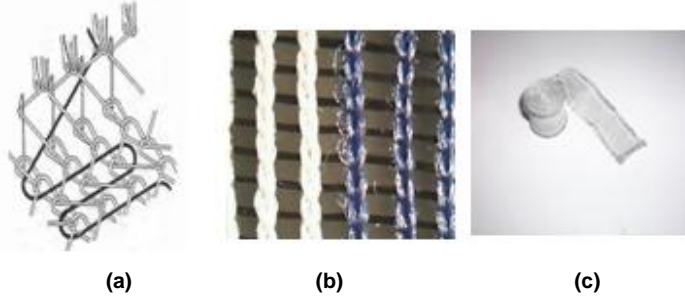


Figure 1

- a) General production procedure of heating panel b) The parallel structure of conductive yarns
c) General view of narrow width conductive fabric band

10 cm-long fabric bands were chosen as a unit ply for heating panels. To compare the different heating levels; single, double, 3 and 4-ply heating pads have been produced. For each ply amount, 3 heating pads have been connected to the circuit and 12 V. electric current have been applied. The heating behaviours were observed in point of temperature and electrical characteristics.

3.2. Stainless Steel Yarns

Metal fiber combines flexibility of traditional fiber with high temperatures resistance and thermal-electric conductivity of steel. Metal fibers are obtained by successive wire bundle-drawings. Because of its mechanical properties, AISI 316L alloy is the most common alloy.

In this study, a special range of continuous stainless steel filament yarns was used to obtain heating function. These yarns have a very precise electrical resistance. Some characteristics of special yarns can be seen on Table 1.

Table1. Some physical characteristics of stainless steel fiber used in heating panels

Average linear resistivity	71 (Ω/m)
Variation linear resistivity	\pm % 14
Yarn count	110 tex
Av. breaking load	23 N

3.3. Electronic Circuit Design for Activating the Heating Panel

In this study, to observe the heating behavior of metallic textile structure, an electronic circuit is designed to meet the electrical requirements. The circuit activates the heating panel, produced by stainless steel yarns. The small dimension, lightness and low-cost parameters of the circuit are considered owing to the needs of smart-interactive garment design in the future works. Owing to the location in the garment, the dimensional parameters are very important. The circuit should be placed in as small an area as possible.

The use of a high linear temperature sensor for observing the heating behavior with digital output is accurate. The temperature measurement system is implemented by using DS1820 (a one-wire digital temperature sensor). The property of one-wire bus has the capability to connect up to several different one-wire devices into the same bus. This is possible due to a unique address that every one-wire device has. Implementing the one-wire interface with one I/O pin is possible, but because that would have significantly increased the complexity of the software, the one-wire sensors should be connected to the serial multiplexer through a serial one-wire line driver. The sensors have a range of $\pm 0.5^{\circ}\text{C}$. Temperature sensor should be used with a microcontroller. Both devices should be low-cost and small in dimensions. The temperature control values are loaded into the microcontroller by software and the heating functions runs according to these pre-set values.

The general scheme of the circuit is shown on Figure 2.

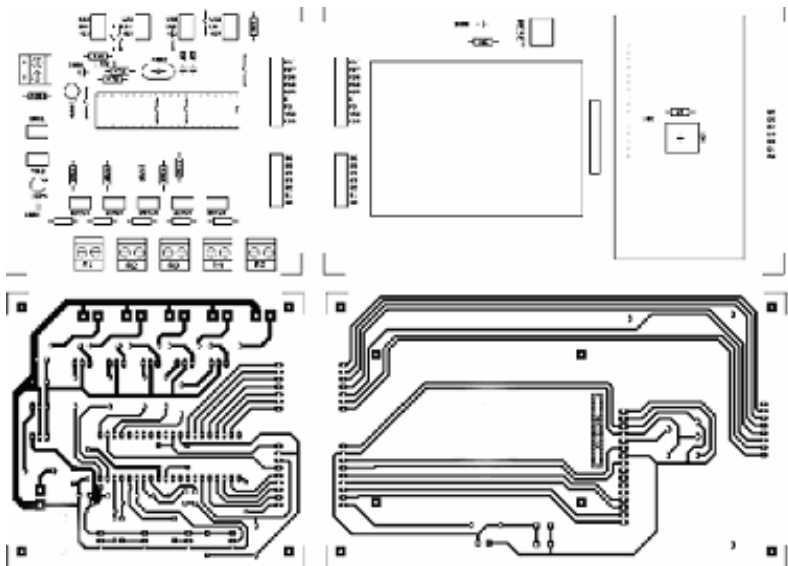


Figure 2. General Scheme of Electronic Circuit Board

4. RESULTS

Figure 3., 4., 5. and 6. indicates the heating behavior of panels containing stainless steel yarns. As seen on Figure 3., single-ply heating pad system provides approximately 15°C heating within about 10 minutes. On the other hand 2-ply systems supplies nearly 25°C as shown on Figure 4.

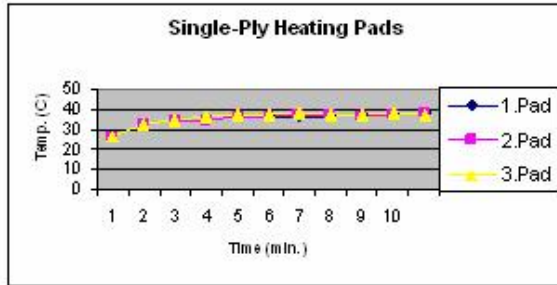


Figure 3. Heating behaviour of single-ply heating pads

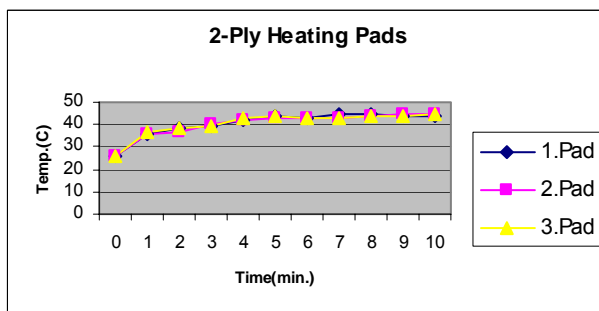


Figure 4. Heating behaviour of 2-ply heating pads

As shown on Figure 5. approximately 30°C heating was obtained by using 3-ply heating pad system within about the same period.

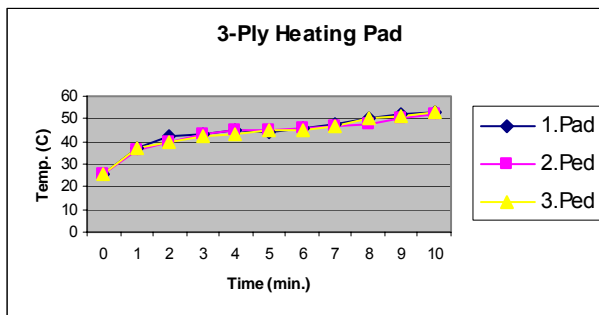


Figure 5. Heating behaviour of 3-ply heating pads

As seen on Figure 6., 4-ply heating pad system provides approximately 40°C within about 10 minutes.

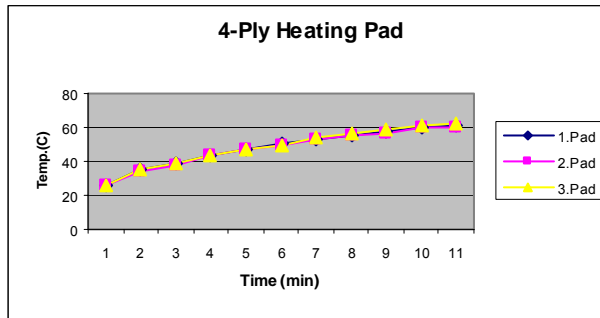


Figure 6. Heating behaviour of 4-ply heating pad

According to the comparison between different-ply heating pads, 4-ply ones reach the maximum value (about 60°C). As expected, the heating levels of the different plies can be arranged 4,3,2 and 1-ply respectively.

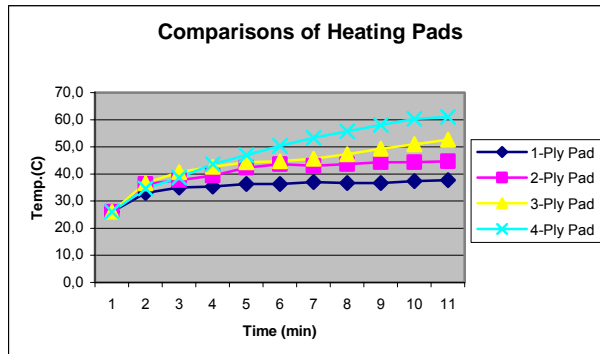


Figure 7. Comparisons of heating pads

Electrical current for the circuit have been supplied from a battery-pack having a capacity of 12 V. Consequently, all pad system starts their performance from this level. However because of the electrical characteristics of the panels such as resistance, they have been served for different time period with same power source as seen on Figure 8.

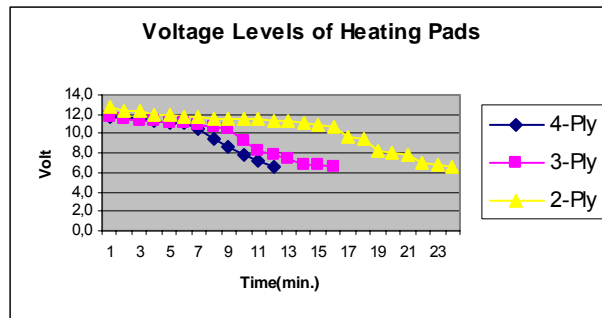


Figure. 8. Voltage levels of heating pads

5. CONCLUSION

Nowadays, conductive fibers are of special interests due to their application possibilities especially for interactive electro-textile products. Various metallic based yarns have been applied for different function.

In this study the heating behaviors of conductive steel fibers were observed and evaluated. A special electronic circuit was designed to assist the system.

Each plies of the heating pad contains the same amount of steel yarns and all heating pads have different number of plies (single, 2, 3 and 4-ply heating pads). It's observed that owing to the different resistance levels, the pads with different number of plies provide different heating degree intervals. Therefore, in the applications of textile based heating elements it's suggested that, the electrical characterization of conductive materials should be examined and the materials that have the most appropriate electrical resistance characteristic must be applied.

Furthermore, in the circuits that used for heating function, the current amount depends on the electrical features of heating structures. Consequently the pads with different plies have various efficient heating in point of time.

It's recommend that the appropriate heating pad dimensions, ply or conductive yarn amounts and sufficient power supply conditions should be evaluated and chosen according to the desired heating level.

On the other hand, in the early stages of the investigations, the combination of electronics and textiles were seemed not to be practicable in view of their opposite properties. With the successful results of scientific studies, the integration of electronic components into textiles offers great advantages. The first samples that combined these systems together were observed in the military and other out-door applications. As a sample of such an application, the temperature controlled heating garment design should have two main divisions. The first step should meet the functional

needs while the second should cover the electronic functions. Being a mobile device, the stability, the time required to operate, and the choice of an adequate mobile power supply unit are the major factors regarding to the design.

Research into the electronic control circuit using pre-set temperature values is on going. In this study, an electronic circuit was designed with the help of previous research. This device will be used in a smart garment with a heating capability in the near future.

REFERENCES

1. Mauch H.P., Nusko R., "New Possibilities With Special Conductive Yarns", Melliland International, pp.224-225, 3/2005.
2. Kukkonen K., Vuorela T., Rantanen J., "The Design and Implementation of Electrically Heated Clothing", IEEE Int. Symp.on Wearable Comp., Proceedings. pp.180-181, 2001.
3. ISO 9886 "Evaluation of thermal strain by physiological measurements"
4. <http://www.maxim-ic.com>; "DS18B20 Programmable Resolution 1-Wire Thermometer".
5. Yazici T., "Temperature Control Unit of an Electrically Heated Clothing", DEU Electrical and Electronics Dept., BSc Project, Advisor: O.Sahin, 2004.
6. <http://www.vdc-corp.com/components/reports/05/br05-09.html> "Smart Fabrics and Interactive Textiles: OEM and End-User Requirements, Preferences and Solution Analysis" Second Ed., 1/2006.
7. Xue, P., Park, K.H., Tao, X.M., Chen, W. Cheng, X.Y., "Electrically conductive yarns based on PVA/carbon nanotubes" Composite Structures Volume 78, Issue 2, April 2007, Pages 271-277
8. Vassiliadis, S., Provatidis, C., Prekas, C., Rangussi, M., "Novel Fabrics with Conductive Fibres", Intelligent Textile Structures - Application, Production & Testing International Workshop - Thessaloniki - Greece - 12-13.05.2005
9. Cottet, D., Grzyb, J., Kirstein, T., Tröster, G. "Electrical Characterization of Textile Transmission Lines", IEEE Transactions on Advanced Packaging, Vol. 26, No.2, pp.182-190, May 2003
10. Kayacan, O., Bulgun, E., Sahin, Ö., "Designing An Electronic Body Temperature Control Unit For Smart Garments" International Conference Futurotextiles, 23-24/11/2006 Lille, France

DESIGNING OF HIGH TECH TEXTILES AND ITS USES AND IMPOTANCE IN TODAY'S FASHION

N.ÖNLÜ, H. HALEÇELİ

Department of Textile, Faculty of Fine Arts, Dokuz Eylül University

ABSTRACT

Intelligent, multi-functional, electronic, etc high tech – produced textiles are those created by the fact that designers, historians, scientists and engineers have got together to discuss difficult and even impossible likelihoods of textiles, on the developmental process of which the third world nations have a great influence. In the consequence of inexpensive output in the third world, the textile industry felt obliged to look for radical remedies to increase prices/ costs of textile items in western nations and Japan, and electronics, computers, nanotechnology and biotechnology practices found uses in textiles.

With the technology adopted in both fiber and finished product by consumers and its increasing role in human life, high-tech progressed and equipped textiles have become the newest field of discovery in the high-tech revolution. High-tech textiles have turned out to be those items used not only in health, defense, safety, communication, etc. but garments in the fashion world as well.

High-tech items in the fashion world have had remarkable effects with their different appearances made of design, tactile and performance. Considerable developments of the 1990's technology created multi-functional futuristic clothes with beautiful and high performing features. In 1990's the fashion world, generally plain and classical silhouettes made of fabric with high-tech materials. The same tendency seems to continue in the 21st century, with fashion phenomenon depending not only on visual features such as color, style and aesthetical parameters but also on high-tech aspects of the cloth. Intelligent properties such as regulating body temperature, changing colors and ability to communicate cause fashion designers to particularly prefer this sort of cloths. For example; Angelina copper fibers are slightly different to a normal fiber as they are not round. 100 per cent copper metal is spun into yarns to impart many health benefits-anti-microbial, thermal regulating, anti-inflammatory, conductive, anti-static, anti-stress and healing properties. Copper can be blended with many other fibers to give added texture, malleability for pleated, crushed and crinkled finishes and rich colors(2). At the same time, this fabric can have been visual effects with aesthetic quality by design.

Therefore; textile and fashion designers attend to open new visions for the 21st fashion through tactile and sensory experiences involving a multitude of ideas and expressions.

Keywords: High Tech Textiles, Intelligent Textiles, Elektronical Textiles, Design, Textile and Fashion Designer, Aesthetic, Fashion

1. INTRODUCTION

High Tech textiles, called multi purpose, intelligent, electronic technical textiles are those designed to perform a particular function. They are manufactured in a way to serve given functions in any textile material, output and / or production method. Industrial textiles are occasionally named high performing high-tech, unconventional and engineering textiles as well (24).

High- tech textiles identified as subgroups of technical textiles by various classifications are products which can meet demands for high technique and quality and provide such functions as mechanical, thermal, electrical and durable features although man - made fibers such as polyester, polypropylene, nylon and viscose and technical textiles produced by glass, cotton and aramide all seem to be a newly progressed textile field, they have actually been used in various areas from natural fibers of cotton, linen and jute tenting, sailing, robe and sack for centuries now. In addition, natural textiles and webs or netting material are evidenced to have been used for road construction and stabilization of marshlands and swamps during and before Roman era centuries ago. The reason why technical textiles are adopted and related investments are involved in this field is that they are accepted as high added value- product and are of economic strategic importance in production. The very influence of the third world nations on the process of technical textiles can not be negligible. Because such countries produce items quite inexpensively, a series of remedies have been sought in order to increase their value price in textile business of western nations and Japan, with high performing textiles and electronic, computerized, nano-technology and bio- technology practiced being started thanks to technological break-through.

Although technical textiles are described as performance or function- based and used rather than aesthetics or non consumer and industrial implementations in a research work by David Rigby association, a British Counseling Firm which has been studying technical textiles for about twenty five years, and in the publication with the name of 'Textiles Terms and Definitions' by the Textile Institute as textile materials and items produced for technical and performing aspects rather than aesthetical or decorative features, high tech textiles have begun to be used in designing and fashion processes as well. Therefore surprising renovations aimed at fibers and fabrics in textile gradually close the present gap and distance between science and designing. For example, increase in uses of flexible materials to serve a given function is sought for a variety of particular requirements. Functional- purpose technological characteristics inherent in new textiles are employed to support various different practices ranging from textile to fashion designs in an aesthetical visional integrity.

Fashion designers who have conceived importance of textile materials since 1990's both create their on textiles and collaborate with other groups of textile designers, which enables them to produce specially designed clothes compatible with their approaches to garments. Simple fashion silhouettes on specifically- designed textiles appreciated and preferred by fashion designers allow them to present fabrics' own features as well.

New fashion collections which have been presented so far provide a perfect promotion for the current multi - functional high-tech textiles. Such a promotion has also started to change pessimistic thoughts of consumers about synthetic items.

High-tech materials have been seen as a contemporary alternative to natural clothes which invaded market in early 1990's. Since then, textiles and fashion designers and textile artists have turned to the sophisticated technology to create what they try to design. Designers and artist-designers are often strongly influenced by break-through and improvements in material and techniques (1)

Renovations created by materials to be used in textiles within the context of high technology provide both textile and fashion designers with new designing possibilities, thanks to which designers manage to produce extraordinary items by forcing through limits of renovation and creativeness. In so doing, they make use of both new production techniques other than renovations of materials and conventional techniques described as traditional ones. Artist designers who present out put- based works together with designers and exhibit them to society, passing on to production try to eliminate the borders between designing and crafts. By means of materials and production techniques.

With such attempts, textiles can become fashion and trade mark items whose added values increase due to high technology. The reason for this development is not only efforts of high- tech textiles produce by for different purposes but also variations in consumer behaviors and trends.

2. DESIGNING IN HIGH-TECH TEXTILES AND ITS USES AND IMPORTANCE IN TODAY'S FASHION

High-tech textiles which are intelligent multi functional and electronic and produced by the fact that so- called impossible processes have been created through the efforts of people from various disciplines such as science experts, engineers, designers, artists, historians and many more are not used for particular functions only. Although high- tech textiles are often described as those with given functions without aesthetical aims in their very definitions, they have come to be accepted as active sports wear and fashion commodities.

1990's witnessed remarkable progresses in textile technology, with both visually beautiful and highly performing futuristic fabrics being acquired in the fashion world. The fashion world has respected integrity and high- tech properties of the material, with plain and classical silhouettes resulting from the output produced with high-tech fibers by sophisticated technology. The purpose is not only to create aesthetical textiles and garments accompanied by fashion but produced multi purpose intelligent and protective items by combining aesthetics with real function as well. In garments, classical

clothes called traditional and high-tech materials were and are used in combination. The same trend continues in 21st century fashion, with fashion phenomenon not depending only on the model, color and aesthetically visual appearance of the fabric. High-tech features of the fabric can also have impact upon the fact that it becomes fashionable. Intelligent aspects such as abilities of the material to regulate body temperature, change colors and communicate cause fashion designers to choose them.

In emergence of smart fibers lie possibilities presented by technological break-throughs and changes the technology has brought about in society. One of the most important factors influencing proliferation of smart fibers is space research and defense-purpose technology (9).

Smart fibers and textiles are those which are capable of sensing light, heat, pressure, electromagnetic waves, sound and ultrasound waves, action and change in motion as well as creating protective and visual effects. Such textiles include an 'actuator' part to realize the response attached to the sensor capable of establishing warming thanks to simulating responses to light, heat and pressure which is unique to single cell creatures, in addition to the means provided by biomimetics technologies (18).

The concept of 'smart materials' is defined as the system that can sense and react to environmental conditions or stimuli by the developments in the field of computer, electronics and textiles. It has been able to integrate electronic component with textile structures to create very smart structures (12).

Beyond being and electronical circuit integration, intelligent textiles have the ability to conceive any effects or changes and respond to them accordingly. If a textile item can only conceive any effects or changes it is called passive intelligent textile product but if it can conceive and respond to any effects, it is named active intelligent textile item, examples of which are as follows: Car seats to wake up drivers who are about to sleep, bed sheets to sense cardiac rhythm, weaving material to change by ambient temperature, life shirt to follow cardiac pulse, inhalation, rate of pulse and body temperature round the clock as vital variables and inform those in charge of sanitation through uncabled communication network when necessary. (23)

Textile and fashion designers endeavour to draw a new horizon for the 21st century fashion through use of perceptual and tactile experiences filled with numerous ideas and expressions.

Unlike its known classical meaning, fashion is the tactic to convince masses of people to adopt it. That is a policy of marketing. Technological fashion however has radical influences on our experiences of mental and communicational activities, health and way of life. What is important and to be asked here is why science has impact on sensuality of aesthetics and fashion. Unintegrated part of daily life, fashion provides for a communication

technology constantly accessible together with garment items, and combines comfortable and aesthetical human body with technology.

Influence of technology allows designer - scientist generations to be born who will be able to utilize technology in new ways and fields. These designers prefer textile intelligence such as personal thermostat, remote control system and warming conduction to seasonal styles and color trends. Their designs are created in various researches in such a way that garments can detect and respond to heat, classify and fight bacteria, show ultra-violet rays, change colors and insulate or keep off dampness. (17).

What is made by designer- scientists is turned into aesthetical output in parallel to their functionality by textile and fashion designers. While designing a textile item, textile and fashion designers not only design its color, motif, design and form- based and aesthetically visual appearance but also start with raw material and complete it as a finished product in the process of designing textiles in the same way as in all productions. Therefore, today, designers work closely with different disciplinary workers as textile engineers .

Since 1990's fashion world has been closely interested in high-tech textiles and such fabrics used in collections by fashion designers. 1990's micro fibers, novel flexible fibers and fabric- included metallic nonwoven surfaces, foams, rubber, fiber optics and electronic textiles drew attention of textile and fashion designers. Textile designers produced distinctly appearing fabrics using such materials. Therefore, fashion designers provided garment forms for them with simple silhouettes without disturbing their visual integrity.

For instance metallic included in novel flexible fiber group are hard and rigid to work in structure. New technology has turned metals into flexible and workable fibers and they have become popular material and textile items, and looked for by textile and fashion designers.

Warp of the fabric called copper satin weave and copper / nylon stripes in 1990 by Irene Van Vilet, a German textile designer are composed of polyamide 6.6, and its weft of copper and polyamide. Lines woven with satin by flexible copper fibers contrast with those thickly woven with plain weave in polyamide fibers, with the surface seeming soft and shimmering (1).

Stainly steel, cotton, polyamide and polyurethane fibers were used in the fabric named 'stainly steel sparkler' by Nuno Company and designed by Reiko Sudo, a Japanese Designer in 1998. Stainly steel fibers were manufactured in 1996 to increase durability and strength of fiber products by a Japanese Tyre Company. Reiko Sudo used stainly steel fiber, cotton and polyamide in combination to create a flexible and soft fabric. Small quantity of polyurethane contained in the material allows a highly shimmering, jeweler - alike stretching metallic textile to be produced. (2).

In the same year, in the fabric called 'Copper Quadra' designed by Keiji Otani and produced by Nuno Company was used copper, cotton, polyamide and polyurethane fibers in combination to create a wonderful metallic surface. Polyurethane was employed to coat the copper fiber lest metal should turn to green and break apart due to corrosion (2).

The above- mentioned examples are typical processes in which high-tech fibers and traditional materials are used in combination. In 1990, high performance fibers were used to carry aesthetical visuality of the fiber to distinctive dimension and create simple garment silhouettes. In addition, multi functional, intelligent and electronic materials were introduced to fashion designing.

A garment prepared for 1995/96 autumn- winter collection by Hussein Callahan, a fashion designer has quite a simple silhouette. The garment was made up of Tyvek, a synthetic fiber called 'envelope paper' in USA. Unlike disposable garment composed of paper in 19960's, that of Callahan is washable, durable and resistant to many chemicals and developed as original protective fabric by DuPont (1).

Helmut Langan, an Austrian fashion designer created aesthetical-purpose and simple saluted garment compatible with its main function from a fabric produced for protective purposes in a way to decrease, absorb and reflect back harmful solar rays, which is part of the collections he formed for 1995/96 autumn-winter season. (1) (Picture 1)

Among the garments which André Courrèges produced for 1994/95 Autumn-Winter season, an overcoat is composed of a metallic textile e to protect the body from elements and manufactured for military purposes. On the sleeves and collar are knitted 19960's synthetics and jersey. (1) (Picture 2)

In March, 1995, Koji Hamai, a textile and fashion designer used a nonwoven surface produced by spread polyester coated with very thin steel in order to heat – insulate on the garment with futuristic appearance called 'Dry Fish'. The textile used is designed to protect those who wear it from uv-rays and electro magnetic waves and allow the skin to perspire as well (Picture 3). The cloth produced by the same designer in the same period called gradation (type I) was used a stretch a polyamide textile covered with very thin titanium on it. The garment permits the skin to perspire just because of the fabric's property, saving the body from UV- UR- Rays and electro magnetic waves simultaneously. It also provides insulation against hot and cold conditions. (1). Both garments designed to be used as overcoats are of simple silhouette which does not conceal appearance of the textiles used. Neither does Koji Hamai design such collections depending on changing fashion trends nor presents them on super garment models during specifically - held fashion shows. He prefers to exhibit his works in art galleries and museums in forms of arrangements- installations to public opinion.

Moreover it seems not impossible to encounter his garments in popular stores run by the system changing twice a year.

Like the above mentioned fashion designers, textile designers utilize performance – increasing, in other words intelligent fabrics such as crease-resistance to create different visions on textile surfaces, as well as producing pattern – focus aesthetical effects by means of using textile structures such color, motif, pattern as designing elements and weaving fabric structures modified to obtain distinctive features. For example, in 1995/96 Philippa Brock, a textile designer, employed wet- finishing process on the fabric she calls 'Formed I'. Cad/Cam (Computer Aided Design/Computer Aided Manufactured) patterned and woven on the jacquard loom as double layer fabric structure, the fabric has white cotton warp and Lycra – mixed linen weft (Picture 4). Wet- finishing process was used to swell the cotton fibers in the fabric to create a nice relief effect on the surface. In the same year wet-finishing process was applied to weaving fabric whose warp and weft are very thin lurex fiber wool creppé named 'Formed IV' by the designer in order to form a relief texture with the wool fibers swollen in it (1)

In 2000's research has rapidly been continuing in fields of high-tech material and textiles as well as in textile and fashion designing. The fabric, 'Wondering Lines-Red' designed and produced in 2001 by the textile designer, Sophie Roet and exhibited in the collection of Victoria Albert Museum, London has the warp made of phosphorescing fibers illuminating like phosphor including bright color silk and polyester / polyamide. Its weft is made up of polyamide mono filament compacted in a way to have wrinkled texture on it. When exposed to condensed light for about two minutes, the fabric absorbs it thanks to its phosphorescing property and illuminates in soft light and the absorbed light gradually fades away. (2)

Innovative fabrics with soft – sea effects developed by SCHOELLER TEXTIL AG were improved by stretch technology. (2).Such functional weaving textiles have an excellent ability to preserve their appearance as well as being soft light and comfortable. They allow for easy perspiration, protecting from wind and water. They do not disturb the skin when in contact with it; conversely feel soft and therefore quite available to create sports wear and contemporary silhouettes in fashion business.

Those developed by the same company were produced with phase-changing materials, called Schoeller-PCM, which all for this purpose include micro capsules and a prespecified temperature interval. (2). These materials can store additional heat when the temperatures both in the body and of external medium increase. When temperature drops, the presorted heat is set free. The overcoat in which Schoeller-PCM was not use gives the heat off. The garment made up of heat- preserving textile fibers can increase comfort which is enables very active people and sports men to have optimum performance in particular.

As in the above mentioned jacket, micro technology and sanitation high technology - based textiles constitute a potential research and development area as well. All developed within this context, new attractive, comfortable and performance - increasing textiles can improve the health of those who wear them. The micro capsules have minute spaces into which to add drugs, natural drugs, vitamins UV protectors, anti- bacterial / anti- microbial agents, insecticides, herbal oil, essences and perfumes which are all invisible to the naked eye and not radically efficient yet. Such micro capsules were actually developed for space technology and its associated uses. Microcapsule textiles have today, started to be utilized in fashion, lingerie and socks businesses. These garments form a rapidly - progressing field in textile sector in Japan. Japanese have recently begun to develop textiles having capsules stuffed with anti-aging and regenerative creams agents used in underwears in close contact with human skin. (2).

Rhovyl, a French Corp produced Rhovyl As fibers which contain an anti-bacterial agent. In this process, a bacteriostatic agent is placed into core of the fiber, preventing bacterial growth as long as bodily activity goes on. The same corp. developed six different high-tech fibers and fabrics, four of which were designed for garments.

Rhovyl'Coton : The properties of Rhovyl® fiber (thermal insulation, wicking of moisture, flame retardancy, resistance to chemical products, atmospheric and biological resistance) combined with those of cotton guarantee warmth, natural skin breath ability and extreme softness. Besides all clothes made of this fiber are machine washable, dry quickly in the open air and need no iron. Rhovyl'Coton® fiber is especially used in clothing. To satisfy growing needs of comfort and softness, products made of Rhovyl'Coton® can be worn as underwear or outerwear.

Rhovyl'Laine: The performances of Rhovyl® fiber (thermal insulation, wicking of moisture, flame redundancy, resistance to chemical products, atmospheric and biological resistance) combined with those of wool guarantee a perfect insulation against cold. Rhovyl'Laine® combines warmth with softness and provides a dry skin in every circumstance. Besides, products made of this fiber that does not felt, are machine washable, dry quickly and need no iron. Rhovyl'Laine® fiber is used in clothing (sweaters, underwear, lingerie and socks).

Rhovyl'On: Rhovyl'On® fiber provides a perfect insulation against cold and dry comfort. It gives you a feeling of well being. The skin breathes and keeps its natural balance. Moreover, Rhovyl'On® fiber is easy care. All clothes made of this fiber are machine washable, dry quickly and have long lasting properties. Rhovyl'On® is the fiber for warm underwear. Ideal for soft warmth in fleecy or napped knits as well as simple interlock.

Rhovyl'Up: The performances of Rhovyl'Up® fiber are obtained by combining Rhovyl® fiber with cellulose fibers or silk. The breathable fiber

ensures optimum evacuation of moisture and offers a dry comfort even during the effort. It provides an optimum heat regulation whatever the atmospheric conditions. Products made of this fiber are machine washable, dry quickly in the open air and need no iron. Rhovyl'Up[®] fiber was developed to meet the requirements of sportsmen. It is used in clothing (sports clothes, technical underwear, hosiery and polar knit) (34).

Of high-tech textiles, another one is electronic textiles, also called e-textiles. Direction of e-textile is towards intelligent textiles practices. Hussein Callahan is one of the designers to create first electronic remote- controlled garments. He uses high technology and high-tech materials able to establish dialogue between the wearing and the surrounding. According to him this way of thinking is the element to further the fashion even if new in the fashion world. McQuenn tends to think similarly. To him, it is new fabrics, engineering and technology which will lead fashion to further horizons (19)

Marks and Spencer, a British Corp introduced smart and fashionable man suits by Bagir Limited into market which have ipods, for fathers' day, 2007 within the context of intelligent fabrics sensitive to tactile effects. The jacket of the suit was tailored with ElekTex[®] tactile sensitive intelligent fabric by Eleksen. It has five - button electronic control panels. Those to wear Elektex are allowed to use and control the ipod's functions. The i pod is hidden in the pocket pouch securely, with an electronic control pad being checked by tactile effects such as off, on, sound and channel changing, which is all ideal and available for the professional bussiness world as a fashionable and functional suit.

Eleksen Corp collaborates with designers to create interactive garment fabrics as well as producing similar wearable technologies. ElekTex fabrics by Eleksen are a textile discovery which is light, flexible, durable, washable and tactile- sensitive. As well as ipod, Mobile Mp3 and cell phone can be attached to the suit. (25)

High-tech textiles are used popularly in active sports wear area. Because active sports wear items have coincided with fashion, high-tech produced sports wear has become integrated into fashion world. With such items being used both in daily living and in sports events. Channel and Hermes have turned out to be trade mark businesses in sports wears and garments in the same way as Nike and Adidas did so previously. Sports wearing sector passed from pitches and courts into streets years ago, becoming today's high fashion icon. The fact that sports wear has become fashionable results from popular figures in cinema, music and show worlds. For example, Madonna and Cameron Diaz wear Puma shirts and shoes, thereby influencing masses of people in what they choose which means that high-tech produced sport wears could reach out to consumers rapidly and become popular and adopted by them. In this way, French luxury giant PPR has acquired Puma, with Gucci and YSL becoming under the same corporate umbrella. Of course, high added value high-tech textiles have

influenced all these processes. Contribution of famous designers to promotion and adoption of high-tech items is inevitably great. For example, Japanese designer Yohji Yamamoto and Stella McCartney design for Adidas. Lacoste and Le Coq Sportif increase and develop their sports wear portfolios as sports wear business enters daily life.

It is women who prefer sports wear items most. With urban woman changing her way of life all over the world, she changed her look at fashion in a way to meet her practical requirements thanks to functionality caused by technological renovations. Women consider comfort, performance and durability in sports wear now, which implies that such items are produced by high technology (17).

3. CONCLUSION

The textiles developed by and equipped with high technology, with consumers adopting technology and its role increasing in life have become the newest discovery and exploration area of high technology revolution. High-tech produced fibers and textiles have turned out to be items used in garments in fashion world over time, in health defence, security and communication thanks to their functional properties as well. High-tech textiles in fashion have created a great impact with their appearance, tactility performance, intelligent properties and health care benefits.

Development of high-tech textiles in design and fashion world has been greatly accounted for by consumer behaviors, trends and expectations. Producers have realized this influence, cooperating with noted designers and trade-mark firms in order to have products adapted to consumers in a rapidly changing world.

The above-mentioned example of i-pod man suit marketed and introduced by Marks and Spencer seems a good process to show that technological textiles can be popular and adopted in connection with changing consumer behaviors and fashion. In Britain, Marks and Spencer and i Pod are among those indispensable of daily life. Eleksen producing the fabric, i Pod and Bagir combining both have three all chosen fashion and trade-mark to promote their commodities among clients. The fact that Marks and Spencer chose Fathers' Day to promote the item is a very element increasing its adoptability and popularity aimed at the sales policy. Ability of Adidas to introduce comfortable, keeping cool, body temperature-regulating high-tech textiles by means of famous fashion designers is an indication that such product are promoted and adopted among consumers through fashion, because renovations can reach out to masses of people via fashion rapidly.

Arzu Kaprol, a Turkish Fashion Designer designed a display concept and costumes for the Project 'Shape the Future' by Basf, one of the greatest chemical producers in the world, using technical textiles called fabrics of future. Basf has promoted and introduced Fixapret® AP, a new high

performance finishing product and anti-microbial fabrics which find a solution to the problem of ironing by means of Arzu Kaprol's designs among fabric producers and clothing sector, wholesalers to provide fabrics and consumers. Fibers of the fabric finished with the new finishing product can be washed and dried and later reversed back to a normal form, with ironing problem disappearing. As the product includes minimal levels of formaldehyde, it is friendly to environment. Its cellulose-based cotton and viscose microbial fabrics are protected from microbes, germs, fungi and yeasts by Fixapret® AP marketed together with Arch Chemicals. (36)

Finally, fashion will serve a different and interrelated functions involving high-tech textiles;

1-It will keep on considering choices of material in individual attempts based on designer and garment producing firms and come forth in textile and fashion world to save its up-to-dateness, with emerging firms stepping into trade market processes.

2- Technology - producing firms will promote their items in order to market their high added value products by means of fashion and thus, they will be adopted among consumers.

In both cases, fashion will function as a first level bridge to convey new technologies to clients. Designers can create much more interesting forms, functions and appearances thanks to the coercion between product and fashion designs (17)



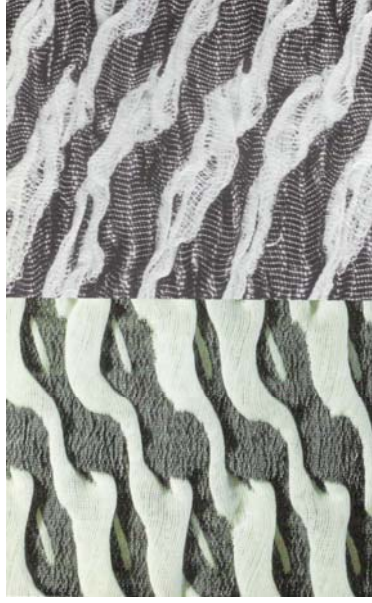
Picture 1. Helmut Lang 1995/1996 Autumn - Winter



Picture 2. André Courrèges 1994/1995 Autumn-Winter



Picture 3. Koji Hamai, 'Dry Fish' March 1995



Picture 4. Philippa Brock, 'Formed I' 1995/96

REFERENCES

1. Braddock, Sarah E. , O'Mahony, Marie; *Techno Textiles – Revolutionary Fabrics for Fashion and Design*, Thames & Hudson,1998,London, England
2. Braddock Sarah E. , O'Mahony Marie; *Techno Textiles 2– Revolutionary Fabrics for Fashion and Design*, Thames & Hudson,2005,London, England
3. Byrne, Chris, *Textiles And Clothing*, Mediatex, Technitex, UK,www.smarttextiles.co.uk/, Eriřim: 12 07 2007.
4. Casselle, Tania, *Sportswear Retailers Continue to Attain Excellent Track Record*, International Market News, July 1999, www.tdctrade.com/imn/imn169/feature3.htm, Eriřim: 17 07 2007
5. Colchester, Chloe, *The New Textiles*, Trends+Traditions,Thames&Hudson,Singapore,1996
6. Emek, Alpaslan, *Teknik Tekstiller Dünya Pazarı, Türkiye'nin Üretim ve İhraç İmkânları,Uzmanlık Tezi*, T.C. Başbakanlık Dış Ticaret Müsteşarlığı İhracatı Geliřtirme Etüd Merkezi,Arařtırma Geliřtirme Başkanlığı Sanayi Dairesi, Ankara, 2004,www.itkib.org. Eriřim: 17 07 2007
7. Giallorenzo, Antonio, *High-tech Textiles and Multi Functional Garments*, 15 October 2002,www.gzespace.com. , Eriřim: 10 08 2007.
8. Gough, Paul, *Wearable Electronics*, www.smarttextiles.co.uk/, Eriřim: 12 07 2007
9. Haleçeli,Havva;Önlü,Nesrin, 'Akıllı Liflerle üretilmiş Textillerin Tekstil Tasarımı Kapsamında Estetik ve Fonksiyonel Nitelikler Açısından İncelenmesi', II.International Technical Textiles Congress, 13-15 July 2005, Cooperation with Teknik Fuarcılık Ltd.řti.İstanbul,Turkey.
10. Hongu, Tatsuya, Philips, Glyn O., *New Fibers*, Wood Head Publishing Limited,1997, England.
11. Hooper, Alan, *Smart Materials- Advanced Materials*, QinetiQ, UK
12. ,www.smarttextiles.co.uk., Eriřim: 12 07 2007

13. Kayacan, Ozan; Bulgun, Yazgan, Ender, 'Akıllı Tekstiller ve Elektrik İleten Tekstil Esaslı Malzemeler', Tekstil ve Mühendis, Yıl:12, Sayı:58, TMMOB Tekstil Mühendisleri Odası,2005,İstanbul, syf:29-34.
14. Lauter, Josef, Fashion Meets Health-bio medical clothes for health enhancement, 15
15. October 2002, www.smarttextiles.co.uk, Erişim:10 08 2007.
16. Malik, Tanveer; Parmar, Shivendra, Value Addition to Textiles, www.fibre2fashion.com, Erişim: 11 07 2007.
17. Miller, Edward, Textiles/Properties, Behaviour, BT Batsford Ltd.,London, 1995.
18. McQuaid, Matilda, Extreme Textiles- Designing for High Performance, Thames& Hudson, National Design Museum, 2005, NewYork.
19. Quinn, Bradley, Techno Fashion, Berg, ,2002, USA.
20. Tao,Xiaoming,Smart Fibers,Fabric and Clothing,Textile Institute,CRC Press,New York,2001.
21. 21.Türkant, Berna, Uluslararası Konferans, Teknik Tekstiller-Yenilikçi Yaklaşım, 24-25 Nisan 2006, Manchester/ İngiltere, Konferans Raporu,AR&GE ve Mevzuat Şubesi, 02.05.2006, İstanbul, www.itkib.org, erişim:12 07 2007
22. Türkant, Berna, Akalın, Mehmet,Uluslararası Konferans, 'Sanayi ve Moda İçin Nano Teknolojiler ve Akıllı Tekstiller, 11-12 Ekim 2006, Londra / İngiltere, Konferans Raporu,AR&GE ve Mevzuat Şubesi, 02.05.2006, İstanbul, www.itkib.org, erişim:12 07 2007
23. Wagner, Philippa, Innovation: materials, WGSN,22.05.07,www.just-style.com, Erişim:4 08 2007
24. Yıldırım, Kenan; Aydın, Nurcan; Çelikkbilek, Aylin; Güçer, Şeref, 'Kaliteli Yaşam İçin Teknik Tekstiller ve Kullanım Alanları',Tübitak - Bursa Test ve Analiz Laboratuvarı (Butal) , www.bilesim.com.tr, Erişim: 10 08 2007
25. Haftanın konusu,www.teknoport.com.tr/, Erişim: 06 08 2007
26. Innovations in Lubricating Technology Natural and Synthetic Fibres, Weaving high-tech fabrics of the future, www.news.com, Erişim: 17 07 2007
27. Marks & Spencer to launch iPod suits for Fathers' Day,www.eleksen.com, 06 08 2007
28. Newscientist-Smart Textiles, 24 February, 2001, www.newscientist.com, Erişim:14 07 2007
29. Scientist Beings Smart Second Skin Dress,www.smartsecondskin.com/main/smartsecondskindress.htm,Erişim: 3 07 2007
30. Sun Protective Clothing, www.exofficio.com/ , Erişim:18 08 2007
31. Sportswear Retailers Continue To Attain Excellent Track Record, International Market News July 1999 ,www.tdctrade.com/ , 18 08 2007
32. Teknik Tekstiller Üzerine Genel ve Güncel Bilgiler, İTKİB Genel Sekreterliği AR&GE ve Mevzuat Şubesi, Mart 2006, İstanbul. www.itkib.org, erişim:12 07 2007
33. Teknik tekstillerin Tanımı ve Gelişimi, www.tekstilteknik.com, Erişim: 11 07 2007
34. www.rhovly.fr, Erişim: 14 08 2007
35. www.materialconnexion.com, Erişim: 14 08 2007
36. www.just-style.com, Erişim:4 08 2007
37. www.textilesintelligence.com/tisttm/ Erişim:3 7 200
38. www.teknikfuarcilik.com/tr/texonline.asp?konu=sayfa&sayfa=33,Erişim:15 08 2007

DESIGNING DIRECTIONALLY ORIENTED WEFT KNITTED STRUCTURES FOR ADVANCED FRP

M. DE ARAUJO, R. FANGUEIRO, F. SOUTINHO

Fibrous Materials Research Group

School of Engineering, University of Minho

ABSTRACT

The application of fibrous materials in the reinforcement of matrixes made from polymers is a very interesting field both from the research and industrial point of view. The importance of these materials, known as FRP (fibre reinforced plastics), is becoming more and more prominent in the replacement of monolithic materials such as metals. In this case, composite materials present various advantages like high specific mechanical properties, due to the low weight, and good heat and corrosion resistance.

The use of weft-knitted structures in composite reinforcements is limited due to their poor mechanical properties. The tensile behaviour of weft-knitted fabrics is strongly restricted by its loop formation. During the application of a tensile load, the loops change their shape in order to accommodate the applied load. In this part of the deformation small loads lead to large displacements, which is the typical behaviour of a low stiffness material. When this type of structure is used as reinforcement, the mechanical properties of the composite material may be considerably hindered, as the resin may bare the initial load and fail before the load is transferred to the reinforcing fibres. However, weft-knitting is the most suitable technique for the production of 3D fabrics for complex shape composite reinforcements and so their stiffness must be improved. This paper reports on the progress that has been made to improving the modulus of elasticity of glass fibre fleece structures in the coursewise direction, in order to enable the production of tubular pre-forms for composite materials with adequate stiffness. The technology developed competes with filament winding and has the possibility of creating complex shapes.

1 INTRODUCTION

The application of fibrous materials in the reinforcement of matrixes made from polymers is a very interesting field both from the research and industrial point of view. The importance of these materials, known as composite materials, is becoming more and more important in the replacement of monolithic materials such as metals. In this case, composite materials present various advantages like high specific mechanical properties, due to the low weight, and good heat and corrosion resistance. The need to design materials with different properties in each direction and to reinforce the thickness direction, in order to overcome delamination, turned textile technologies very attractive for the production of composite reinforcements. The flat knitting technology is mostly suitable to produce complex shaped fabrics and sandwich fabrics [1, 2, 3, 4]. The use of weft-knitted fabrics in composite reinforcements is limited due to their poor mechanical properties

[5, 6, 7]. The tensile behaviour of weft-knitted fabrics is strongly restricted by its loop formation. During the application of a tensile load, the loops change their shape in order to accommodate the applied load. In this part of the deformation small loads lead to large displacements, which is the typical behaviour of a low stiffness material. However, due to this behaviour, knitted fabrics are particularly suitable for applications where resistance to impact and absorption of energy are the main requirements. This paper describes the development work undertaken in order to improving the stiffness in the coursewise direction of fleece glass fibre fabrics to be used in 3D tubular preforms for technical applications. The effects of fibre orientation are analysed by comparing the tensile testing results obtained for different types of fleece structures. The fleece structure is chosen for the current work, as it uses less knitting yarn per unit area and may be manufactured in 3D complex shapes in electronic flat knitting machines with the obvious advantages of versatility. For some applications, the knitting yarn works as a scaffold to hold the laid-in or the pile yarn, which is the reinforcing yarn, in the adequate position, for increasing stiffness in the coursewise direction [5].

2 EXPERIMENTAL

2.1 Materials

The present work has the objective of studying the load-elongation behaviour of various weft-knitted fleece fabrics in the coursewise direction, so that the tensile properties and particularly the initial modulus may be improved. The variations introduced to the samples consisted in varying the fleece yarn linear density, altering the course density and altering the knitted structure (tuck and miss sequence).

Figure 1 illustrates an example of one of the modified 1X3 glass fibre fleece structures developed.

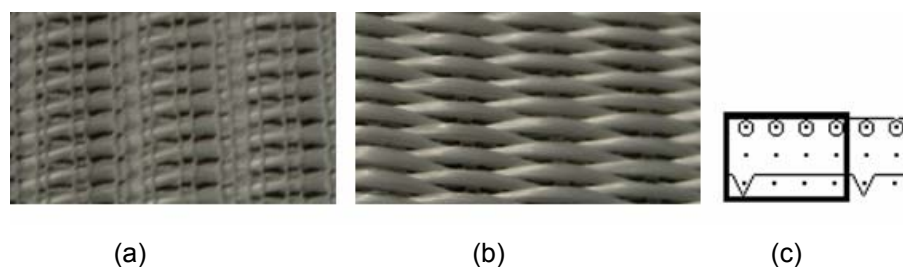


Figure 1. Modified Fleece (1 X 3 structure) (sample A7)

(a) Technical face (b) Technical back (c) Diagram

Table I shows the specifications of the samples developed for this work. The ground yarn used was in all cases a 15 Tex continuous multifilament polyamide yarn. The fleece yarn was a continuous multifilament glass fibre yarn of varying linear density (204, 408 and 544 Tex).

Table 1.Specifications of the sample materials

Fleece structure	Tex _f (glass fibre fleece yarn)	l_g (cm)	l_f (cm)	c (couses/cm)	Sample code
1 X 3	204	0.45	0.17	14	A1
		0.48	0.20	10	A2
		0.60	0.20	08	A3
	408	0.44	0.20	13	A4
		0.51	0.19	09	A5
		0.58	0.20	07	A6
	544	0.48	0.22	12	A7
		0.50	0.24	08	A8
		0.61	0.24	06	A9
1 X 4	204	0.37	0.18	15	B1
		0.39	0.21	11	B2
		0.44	0.20	07	B3
	408	0.55	0.25	13	B4
		0.59	0.24	10	B5
		0.59	0.25	07	B6
	544	0.58	0.22	13	B7
		0.58	0.21	10	B8
		0.60	0.22	07	B9
1 X 5	204	0.29	0.20	14	C1
		0.33	0.20	11	C2
		0.35	0.22	10	C3
	408	0.37	0.21	15	C4
		0.39	0.23	10	C5
		0.40	0.23	07	C6
	544	0.38	0.23	14	C7
		0.42	0.23	10	C8
		0.45	0.23	06	C9

Legend:

1 X 3 fleece structure = 1 tuck/ 3 miss (float)

1 X 4 fleece structure = 1 tuck/ 4 miss (float)

1 X 5 fleece structure = 1 tuck/ 5 miss (float)

l_g = average loop length of the ground yarn (cm)

l_f = average loop length of the fleece yarn (cm)

c = course density (courses per cm)

Tex_f = linear density of the fleece yarn

All samples were produced in a 10 gauge Stoll CMS 320 TC electronic V-bed knitting machine equipped with IRO NOVA storage yarn feeders.

2.2 Test Methods

2.2.1 Structural Parameters

After knitting all samples were dry relaxed by laying them flat on a polished surface in a standard atmosphere for 48 hours before testing. The average course density was measure with the aid of a counting glass. The average loop length was measured with the aid of the HATRA course length tester.

2.2.2 Tensile Properties

Tensile testing of the knitted structures was conducted in the coursewise direction. Ten samples of each structure were prepared and tested using a HOUSFIELD H10KS universal tensile tester. The Grab method was used. The effective width of the specimens was the width of the jaws which was 2.5 cm. The effective length of the specimens was the distance between jaws which was 10 cm. The initial pre-tension was set at 25 N. The test was conducted at a cross-head speed of 5 mm/min

The load-elongation curves were registered for all samples tested.

2.3 Results and Discussion

2.3.1 Structural Parameters

The average fabrics structural parameters measured are shown in Table I.

There are limitations to what it is possible to knit in a knitting machine, especially, when difficult to knit yarns, such as glass fibre yarns, are used. Therefore, great care was taken to avoid breaking any filaments during knitting. This was achieved by careful setting up of the knitting machine for any particular sample produced and using storage yarn feeders. For any particular structure and fleece yarn tex, as the loop length of the ground yarn (l_g) decreases the course density (c) increases and therefore the course spacing ($1/c$) decreases. This is to be expected as the fabric becomes tighter. There are practical limitations to this as very tight fabrics become difficult to knit because of the size of the needles being too large relatively to the loop length and open fabrics become unstable and difficult to handle. For any particular structure and fleece yarn tex, there is no clear relationship between the loop length of the ground yarn (l_g) and that of the fleece yarn (l_f). This, seems reasonable, as the latter is more related to machine gauge and fleece yarn in-put tension.

2.3.2 Tensile properties

The results for the tensile properties of the samples tested are shown in Table II.

Table 2. Tensile properties of the fabric samples in the coursewise direction (Grab method)

Sample code	Fibre mass/cm (g)	Breaking load (N)	Breaking Load per Course (N)	Strain at Break	E (kN)
A1	0.286	408.0	11.66	0.65	34.53
A2	0.204	351.6	14.06	0.43	6.85
A3	0.163	319.2	15.96	0.99	0.68
A4	0.530	501.0	15.42	0.48	123.71
A5	0.367	437.0	19.42	0.60	42.68
A6	0.286	389.6	22.26	0.79	23.86
A7	0.653	677.0	22.57	0.28	143.48
A8	0.435	478.0	23.90	0.77	68.53
A9	0.326	404.0	26.93	1.16	30.56
B1	0.306	533.0	14.21	0.89	39.59
B2	0.224	389.6	14.17	0.73	8.92
B3	0.143	313.6	15.68	0.78	3.09
B4	0.530	506.0	13.49	0.40	87.53
B5	0.408	516.0	18.76	1.06	18.76
B6	0.286	221.0	12.63	0.60	14.41
B7	0.707	569.0	17.51	0.25	147.20
B8	0.544	494.0	19.76	0.77	37.31
B9	0.381	671.0	38.34	1.47	12.58
C1	0.286	517.0	14.77	0.68	49.67
C2	0.224	359.6	13.08	0.43	18.33
C3	0.204	340.8	13.63	0.70	0.70
C4	0.612	507.0	13.52	0.69	21.90
C5	0.408	444.5	17.78	0.59	18.95
C6	0.286	474.0	27.09	1.02	13.00
C7	0.762	728.0	20.80	0.58	134.57
C8	0.544	435.0	17.40	0.67	35.81
C9	0.326	336.8	22.45	0.44	44.06

Legend:

Breaking load per course (N) = breaking load/ 2.5c

strain = elongation at break/ initial length

E (kN) = Modulus of elasticity = δ/ϵ measured at the initial stage (straight part of the curve)

Fibre mass/ cm (g) = $c \text{ Tex}_f 10^{-4}$ = estimated mass of load bearing fibres in the coursewise direction per cm of fabric width

The initial pre-tension of 25N was used to assure that the fleece yarn was kept straight from the beginning of testing. The ground yarn loop length (l_g) has a considerable effect on the tensile properties of the fabrics as can be shown in the example of Fig. 2. For each structure, a shorter value of l_g increases the initial modulus of the fabrics. With the exceptions of fabrics B5, B9 and C6, this is also the trend for the relationship between l_g and the breaking load. This can be explained by an increase in course density, thus resulting in a greater number of fleece yarns bearing the load. There is a general trend for the breaking load per course to increase as l_g increases. This is possibly due to the individual fleece yarns being in a straighter configuration in a looser fabric.

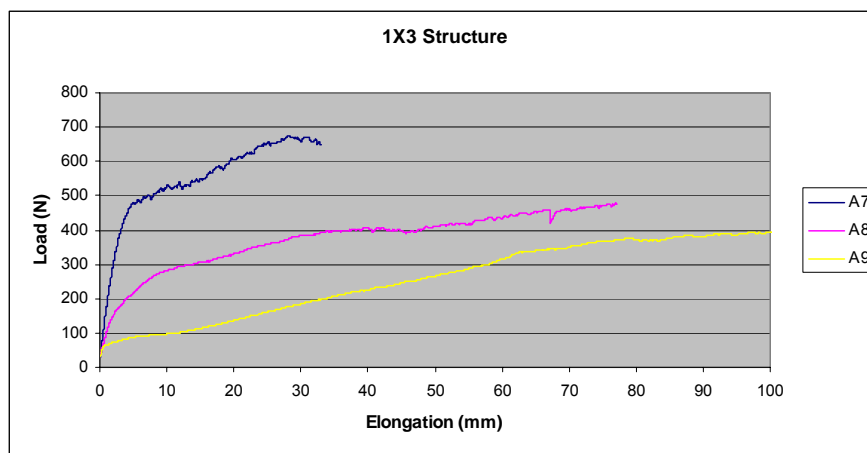


Figure 2. Effect of ground yarn loop length (l_g) and course density (c) on the load-extension curve for 1 x 3 structures with 544 tex fleece yarn

The fleece yarn linear density has a considerable effect on the tensile properties of the fabrics as can be seen in the example of Fig. 3. For each structure there is a general increase of breaking load, breaking load per course and initial modulus as the yarn Tex increases. This may be due to a greater number of fibres being available to bare the load as yarn tex increases.

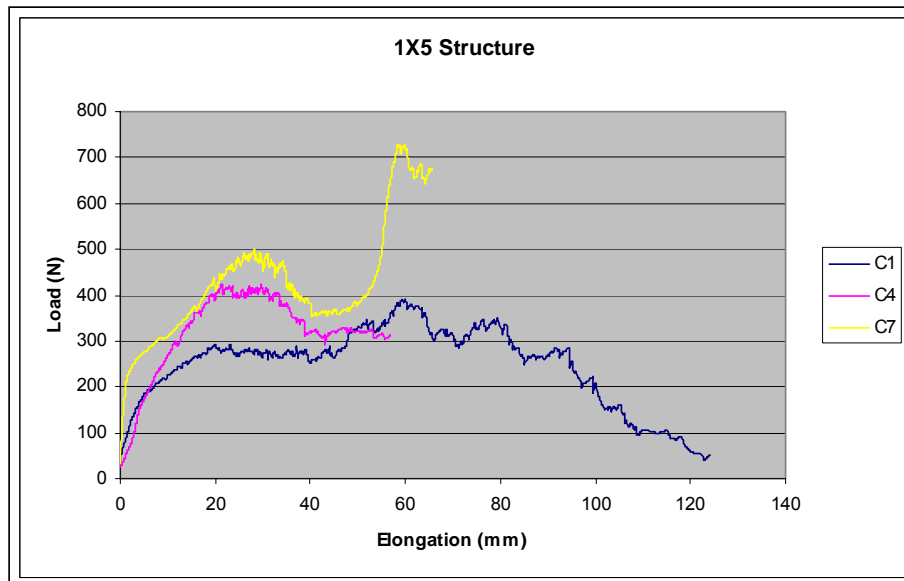


Figure 3. Effect of fleece yarn linear density on the load-extension curve for 1 x 5 structures

The effect of the float length on the tensile properties of the fabrics does not seem to be an important one as can be shown in the example of Fig. 4. This may be due to the fact that it makes no difference to the amount and alignment of the fibres that bare the load.

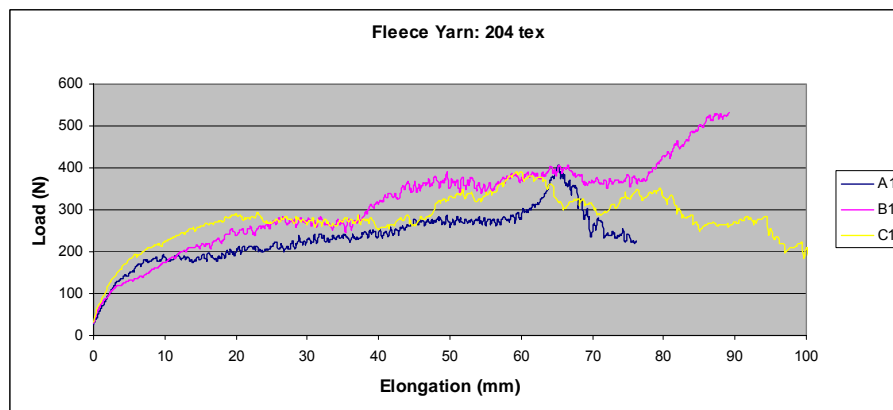


Figure 4. Effect of different float lengths on the load-extension curve of structures produced with the 204 tex fleece yarn

Overall, fabrics A7, B7 and C7, which have different float lengths, exhibit a higher breaking load, a lower strain at break and a higher initial modulus and so are considered the best performers. This is essentially due to a shorter loop length of the ground yarn, increased course density and the use of a heavier yarn as fleece, as can be shown in Fig. 5.

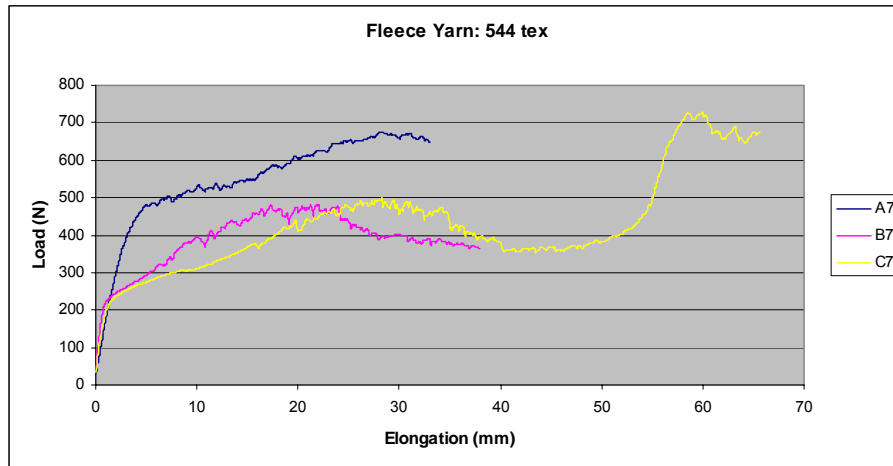


Figure 5. Effect of fibre mass/ cm on the load-extension curve of structures produced with the 544 tex fleece yarn

It seems that, if the properties of the fleece yarn component filaments are the same, the important parameter to consider is the fleece fibre mass/ cm available to bear the load in the particular direction. In fact, the correlation coefficient between the fibre mass/cm and the fabrics breaking load is 0.75 and the one between the fibre mass/cm and the fabrics initial modulus is 0.80, thus revealing a good positive relationship between the two sets of properties.

3 CONCLUSIONS

Directionally oriented weft knitted structures were developed and the effect of structural parameters on their tensile properties was assessed. The fleece fibre mass/ cm, which is the combined effect of ground yarn loop length and fleece yarn linear density, are the most important parameters affecting the tensile properties. As l_g decreases and the fleece yarn linear density increases there is a considerable improvement in breaking load and initial modulus in the coursewise direction. The length of the float in the structure does not seem to influence the tensile properties of these fabrics. It was possible to develop a set of fabrics with improved properties in the coursewise direction and appropriate to be used in FRP hoses and tubes as the reinforcing material.

ACKNOWLEDGEMENTS

The authors want to acknowledge the Agência de Inovação (Portugal) for providing research funds under the POCTI program (PRETUBE project) and the University of Minho, Portugal for providing research facilities.

REFERENCES

1. H. Hong, A.A. Filho, R. Figueiro and M. D. de Araujo, Flat Knitting
2. Machines for the Production of 3D Shaped Fabrics for Technical Applications, Melliand Textilberichte English, Germany, 1+2/ 1996, p. E13-E14. (English and German)
3. M.D. de Araujo, H. Hong and R. Figueiro, Production of 3D Shaped
4. Reinforcing Fabrics by Knitting to Shape, Melliand Textilberichte English, Germany, 5/1996, p.E66-E67.(English and German)
5. M. D. de Araújo, R. Figueiro, O. Ciobanu, H.Hong, L. Ciobanu, Weft-knitting Fabric Design for Technical Applications, Proceedings of 30th Textile Research Symposium at Mount Fuji (Ed. S. Kawabata), Shizuoka, Japan, 30 July-1 August, 2001
6. H. Cebulla, O. Diestel, P. Offermann, Modeling and Production of Fully Fashioned Biaxial Weft Knitted Fabrics, Proceedings of TECNITEX 2001: 1st AUTEX Conference (Ed. M. de Araujo), Povia de Varzim, Portugal, 29-30 June, 2001
7. M. D. de Araújo, H. Hong and R. Figueiro, "Improving the Mechanical Properties of Composite Materials Reinforced by Weft-knitted fabrics", October, Proceedings of Textile Technology Forum/ IFAI, Charlotte, USA, 2002.
8. M. D. de Araújo, R. Figueiro and H. Hong, Modelling and Simulation of the Mechanical Behaviour of Weft- Knitted Fabrics for Technical Applications, Part I: General considerations and experimental analyses, AUTEX Research Journal, www.autexrj.org, Vol. 3, No. 3, September 2003
9. M. D. de Araújo, R. Figueiro, H. Hong, "The Mechanical Behaviour of Weft-knitted Fabrics for Technical Applications", Proceedings of 2004 International Textile Congress: Technical Textiles: World Market and Future Prospects (Ed. A. Naik), UPC, Tarrassa, Spain, 18 – 20 October, 2004

MODELING FIBROUS REINFORCEMENTS AND COMPOSITES USING FIBER BUNDLE CELLS

L.M. VAS¹, P. TAMAS²

¹Department of Polymer Engineering, Budapest University of Technology and Economics

²Department of Information Engineering, Budapest University of Technology and Economics

ABSTRACT

This paper presents a statistical modeling method based on some earlier results and the widely used averaging techniques using some idealized fiber bundle cells as model elements. The expected mechanical response of the fiber bundle cells including the damage process can be calculated. For phenomenological applications a modeling software FiberSpace has been elaborated. To demonstrate its applicability to both phenomenological and structural-mechanical modeling some results obtained for real fibrous structures and composites subjected to mechanical load are presented and compared to the measurements.

Key Words: Fiber bundle, statistical modeling, fibrous reinforcement, polymer composite

1. INTRODUCTION

Reinforcements of polymer composites such as rovings, fiber mats, fleeces, fabrics, and braided or knitted structures [1] are important kinds of technical textiles. In case of short fiber reinforced composites reinforcement can be considered as a fiber flow [2]. Composites are a kind of uniting of fibrous reinforcement and embedding matrix material where the good adhesion between fibers and matrix provides outstanding mechanical properties by means of suitable cooperation [1]. According to experiences the so called fiber bundles, representing statistical geometrical and mechanical properties of the structure, play an important role in the mechanical behaviour of fibrous structures [2]. Fiber bundles are created e.g. by fibers between two bonds in a fabric or fibers intersecting a cross section in a roving, a yarn, or a fiber flow. Fiber bundles, above all the so called classic type, have been studied since the first third of the last century [3] and among others the results of Weibull [3-5], Peirce [3-5], Daniels [3-5], Harlow and Phoenix [4], and Phoenix [5,6] focusing mainly on the estimation of the strength probability have proved to be of fundamental importance. Based on some earlier results [7-12] and the widely used averaging techniques [1,13-16] a modeling method and software has been developed using some idealized fiber bundle cells as model elements. To demonstrate its applicability to both phenomenological and structural-mechanical modeling some results obtained for real fibrous structures and composites are presented.

2. MODELING METHOD BASED ON FIBER BUNDLE CELLS

Idealized fiber bundles as model elements are used for modeling in themselves or in form of a network.

2.1 Idealized Fiber Bundle Cells

Fibers in a fibrous structure can be classified according to their geometry (shape, position) and mechanical behaviour (strain state, gripping). These fiber classes are called fiber bundle cells (FBCs) (Figure 1). Fibers of these FBCs are supposed to be perfectly flexible, linearly elastic and to break at a random strain (ε_S). They are straight in the E-bundle, loose ($\varepsilon_o < 0$) or pretensioned ($\varepsilon_o > 0$) in the EH-bundle, and oblique (fiber angle $\alpha \neq 0$) in the ET-bundle, and gripped ideally in these cases. Fibers in the ES-bundle are straight but they may slip out of their grip at a strain level ($\varepsilon_b < \varepsilon_S$) or create fiber-chains with slipping bonds. Both the shape, position, and strength parameters of fibers are assumed to be independent stochastic variables.

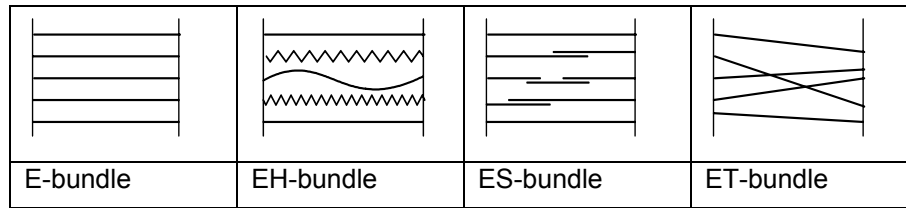


Figure 1. Structural scheme of the idealized fiber bundle cells

Considering a constant rate elongation tensile test the tensile force ($F(u)$) creates a stochastic process as a function of the bundle strain (u). Being aware of the relationship between the bundle (u) and fiber strains (ε), the expected value of the tensile force of the FBCs ($E(F) = \bar{F}$) could be calculated as a sum of the single fiber forces using the suitable formulas developed [7, 12]. Dividing the expected value by the mean breaking force of fibers, the normalized tensile force of bundle is computed as follows:

$$0 < FH(z) = \bar{F}(z) / n\bar{F}_S \leq 1, \quad z = u / \varepsilon_S \quad (1)$$

where n and \bar{F}_S are the number and the mean breaking force of fibers, respectively, and z is the bundle strain normalized by the mean breaking strain of fibers. Figure 2 shows the graphic relationship between the strain of individual fibers and the bundle as well as in Figure 3 the typical normalized expected value processes calculated at different parameter values are plotted for the FBCs. In case of ES-bundle ε_{bL} is the relative slippage way of fibers.

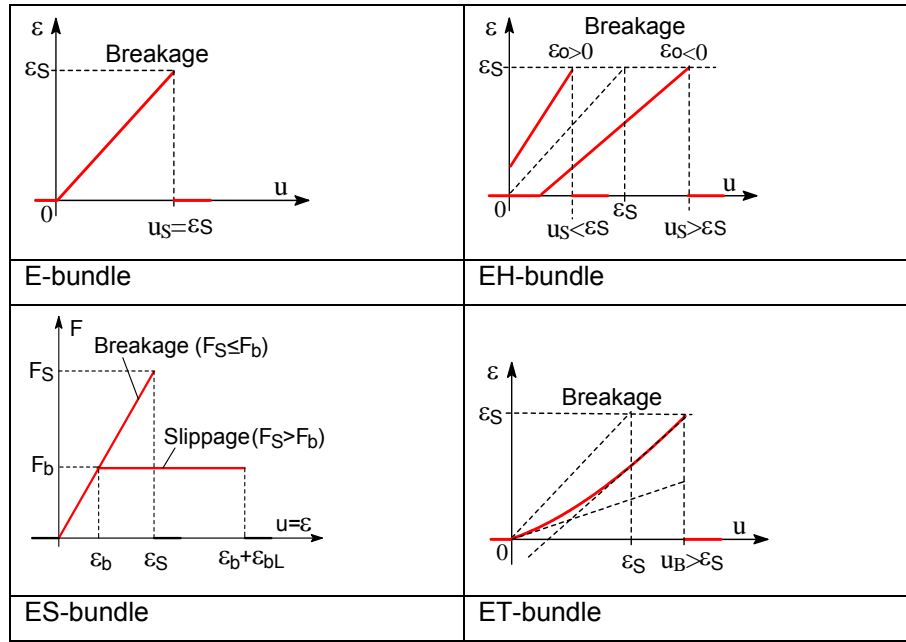


Figure 2. Fiber strain versus bundle strain curves of the FBCs

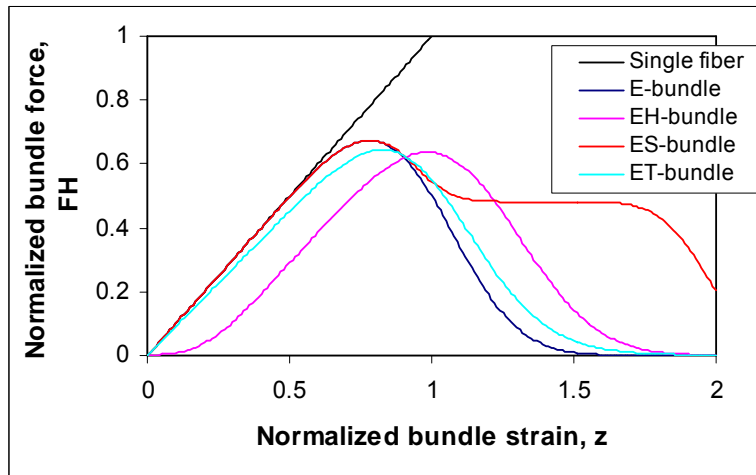


Figure 3. Expected value of typical normalized force-strain curves of the FBCs: E ($\bar{\epsilon}_S = 0.1$, $\sigma_{eS}/\bar{\epsilon}_S = 0.2$), EH ($\bar{\epsilon}_o/\bar{\epsilon}_S = -0.2$; $\sigma_{eo}/\bar{\epsilon}_S = 0.1$), ES ($\bar{\epsilon}_b/\bar{\epsilon}_S = 1$, $\sigma_{eb}/\bar{\epsilon}_S = 0.1$, $\bar{\epsilon}_{bL}/\bar{\epsilon}_S = 1$, $\sigma_{ebL}/\bar{\epsilon}_S = 0.1$), and ET-bundle ($\tan \alpha = 0.2$, $\sigma_{\tan \alpha} = 0.3$)

For the numerical calculations all random parameters were assumed to be of normal distribution.

2.2 Modeling Method

From Figures 3 it is obvious that the FBCs can model rather complicated mechanical behaviours such as the initial convex part caused by crimped fibers (EH-bundle) or the slippages generated plateau beyond the peak (ES-bundle) even if they are used in themselves. In general, however, several types of FBCs are needed to model the response of the structure tested. In most cases the parallel connected FBCs (Figure 4.a) called composite bundle provide a suitable model and the resultant expected value process is calculated as the weighted sum of the single FBC responses where the weights are the fiber number ratios. In case the size effect such as the gauge length on strength are examined serial connection of the same type of FBCs is suitable to use (Figure 4.b).

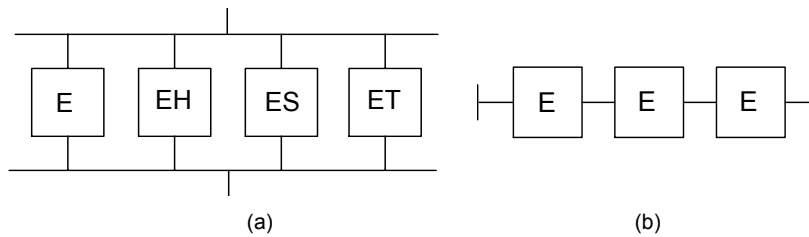


Figure 4. (a) Parallel and (b) serial connections of FBCs

2.3 Modeling Software

A program package named FiberSpace has been developed in Delphi Code in order to assist the construction of a suitable FBC model for a given material or studying the behavior of model structures. The menu driven FiberSpace works together with Visual Basic supported MS Excel (Figure 5). By Excel measured data can be received and converted as well as function procedures can be developed utilizing its graphic and other possibilities.

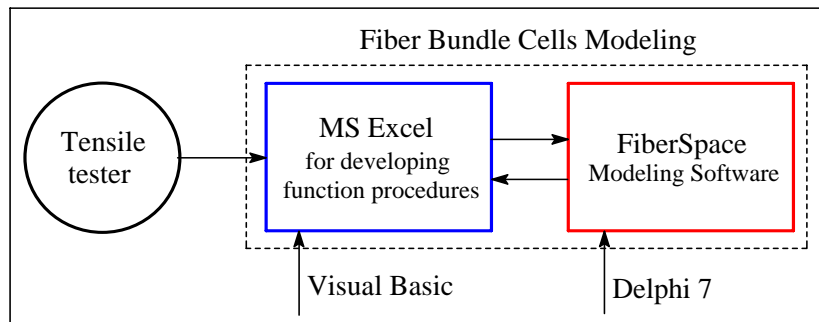


Figure 5. System of measuring and modeling real fibrous structures

3. MODELING FIBROUS REINFORCEMENTS AND COMPOSITES

FBCs can be used for creating phenomenological or structural-mechanical models. The applicability of the fiber-bundle-cells method and the elaborated modeling program is demonstrated by modeling the loading and damage process of different fibrous structures and composites during tensile or flexural test and comparing them with the measurements.

3.1 Phenomenological Modeling Of Fibrous Structures

In this case the best approximation of the measured load-deformation curve is determined as a response of a model composite bundle using a fitting procedure based on the least squares method. Software FiberSpace makes it possible to describe the structure of the fibrous material in terms of FBCs and their weights on the basis of a tensile test, moreover to estimate the mean single fiber breaking strain and load as fitted normalizing factors more precisely than calculating from the load peak directly. Figure 6 shows the normalized measured and modeled tensile load-elongation (gauge length $l_o=30$ mm) relationships of Vertan EC13 glass fiber roving (140x18=2520 tex, $n_f=6750$ fibers). For modeling a single ES-bundle was used.

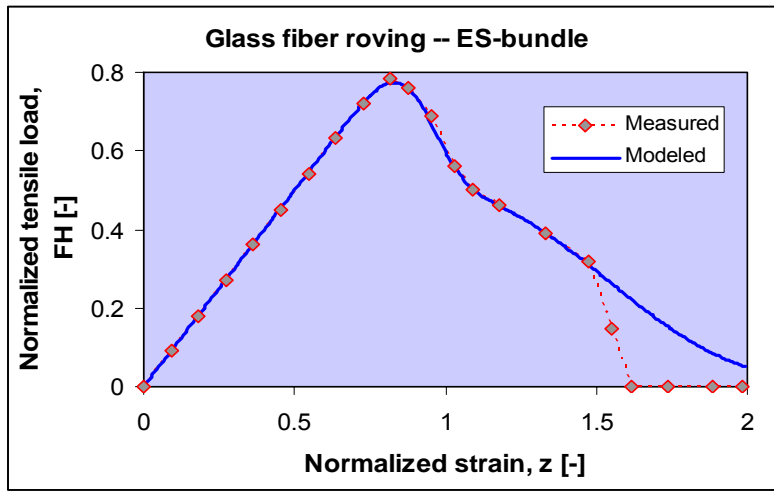


Figure 6. Measured and modeled tensile load-strain curves of a fiber glass roving

The load and elongation values of the measured load peak were $F_{RS}=740$ N and $\Delta l_{RS}=0.79$ mm, respectively, from which calculated strength values of the single fibers could be calculated:

$$\bar{F}_{S1} = F_{RS} / n_f \approx 109.6 \text{ mN}, \quad \bar{\varepsilon}_{S1} = \Delta l_{RS} / l_o \approx 2.63\% \quad (3)$$

The peak values of the normalized modeled curve were $FH(z^*)=78.6\%$, $z^*=81.8\%$. Thus corrected fiber strength data can be obtained as follows:

$$\bar{F}_{S2} = \bar{F}_{S1} / FH(z^*) \approx 139 \text{ mN}, \quad \bar{\varepsilon}_{S2} = \bar{\varepsilon}_{S1} / z^* \approx 3.22\% \quad (4)$$

In Figure 7 the normalized result of a so called flat bundle test of cotton fibers (UHM=27.2 mm, mean linear density of cotton fibers $q_f=1.9$ dtex [17]) measured by a SpinLab 900 HVI Fibrograph with the gauge length of $l_0=3.175$ mm is depicted. A composite bundle fitted and constructed from E-, EH-, and ES-bundles with the respective weights 9.7%, 71.8%, and 18.5% provides a good model to describe the whole variation of the tensile force including the initial part of small slope and the plateau of the last part (Figure 9). The mean squared relative error of fitting is 0.34%.

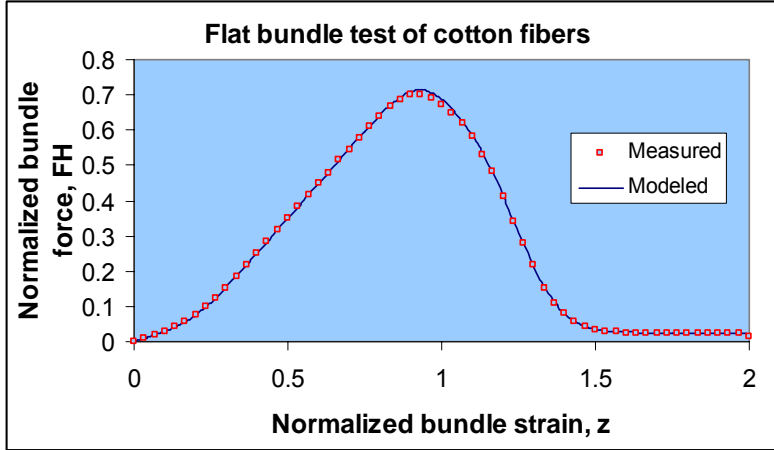


Figure 7. Measured and modeled tensile load-strain curves of a flat bundle of cotton fibers

The load and elongation values of the measured load peak were $F_{BS}=94.8$ N and $\Delta l_{BS}=0.23$ mm, respectively, where the bundle strain was $\varepsilon_{BS}=7.24\%$. The peak values of the normalized modeled curve came about $FH(z^*)=70.2\%$, $z^*=92\%$. Hence the strength data of single fibers can be estimated as follows:

$$\bar{F}_{BS}^* = F_{BS} / FH(z^*) \approx 135.1 \text{ N}, \quad \bar{\varepsilon}_{S2} = \bar{\varepsilon}_{BS}^* = \varepsilon_{BS} / z^* \approx 7.87\% \quad (5)$$

The Spinlab HVI System gives the bundle or fiber strength as tenacity in cN/tex (or g/tex). In this case the measured and corrected specific strength of the fibers might be estimated with a linear bundle density of $q_{fB}=453$ tex:

$$\bar{f}_{S1} = F_{BS} / q_{fB} \approx 20.9 \text{ cN/tex}, \quad \bar{f}_{S2} = \bar{F}_{BS}^* / q_{fB} \approx 29.8 \text{ cN/tex} \quad (6)$$

3.2 Structural mechanical modeling of composites

In order to create a structural mechanical model one has to be aware of the structural element properties and the structure of the fibrous material in question [1,2,13,14]. The reinforcement of a unidirectional short fiber

composite creates a so called fibre flow in which the adhesion length of fibres is the half of the critical one ($L_S = L_{crit}/2$) and determined by the specific adhesion (f_b) and the mean fibre breaking load $F_S = f_b L_S$. During a tensile test fibres intersecting the breaking cross section break or slip out of the grip realized by the matrix (Figure 8) depending on whether their minimal part-length ($l_m = \min(l, l')$) on the two sides of the cross section is larger than L_S or not [10,11]. Under load slippages and breakages take place gradually one after the other determining a kind of damaging or breaking process characterized by the changes in the measured tensile force.

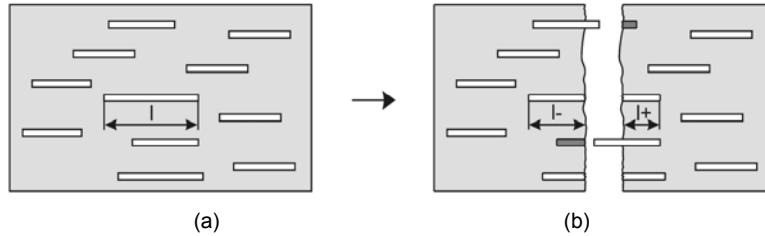


Figure 8. Short fiber reinforced composite (a) before and (b) after fracture

Fibers intersecting the breaking cross section can be considered as an embedding ES-bundle thus the expected value process of the bundle force can be calculated and its maximum can be treated as the strength of the composite. For the sake of simplicity the calculations were performed for constant fiber length (L) and fiber breaking strain (ε_{fS}). The result obtained for the reinforcing fiber flow consists of two parts: an initial straight line (Section I) and a hyperbole (Section II) (Figure 9).

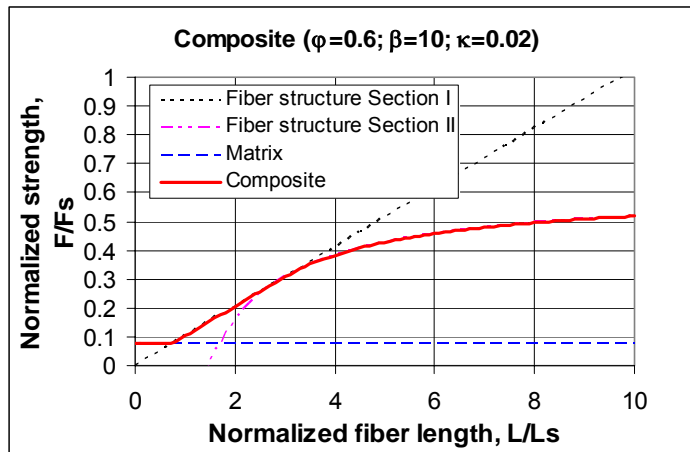


Figure 9. Normalized theoretical strength of short fiber composites as a function of the normalized mean fiber length (ϕ - fiber content; $\beta = \varepsilon_{mS}/\varepsilon_{fS}$, $\kappa = E_m/E_f$; ε_{mS} , ε_{fS} and E_m , E_f are the mean breaking strain and the tensile modulus of the matrix and the fibers, respectively)

The resultant for the composite was calculated with the rule of mixture hence the initial horizontal section is determined by the matrix strength. As an other example for structural-mechanical application the 3P bending test of a unidirectional Zoltek Panex PX33TW-048-131 carbon fiber/CIBA LY556 epoxy resin composite beam [18] is considered. The flexural test was carried out with $l=60$ mm span length. The rectangular cross section of the beam (4×10 mm²) was built up of resin matrix impregnated fiber layers which were assumed to be flat fiber bundles of E-type where the fibers and their matrix vicinity formed kinds of composite elements. Based on the classical bending theory and assuming that gradual fracture of the composite layers with layer breaking strain ε_L ($Eps0=E(\varepsilon_L)=1.2\%$, $Eps1=D(\varepsilon_L)=0.12\%$) of normal distribution took place on the stretched side, the expected value and the standard deviation of the bending force ($F(u)$) process could be computed [12,18]. In Figure 10 the measured values of the bending load, calculated point by point as the average of 4 measurements ($N=4$) [18], go inside the field of confidence interval of the expected value process computed from the standard deviation at probability level 95% until they cross the border at the ultimate fracture.

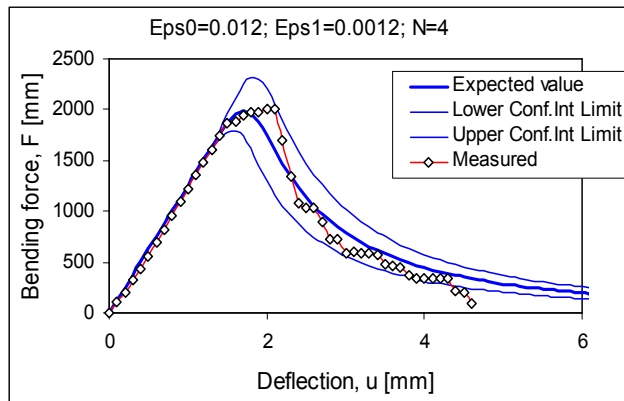


Figure 10. Measured and modeled bending load-deflection curves of an unidirectional composite beam

4. CONCLUSIONS

The idealized statistical fiber-bundle-cells (FBCs) and the modeling method developed are suitable for modeling both fibrous reinforcements and fiber reinforced composites. Phenomenological modeling makes it possible to analyze fibrous structures on the basis of evaluating measurements. Besides providing some structural information about the fibrous material tested in the cases above the single fiber strength data obtained with FiberSpace model were proved to be larger by about 27% for the glass fibers and 43% for the cotton fibers than those calculated from the measured peaks. Consequently, by using the FBC modeling method one can achieve a

significant improvement in determining the single fiber data. Parallely, FBCs can be applied to creating structural-mechanical models of composites without meshing or using iterative simulation cycles.

ACKNOWLEDGEMENTS

This work has been supported by OTKA Hungarian Scientific Research Fund through grant T049069.

REFERENCES

1. Chou, T-W., Ko, F.K. (Editors) (1989), "Textile Structural Composites"; Elsevier, New York.
2. Zurek, W. (1975), "The Structure of Yarn". 2nd revised edition. Warsaw (Poland), 1971, Springfield (Virginia, USA).
3. Sutherland, L.S. and Guedes Soares, C. (1997), "Review of Probabilistic Models of the Strength of Composite Materials". Reliability Engineering and System Safety, Vol.56. 183-196.
4. Harlow, D.G. and Phoenix, S.L. (1978), "The Chain-of-Bundles Probability Model For the Strength of Fibrous Materials I: Analysis and Conjectures". Journal of Composite Materials Vol.12. 195-214. "II: A Numerical Study of Convergence". Vol.12. (July) 314-334.
5. Phoenix, S.L. (1979), "Statistical Aspect of Failure of Fibrous Materials". Composite Materials: Testing and Design (Fifth Conference), ASTM STP 674, 455-483.
6. Phoenix, S.L. (1980), "Statistical Models for the Tensile Strength of Yarns and Cables". In: Mechanics of Flexible Fiber Assemblies (edited by Hearle J.W.S., Thwaites J.J., and Amirbayat J.) NATO Advanced Study Institutes Series. Series E: Applied Sciences – No. 38. Sijthoff & Nordhoff, Alphen aan de Rijn, The Netherlands; Germantown, ML. USA. 113-141.
7. Vas, L.M. (1992), "Latest Results in the Tensile Test Theory of Fiber and Yarn Bundles Ordered into Plane" (in Hungarian). Magyar Textiltechnika Vol.45. (3) 71-75, (5-6) 137-142, (7-8) 187-191.
8. Vas, L.M. and Csanzi, F. (1993), "Use of Composite-Bundle Theory to Predict Tensile Properties of Yarns". Journal of the Textile Institute Vol.84. (3) 448-463.
9. Vas, L.M. and Halász, G. (1994), "Modelling the Breaking Process of Twisted Fibre Bundles and Yarns". Periodica Polytechnica Vol.38. (4) 297-324.
10. Vas, L.M. (2006), "Strength of Unidirectional Short Fiber Structures as a Function of Fiber Length". Journal of Composite Materials Vol.40. (19), 1695-1734.
11. Vas, L.M. (2006), "Statistical Modeling of Unidirectional Fiber Structures", Macromolecular Symposia. Special Issue: Advanced Polymer Composites and Technologies Vol.239. (1) 159-175.
12. Vas, L.M., Rácz Zs., and Nagy P. (2004), "Modeling and Testing the Fracture Process of Impregnated Carbon Fiber Roving Specimens During Bending" Part I. "Fiber Bundle Model". Journal of Composite Materials Vol.38. (20), 1757-1785. Part II. "Experimental Studies". Vol.38. (20), 1787-1801.
13. Gibson, R.F. (1994), "Principles of Composite Material Mechanics". McGraw Hill, New York.
14. Valavala, P.K. and Odegard, G.M. (2005), "Modeling Techniques for Determination of Mechanical Properties of Polymer Nanocomposites" Review on Advanced Materials Science. Vol.9. (1) 34-44.

15. Tumino, D., Cappello, F., and Catalanotti, G. (2007), "A Continuum Damage Model to Simulate Failure in Composite Plates under Uniaxial Compression". Express Polymer Letters Vol.1. (1) 84-91
16. Vas, L.M., Poloskei, K., Felhos, D., Deak T., and Czigany, T. (2007), "Theoretical and Experimental Study of the Effect of Fiber Heads on the Mechanical Properties of Non-continuous Basalt Fiber Reinforced Composites". Express Polymer Letters Vol.1. (2) 109-121.
17. Bobeth, W. (Hrsg.) (1993), "Textile Faserstoffe. Beschaffenheit und Eigenschaften" Springer Verlag, Berlin.
18. Rácz, Zs. (2006), "Analyzing the Bending Characteristic and Damage Process of Unidirectional Composite Beams" (in Hungarian) PhD Thesis. Budapest University of Technology and Economics, Budapest, Hungary.
19. László M. Vas, Associate Professor, Budapest University of Technology and Economics, Department of Polymer Engineering, 1111 Budapest, Hungary, E-Mail: vas@pt.bme.hu; Phone: +36 1 463 1529, FAX: +36 1 463 1527.
20. Péter Tamás, Research Fellow, Budapest University of Technology and Economics, Department of Information Engineering, 1111 Budapest, Hungary, E-Mail: tamas@inflab.bme.hu, tamas@git.bme.hu; Phone: +36 1 463 1691, FAX: +36 1 463 1689.

FIBER SURFACE TREATMENTS FOR IMPROVING FIBER-MATRIX INTERFACE BOND STRENGTH IN NATUREL FIBER REINFORCED POLYMER COMPOSITES

K. SEVER¹, V. ÇEÇEN¹, M. SARIKANAT²,

H. YILDIZ², I. TAVMAN¹,

¹ Department of Mechanical Engineering, Dokuz Eylul University

² Department of Mechanical Engineering, Ege University

ABSTRACT

Nowadays, glass, carbon, boron and kevlar fibers are being used as reinforcing materials in polymeric composites which have been widely used for structural applications. However these fibers are resistant to biodegradation and can pose environmental problems. Natural fibers from plants such as jute, bamboo, coir, sisal and pineapple have advantages in comparison to other fibers in that they form a renewable and biodegradable. At the same time these fibers have low density, high toughness and acceptable strength properties. All natural fibers have hydrophilic properties. This can cause a very poor interface bond strength between natural fiber and the hydrophobic matrix. There are several surface treatment methods to improve the natural fiber-matrix interface in natural fiber composite. Fiber-matrix adhesion has to be optimized for ensuring good mechanical properties. In this study, Surface treatments which are used on natural fibers will be emphasized.

Key words: Natural fiber, Surface treatment, Adhesion, Polymer composite

1.INTRODUCTION

Synthetic fibres such as nylon, rayon, aramid, glass, polyester and carbon are extensively used for the reinforcement of plastics. Nevertheless, these materials are expensive and are non-renewable resources. Because of the uncertainties prevailing in the supply and price of petroleum based products, there is every need to use the naturally occurring alternatives. In many parts of the world, besides the agricultural purposes, different parts of plants and fruits of many crops have been found to be viable sources of raw material for industrial purpose. In recent years, polymer composites containing vegetable fibers have received considerable attention both in the literature and in industry. The interest in natural fiber reinforced polymer composites is growing rapidly due to the high performance in mechanical properties, significant processing advantages, low cost and low density[1]. Advantages of natural fibers are abundant, renewable, recyclable, low cost, high toughness, low density, good specific strength properties, reduced tool wear

(nonabrasive to processing equipment), CO₂ neutral when burned and biodegradability [2-6]. The extent of environmental pollution caused is less compared to synthetic fibers. [2]. The disadvantages and limitations of natural fibers, when used as reinforcement for composites, are related to the lack of proper interfacial adhesion, poor resistance to moisture absorption, limited processing temperature to about 200°C, and low dimensional stability (shrinkage, swelling)[3]. The hydrophilic nature of natural fibers is a major drawback for their application as reinforcement for composites. The poor moisture resistance of natural fibers leads to incompatibility and poor wettability with hydrophobic polymers, and this reduces the interaction bonding at fiber/matrix interface[5,7]. The fiber/matrix interface plays an important role in the physical and mechanical properties of composites. To improve the interfacial properties, natural fibers are subjected to surface treatments.

2. CLASSIFICATION AND STRUCTURE OF NATURAL FIBERS

Natural fibers are classed according to their source; plants, animals or minerals. In general, it is the plant fibers that are used to reinforce plastics in the composite industry [8]. Fibers obtained from the various parts of the plants are known as vegetable fibers. These fibers are classified into three categories depending on the part of the plant from which they are extracted [1-2].

1. Bast or Stem fibers (jute, flax, banana etc.)
2. Leaf fibers (sisal, pineapple, screw pine etc.)
3. Fruit fibers (cotton, coir, oil palm etc.)

The physical properties of natural fibers are mainly determined by the chemical and physical composition, such as the structure of fibers, cellulose content, angle of fibrils, cross-section, and the degree of polymerization, which are affected by the nature of the plant, area of growth, its climate, age of the plant, and the extraction method used [1-2,9-10]. Furthermore, there is an enormous amount of variability in fiber properties depending upon whether the fibers are taken from which part of the plant, the quality of plant and location. Different fibers have also different defects such as micro compressions, or pits or cracks[2].

With the exception of cotton, the components of natural fibers are cellulose, hemicellulose, lignin, pectin, waxes and water soluble substances, with cellulose, hemicellulose and lignin as the basic components with regard to the physical properties of the fibers[9,11]. Other components, usually regarded as surface impurities, are the pectin and wax substances[12].

A single fiber of all plant-based natural fibers consists of several cells. These cells are formed out of crystalline microfibrils based on cellulose, which are connected to a complete layer, by amorphous lignin and hemicellulose[11].

Cellulose fibrils are aligned along the length of the fiber, irrespective of its origin, i.e. whether it is extracted from stem, leaf or fruit. [1]. These microfibrils are found to be 10–30 nm wide, less than this in width, indefinitely long containing 2–30,000 cellulose molecules in cross-section[8]. Multiple layers of such cellulose-lignin/ hemicellulose in one primary and three secondary cell walls stick together to form a multiple-layer-composite, the cell. These cell walls differ in their composition (ratio between cellulose and lignin/hemicellulose) and in the orientation (spiral angle) of the cellulose microfibrils. The spiral angle of the fibrils and the content of cellulose generally determine the mechanical properties of the cellulose-based natural fibers[11].

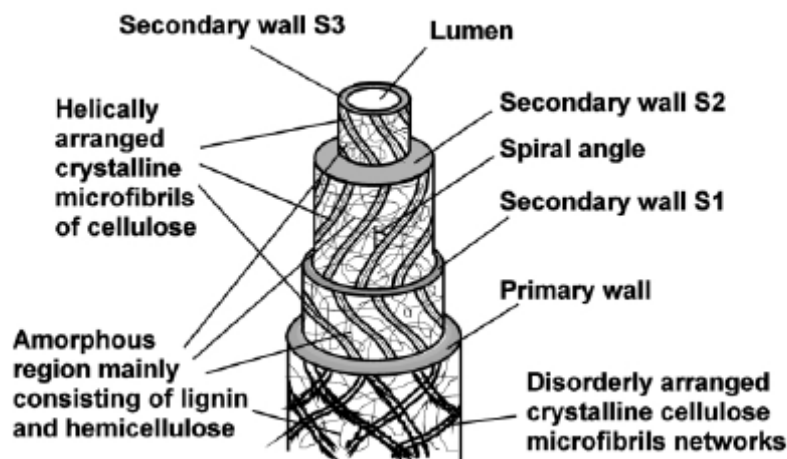


Figure 1. Structural constitution of a natural vegetable fiber cell[13]

Cellulose is the main component of the vegetable fibers. Cellulose is a natural polymer with high strength and stiffness per weight, and it is the building material of long fibrous cells[3]. The chemical structure of cellulose contains three hydroxyl groups, which in the macromolecular cellulose structure form hydrogen bonds. Two of these hydroxyl groups form intermolecular bonds, while the third one forms intramolecular hydrogen bonds. Therefore all plant fibers are hydrophilic in nature[1-2,12]. Higher cellulose content leads to higher stiffness and, therefore, will be most suitable for resin reinforcement[12].

Lignin is a hydrocarbon polymer with a highly complex structure consisting of aliphatic and aromatic constituents and forms the matrix sheath around the fibers that holds the natural structure (e.g. trees) together[8-9] and have the least water sorption of the natural fiber components[14]. The distinct cells of hard plant fibers are bonded together by lignin, acting as a cementing material. The lignin content of plant fibers influences its structure, properties and morphology[1].

The other component of natural fibers is hemicellulose. Hemicellulose is strongly bound to cellulose fibrils presumably by hydrogen bonds. Hemicellulosic polymers are branched, fully amorphous and have a significantly lower molecular weight than cellulose. Because of its open structure containing many hydroxyl and acetyl groups, hemicellulose is partly soluble in water and hygroscopic[14]. Unlike cellulose, the constituents of hemicellulose differ from plant to plant. The mechanical properties are lower than those of cellulose[9].

Both the hemicellulosic and pectin materials play important roles in fiber bundle integration, fiber bundle strength, and individual fiber strength as well as water absorbency, swelling, elasticity, and wet strength[3].

Plant fibers are highly polar due to the presence of the hydroxyl groups. On the other hand, plant fibers are covered with pectin and waxy substances, thus hindering the hydroxyl groups from reacting with polar matrices, and forming mechanical interlocking adhesion with nonpolar matrices. Also, hydrophilic nature is a major problem for all cellulose-fibers if used as reinforcement in plastics. High water and moisture absorption of the cellulose fibers causes swelling and plasticizing effects, resulting in dimensional instability and poor mechanical properties. This limits the application of plant fibers as reinforcement for polymeric materials[12]. To produce the reactive hydroxyl groups and the rough surface for adhesion with polymeric materials, plant fibers need to undergo physical and/or chemical treatment to modify the surface and structure.

3. USED METHODS TO MODIFY THE NATURAL FIBER SURFACE

3.1. Plasma Treatment and Plasma Polymerization

Plasma treatment and plasma polymerization offer new approaches to the modification of natural fiber surfaces. Cold-plasma techniques are dry, clean processes without environmental concerns[15].

Organic fibers generally have smooth surfaces and little superficial energy, which result in low adherence to the matrix. These fibers usually do not have chemical functional groups to form covalent bonds in the fiber–matrix interface. The most common treatments modify the fibers by removing the superficial layer, changing the topography and the chemical nature of the surface. Plasma treatment improves fiber-matrix adhesion largely by introducing polar or excited groups or even a new polymer layer that can form strong covalent bonds between the fiber and the matrix, and sometimes by roughening the surface of fibers to increase mechanical interlocks between the fiber and the matrix[16-17].

Glow discharges are efficient in creating a high density of free radicals in the gaseous phase and on the surface of the material being exposed to, including the most stable polymers. Plasma treatments change the superficial properties of the material based on the formation of free radicals

on the surface as a result of the impacts with the energetic particles (electrons, ions, etc) traveling in the plasma. The superficial free radicals created by the plasma can react with each other or with other components activated in the plasma environment to form different chemical compounds. They also increase the superficial energy of the fibers and modify the wet ability of the surfaces exposed to the plasma[17] .

Proper selection of starting compounds and external plasma parameters (e.g. power, pressure and treatment time) allow creation of desired characteristics on lignocellulosic substrate surfaces. In a cold plasma treatment system, depending on the type and nature of the gases used, a variety of surface modifications can be achieved. Surface energy can be increased or decreased, crosslinking can be introduced, and reactive free radicals and groups can be produced[9,15,18]. Surface free energy of a material is the work required in creating a new surface. Both surface free energy and contact angle are used to define the wettability of one material to another. The higher the surface energy and the smaller the contact angle, the stronger the adhesion between the two surfaces. Generally, plasma treatments introduce unpaired electrons and create new excited sites on the surface, which leads to an increase in surface energy and a decrease in contact angle[16]. Such as, the treatment of rayon fibers with oxygen plasma results in increasing the total as well as in the polar part of the free surface energy with increasing treatment time, because of the increased O/C ratio[9]. With an oxygen plasma, various polar groups such as -C-OH, -C=O, -COOH and -CO₂ introduce on the surface of treated fibers[16].

Plasma modification is believed to modify the crystalline and amorphous topographies of cellulosic substrates. Since cellulose and hemicellulose are more reactive to plasma, they are more easily etched away by plasma treatments, leaving more non-polar lignin on the fiber surface, which contributes to the improvement of interfacial adhesion[15].

Plasma polymerization is the simultaneous polymerization of monomers compatible to the fiber and to the matrix. The film formed in this way should have good adhesion to the fibers and to the matrix, but it should not alter the global properties of the fibers, because it solely modifies the surface. Thus, the surfaces of the fibers treated with plasma polymerization can result in stronger bonds with the matrices[17].

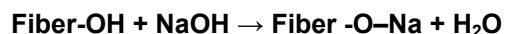
The influence of plasma treatments on the tensile strength of fibers is one of the most controversial issues. The results could be negative, unchanging or positive, depending on the situation. When corrosive gases such as air, oxygen and ammonia are used, a moderate plasma treatment will introduce only surface modification without any ablation so that the tensile strength of the fiber remains unchanged. However, an intensive plasma treatment will likely etch the bulk of the fiber, which certainly harms its mechanical properties. If polymeric gases are used, plasma polymerization will take place on the fiber surface under suitable conditions. This layer of polymer,

due to its crosslinked network of molecular chain structure, may behave stronger than the fiber itself. As a result, the mechanical properties of fibers are enhanced by the plasma treatment. The chemical composition of the fiber surfaces can be changed obviously by both plasma ablation and plasma polymerization[16].

3.2. Alkali Treatment

Alkaline treatment or mercerization is one of the most used chemical treatment for natural fibers when used to reinforce thermoplastics and thermosets[14]. Alkali treatment of the fiber can clean the fiber surface, chemically modify the surface and increase the surface roughness. It has been widely used on cotton textiles, jute, hemp, sisal, kenaf fibers[12,19]. An alkali treatment of cellulose-fibers depends on the type and concentration of the alkaline solution, its temperature, time of treatment, tension of the material as well as on the additives[2,9,18].

The reaction of sodium hydroxide with cellulose is shown below. Addition of aqueous sodium hydroxide (NaOH) to natural fiber promotes the ionization of the hydroxyl group to the alkoxide. Modification done by alkaline treatment is the disruption of hydrogen bonding in the structure[14].



Surface impurities can remove from fiber surface with various concentrations of alkaline solution and increase of uniformity can contribute to increase in tensile strength. However, a low concentration of the solution can not be good enough to effectively remove impurities from fiber surfaces and a very high concentration of the solution would certainly damage fibers and consequently reduce tensile strength of fibers[19]. Moreover, alkali treatment removes hemicelluloses, lignin, pectin, waxy substances, and natural oils covering the external surface of the fiber cell wall. This reveals the fibrils, and gives a rough surface topography to the fiber, Figure 2 [10, 12, 20-21]. Alkali treatment also leads to fiber bundle fibrillation, that is, breakdown of the composite fiber bundle into smaller fibers, which increases the effective surface area available for contact with the wet matrix[20, 22].

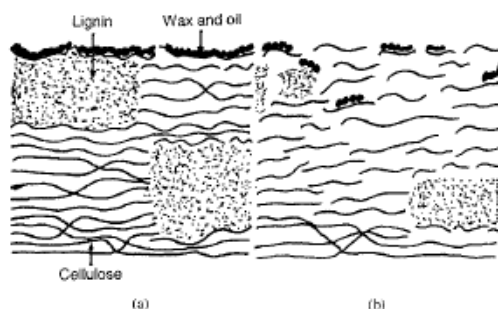


Figure 2. Typical structure of (a) untreated and (b) alkalinized cellulosic fiber[12].

Alkali treatment influences chemical composition of fibers, degree of polymerization and molecular orientation of cellulose crystallites, due to removal of cementing substances such as lignin and hemicellulose[3,14,23]. Alkalis, particularly sodium hydroxide, readily react with hemicellulose but have little effect on lignin at low concentrations[11]. It increases the amount of cellulose exposed on the fiber surface, thus increasing the number of possible reaction sites [3,14]. Treatment with NaOH leads to a decrease in the spiral angle, i.e. closer to fiber axis, and increase in molecular orientation[9,24].

Additional to the increase of the fiber properties through alkalization, an increase of composite quality are to be expected of laminates due to the improved fiber–matrix adhesion.

3.3. Treatment with Silane Coupling Agents

The general chemical formula of silane is $X_3\text{-Si-R}$, a multifunctional molecule that reacts at one end with the cellulose fiber surface and the other end with the polymer phase. R is a group, which can react with the resin, and X is a group, which can hydrolyze to form a silanol group in aqueous solution, and these react with hydroxyl group of the cellulose surface. R-groups may be vinyl, γ -aminopropyl, γ -methacryloxypropyne etc. The X-group may be chloro, methoxy, ethoxy etc. Bifunctional silane molecules act as a link between the resin and the cellulose by forming a chemical bond with the surface of cellulose through a siloxane bridge while its organofunctional group bonds to the polymer resin. This co-reactivity with both the cellulose and the polymer via covalent primary bonds gives molecular continuity across the interface region of the composite. It is essential that the R-group and the functional group be chosen so that they can react with the functional group in the resin under given curing conditions. Furthermore the X-group must be chosen that can hydrolyze to allow reactions to take place between the silane and the OH-group on the cellulose surface. When the treated fibers are dried, a reversible condensation takes place between the silanol and -OH groups on the cellulose fiber surface, forming a polysiloxane layer, which is bonded to the cellulose surface. When the silane coated cellulose surface in contact with the resin, the R-groups on the fiber surface react with the functional groups present in the polymer resin, forming a stable covalent bond with the polymer. Once all these reactions occur, the silane coupling agents may function as a bridge to bond the cellulose fibers to the resin with a chain of primary strong bond[2]. Also, the coupling agent-resin matrix interface is a diffusion boundary where intermixing takes place, due to penetration of the resin into the chemisorbed silane layers and the migration of the physisorbed silane molecules into the matrix phase[7]. Fig. 3 is a representation of the bonding of the siloxane to the polymer through a combination of interpenetration and chemical reaction .

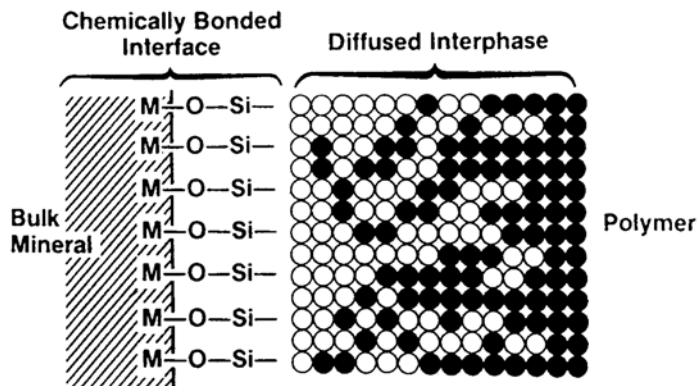


Figure 3. Bonding siloxane to polymer through diffusion[25]

Treatment of fibers with silane coupling agents significantly improves the interfacial adhesion and therefore the mechanical properties of the composites[2]. The interaction between the silane coupling agent modified fiber and the matrix was much stronger than that of alkaline treatment, which led to composites with higher tensile strength from silane treated than alkaline-treated fiber[14,26].

A number of factors affect the microstructure of the coupling agent. They are the silane structure, its organofunctionality, acidity, drying conditions and homogeneity, the topology and the chemical composition of fiber surface[2].

The general mechanism of how alkoxy silanes form bonds with the fiber surface which contains hydroxyl groups is as follows: Alkoxy silanes undergo hydrolysis, condensation and the bond formation stage(Figure 4). In addition to this reactions of silanols with hydroxyls of the fiber surface, the formation of polysiloxane structures can take place[9,18].

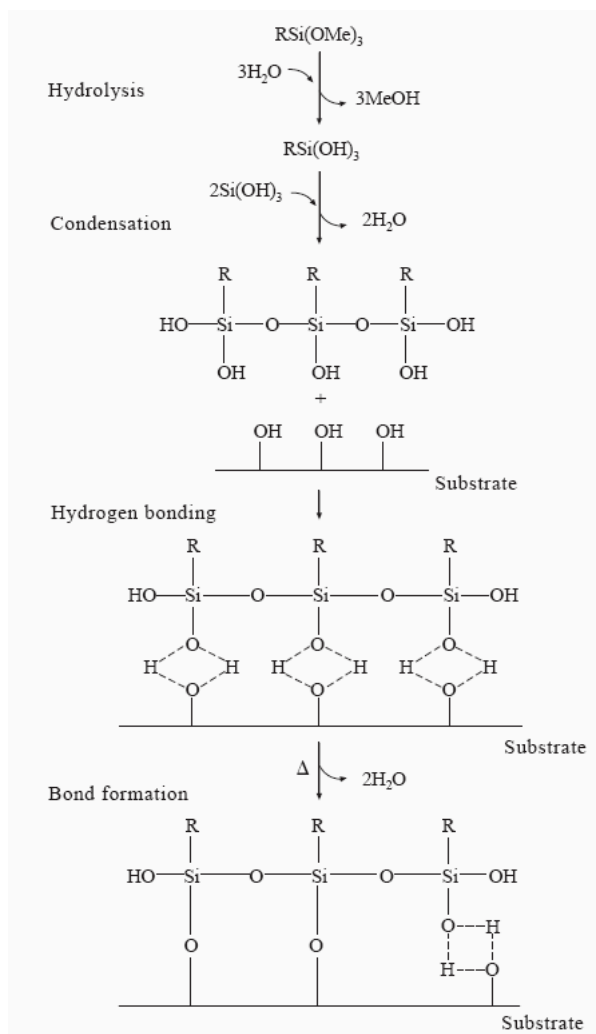
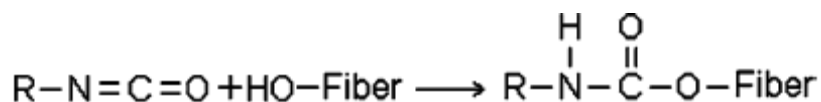


Figure 4. Reactions and Bonding of alkoxy silanes (Arkles et al., 1992)[27]

3.4. Treatment with Isocyanates

An isocyanate, the poly(methylene) poly(phenyl) isocyanate (PMPPIC), is a compound containing the isocyanate functional group $-\text{N}=\text{C}=\text{O}$, which is highly susceptible to reaction with the hydroxyl groups of cellulose and lignin in fibers and forms strong covalent bonds, thereby creating better compatibility with the polymer matrix in the composites. An isocyanate treatment has also significant influence on the properties of composites, i.e., increased thermal stability, reduced water absorption etc. The reaction between fiber and isocyanate coupling agent is shown below :



therefore a urethane linkage is formed. The urethane group results from the interaction of an isocyanate and hydroxyl compound. The better performance is due to the formation of urethane linkage between –OH group of the fiber and –N= C= O group of PMPPIC. R could be different chemical groups (such as alkyl)[2-3, 11,14].

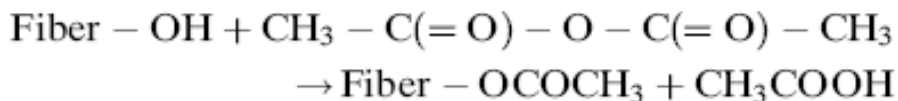
Comparing both methods, treatment with silanes or treatment with isocyanates, isocyanatic treatment is more effective than the treatment with silane[9,18]. Isocyanates provided better interaction with thermoplastics[3].

3.5. Acetylation Treatment

Acetylation of natural fibers is a well-known esterification method causing plasticization of cellulosic fibers. Acetylation is based on the reaction of cell wall hydroxyl groups of lignocellulosic materials with acetic or propionic anhydride at elevated temperature (usually without a catalyst). The reaction involves the generation of acetic acid (CH₃COOH) as by-product which must be removed from the lignocellulosic material before the fiber is used[14].

The procedure included an alkaline treatment initially, followed by acetylation. Fibers were pretreated with sodium hydroxide in order to activate the OH groups on the cellulose and lignin. Fibers were then subjected to acetylation with acetic anhydride in acetic acid medium[14]. Acetylation, with acetic acid only, reaches probably no other than the easily accessible hydroxyl groups[9].

Chemical modification with acetic anhydride (CH₃-C(=O)-O-C(=O)-CH₃) substitutes the polymer hydroxyl groups of the cell wall with acetyl groups, modifying the properties of these polymers so that they become hydrophobic[14]. The reaction of acetic anhydride with fiber is shown as :



Acetylation can reduce the hygroscopic nature of natural fibers and increases the dimensional stability of composites. Acetylation treatment of fiber improves the fiber–matrix adhesion[14].

4. RESULTS

Natural fibers are considered as a potential material in place of synthetic fibers in composite materials. Although natural fibers have advantages of being low cost and low density, natural fibers have strong polar character. Large amount of hydroxyl group in cellulose gives natural fiber hydrophilic

properties when used to reinforce hydrophobic matrices; the result is a very poor interface and poor resistance to moisture absorption. Surface treatments are potentially able to overcome the problem of incompatibility. Surface treatments can increase the interface adhesion between the fiber and matrix, and decrease the water absorption of fibers.

REFERENCES

1. A Review on Sisal Fiber Reinforced Polymer Composites, Kuruvilla Joseph, Romildo Dias Tolêdo Filho, Beena James, Sabu Thomas, Laura Hecker de Carvalho, *Revista Brasileira de Engenharia Agrícola e Ambiental*, v.3, n.3, p.367-379, 1999 Campina Grande, PB, DEAg/UFPB
2. A Review on Interface Modification and Characterization of Natural Fiber Reinforced Plastic Composites Jayamol George, M. S. Sreekala, Sabu Thomas, *Polymer Engineering and Science*, September 2001, Vol. 41, No. 9
3. Natural Fiber Eco-Composites, G. Bogoeva-Gaceva, M. Avella, M. Malinconico, A. Buzarovska, A. Grozdanov, G. Gentile, M.E. Errico, *POLYMER COMPOSITES—2007*
4. Natural Fiber Polymer Composites: A Review, D. Nabi Saheb, J. P. Jog, *Advances in Polymer Technology*, Vol. 18, No. 4, 351–363 (1999)
5. Chemical Modification of Jute Fibers for The Production of Green-Composites, F. Corrales, F. Vilaseca, M. Llop, J. Gironès, J.A. Méndez, P. Mutjé, *Journal of Hazardous Materials* 144 (2007) 730–735
6. Biofiber-Reinforced Polypropylene Composites, Rajeev Karnani, Mohan Krishnan, Ramani Narayan, *Polymer Engineering And Science*, February 1997, Vol. 37, No. 2
7. Interaction of Silane Coupling Agents with Cellulose, Mekki Abdelmouleh, Sami Boufi, Abdelhamid ben Salah, Mohamed Naceur Belgacem, Alessandro Gandini, *Langmuir* **2002**, 18, 3203-3208
8. Review Current International Research Into Cellulosic Fibres and Composites, S. J. Eichhorn, C. A. Baillie, N. Zafeiropoulos, L. Y. Mwaikambo, M. P. Ansell, A. Dufresne, K. M. Entwistle, P. J. Herrera-Franco, G. C. Escamilla, L. Groom, M. Hughes, C. Hill, T. G. Rials, P. M. Wild, *Journal of Materials Science* 36 (2001) 2107 – 2131
9. Composites Reinforced with Cellulose Based Fibres, A.K. Bledzki, J. Gassan, *Prog. Polym. Sci.* 24 (1999) 221–274
10. Oil Palm Fibers: Morphology, Chemical Composition, Surface Modification, And Mechanical Properties, M. S. Sreekala, M. G. Kumaran, Sabu Thomas, *Journal Of Applied Polymer Science*, Vol. 66, 821–835 (1997)
11. A Review on Pineapple Leaf Fibers, Sisal Fibers and Their Biocomposites Supriya Mishra, Amar K. Mohanty, Lawrence T. Drzal, Manjusri Misra, Georg Hinrichsen, *Macromol. Mater. Eng.* 2004, 289, 955–974
12. Chemical Modification of Hemp, Sisal, Jute and Kapok Fibers by Alkalization, L. Mwaikambo, M. Ansell, *Journal of Applied Polymer Science* 84 (12) (2002) 2222–2234.
13. The Effect of Fiber Treatment on The Mechanical Properties of Unidirectional Sisal-Reinforced Epoxy Composites, Min Zhi Rong, Ming Qiu Zhang, Yuan Liu, Gui Cheng Yang, Han Min Zeng, *Composites Science and Technology* 61 (2001) 1437–1447
14. Chemical Treatments of Natural Fiber for Use in Natural Fiber-Reinforced Composites: A Review, Xue Li, Lope G. Tabil, Satyanarayan Panigrahi, *J Polym Environ* (2007) 15:25–33

15. Effects of Plasma Treatment in Enhancing the Performance of Woodfibre-Polypropylene Composites, Xiaowen Yuan, Krishnan Jayaraman, Debes Bhattacharyya, Composites: Part A 35 (2004) 1363–1374
16. Application of Plasma Technologies in Fibre-reinforced Polymer Composites: A Review of Recent Developments, Rongzhi Li, Lin Ye, Yiu-Wing Mai, Composites Part A 28A (1997) 73-86
17. Plasma Modification of Cellulose Fibers for Composite Materials, J. Morales, M. G. Olayo, G. J. Cruz, P. Herrera-Franco, R. Olayo, Journal of Applied Polymer Science, Vol. 101, 3821–3828 (2006)
18. Properties and Modification Methods for Vegetable Fibers for Natural Fiber Composites A. K. Bledzki, S. Reihmane, J. Gassan, Journal of Applied Polymer Science, Vol. 59, 1329-1336 (1996)
19. Chemical Modification of Kenaf Fibers, A.M. Mohd Edeerozey, Hazizan Md Akil, A.B. Azhar, M.I. Zainal Ariffin, Materials Letters 61 (2007) 2023–2025
20. Sisal Fibre and Its Composites: A Review of Recent Developments, Yan Li, Yiu-Wing Mai, Lin Ye, Composites Science and Technology 60 (2000) 2037-2055
21. The Role of Fibre/Matrix Interactions on The Dynamic Mechanical Properties of Chemically Modified Banana Fibre/Polyester Composites, Laly A. Pothan, Sabu Thomas, G. Groeninckx, Composites: Part A 37 (2006) 1260–1269
22. Composites Based on Jute Fibers and Phenolic Matrices: Properties of Fibers and Composites, I. A. T. Razera, E. Frollini, Journal of Applied Polymer Science, Vol. 91, 1077–1085 (2004)
23. Effect of Fiber Surface Treatment on The Fiber–Matrix Bond Strength of Natural Fiber Reinforced Composites, A. Valadez-Gonzalez, J.M. Cervantes-Uc, R. Olayo, P.J. Herrera-Franco, Composites: Part B 30 (1999) 309–320
24. Possibilities for Improving the Mechanical Properties of Jute/Epoxy Composites by Alkali Treatment of Fibres, Jochen Gassan, Andrzej K. Bledzki, Composites Science and Technology 59 (1999) 1303-1309
25. Tailoring of Interfaces in Glass Fiber Reinforced Polymer Composites: A Review, A.T. DiBenedetto, Materials Science and Engineering A302 (2001) 74–82
26. Effect of Fiber Surface Treatment on the Properties of Biocomposites from Nonwoven Industrial Hemp Fiber Mats and Unsaturated Polyester Resin, Geeta Mehta, Lawrence T. Drzal, Amar K. Mohanty, Manjusri Misra, Journal of Applied Polymer Science, Vol. 99, 1055–1068 (2006)
27. Silanes and Other Coupling Agents, Arkles, B., Steinmetz, J.R., Zazyczny, J., & Mehta P., K.L. Mittal (Ed.). (1992). (p. 92). The Netherlands: VSP.

PERFORMANCE OF NYLON 66 TYRE CORDS WITH DIFFERENT LINEAR DENSITIES

A. AYTAÇ¹, B. YILMAZ², V. DENİZ¹

¹Department of Chemical Engineering, Kocaeli University

²KORDSA Global Industrial Yarn and Tyre Cord Fabric Manufacturing and Trading Inc.

ABSTRACT

The performance of nylon 6.6 tyre cords with different linear densities (dtex) was investigated by measuring different mechanical and physical properties. The breaking strengths are increased with the increasing linear densities of cords, but decreased with the increasing twist level. Adhesion values have been increased with the increasing linear density and twist level almost in all cases. It is observed that increasing in the twist levels of cords significantly improved the fatigue resistance for 1400 and 1880 dtex cords. On the other hands, no changes are observed in the strength retention values for 940 dtex cords. The authors have concluded that the fatigue resistances of the cords with the lower linear densities are better than higher linear densities cords.

Key Words: Tyre cord, mechanical properties, twist level, dtex, nylon 66, fatigue, adhesion.

1. INTRODUCTION

Tyres, conveyor belts, hoses, v-belts are typical examples of textile reinforced technical rubber goods and considered as composite materials. These materials are composed of three components such as textile (cord fabric), rubber and an interface adhesion layer (Resorcinol-Formaldehyde-Latex, RFL) (1). Cord fabric is the basic textile material, which is used to reinforce the pneumatic tyre. Several important properties of reinforcing materials are tensile, modulus, dimensional stability, fatigue and adhesion under tyre running conditions (2). Cord fabric consists of parallel warps and rare wefts. Cords can be produced by using different type of yarns. Production of reinforcing cord fabric has mainly three process steps: twisting, weaving and treating (dipping-heat setting).

Adhesion is an important factor in using textile materials together with rubber as well as individual properties of each material. The role of adhesion may be to give desirable properties, to improve durability, and maintain the shape of the composite. Tyres, belts, and transmission belts are used under severe conditions. Adhesion strength between cord and rubber matrix can affect performance of products; therefore, very high levels of adhesion are required (3).

RFL has been used to promote cord/rubber adhesion since 1935. No other resin has been replaced RF resin and no other latex has been replaced 2-

vinylpyridine–butadiene–styrene (15:70:15, w/w/w). Cords must be coated in RFL dip followed by pre-curing in a hot zone. After pre-curing, solution onto cord surfaces is crosslinked and is transformed to an insoluble system. The latex gives required flexibility to adhesive and reactivity to rubber. Moreover, RF resin provides a desirable heat and fatigue resistance by forming a three-dimensional network (4).

The demand for certain characteristics for automobiles, trucks, and aircrafts make fatigue analysis for tyre cords another important factor in predicting tyre performance. The cords in a tyre are constantly flexed, extended, and compressed. Therefore, the reinforcing fibers must withstand a large number of flexing cycles without the loss of properties (5). At the side walls of a tyre, cords should be flex material which is necessary for tyre running. In respect to this, nylon 6.6 is superior to most tyre-reinforcing materials (6).

This paper emphasizes on the mechanical and fatigue properties of Ny 6.6 greige and dipped cords in different linear densities. The effects of the linear density and twist level of Ny 6.6 tyre cords have been investigated.

2. EXPERIMENTAL

2.1. Material

The materials used for experimental purposes were 940-1440 -1880 dtex Ny 6.6 yarns, untreated cord (known as greige cord) and treated cords (known as dipped cords as the cords were dipped in RFL resin. All samples (yarns and cords) are obtained from KORDSA Global (Turkey). Tyre cords were prepared by twisting the yarns into two-ply construction with different twist level and subsequently they were dipped.

2.2.1 Twist

Cord twists (in twist per meter, tpm) of the greige and dipped cords were measured using a Zweigle twist tester (Germany), according to ASTM D885.

2.2.2 Tensile Tests

Tensile tests were performed by using Instron tester 4502, with cross head speed of 300mm/min and gauge length of 254 mm according to ASTM D885. An average of 5 test runs has been reported for each type cord.

2.2.4 H-Adhesion Test

Rubber strips were placed in the channels of a stainless steel die. Then dipped cords were placed on rubber strips. The ends of cords were stretched by 50 g weights. Another rubber strips were put on the cords in order to cover the cords totally. Samples then were vulcanized at 153 °C and pressure of 3.2 MPa for 25 min. Then the products were cut into H-shape samples. Static adhesion was evaluated by measuring cord pull out force in Instron tester 4502 at 25 °C, (ASTM D4776). An average of 8 test runs has been reported for each type cord.

2.2.5 Fatigue Test

Fatigue properties of the cords were measured using Wallace test equipment. The equipment has five hubs and is capable of testing up to five

specimens at one time. The prepared test specimens were mounted to the hubs. Then the equipment runs up to 100,000 cycles. The number of cycles in each test is being recorded by a counter affixed to each rocker arm (ASTM D 430). A set of sample is not flexed and is kept for comparison. The evaluation of the results has been made by comparing residual breaking strengths and adhesion values of flexed samples with the values of un-flexed samples.

3. RESULTS AND DISCUSSION

There are many demands for mechanical properties of industrial yarns. The parameter obtained from load-elongation (stress-strain) curves, such as the breaking strength, breaking elongation, braking energy and initial modulus are useful but not able to completely meet all the requirements. Moreover, adhesion and fatigue properties should be known.

Load - elongation (%) curves for Ny 6.6 tyre cords with three different linear densities and twist levels are shown in Fig.1. The typical mechanical properties of greige cords are given in Table 1. The mechanical properties of a cord are very depending on the linear density and the amount of twist applied. As it can be seen in Fig.1, the breaking strengths are increased with the increasing linear densities of Ny 6.6 cords, but decreased with the increasing twist level. When the linear density of the cords is changed, the initial modulus and breaking energy of the cords are increased. It can be seen from Table 1 that increasing linear density enhances the initial modulus and breaking energy. On the other hand, increasing the twist level increases the breaking energy, whereas decreases the initial modulus.

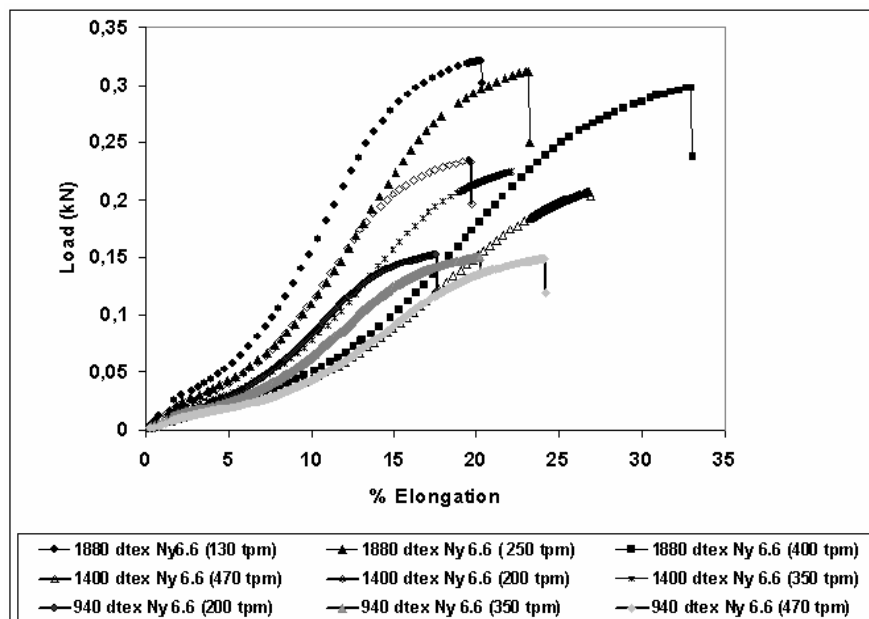


Figure 1. Load – elongation (%) curves of greige Ny 6.6 cords with different twist levels and linear densities.

Table 1. Tensile properties of Greige Ny 6.6 cords with different linear densities

Linear density (dtex)	Twist Level of Ny 6.6	Breaking Strenght (N)	Breaking Elongation (%)	Breaking Energy (Joule)	Initial Modulus (N/mm)
940	200	156	19,07	3,67	5,88
940	350	155	22,39	3,91	5,10
940	470	152	26,11	4,57	4,21
1400	200	236	20,28	6,34	8,43
1400	350	228	23,43	6,73	6,86
1400	470	216	29,08	7,41	5,10
1880	130	321	20,48	9,12	11,47
1880	250	314	23,85	9,87	9,31
1880	400	298	32,94	11,98	6,47

Mechanical properties of the dipped cords are shown in Table 2. The breaking strengths of the dipped cords are slightly lowered by dipping and heat treatment. Dipping also decreased final elongations values of the cord. Therefore the breaking energy of the dipped cords lowers than greige cords. The typical mechanical properties of dipped cords are given in Table 2. Those differences among the mechanical properties of greige and dipped cords can be easily seen by comparing the Tables 1 and 2.

Adhesion strength between cord and rubber matrix can affect performance of tyres. During tyre cord dipping process, an adhesive was applied and the fabric is treated under controlled condition of time, temperature and tension (3T). H-adhesion test method was used for the adhesion evaluation. The results of H-adhesion values were presented in Table 2.

Table 2. Tensile properties of Dipped Ny 6.6 cords with different linear densities

Linear density (dtex)	Twist Level (tpm)	Breaking loads (N)	Breaking Elongation (%)	Breaking Energy (Joule)	Thickness(mm)	H-dhesion (N)
940	200	151	19,26	3,57	0,56	108
940	350	147	21,46	3,92	0,56	123
940	470	146	24,33	4,37	0,57	121
1400	200	239	20,99	6,55	0,65	140
1400	350	228	25,14	7,03	0,70	191
1400	470	216	24,49	6,27	0,69	192
1880	130	301	19,32	7,99	0,75	152
1880	250	286	22,01	8,70	0,78	187
1880	400	258	24,05	8,12	0,74	222

The adhesion values of cords with different linear densities versus the increasing twist levels are given in Fig.2. Increase in linear density and twist level can cause to increase adhesion almost in all cases. The thickness of the cords increases with the increasing linear densities. Tensile properties of dipped cords with different linear densities are seen in Table 2. As can be seen from Table 2, when the cord thickness is increased, the adhesion value is also increased. This increasing adhesion may be explained with the increasing of cords' surface areas with the increase of twist level.

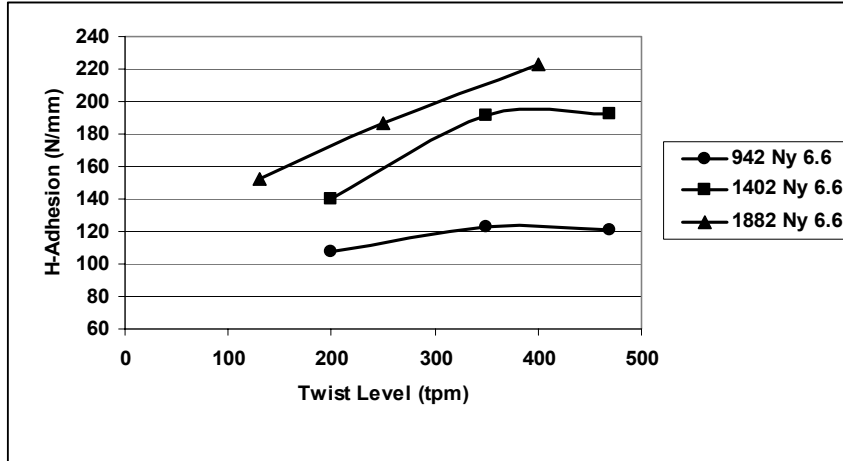


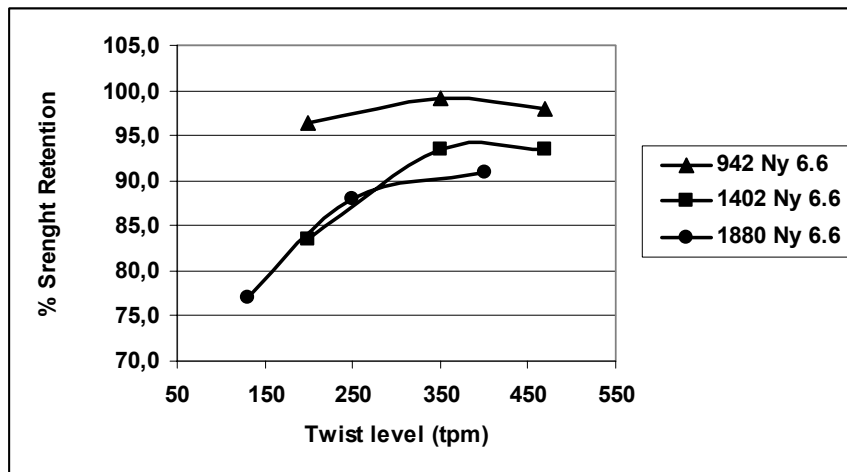
Figure 2. Changing of adhesion values of Ny 6.6 cord with different linear densities by increasing twist levels

Flex fatigue test was carried out on cords with different linear densities and twist levels at standard atmospheric conditions of %65 relative humidity and room temperature. Flex fatigue resistance test results for dipped cords is given in Table 3.

Two sets of samples were flexed applying 100.000 cycles at test equipment. A set of sample is not flexed and is kept for comparison. The evaluation of the results has been made by comparing strength retention and adhesion values of flexed samples with the values of un-flexed samples.

Table 3. Tensile Properties of Dipped and Flexed Ny 6.6 tyre Cords

Linear Density of Ny 66	Twist Level (tpm)	Adhesion(N)		% Adhesion Retention	Breaking Strength(N)		%Strength Retention
		Unflexed sample (N)	Flexed sample (N) (100 000 cycle)		Unflexed sample	Flexed Sample	
940	200	205	181	88	141	67	48
	350	307	256	83	147	92	63
	470	299	248	83	137	110	80
1400	200	283	194	69	202	169	84
	350	355	250	71	225	211	94
	470	360	273	76	222	208	93
1880	130	305	264	87	264	205	77
	250	339	259	76	281	247	88
	400	389	244	63	291	264	91


Figure 3. Strength retention of Ny 6.6 at different linear densities

Strength retention (%) - twist level curves for cords at three different twist levels and linear densities are shown in Fig.3. It is observed that the fatigue resistance was improved significantly when the twist levels of cords were increased for 1400 and 1880 dtex cords. On the other hands, no changes

are observed in the strength retention values for 940 dtex tyre cords. It has been found that fatigue resistance of cords with lower linear densities is better than that of higher linear densities cords. This is most probably due to that internal friction among the fibers is increased with the increasing linear density. Therefore, higher cycles need to be applied to lower linear density tyre cords for deteriorations for 940 dtex Ny 6.6.

3. CONCLUSIONS

The mechanical properties of a cord are very depending on the linear density and the amount of twist applied. The breaking strengths were increased with the increasing linear densities of Ny 66 cords whereas tensile strength values were decreased with the increasing twist level. An increase linear density and twist level cause to increase adhesion almost all cases.

It is observed that increasing of the twist levels significantly improved the fatigue resistance for 1400 and 1880 dtex cords. On the other hands, no changes are observed in the strength retention values for 940 dtex cords. The fatigue resistances of the lower linear densities cords are better than higher linear densities cords.

REFERENCES

1. Yilmaz. B. (2003). The Effect of Ambient Conditions on Aging of Tire Cord Fabric Adhesion. Tire Technology International.
2. Bhakuni, R.S., Rye, G.W. and Domchick, S.J., (1978), Adhesive and processing concepts for tire reinforcing materials, ASTM Symposium, Akron, Ohio.
3. Darwish. N. A., Shehata. A. B., Lawandy. S. N., Abou-Kandil. A. I. (1999). Effect of Non-Oiled Sulfur Concentration on the Adhesion between Nitrile Rubber and Nylon Cord. Journal of Applied Polymer Science. Vol. 74. 762–771.
4. Jamshidi. M., Afshar. F., Mohammadi. N. and Pourmahdian. S., (2005) Study on cord/rubber interface elevated temperatures by H-pull test method. Applied Surface Science. vol 249. 208-215.
5. Cho. H.H., Lee. K.H. and Bang Y.H., (2000). Effect of Fine Structure on Fatigue Resistance Property of Poly(ethylene terephthalate) Tire Cord Fibers. Journal of Applied Polymer Science. Vol. 78. 90–100.
6. Nkiwane. L. and Mukhopadhyay. S.K. (2000). A study of flex fatigue characteristics of nylon 6.6 tire yarns and cords. Journal of Applied Polymer Science. Vol. 75. p. 1045-1053.

INVESTIGATION OF THE IMPACT BEHAVIOUR IN GLASS FIBER REINFORCED COMPOSITE MATERIALS

M. KARAHAN¹, N. KARAHAN¹, S. GÜNDOĞAN²

¹ University of Uludag Vocational School of Technical Sciences, Textile Dep.

² University of Uludag Eng.&Arch. Fac. Textile Dep.

ABSTRACT

In this research, an investigation was conducted on the impact resistances of polyester resin composites that are used in automotive industry, reinforced with randomly distributed discontinuous and continuous glass fiber mat and glass fibers produced by hand lay-up, RTM and SMC molding methods. Firstly, tensile strength and elasticity module were found in order to determine the mechanical properties of the composite plates. Impact strength was determined by charpy test. In order to determine the deformation on the materials after impact, the samples exposed to low speed weight drop, were applied the 3-point bending test and their strength losses were determined. It was determined that the increase in fiber volume fractions increased the impact strength of the composite materials. But however it was observed that the use of filler materials in composite structure decreased the mechanical properties and impact strength of composites.

Key Words: Glass fiber-polyester composites, SMC, RTM, hand lay-up, impact strength.

1. INTRODUCTION

Today, automotive industry is one of the greatest and most prevalent sectors in the world and has become a very important consuming area for engineering materials. Although metallic materials are mostly used in this sector, the cultural and economic changes in recent years caused important changes in material preferences as well as design. The developments in polymer composite materials have become an important and supportive parameter in this change [1, 2]. Four factors are very important in composite materials usage becoming widespread in automotive industry: Weight saving, security, product quality, production easiness and flexibility [3]. The high energy absorption ability of composite materials makes them more advantageous compared with classic materials such as aluminum and steel and due to these properties, their usage have been increased in automotive parts that are exposed to collision [4]. A chassis made of composite material absorbs 80% more energy compared with a steel chassis in case of a collision [5].

The easy molding properties of composites provide many production advantages. The production of big structural complex parts being produced as a whole removes the necessity of part combining and montage and this allows materials to be produced with higher resistance and lower cost.

Molding processes being easy and coloring ability during molding, decreases the production time and cost, and also allows more color options and aesthetic features. As a result, composite materials are being used in production of outer body parts in automotive industry [6].

Automotive manufacturers today, are under the pressure of ability to produce low-cost automobiles that are resistant to environmental factors, having a high security level, very good comfort and equipment and consuming less fuel. Under this circumstances, composite materials are seen as the most convenient material that can be used instead of aluminum and steel. The easiest method in establishing lightweight without concession from strength is the usage of carbon fiber reinforced composites. However, carbon fibers are found expensive for some automotive applications. On the other hand, glass fiber have found a very prevalent application area in automotive industry together with the thermoplastic and thermoset resins, due to its high rigidity and low cost [7, 8]. Thanks to the new developments in production processes and molding techniques, glass fiber mats are being used in lightweight and high-performance automotive parts [9]. Some of the important molding methods in production of the automotive composites are hand lay-up method, sheet molding compounds (SMC), bulk molding compounds (BMC) and resin transfer molding (RTM). Products that are produced with these methods are used in side beams, ceiling and bottom panels, exterior body panel, bumpers and mudguard. While ready fiber-resin mixture is used in the production of these parts with SMC and BMC methods, discontinuous and continuous fiber mat, woven, knitting and uni-directional fabrics can be used as reinforcement with the other methods such as RTM and hand lay-up [10]. Generally, performance features such as high impact strength, high tensile strength, high fatigue resistance and preserving the strength at different temperatures are expected from automotive composites.

Especially collision resistance is very important in automotive parts and generally researches are concentrated on impact strengths and mechanical properties of the automotive composites. One of the comprehensive studies about this subject was made by Simunovich and Lee [11]. In this research, damage behavior and propagation properties for randomly glass fiber mat-polyester resin composite materials, were determined by experimental studies and damage behavior of the composite parts was modeled by the DYNA3D simulation program. Santulli et al. [12] investigated the impact strengths in glass fiber-polypropylene thermoplastic composites by charpy test. In a different research, Piry and Michaeli [13], studied the impact strengths and damage analysis of glass fiber-polyester resin composites produced by SMC method. The impact strength in case of fiber distribution and fiber volume fraction being changed in the structure was theoretically determined by EXPRESS simulation program, the loading amounts for initializing a crack and total energy amounts for the structure to fracture were theoretically calculated and results were compared with experimental data.

Oldenbo et al. [14], investigated the mechanical properties and fracture toughness of standard and low fiber volume fraction glass fiber–polyester resin SMC composites and found out that SMC composites with lower densities are more resistant to small collisions. In a similar research, Gregl et al. [15] found out that Young module was realized 20% lower when 10% of glass spheres were added to SMC composition as filler. Ming-Fa et al. [16] found out that 30% weight was saved when glass fiber–vinyl ester composites produced by RTM method, were used in bus bodies that operated with electricity and they studied the mechanical properties and impact strengths of glass fiber–vinyl ester composites. Kim and Lee [17], studied the relation between surface qualities and shrinkage ratios after curing of glass fiber–polyester resin composite parts produced by RTM method. They experimentally measured surface qualities and formations of the surface contour lines related with fiber volume fraction and then design and production of the bus inner panels were made according to the obtained results. Studies about RTM glass fiber–polyester composites have been concentrated mainly about shrinkage and warpage problem of these materials after the curing [18-21].

The purpose of this study is to investigate impact resistances of polyester resin composites that are used in automotive industry, reinforced with randomly discontinuous and continuous glass fiber mat and glass fibers produced by hand lay-up, RTM and SMC molding methods. For this purpose, firstly, the mechanical properties of the composite plates were determined. Impact strength was determined by charpy test. In order to determine the deformation on the materials after impact, the samples exposed to low speed weight drop were applied the 3-point flexural bending test and their strength losses were determined.

2. MATERIAL AND METHOD

2.1. Material

The reinforcement materials and their properties that were used in hand lay-up and RTM methods are given in Table 1. CE 92 N8 type unsaturated polyester was used as resin. 50% active Methyl Ethyl Ketone Peroxide was used with a ratio of 2%. And 6% Cobalt Naphthalate was used with a ratio of 0.25% as hardener and catalyst.

In SMC method, two ready compounds with different fiber volume fractions were used. The compound is in a form of non-cured layer including fiber, resin and other filler and additives. The ratios of used SMC composite contents are given in Table 2.

Hand lay-up, RTM and SMC molding methods were used in production of composite plates with dimensions of 300x300x4 mm. In Table 3, the reinforcement elements and resin amounts in plates produced by hand lay-up and RTM methods can be found.

Table 1. The reinforcement material types used in hand lay-up and RTM samples.

Material Type	Glass Fiber Type	Weight (gr/m ²)	Supplier
Randomly continuous glass fiber mat-U850	E-glass continuous filament	300	Vetrotex-Saint Gobain
Randomly discontinuous glass fiber mat-EMAT-1	E-glass discontinuous fiber	450	Cam Elyaf Inc.
Randomly discontinuous stitched glass fiber mat	E-glass discontinuous fiber	450	Cam Elyaf Inc.

Table 2. The ratios of SMC composite compositions the thicknesses of SMC composite plates

SMC materials	SMC-1	SMC-2
Discontinuous glass fiber (%)	22	28
Poliester resin (%)	26	28
Calcium Carbonat filler (%)	48	40
Pigment and thickener additives (%)	4	4
Total (%)	100	100
The thickenesses of finished plates (mm)	3.8	4

Table 3. The reinforcement elements and fiber volume fractions used in composite plates produced by hand lay-up and RTM methods.

Production Method	Reinforcement materials	Total weight of reinforcement materials (gr)	Weight of finished plate (gr)	Fiber volume fraction (%)	Thickness of finished plate (mm)
Hand lay-up	3 plies EMAT-1 discontinuous mat	121.5	587.85	20.66	4.4
RTM-1	3 plies U850 continuous mat	81	442.24	18.32	3.6
RTM-2	2 plies stitched mat + 1 ply U850 continuous mat	108	486.73	22.18	4

In hand lay-up operation, resin was applied to glass fiber mats by a roll and left for curing. In RTM method, resin injection was made with 3 bar pressure.

Material was left under press in room temperature for 45 minutes for curing. In SMC method, molding was made under 60 kg/cm² pressure at 140°C temperature. Samples were left for 5 minutes for curing.

2.2. Method

In order to determine the mechanical properties of the materials, primarily their tensile strengths and modules were found. For this purpose, first of all breaking load and breaking strain were determined. Tests were performed with HTE Hounsfield tension test device with 50 kN capacity, according to ASTM 1 D638 standards. Tensile strength and module was calculated by the equation below [22]:

$$\sigma_c = \frac{F}{w.t} \quad (1)$$

Here, σ_c is tensile strength (Mpa), F , maximum load (N), w , sample width (mm), t sample thickness (mm)

$$E_c = \frac{\sigma_c}{\varepsilon} ; \varepsilon = \frac{\Delta l}{l_0} \quad (2)$$

Here, E_c , is elasticity module, ε , breaking strain, l_0 , initial sample length, (mm), Δl , breaking elongation (mm).

In order to determine the impact resistances, low speed weight dropping method used. The spherical ended weights of 1 kg, with 45 mm diameter dropped from 1 m height on the samples and then their strength losses were determined with 3 point flexural bending test. Samples were attached from 2 sides during the weight drop as seen in Figure 1.

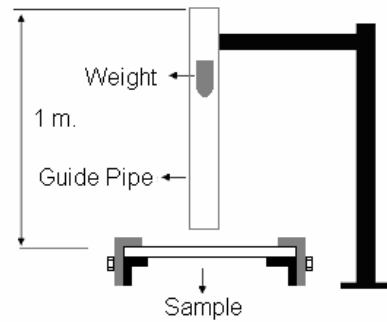


Figure 1. Fixing of the samples from two sides during weight drop.

Strength losses were observed by comparing with samples on which weight was not dropped. 3 point bending tests were made according to ASTM 1 D7 90 standards in 4301 Instron device. Bending strength and bending module were calculated from the equations below [22]:

$$\sigma_{CF} = \frac{3.F.l}{2.w.t^2} \quad (3)$$

$$E_{CF} = \frac{m.l^3}{4.w.t^3} \quad (4)$$

Here, σ_{CF} is the bending strength of the composite plate, E_{CF} , is the bending module of the composite plate, F : Maximum force (N), l : composite plate length (mm), w :plate width (mm), t : plate thickness (mm), m : $\tan \alpha$, is the slope of the load-elongation curve of the elastic region.

The impact strengths of the samples were determined by the KSG-70 type Charpy test device according to the DIN 53453 standards. Samples were tested without notches. At the end of Charpy tests, impact strength was calculated by the equation below: [22]

$$K_C = \frac{A_C \cdot 10^9}{w.t.l} \quad (5)$$

Here, K_C , is impact strength (J/m³), A_C , fracture energy (J), l : composite plate length (mm), w :plate width (mm), t : plate thickness (mm)

3. RESULTS AND DISCUSSION

3.1. Mechanical Properties

In order to determine the mechanical properties of the composite plates produced with different methods, initially tensile load and breaking strain were found and then according to these results, tensile strength and elasticity module were calculated by using equation 1 and 2. Results are given in Table 4.

Table 4. The mechanical properties of composite plates produced by hand lay-up, RTM and SMC methods

Production method	Maximum load-F (kN)	Breaking Strain- ϵ	Tensile strength- σ_c (MPa)	Elasticity Modüle- E_c (MPa)
Hand lay-up	4.43 ± 0.96	0.090±0.01	50.30 ± 10.92	587.20 ± 101.92
RTM-1	4.06 ± 0.13	0.060±0.01	56.44 ± 1.80	891.47 ± 71.54
RTM-2	4.65 ± 0.40	0.048±0.005	58.15 ± 4.99	1227.64 ± 214.47
SMC-1	2.65 ± 0.081	0.044±0.003	34.89 ± 1.062	790.46 ± 58.29
SMC-2	5.77 ± 0.22	0.070±0.01	72.18 ± 2.75	984.89 ± 127.76

In the hand lay-up method, discontinuous and randomly distributed mat was used and nearly 20% fiber volume fraction was obtained in the produced composite plate. Tensile strength for this plate is around 50 MPa but a 20% deviation in strength and module values is interesting. The reason of this phenomenon is considered as air voids in the plate, which weaken the structure. Figure 2 shows the air voids within the composite plate structure produced by hand lay-up method.



Figure 2. The air voids between the fibers of the composite plate produced by hand lay-up method and resin-rich regions.

Also in the structure produced by random distributed felt, fibers are gathered during the resin impregnation, which causes resin-rich regions to occur, and the homogeneity of the structure is deteriorated. This can be considered as another factor for the deviation between the values. No air void is left in the composite plate structure produced by RTM molding method so structure is more dense. Fiber volume fraction is about 18% in the RTM-1 composite plates produced by continuous felt. The volume fraction of this plate is lower compared with the hand lay-up method but tensile strength is 12% higher and elasticity module is 50% higher. This shows that the stiffness of the continuous felt reinforced composite plate produced by RTM method is higher. Besides the low standard deviation, shows the homogeneity of the structure.

Continuous mat reinforced RTM composites are a good solution for obtaining high strength and high stiffness at the same time. However due to the high cost of continuous mats, they are used together as hybrid with discontinuous felts in RTM process while producing the parts for automotive industry. Practical applications have shown that if discontinuous random distributed felts are used in RTM process, fibers disintegrate during resin injection, which prevents a homogenous structure to be obtained. For this reason, stitched discontinuous randomly distributed felts have been developed. These structures are generally suitable for resin injection but cannot be used alone. They are generally used together with the continuous felts. In the RTM-2 composite plate, 2 layers of stitched random distributed felts were used together with 1 layer of continuous randomly distributed felt. The fiber volume fraction in this felt is about 22%. Although this

ratio is 4% higher than RTM-1 composite plate, the increase in tensile strength is not significant. However, the elasticity module is 37% higher. But, there has been a 17% standard deviation in the module values of RTM-2 composites.

Although the fiber volume fraction of SMC-1 composite plate is 22%, the tensile strength has been determined around 35 MPa. As it is produced under high pressure, there are no air voids in the structure. However, in the SMC composition, important amount of calcium carbonate is used as filler besides fiber and resin. Calcium carbonate behaves as air voids in the structure and decreases the strength seriously. Figure 3, compares the SMC, hand lay-up and RTM composite. However, considering the elastic module value, it seems that calcium carbonate increases the stiffness. The fiber volume fraction in the SCM-2 plate is 28%. The 6% increase in the ratio, raised the tensile strength more than two times. However, the increase in elasticity module compared with SCM-1 is 24%. The decrease of filler ratio and increase of resin ratio, cause the ductility of the structure to increase slightly. Although there is a significant increase in strength due to glass fiber volume fraction, the same increase did not occur in the stiffness of the material.

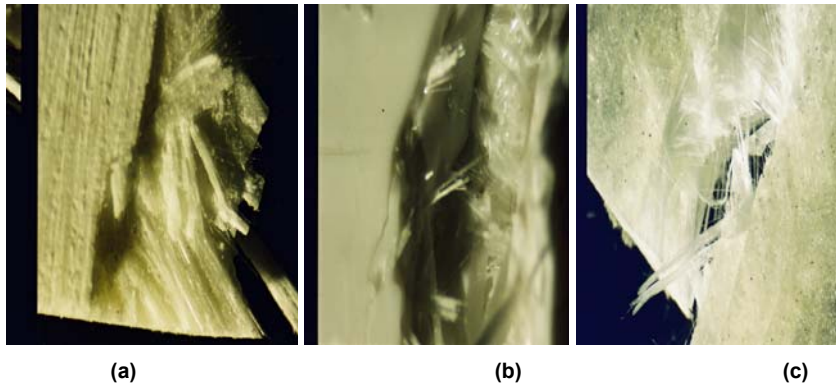


Figure 4. The comparison of surface and inner structures of SMC
(a) RTM (b) and hand lay-up (c) composites

3.2. Impact Strength

Most important performance parameters in automotive composites are impact strength and amount of energy required for fracture. Impact strengths of the materials produced for that purpose were determined by charpy test. Impact strengths were calculated by equation 5. The results are in Table 5. When the results are analyzed, it was seen that the minimum impact strength were obtained in SMC-1 composite material. According to this result, we can say that the high amount of filler decreases the toughness of the structure. In SMC composites, impact strength and toughness of the structure increases related with fiber volume fraction. Although there is important amount of air voids in composite plates produced by hand lay-up method, they have more impact strength compared with SMC-1 composite materials. However, there is around

30% of deviation in the impact strength values of the composites produced with hand lay-up method. The reason of this phenomenon is the resin-rich regions formed due to air voids and disordered distribution of fibers in the structure. Impact strength in RTM-1, continuous felt reinforced composite material is more than part produced with hand lay-up method despite of the lower fiber volume fraction. In RTM-2 composite part, 4% increase in fiber volume fraction causes 23% increase in fracture strength. A hybrid structure being used in RTM-2 composite material has some advantages. The stitched mat increase the fiber volume fraction and toughness while discontinuous mat prevents rupture after fracture and increases the ductility of the material at the same time. As a result, the energy amount for breaking these materials increases. In Figure 5, it can be seen that while fibers of discontinuous felt break completely after impact, thinner filaments of the continuous felt do not break and keep the structure as one piece.

Table 5. Impact strengths of the composite plates produced by Hand lay-up, RTM and SCM methods

Production Method	Fracture Energy- A_c (J)	Impact Strength- K_c (kJ/m ³)
Hand lay-up	1.16 ± 0.38	478.16 ± 155.73
RTM-1	1.18 ± 0.21	596.68 ± 102.92
RTM-2	1.61 ± 0.32	731.06 ± 145.46
SMC-1	0.64 ± 0.11	304.17 ± 51.45
SMC-2	1.39 ± 0.18	629.87 ± 84.74

Impact strengths and elasticity module values of the composite plates produced by Hand lay-up, RTM and SCM methods are compared in figure 6. As seen in the figure, impact strength increases similarly to module. However, this is not valid for SMC-1 plates. The toughness of the structure is very low due to excess filler amount in SMC-1 composite parts however by the 6% increase of the fiber volume fraction, the toughness and energy absorption capability of the structure increase approximately two times. In this case, we can say that the increase in the fiber volume fraction has the biggest effect in impact strength.

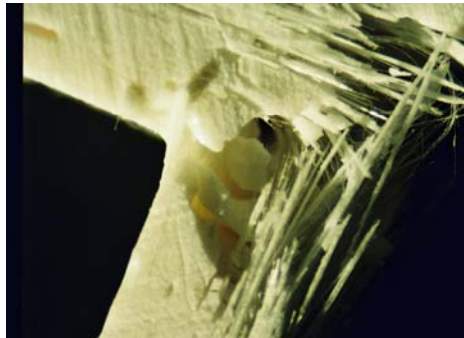


Figure 5. The fracture in RTM-2 composite part after impact

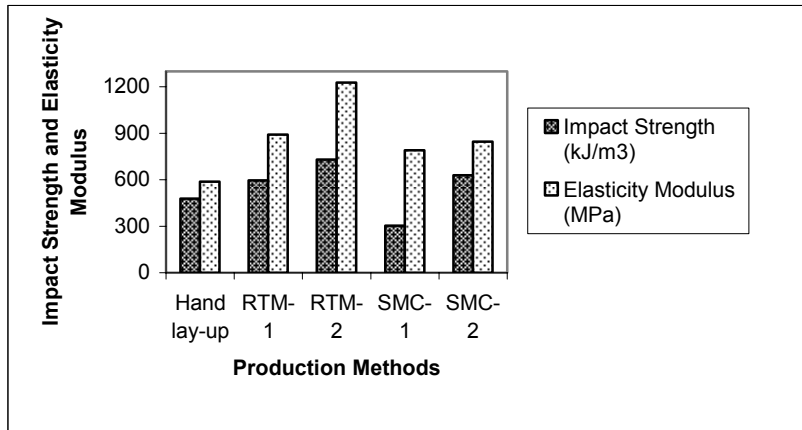


Figure 6. The impact strengths and elasticity modules of Hand lay-up, RTM and SCM composites

3.3. The Residual Strength after Impact

In automotive composites, one of the biggest problems in especially exterior body and bonnet parts, are the small bumps during parking. This causes small cracks in the composite parts and decreases the strength of the structure. In this study, this problem was simulated by low-speed weight drop method. The bending strength and module values of the weight dropped samples were determined by 3 point flexural bending test and losses in strength and module values were compared with parts on which no weight was dropped. Bending strength and module were calculated respectively by equation 3 and 4. Results are given in Table 6. According to these results, it can be seen that bend strength and module increase with increasing fiber volume fraction but there are losses in bending strength after the impact. Composite parts produced by hand lay-up method, have low bending strength but due to their ductile structure, bending strength loss after the impact is low. Besides, the bending strength in RTM composites have increased 3 times according to the 4% increase in fiber volume fraction. However, as the fiber volume fraction increases, the loss in bending strength after impact also increases. It is observed that bending strength is halved in RTM-2 composite parts. However, it is interesting that the decrease in bending module is limited. The displacement value decreasing at the same time with decreasing strength limits the change in module. This phenomenon can be clearly observed in the load-displacement curve in figure 7. The cracks occurred in the structure after weight drop, decreases the elasticity of the structure and rupture occurs where cracks are gathered (Figure 8). In this case, bending and displacement amount decrease.

Table 6. The 3 point bending test results of composite plates produced by hand lay-up, RTM and SMC methods (% Diff. : % Difference)

Production method	Bending (Mpa)	Strength.- σ_{CF}	% Diff.	Bending (Mpa)	Module- E_{CF}	% Diff.
	Non-impacted	Impacted		Non-impacted	Impacted	
Hand lay-up	28.92±7.2	27.01±7.5	6.6	658±132	621±137	5.6
RTM-1	25.83±2.8	21.08±4.2	18.3	1143±86	1086±94	4.9
RTM-2	76.53±4.8	34.56±5.1	54.8	2276±287	2162±264	5
SMC-1	15.27±2.5	15.11±2.2	1.04	976.9±72	922±86	5.5
SMC-2	50.88±6.1	42.34±5.7	16.8	1687±182	1618±195	4.1

In SMC composites, with the 6% increase in the fiber volume fraction, bending strength increases 3 times. Loss in bending strength also increases after impact due to increase in fiber volume fraction but this loss is not as much as the losses in RTM composites. The decrease in bending modules is around 5% like the others. As a result, we can say that while fiber volume fraction increases, the bending strength increases but bending strength losses after impact also increases. Besides, important changes do not occur in bending module after impact.

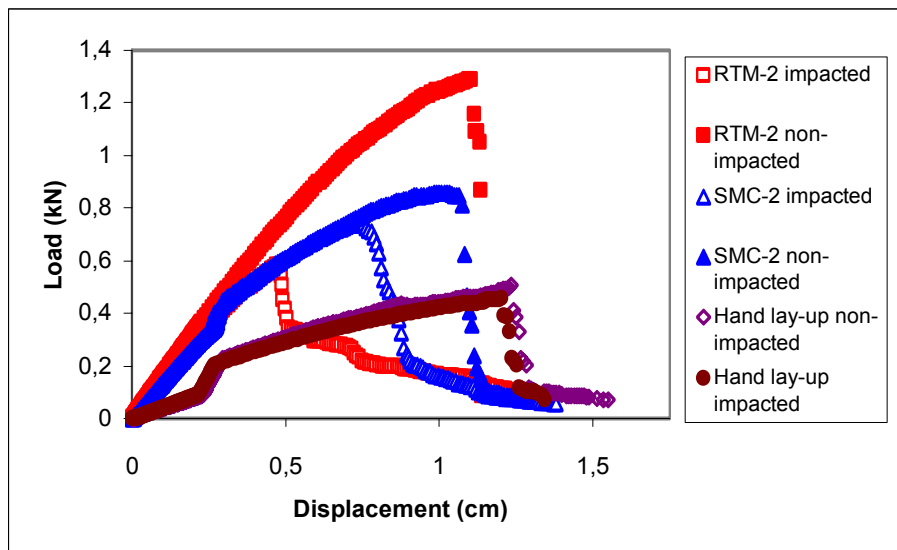


Figure 7. Load-displacement results of the 3 point bend test results applied on impacted and non-impacted samples



Figure 8. Cracks occurring on the surface after weight drop
(brown powder is placed on cracks in order to make them more visible).

4. CONCLUSION

Following conclusions were obtained from these studies:

- With increasing fiber volume fraction values, mechanical properties and impact strength increase. However, calcium carbonate used as a filler, decreases the mechanical properties and impact strength of composite structure and makes the structure more brittle.
- It is very difficult to maintain homogeneity in composite parts produced by hand lay-up method. The mechanical performances of such parts are limited and they should not be used in important places where strength is required.
- The mechanical properties of composite parts produced with RTM method increase related with fiber volume fraction. Such parts can be used in places where high performance is required. Their energy absorbing capability and impact strengths are higher compared with composites produced by hand lay-up and SCM methods. However RTM composites lose most of their strengths after impact.
- Mechanical properties develop in SCM composites related with fiber volume fraction. However due to the high filler amount in its structure, compare to RTM composites, mechanical properties and energy absorbing capability decrease more when fiber volume fraction is low. As fiber volume fraction increases, these disadvantages decrease. Besides, the strength losses of SMC composites after impact are less than RTM composites.
- Although strength losses occurred after impact, losses in modules were very limited.

ACKNOWLEDGEMENT

We would like to thank to Arpacilar Ltd. Sti. for supplying the materials used in this research and for production of the composite plates

REFERENCES

1. Hazen J.R., Musselman M., Black S., Automotive Composites, Ray Publishing Inc., Wheat Ridge, CO, 2006.
2. Lovins A., Hypercars: The Next Industrial Revolution, Proceedings of the 13th International Electric Vehicle Symposium, p. 113-120, Osaka, Japan, 1996
3. Brylawski M., "Uncommon Knowledge: Automotive Platform Sharing's Potential Impact on Advanced Technologies", SAMPE-ACCE-DOE Advanced Composites Conferences, p: 293-308, September 27-28 1999.
4. Kindervater C., "Crash Resistance and Strength of High Performance Composite Light Vehicle Substructure", ISATA (International Symposium on Advanced Transportation Applications), p. 741-751, Aachen Germany, 1994.
5. McConnel V., "Future Cars Take Shape with Composites", Reinforced Plastics, Vol:43, No:5, p. 44-48, May 1999.
6. Jacop A., "Chrysler Rethinks the Composite Car", Reinforced Plastics, Vol:41, No:11, December 1999.
7. Hartness T., Humsan G., "The Evaluation of a New Process to Produce Low Cost, High Performance Fiber Reinforced Thermoplastic Composites", 45th International SAMPE Symposium, p. 2070-2080, 21-25 May 2000.
8. Brast K., "The Direct Strand-Deposition Process-New Methods in Compression Molding of Long Fiber Reinforced Thermoplastics", 45th International SAMPE Symposium, p. 2357-2368, 21-25 May 2000.
9. Hodgkin J.H., Rabu N., "A New Development in High Speed Composite Fabrication for Aerospace, Automotive and marine Application", 45th International SAMPE Symposium, p. 2274-2282, 21-25 May 2000.
10. Cam Elyaf Sanayi A.Ş., "CTP (Cam Takviyeli Plastik) Teknolojisi, www.camelyaf.com.tr
11. Simunović S. and Lee H.K., "Damage Behaviour of Aligned and Random Fiber Reinforced Composites For Automotive Applications", SAMPE-ACCE-DOE Advanced Composites Conferences, September 27-28 1999, pp: 196-203.
12. Santulli C.; Brooks R.; Long A.C.; Warrior N.A.; Rudd C.D., "Impact properties of compression moulded commingled E-glass-polypropylene composites" Plastics, Rubber and Composites, Vol:31, No:6, p.270-277, 2002.
13. Piry M., Michaeli E.h.W., "Stiffness and Failure Analysis of SMC Components Considering the Anisotropic Material Properties", 45th International SAMPE Symposium, p. 2344-2356, 21-25 May 2000.
14. Oldenbo M., Fernberg S.P., Berglund L.A., "Mechanical behaviour of SMC composites with toughening and low density additives" Composites: Part A, Vol:34, p. 875-885, 2003.
15. Gregl BV, Larson LD, Sommer M, Lemkie JR. "Formulation advancements in hollow- glass filled SMC". SAE Technical paper series, no 1999-01-0980; 1999.
16. Ming-Fa S., Yung-Kun L., Yu-Hwey C., "The Process Development for Composite Electric Bus Body Using Resin Transfer Molding Technology", 45th International SAMPE Symposium, p. 2332-2344, 21-25 May 2000.
17. Kim P.J., Lee D.G., "Surface quality and shrinkage of the composite bus housing panel manufactured by RTM", Composite Structures, Vol: 57, p. 211-220, 2002.

18. Huang MC, Tai CC. "The effective factors in the warpage problem of an injection-molded part with a thin shell feature", Journal of Material Processing and Technology, Vol:110, p. 1-9, 2001.
19. Vu-khanh T, Do-thanh V. "Predicting Shrinkage in polyester reinforced by glass fabrics" Journal of Composite Materials , Vol 34, No: 12, p.998-1008, 2000.
20. Jain LK, Lutton BG, Mai YW, Paton R. "Stresses and deformations induced during manufacturing. Part II: a study of the springin phenomenon", Journal of Composite Materials, Vol:31, No:7, p.696-719, 1997.
21. Kikuchi H, Koyama K. "Generalized warpage parameter", Polymer Engineering Science, Vol:36 No:10, p.1309-1316, 1996.
22. Geier M.H., Quality Handbook for Composite Materials, Chapman&Hall, London, 1994.

INVESTIGATION OF PROCESSING CONDITIONS ON THE MORPHOLOGY AND PROPERTY ENHANCEMENT IN EXTRUSION-CAST HDPE-CLAY NANOCOMPOSITE FILMS

A. ESFANDIARI ¹, M.HAJILARI ²

¹ Islamic Azad University, Department of Textile, Young Researchers Club

² Islamic Azad University, Department of Textile

ABSTRACT

High density polyethylene (HDPE) nanocomposite was extrusion cast into films, and the effect of decreasing film thickness on the orientation of intercalated clay layers is studied. The effect on the pseudo-static and dynamic tensile properties is investigated. Change in the morphology of the nanocomposite film due to deformation during tensile measurement is discussed and related to the tensile properties. A model to theoretically predict the tensile modulus based on the degree of platelet orientation is developed and compared to data.

Key Words: Conditions, nanocomposite, extrusion, clay, film.

1. INTRODUCTION

Recently, much effort has been made towards development of polymer-clay nanocomposites, and to understand the enhancement in properties upon addition and dispersion of organo-clay in polymers. Reports have mentioned that orientation of the clay layers, the polymer structures and their relative orientation with respect to each other could play an important role in property enhancement [1-4 and 16]. In order to change the orientation of both polymer and clay structures, and relate the change to the property enhancement, various studies have used injection molding, due to its ability to generate high degree of shear on the melt [1, 3, and 5]. Dynamic mechanical properties and tensile properties are a few of the most commonly studied properties [6-10].

2. EXPERIMENTAL

2.1. Materials

Natural montmorillonite treated with quaternary ammonium salt (Cloisite 20A, Southern Clay Products) was used as reinforcement, maleic anhydride grafted polyethylene (Mw = 79900 g/mol, Mw/Mn = 4.9 and MA content = 2 %) (PEMA) was used as a compatibilizer and high density polyethylene (Mw = 139200 g/mol, Mw/Mn = 9.13, MI = 0.3 g/10min and density = 0.95 g/cc) was used as a base resin for preparing polyethylene-clay nanocomposite.

2.2. Preparation of Nanocomposite

In order to obtain a uniform mixing between the clay (powder), PEMA (pellets) and HDPE (pellets) the pellets were ground into a 35 mesh powder using a large 1000lbs capacity grinder. Master batch (MB12) containing 10 wt. % clay, 20 wt. % PEMA and 70 wt. % HDPE was made by melt mixing the powders in a large Banbury mixer. The clay to compatibilizer ratio was 1:2. The temperatures in the mixer varied from 220-300 °F and the rotor speed was set at 120 rpm. The partially melted mixture from the mixing zone of the Banbury mixer was extruded into thin strands using a single screw extruder and then pelletized. The temperatures in the extruder varied from 220-300 °F and the screw speed was set at 18 rpm.

The pellets of the master batch, MB12, were then let down into HDPE using a Berstorff twin screw extruder. Nanocomposite HD510 with 5 wt. % organo-clay and 10 wt. % compatibilizer loading was made from the master batch MB12. HDPE containing no clay and compatibilizer, HD000, was also passed through the twin screw extruder and pelletized in order to maintain similar processing history on all the resins. The temperature in the extruder varied from 360-405 °F from zone 1 to zone 9 and was 370 °F in the die. The screw speed was maintained at 195 rpm. The nanocomposites were extruded into thin strands and then finally pelletized using a pelletizer. The final composition of the 3 samples is shown in table 2.1.

Table 2.1. Composition of the nanocomposites

Sample designation	Composition (wt. %)		
	Clay	PEMA	HDPE
HD000	0	0	0
HD510	5	10	85

2.3 Extrusion Film Casting

Resin HD000 and HD510 were cast into films using an OCS extrusion cast line fitted with a coat-hanger die of 20 mil (0.49 mm) die gap. From each resin four different films varying in thickness were made by changing the draw down ration (DDR). The effect of varying the DDR on the orientation of clay in these films and its effect on the properties was studied. DDR of 20:1, 8:1, 5:1 and 2.5:1 was used for casting 1, 2.5, 4 and 8 mil films respectively. The temperature in the extruder varied from 356°F-365 °F and was 372 °F at the die. The temperature of the chill roll was 90 °F. The films cast from base resin HD000 and nanocomposite HD510 are designated as HD000X and HD510X respectively where X is the film thickness.

2.4. Characterization

2.4.1. Small Angle X-Ray Scattering

Since in this study our aim was to relate the orientation of the modified clay structures to the property enhancement in the nanocomposite films, and

since 2D SAXS measurements can give data on the orientation and dispersion of the modified clay structures, only SAXS 2D measurements were conducted on an x-ray instrument described previously [11]. The 2D measurements are useful in determining both size and relative orientation of modified clay and polymer lamellae structures in the polymer-clay nanocomposite films. The films were laid over one another, to form a 2 mm thick stack, for measurement. Care was taken that the films were stacked in such a manner that all the films in a stack had their machine direction (MD), transverse direction (TD) and normal direction (ND) aligned.

2.4.2 Dynamic Mechanical Analysis

Dynamic mechanical analysis of the materials was carried out using TA instruments, DMA Q800 to study the mechanical transitions in the temperature range from -150°C to 50°C at 1 Hz frequency. The samples were first cooled down to -150°C and then the temperature was raised at a rate of 3°C/min. The change in storage modulus, loss modulus and $\tan \delta$ along the sample machine direction (MD) was studied. Samples of size 1 ¼ in. length and ¼ in. width were cut along MD in the films. The ratio of storage modulus, loss modulus and $\tan \delta$ for all the nanocomposite films to that of the corresponding HDPE films was then plotted against temperature to study the change as a function of temperature. This kind of analysis gives a clear picture of the effect of change in morphology, due to change in temperature, on the change in properties.

2.4.3 Tensile Properties

The tensile properties of the films along the MD were studied. The tensile strengths and elongation at yield and at break were obtained in accordance to ASTM D882 and 1% secant modulus was obtained in accordance to ASTM E111 using Sintech1S universal tensile testing machine.

3. RESULTS AND DISCUSSION

3.1. 2-D Small Angle X-Ray Scattering (SAXS)

3.1.1 SAXS Analysis

In order to study the 3D orientation of various structures in the nanocomposite films, x-ray measurements need to be carried out for at least two orientations of the sample with respect to the x-ray beam as shown in figure 2.1 and described in previous chapter. Projections are designated by the three principal sample axes, M, machine direction, T, transverse direction and N, normal direction. Figure 2.1 shows the three sample orientations used for the SAXS measurements. Corrected 2D SAXS patterns for the different orientations are shown in Figure 2.2. The sample orientations are designated with reference to Figure 2.1.

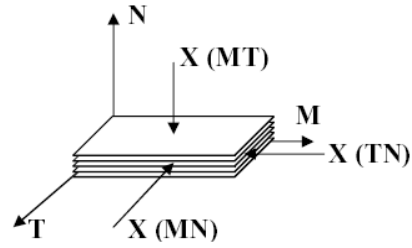


Figure 2.1. Orientation MT, MN and NT with the x-ray beam normal to the MT, MN and NT plane of the sample respectively.

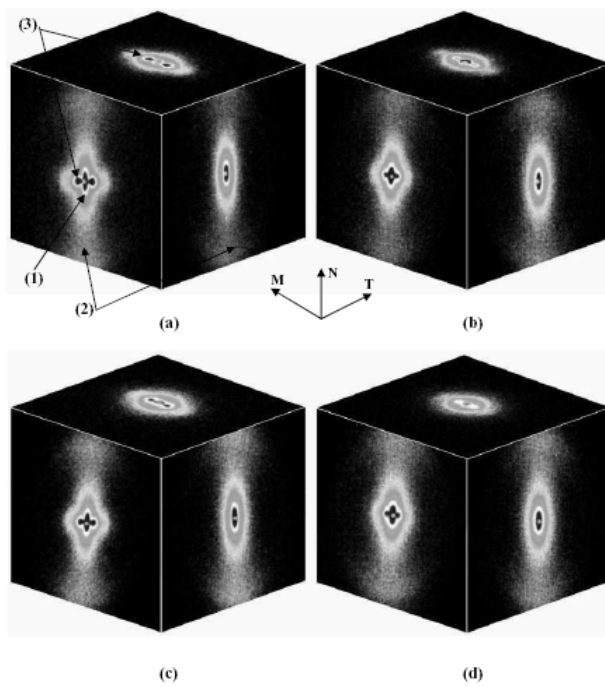


Figure 2.2. 2-D SAXS patterns for orientation MN (left face), NT (right face) and MT (top face) of films a) HD510 CF 1, b) HD510 CF 2.5, c) HD510 CF 4 and d) HD510 CF 8. The numbers in parenthesis represent the reflections from (1) Clay tactoid (002) planes, (2) Intercalated clay (002) planes and (3) Polymer lamellar (002) planes. The sample orientations are designated with reference to Figure 2.3.

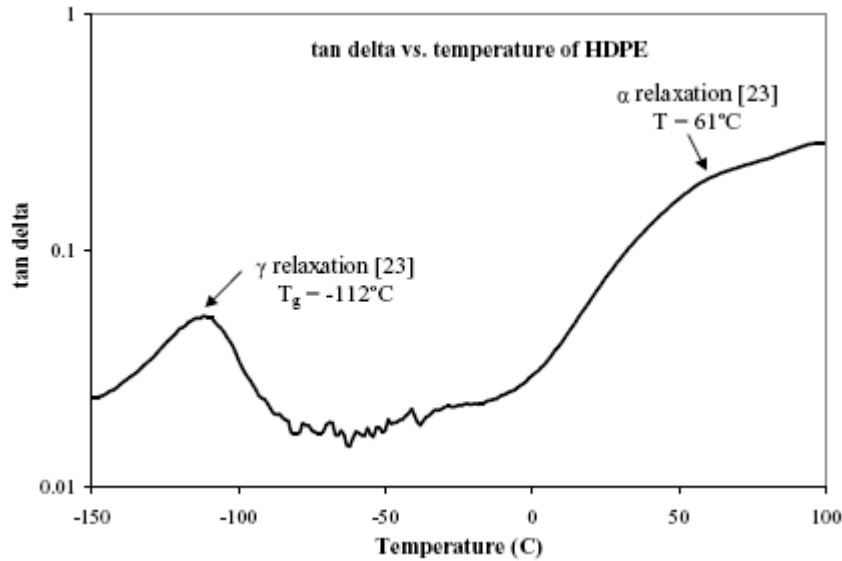


Figure 2.3. Tan delta plot of HDPE.

For the TN and MT orientations, the radial average of the 2D patterns (figure 3.8) yield figure 2.4 [11], showing the intensity versus scattering vector $q = 4\pi [\sin(\theta/2)]/\lambda$, where θ is the scattering angle and $\lambda = 1.542\text{\AA}$ is the wavelength. The d-spacing is calculated using Bragg's law. The radial plots obtained from the SAXS measurements give data on periodicity (dispersion) of a) intercalated clay platelet (002) planes and b) polymer lamellae (002) planes similar to [11].

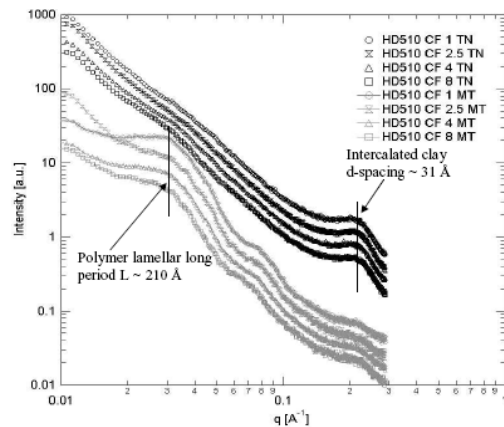


Figure 2.4. SAXS Log-log radial plots for HD510 CF 1 and HD510 CF 4 in orientation MT and TN. Here L represents the polymer lamellar long period and d represents the spacing of the intercalated/modified clay in the nanocomposite films.

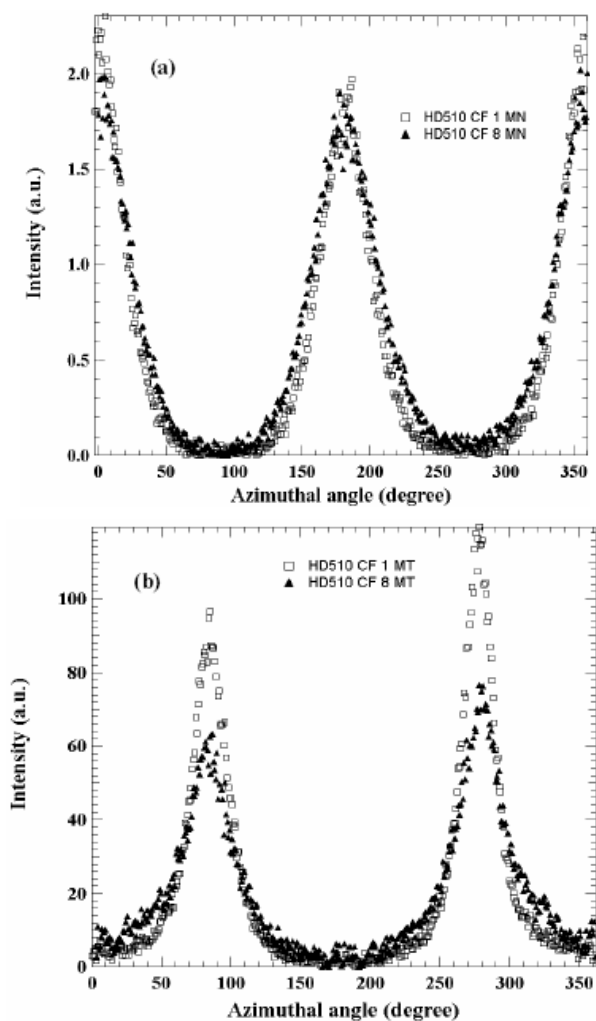


Figure 2.5. Azimuthal plot for films HD510 CF 1 and HD510 CF 8 showing the orientation of a) intercalated clay (002) plane normals in the MN orientation and b) polymer lamellar (002) plane normals in the MT orientation. For any periodic structure, the sharpness of the azimuthal peak reflects the extent of orientation.

For the MN and MT orientations the azimuthal average of the 2D patterns yield figure 2.5, showing intensity as a function of azimuthal angle (Φ) similar to [11]. For each sample orientation, azimuthal plots for clay and polymer lamellar can be made. Figures 2.5 a and 2.5b compare the orientation data obtained from SAXS for the intercalated clay platelets and polymer lamellar structures respectively in films HD510 CF 1 and HD510 CF 8. The azimuthal plots for films HD510 CF 2.5 and HD510 CF 4 lie between those of films HD510 CF 1 and HD510 CF 8 and were not plotted in figure 2.5 for the

reasons of clarity. For any periodic structure, the sharpness of the azimuthal peak reflects the extent of orientation.

The azimuthal plot (figure 2.5) can be used to calculate the average cosine square of the normal to the plane of reflection [11] for the particular projection. For example, the MN planar projection, $\langle \cos^2 \Phi_{MN} \rangle$, can be calculated by,

$$\langle \cos^2(\phi_{MN}) \rangle = \frac{\int_0^{2\pi} I(\phi_{MN}) \cos^2(\phi_{MN}) d\phi_{MN}}{\int_0^{2\pi} I(\phi_{MN}) d\phi_{MN}}$$

The Φ_{MN} value from orientation MN is used along with Φ_{TN} value from orientation TN, or Φ_{MT} value from orientation MT, to determine the 3D orientation of the structural normals to the intercalated clay layers, or polymer lamellar planes, respectively in the three principle film axes represented by Φ_M , Φ_T and Φ_N using the calculations presented earlier [11]. Values of the angle and the cosine square of the angle made by normal of the intercalated clay platelet (002) planes and polymer lamellar (002) planes, with MD, TD and ND of all nanocomposite films is presented in table 2.2.

Table 2.2. Values of angle and cosine square of angle made by the normal of intercalated clay platelet (002) planes (extension: clay) and polymer lamellar (002) planes (extension: poly), with MD, TD and ND in all films.

Sample	HD510 CF 1	HD510 CF 2.5	HD510 CF 4	HD510 CF 8
$\langle \cos^2 \Phi_M \rangle$ clay	0.117	0.140	0.171	0.225
$\langle \cos^2 \Phi_T \rangle$ clay	0.132	0.139	0.134	0.15
$\langle \cos^2 \Phi_N \rangle$ clay	0.751	0.722	0.694	0.626
$\langle \Phi_M \rangle$ clay	69.98	68.05	65.53	61.71
$\langle \Phi_T \rangle$ clay	68.65	68.14	68.5	67.2
$\langle \Phi_N \rangle$ clay	29.97	31.82	33.56	37.71
$\langle \cos^2 \Phi_M \rangle$ poly	0.841	0.790	0.732	0.655
$\langle \cos^2 \Phi_T \rangle$ poly	0.084	0.110	0.162	0.170
$\langle \cos^2 \Phi_N \rangle$ poly	0.075	0.100	0.106	0.176
$\langle \Phi_M \rangle$ poly	23.52	27.24	31.19	35.99
$\langle \Phi_T \rangle$ poly	73.09	70.63	66.28	65.65
$\langle \Phi_N \rangle$ poly	74.11	71.58	70.95	65.22

The average cosine square projection of the structural normals from the 'i' axis, $\langle \cos^2 \Phi_i \rangle$ can be used in a Wilchinsky triangle [12-14] (Figure 2.6).

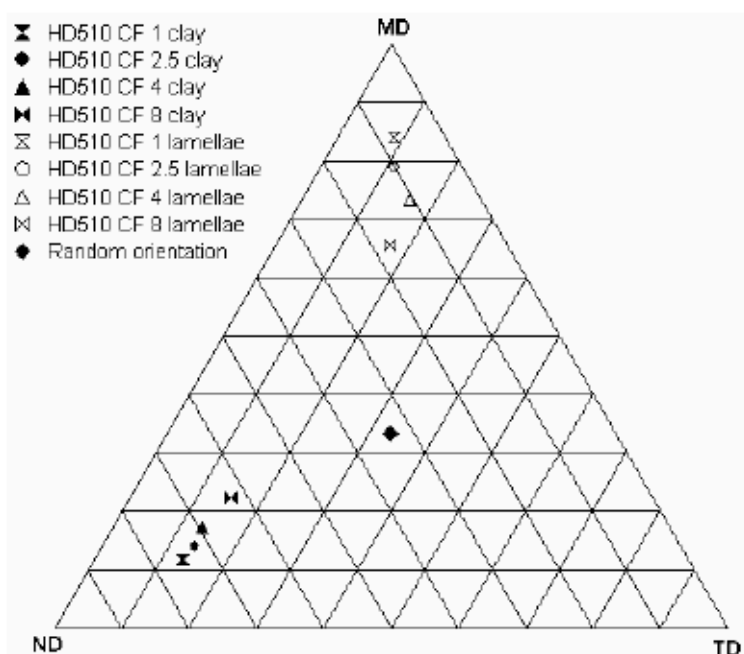


Figure 2.6. Wilchinsky triangle [12-14] for average normal orientation of intercalated clay (002) plane (filled markers), and polymer lamellar (002) planes (unfilled markers) in all the films examined here. For a randomly oriented sample a point in the center results.

The Wilchinsky triangle is a ternary plot that graphically displays the average direction of the structural normal orientation with a single point. It is constructed by counting from the opposite side of a direction 'i' the value of $\langle \cos^2 \Phi_i \rangle$ and making a point where the three $\langle \cos^2 \Phi_i \rangle$ values intersect. For a randomly oriented sample $\langle \cos^2 \Phi_M \rangle = \langle \cos^2 \Phi_N \rangle = \langle \cos^2 \Phi_T \rangle = 0.333$ and a point in the center of the Wilchinsky triangle results (circle, figure 2.6). For perfect orientation of a plane in MT the normal points in the N direction and a point at the ND corner results.

CONCLUSION

High density polyethylene (HDPE) nanocomposite was extrusion cast into films, and the effect of decreasing film thickness on the orientation of intercalated clay layers is studied. The orientation of intercalated clay platelet normals and polymer lamellar (002) plane normals in the nanocomposite films increased along the film ND and MD respectively with decreasing thickness or increasing draw down ratio (DDR).

Pseudo-static and dynamic mechanical properties of all the films were studied and related to the intercalated clay platelet orientation. Percent increase in the tensile strength at yield and at break for the nanocomposite films increased non-linearly and linearly, respectively, with decreasing film thickness. Change in the morphology of the nanocomposite films due to deformation during tensile measurement was discussed and related to the tensile properties. A model to theoretically predict the tensile modulus based on the degree of platelet orientation was developed and compared to data. Increase in the storage modulus ratio and decrease in $\tan \delta$ ratio was observed with decreasing film thickness which indicated increased reinforcement with decreasing film thickness.

In all 4 nanocomposite films the intercalated clay platelet dispersion remained the same while their degree of orientation along the film MD varied considerably. Significant difference observed in the tensile and dynamic mechanical properties of the nanocomposite films, of different thickness, indicated the importance of considering the orientation of the clay layers along with its dispersion for understanding the structure property relationship in polymer-clay nanocomposite systems. Although Bicerano *et al.* [15] recently developed models and predicted that the relative modulus of the nanocomposite with respect to the base resin would increase with increasing orientation of the clay basal plane normal along the ND, our study is the first of its kind to experimentally demonstrate the relationships between processing condition, orientation, and the tensile and dynamic properties.

REFERENCES

1. K. Varlot, E. Reynaud, G. Vigier, J. Varlet (2002) "Mechanical properties of clay-reinforced polyamide", *J. Polym. Sci. Part B: Polym. Phys.*, 40, 272-283.
2. T. Fornes, P. Yoon, H. Keskkula, D. Paul (2001) "Nylon 6 nanocomposites: the effect of matrix molecular weight", *Polym.*, 42, 9929-9940.
3. Y. Kojima, A. Usuki, M. Kawasumi, A. Okada, T. Kurauchi, O. Kamigaito, K.Kaji (1995) "Novel preferred orientation in injection-molded nylon 6-clay hybrid", *J. Polym. Sci., Polym. Phys.*, 33, 1039-1045.
4. R. Krishnamoorti, K. Yurekli (2001) "Rheology of polymer layered silicate nanocomposites", *Current Opinion in Colloid Interface Sci.*, 6, 464-470.
5. K. Varlot, E. Reynaud, M. Kloppfer, G. Vigier, J. Varlet (2001) "Clay-reinforced polyamide: Preferential orientation of the montmorillonite sheets and the polyamide crystalline lamellae", *J. Polym. Sci., Polym. Physc.*, 39, 1360-1370.
6. M. Jisheng, Q. Zongneng, H. Youliang (2001) "Synthesis and characterization of polypropylene/clay nanocomposites", *J. App. Polym. Sci.*, 82, 3611-3617.
7. M. Alexandre, G. Beyer, C. Henrist, R. Cloots, A. Rulmont, R. Jerome (2001) "Preparation and properties of layered silicate nanocomposites based on ethylene vinyl acetate copolymers", *Macromol. Rapid. Commun.*, 22, 643-646.
8. N. Ogata, G. Jimenez, H. Kawai, T. Ogihara (1997) "Structural and
9. thermal/mechanical properties of poly (lactic)-clay blend", *J. Polym. Sci., Polym.Physc.*, 35, 389-396.

10. A. Oya, Y. Kurokawa (2000) "Factors controlling mechanical properties of clay/polypropylene nanocomposites", *J. Mater. Sci.*, 35, 1045-1050.
11. Q. Zhang, Y. Wang, Q. Fu (2003) "Shear induced change of exfoliation and orientation in polypropylene/montmorillonite nanocomposites", *J. Polym. Sci., Polym. Phys.*, 41, 1-10.
12. A. Bafna, G. Beaucage, F. Mirabella, S. Mehta (2003) "3D hierarchical orientation in polymer-clay nanocomposite films", *Polym.*, 44, 1103-1115.
13. A. Bafna, G. Beaucage, F. Mirabella, G. Skillas, S. Sukumaran (2001) "Optical properties and orientation in polyethylene blown films", *J. Polym. Sci., Polym. Phys.*, 39, 2923-2936.
14. R. Roe (2000) "In: methods of X-ray and neutron scattering in polymer science", Oxford University Press, NY, 199.
15. L. Alexander (1985) "In: X-ray diffraction methods in polymer science", R. E.Krieger Publications: Florida, 245.
16. D. Brune, J. Bicerano (2002) "Micromechanics of nanocomposites: comparison of tensile and compressive elastic moduli, and prediction of effects of incomplete exfoliation and imperfect alignment on modulus", *Polym.*, 43, 369-387.
17. A.H. Esfandiari;H.Nazokdast;A-S. Rashidi;M-E. Yazdanshenas (2007) "Investigation of Effect of Organoclay and Compatibilizer on Microstructure and Mechanical Properties of PP/PA6/Montmorillonite Nanocomposite", 6th International Conference of Textile Science (TEXSCI 2007), Liberec, Czech Republic, Book of Abstracts, pp:31-32.

DESIGN AND COMPUTATION OF WOVEN TEXTILE COMPOSITE STRUCTURES UNDER IMPACT CONDITIONS

İ. KAYNAK

Dumlupınar University, Faculty of Technical Education, Department of Mechanical Education

ABSTRACT

The aramide fiber textiles of woven composite structures in terms of their strength is a complex task because many different woven types are involved in the damage and fracture to which these materials are subjected. The woven and unidirectional patterns are investigated for theoretical estimations and simulation approximations are contributed to impact behaviors of design and computation textile composite structures. The several of damage mechanisms and its evolution models make it extremely difficult to estimate the strength margins. The designs of woven textile composite structures patterns are simulated and computation part is completed with the analytically. The strategy adopted in the study on designing unidirectional laminated composite structures is based on the choice of materials (woven and unidirectional plies) and the use of simple models (focusing on the fracture of the first ply) with which industrial impact structural analysis can be carried out. The choice of woven textile composite materials does not only depend upon mechanical criteria but also on the simplicity of the corresponding modeling procedures.

Keywords: Woven aramide fibers, Woven Textile Design, Textile composites.

1. INTRODUCTION

Composites are designed to achieve unique high strength, high stiffness, superior performance characteristics and lightweight materials for structural applications, not possible with traditional material production methods. Ability of woven textile composite structures to have controlled damage deformation under impact condition and can be also crucial for design and computation of laminated composite structure' applications (e.g. shock absorbers, displacement gauges, pressure and force).

By using advanced technologies in a number of different weave architectures in the field of woven textile composites that have been improved a number of weaving methods to produce multilayer, structural performs which have three dimensional fiber architectures.

There are many type of woven and unidirectional textile composite components, however, are fabric manufactured using the widely available of their reinforcements, thanks to good formability characteristics. In the composite structural applications, impact loads can be classified into three sections: one of them is low velocity impact, second one is high velocity impact and the last one is hyper velocity impact. The reason of this classification, energy transfer between the target and projectile, energy

dissipation and damage propagation mechanism under drastic changes as the velocity of projectile changes [1]. A large variety of the orientation of fibers architectures is dependent both on the initial fiber geometry adopted during weaving and also on the effects of at every point on the plane woven or unidirectional fibers.

Rose and Sierakowski [2] studied the effects of impacts exerted by conical head impactors and observed delamination in glass epoxy plates by using a powerful light source. It has been shown that 3D woven composites have unique mechanical and physical properties compared with their 2D counterparts [3, 4].

They have a reasonable cost due to their relatively simple resin impregnation process [5] and high performance because of their resistance to delamination [6, 7].

2. EXPERIMENTAL

In the graphs the segments which emanate from the center in a radial direction represent the magnitudes of stresses; positive quantities are indicated outward from the center in Figure 1. The broken curves are graphs of the stresses in isotropic plates under same conditions. The schematic representation of woven unit cell of a fabric structure can be seen in Figure.2, where a typical woven structure is shown the warp (lengthwise) and fill (crosswise) yarns forming the fabric make angle $\alpha \geq 0$ with the plane of the fabric layer.

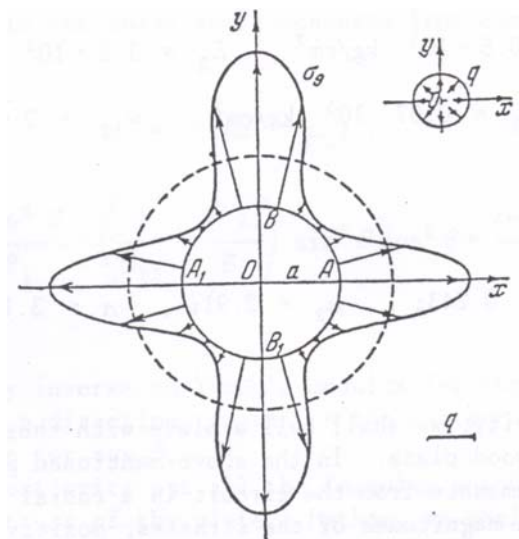


Figure. 1. A normal pressure is distributed uniformly along the edge of the cavity, q is the pressure per unite area. [1]

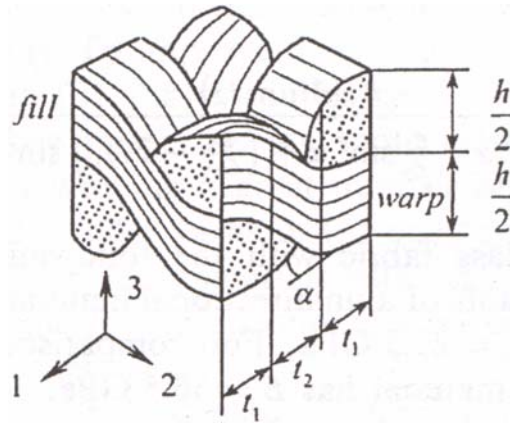


Figure 2. Micro-structural model are chosen as a unit cell of a fabric structure of woven textile composites. [2]

A normal pressure is distributed uniformly along the edge cavity in Figure. 1 and the stresses is given by

$$\sigma_{\theta} = q(E_{\theta}/E_1) [\mu_1\mu_2 + n(\sin^2\theta - \mu_1\mu_2 \cos^2\theta) + (1+(\mu_1)^2)(1+(\mu_2)^2) \sin^2\theta \cos^2\theta] \quad (1)$$

and q is the pressure per unit area. For an isotropic plate $\sigma_{\theta} = q$. In an orthotropic plate the stresses can be seen at the above equation (1), are distributed along the contour non uniformly [8]. In this study, the first layer of the textile composite layer under high velocity impact perforation is represented with experimentally. Therefore the results are compared with analytical solution are directly convenient to the results and can be seen at the Figure 3.

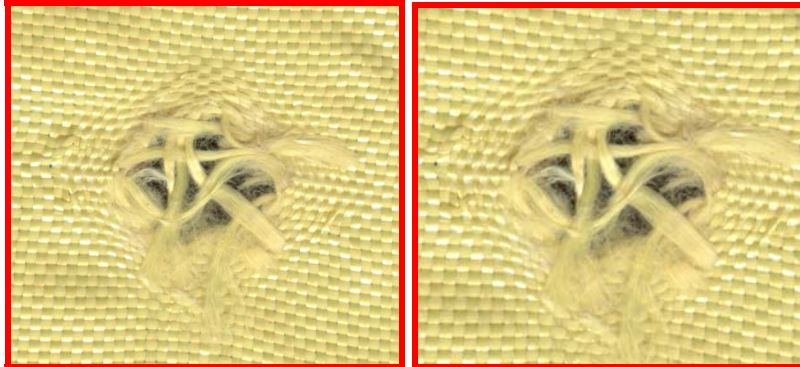


Figure.3 Micro-structural model and unit cell in front of view are chosen as a unit cell of a fabric structure of woven textile composites.

The experimental results in Figure.3 and in Figure.4 can be seen easily in the perforation first layer parts are chosen two types of views can be seen that therefore analytically and theoretically convenient in Figure.1 and in Figure 2.

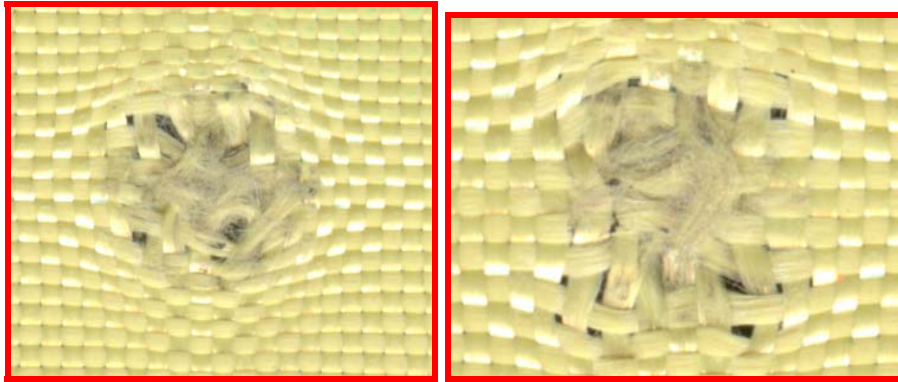


Figure 4. Micro-structural model and unit cell in back of view are chosen as a unit cell of a fabric structure of woven textile composites.

3. CONCLUSION

The high velocity impact properties were tested. In the Figure .1, indicates the distribution of the stresses along the contour of the cavity in woven textile first plate composites (the direction of the x -axis is parallel to the grain). The maximum value of the stress σ_0 is equal to approximately three times bigger than q and is obtained at points B (y - direction) upper and down B_1 . The minimum stress occurs only near $0.1q$.

REFERENCES

1. Naik N.K. , Shrirao P., Reddy B.C.K., Ballistic impact behavior of woven fabric composites: Formulation, Int. J. of Impact Engineering, 2006,(32),p.1521-1552.
2. Hosseinzadeh R., Shokkrieh M. M., Lessard L., Damage behavior of fiber reinforced composite plates subjected to drop weight impacts, Composites Science and Technology, 2006, (66), p. 61-68.
3. J. Brandt et all. , Manufacture and performance of carbon/epoxy 3D woven composites. In. Proceedings of the 37th international SAMPE symposium, Anaheim, CA, 1992.
4. Brandt J., Drechsler K., Arendts F.J., Mechanical performance of composites based on various three-dimensional woven-fiber performs. Composite science and Technology,1996, (56), p.381-386.
5. Tan P. et all., Composite: Part A., 2000., (31), p. 259-271.
6. Mouritz A.P. et all., rewiev of applications for advanced three-dimensional fibre textile composites., Composite: Part A., 1999., (30), p. 1455-11461.
7. Chow TW., Ko F.K., Textile structural composites. Distributors for the U.S. and Canada. Amsterdam (NY, USA) Elsevier science: 1989.
8. S.G. Lekhnitskii "The theory of elasticity of an anisotropic elastic body", p.166-167, Holden-Day Inc., California, 1963.

Figures:

- 1-S.G. Lekhnitskii "The theory of elasticity of an anisotropic elastic body", p.163-174, Holden-Day Inc., California, 1963.
- 2-Valery V. Vasiliev, Evgeny V. Morozov "Mechanics and analysis of composite materials", p.205-212, Elsevier Science, Oxford, UK., 2001

NANOSTRUCTURED TEXTILE SURFACES USING PLASMA COATINGS

D.HEGEMANN

Empa, Swiss Materials Science & Technology

ABSTRACT

Nanostructured surfaces are of great interest, since they provide a high surface area. A high functionality can thus be obtained by ultrathin coatings. Plasma polymerization of hydrocarbons mixed with reactive gases was used in a regime where both deposition and etching processes took place yielding a nanoporous, crosslinked network with accessible functional groups. Using plasma co-sputtering of a silver target, Ag nanoparticles can be in-situ embedded within the growing plasma polymer yielding a well-defined size and distribution of nanoparticles at the coating surface. Hence, an anti-microbial activity was achieved. Multifunctional textile surfaces can thus be obtained by adjusting combined properties such as wettability, functional group density as well as anti-bacterial and bio-responsive surfaces.

1. INTRODUCTION

The formation of nanostructured surfaces gained high interest due to their large surface area which might yield a highly functional surface. The main approach is the incorporation of nanoparticles into wet-chemical coatings or compounds. However, some difficulties during the handling of nanoparticles (agglomeration, nano toxicology) and concerning the distribution of nanoparticles at the surface as well as mechanical durability occur. Nanoporous structures, on the other hand, which can be obtained by plasma polymerization/etching processes might avoid these issues and yield an even higher surface area [1,2]. Furthermore, nanoparticles with homogeneous size and spatial distribution can also be embedded in-situ by a plasma polymerization/co-sputtering process.

Products made with the help of textiles and fibers become more and more sophisticated and "multifunctional". Tailored surface modifications are required to meet customer needs and to assure a share in the market.

Plasma treatment as a dry and eco-friendly technology, is offering an attractive way to add new functionalities such as water repellence, long-term hydrophilicity, mechanical, electrical and antibacterial properties as well as biocompatibility due to the nano-scaled modification on textiles and fibers [1]. At the same time, the bulk properties as well as the touch of the textiles remain unaffected.

Therefore, we investigated gases mixtures of hydrocarbons mixed with ammonia within low pressure RF discharges to obtain nanoporous coatings by controlling the rivaling deposition/etching processes and to incorporate Ag nanoparticles from a silver target during film growth [3].

2. EXPERIMENTAL

RF plasma reactors working at 13.56 MHz coupled to an internal electrode were used for plasma polymerization. Beside a cylindrical batch reactor with plane parallel electrodes (\varnothing 30 cm), a reel-to-reel web coater with a rotating drum (\varnothing 58 cm, 65 cm wide) used as electrode and an air-to-air fiber coater with an RF antenna, where the fibers are led several times through the plasma zone, are present at Empa to demonstrate industrial scale-up. Plasma polymers of amino-functionalized hydrocarbons were deposited on Si wafer, glass slides, and textile fabrics/fibers at a pressure of 10 Pa and varying C_2H_2 or C_2H_4/NH_3 ratio and energy input. A silver target was used for co-sputtering by addition of Ar to the gas discharge.

3. RESULTS AND DISCUSSION

As it is well-known, plasma polymerization – that means radical-promoted – processes are governed by the composite parameter power input per gas flow, which relies on the concept of macroscopic kinetics [4]. Therefore, the energy input into the active plasma zone can be used to control plasma polymerization processes.

By the admixture of ammonia (NH_3) to hydrocarbon discharges (e.g. C_2H_2 , C_2H_4) etching processes are introduced depending on the NH_3/C_xH_y ratio, which leads to a reduction in deposition rate. Thus, regimes of rivaling deposition/etching were identified which generated nanoporous plasma coatings consisting of a crosslinked hydrocarbon network with nitrogen functional groups (a-C:H:N). Fig. 1 shows the topography of a nanoporous plasma coating indicating voids, which are smaller than 25 nm, within a branched plasma polymer network. These coatings were found to be mechanically stable and durable.

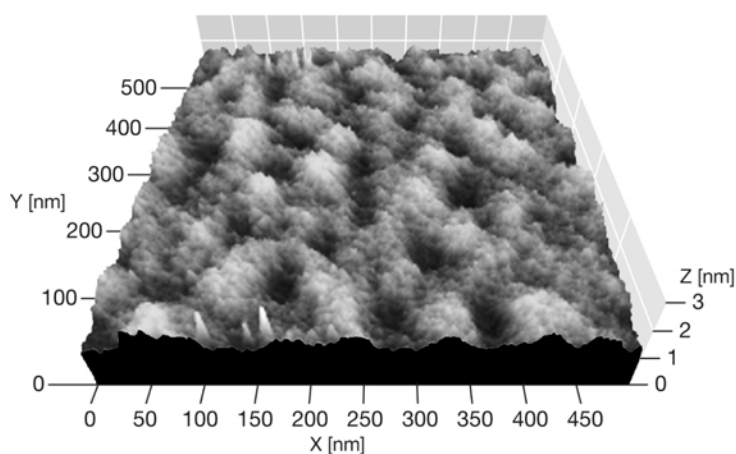


Figure 1. AFM topography of a nanoporous a-C:H:N plasma coating

However, further analyses were required to prove the nanoporous character and to show the formation of functional groups. Therefore, we used dyeing of plasma coated PET fabrics by acid dyes (C.I. Acid Blue 127:1) that can be attached to amine groups (within the a-C:H:N coatings), whereas PET fabrics are not colored by these dye stuffs. We found that the color intensity linearly increased with the film thickness. Therefore, it can be assumed that the dye molecules enter the entire film thickness through connected voids within the crosslinked plasma polymer network [5].

Using plasma sputtering metallizations can be applied to fabrics and fibers to obtain an anti-static treatment and conductive fibers [6]. A homogeneous all-side treatment assures a good electrical conductivity by maintaining the textile properties of yarn and monofilament fibers. However, for anti-microbial activity monovalent Ag ions are required which can be solved from the surface [7]. Thus, a high surface area with respect to the bulk (metallic) silver is advantageous that can be given by nanoparticle embedding.

Especially, co-sputtering of silver during plasma polymerization enables the controlled incorporation of Ag nanoparticles into a functional plasma polymer matrix such as a-C:H:N in a one-step process inducing an anti-bacterial activity. Homogeneous size and spatial distributions of nano particles were obtained by plasma polymerization/co-sputtering (Fig. 2). Hence, nanostructured, multifunctional textile surfaces can be achieved regarding wetting properties, type and density of functional groups as well as bio activity.

However, suitable plasma reactors and scalable processes are required for an economical treatment of textiles. The scale-up of plasma processes is thus an important issue and was demonstrated using continuous web/fiber coaters [2,8]. The presented plasma coatings are not limited to textile substrates, but can be applied to other surfaces as well.

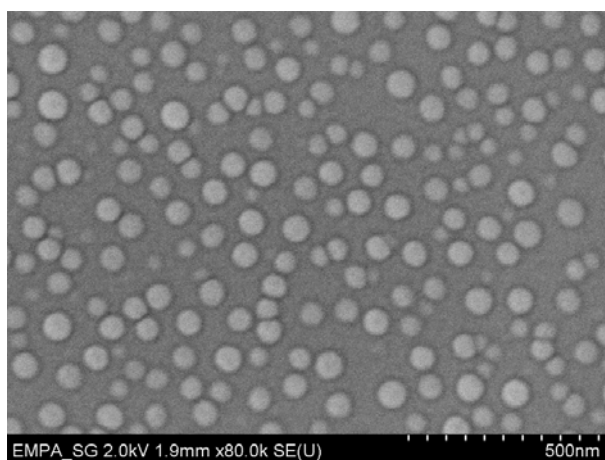


Figure 2. Distribution of Ag nanoparticles within a-C:H:N plasma coating (HRSEM picture)

4. CONCLUSIONS

While using RF discharges with hydrocarbons, the growth mechanism of plasma-polymerized a-C:H coatings can be modified by admixture of NH₃ to induce etching processes during deposition. Rivaling deposition/etching processes thus supported the generation of nanoporous, highly crosslinked plasma coatings containing accessible functional groups. Co-sputtering of a silver target with Ar enabled the in-situ incorporation of Ag nanoparticles within the functional plasma polymers (a-C:H:N) to add anti-microbial properties. A homogeneous distribution of Ag nano particles present at the coating surface was obtained. Low amounts of silver incorporation was proven to be antimicrobial, yet allowing cell growth. Hence, the deposition of plasma coatings using combined deposition/etching/sputtering processes enabled the formation of multifunctional surfaces.

REFERENCES

1. D. Hegemann, Indian J. Fib. Text. Res. 31 (2006) 99.
2. D. Hegemann, D.J. Balazs, in: Plasma Technologies for Textiles, ed. R. Shishoo, Woodhead Publ., Cambridge, 2007.
3. D. Hegemann, M.M. Hossain, E. Körner, D.J. Balazs, Plasma Process. Polym. 4 (2007) 229.
4. A. Rutscher, H.-E. Wagner, Plasma Sources Sci. Technol. 2 (1993) 279.
5. D. Hegemann, M.M. Hossain, D.J. Balazs, Progr. Org. Coatings 58 (2007) 237.
6. M. Keller, A. Ritter, P. Reimann, V. Thommen, A. Fischer, D. Hegemann, Surf. Coat. Technol. 200 (2005) 1045.
7. D.J. Balazs, K. Triandafillu, P. Wood, Y. Chevolot, C. van Delden, H. Harms, C. Hollenstein, H.J. Mathieu, Biomaterials 25 (2004) 2139.
8. D. Hegemann, in: Plasma Polymers and Related Materials, ed. M. Mutlu, Hacettepe Univ., Ankara, 2005, p.191.

NANOSTRUCTURED TEXTILE SURFACES USING PLASMA COATINGS

D.HEGEMANN

Empa, Swiss Materials Science & Technology

ABSTRACT

Nanostructured surfaces are of great interest, since they provide a high surface area. A high functionality can thus be obtained by ultrathin coatings. Plasma polymerization of hydrocarbons mixed with reactive gases was used in a regime where both deposition and etching processes took place yielding a nanoporous, crosslinked network with accessible functional groups. Using plasma co-sputtering of a silver target, Ag nanoparticles can be in-situ embedded within the growing plasma polymer yielding a well-defined size and distribution of nanoparticles at the coating surface. Hence, an anti-microbial activity was achieved. Multifunctional textile surfaces can thus be obtained by adjusting combined properties such as wettability, functional group density as well as anti-bacterial and bio-responsive surfaces.

1. INTRODUCTION

The formation of nanostructured surfaces gained high interest due to their large surface area which might yield a highly functional surface. The main approach is the incorporation of nanoparticles into wet-chemical coatings or compounds. However, some difficulties during the handling of nanoparticles (agglomeration, nano toxicology) and concerning the distribution of nanoparticles at the surface as well as mechanical durability occur. Nanoporous structures, on the other hand, which can be obtained by plasma polymerization/etching processes might avoid these issues and yield an even higher surface area [1,2]. Furthermore, nanoparticles with homogeneous size and spatial distribution can also be embedded in-situ by a plasma polymerization/co-sputtering process.

Products made with the help of textiles and fibers become more and more sophisticated and “multifunctional”. Tailored surface modifications are required to meet customer needs and to assure a share in the market.

Plasma treatment as a dry and eco-friendly technology, is offering an attractive way to add new functionalities such as water repellence, long-term hydrophilicity, mechanical, electrical and antibacterial properties as well as biocompatibility due to the nano-scaled modification on textiles and fibers [1]. At the same time, the bulk properties as well as the touch of the textiles remain unaffected.

Therefore, we investigated gases mixtures of hydrocarbons mixed with ammonia within low pressure RF discharges to obtain nanoporous coatings by controlling the rivaling deposition/etching processes and to incorporate Ag nanoparticles from a silver target during film growth [3].

2. EXPERIMENTAL

RF plasma reactors working at 13.56 MHz coupled to an internal electrode were used for plasma polymerization. Beside a cylindrical batch reactor with plane parallel electrodes (\varnothing 30 cm), a reel-to-reel web coater with a rotating drum (\varnothing 58 cm, 65 cm wide) used as electrode and an air-to-air fiber coater with an RF antenna, where the fibers are led several times through the plasma zone, are present at Empa to demonstrate industrial scale-up. Plasma polymers of amino-functionalized hydrocarbons were deposited on Si wafer, glass slides, and textile fabrics/fibers at a pressure of 10 Pa and varying C_2H_2 or C_2H_4/NH_3 ratio and energy input. A silver target was used for co-sputtering by addition of Ar to the gas discharge.

3. RESULTS AND DISCUSSION

As it is well-known, plasma polymerization – that means radical-promoted – processes are governed by the composite parameter power input per gas flow, which relies on the concept of macroscopic kinetics [4]. Therefore, the energy input into the active plasma zone can be used to control plasma polymerization processes.

By the admixture of ammonia (NH_3) to hydrocarbon discharges (e.g. C_2H_2 , C_2H_4) etching processes are introduced depending on the NH_3/C_xH_y ratio, which leads to a reduction in deposition rate. Thus, regimes of rivaling deposition/etching were identified which generated nanoporous plasma coatings consisting of a crosslinked hydrocarbon network with nitrogen functional groups (a-C:H:N). Fig. 1 shows the topography of a nanoporous plasma coating indicating voids, which are smaller than 25 nm, within a branched plasma polymer network. These coatings were found to be mechanically stable and durable.

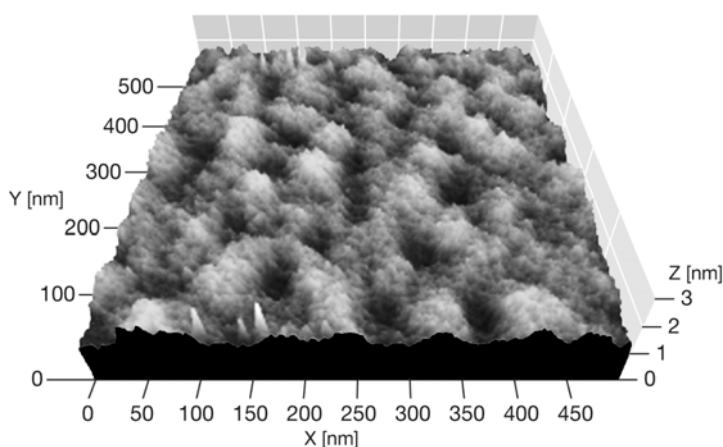


Figure 1. AFM topography of a nanoporous a-C:H:N plasma coating

However, further analyses were required to prove the nanoporous character and to show the formation of functional groups. Therefore, we used dyeing of plasma coated PET fabrics by acid dyes (C.I. Acid Blue 127:1) that can be attached to amine groups (within the a-C:H:N coatings), whereas PET fabrics are not colored by these dye stuffs. We found that the color intensity linearly increased with the film thickness. Therefore, it can be assumed that the dye molecules enter the entire film thickness through connected voids within the crosslinked plasma polymer network [5].

Using plasma sputtering metallizations can be applied to fabrics and fibers to obtain an anti-static treatment and conductive fibers [6]. A homogeneous all-side treatment assures a good electrical conductivity by maintaining the textile properties of yarn and monofilament fibers. However, for anti-microbial activity monovalent Ag ions are required which can be solved from the surface [7]. Thus, a high surface area with respect to the bulk (metallic) silver is advantageous that can be given by nanoparticle embedding.

Especially, co-sputtering of silver during plasma polymerization enables the controlled incorporation of Ag nanoparticles into a functional plasma polymer matrix such as a-C:H:N in a one-step process inducing an anti-bacterial activity. Homogeneous size and spatial distributions of nano particles were obtained by plasma polymerization/co-sputtering (Fig. 2). Hence, nanostructured, multifunctional textile surfaces can be achieved regarding wetting properties, type and density of functional groups as well as bio activity.

However, suitable plasma reactors and scalable processes are required for an economical treatment of textiles. The scale-up of plasma processes is thus an important issue and was demonstrated using continuous web/fiber coaters [2,8]. The presented plasma coatings are not limited to textile substrates, but can be applied to other surfaces as well.

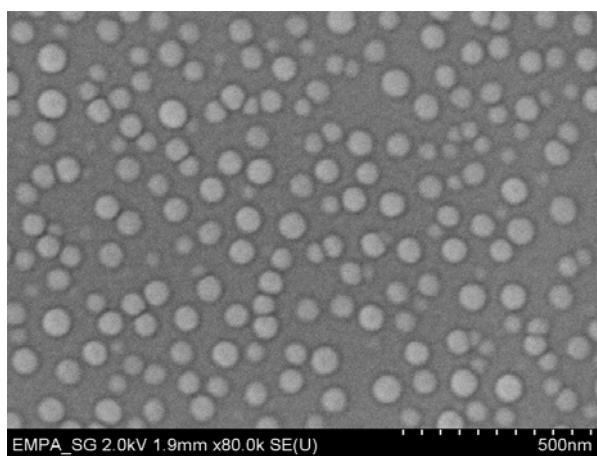


Figure 2. Distribution of Ag nanoparticles within a-C:H:N plasma coating (HRSEM picture)

4. CONCLUSIONS

While using RF discharges with hydrocarbons, the growth mechanism of plasma-polymerized a-C:H coatings can be modified by admixture of NH₃ to induce etching processes during deposition. Rivaling deposition/etching processes thus supported the generation of nanoporous, highly crosslinked plasma coatings containing accessible functional groups. Co-sputtering of a silver target with Ar enabled the in-situ incorporation of Ag nanoparticles within the functional plasma polymers (a-C:H:N) to add anti-microbial properties. A homogeneous distribution of Ag nano particles present at the coating surface was obtained. Low amounts of silver incorporation was proven to be antimicrobial, yet allowing cell growth. Hence, the deposition of plasma coatings using combined deposition/etching/sputtering processes enabled the formation of multifunctional surfaces.

REFERENCES

1. D. Hegemann, Indian J. Fib. Text. Res. 31 (2006) 99.
2. D. Hegemann, D.J. Balazs, in: Plasma Technologies for Textiles, ed. R. Shishoo, Woodhead Publ., Cambridge, 2007.
3. D. Hegemann, M.M. Hossain, E. Körner, D.J. Balazs, Plasma Process. Polym. 4 (2007) 229.
4. A. Rutscher, H.-E. Wagner, Plasma Sources Sci. Technol. 2 (1993) 279.
5. D. Hegemann, M.M. Hossain, D.J. Balazs, Progr. Org. Coatings 58 (2007) 237.
6. M. Keller, A. Ritter, P. Reimann, V. Thommen, A. Fischer, D. Hegemann, Surf. Coat. Technol. 200 (2005) 1045.
7. D.J. Balazs, K. Triandafillu, P. Wood, Y. Chevolot, C. van Delden, H. Harms, C. Hollenstein, H.J. Mathieu, Biomaterials 25 (2004) 2139.
8. D. Hegemann, in: Plasma Polymers and Related Materials, ed. M. Mutlu, Hacettepe Univ., Ankara, 2005, p.191.

CONDUCTING POLYMER COATED FABRICS FOR POTENTIAL APPLICATIONS IN MICROWAVE FREQUENCIES: A STUDY OF ELECTROMAGNETIC PROPERTIES

E. HÅKANSSON¹, A. KAYNAK²

¹ Centre for Materials and Fiber Innovation, Geelong Technology Precinct, Deakin University

² School of Engineering and Information Technology, Deakin University

ABSTRACT

The microwave reflection, transmission and complex permittivity of para-toluene-2-sulfonic acid doped conducting polypyrrole (PPy/pTSA) coated Nylon-Lycra textiles in the 1-18 GHz frequency were investigated. The real part of permittivity increased with polymerization time and dopant concentration, reaching a plateau at certain dopant concentration and polymerization time. The imaginary part of permittivity showed a frequency dependent change throughout the tested range. All the samples had higher values of absorption than reflection. The total electromagnetic shielding effectiveness exceeded 80% for the highly pTSA doped samples coated for 3 hours.

Keywords: Polypyrrole, Permittivity, Aging, Electromagnetic Interference Shielding, Microwave frequencies

1. INTRODUCTION

Conducting polymers may be used as alternatives to some commonly used metallic shielding materials. In contrast to metallic shielding materials, conducting polymers not only reflect but also absorb electromagnetic radiation in the microwave frequency range of 30 MHz to 30 GHz [1,2]. Conducting polymer coated textiles may have potential applications in the minimization of EMI interference by fabricating frequency selective fabric absorbers. A non-contact non-destructive free space method has been refined and used for investigations on thin and flexible specimens of sample sizes greater than 150 by 150 mm across broad microwave bandwidths [3]. Investigation of a range of materials with the free-space transmission method has yielded satisfactory results [4,5] while an extensive investigation of conducting textiles using this method was lacking. In this paper the reflection, transmission and complex permittivity of PPy/pTSA coated Nylon-Lycra textiles in the 1-18 GHz frequency were investigated using the free space transmission methods.

2. EXPERIMENTAL

2.1 Synthesis of Polypyrrole on Textile Substrates

A 0.53 mm thick double-sided basket-weave Nylon-Lycra® with an average Lycra content of 20% was used as substrate textile. After drying fabric

samples in a Binder FED 115 Lab oven at 105°C and cooling to room temperature, the samples were introduced into an aqueous solution containing pyrrole monomer (98%, Aldrich), the dopant para-toluene sulphonic acid (pTSA) (98%, Sigma-Aldrich), and the wetting agent Albegal FFA (Ciba) at a concentration of 0.01 % (w/w). Pyrrole was distilled under vacuum and used at a fixed concentration of 0.045 mol/l in all experiments. The oxidant ferric chloride hexahydrate (min 98%, Fluka) was added to the solution and a film of conducting polypyrrole was formed directly on the textile substrate through oxidative polymerization [6]. The optimized ratio of the oxidant ferric chloride hexahydrate (FeCl_3 , Aldrich) to monomer of 1:2.23 was used [7], resulting in a fixed concentration of 0.1 mol/l FeCl_3 , while pTSA was used in concentrations up to 0.036 mol/l. The synthesis was performed at room temperature with a varying polymerization times from 60 to 240 minutes. After PPy coating and drying, the samples were cut to size (305×305 mm or 500×500 mm) and stored at 20°C at 65 % RH.

2.1 Physical Characterization

A LEO 1530 FEG-SEM scanning electron microscopy (SEM) was used to perform a surface morphology study of the conducting textiles. Due to the sufficient conductivity of the polypyrrole coatings, no further conductive coating prior to imaging was necessary.

Fabric thickness measurements were made on preconditioned textile samples in a standard atmosphere using a textile thickness tester (DGTW01B, Mitutoyo, Japan) in accordance with ISO 9073-2 standard (0.5 kPa). The average thickness value from 20 measurements on each sample was used to obtain good accuracy. The original thickness of the uncoated substrate material was 0.53 mm. After in-situ polymerization, an approximate thickness of 0.53-0.55 mm was obtained. Fiber diameter measurements of the uncoated and coated fibers were carried out using an optical fiber diameter measurement analysis (OFDA) using an OFDA 2000, which uses optical image analysis to measure the fiber diameters of 2 mm snippets of fibers between two 70 mm square glass slides. A minimum of 35000 fibers from each sample were measured and averaged. Optical transmission microscopy analysis was performed on 8 μm microtome transverse sections of PPy coated fabric set in Technovit 7100 resin using an Olympus BX51 equipped with a DP12 camera (3.34 Mpixel).

The surface resistivity of the conducting fabrics was measured according to AATCC test method 76-1995 [8] using a 34401A multimeter (Agilent Technologies) after conditioning in a standard atmosphere (20°C, 65% RH). In the case of coated fabrics, rather than resistivity in Ω/m , surface resistivity R_s in Ω/sq ('ohms per square') is used to express the electrical property.

2.2 Dielectric Characterization

Permittivity of the conducting textile substrates was performed using a free space transmission method in conjunction with a mathematical diffraction reduction

method as described by Amiet [4]. The conducting textile sample was placed horizontally flat between two broadband DRG118-A horns operating in the 1-18 GHz frequency range. A radiation output system consisting of an 8510C vector network analyzer (Agilent Technologies) and an 8517A S-parameter test set (Agilent Technologies) with an 83651B synthesized frequency source (Agilent Technologies) generated a swept signal across the pre-set frequency range and collected the data from the measurement. The system covers the frequency range of 45 MHz to 50 GHz, where the vector network analyzer has a dynamic range of greater than 100 dB with resolutions of 0.01 dB in magnitude and 0.01 degrees in phase. Software written by Amiet controls the system and to improve accuracy of the permittivity measurements, the diffraction signal was removed using a mathematical method involving two Fast Fourier Transforms (FFT) and one inverse FFT [3]. A time-gate of 1.0 ns, using a Kaiser-Bessel window, was applied to the frequency domain measurement data, which was converted to time domain to include only signals that reached the output port within the predetermined amount of time. The system was calibrated at least every 5 minutes during the transmission measurements in order to adjust for changes in the ambient temperature and humidity with time.

The interaction of a material with electromagnetic fields can be characterized by complex permittivity ϵ^* (related to the electrical component of field), complex permeability μ^* (related to the magnetic component of field), and total (ac + dc) conductivity σ_{tot} . The relative complex permittivity ($\epsilon^* = \epsilon_0 \epsilon_r$ where $\epsilon_0 = 8.854 \times 10^{-12}$ F/m) of a material consists of a real part (ϵ'), mainly associated with amount of polarization occurring in the material, and an imaginary part (ϵ''), related to dissipation of energy in the material as per

$$\epsilon_r = \epsilon'_r + i\epsilon''_r \quad (1)$$

The shielding effectiveness (SE) in [dB] can be calculated as per [9]

$$SE = 10 \cdot \log_{10} (T[\%]/100) \quad (2)$$

A material is considered a good conductor if $\sigma_{tot} \gg -\omega\epsilon_0\epsilon_r$ and a good dielectric if $\sigma_{tot} \ll -\omega\epsilon_0\epsilon_r$ ($\sigma_{tot} > 0$). This inequality determines how to approximate the skin depth as shown

$$\text{For good conductors: } \delta \cong \sqrt{\frac{2}{\omega\mu_0\sigma_{tot}}} \text{ [m]} \quad (3)$$

$$\text{For good dielectrics: } \delta \cong \frac{2}{\sigma_{tot}} \sqrt{\frac{\epsilon'\epsilon_0}{\mu_0}} \text{ [m]} \quad (4)$$

In the case of the conducting polymers investigated $\sigma_{tot} \approx -\omega \epsilon_0 \epsilon_r$. The materials tested in this work are thin conductive films deposited on non-conductive fabrics, where the skin depth almost exclusively is larger than the total thickness of the material. The free space method used here produces information about the magnitude and percentages of all amounts of radiation being reflected, absorbed and transmitted through the fabric.

3 RESULTS AND DISCUSSION

3.1 Physical Characterization

The morphology of the Nylon-Lycra filaments coated with PPy-pTSA was smooth and free from cracks (Figure 1). As the polymerization time was increased, the amount of nodular particles on the surface increased. These nodular particles are not strongly adherent to the coating surface, and they can be minimized via control of the process parameters.

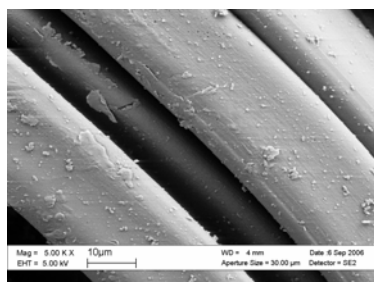


Figure 1. SEM images of PPy-pTSA (0.027 mol/l) coated Nylon Lycra. Polymerization time= 180 min.

A thin layer of conducting PPy on the filament is shown in Figure 2. When the elastomeric Lycra fibers are cut off for imaging, they contract slightly, thus causing wrinkling of the coating in the vicinity of the cut ends. The wrinkling, instead of cracking or delaminating of the conducting layer, indicates good adherence and elasticity of the applied coating.

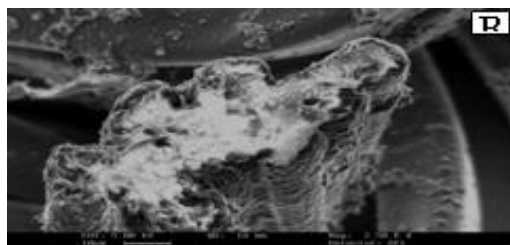


Figure 2. Micrograph of coated coated Lycra® fiber (B) ends. Polymerization time: 180 minutes, concentration 0.018 mol/l pTSA. Magnification: 2500 x. Scale bar = 10μm.

Upon coating by PPy doped with pTSA a color change occurs in the Nylon textile as can be seen in Figure 3. As the coating progressed the fabric colour changed from light grey (uncoated), to yellowish, towards and finally towards brown. The handle and flexibility of the fabric after coating were very close to that of the untreated fabrics. The PPy coatings had little influence on the mechanical properties of the substrate on which it was formed.

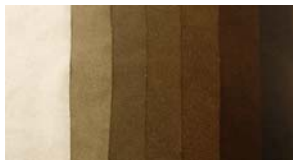


Figure 3. Color change in the PPy-pTSA coated Nylon-Lycra at different polymerization times. From left to right: Uncoated, 5 min, 15 min, 30 min, 60 min, 120 min, 300 min.

The color change of the fabric was accompanied by an increase in the fiber diameter as the polymerization time was increased. The fiber diameter analysis showed that the mean diameter of the pristine Nylon-Lycra fibers was $23.84 \pm 0.1 \mu\text{m}$. During polymerization, the mean fiber diameter increased with time as the polymer deposited on the fabric. The rate of mean fiber diameter increase was higher in the initial stages of polymerization and slower at longer polymerization times due to the higher polymer formation rate in the early stages of coating. The variation of coating thickness with

polymerization time was approximated by $d = \frac{1}{20}\sqrt{t}$, where, d is the

coating thickness in μm and t is the time in minutes. Optical transmission microscopy analysis showed that the coating of PPy surrounded each fiber (Fig.4). The coating was adherent to the fiber even after setting in resin, microtome sectioning and application onto glass slides. The thickness of the coating layer increased as the polymerization time increased and the appearance of bulk polymer (nodular) particles became more pronounced. At long polymerization times of 180 minutes or more, the coating started to crack due to its larger thickness and incipient brittleness, as indicated by arrow in Figure 4b.



Figure 4. Optical transmission microscope images of transverse sectioned Ppy-pTSA coated Nylon-Lycra with different polymerization times: 60 min (a), 90 min (b), 120 min (c) and 180 min (d). Scale bar = $50 \mu\text{m}$.

The surface resistivity as a function of concentration of pTSA at a set polymerization time showed that the surface resistivity dropped quickly as even small amounts of pTSA was added (Fig.5). The initial decrease in surface resistivity for FeCl_3 when compared with $\text{FeCl}_3 + 0.004 \text{ mol/l}$ pTSA was 65% (from 1010 to 350 Ω/sq). The surface resistivity continued to drop with an increase in dopant concentration, however at a much lower rate than at the initial drop.

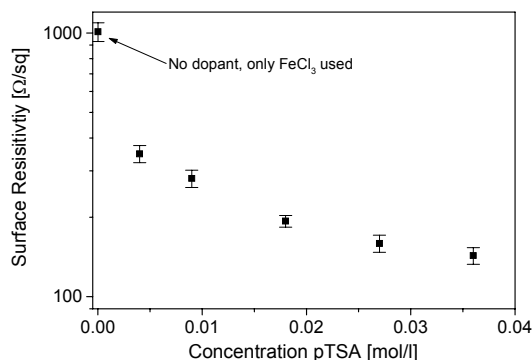


Figure 5. Surface resistivity versus dopant concentration for PPy-pTSA coated Nylon-Lycra. Polymerization time: 180 minutes.

3.2 Microwave Frequency Dielectric Characterization

3.2.1 Permittivity of Conducting Textiles

The imaginary part of permittivity was almost 200% larger for the long polymerization time than that of the short time (Fig.6). The difference in surface resistivity between the two samples was approximately one order of magnitude. The real part of permittivity was between 60% (0.027 mol/l) and 80 % (0.015 mol/l) higher for a long polymerization time than the short time. The increase in the real part of permittivity upon addition of larger amounts of dopant may be indicative of the added dopant actively taking part in the charge storage in the material. The same situation was present at the longer polymerization time, however the differences in magnitude between the different dopant concentrations were less pronounced. The smaller effects of higher dopant concentrations on the real part of permittivity at long polymerization times indicates that the increase in energy storage capacity may be possible only up to a certain level of added dopant. Above this concentration, the addition of further dopant ions does not contribute to any further capacitive behaviour of the material.

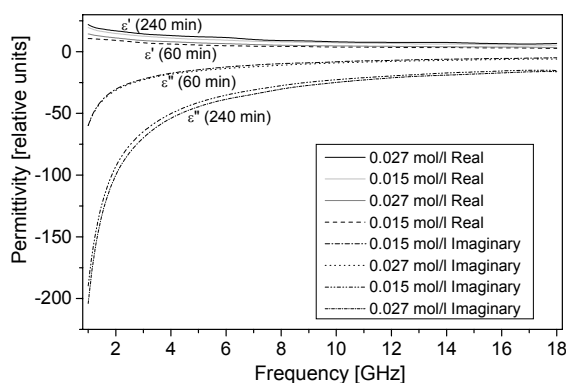


Figure 6. Permittivity response for PPY-pTSA coated Nylon-Lycra with 0.015 mol/l or 0.027 mol/l pTSA and 60 or 240 minutes polymerization time.

3.2.2 Reflection, Transmission and Absorption of Conducting Textiles

The results of reflection and absorption of PPy coated Nylon is in accordance with those of Kim et al up to 1.5 GHz. PPy-coated plain-weave PET fabrics had a reported contribution to shielding from absorption of up to 7% at frequencies up to 1.5 GHz. The absorption contributions to shielding obtained for PPy coated fabrics investigated here were up to 6 times higher. Another study of similar materials showed a maximum absorption of 33% at a resistivity of 2.85 S/cm at 1.5 GHz [10,11]. A common feature of the results is that the longer the polymerization time and the higher the dopant concentration, the lower the transmission and the higher the reflection in the conducting textile samples. The reflection values increase with an increase in frequency. This is expected because the higher frequency will have a smaller penetration depth of radiation and hence less interaction with the polymer. Results indicated that the *combination* of high values of both real and imaginary parts of permittivity were responsible for the resulting total shielding of radiation.

When pTSA was excluded, significantly lower value of reflection, and almost half the level of absorption was obtained. This is indicative of the dopant ions in the material actively contributing to the conductivity, which has been confirmed by published data [12,13]. The absorption increases by over 40% (average value over whole frequency range) with the addition of only small amounts of dopant ions. This is an effective way of improving the microwave absorption in PPy-coated fabrics. The absorption level for a sample doped with 0.018 mol/l pTSA was twice that of a sample with no additional dopant. The amount of reflection steadily increased with the increase in concentration of the dopant in the polymerization bath, reaching maximum levels of 31.36%, whereas the sample without dopant displayed an average reflection value of less than 5%. The transmission decreased with the

increase in the dopant concentration and frequency. Conversely, the reflection levels increased with frequency. Figure 7 shows the average values of reflection, transmission and absorption for samples with different dopant concentrations, but a constant polymerization time of 180 minutes.

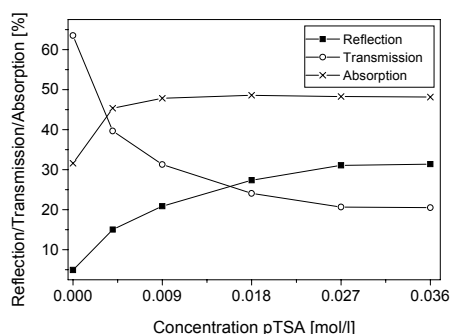


Figure 7. Reflection, transmission and absorption values for PPy-pTSA coated Nylon-Lycra in 1-18 GHz frequency range for different dopant concentrations. Polymerization time: 180 minutes.

As discussed above, the conductivity increased with an increase in the dopant concentration and/or polymerization time. There was an upper limit for the conductivity of PPy-coated textiles and some samples with long polymerization times would have approached their threshold conductivity. This is why the total transmission loss reached a plateau at polymerization times above 180 minutes and dopant concentrations beyond 0.027 mol/l.

The variations in total transmission loss with frequency decreased with an increase in dopant concentration, especially at long polymerization times. This is in accordance with previous reported results for PPy-loaded paper in the 2-18 GHz range. The transmission loss for the samples with a 60 minute polymerization time was the lowest, and an increase in total transmission loss was obtained when the polymerization time was extended. However, the increase in the total transmission loss at a very long polymerization time of 240 or 300 minutes was only a few percent higher compared to that obtained at 180 minutes.

4 CONCLUSION

The permittivity of PPy-coated textiles was measured using a free space transmission measurement technique over the frequency range 1–18 GHz. The measurements are relatively free from diffraction aberration, which indicates that the free space transmission measurement method is suitable for use with the flexible and thin conducting textiles. The real part of complex relative permittivity increased with polymerization time but stabilized after 120 minutes. The change in the real part of permittivity was not significant beyond 12 GHz irrespective of polymerization time. The imaginary part of

permittivity changed with an extension of the polymerization time and varied throughout the frequency range. The influence of an increase in dopant concentration on the permittivity response was also confirmed. Both the real and imaginary parts of permittivity remained stable above dopant concentrations of 0.018 mol/l pTSA.

The polymerization time, dopant concentration and choice of dopant influenced the permittivity and hence reflection, transmission, absorption as well as total shielding effectiveness of the conducting textiles. However, it was difficult to distinguish either of these two factors as being exclusively deterministic of shielding behaviour. All conducting Nylon-Lycra textiles had higher values of absorption than reflection. The highest absorption levels of around 48.27 % to 48.78 % are obtained for samples with a polymerization times of 120 or 180 minutes in combination with a dopant concentration of 0.018 or 0.027 mol/l pTSA. The shielding analysis showed that chemical structure influences the shielding effectiveness. The absorption dominated, considerably high shielding proves that conducting polymer coated textiles are good light-weight candidates as shielding materials.

REFERENCES

1. Kaynak, A., Unsworth, J., Beard, G.E. and Clout, R. *Mater. Res. Bull.* 1993; 28:1109-1125.
2. Kaynak, A. *Mater. Res. Bull.* 1996; 31(7):845-860
3. Amiet, A., *Free Space Permittivity and Permeability Measurements at Microwave frequencies.* (PhD Thesis), Monash University, Australia, 2003
4. Amiet, A. and Jewsbury, P. In *2000 Asia Pacific Microwave conference*. 2000. Sydney, NSW Australia Truong, V.-T., Riddell, S.Z. and Muscat, J. *Mater. Sci.* 1998; 33:4971-4976
5. Kaynak, A. and Beltran, R. *Polym. Int.* 2003; 52:1021
6. AATCC Technical Manual, Electrical resistivity of fabrics. 1996, American Association of Textile Chemists and Colorists. p. 100-101
7. Balanis, C.A., *Advanced Engineering Electromagnetics* John Wiley and Sons, 1989
8. Kim, M.S., Kim, H.K., Byun, S.W., Jeong, S.H., Hong, Y.K., Joo, J.S., Song, K.T., Kim, J.K., Lee, C.J., and Lee, J.Y. *Synth. Met.* 2002; 126:233-239
9. Lee, J.Y., Kim, H.K., Kim, M.S., Joo, J.S., Jeong, S.H., Kim, S.H., and Byun, S.W. In *American Chemical Society Division of Polymeric Materials, Science and Engineering Meeting 2002*. 2002
10. Rodriguez, J., Grande, H.-J. and Otero, T.F., Polypyrroles: from basic research to technological applications, In: H.S. Nalwa, Editor. 1997, John Wiley and Sons. p. 415-442
11. Nalwa, H.S., ed. Charge transport in conducting polymers. *Handbook of organic conductive molecules and polymers*, ed. H.S. Nalwa. Vol. 4. 1997, John Wiley and Sons
12. Håkansson, E., Lin, T., Wang, H. and Kaynak, A. *Synth. Met.* 2006; 156(18-20):1194-1202

SURFACE MODIFICATION AND CHARACTERIZATION OF COTTON AND POLYAMIDE FABRICS BY PLASMA POLYMERIZATION OF HEXAMETHYLDISILANE AND HEXAMETHYLDISILOXANE

B. KILIÇ¹, A. AKŞİT¹, M. MUTLU²

¹Dokuz Eylül University, Engineering Faculty, Textile Engineering Department

²Hacettepe University, Engineering Faculty, Plasma Aided Biotechnology and Bioengineering
Research Group (PABB)

Plasma, as a very reactive material, can be used to modify the surface of a certain substrate (typically known as plasma activation or plasma modification), depositing chemical materials (plasma polymerization or plasma grafting) to impart some desired properties, removing substances (plasma cleaning or plasma etching) which were previously deposited on the substrate. Plasma technologies offer a wide spectrum of possible treatments of materials. Plasma-chemical conversion of the feed gas produces chemically active particles that are able to modify textile surface molecules via chemical reactions after impinging on the surface. The radicals generated inside the plasma region must be given the opportunity to move to the reaction place at the textile fiber surface.

In the last few years, a great deal of work has been produced in the field of plasma deposition of organo-silicon compounds (SiO_x). The first target of these studies was the production of SiO₂-like films devoted to micro-electronics applications. However, plasma-deposited SiO₂-like materials are also characterised by other very important properties such as good biocompatibility, resistance to chemicals and abrasion. In addition to these silicone and silica based compounds are well known fire retardants and appear to work by a protective surface layer mechanism [1-4].

The aim of this study was the investigation of the influence of hexamethyldisiloxane (HMDSO) and hexamethyldisilane (HMDS) plasma conditions on the surface characteristics of cotton and polyamide fabrics being treated with plasma. For this purpose, 100% cotton and %100 polyamide fabrics were treated in the hexamethyldisiloxane and hexamethyldisilane plasmas. The modification of surfaces was carried out at low pressure (<100Pa) and low temperature (<50°C) plasma conditions. Plasma treatments were performed in PICO RF (radio frequency, 13.56

MHz) low pressure plasma system (Diener electronic GmbH + Co. KG, Germany). Variables of the processes were discharge power and exposure time. The changes in the characteristics of the cotton and polyamide fabrics were evaluated by FTIR-ATR analysis, contact angle measurements and vertical flammability tests.

100% cotton and 100% polyamide fabrics were used. The sample sizes of fabrics were 36 in warp and 22 cm in weft direction. Hexamethyldisiloxane and hexamethyldisilane (Aldrich Chemical) were used as monomers in radio frequency glow-discharge plasma system.

Plasma polymerization treatments were carried out in PICO RF (radio frequency-13.56 MHz) Plasma Polymerization System (Diener electronic GmbH + Co. KG, Germany). Power loss was minimized by means of a matching network. At first, the reactor was evacuated to 26-30 Pa and then monomer inlet was opened and monomer (HMDSO or HMDS) vapor was allowed to flow through the reactor. The details of the steps of the plasma treatment of fabrics were given in our previous paper [5]. Cotton and polyamide fabrics were modified in various plasma polymerization conditions (discharge power: 20, 40, 60 W and exposure time: 5, 10, 15 min). The effects of power and exposure time parameters on the contact angles and vertical flammability properties were evaluated by statistical software, MINITAB® for Windows. FTIR-ATR analyses were conducted to obtain the changes in surface structures after plasma treatments.

Contact angle of the fabrics were measured by KSV CAM 100 goniometer. Flame spread (in warp direction) times of the cotton and polyamide fabrics were evaluated according to TS 5569 EN ISO 6941 with vertical flammability tester. In this method, a vertical fabric with the sizes of 560 X 170 mm² is exposed to the flame of a horizontal burner at a distance of 2 cm from the short bottom side. The flame spread times to the marking threads at 24 cm, 39 cm and 54 cm distances from the bottom are recorded for the evaluation. However, our sample length was small than the length in the standard. Therefore, we could obtain only the flame spread time of the first thread at 24 cm. The ATR-IR spectroscopic measurements were performed using a Thermo Nicolet Nexus 470 FTIR spectrometer equipped with diamond ATR crystal. All ATR-IR spectra are calculated from 32 scans at 8 cm⁻¹ resolution.

Key Words: Surface modification, plasma polymerization, cotton, polyamide, hexamethyldisilane, hexamethyldisiloxane

REFERENCES

- Jama, C. and Delobel, R., (2007). "Cold Plasma Technologies for Surface Modification and Thin Film Deposition" in *Multifunctional Barriers for Flexible Structure Textile, Leather and Paper*, Springer Series in Materials Science, Volume 97, Duquesne, S., Magniez, C. and Camino, G. (Eds.), pp.109-124

- Schartel, B., Kühn, G., Mix, R. and Friedrich, J., (2002). *Macromolecular Materials and Engineering*, Vol.287, pp.579-582
- Hegemann, D., Brunner, H. and Oehr, C. (2003). *Surface and Coatings Technology*, Vol. 174-175, pp.253-260
- Zanini, S., Ricardi, C., Orlandi, M., Esena, P., Tontini, M., Milani, M. and Cassio, V. (2005). *Surface & Coatings Technology*, Vol. 200, pp.953-957
- Cireli (Aksit), A., Kutlu (Kilic), B. and Mutlu, M. (2007). *Journal of Applied Polymer Science*, Vol.104, pp.2318-2322

SILANE TREATED GLASS FIBER

K. SEVER¹, V. ÇEÇEN¹, M. SARIKANAT², İ. TAVMAN¹

¹Department of Mechanical Engineering, Dokuz Eylul University

² Department of Mechanical Engineering, Ege University

ABSTRACT

Fiber-reinforced composite materials are being more widely used in many applications. With the increasing applications of these materials, more and more knowledge is needed to get a better understanding of the bonding of the materials, which can lead to different mechanical properties of the materials. The high specific strength along the fiber direction is an important advantage for fiber reinforced polymer composites and the fiber/matrix interface is generally the weakest part of the composites. Thus, the interface/interphase in fiber reinforced composites plays a very important role in determining the composite mechanical properties. In order to achieve the best composite mechanical properties, many efforts have been made to improve interfacial properties. Fiber surface treatments are often used to create a fiber/matrix interface possessing different characteristics so that the fiber strength is utilized effectively under an optimum bonding. There are many methods or treating agents for surface treatment of glass fibers based on protecting fibers from damage and improving the adhesion between fiber and matrix. In general, the silane coupling agents are applied to fibers as a chemical surface treatment and provides a good adhesion between glass fibers and resin matrix. In this study, influences of silane treatment onto glass fiber at fiber-matrix interface were emphasized.

Key words: Glass fiber, Silane treatment, Interface, Polymer composite

1. INTRODUCTION

Fiber reinforced materials are basically composed of two constituents, fiber and matrix, where generally the fiber acts as a reinforcement of the matrix material or, alternatively, the matrix acts as an adhesive between the fibers[1]. In fact, fibrous polymer composite materials have three components: fiber, matrix and interface (interphase)[2]. The fibers ensure the strength of the material, while the matrix helps to keep the shape of the part; the interface, as a key element of the composite, transfers the load from the matrix to the fibers and, thus, it is responsible for the effect of "reinforcement"[3]. However, the fiber/matrix interface is generally the weakest part of the composites[4].

Interfaces in composites form in the vicinity of fiber surfaces and may exhibit significantly different material characteristics than the bulk resin properties. The chemical composition, as well as the microstructure, of the material at the interphase region mainly controls the properties of the interphase. The thickness of the interphase ranges from 1 to 1000 nanometers depending on materials, sizing and process conditions. The properties of the interphase

and degree of adhesion between the fiber and matrix govern load transfer between the composite constituents [5,6]. The properties of the interphase are critical to global composite performance such as strength, toughness, durability and impact/ballistic resistance [6].

With glass fibres, other problem was the hydrophilic nature of the glass surface. The fiber surface attracted water, resulting in much loss of strength for polymer composites. In severe cases, the water leached ions from the glass, and the ionic solutions created in the interface regions developed osmotic pressure. This pressure caused the spalling of surface layers, seriously damaging structures such as boat hulls [7].

There is a need for appropriate methods to assess changes in the strength and stability of the interface. There are many methods and treating agents for surface treatment of glass fibres based on protecting fibres from damages and improving the adhesion between fibre and matrix. In general, the silane coupling agents are applied to fibers as a chemical surface treatment and provides a good adhesion between glass fibers and resin matrix[4].

2. SILANE COUPLING AGENT

A silane coupling agent to glass fibers is applied to improve the mechanical bond between the glass fiber and the polymer matrix and form a barrier which is impervious to water, between the glass fiber and the polymer matrix and hence improve moisture sensitivity[8].

2.1. The Reactions of a Silane Coupling Agent in Aqueous Solutions and Bond Formation onto the Glass Fibers

Organofunctional silanes are the most widely used coupling agents for improvement of the interfacial adhesion in glass reinforced materials. Organosilanes have the general structure, X_3Si-R . These multi-functional molecules that react at one end with the glass fiber surface and the other end with the polymer phase. R is a group which can react with the resin, and X is a group which can hydrolyze to form a silanol group in aqueous solution (Figure 2(a)) and thus react with a hydroxyl group of the glass surface. The R-group may be vinyl, γ -aminopropyl, γ -methacryloxypropyl, etc.; the X-group may be chloro, methoxy, ethoxy, etc. [9]. Several organofunctional silanes are used commercially since each functional group is somewhat specific for a resin type (Table 1). The total amount of silane coupling agent applied is generally 0.1-0.5 % of the weight of glass.[10]. In particular, the concentration of silane coupling agent is a critical factor in determining the mechanical performance and fracture behaviour of the composite[11].

Table 1. Typical Commercial Silane Coupling Agents (Plueddemann, 1974)

Silane Name	Resin type
Vinylbenzylcationicsilane	All Resins
Vinyl-tris(β -methoxyethoxy)silane	Unsaturated polymers
Vinyltriacetoxysilane	Unsaturated polymers
γ -Methacryloxypropyltrimethoxysilane	Unsaturated polymers
γ -Aminopropyltriethoxysilane	Epoxies, Phenolics, Nylon
γ -(β -aminoethyl) aminopropyltrimethoxysilane	Epoxies, Phenolics, Nylon
γ -Glycidoxypropyltrimethoxysilane	Almost all resins
γ -Mercaptopropyltrimethoxysilane	Almost all resins
β -(3,4-epoxycyclohexyl)-ethyltrimethoxysilane	Epoxies
γ -Chloropropyltrimethoxysilane	Epoxies

The structure of the silane layer depends on a number of factors including the layer thickness and amount of adsorbed material, the deposition procedure (i.e., solvent polarity, water content, pH, and substrate isoelectric point), the hydrolysis and condensation kinetics of the coupling agent, and the substrate/coupling agent interaction [12–16, 8]. Furthermore, the structure of the silane layer depends on the silane structure in the treating solution and its organofunctionality, drying conditions, the morphology of the fibre and the chemical composition of the surface[11].

Silane coupling agents are generally applied onto the glass fiber surfaces from dilute aqueous solutions, where three time-dependent processes, silane hydrolysis, silane condensation and silane adsorption occur simultaneously [17]. Arkles, Steinmetz, Zazyczny & Mehta (1992) [18] showed that the reactions of alkoxysilanes in aqueous solutions and bond formation onto the glass fibers in Figure 1.

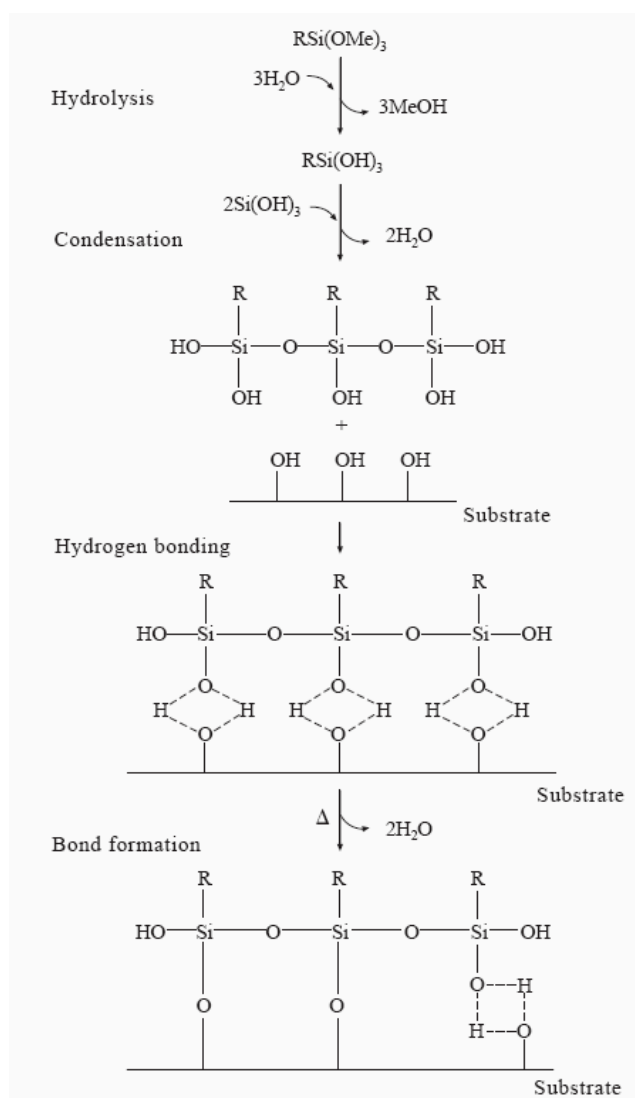


Figure 1. Reactions and Bonding of alkoxy silanes (Arkles et al., 1992)

The trihydroxy silanols, Si(OH)_3 , are able to compete with water at the glass surface by hydrogen bonding with the hydroxyl groups at the surface (Figure 2(b)), where M stands for Si, Fe, and/or Al.

When the treated fibers are dried, a reversible condensation takes place between the silanol and M-OH groups on the glass fiber surface, forming a polysiloxane layer which is bonded to the glass surface (Figure 2(c)).

Therefore, once the silane coated glass fibers are in contact with uncured resins, the R-groups on the fiber surface react with the functional groups present in the polymer resin, such as methacrylate, amine, epoxy and styrene groups, forming a stable covalent bond with the polymer (Figure 2 (d)).

It is essential that the R-group and the functional group be chosen so that they can react with the functional groups in the resin under given curing conditions. Furthermore, the X-groups must be chosen, that can hydrolyze to allow reactions between the silane and the M-OH group to take place on the glass surface. Once all these occur, the silane coupling agents may function as a bridge to bond the glass fibers to the resin with a chain of primary strong bond [9].

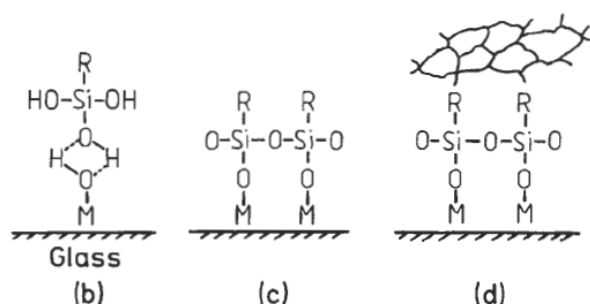


Figure 2. Functions of a coupling agent: (a) hydrolysis of organosilane to corresponding silanol; (b) hydrogen bonding between hydroxyl groups of silanol and glass surface; (c) polysiloxane bonded to glass surface; (d) organofunctional R-group reacted with polymer (Kim & Mai, 1998. p. 177).

2.2. Bonding Theories between Glass Fiber and Polymer Matrix after Silane Treatments of Glass Fibers

There are two bonding theories. These are chemical bonding theory and interpenetrating polymer network (IPN).

2.2.1. Chemical Bonding Theory

In the chemical bonding theory, the bifunctional silane molecules act as a link between the resin and the glass by forming a chemical bond with the surface of the glass through a siloxane bridge, while its organofunctional group bonds to the polymer resin. This co-reactivity with both the glass and the polymer via covalent primary bonds gives molecular continuity across the interface region of the composite[9]

2.2.2. Interpenetrating Polymer Network

The chemical bonding theory explains successfully many phenomena observed for composites made with silane treated glass fibers. However, a layer of silane agent usually does not produce an optimum mechanical

strength and there must be other important mechanisms taking place at the interface region. An established view is that bonding through silane by other than simple chemical reactivity are best explained by interdiffusion and interpenetrating network (IPN) formation at the interphase region.

The coupling agent-resin matrix interface is a diffusion boundary where intermixing takes place, due to penetration of the resin into the chemisorbed silane layers and the migration of the physisorbed silane molecules into the matrix phase[9]. Fig. 3 is a representation of the bonding of the siloxane to the polymer through a combination of interpenetration and chemical reaction [19].

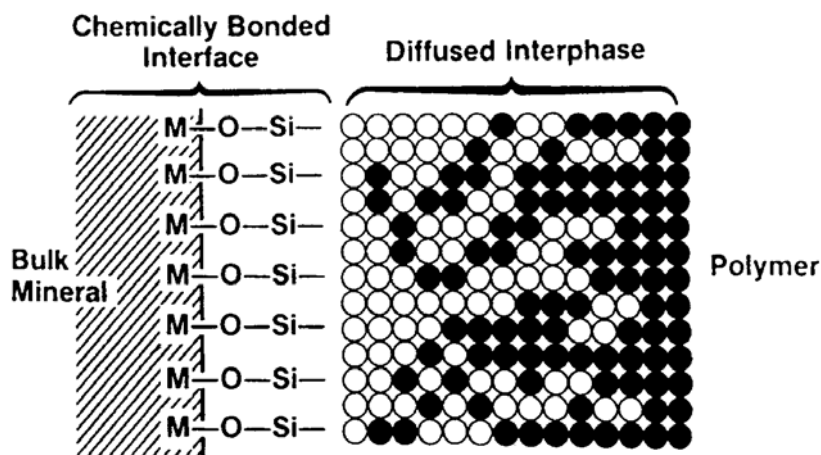


Figure 3. Bonding siloxane to polymer through diffusion

2.3. Silane Layers on Glass Fiber Surface

When glass fibers are treated with a silane solution in an organic solvent, two layers are formed on the glass surface (Figure 4). Coupling agents deposited on glass surfaces are usually heterogeneous layers of physisorbed and chemisorbed fractions.

A physisorbed silane layer: It could consist of as much as 270 monolayer equivalents, and although insoluble in benzene, was rapidly removed by the cold water[20]. As the silane concentration increases, a physisorbed layer is formed on the chemisorbed layer formed previously. This layer cause a lubrication effect[21,25]. Therefore, the mechanical interfacial properties of the composites decrease at a higher silane coupling agent concentration[25]. Also, the physisorbed silane prevents the reaction between the chemisorbed silane and the matrix resin[24]. The outer physisorbed layers of silane are capable of mixing with and plasticizing the matrix network[22].

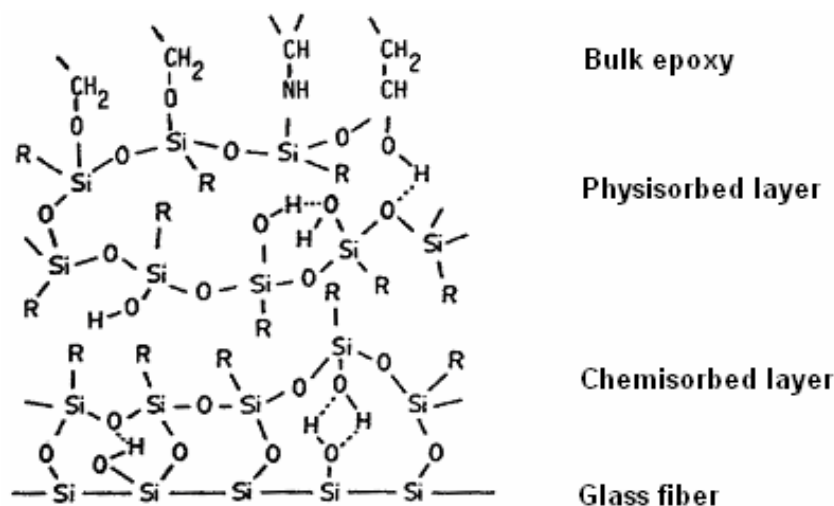


Figure 4. Schematic model of the glass-silane coupling agent interphase[24].

A chemisorbed silane layer: The layer was covalently bonded and thus not easily removed[26-27]. The layer could consist of about ten monolayer equivalents. Most of chemisorbed layer can be removed from bare glass by boiling in water for a few hours. The residue appears to be especially strongly bound to the surface[20]. Because, strongly chemisorbed portion of the layers closest to the glass surface[23]. When resin is applied to finished glass to form a proper glass-coupling agent-resin adhesive bond, the interface can remain stable in the presence of boiling water for many weeks, even under load. Chemisorbed layer is responsible for wet strength retention in glass-resin laminates. physisorbed hydrolysate of coupling agent is either ineffective or deleterious[20].

3. EFFECT OF SILANE COUPLING AGENT FOR GLASS FIBER-REINFORCED POLYMER COMPOSITES

Their effectiveness depends on the nature and pretreatment of the substrate, the type of silane used, the thickness of the silane layer and the process by which it is applied. In a relatively dry state, the proper choice of a silane coupling agent is an effective means of promoting interfacial adhesion and enhancing mechanical properties[19]. Because, the chemical bonds formed between the fiberglass and polymeric resin, through the use of a silane coupling agent, improve the mechanical strength of composites [28].

In wet state, glass fiber/polymer composites are sensitive to moisture. They absorb moisture in humid environments and undergo dilatational expansion. The presence of moisture and the stresses associated with moisture-induced expansion may cause lowered damage tolerance and structural durability. The structural integrity and lifetime performance of fibrous

polymeric composites are strongly dependent on the stability of the fiber/polymer interfacial region. The absorbed water molecules in polymer composites are known to have significant effects on their final performance of composite structures especially in their long-term utilization [29]. Glass fiber/polymer matrix interface uptakes a lesser amount of water when the fiber is treated with a silane coupling agent [29,30]. Thus, shear strength loss of the untreated composite was higher than that of the silane treated materials.

4. RESULTS

A silane coupling agents are applied to glass fibers as a chemical surface treatment and provides a good adhesion between glass fibers and resin matrix. The silane coupling agents function as a bridge to bond the glass fibers to the resin with a chain of primary strong bond. Thus, the presence of coupling agents enhances mechanical properties of polymer composites as well as environmental stability.

REFERENCES

1. Mechanical Properties of Polymer Composites Based on Commercial Epoxy Vinyl Ester Resin and Glass Fiber, A.L. Nazareth da Silva, S.C.S. Teixeira, A.C.C. Vidal, F.M.B. Coutinho, *Polymer Testing* 20 (2001) 895–899
2. Interfacial Effects in Glass Fibre Composites As A Function of Unsaturated Polyester Resin Composition, K. Rot, M. Huskić, M. Makarović, T. Ljubić Mlakar, M. Zigon, *Composites: Part A* 32 (2001) 511–516
3. Characterization of Fiber/Matrix Interface Strength: Applicability of Different Tests, Approaches And Parameters, Serge Zhandarov, Edith Mäder, *Composites Science and Technology* 65 (2005) 149–160
4. Effect of Interfacial Adhesion and Statistical Fiber Strength on Tensile Strength of Unidirectional Glass Fiber/Epoxy Composites. Part I: Experiment Results, F.M. Zhao, N. Takeda, *Composites: Part A* 31 (2000) 1203–1214
5. Dynamic Stress/Strain Response of the Interphase in Polymer Matrix Composites, M. Tanoğlu, S.H. McKnight, G. R. Palmese, J.W. Gillespie, *Polymer Composites*, October 2001, Vol. 22, No. 5
6. The Effects Of Glass-Fiber Sizings On The Strength And Energy Absorption Of The Fiber/Matrix Interphase Under High Loading Rates, M. Tanoglu, S.H. McKnight, G.R. Palmese, J.W. Gillespie Jr., *Composites Science and Technology* 61 (2001) 205-220
7. Why Interface Testing by Single-Fibre Methods Can Be Misleading, M. R. Piggott, *Composites Science and Technology* 51(11:397) 965-974
8. Substrate Effects on The Chemisorbed and Physisorbed Layers of Methacryl Silane-Modified Particulate Minerals, H. Ishida, J.D. Miller, *Macromolecules* 17 (1984) 1659-1666
9. Surface Treatments of Fibers and Effects on Composite Properties. Engineered Interfaces in Fiber Reinforced Composites, Kim JK, Mai YW. (Ed.1), 1998, pp. 171-237, U.K.: The Netherlands
10. Mechanisms of Adhesion Through Silane Coupling Agents, Interfaces in Polymer Matrix Composites, Plueddemann EP, In: Plueddemann EP, Editor. New York: Academic Press, 1974. p. 173-215.
11. Impact response of woven glass fabric composites- I.Effect of fibre surface treatment, Yasunobu Hirai, Hirayuki Hamada, Jang-Kyo Kim, *Composite Science and Technology* 58 (1998) 91-104

12. Characterization of Sizing Layers and Buried Polymer/sizing/substrate Interfacial Regions Using a Localized Fluorescent Probe, Joseph L. Lenhart, Joy P. Dunkers, John H. van Zanten, Richard S. Parnas, *Journal of Colloid and Interface Science* 257 (2003) 398–407
13. N. Nishiyama, R. Schick, H. Ishida, *J. Colloid Interface Sci.* 143 (1991) 146.
14. Reactions of a Trifunctional Silane Coupling Agent in the Presence of Colloidal Silica Sols in Polar Media, M.W. Daniels, J. Sefcik, L.F. Francis, A.V. McCormik, *J. Colloid Interface Sci.* 219 (1999) 351-356.
15. Structure of 3-Aminopropyl Triethoxy Silane on Silicon Oxide, E.T. Vandenberg, L. Bertilsson, B. Liedberg, K. Uvdal, R. Erlandsson, H. Elwing, I. Lundström, *J. Colloid Interface Sci.* 147 (1991) 103-118
16. Structure of Silane Coupling Agents Adsorbed on Silicon Powder, S.R. Culler, H. Ishida, J.L. Koenig, *J. Colloid Interface Sci.* 106 (1985) 334-346
17. Adsorption of an Isocyanurate Silane on E-Glass Fibers from Ethanol and Toluene, Anne E. E. Norström, Pasi J. Mikkola, Janis G. Matisons, Jarl B. Rosenholm, *Journal of Colloid and Interface Science* 232, 149–155 (2000)
18. Silanes and Other Coupling Agents, Arkles, B., Steinmetz, J.R., Zazyczny, J., & Mehta P., K.L. Mittal (Ed.). (1992). (p. 92). The Netherlands: VSP.
19. Tailoring of Interfaces in Glass Fiber Reinforced Polymer Composites: A Review, A.T. DiBenedetto, *Materials Science and Engineering A302* (2001) 74–82
20. M.F. Schrader, *Radioisotope Studies of Coupling agents at the interface*, 110-129
21. Effect of Surface Treatment on the Mechanical Properties of Glass Fiber/Vinylester Composites, Rohchoon Park, Jyongsik Jang, *Journal of Applied Polymer Science*, Vol. 91, 3730–3736 (2004)
22. Investigation of Waterborne Epoxies for E-Glass Composites, Robert E. Jensen, June 9, 1999, Blacksburg, Virginia, Doctoral Thesis
23. Characterization of Sizing Layers And Buried Polymer/Sizing/Substrate Interfacial Regions Using A Localized Fluorescent Probe, Joseph L. Lenhart, Joy P. Dunkers, John H. van Zanten, Richard S. Parnas, *Journal of Colloid and Interface Science* 257 (2003) 398–407
24. The Influence of Sizing Conditions on Bending Properties of Continuous Glass Fiber Reinforced Polypropylene Composites, H. Hamada, K. Fujihara, A. Harada, *Composites: Part A* 31 (2000) 979–990
25. Effect of Silane Coupling Agent on Mechanical Interfacial Properties of Glass Fiber-Reinforced Unsaturated Polyester Composites, S-J Park, J-S Jin, *Journal of Polymer Science: Part B: Polymer Physics*, Vol. 41, 55–62 (2003)
26. Treated Glass Fibers—Adsorption of an Isocyanurate Silane from CCl₄, Anne E. E. Jokinen, Pasi J. Mikkola, Janis G. Matisons, Jarl B. Rosenholm, *J. Colloid Interface Sci.* 196 (1997) 207-214
27. Silicones in Coatings, P. Arora, L.G. Britcher, D.C. Kehoe, J.G. Matisons, R. St C. Smart, The Paint Research Association, Paper 16, Middlesex, February 1996
28. Interfacial Behavior of Epoxy/E-Glass Fiber Composites Under Wet-Dry Cycles by Fourier Transform Infrared Microspectroscopy, W. Noobut, J. L. Koenig, *Polymer Composites*, February 1999, Vol. 20, No. 1
29. Temperature Effect During Humid Ageing on Interfaces of Glass And Carbon Fibers Reinforced Epoxy Composites B.C. Ray, *Journal of Colloid and Interface Science* 298 (2006) 111–117
30. Water at the Polymer /Substrate Interface and its Role in the Durability of Polymer/Glass Fiber Composites, T.Nguyen, E.Byrd, D.Aished, K.Aouadi, J.Chin, *Durability of Fibre Reinforced Polymer Composites for Construction*, 1.st International Conference, 1998, Canada, B. Benmokrane, H.Rahman, Editors, 451-462 pp

RECYCLED WOOL-BASED NONWOVEN MATERIAL FOR DECOLORISATION OF DYEHOSE EFFLUENTS

M. RADEVIC, D. RADOJEVIC, V. ILIC, D. MIHAILOVIC, P. JOVANCIC

Textile Engineering Department, Faculty of Technology and Metallurgy, University of Belgrad

ABSTRACT

The aim of this study was investigate the possible application of recycled wool-based nonwoven material for removal of different dyes that are used in textile dyehouses. Basic, reactive, direct and metal complex dyes were investigated. The sorption kinetics, the influence of initial dye concentration, pH and temperature were analyzed. The sorption properties were highly influenced by type of the dye due to differences in their chemical structure and thus, the mechanism of binding to wool. Modification of material with chitosan and hydrogen peroxide improved the sorption capacities and sorption rates but no general trend could be established. Consequently, the sorption behavior had to be analyzed separately for each type of the dye studied. The results indicated that recycled wool-based nonwoven material can be used as an efficient, low-cost sorbent for decolorisation of effluents.

Keywords: Wool, sorbent, dye, chitosan, hydrogen peroxide

1. INTRODUCTION

Nowadays, textile industry must deal with increasing environmental demands for purification and control of effluents since it generates huge quantities of wastewater. In addition to the limitation of BOD, COD, metal ion and some organic compounds in industrial effluents, the request for almost complete decolorisation of wastewater was introduced [1]. Therefore, these regulations had strong impact on the textile dyehouses, which produce very complex effluents containing a wide range of dyes and auxiliaries. Normally, the dyehouse effluent contains about 10-50 mg/L of dyes, colour being noticeable at concentrations above 1 mg/L [2]. It is estimated that the BOD of mixed wastes from dyehouses is typically 200-3000 mg/L, COD 500-5000 mg/L, suspended solids 50-500 mg/L, with pH in the range 4-12 [2]. The amount of dye released in effluent through the exhaust and wash baths strongly depends on the type of dye, depth of shade, dyeing method, liquor ratio, etc [2].

Many efforts have been made to develop treatment or combination of treatments for decolorisation and removal of dyes from wastewater that would meet the demands of high efficiency and economical feasibility [3-4]. Dyes are usually very difficult to decolorize because of their complex structure and synthetic origin [5]. There is a wide range of dyes differing in chemical structure, which require specific and selective treatments. Dyehouse effluents cannot be aerobically treated in municipal sewerage

systems [6]. Textile effluent decolorisation treatments are divided into three categories: biological, chemical and physical. Currently, physical and chemical treatments are mainly used for removal of dyes from effluents [5].

Adsorption seems to be a viable treatment as it provides removal of dyes that are too stable for conventional methods. It is highly affected by numerous physico-chemical factors such as pH, sorption time, temperature, sorbent/dye interaction, sorbent surface area, particle size, etc [7]. Many different sorbents are currently available, but activated carbon in powder and granulated form is the most commonly used [2, 8]. Although it is extremely efficient for removal of different kinds of dyes, it is also very expensive [5]. Thus, many low-cost natural sorbents such as chitin, chitosan, peat, wood chips, fly ash and coal mixture, corn cobs, silica gel, natural clay, rice hulls, palm kernel fibre, coconut hard shell are studied [2, 5, 9-13].

It is well documented that wool has excellent sorption properties for metal ions and oils [14-15] but there are only few available data on the sorption properties of wool for dyes [16]. This study was aimed at investigating the possibility of using the recycled wool-based nonwoven material (RWNM) developed by our group as a sorbent for removal of basic, reactive, metal complex and direct dyes. To improve the sorption properties, the material was treated with biopolymer chitosan and hydrogen peroxide. The influence of pH, temperature and initial dye concentration on dye uptake as well as sorption kinetics were studied.

2. EXPERIMENTAL

2.1 Material

The recycled wool-based nonwoven material (78% wool/22% polyester) was produced from secondhand military knitted pullovers of the constant characteristics that were torn off, washed, decolorised with reducing agent, dried and garneted in industry. To avoid the effect of chemical binders on dye sorption, needlepunch process was chosen to produce the nonwoven material. The material was produced from recycled fibres on Dilo (Germany) needle loom.

C.I. numbers and commercial names of investigated dyes are given in Table 1.

Table 1. C.I. numbers and commercial names of investigated dyes

Commercial name	C.I. number	Manufacturer
Tubantin blue GLL 300%	C.I. Direct Blue 78	Bezema
Bezacryl goldyellow GL fl.	C.I. Basic Yellow 28	Bezema
Lanaset yellow 4GN	C.I. Reactive Yellow 39	Ciba
Lanaset gray G	C.I. Acid Blue 317	Ciba

2.2 Treatments

The treatment of RWNM with biopolymer chitosan (CHT) was based on immersion of samples in 0.3% CHT (liquor ratio 30:1), which were shaken for 20 minutes, squeezed out through laboratory squeeze rolls and dried at room temperature. Subsequently, they were washed with tap water and dried at room temperature. 0.3% solution of chitosan was prepared according to the following procedure: 3.00 g of chitosan was stirred in 0.4% acetic acid. Volumetric flask of 1L was filled up with 0.4% acetic acid and solution left overnight ready for the application to material.

Hydrogen peroxide treatment (H_2O_2 , 20 mL/L; $\text{Na}_4\text{P}_2\text{O}_7$, 1.5 g/L and NH_3 , 2.5 mL/L) was done in static conditions (without shaking). Samples were treated in the solution for 1 hour (liquor ratio 30:1) at 70°C and pH 9.40, washed with tap water and dried at room temperature.

2.3 Methods

The dye uptake (q , mg/g) was determined as a difference between the initial concentration of dye in the solution (C_0 , mg/L) and the final concentration of dye in the solution (C_f , mg/L) (Equ. 1). UV/VIS Spectrophotometer (Shimatzu 1700, Japan) was used for determination of the concentration of dyes in the solution.

$$q = \frac{(C_0 - C_f) \cdot V}{m} \quad (1)$$

The symbol V presents the solution volume (L) and m is the mass of sorbent material (g).

The following processes and parameters have been studied:

- the sorption kinetics - 1.00 g of material was shaken in 50 mL of dye solution ($C_0=100$ mg/L) for 0.25, 0.5, 1, 3, 6, 12 and 24 h at pH 5.00 for basic dyes and pH 3.30 for metal complex, reactive and direct dyes;
- the influence of initial dye concentration on sorption process – 1.00 g of material was shaken in 50 mL of dye solution of different concentrations ($C_0=10, 50, 100$ and 500 mg/L) for 3 h at pH 5.00 for basic dyes and pH 3.30 for metal complex, reactive and direct dyes;
- the influence of temperature on sorption process – 1.00 g of material was shaken in 50 mL of dye solution ($C_0=100$ mg/L) for 1 h at pH 5.00 for basic dyes and pH 3.30 for metal complex, reactive and direct dyes, in water bath WB14 (Mettmert, Germany) supplied with shaking device. Temperature of the solutions were maintained at 20 °C, 40 °C and 60 °C;
- the influence of pH on the sorption process – 1.00 g of material was shaken in 50 mL of dye solution ($C_0=100$ mg/L) for 1 h. Appropriate initial pH values of the solutions (pH_0) were adjusted with CH_3COOH (1.00 g/L) and

KOH (0.100 M). After the sorption, final pH values of the solutions (pH_f) were measured using an Inolab 730 (WTW, Germany) pH-meter. Initial pH values were adjusted to 3.30, 5.00 and 7.00.

3. RESULTS AND DISCUSSION

Sorption kinetics for direct, basic, reactive and metal complex dyes is shown in Fig. 1. Sorption of direct dye (Fig. 1a) on untreated and H_2O_2 treated RWNM is almost unaffected by prolongation of sorption time. After the rapid sorption on CHT treated RWNM in the first 3 h, process slowed down and equilibrium was reached after 6 h. Uptake of direct dye on untreated RWNM was low. Selected direct dye has high molecular weight with several sulphonate groups. The affinity of dye might decrease with an increase in degree of sulphonation of the dye and after the first sulphonate group, each additional group likely has a negative influence on the sorption, facilitating desorption of the dye from RWNM. However, H_2O_2 and particularly CHT treatment significantly improved uptake of direct dyes. Superior sorption behavior of CHT treated RWNM can be attributed to existence of new amino groups on wool originating from chitosan that contribute to the increase in the positive zeta-potential of the fibre surface [17]. Amino groups in acidic conditions are protonated and ionic interaction between sulphonate groups of direct dyes and protonated amino groups of wool are expected.

Basic dye uptake on H_2O_2 treated RWNM (Fig. 1b) was remarkably higher compared to untreated and CHT treated RWNM. In the case of H_2O_2 treated RWNM equilibrium was reached already after 1 h of sorption. Untreated and CHT treated samples performed similar behavior. Higher dye uptake on H_2O_2 treated RWNM is suggested to be due to wool oxidation and formation of appropriate functional groups [18]. The binding of basic dyes to wool is carried out via carboxylic groups. Electrostatic attraction between deprotonated, negatively charged carboxylic groups of wool and positively charged cationic basic dyes could be established at operated pH.

Each modification of RWNM brought about increase in uptake of reactive dye (Fig.1c). In the first several hours, CHT treated sample showed higher uptakes in comparison with H_2O_2 treated RWNM, but the sorption decreased within last 12 h, causing almost the same final uptake (24 h) for the both samples. Similar behaviour occurred during the sorption of metal complex dye (Fig 1.d).

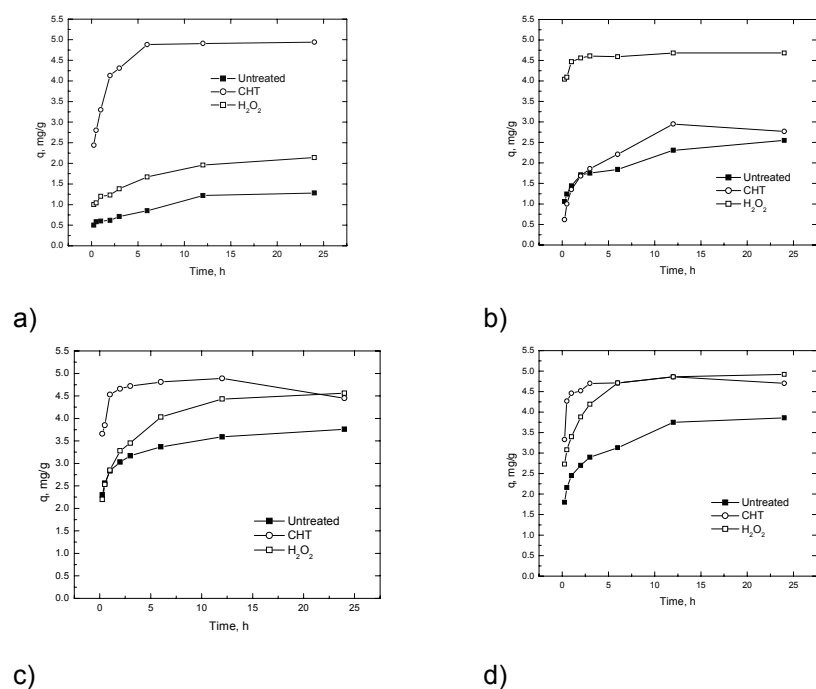


Figure 1. Sorption kinetics for

a) Tubantin blue GLL; b) Bezacryl gold yellow GL; c) Lanaset yellow 4GN; d) Lanaset grey G.

The influence of initial dye concentration in solution on dye uptake of direct, basic, reactive and metal complex dyes is demonstrated in Fig. 2. The results on sorption kinetics pointed out that high percentage of dyes was removed within the first 3 h of sorption, this being the reason to select the sorption time of 3 h for a study on influence of initial concentration on dye uptake. The increase in initial concentration brought about rise of dye uptake. At low initial dye concentrations (50 mg/L), there was a slight difference between untreated and differently treated samples. However, at higher initial dye concentrations treated samples started to demonstrate their advantages. Although uptake of dyes increased, the percentage of dyes adsorbed by untreated and differently treated materials decreased. Reduction of the fraction of dyes adsorbed indicates that higher amounts of dyes are left in the solution.

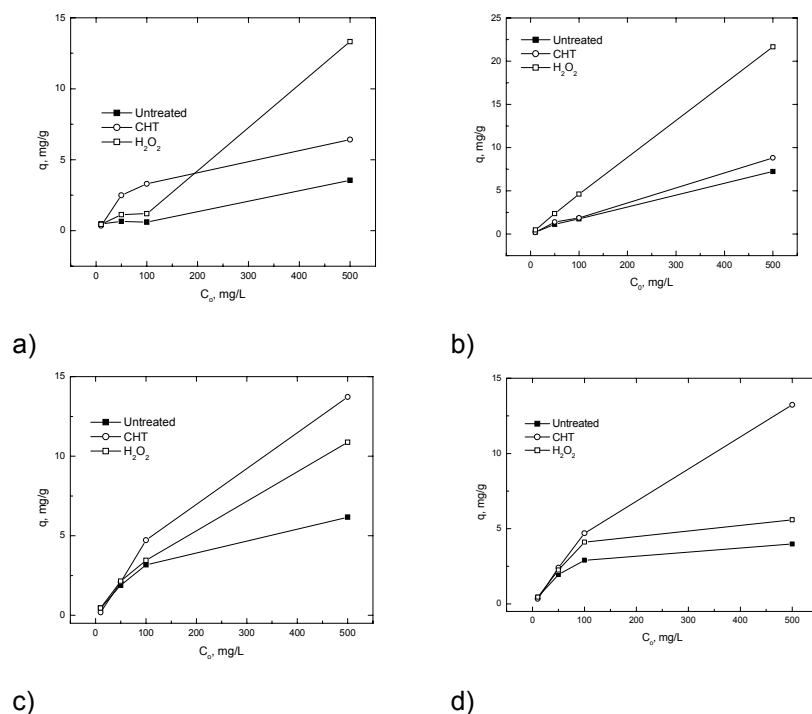


Figure 2. The influence of initial concentration on uptake of

a) Tubantin blue GLL; b) Bezacryl gold yellow GL; c) Lanaset yellow 4GN; d) Lanaset grey G.

The influence of temperature on dye uptake of direct, basic, reactive and metal complex dyes is demonstrated in Fig. 3. Temperature positively affected sorption of direct dye on untreated and H_2O_2 treated RWNM. The rise of temperature induced the increase in direct dye uptake at 40°C on CHT treated RWNM. However, at 60°C dye uptake decreased to the level of sorption at 20°C. Basic dye uptake is not considerably affected by temperature independently on RWNM studied. In the case of reactive and metal complex dyes, the rise of temperature led to an increase in dye uptake for untreated and H_2O_2 treated RWNM. On the contrary, sorption on CHT treated sample decreased with an increase in temperature.

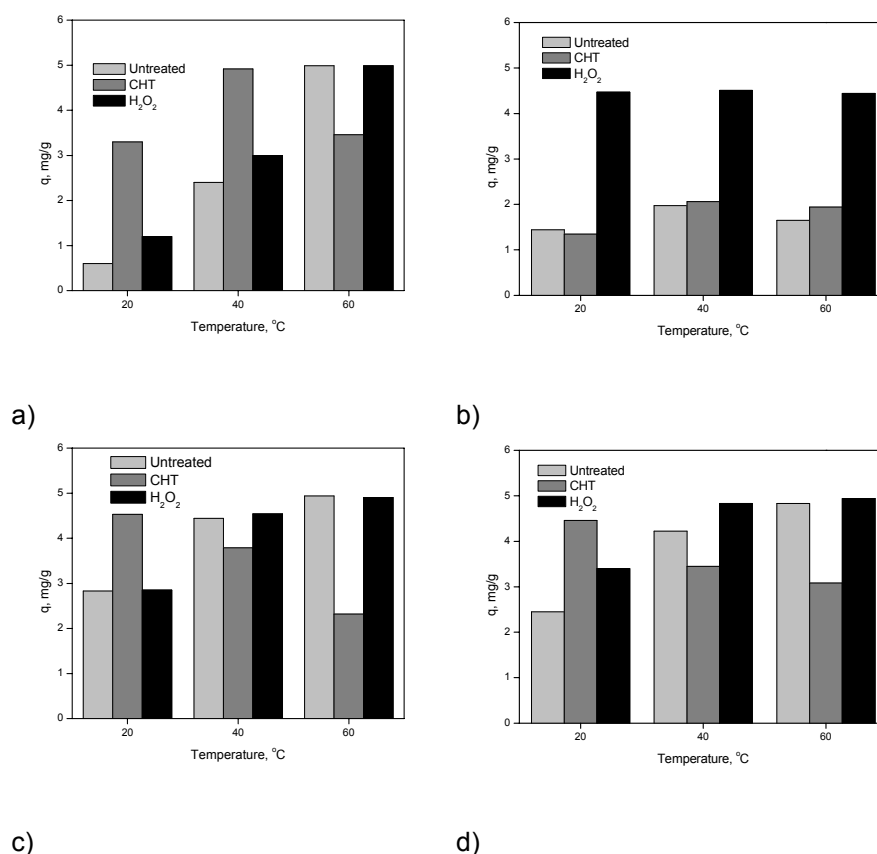


Figure 3. The influence of temperature on uptake of

a) Tubantin blue GLL; b) Bezacryl gold yellow GL; c) Lanaset yellow 4GN; d) Lanaset grey G.

The influence of pH on dye uptake of direct, basic, reactive and metal complex dyes is demonstrated in Fig. 4. The increase in pH negatively influenced the sorption of direct dyes. Such behavior was expected since the rise of pH caused the inhibition of the protonation of amino groups that are the main site on wool for establishing the ionic interaction with sulphonate groups of dyes. On the contrary, the rise of pH induced significant increase in basic dye uptake. This effect was particularly pronounced in the case of H₂O₂ treated RWNM. Such behavior could be anticipated since at higher pH values, carboxylic groups are deprotonated and thus negatively charged, providing the electrostatic attraction with cationic basic dyes. The influence of pH on sorption of reactive and metal complex dyes is similar to that obtained for direct dyes. CHT treated samples are not remarkably affected by pH.

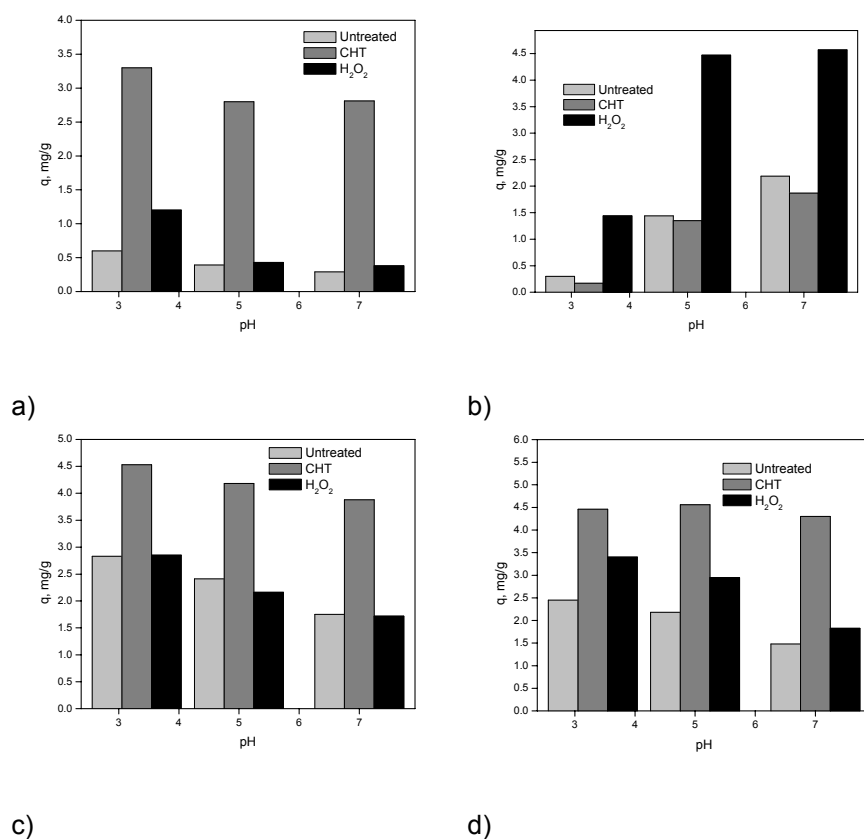


Figure 4. The influence of pH on uptake of

a) Tubantin blue GLL; b) Bezacryl gold yellow GL; c) Lanaset yellow 4GN; d) Lanaset grey G.

4. CONCLUSIONS

The recycled wool-based nonwoven material can efficiently remove basic dye Bezacryl gold yellow GL, reactive dye Lanaset yellow 4GN and metal complex dye Lanaset grey G from water. However, insufficient sorption of direct dye Tubantin blue GLL occurred either on untreated sorbent or sorbent treated with biopolymer chitosan or hydrogen peroxide. Sorption of studied dyes was significantly affected by initial dye concentration, pH and temperature.

The latest results indicated that recycled wool-based nonwoven material can be efficiently used for purification of real effluents from textile dyehouses.

ACKNOWLEDGEMENT

We gratefully acknowledge the support from European Community FP6 Programme through financing the EMCO project INCO CT 2004-509188 and Ministry of Science and Environmental Protection of the Republic of Serbia for project TD-7017B. This research reflects only the author's views and the European Community is not liable for any use that maybe made on the information contained therein.

REFERENCES

1. Hönings R, Peters R, Müller B M, Thomas H, Höcker H, *Proceedings, 9th International Wool Textile Research Conference*, (International Wool Secretariat, Biella) Vol. I (1995) 300.
2. Laing I G, *Rev Prog Color*, 21 (1991) 56.
3. Tünay O, Kabdasli I, Eremektar G, Orhon D, *Wat Sci Tech*, 34 (1996) 9.
4. Smith B, Koonce T, Hudson S, *Am Dyest Rep*, 82 (1993) 18.
5. Robinson T, McMullan G, Marchant R, Nigam P, *Bioresource Technology*, 77 (2001) 247.
6. Willmot N, Guthrie J, Nelson G, *JSDC*, **114** (1998) 38.
7. Rao KLLN, Krishnaiah K, Ashutush, *Indian J. Chem. Technol.*, **1** (1994) 13.
8. Kumar MNVR, Sridhari TR, Bhavani KD, Dutta PK, *Colorage*, **40** (1998) 25.
9. McKay G, Blair HS, Gardner JR, *J. Appl. Polym. Sci.*, 29 (1984) 1499.
10. Carlough M, Hudson S, Smith B, Spadgenske D, *J. Appl. Polym. Sci.*, 42 (1991) 3035.
11. Yoshida H, Fukuda S, Okamoto A, Kataoka T, *Wat. Sci. Tech.*, 23 (1991) 1667.
12. Ofomaja OE, Ho YS, *Dyes and Pigments*, 74 (2007) 60.
13. Pathak J, Rupainwar DC, Talat M, Hasan SH, *Journal of Indian Chemical Society*, 83 (2006) 1253.
14. Maclaren J A, Milligan B, *Wool Science - The Chemical Reactivity of the Wool Fibre* (Science Press, Marickville, Australia) (1981).
15. Choi H M, Moreau J P, *Microscopy Res Tech*, 25 (1993) 447.
16. Weltrowski M, Patry J, Beaudoin B, *Proceedings, 9th International Wool Textile Research Conference*, (International Wool Secretariat, Biella), Vol. IV (1995) 343.
17. M. Radetic, D. Jocic, P. Jovancic, Lj. Rajakovic, H. Thomas, Z.Lj. Petrovic, *J. Appl. Polym. Sci.*, 90 (2003) 379.
18. Jovancic P, Jocic D, Molina R, Juliá MR, Erra P, *Textile Res. J.*, 71 (2001) 948.

THE APPLICATION OF MICROCAPSULES OF PCM IN FLAME RESISTANT NON-WOVEN MATERIALS

I. CARDOSO¹, J. R. GOMES²

¹Micropolis SA

²Department of Textile Engineering, University of Minho

ABSTRACT

The use of organic PCM microcapsules (mPCM) has been gaining ground in technical textiles as a temperature regulating medium and hence a means of keeping the body at a comfortable temperature when wearing impermeable protective clothes. However, for such applications as fire fighter's protective clothes, the standards require that all the material composing the material be fire resistant. The application of mPCM is usually through the use of binder applied on the fibres by padding, such as is used on non-woven wads, or immersed in a PU coating applied on one side of the textile fabric. These methods imply that significant amounts of binder are present in the substrate. Binders are inevitably inflammable which means that such applications are not appropriate for fire resistant materials. More recently other ways of fixing mPCM to the fibres with a lot less binder present was proposed using coated microcapsules with an outer thermoplastic wall as binder. This method was first tested for fixing mPCM but the non-woven still didn't pass the test according to the standard EN532. Microcapsules without the second thermoplastic wall were alternatively fixed with MF resin, non-flammable, and by applying flame retardant recipes it was possible for the samples to pass the test. However, since the amount of flame retardant necessary for the mPCM to stand the test, and the resin to thermo fix it was very high, the material became unacceptably stiff. Based on a new approach where reactive microcapsules without any binder were used, it was possible to use a lot less flame retardant and resin, and the material was resistant to the standard EN532. In this standard the material has to resist washing and still be flame retardant. The thermal effect was evaluated in a prototype plate calorimeter. Washfastness was evaluated in SEM photographs and by weight, showing that there was a small loss of microcapsules and of fire retardant material after the first wash, but little loss in the subsequent washes, in accordance to the requirements of the EN532 test

INTRODUCTION

Protection clothes for firefighters are made in a way that they protect them from external heat. The materials used are usually thick and heavy so as to provide the necessary insulation to heat. Whereas they perform as expected during the firefighting, the energy the firefighter spends on the exercise of firefighting and accessory tasks, aggravated by the fact that the firefighting clothes are heavy and non-breathable, makes him experience discomfort and extra stress. The use of organic microcapsules of phase change materials (mPCM) has been gaining ground in technical textiles as a temperature regulating medium and hence as a means of keeping the body at a comfortable temperature when wearing impermeable protective clothes.

They work by absorbing the extra energy the body releases, and then giving it back when the body cools down. This exchange of energy happens around the phase change temperature (melting point) of the PCM which in this case is 28°C, which is also considered the comfort temperature for the body. However, for such applications as fire fighter's protective clothes, the standards require that all the material composing the material be fire resistant. Since PCM are flammable paraffins, they should be microencapsulated in heat resistant material so that they don't become exposed to the flames due to deterioration of the microcapsule shell. The most common material used as shell material is melamine-formaldehyde, since it is heat resistant. It is also in itself a fairly good flame resistant material.

In this work the mPCM had to be applied to a non-woven material made of aramid fibre, which is a flame resistant, in such a way as not to bind it with flammable binders. Most applications of microcapsules are with thermoplastic binders such as acrylic or polyurethane. In a first attempt to avoid this problem, instead of immersing the microcapsules in a binder, the microcapsules were coated with a second wall made of binder material (Gomes et al, 2003), PMMA, and this second wall was treated with flame retardant products. To fix the microcapsules and the fire retardant a cross-linking resin, also based on melamine-formaldehyde was used, which altered the non-woven material making it too stiff. Other solutions were tested such as the direct binding of the microcapsules with melamine-formaldehyde resins without the use of acrylate thermoplastic binders and the application of alternative fire retardant products. The different fire retardant products tested were of different types, and chosen so as to bind onto the microcapsules or/and bind onto the material. In the first case a halogenated copolymer was used on the coating of the MF mPCM for one trial and a metal oxide was bound by ion exchange to a polymer coated onto the MF mPCM on another trial. For the non coated mPCM, finishing products based on phosphorous were applied on the material containing the microcapsules, Pyrovatex (n-hydroxy-methyl-3-dimethylphosphonopropionamide) and phosphoric acid. To complement the fire retardant treatment, Boric acid was first applied to the microcapsules as it could react with the MF wall of the PCM microcapsules.

The flame retardancy compared to the non-treated microcapsules was tested according to the standard test EN532 which included washing (5 times in washing machine). The washfastness was evaluated by weight measurement, before and after washing. The stiffness of the material was screened by different observers and only those materials which didn't alter too much their drape and tactile properties were accepted.

The thermal effect was tested in a prototype plate calorimeter.

EXPERIMENTAL

Equipment

The microcapsules' emulsion was applied in a Werner Mathis laboratory machine, the pressure being pneumatically controlled. Thermal fusion of double walled microcapsules and curing of melamine-formaldehyde resin was carried out in a Werner Mathis drying/curing chamber at 150°C.

The calorimeter used was a prototype consisting of two plates through which a heat flux is produced. The top plate is heated to 45°C and the bottom plate kept at 25°C. The heat sensor in the bottom plate measures the heat flux through the non-woven placed between the plates (Hes, 2000).

Starting Materials

Non-Woven (needled) supplied by Duflot Industries (France)

Fibre: Nomex (Aramid)

Mass: 110g/m²

Microcapsules of octadecane PCM with a Melamine-formaldehyde shell were supplied by Micropolis (Portugal).

The melamine-formaldehyde precondensate was supplied by BASF (Lyofix MLF and Kaurit TX).

Pyrovatex was supplied by CIBA (Pyrovatex CP new)

FIRE RETARDANT MICROCAPSULES

mPCM coated with PMMA-PPBBA co-polymer

Microcapsules were coated with PMMA (polymethylmethacrylate) copolymerized with a fire retardant monomer, PPBBA (poly-pentabromobenzylacrylate) by radical polymerisation around the MF microcapsules of PCM.

mPCM coated with PMMA-PMA co-polymer treated with zinc oxide

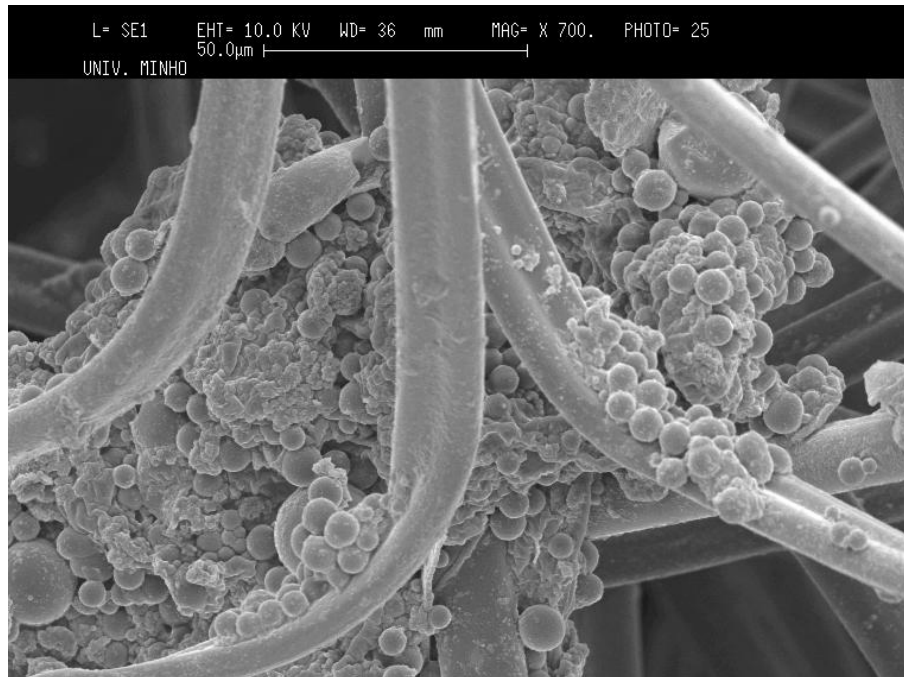
A copolymer of PMMA with PAM (polymethacrylic acid) coated in the same way as above onto the MF mPCM, was treated with zinc oxide so as to attach zinc ions onto the carboxylic groups of the PAM polymer.

mPCM with Boric acid

Boric acid was applied to the PCM microcapsules, and the mPCM were subsequently washed and applied to the non-woven.

RESULTS FOR ARAMID NON-WOVEN CONTAINING MPCM

SEM photographs of Non-woven containing mPCM treated with Boric Acid



Thermal Effect of non-woven

A Thermograph for Aramid Non-woven was taken in the plate calorimeter, first for the sample without mPCM and then for comparison, on the same graph, for the non-woven containing double walled mPCM, fire retardant (pyrovatex) and melamine-formaldehyde resin. The time the flux takes to reach half the maximum flux was measured. The graph is on figure 2 and the results for the flux are on table 1.

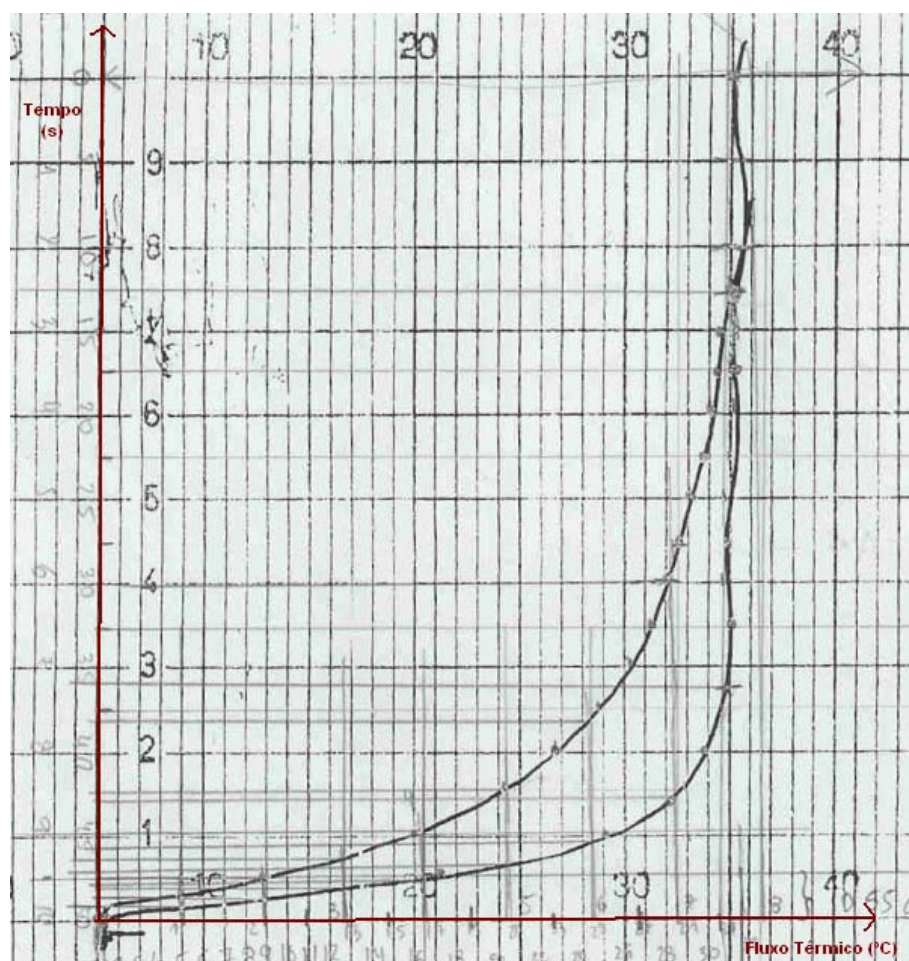


Figure1. Thermograph for non-woven containing double walled mPCM

Table 1. Half-time of flux

Sample	½ time
Non-woven	13.2
Non-woven with double walled mPCM	26.2

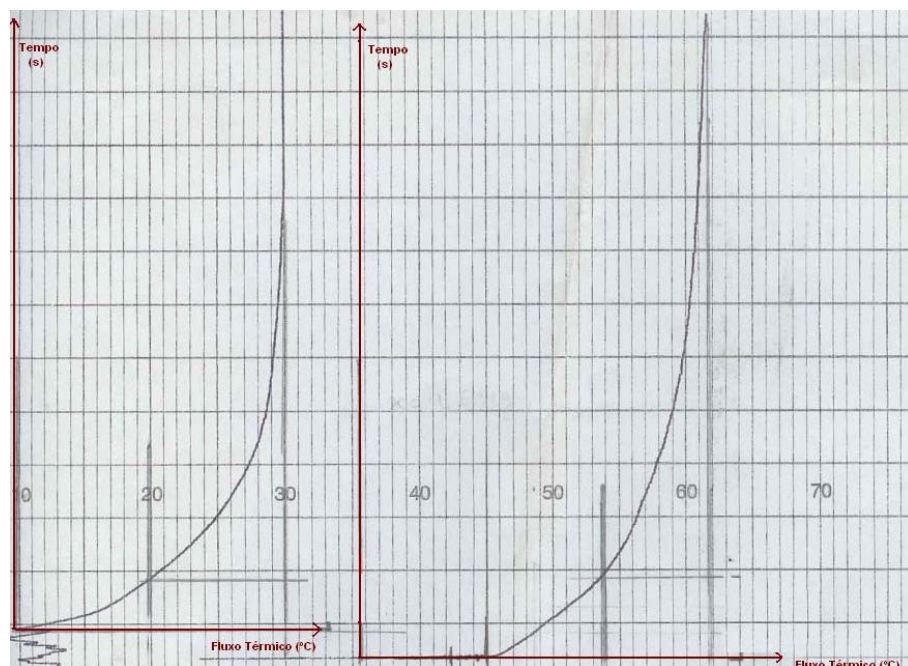


Figure 2. Thermograph for non-woven containing single walled mPCM treated with Boric Acid

Table 2. Half-time of flux for non-woven containing single walled mPCM treated Boric Acid

Sample	½ time
Non-woven	10
Non-woven with double walled mPCM	23

WASHFASTNESS RESULTS

Double walled microcapsules

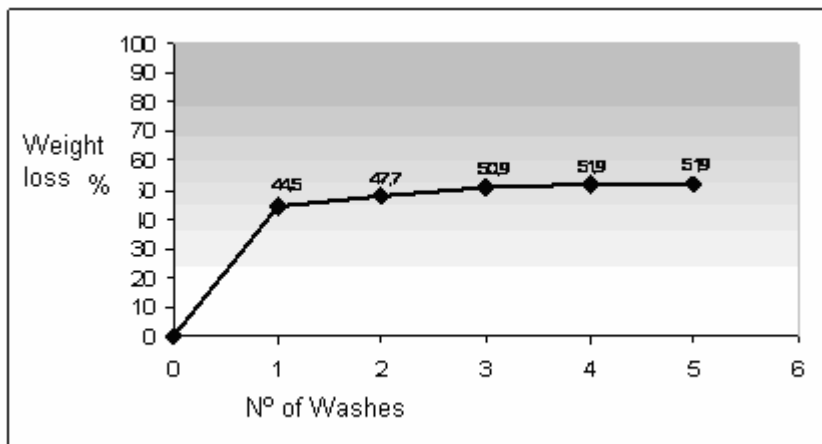


Figure 3. Weigh loss of non-woven with double walled a PCM after 5 times washes

Single walled microcapsules with boric acid

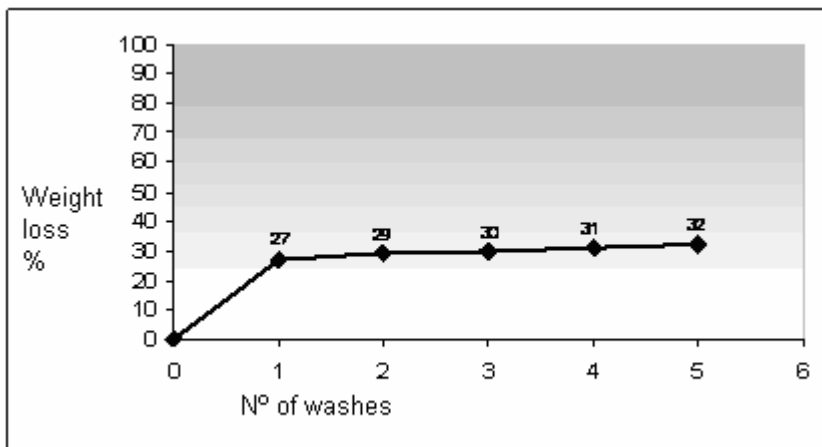


Figure 4. Weigh loss of non-woven containing single walled MF a PCM treated with boric acid

FLAME-RETARDANCY RESULTS

The non-woven samples with different types of double walled mPCM were tested according to standard EN532. The results are on table 3.

Table 3. Flame retardancy double walled PCM

Microcapsules	Speed of flame propagation	Time of burning (seconds)	Extent of burning
Double walled mPCM	Fast	>5	Total
Double walled mPCM with PMBBA	Fast	> 5	Partial
Double walled mPCM with Zinc	Medium	3-5	Partial

The non-woven samples containing a flame retardant mixture of Pyrovatex (n-hydroxy-methyl-3-dimethylpropionamide)+phosphoric acid and two types of MF mPCM were tested according to standard EN532. The results are on table 4.

Table 4. Flame retardancy of MF mPCM

Microcapsules	Speed of flame propagation	Time of burning (seconds)	Extent of burning
MF mPCM	Fast	>5	Total
MF mPCM in non-woven with Pyrovatex+phosphoric acid	None	0	None
mPCM with Boric Acid in non-woven with Pyrovatex + phosphoric acid	None	0	None

TACTILE (HANDLE), DRAPE (rigidity) AND OTHER PROPERTIES OF MATERIALS

Other properties important for the commercial viability of the material, such as tactile properties (handle), adhesion of microcapsules when shaking and applying friction to the material, other noticeable characteristics such as smell, were evaluated by independent observers. The results are on table 5.

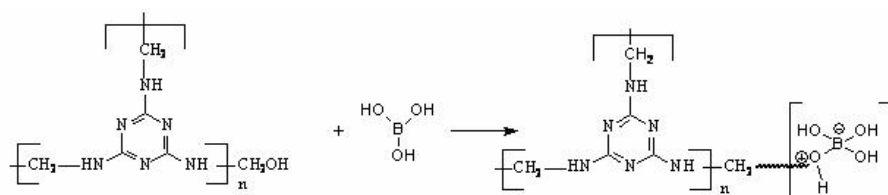
Table 5. Properties of Non-woven material containing microcapsules

Microcapsules	Handle	Rigidity	Other
Non-woven with Double walled mPCM treated with zinc oxide	harsh	Medium	Low adhesion of mPCM to fibres
MF mPCM in non-woven with Pyrovatex+phosphoric acid	Medium	Hard	Strong odour (fish)
mPCM with Boric Acid in non-woven with Pyrovatex + phosphoric acid	Soft	Low (High drape)	None

DISCUSSION OF THE RESULTS

Treated double walled microcapsules were not sufficiently flame-retardant to withstand the standard test EN532 as can be seen in table 3 and figure 3. Single walled MF microcapsules bound by MF resin and non-woven treated with flame retardancy products, resisted the flame test EN532, as seen in table 4, but altered considerably the properties of the original non-woven material with respect to handle and rigidity. They also released a strong unpleasant fish odour, due to the large quantity of Pyrovatex needed for withstanding the flame test.

When this product was replaced partially by Boric acid, these properties improved a lot. Boric acid gave the best results and did not wash-off from the microcapsules nor from the non-woven material. The reason must be that they react with both the microcapsules MF wall and with the MF resin, according to the equation:



The washfastness of the single walled MF microcapsules with Boric acid, bound by MF resin and with Pyrovatex and phosphoric acid, also gave the best results for washfastness which suggests that there was a reaction between the MF wall of the mPCM, the MF resin and the n-hydroxy-methyl-3-dimethylphosphonopropionamide (Pyrovatex).

CONCLUSIONS

For achieving the flame retardancy standard in a non-woven lining inside firefighters' protective clothes, of the different technologies tested, it was found that only a conjugation of both microcapsule protection and non-woven flame retardant finishing, was appropriate. It was also found that even the use of small quantities of thermoplastic binder around the microcapsules was sufficient for the material to fail the test. Boric acid previously applied on the mPCM was found to be a good complement to the standard flame retardancy finishing based on phosphorous and applied on the non-woven. In this way tactile and other properties of the original non-woven material were preserved.

REFERENCES

1. Pushaw R J, *Coated skived foam and fabric article containing energy absorbing phase change material*, US Patent 1997, US5677048
2. Colvin D P, Bryant Y G, *Fiber with reversible enhanced thermal storage properties and fabrics made therefrom*, European Patent 1989, EP0306202
3. Lenox-Kerr P, *Technical Textiles*, July/August 1998

4. Sports Trends, July 2000
5. Gomes, J.I.N.R., Lima, C.J.E., "Microcapsules applied in thermal insulation", *Materials Society*, Guimarães, June 1999
6. Hes, L., *Fundamentals of Clothing Comfort*, China Textile Institute, Taipei (2000)
7. Gomes J.I.N.R., Cardoso I., Santos P. "Application of microcapsules of phase change materials to textiles for thermal insulation and comfort without loss of permeability", 2nd international Autex conference, June 2003, Gdansk, Poland.

INVESTIGATION OF PRESENCE OF SOME PATHOGENIC MICRO ORGANISM ON ACRYLIC CARPET

A. ASHJARAN¹, R. KHAJAVI², M. SATTARI³

¹Faculty Member of Islamic Azad University Share Rey Branch

²Faculty Member of Islamic Azad University Of South Of Tehran

³Faculty Member of Tarbiyat Modares University

ABSTRACT

Carpets are considered as an appropriate medium for micro organisms to grow, especially when are remained in public place, such as mosques for a long period of time and are washed at long intervals. Machine-made acrylic carpets are commonly used in Iran. Due to the direct touch of people with carpets and the need for keeping the carpets in a hygienic condition, existence of some harmful microbes, such as *Escherichia coli* and *pseudomonas* has been examined in acrylic carpets.

As a result of this research, several carpets were spread at a mosque for a period of one month. Then the related tests for cultivation and separation of micro organisms, grown into the carpets, were conducted using the two methods of enrichment in nutrient environments: i) thioglycolate and noutrunt brath, and ii) shake the dust off the carpet onto cultivation mediums such as blood agar and noutrunt agar.

After the micro organism colonies are grown, in cultivation environments, the colonies were separated and some tests including catalase and sitrat were carried out in five phases on the colonies for identifying the varieties of bacterium. As a result of tests, types of bacterium, such as *Escherichia coil*, *enterobacter*, *staphylococcus saprophytic us*, *pseudomonas* and *bacillus* were identified. Each of the mentioned bacteria can be seriously harmful for the health of human.

Key Words: Carpet, micro organism, *pseudomonas*, *Escherichia coli*, noutrunt brath, thioglycolate

INTRODUCTION

Micro organism is part of our life. These creatures affect human being in different ways. Micro- organisms can adopt themselves with different environmental conditions and generally they need moisture, material and suitable temperature to order to grow. This growing condition depends on principal kind of wear and direct contact of man potentially ready in loom items. They often need a thin of water that can be found on skins, looms and carpets.

In Iran's culture, carpet is the first choice for covering the floor, and the carpets fuzz is suitable place for micro organism growing. It is clear that growing and increasing the microbes make the conditions unfavourable, loosing the quality of loom items and the customers are in danger.

Nowadays using the synthetic fibre carpets and particularly those with acrylic are usual, because of softness. It is very important to pay attention to the healthy and cleanliness. In this research, the acrylic carpet is examined in a period of time, for the activity of the Bacteria by using morphological bacteria and suitable condition some dangerous bacteria were observed.

The steps of the test were as follows:

- A) Placing the carpets in the mosques for one month
- B) Providing the conditions in order to grow the colony of the bacteria's on the carpets is in tow ways: riching and shaking
- C) Separating the grown colonies and testing them for identifying the genre and type of the bacteria

The procedure and general description of test:

A) Placing the carpets in the mosque for one month

Some acrylic carpets are placed with the same quality in the mosque for one month that the amount of stepping on them is 200 daily and is about 5200 monthly. Characteristics of the carpet are shown in Table 1.

Table 1. Characteristics Of Negin Mashhad Carpet

Yarn String	Length of pile
Material	11+- 1 mm
100 % Acrylic	
Warp yarn	Siz
Cotton 35 %	3*2 m
Polyester 65 %	
Weft yarn = joot	Color :
	White cream

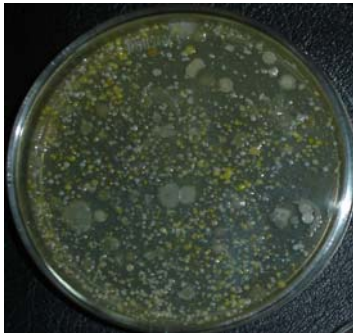
B) Providing the growth conditions for bacteria colonies In the carpets in two ways: i) riching and ii) shaking. Growing of the bacteria is in figure1&2.

B-1) Richening the bacteria on fibbers in rich bath.

In this Method, we choose some samples of fibres from Different parts of carpets and placed them in rich bathes like thioglycolate and nutrient broth to help the micro organism to rich. And after 24 hours, this Liquid of bathes were in the platting-out method in rich blood agar, nutrient agar and EMB position. We provide growing conditions as follows: the temperature was 37 °C, and the time period was 48 hours. This procedure results in bacteria colonies.

B-2) Shaking methods on the enrichment environment.

This method was for paying more attention and completing the previous method. In this method, different parts of Carpet were shaken on prepared environment like thioglycolate, Nutrient agar, EMB and they prepare the suitable conditions, so that we observed the micro organism colonies after a certain time.



(A)



(B)

Figure 1. Growing of bacteria with shaking (a) and riching(b) method on Nutrient agar plate



Figure 2. Growing of bacteria with shaking (a) and riching (b) method on blood agar plate

C) Separating the grown colonies and testing to determine the kind of bacteria:

In this level, exiting colonies on the culture medium were separated carefully with phildopelatin contribution, and each one of these colonies was performed on 6 levies of bacteriology experiment and specialized test.

These experiments included thermal colony Catalase, Oxidas, Simon citrate, urea and TSI tests.

C-1) Thermal - colouring test:

Recurring instances: 1- Viole dojansin, 2-Logol, 3- AlcoholAcetone, 4- Fuchsine

First, take a colony isolated from the bacteria from culture medium and dilute it by physiological saline and appoint it on the lamina within 60 seconds in the vicinity with a drop of violet doxanin matter. Then lamina is carried under the faucet and a drop of logol is trickled onto the lamina. After 30 seconds, lamina is again carried under faucet, and acetone alcohol drop is added to it. In the case of the positive warm bacteria, colour of the background remains violet, but in the case of the negative warm bacteria's, violet colour disappears. Afterwards, surface of lamina is carried under faucet and a drop of fuchsin is trickled to it and the result is studied after 30 seconds. There was no colouring for the positive warm bacteria, but in the case of the Negative warm bacteria, red-colour is appeared.

C-2) Catalase:

A drop of eau oxygenise is added to microbes suspension, and the result is examined from its oxygen bubbles Point of view. If gas is not created, it shows the experiment is negative. Such an observation fact could be very different for bacteria's according to their negative or positive manner.

C-3) Oxidase:

To perform for this experiment, one-percent Parapheny lend amine-chloride dimethyl solution is used. In this case, several millilitre of this consume were trickled up to the colonies which are under experiment. If after 30-40 seconds, reddish brown is appeared, it indicates the Positive ness and if it was colourless, it shows that the experiment was negative.

C-4) Citrate test:

Microbe colonies are inoculated in Simon citrate. After 2 hours, if the blue colour is observed on this medium, it indicates to having a positive experiment, and if there wasn't at serviced any change of colour and the medium keeps its green colour, it represents that experiment is negative.

C-5) Urea test:

Some of the under-test microbe colonies pumped to a Urea circum ference and put it in 37°C temperature. Colour reaction result is studied after, 24 hours If the reddish colour is abserved refer to positive and if no enrages of colour is showed, it refer to a negative experiment.

C-6) Tsi test:

It is a red colour medium to control and recognize Aerobic and anaerobic bacteria. This medium is inoculated by the aerobic and anaerobic bacteria and The related medium acidized in surface for aerobic Bacteria and in under-mentioned for anaerobic bacteria Changes to yellow colour.

Finally, the result of reactions of all colonies to these tests. Leded to the observation of five Bacteria that their names and chemical properties of them are shown in Table 2.

Table 2. Properties Chemical of organized micro organisms

number	micro organisms	Thermal - coloring test	Catalase	Oxidase	Citrate test	Urea test	Tsi test
1	<i>Escherichia coli</i>	Bacille -	+	-	-	-	Acid/ Acid
2	<i>enterobacter</i>	Bacille -	+	-	+	-	Acid/ Acid
3	<i>staphylococcus saprophytic us</i>	Cocce -	+	*	-	-	*
4	<i>pseudomonas</i>	Bacille -	+	-	-	-	Alk/ Alk
5	<i>bacillus</i>	Bacille +	+	-+	-	-	Alk/ Alk

CONCLUSION

Carpet that is a common worn fabric in Iranian culture could be a way of transition of pathogen microbes. In this research, the result gained from bacteria loges experiments on to acrylic- machine carpet that used in public places has shown that in the above conditions, five types of Bacteria's namely (*Escherichia coli*, *Enterobacter*, *Staphylococcus-Saprophytic us*, *Pseudomonas* and *Bacillus*) had grown. Each of these micro- organisms could be dangerous for human and woven fabric health.

REFERENCES

1. Anand, S.C.J.F Kennedy M.Mirafteb and S.Rajendran2006, Medical textiles and Biomaterials fir Healthcare. Woodhead Publishing Limited, Cambridge England, PP: 177-186
2. Bahgat, M.A, A.El- Falaha, A.D. Russell, J.R. Furr and D.t.Rogers, 1985. Activity of Benzalkonium Chloride and Chlorhexidine Diacetate Against Wild-Type and Envelope Mutants of *Escherichia Coli* and *Pseudomonas aeruginosa*. Intl. J. Pharmaceutics, 25:329-337
3. Cai, Z. and G. Sun, 2004, Antimicrobial Finishing of Acrilan Fabrics With Cetylpyridinium Chloride. J. Applied Polymer Sci, 94:243-247
4. Diz, M, M.R. Infante and P. Erra, 2001. Antimicrobial activity of wool treated with a new thion cationic surfactant Textile Res. J, 71: 695-700
5. Gloor, M, B. Schorch and U. Hoeffler, 1979. The feasibility of replacing antibiotics by quaternary ammonium compounds in topical antimicrobial acne therapy .Arc. Dermato . Res ., 265: 207 – 212

6. Han, S. and Y. Yang, 2005. Antimicrobial activity of wool fabric treated with curcumin. *Dyes and Pigment*, 64: 157– 61.
7. Huang, R, Y. Du, L. Zheng, H. Liu and L. Fan, 2004. A new approach to chemically modified chitosan sulfates and study of their influences on the inhibition of *Escherichia coli* and *Staphylococcus aureus* growth *Reactive and Functional Polymers* , 59 : 41-51.
8. Kim, Y.H.and G. Sun, 2001. Durable antimicrobial finishing of nylon fabrics with acid dyes and a quaternary ammonium salt . *Textile Res. J.*, 71: 318–323.
9. Lim, S. and S. M. Hundson, 2004. Application of a fiber-reactive chitosan derivative pp 123-128.
10. *Schindler, W.D. and P.J Hauser, 2004. *Chemical Finishing of Textiles*. Woodhead Publishing Limited, Cambridge England, PP: 165– 174.
11. Shao, H., L. Jiang, W. Meng and F. Qing, 2003. Synthesis and antimicrobial activity of a Perfluoroalkyl-Containing quaternary ammonium salt . *J. Fluorine Chem.*, 124: 89-91

DEVELOPMENT OF A NOVEL AIR-JET TEXTURING+TWISTING (AJT²) TECHNOLOGY

E. ÖZNERGİZ¹, U. TURGUTER², Ö. ÇALIŞKAN¹, A. DEMİR¹

¹Istanbul Technical University, Department of Textile Engineering

²Arçelik Research Center

ABSTRACT

A novel and innovative air-jet texturing + twisting (AJT²) technology has been developed and patented (TPE Document Code: 69065, Registration No: 20072344). This paper defines this novel process and elaborates on the potentials of this new technology in the field of technical textiles. The novel technology on-line combines the air-jet texturing operation with the twisting operation. Figure 1 illustrates the principles of this new technology and Figure 2 shows the prototype machine designed and manufactured to realise this technology.

Since the air-jet texturing is the only process to texturise the non-thermoplastic, especially glass, carbon and metallic fibres, this new technology has the unique features of combining these fibres to create composite fibres for technical applications. This is the only technique that a metallic wire could be inserted into the centre of a yarn in one single operation to create hybrid yarns. This technology has been developed by the support of TÜBİTAK research grant no: 105M134.

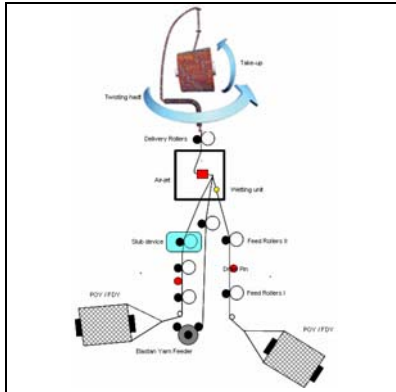


Figure 1 Principles of the AJT2 process



Figure 2 Prototype machine has been designed and developed to realise the possibility and potentials of the new technology

Keywords: Air-jet Texturing, Direct Twisting, Combined Yarns, Hybrid yarns, composite yarns.

1. INTRODUCTION

The air-jet texturing process forms a yarn with tightly convoluted, entangled and looped filaments resembling yarns spun from staple fibres such as

cotton and wool. In this process of air-jet texturing, multi filament yarn is fed into a narrow channel where it meets with a flow of compressed air and taken away from that channel at a lower speed than the feeding speed (called overfeed) and makes a right turn just after the narrow channel. At the exit of the narrow channel a supersonic, highly turbulent air jet is formed by the compressed air flow that pushes the freely available filaments in any direction in such a way that they entangle, convolute and loop with each other. Such converted yarn is much softer, bulkier and gives warmer feeling to wearer and possesses natural look and appearance than the supply yarn which may be composed of one or many filament yarns be thermoplastic, organic or metallic. Such a process has been the subject of many international patents so far. Nevertheless, all of these patents describe and claim processes with the produced yarn wound on tubes to form a simple package be it parallel or conical in shape.

The developed work has resulted in a novel process which on-line combines the air-jet texturing operation with the twisting operation. Yarn twisting process is a well known textile process. Although there has been many twisting methods developed, there are only three distinct types of twisting techniques industrially widespread used. The rest is of a property of patent literature. These widespread used twisting techniques are ring twisting, two-for-one twisting and direct twisting. In the ring twisting process, the tube on which the yarn is accumulated to form a package is turned. Since the mass of the tube and package increases as the twisting process continues, the size of the package holding tubes (mostly called kops) are kept as small as possible and the operation speed of such a ring twisting is limited to the low speeds of 10–20 m/min. On the other hand, during the two-for-one twisting the yarn holding package is not rotated. In addition to that, one revolution of the twist generating spindle forms two turns (hence two twists) on the yarn. That is why this process is named as two-for-one twisting. The operation speed of two-for-one twisting is in the range of 100-200 m/min. Yet, in this process, the supply bobbin has to have a hollow tube through which an unwound yarn is passed and directed to the radially positioned exit of the rotating spindle. The supply package is magnetically stabilized on this rotating spindle. The radially out fed yarn is then threaded through the yarn guide positioned above the spindle and then wound onto cross wound bobbin in the form of cylindrical or conical shape. By one rotation of the spindle, the yarn is twisted once while it is fed from the package to the spindle and twisted again from the spindle to the yarn guide positioned above the spindle forming the twisting balloon. In the process of two-for-one twisting, the supply yarn is limited to one or two bobbins stacked one above the other on the rotating spindle.

Relatively recently invented [1,2] and developed third method of twisting involves a rapidly rotating spindle where the supply yarn(s) are fed through the centre and led out from the radially positioned tunnel. The rotating and hence twisted yarn is then directed to the yarn guide positioned above the

spindle axis. The yarn is finally wound onto bobbin by the winder located within the sphere of the yarn balloon. The movement and energy transfer into the sphere formed by the rotating yarn balloon is the subject of another granted patent [3]. By such a process there is no limit of the number and shape of the supply yarn to be twisted.

This current development has been enabled by this third twisting technique. One or more multifilament yarn (FDY=Fully Drawn Yarn) or flat filament yarn may be directly fed by the BS1 (Feeding Cylinder 1) into the yarn channel of the air-jet nozzle at a higher speed than it is taken away from. In case of using a semi-finished yarn such as POY (Partially Oriented Yarn) as supply yarn, the yarn has to be fed by the ÇS drawing cylinders at lower speed than the BS1 in order to create a draw between the ÇS and BS1. The drawing cylinders may be cold or hot depending on the material of the yarn. After the drawing operation, the yarn is then ready as finished yarn to be fed in the yarn channel of the air-jet nozzle by the BS1 feed cylinders. Just before the entry of the feed yarn into the yarn channel, it is wetted by a water jet to wash off most of the spin finish oils as well as to reduce the friction between the filaments and between the filaments and all surrounding yarn guides including the yarn channel of the air-jet nozzle itself. Reduction of the friction improves the texturing tremendously. Such overfed and wetted filaments encounter the air flows coming from a 6-10 bar pressurised air source. The air flow(s) drag and separate the filaments to the exit of the yarn channel where a supersonic, turbulent free air jet is created and where the filaments are forced to turn at a right angle and pulled at a lower speed by the AS the delivery rollers that rotates slower than the BS1 rollers. The supersonic and highly turbulent jet of air blows the filaments in all possible directions and hence causes them to entangle and mix together

Such entangled, looped, convoluted and mixed filament bundle is fed into the central bore of the rotating spindle through which it is twisted and simultaneously wound up.

Since this novel process imparts at least two distinct improvements to the air-jet textured and mixed filaments by giving additional cohesion to the filaments. In the first distinct improvement, the air-jet texturing process may be carried out at much lower pressures (for example 5 bar instead of 9 bar air pressure) providing economical benefits. The other improvement is due to a novel character obtained in the final yarn. While the air-jet texturing forms all sorts of fancy yarns by mixing different colour, material, number of filaments, this novel combined process doubly widens this scope by adding all sorts of natural and/or spun staple yarn the air-jet textured yarns. In this way, the high tenacity and high wear resistance of the filament yarns is combined with the natural look and appearance as well as soft and warm feeling of spun staple yarns.

Another advantage enabled by this novel process is that two or more simultaneously air-jet textured yarns may be combined (doubled, folded) to

obtain softer yarns and hence fabrics. In the conventional ring or rotor spinning of staple fibres, a single end yarn is spun. Such single end spun yarns have inherent low tenacity, high irregularity and high rigidity. Such adverse properties are eliminated by the doubling or three-folding of such single end spun yarns. In similar fashion, the rigidity of the single end textured yarns are eliminated or reduced by the folding process enabled by this novel combined process.

This current developed technology gives the possibility of combining carbon, metal or all kinds of non-thermoplastic mono or multi-filament yarn with air-jet textured filament yarns and/or spun staple yarns to create totally different technical yarns.

2. PROCESS AND YARN EXAMPLES

The following process and yarn examples are for explanation only and therefore the newly developed technology is not limited with these examples.

2.1 Single End Yarn Air-Jet Texturing-Twisting

A polyester 250 dtex POY is placed on the creel of the machine. The yarn is pneumatically sucked from the bobbing via closed tubes and brought to the front of the machine. Having passed through the yarn cutter which cuts the yarn in case of any yarn breaks that hinders that yarn to reach yarn presence sensor just before the twisting spindle, the yarn is heated up to above its glass transition while it is wrapped three or four times over and forwarded at a speed of 220 m/min by the heated rollers with 95°C. During the wrapping of the yarn around the heated rollers, the friction between the incoming and outgoing yarns is eliminated by the separator roller placed beside the heated roller at an inclined axis. This separator roller is not driven and has much smaller diameter than the heated roller. The wrapping of the yarn around the heated roller provides both better heating and hence softening and gripping the yarn for effective drawing. Such forwarded yarn then reaches the BS1, the feed roller. The BS1 rotates to provide a surface speed of 360 m/min. As soon as the yarn is firmly nipped between this surface and the rubber coated idle rotating pressure roller, it is subject to a draw ratio of 1.6363 that creates orientation of the linear macromolecules in parallel with the filament axis. This drawing and hence orientation makes the yarn ready to use. The finished yarn is then passed through the eyelet of the noise and mist abatement chamber and the wetting head to reach the yarn channel of the air-jet texturing nozzle where it meets with the air flow coming from the compressed air reservoir with 6 bar pressure. For example the air-jet texturing jet of Heberlein type T311 is a suitable jet for this purpose. The three incoming air flow of T311 nozzle is pressurised at 6 bar. These three air flows drag and accelerate the wetted and overfed filaments. As the separated and accelerated filaments turn with 90° angle at the very exit of the yarn channel, the filaments move relative to each other and hence tangle and mix by the effect of turbulent and supersonic air to form a highly tangled,

looped, convoluted and thus textured compact yarn. The textured yarn is then taken out of the noise and mist abatement chamber and delivered at 300 m/min by the rotation of the chrome or ceramic plated delivery rollers. This yarn assumes a linear density of 180 dtex. Finally this yarn is fed to the twisting spindles which rotate at 4800 rpm to give a twist of 16 tpm. This twisted yarn (Figure 3) is wound up onto conical tube to form a conical bobbin.

Thus produced yarn obtains equal mechanical properties such as tenacity, break elongation, to yarns normally textured at a pressure of 9 bar. In addition, this yarn (Figure 3) obtains better compactness that results in desirable surface appearance in knitted and woven fabrics.

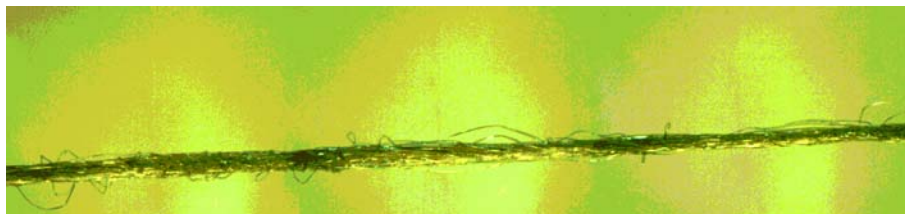


Figure 3. Single end textured and twisted yarn

2.2 Textured and Twist Doubled Yarn

Two filament yarns textured in the same way as described above are fed into the twisting spindle. At a rotational speed of 6000 rpm, the yarn assumes 20 twists per meter. Thus textured and twisted double yarn is wound onto conical bobbin.

Such produced yarn has both equal mechanical properties compared to air-jet textured yarn produced at 9 bar air pressure and assumes softer hand and touch to yarn textured as single 360 dtex yarn (Figure 4). This yarn results in improved drape in both knitted and woven fabrics.



Figure 4. Textured and twist doubled yarn

2.3 Combined Yarn of Filament Air-Jet Textured Yarn With Spun Staple Fibre Yarn

The above described single end textured 180 dtex yarn is fed into the twisting spindle together with a Ne40 combed cotton yarn. By the rotational

speeds of 2000-20000 rpm, preferably 6000 rpm of the twisting spindle, 20 tpm is imparted to combine both yarns. This combined yarn (Figure 5) is then wound onto conical package.



Figure 5. Textured yarn twist assembled with and spun staple yarn

Such combined yarn has better touch and warmth and natural appearance in comparison with the 320 dtex single and or doubled yarn. By this yarn, the knitted and woven fabrics get improved natural appearance and feel.

4. CONCLUSIONS

This work has developed a novel combined process by which the air-jet texturing and twisting processes are carried out simultaneously on a filament and staple spun yarn. In the conversion of the thermoplastic or organic filament yarns into a yarn with improved and better qualities, the air-jet texturing plays an important role. But this process is limited in widespread use due to high amount of compressed air consumption. On the other hand, the twisting operation achieved by the rotation of an end of a yarn brings together the yarn forming fibres or filaments together hence increase the cohesion and imparts strength as well as creates fancy and high value yarns from simple yarns. This new developed technology involves a combined single one step process in which the air-jet texturing and twisting processes both of which are individually unique processes. The combined process offers both improved process economics as well as limitless possibilities to create fancy effects on filament and spun staple yarns.

The combined process also offers covering of non-thermoplastic yarns such as metallic, carbon, ceramic, glass mono- or multi-filament yarns to be used in intelligent textiles for the electrical conductivity or heat dissipation.

REFERENCES

1. European Patent EP 1 544 333 A1
2. European Patent EP 1 566 474 A3
3. European Patent Application PCT/EP2004 000301

EFFECT OF FIBERS CHARACTERISTICS ON POLYESTER FIBERS DISPERSION FOR WET-LAY NONWOVEN

A. SAFAVI, M. LATIFI, M.R. BABAEI

Department of Textile Engineering, Amirkabir University of Technology

ABSTRACT

At the present study, an on-line vision system was designed to observe the dispersion behavior of polyester fibers. The effects of fiber length and fineness on defects (namely logs and ropes), created in dispersion process, were studied. Also the effects of length and fineness on dispersion speed, were considered. The results indicated that the defects increase by increasing fiber length and fineness. It also showed that by increasing the fiber length and fineness, the highest break-up fiber clumps time, decreases. In other words, when the fiber length and fineness are increased, the dispersion speed increases.

Key Words: dispersion, finesse, length, clumps, break-up

1. INTRODUCTION

The wet-laid nonwoven manufacturing can be divided into fiber dispersing and blending, lay-down process (web formation), drying and finally bonding. Fiber dispersion is the most challenging step of the wet-laying process. This process usually involves the suspension of fibers in water. A wet-laid nonwoven is then formed by draining this solution through a forming mesh (a monofilament woven screen). At this stage the majority of fibers are in the form of separable clumps and need to be separated into individual fiber in a mixing tank through the shear exerted on them by the flow field. To form a uniform nonwoven, fibers must be well-dispersed prior to be laid-down otherwise they may stay as fiber bundles and appear as defects (the so-called log defects) in the final product. In most cases, the cut ends fibers in logs remain aligned. Logs usually appear in the fabric because of fibers agitation during the initial dispersion. An analytical study accompanied with experimental observation [1] has showed that the break-up rate of logs increases by increasing shear rate agitation speed). Rope formation is a major concern especially when fibers with varying degree of stiffness are mixed. In this case, the more flexible fibers will twist and wrap around the stiffer fibers[4].

The surface properties of wet-laid fibers are reported in different pioneer works [2-3,5]. In almost all the previous works, dispersed fibers were first deposited onto a forming surface then dried and analyzed using image analysis tools. This can become an exhausting process when investigating several different fibers and for several different dispersion times[6]. In this

study, to skip the deposition and drying steps, an on-line computer vision system were developed to monitor the quality of dispersion over time while mixing different fibers under different shear fields were carried out. the experimental work is presented in the next section.

2. EXPERIMENTAL WORK AND IMAGE PROCESSING

A laboratory camera, a collimated backlight source, a flat bottom glass beaker and a magnetic stirrer were set up (figure 1). To avoid extra light, all tests were done in a dark room.

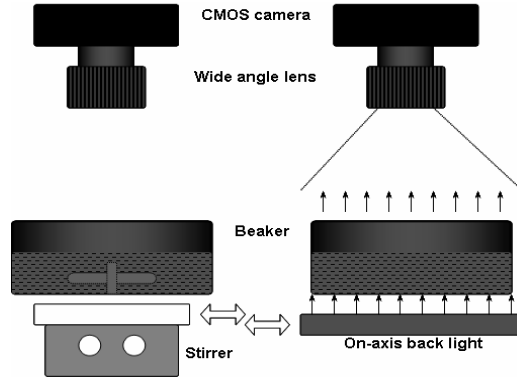


Figure 1. A Schematic of the set-up[6]

Polyester fiber with 16, 21 and 26 μ m diameters and 8, 11 and 15mm lengths were used. Each experiment was repeated three times. In total 27 samples were experimented and the crowding factor, n_f was calculated using equation 1:

$$n_f = \frac{2}{3} C_v \left(\frac{l}{d} \right)^2 \quad \text{equation 1}$$

Where C_v , l and d are volume fraction, fiber length and fiber diameter respectively [7].

The appropriate amounts of samples were selected so that the crowding factor of all samples remained equal. Table 1 shows the results.

Each Sample was dispersed in a beaker containing 200ml of water and the liquid was being agitated with the stirring speed of 540rpm[6] for 12min.

One image per 30 seconds was taken during the first 3 minutes and followed by one image per 60 seconds for the rest of the dispersion period. Figure 2 illustrates several images. An appropriate computer program in "MATLAB" was written and several Image processing techniques were applied to process the images. Finally the overall area of the defects (logs and ropes) was counted in the unit of pixels and reported.



Figure 2. step by step images in dispersion process

Tablo 1. The sample weight (gr)

		diameter (mm)		
		0.026	0.021	0.016
length (mm)	8	0.1	0.065	0.038
	11	0.053	0.034	0.02
	15	0.028	0.019	0.01

3. RESULTS AND DISCUSSIONS

3.1 The Effect of the Fiber Length on the Defects

The effect of the fiber length on the defected areas was studied. Figure 3 demonstrates the results. It shows that the defect number decreases when the length of the fibers increase.

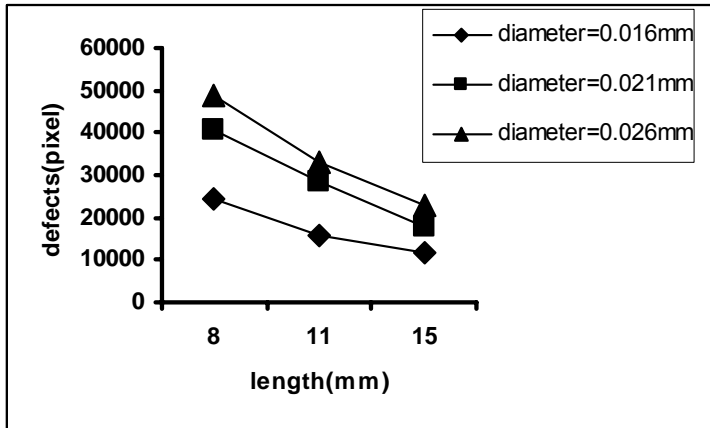


Figure 3. The defects vs. the fiber length for the different fiber fineness

3. 2 The Effect of the Fiber Fineness on the Defects

The effect of the fiber fineness on the defected regions was considered.

Figure 4 displays the results. It confirms that the defect number decreases while the fineness of the fibers increase.

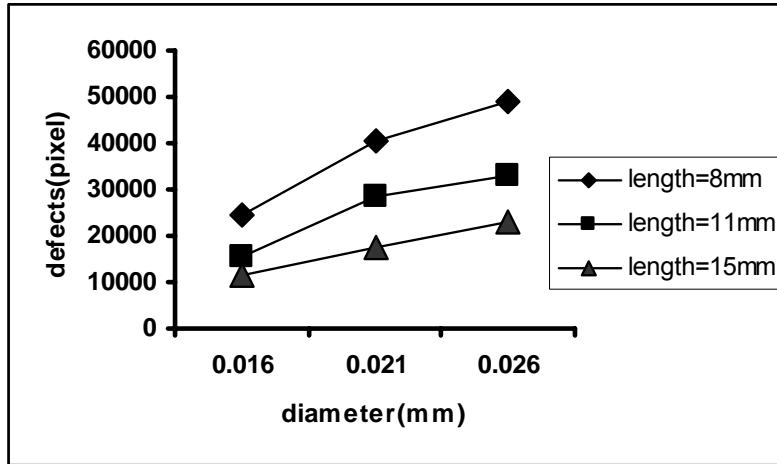


Figure 4. The defects vs. the fiber diameter for the different fiber lengths

3.3. The Effect of the Optimum Dispersing Time on the Defects

The optimum dispersing time is the time in which the number of the fiber clumps is minimum. The effect of the dispersing time was investigated. It seems that the optimum dispersing time decreases when the fiber fineness increases resulting lesser defects (Figure 4). The results also show that the optimum dispersing time decreases when the fiber length increases (Figure 5). Table 2 reveals the optimum dispersing time at different fiber lengths and diameters.

Tablo 2. optimum dispersing time (sec)

		diameter (mm)		
		0.026	0.021	0.016
Length(mm)	8	360	150	120
	11	300	120	90
	15	90	90	90

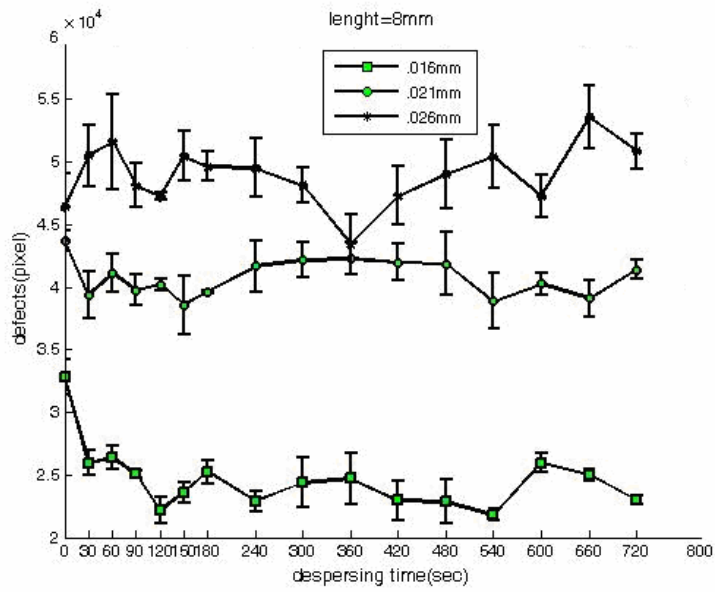


Figure 5. Dispersing time vs. defects (the fiber length is 8mm)

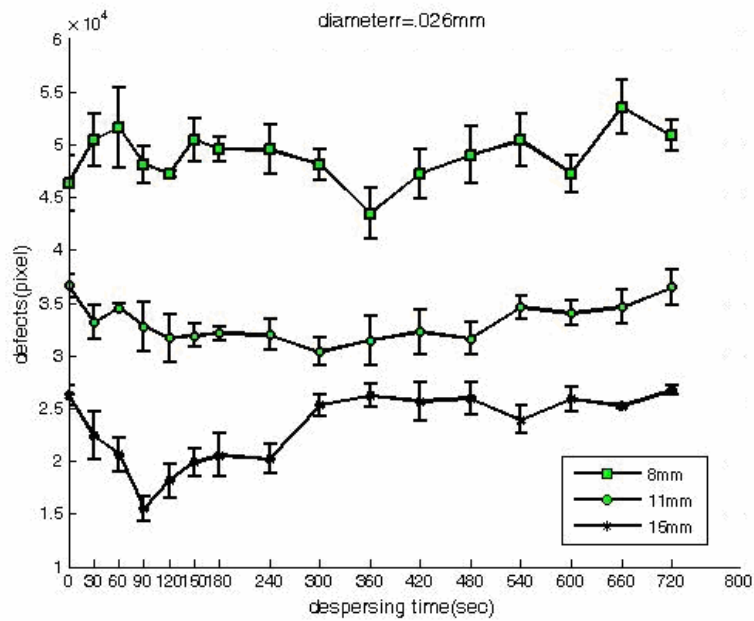


Figure 6. Dispersing time vs. defects (the fiber diameter is 0)

3.4. DISCUSSION

As the crowding factor of all samples is the same, the number of fibers in the sample decreases when the fiber length increases. The lesser the number of fibers, the smaller the chance of contact points between the fibers. As a result the number of defected areas decreases when the fiber length increases.

According to the earlier studies [1], when the fiber diameter increases, the required energy for separating the fibers from each other, increases. Also by increasing the fiber diameter, the surface tension force that resists against shear forces, caused by the flow field, increases. So the required energy for separating the fibers, increases. Therefore an increase in the fiber diameter in constant condition (i.e. shear forces (dispersing speed) and fiber length), causes an increase in defects.

Based on shiffler's researches [1] the required energy for clumps separation, has direct relation with fiber diameter. *i.e.* when the fiber diameter is increased, this energy increases too. In a constant condition (specially at equal shear forces), when this energy increases, it is clear that the time required to separate fibers, increases. In other words, an increase in fiber diameter, raises the time required to separate fibers.

As mentioned earlier, by increasing the fiber length, the number of fibers in the samples, decreases. Therefore the number of contact Points decreases and as a result the required time to separate fibers, *i.e.* the optimum dispersing time decreases and minimum defects are built up.

It is resulted that in smaller fiber lengths, dispersion process is done more evenly. Also the average time which is required to reach minimum defects (maximum fiber clumps break-up), for the smaller fiber lengths, is lesser than longer one. By increasing the fiber length, the required time decreases. But the dispersion process becomes uneven. It could be observed that the defects increase significantly when the dispersing time exceeds the optimum dispersing time. In fact after breaking up the logs, the ropes increase intensively. So if the longer fibers are used in the dispersion process, the control of time is important. On the other hand, there is no significant difference between the minimum and the average defects, when the smaller fiber length is used. By increasing the fiber length, this difference becomes larger and needs more attention.

The same as fiber length, in the case of less fiber fineness (*i.e.* more fiber diameter), the dispersion process is done evenly. Also the average required time to reach to the minimum defects, decreases. However, control of the dispersing time is important.

4. CONCLUSION

In this work, polyester fibers at three different lengths and diameters were dispersed in water and agitated. The dispersion behavior of fibers and their effects on the amount of defects were considered. The results indicated that by increasing the fiber length and fineness, the number of defects decreases and the required time for fiber clumps to be opened and changed to the separated fibers decreases. It could be found that control of time during dispersing process is more important specially when longer and /or finer fibers are used.

REFERENCES

1. Shiffler,D,A, (1985), "Characterizing the dispersion kinetics of synthetic fibers in water", TAPPI Journal,68(8),88-91
2. Keit, J.M., (1994), "dispersion of synthetic fiber for wet-lay nonwoven", TAPPI Journal , 77(6), 207-210.
3. Vaidya,N.; Pourdeyhimi, B.; Shiffler,D.A. and Acar,M.,(2003),"The manufacturing of wet-laid Hydroentangled glass fiber Composites: preliminary Results", International nonwovens Journal,12(4).55-59.
4. Shiffler, D.A., (June1988)" Defective fibers in wet-lay nonwoven fabrics" TAPPI Journal , P117
5. Parrinello, L.M, (1991), " Fiber geometry effects on Physical Properties of Chopped Fiber Composites", TAPPI Journal, 74(1), 85-88.
6. M. Latifi , H. V. Tafreshi , B. Pourdeyhimi " On line observation of Glass and Polyester Fiber Dispersion in Wet-Laid Nonwoven Process "
7. <http://www4.ncsu.edu/~hubbe/Defnitsns/CrowdFac.htm>.

THE EFFECT OF THE YARN TWIST DIRECTIONS ON THE SHEARING BEHAVIOR OF THE WOVEN FABRICS

A. ALAMDAR YAZDI¹, G. ÖZÇELİK²

¹Department of Textile Engineering, Yazd University

²Department of Textile Engineering, Ege University

ABSTRACT

This experimental work deals with the shearing properties of woven fabrics. A total of 16 plain woven fabrics (four groups, each with four samples) were produced by using Solo spun yarns as warp and weft threads. The shearing rigidity of each fabric was measured in two systems: Concentrated loading method and Kawabata evaluation system. The results indicate that fabric's shearing characteristic is affected by the yarn twist direction. That is, fabrics in which the twist direction of warp and weft yarns are the same (Z & Z), the shearing rigidity is higher than the fabrics in which the twist direction is opposite to each other (Z & S). In addition, it showed that increasing in twist multiplier of the yarns in fabrics which the twist direction of the warp and weft is the same, cause increment in the shearing rigidity due to nesting of the yarns at crossing points.

Key Words: Concentrated Loading Method, shearing property, bending length, woven fabric

1. INTRODUCTION

The ability of a woven fabric to accept shear deformation is a necessary condition for a conformable fitting to a general three dimensional surface and is the bases for the success of woven textiles as clothing materials. This property is affected by the yarn characteristic and fabric structure.

The twist of the threads in which the fabrics are made of, is one of the main parameter affecting the fabric behaviours including shearing property.

In one hand yarn twist affects the yarn properties like surface characteristics of the yarn and on the other hand it effects the relation between the warp and weft yarns, at interlacing points.

The leading tools, which are used to measure the shearing property, are KES-FB1 shearing tester and FAST 3 extensibility tester. It could also be evaluated by the concentrated loading methods [2].

In this work we examine the effects of the yarn twist direction on the shearing movement of the fabric produced with Solo spun yarns by considering the local surface helix angles of bent yarn at crossing point.

2. MATERIALS AND METHODS

To examine the effect of twist direction on the interaction between the warp and weft at crossing points, two sets of yarns (S & Z) each containing 4 different twist levels were produced. In order to have pure single yarn (without any weaving preparation treatment) Solospun yarn with advantage of lower hairiness, was used. The details of the material and yarn specification are shown in Table 1.

Table 1. Specification of the fibres and produced yarns.

Fibres	Yarns				
	Blend	Twist	Count (Nm)		Surface helix angle at contact point
1- Australian merino fleece wool top as per international standard (IWTO) Wool specification: 22 micron (maximum average), 65 mm (minimum average), sliver weight 20 gr/m	45%		30	24	
		Direction	S & Z	S & Z	
2- DuPont Polyester Tops, 20gr/m Polyester tops, 3 den, 76 mm, raw white, semi dull, low pilling.	55%	Multiplier (α_m)	127	127	43.3
			115	115	40.4
			105	105	38.1
			100	100	36.5

Based on the specifications shown in Table 2, two warp beams were prepared (without any waxing treatment).

Table 2. Specification of warp thread

Beams	Yarn count	Twist direction	Turns/meter	Ends/10 cm.	Twist angle
A	1/24	Z	622	200	43.3
B	1/30	Z	695	230	43.3

Using the same yarn count but different levels of twist (twist multipliers of 3, 3.5, 3.8 and 4.2) as weft yarn, 8 fabric samples were woven on each beam, therefore totally 16 samples were produced. Fabrics were woven on the Lens-1966, shuttle loom, 120 picks per minute, with low level of tension for the warp yarns and relatively higher level of tension for the weft yarns.

Figure 1 shows the complete line of the samples production with the necessary information.

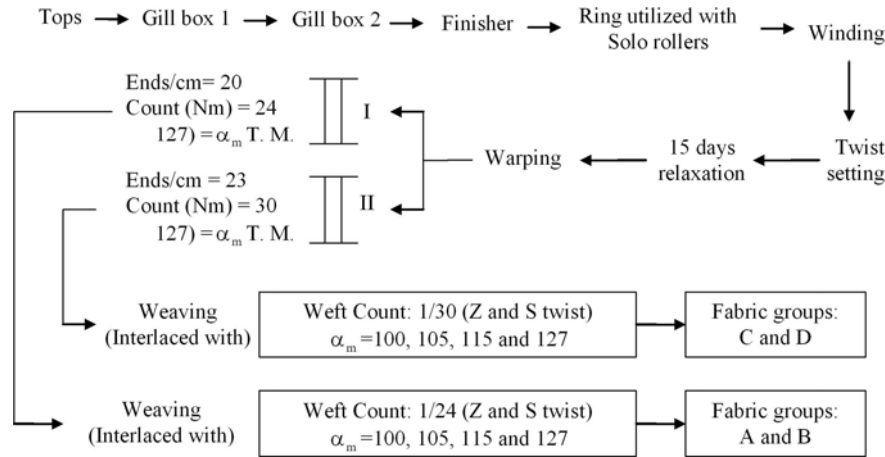


Figure 1. Production line diagram

Tests

a) Kawabata Evaluation System

Shear rigidity in warp and weft directions were measured by Kawabata tensile and shear tester. For this purpose 4 samples in the dimensions of 20×20 cm, were cut from each fabric. Fabric shearing rigidity was the average value of the warp and weft shearing rigidity.

b) Concentrated loading method

A rectangular specimen 24 cm in lengthwise and 5 cm in transverse directions was cut from every sample fabric, at angle of 45° to the warp direction, (which is the same to the weft direction) using a special template. The strip is then folded in half to form a double ply of face to face fabrics 12-cm in lengthwise. The puncher is inserted an eyelet 1-cm from the ply ends opposite to the fold and the second eyelet is inserted 10-cm far from the first one after possible slack is removed. (Doubling the strip makes the samples free from any shear strain, which could be developed under tensile stress).

The samples were then subjected to a single loading-unloading cycle at a rate of 10 mm/min with a 200 g maximum force using a simple attachment to the jaws of Testometric-micro 350 made in the Shirley developments, with 4kg load cell. The gap area above the critical point of the concentrated load curve, (AGA,-Fig. 2) was measured to calculate the stiffness of the shearing movement [2].

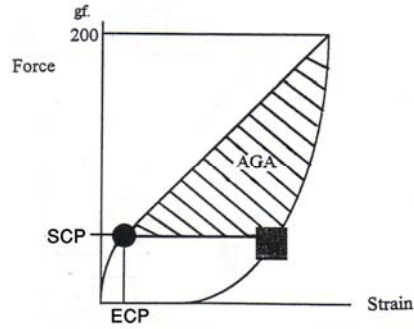


Figure 2. The features extracted from the concentrated loading curve.

3. RESULTS AND CONCLUSION

Table 3 shows the measured rigidity of the fabrics (A1-A4, B1-B4, C1-C4 and D1-D4). Comparison of the shearing rigidities in each beam (Bs to As and Ds to Cs) shows that the fabrics with the same twist directions perform higher rigidity.

Table 3. The weft twists helix angle and the values of shearing rigidity.

Fabrics	Weft twist multiplier		Beam I		Beam II	
			A	B	C	D
1	127	Weft twist direction	Z	S	Z	S
		Fabric shear rigidity (G)	0.680	0.660	0.700	0.650
2	115	Weft twist direction	Z	S	Z	S
		Fabric shear rigidity (G)	0.665	0.640	0.680	0.700
3	110	Weft twist direction	Z	S	Z	S
		Fabric shear rigidity (G)	0.657	0.650	0.680	0.660
4	105	Weft twist direction	Z	S	Z	S
		Fabric shear rigidity (G)	0.650	0.660	0.660	0.680

Figure 3 shows fabric shear rigidity values versus the weft twist multipliers for all the fabrics. For the both beams the fabrics (–A and C–) with the same twist direction (Z & Z twist) perform higher shear rigidity and are affected by the change of weft twist multipliers. However the fabrics with opposite twist directions (–B and D–) are not affected by the twist changes.

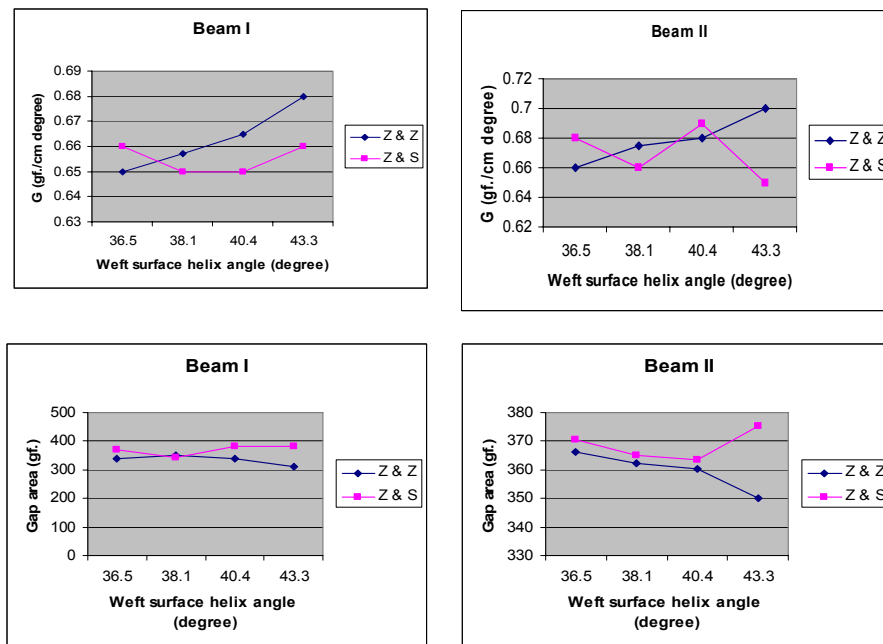


Figure 3. The effect of twist (direction and the amount) on the shearing property of the woven fabrics

Table 3 also indicates that change in weft twist multipliers does not affect the shear rigidity of the B and D groups of fabrics. The only difference between A and B or C and D, is the twist direction of the weft yarns. B and D group of fabrics are made of warp yarn Z and weft yarn S twist. Thus, the difference could be due to the bedding of the warp and weft yarns at crossing points.

This is because when the twist direction is the same, the fibres of the two sets of yarns (warp and weft) are engaged, making the shearing movement difficult, causing delay in the buckling point (out of plane deformation) of the fabric.

Table 4 compares the critical point specification (buckling point) of the fabrics. It indicates that buckling phenomenon is irregular for the fabrics in which the warp and weft twist direction are not the same, in comparison to those in which the warp and weft twist direction are unidirectional.

Table 4. Specification of the buckling points extracted from the concentrated loading curves

	<i>Beam I</i>				<i>Beam II</i>			
<i>Fabric</i>	<i>A</i>		<i>B</i>		<i>C</i>		<i>D</i>	
<i>F.T. Direc.</i>	<i>Z & Z</i>		<i>Z & S</i>		<i>Z & Z</i>		<i>Z & S</i>	
<i>F.T. Angle</i>	<i>gf.</i>	<i>%</i>	<i>gf.</i>	<i>%</i>	<i>gf.</i>	<i>%</i>	<i>gf.</i>	<i>%</i>
36.5°	13.725	0.230	12.940	0.240	14.181	0.198	11.197	0.218
38.1°	14.111	0.186	9.555	0.330	14.522	0.171	13.237	0.251
40.4°	15.231	0.144	14.333	0.195	15.327	0.166	10.444	0.243
43.3°	15.663	0.152	10.125	0.256	15.924	0.160	16.329	0.166

In fact, when warp and weft twist directions are the same, the twist on the underside of the top thread is in the same direction as that on the upper side of the lower thread. Such condition is favourable for the threads to bed into each other and put the fabric at the equilibrium status, giving uniform deformation. In other words, free self movement of the yarns in the structure is limited and depending upon the depth and the area of compactness, the movement is controlled. Such condition makes fabric deformation uniform, and load distribution regular.

When the twist direction for warp and weft is not the same, the twist on the underside of the top thread is in the opposite direction of that on the upper side of the lower thread. In this case the condition is such that the threads can not bed into each other. They do not form a compact cloth (the weave and threads structure is distinct) especially when the twist is high, and as a result the effect of any torque existing in the yarn will affect the distortion of the fabric [3].

The highest shear rigidity belongs to the fabrics with Z & Z twist direction and twist multiplier of 127 for warp and weft. That is, twist angle at crossing points is 43.3 degree for both warp and weft yarns, making a total of almost 90° which enables the yarns bed into each other and as a result increasing the yarn compactness at crossing points causing delay in "out of plane deformation".

4. CONCLUSIONS

- 1- Shearing property of the fabric is affected by the conditions of the contact points.
- 2- Fabrics for which the warp and weft twist are unidirectional (Z & Z twist direction), perform higher shearing rigidity, (smooth rounded

curvature) in comparison to those for which the warp and weft twist directions are opposite to each other.

- 3- Increase in twist multiplier of the fabrics in which the twist direction of the warp and weft is the same causes increment in the shearing rigidity due to the bedding of the yarns at crossing points.
- 4- The best condition belongs to the fabric in which the warp and weft twist multiplier was 127.

REFERENCES

1. Bishop, d.p. (1996), "Fabrics: Sensory and Mechanical Properties", Vol. 26, No. 3, Textile Progress,
2. Alamdar-Yazdi, A. (2004), "A new method to evaluate low-stress shearing behaviour of woven fabrics", Vol. 29, Indian Journal of Fibre & Textile Research.
3. Alamdar-Yazdi, A. and Khojasteh, M. (2006), "The effect of twist liveliness on the woven fabric distortion", Vol. 7, No. 1, Fibers and Polymers.

PHOTOVOLTAIC APPLICATIONS FOR TEXTILES

A. ÇELİK¹, A. DEMİR², Y. BOZKURT¹

¹Dokuz Eylül University, Textile Engineering Department

²İstanbul Technical University, School of Textile Technologies and Design

ABSTRACT

Photovoltaic energy generation technology, among various technologies, provides a source of renewable energy in a variety of form factors for commercial, government and consumer applications by converting sunlight into electricity and presenting clean and sustainable products. Researchers have been studying on producing economical, efficient and versatile photovoltaic devices in many areas and developing prototype solutions into manufacturable forms. These intelligent materials generate a great power potential in widespread areas for many usage. Until very recently, nearly all photovoltaic devices were hard silicon semiconductor based cells and therefore they were very limited in widespread applications. Flexible polymeric semiconductors are now opening a new area in which films and fibres are becoming a potential application form. Fibres and textiles are maturing fields for photovoltaic cells with promising different applications. Photovoltaics based on textiles can positively increase the number of applications available to solar technology by delivering lightness and flexibility of photovoltaics and extending integration to other textile materials. This paper summarizes photovoltaic technology, devices including possible new uses in fibres and textiles with advanced properties.

Keywords: Organic semiconductor, photovoltaic cell, solar technology, fibre, textile.

1. PHOTOVOLTAIC TECHNOLOGY AND FEATURES

There is an increasing demand to develop and use the clean energy technologies which can produce environmentally friendly energy, in recent years. Among these methods, the most remarkable one is producing energy by using sun which is limitless energy source (and other UV sources).

Solar cells are based on semiconductor materials which directly convert sun light that comes to cell surface into electricity. This technology is used for calculators, buoys, urgent telephone call boxes, road signs and satellites effectively. Today, special materials and semiconductors such as silicon are used in a photovoltaic cell which is formed by words photo=light and voltaic=electricity, widespread. Working principle of the cell is absorption of part of photons by semi transmissive material when they come into solar cell. Energy of photons causes excitation in electrons and to flow in a way by forming electrical current. These electrons contact with a metal in the cell and current is taken out by this conductive structure from the cell to use [1-2]. Silicon is used mostly in production of photovoltaic cell because of its efficiency. Besides other inorganic semiconductor based materials such as Gallium Arsenide (GaAs), Cadmium Telluride (CdTe) and Cadmium sulfide

(CdS) are used [3]. In organic solar cells, many kinds of organic chemical materials, aromatic colorful dyes, titanium dioxide and other semiconductor oxides are also used [4].

Photovoltaic systems produce electricity by using light comes from sun. Some advantages of this technology began to develop with space applications in the middle of the 20th century, are Being modular (no moving parts) and clean (no waste), easy maintaining, buildable where it is required. With this system, electricity is used directly and it can be stored regionally or it can be fed into an existing electricity network. When its cost is decreased, photovoltaic energy which can be compete against other energy production types, will help to struggle with threat of global climate change and provide world energy demand.

However studies are limited, today, solar technology has an increasing widespread use. Application of this technology to textiles and especially developing a photovoltaic fibre will be very important for future possibilities in both commercially and scientific meaning.

In the study about developing a photovoltaic fibre is carried on by authors as a doctoral thesis in university. For this study, using the fibre raw material and other chemical materials which have determined physical and chemical properties, fibre designs are made and these fibres will be also produced with methods of spinning and coating. With this study, various textile surfaces will become intelligent structures which will produce energy.

2. IMPORTANCE FOR TEXTILES

Textile materials which have different properties by attracting attention caused new and rapid developments. Apart from the traditional wearing and covering, advanced textile products are materials which are looked for technical uses. After various photovoltaic materials which have appropriate features for textile materials are selected and gathered, solar technology will be used as a textile structure or integrated to existing structure easily. From this view, using this fibre, the textile materials' base material becomes photovoltaic. So, new practical and portable products which are made from photovoltaic fabrics or used with them in the form of electronic devices will be presented to the markets. In the future, obtaining any photovoltaic textile structure depend on a photovoltaic fibre which has a good electrical performance and appropriate to active using beside many kinds of physical properties like strength, fineness and flexibility

3. APPLICATIONS OF SOLAR CELLS TO TEXTILES

Photovoltaic textiles, in theoretically, are tried to fabricate as a photovoltaic fibre or material which will be used easily in any textile structure. In this wise, production of a flexible photovoltaic structure appropriate to textile material, excepting the integrated materials, will be actualized with flexible and effective

photovoltaic fibre which will be provided by specific production methods and materials [5].

In recent years, utilization the photovoltaic materials based on compound of copper, indium, gallium and selenium (CIGS) which doesn't contain silicon and is environmentally friendly because of less carbon dioxide propagation began to increase beside silicon which is used widespread in flexible solar cell applications for textiles [6].



Figure 1. Rollable flexible silicon based solar panel [7]

Researchers developed a ski-jacket prototype which produces energy (2.5 Watt) under optimum sun light conditions. Incoming cells using amorphous silicon are 0.5 mm fineness and works with %5 efficiency. Therefore photovoltaic elements have been put on places where is most appropriate for sun light and most ergonomic for user (shoulders and back). Because of thinness, cells are flexible which wearer will take comfort. A converter changes the voltage that cells produce, to constant current with 4.5 volt. Very thin and washable micro cables have been sewn into material and electrical current has been directed to many kinds of devices or chargeable batteries with these cables [8-9].



Figure 2. A ski-jacket on which solar energy cells are integrated [9]



Figure 3. A commercial solar jacket which produces electricity for working of portable small devices [10]

Electrical energy obtained from three military tents given below is approximately between 200 Watt and 1 Kilowatt. Number of tents can be increased when more energy required. Produced energy can be charged in batteries. This kind of product can be used for compensating of energy demand for many aims such as lighting, ventilation, GPS systems, rechargeable cells and laptops [11].



Figure 4. Military tent on which solar energy cells are integrated [11]

Hynek et al. have put flexible silicon based solar cells on a tie surface made from cotton sateen fabric. Also digital textile printing technique has been used for the design structure on tie. Surface of the solar cells has been coated with a lamination to be protected. Although some disadvantages (lustre of the surface, width and knot of tie), it has been told that problems could be overcome with method of digital textile printing and using advanced solar cells [12].



Figure 5. A photovoltaic tie and jacket on which solar energy cells are integrated [12]

Shur et al. has used polycrystalline semiconductor CdS based solar cells and CuS based metal films in their studies which have been made to obtain semi conductive yarns beside these studies which the integration of inorganic semiconductor based solar cells to textiles have been explained above. In that way CdS/Cu_{2-x}S based films have been deposited on synthetic yarn and formed into a fabric and photovoltaic efficiency is measured [13,14].

However among all solar cell materials, organic based solar cells are more appropriate to textiles with regard to important features such as flexibility, performance and inexpensiveness. In scientific studies about solar cells related with textile materials, integration or production of a fibre is concerned. Integration of organic solar cells to textile structures must be appropriate to consumer demands otherwise it can cause negative results for commercially. Photovoltaic films must be also placed on fabric or apparel in a way which will take sun light to obtain maximum energy.

By developing versatile polymeric photovoltaic materials which are lighter and more flexible than traditional solar cells, plastic based, cheaper and coatable organic photovoltaic material technology for various applications has been appeared. According to a commercial application, the photovoltaic material under indoor and outside light, using photovoltaic nanotechnology to provide electricity to many electronic devices, uses wider light spectrum than traditional solar cells. These photovoltaic materials on flexible substrates can be printed and coated cheaply and same machine and technologies can be also used. They have various color, design and transparency and can be used on many surface and products [15]. Beside the camp tents and shelters, many kinds of thing even daily bag can produce electricity [16-18]. Number and area of applications will be increased if studies about producing the woven fabric which will have good electricity properties from fibres give positive results. Thus every type of fabric will be photovoltaic based and generate energy [19].

In 2005, researchers studied screen printing for the deposition of the active layer of a bulk donor-acceptor heterojunction solar cell using a poly (phenylenevinylene) derivative as donor and PCBM (a C_{60} derivative) as acceptor material related with production of organic solar cell integrated to textiles in. Solar cells were realized with energy conversion efficiency of 1.3% [20].



Figure 6. A photovoltaic suitcase on which solar energy cells are integrated [20]

Krebs et al. used two different strategies for the incorporation of polymer photovoltaics into textiles in 2006. Basic incorporation of a polyethyleneterphthalate (PET) substrate carrying the polymer photovoltaic device prepared by a doctor blade technique necessitated the use of the photovoltaic device as a structural element. The second strategy was more elaborate and involved the lamination of a thin layer of polyethylene onto a textile material followed by plasma treatment and application of a PEDOT electrode onto the textile material. It was shown that solar cells produced can be applied to textile surfaces efficiently and the degradation resulting from transport of oxygen and/or water into the device are more pertinent than the mechanical stability on the timescale of those experiments [21].



Figure 7. Photovoltaic apparels on which solar energy cells are integrated [21]

A project (SOLTEX) was organized to develop a flexible organic (plastic) solar cell that can be integrated with textile surfaces by lamination technology. In the project, firstly, researchers started from proven organic solar cell technology and adapt this in order to obtain a solar-cell sheet that is suitable for lamination with textiles. Secondly, researchers selectively replace certain parts of the solar cell in order to improve its performance in the demanded environment [8]. Researchers studied about adaptation of solar cell technology to fibre form which could be directly incorporated into applications where high flexibility and small diameter were necessary, in 2002. In their research, a long, flexible tubular solar cell was assembled by building up the solar cell from the inside out and a conductive stainless steel was used as internal electrode coated with semiconductive nanosized TiO_2 powder which different organic dyes were used to sensitize. The mounting of electrode, ceramic powder and electrolyte was incorporated into a transparent polymer tube that has been coated with conductive polymer on the inside [22]. In 2005, in a patented research shown in Figure 8, the material had photovoltaic effect (0), included a fibre core (1) having an outer surface, a photosensitized nanomatrix material (2), and a charge carrier material (3), where the photosensitized nanomatrix material and the charge carrier material were disposed between the outer surface of the fibre core and the light-transmissive electrical conductor (4) and one or more wires (4) inserted in it. There is also a protective layer (6) and thus, realized the fibre role [5].

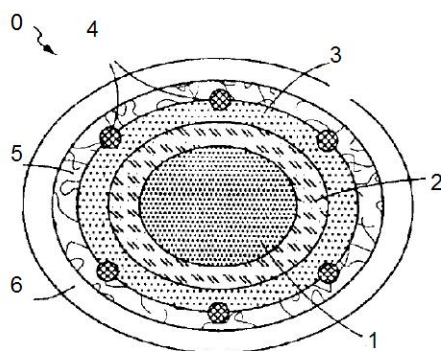


Figure 8. Cross section of the photovoltaic fibre [5]

Researchers studied about a cylindrical flexible solar cell which is made of only flexible materials in order that the cell could freely bend, had a cylindrical shape that allows the cell to absorb solar light at any angle of illumination, and had a large surface area and high efficiency, and developed a method of producing the same, in 2006. Generally, solar cell in the invention has many layers; however the most important one is the semiconductor electrode which includes a conductive transparent substrate, a light absorbing layer (metal oxide layer) and a sensitizer (dye) [23].

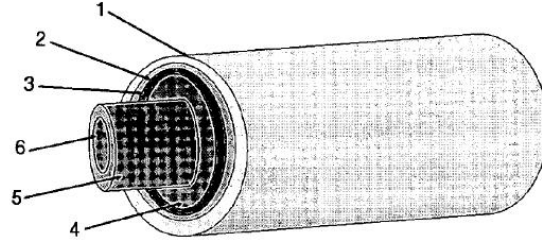


Figure 9. In photovoltaic fibre; a cylindrical waveguide (6), a counter electrode(5), an electrolyte layer(4), a semiconductor electrode: transparent substrate (1), a light absorbing layer (metal oxide layer) (2), and a sensitizer (dye) (3) [23].

Liu et al. have fabricated organic photovoltaic devices using thin film geometries, onto multimode optical fibres (0,6-1,5 mm in diameter). It was shown that small fibres (0,6 mm transmitted most of the energy through back and so, optical loss into the device increased as the fibre diameter decreased (%0,1 efficiency in 1,5 mm diameter and %0,6 efficiency in 0,6 mm). In the study, optical fibres have been coated with ITO, PEDOT:PSS, P3HT:PCBM, LiF and Aluminum layers [24].

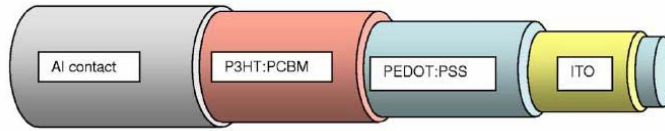


Figure 10. Photovoltaic fibre [24]

5. RESULTS

Efficiencies of organic solar cells show an increase by development and advances in materials which are used in recent years [25,26]. Flexibility, inexpensiveness and lightness of organic solar cells allow them widespread using in many systems and areas from industry to defense. An active textile fibre and a fabric produced from it, in second step, in the future, will be used in every part of life and open new windows for versatile materials which will generate energy. Demand of photovoltaic textile materials (fibre, fabric and etc.) and photovoltaic thin films which are integrated on apparels is related with fashion strong [12]. In textile sector which consumer wants are considered, to get commercial success, these types of materials must show an attractive appearance and full completeness with textile structure beside duty of production electricity energy from sun light.

REFERENCES

1. T. Yöney, Güneş Pilleri Nasıl Çalışır, Tübitak Bilim Teknik Dergisi, Aralık 2002 sayfa 97.
2. Organik Güneş Hücreleri, Tübitak Bilim Teknik Dergisi, Aralık 2005 sayfa 42

3. E.Çetin, B.S.Sazak, Fotovoltaik Hücre Yapısı ve Sistem Verimine Etkisi, 10.Denizli Malzeme Sempozyumu ve Sergisi, 14-15-16 Nisan 2004, 369-374
4. Türkiye'de Güneş Enerjisi, Tübitak Bilim Teknik Dergisi, Temmuz 2006 sayfa: 34-41.
5. Patent US 6,913,713 B2
6. M.B.Schubert, J.H.Werner, *Materialstoday*, 6, 9, (2006).
7. http://www.sailgb.com/p/powerfilm_rollable_solar_panels/
8. Research Project PA/09, Flexible, organic solar cells for power generating textiles SOLTEX. <http://www.belspo.be/belspo/fedra/proj.asp?l=en&COD=PA/09#docum>
9. www.maier-sports.de/
10. www.scottevest.com/pressrelease/sev_solar/images/Solar_Jacket_Scott_HI_RES.jpg
11. www.powerfilmsolar.com/products/military/armytents/
12. www.tx.ncsu.edu/jtatm/volume4issue3/digital_printing.htm
13. M.S.Shur, J.Sinius, R.Gaska, S.Rumyantsev, *Electronic Letters*, 8, 37, (2001).
14. M.S.Shur, G.Gaskiene, S.L.Rumyantsev, R.Rimeika, R.Gaska, J.Sinius, *Electronic Letters*, 16, 37, (2001)
15. <http://www.konarkatech.com/>
16. Special Report: A Low-Cost Energy Future, (2005).
http://www.businessweek.com/technology/content/sep2005/tc20050920_6204_tc_217.htm
17. <http://www.time.com/time/magazine/article/0,9171,1122044-2,00.html>
18. C. Feinberg, The solar-powered soldier, *Globe Newspaper Company*, (2005).
http://www.boston.com/news/globe/ideas/articles/2005/07/31/the_solar_powered_soldier/
19. <http://www.imec.be/wwwinter/mediacenter/en/SR2006/681465.html>
20. <http://www.imec.be/wwwinter/mediacenter/en/SR2005/html/142357.html>
21. F. C. Krebs, M. Biancardo, B. Winther-Jensen, H. Spanggard, J Alstrup, *Solar Energy Materials & Solar Cells*, 90 (2006).
22. B. Baps, M.Eber-Koyuncu, M.Koyuncu, *Key Engineering Materials*, 206-213, (2002).
23. J.Nam, S.Park, W.Jung, Y.Park, Patent Application Pub.No.:US 2006/0185714 A1, (2006)
24. J. Liu, M. A. G. Namboothiry, D. L. Carroll, *Applied Physics Letters* 90, 063501 (2007)
25. K. Kim, J Liu, M. A. G. Namboothiry, D. L. Carroll, *Applied Physics Letters*, 90, 163511, (2007)
26. S. Lu, *The international society of Optical Engineering*, SPIE, 10.1117/2.1200703.0649, (2007).

FLAME RETARDANT/ANTIBACTERIAL BI-FUNCTIONAL COATINGS ON TEXTILES

B. AKKÖPRÜ, S. ÜN, C. DURUCAN

Department of Metallurgical and Materials Engineering Middle East Technical University

ABSTRACT

Silver and silver/phosphorus doped hybrid silica coatings on polyester-based fabrics have been developed for obtaining antibacterial and dual functional - antibacterial/flame retardant – textile finishes. The effects of fabric surface pretreatment on coating morphology, erosion of silica, silver and phosphorous have been investigated. Coating durability was evaluated by DI water and alkaline detergent laundering. The effects of washing on antibacterial performance and degradation of the coatings were examined by using SEM, EDX and XRD together with antibacterial and flammability tests.

Key Words: Antibacterial, flame retardant, sol-gel, technical textiles

1. INTRODUCTION

The growth of bacteria on textiles is very easy as fabrics are appropriate environments for microorganisms providing, nutrition, moisture, oxygen, and heat. Therefore, there is a great demand for antimicrobial finishes on textiles to control the growth of microorganisms, and prevent the textiles from staining, odor, and health concerns caused by such microorganisms [1]. Antimicrobial textiles can be prepared by incorporating silver biocide particles onto fibers or fabrics. Silver and its ionic compounds are unique compared to other antimicrobial agents because of their nontoxic and non carcinogenic properties [2]. Silver is also biocompatible with human soft tissue and does not cause skin irritation [3]. Long term antibacterial function and durability of such antibacterial textile finishes involve efficient inclusion of silver in a robust coating. Sol-gel techniques can be employed in making such coatings as they simply lead to inert glassy silica network starting from an aqueous solution. Low processing temperatures and aqueous based approaches of sol-gels are easily adaptable for textile finishing processes. Sol-gel also provides practical ways for achieving uniform distribution of silver particles in silica matrices with an additional control on the size, and the chemical state of silver by proper manipulation of solution chemistry and subsequent thermal treatments. Current efforts in developing value added technological textiles rely on achieving multi-functions in the finished products. Along this line, accompanying antibacterial function with one other important property for clothing, household and medical textiles is flame retardancy. Several technologies have been used to improve the flame retardancy alone. [4-6]. halogen-containing and halogen-free products have been used extensively for

this purpose. Recently, as a result of environmental concerns halogenfree flame retardants have become more popular. Most of the common non halogeneous flame retardants are basically phosphorus based products [7].

In the present study, preparation of silver-doped phosphorus containing hybrid sol-gel coatings on textiles for obtaining dual functionantibacterial/ flame retardant- has been reported. We have examined the effects of initial textile surface preparation and laundering on coating morphology, formation of metallic silver nanoparticles and phosphorus compounds in the sol-gel derived silica based coatings. These have been achieved by combination of a variety of analytical materials characterization tools using x-ray diffraction (XRD), scanning electron microscopy (SEM) and energy dispersive x-ray analysis. The changes in coating properties and degradation of silver and phosphorous compounds after different laundering conditions were discussed in relation with the microstructural, antibacterial and flame retarding performance of the coated fabrics.

2. EXPERIMENTAL PROCEDURE

2.1.1 Preparation of Silver-Doped Antibacterial Coating Sol

In preparation of antibacterial coating sol tetra-ethyl-orthosilicate (TEOS, $\text{Si}(\text{OC}_2\text{H}_5)_4$, Aldrich), silver nitrate (AgNO_3 , Aldrich), ethanol ($\text{C}_2\text{H}_5\text{OH}$, Merck) and distilled (DI) water were used. (AgNO_3)/(TEOS) molar ratio was 0.015. Prepared formulations are shown in Table 1. First, required amount of AgNO_3 was dissolved in DI water. Then 0.1 M HNO_3 and half of the ethanol were added to this solution. This mixture was stirred for 20 min at room temperature to form solution-A. In another beaker, TEOS and the remaining portion of ethanol were mixed for 20 min to obtain solution-B. Then solution-A was slowly added into solution-B under stirring. After complete addition, the mixture was stirred for 100 min at room temperature.

2.1.2 Preparation of Antibacterial/Flame Retardant Dual Function Coating Sol

The antibacterial/flame retardant dual functional coating sol was prepared by adding di-ammonium hydrogen phosphate ($(\text{NH}_4)_2\text{HPO}_4$, Merck) solution into the antibacterial coating sol. First, $(\text{NH}_4)_2\text{HPO}_4$ was dissolved in DI water. The solution pH changed to pH=2 by adding 1M HNO_3 to adjust the pH to same value as silver-doped antibacterial coating. Then, mixed solutions were stirred for 30 min at 40-50°C. The formulation for this sol is also outlined in Table 1.

2.2 Textile Pretreatment, Coating and Post-Treatment

In both case, sols were applied to textiles after 2 days of aging. Prior to coating, polymer-based fabric samples (typically 1.5x1.5 cm) were chemically treated. Pretreatment was performed by immersing the samples either in ethanol (Merck, 200 proof) or hydrogen peroxide (H_2O_2 , Merck 30

%) for 10 Table 1. Formulations of hybrid sols used in this study min at room temperature. Coatings were applied on wet, fresh pre-treated fabrics by submerging into the coating sols for 15 min. The coated fabrics were then heated in an oven at 100°C for 1h. Coated samples were washed in DI water or detergent at 70°C for 15 min. Selected samples were kept in as-prepared condition.

Table 1. Formulations of Hybrid Sols Used in This Study

Silver-doped antibacterial coating sol	
$[AgNO_3]/[TEOS] = 0.015$	
Formulation	TEOS:AgNO ₃ :C ₂ H ₅ OH:H ₂ O:HNO ₃
(Molar ratio)	1:0.015:2:8:0.015
Gelation time	4–5 days
Antibacterial/flame retardant dual function coating sol	
$[AgNO_3]/[TEOS] = 0.015$	
Formulation	TEOS:AgNO ₃ :(NH ₄) ₂ PO ₄ :C ₂ H ₅ OH:H ₂ O:HNO ₃
(Molar ratio)	1:0.015:0.2:3:12.4:0.6
Gelation time	7-8 days

3. CHARACTERIZATION

XRD: X-ray diffraction analyses were performed using a Rigaku D/Max-2000 PC model diffractometer. X-ray source was Ni-filtered CuK α radiation. The xray source operating voltage was 40 kV and the scan rate was 2°/min.

SEM: The visual examination of the coated fabrics, coating morphology and coverage were performed by using JSM-6400 model SEM operated at 20 kV. For determination of silver and silicon concentration before and after washing experiments, energy dispersive x-ray analyses were used. All EDX spectra were obtained from a selected area (at 2500X) at the center of the samples.

Antibacterial Performance Tests: The antibacterial properties of coated fabrics before and after washing process were quantitatively determined against Escherichia coli, where coated fabrics were placed in to bacteria seeded agar plates and incubated for 24 h and the decrease in the number of bacteria colony was monitored. Throughout the antibacterial performance tests a b are (uncoated) fabric was used as control and evaluated in the same testing conditions in parallel with the coated samples.

Flame Retardancy Test: The flame resistance of the coated samples was tested by monitoring the progression of the flame as a function of time within a frame of 0-30 sec. Flame resistance measurements were performed in open air using coated strip samples of (1x15 cm). Antibacterial/flame retardant dual function coating sol

4. RESULTS and DISCUSSION

4.1 Effect of Pretreatment on Coating Morphology and Stability:

Figure 1 discloses the SEM micrographs of coated fabrics of different pretreatment history with identical coating and post treatment processes. In both cases coating solution was silver nitrate containing antibacterial sol and post treatment was 1 hour heating at 100°C.

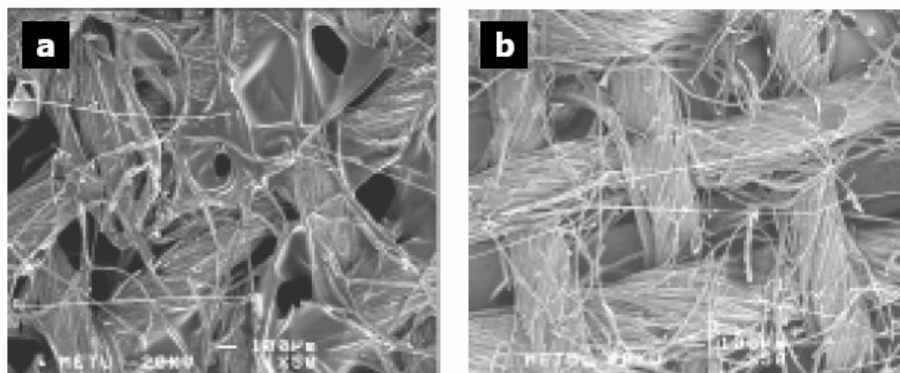


Figure 1. SEM micrographs of silver-doped antibacterial coated fabrics pretreated a) in ethanol, b) in hydrogen peroxide. Both samples were heat treated for 1h at 100°C after coating process.

As shown in Figure 1, ethanol treated textile surface is partially overflowed with coating material exhibiting relatively more intense and locally accumulating coverage on the fibers and somewhat better adhesion compared those for hydrogen peroxide treated samples in as-prepared condition. Accompanying SEM micrographs in Figure 2 show the same coated fabrics with a detailing magnification at around size of individual fiber of the yarn but this time after washing treatments. These SEM images clearly present the effects of laundering on the stability and morphology of the sol-gel derived coatings. Both DI water and detergent washing remove a moderate amount of the coating from the fabrics. Erosion of coating is more severe in the case of ethanol pretreatment where excess coating material filling the space in between individual fibers was leached out after washing and isolated fibers can be clearly observed. On the other hand, sol-gel coatings attach effectively on hydrogen peroxide pretreated textiles as single yarn in the fabric is still composed of bundled fibers where the coating material is confined. The hydrogen peroxide treated fibers also contain reticulated surface features resembling relatively more remains of the coating. These suggest different attachment mechanism and chemistry of the sol-gel coating on the fabrics governed by the prior surface treatment and possibly improved coating durability in the case of hydrogen peroxide treatment. The XRD results presented in Figure 3 also support the SEM findings on how significant the surface treatment is in terms of coating attachment efficiency. Figure 3 shows

the XRD patterns of bare and silver-doped antibacterial sol coated fabrics treated with ethanol or hydrogen peroxide in as-prepared condition. For all XRD patterns, three main neighboring peaks in the range of $2\theta=15^{\circ}$ - 30° and $2\theta\approx 33^{\circ}$ and $2\theta\approx 47^{\circ}$ are assigned for polyester-based fabric. In XRD data the identifying peak for the coating can be from crystalline silver dopant or some silver compound as the matrix is amorphous sol-gel derived silica. This fingerprint silver peak located at $2\theta \approx 38^{\circ}$ is only present on the pattern of coated samples when ethanol was the pretreatment agent as shown in Figure 3b. This peak is relatively hard to resolve in the background in the complete 2θ range of the spectrum. However, the inset showing the XRD patterns of bare and coated fabric pretreated with ethanol for detailed comparison in the 2θ range where the most intense silver peak is located. On the other hand, as shown in Figure 3c, i.e. for hydrogen pretreated coated textiles, no peak for silver is present. Given to promising sol-gel coating attachment efficiency, ethanol was used as a standard surface pretreatment agent in making dual antibacterial and flame retardant bi-functional coatings.

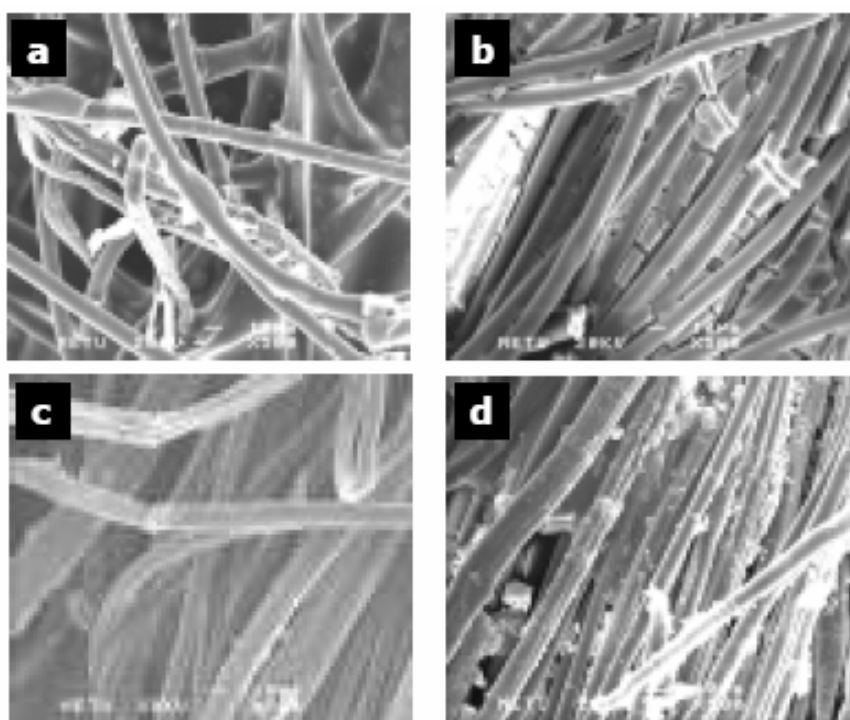


Figure 2. SEM micrographs of silver-doped antibacterial coated fabrics pretreated with different pre-treatment history. Ethanol pre-treated fabrics after a) DI water and b) detergent wash. Hydrogen peroxide pre-treated fabrics after c) DI water and d) detergent wash.

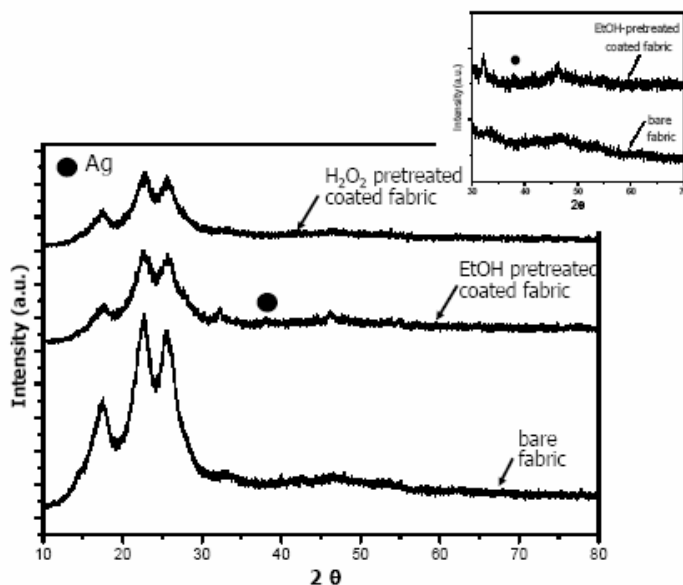


Figure 3. XRD patterns of bare and silver-doped antibacterial sol coated fabrics initially pre-treated with ethanol or hydrogen peroxide for 15 min at room temperature. The inset shows the detailed patterns of bare and coating with ethanol pre-treatment better resolving the silver peak.

4.3 Effect of Laundering on the Erosion of Coatings

In order to assess the durability of coated textile fabrics, they were washed in two different media; with DI water at pH 5.5 and in detergent solution at a pH value around 10-12. In both treatments, the temperature was adjusted to 70°C. Figure 4 shows the EDX spectra of bare textile fabric together with those for silver doped antibacterial sol coated textile fabric before and after two different laundering treatments. Figure 4a presents EDX spectra of bare textile and all the radiation correspond to polyester. On the contrary, silver (3 keV) and silicon (1.7keV) radiations are observable for coated fabrics as shown in Figure 4b, with a corresponding Ag/Si atomic ratio of 0.03. The washing treatments affected the silver radiation. As it can be seen from EDX patterns (Figure 4c) silver amount was reduced significantly after DI washing and but silicon leach out was relatively low with a very small Ag/Si ratio 0.01 for the washed fabric. Detergent washing produces different effects on relative leaching rate of the coating components, i.e. silicon and silver. As shown in Figure 4d detergent washing produces an apparent decrease in the intensity of silicon EDX peak. The measured Ag/Si ratio was this time 0.8, implying preferential degradation of silica during alkaline detergent washing. Similar trends in leaching for silver and silicon were observed for dual function silver/phosphorus coated fabrics as somewhat implied by XRD findings in Figure 5. This figure also provides some insights about the

interpretation of the aqueous durability of the flame retardant component of the coating, i.e phosphorus. In general, washing treatment with DI water also leads to erosion of the phosphorous from the coating but relatively at a smaller extent. Again, similar to silver-doped coatings, for dual functional coatings most of the silver leached out after DI water wash whereas silver was still on the fabric after detergent washing. (not shown here)

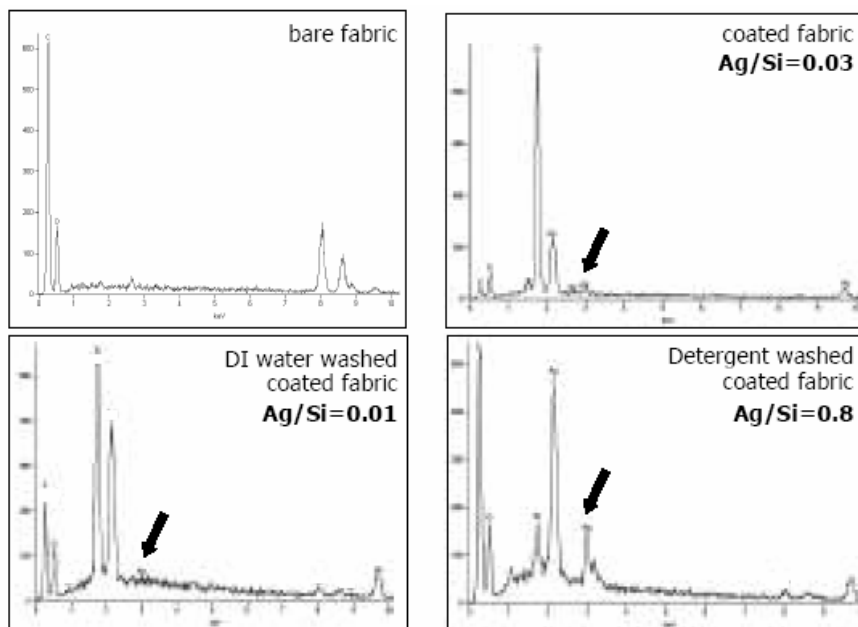


Figure 4. EDX spectra of a) bare, silver-doped antibacterial sol coated fabrics b) as-prepared, after c) DI water and d) detergent washed conditions.

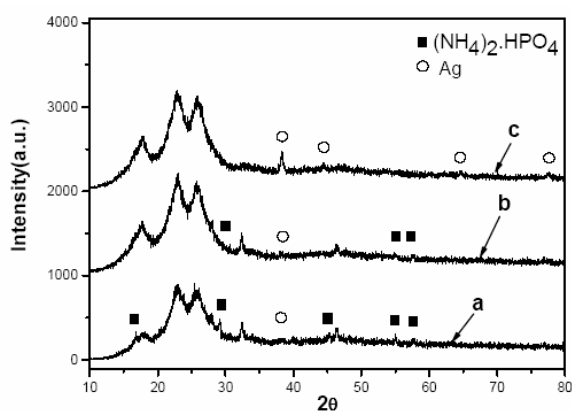


Figure 5. XRD patterns of antibacterial/flame retardant dual function sol coated fabrics a) in s-prepared condition and b) after DI water and (c) after detergent washing.

4.4 Antibacterial Performance

Antibacterial performance tests were only applied to ethanol pre-treated, silver-doped silica coated fabrics. Table 2 summarizes the antibacterial tests results for duplicate samples for bare, asprepared, and washed fabrics. Bare fabrics do not show any antibacterial property, the initial number of colony was 600 and it remained unchanged after antibacterial performance test. Coated fabrics exhibit excellent antibacterial property in as-prepared condition. The number of colony for coated fabrics dropped to approximately 20 at the end of test. Antibacterial performance of the coated textiles after washing treatment at 70°C weakened especially for DI water laundering. The weakening of antibacterial performance was not that severe in the case of alkaline detergent washing where almost half of the bacterial colonies were ceased even for the washed samples. The total colony number was around 100-200. This is due to relatively higher amount of silver which remains after washing in this particular environment as it has been previously discussed.

Table 2. Antibacterial Test Results For Silver-Doped Hybrid Coatings In Different Conditions

	Number of bacteria colonies
Bare fabric	600
Ethanol pretreated coated fabric	26, 21
Coated fabric washed with DI water at 70°C	> 500, > 500
Coated fabric washed with Detergent at 70°C	100, 200

4.5 Flame Retardancy

Phosphorous-compound addition to the silver doped silica solution enhances the flame retardant properties of the antibacterial coatings as point out in Figure 6.

This figure shows the comparative upward advancement of a flame for phosphate added silver-doped silica solution coated fabrics and bare fabric sample. In a follow up time up to 22 s flame propagates always faster for non-coated fabric. As shown in the final frame of Figure 6 corresponding to 22 s, the flame was terminated for uncoated fabric where polyester based fabric was completely ceased and burn out, whereas the dual function coated fabric was still in some intermediate phase of burning indicating an improvement in flame resistance.

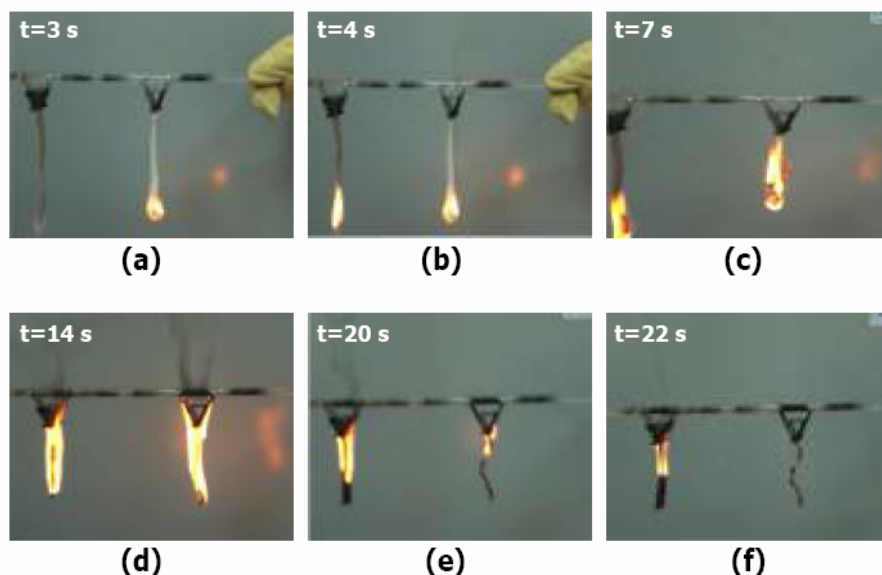


Figure 6. Pictures showing the flammability behavior of antibacterial/flame retardant dual function sol coated fabrics (left) and bare fabric (right) at different times after burning. (a) 3 sec. (b) 4 sec. (c) 7 sec. (d) 14 sec. (e) 20 sec. (f) 22 sec.

5. CONCLUSIONS

Ethanol and hydrogen peroxide pretreatments lead to different attachment efficiencies of sol-gel derived silver-doped silica hybrid coatings on polyester-based fabrics. Ethanol treatment basically enhances the attachment of the ethanol based immature organic sols probably by meeting proper wetting conditions. This produces better coverage and enables relatively more swelling of the deposited material on ethanol treated fabrics compared those obtained by hydrogen peroxide pretreatment. Ethanol pretreated coated fabrics exhibit excellent antibacterial potential with some degeneration after laundering, but still show promising biocidal activity after aggressive detergent washing. Silver leaching potential of the laundering environment is found more critical than disintegration of silica network in terms of antibacterial performance. Adding flame resistant phosphorous compound and achieving dual function in these silver-doped coatings seems quite possible as phosphorus discharge from such coatings in low pH medium due to laundering was less prominent compared to leaching of silver biocide.

ACKNOWLEDGEMENTS

The authors acknowledge the financial support through TUBITAK 106M061, ODTU-OYP Program and ODTU-BAP 2006-03-08-04.

REFERENCES

1. Mahltig, B., Haufe, H., Böttcher, H. (2005) *J Mater Chem* 82:238.
2. Stillman M. J., Presta A., Gui, Z. Q., Jiang, D. T (1994) *Metal-Based Drugs* 1:375.
3. Rong, M. Z., Zhang, M. Q., Zheng, Y. X., Zeng, H. M., Friedrich, K. (2001) *Polymer* 42:3301.
4. Chan, C. M. (1994) "In Polymer Surface Modification and Characterization" Hanser; New York pp 1–4.
5. Feast, W. J., Munro, H. S., Richards, R. W. (1993), *Polymer Surfaces and Interfaces II*; Editors; Wiley: Chichester, UK, pp 1–290.
6. III. International Technical Textiles Congress 1-2 December 2007 ISTANBUL
7. Kandola, B. K., Horrocks, A. R., Price, D., Coleman, G. V. (1996), *J Macromol Sci Rev Macromol Chem Phys*, 36:721.
8. Levchik, S. V., Weil E. D., (2006), *J Fire Sciences*, 24:34

RESISTIVITY OF BASALT FIBER REINFORCED SILICON OXYCARBIDE – NUMERICAL SIMULATION AND EXPERIMENTAL MEASUREMENT

B. TOMKOVÁ, M. MARŠÁLKOVÁ

Department of Textile Materials, Technical University of Liberec

ABSTRACT

The determination of electrical properties of basalt fiber reinforced silicon oxycarbides (SiOC) are objectives of presented paper. Studied specimen have been prepared due to pyrolysis of polymer precursors. The numerical model for prediction of specimen conductivity is based on multi-scale modelling method. The conductivity of specimen is determined as reciprocal to resistivity. Experimental measurement of specimen resistivity has been realized with the use of HP 4339B High Resistance Meter measurement device. The measured values of conductivity have been compared to the numerical ones, the calibration of SiOC input parameters followed.

Keywords: basalt fibres, reinforced silicon oxycarbides, electrical properties, numerical simulation, properties prediction, measurement of resistivity

1. INTRODUCTION

Reinforced silicone oxycarbides (SiOC) are newly developed ceramics based on polysiloxane resins supposedly applicable as structural materials possessing high heat resistance in oxygen atmosphere [1]. Their structure and properties depend on both, the type of reinforcement and matrix precursor, and time-temperature regime of polysiloxane precursor pyrolysis. The reinforcement is either particular (metals or alloys particles) or fibrous (inorganic fibres).

As for fibrous reinforcement ceramic fibres are the only ones commercially applied nowadays [7]. Those are materials efficient for high-tech applications (aeronautics or astronautics) but too expensive for common use. In this case the utilization of low cost reinforcing fibres appears as most suitable approach to minimize the composites costs. The tests of glass fibres reinforcement have been realized but those have proved there is impossible to reach the temperature of pyrolysis necessary for complete transformation of polysiloxane precursors (over 1000°C) into SiOC as the glass starts to melt in temperatures over 800°C [8]. Regarding this knowledge the basalt fibers have been proposed as potential reinforcement. These low cost fibers have properties comparable to glass fibres but possess higher melting temperature (up to 1400°C).

The ceramic specimen studied in our research are composed of basalt fibres (commercial product of Kamenny Vek), and pyrolysed silicone resin Lukosil

M130 (commercial product of Lucebni zavody Kolín). Due to technical reasons the pyrolysis have been realized in oxygen atmosphere. The internal structure and basic thermomechanical properties of the composites have been described in [6]. The prediction of transport properties (the charge transport) of studied specimen are objective of presented paper. The numerical simulation of specimen electrical conductivity have been realized with the use of multiscale-modelling approach [2]. The results have been compared to the experimental measurements. Good agreement between numerical results and the experimental ones shows applicability of generated multiscale geometry model of composite specimen for prediction of further material properties, e.g. thermal conductivity or thermal expansion, etc.

2. EXPERIMENTAL PROCEDURE

2.1 Composite Specimen Preparation

Basalt fiber rovings have been treated by acetone to clear off the surface sizing which may undesirably effect the adhesion between the fiber reinforcement and polymer matrix. Pure fibres have been impregnated by silicone resin Lukosil M130 (polymethylsilicone resin dissolved in xylene). Next the specimen have been cured at the temperature of 100°C for 24 hours to prepare polymer precursors (basalt fiber reinforced composites with cured polysiloxane resin).

The basalt-polysiloxane precursors have been finally pyrolysed in air at heating rate 50°C per hour. Final temperature (heat treatment temperature) has been set on 1000°C, see Table 1. Within the pyrolysis cured polysiloxane resin should be transformed into heat resistant porous silicon oxycarbide glass [1].

Table 1. Time-temperature regime of basalt-polysiloxane pyrolysis

Heating rate	Heat treatment temperature	Dwell time
50 °C per hour	1000°C	60 minute
Cooling rate		
100°C per hour	25°C	60 minute

2.2 Simulation of composite specimen electrical conductivity

Numerical simulation of material properties requires the geometry description of the area or volume representing the internal structure. The geometry should be simplified to make the computation possible. To prepare geometry model suitable for numerical simulation yet to respect the real structure of composite specimen the multiscale geometry modelling

approach appears as optimum for complex structures [2]. The basic structural information are acquired by the use of computer aided image analysis.

■ Structural analysis of composite specimen

Micrographs of composite specimen have been acquired by the image analysis system LUCIA (Laboratory Universal Computing Image Analysis). Complete imaging workstation is composed of microscopes, cameras, stands, illuminators, PCs and other accessories. The mezo-structure of composite have been scanned by optical microscope Nikon ME600 Eclipse, the analysis of microstructure have been realized with the use of scanning electrone microscope VEGA-TESCAN, see Figure 1.



Figure 1. Image analysis workstation:

(a) optical microscope Nikon ME600 Eclipse **(b)** scanning electrone microscope VEGA-TESCAN

The micrographs allowed us to study the morphology of cured and pyrolysed composite specimen, analyse the influence of curing and pyrolysis on the structure of fiber reinforcement and matrix, evaluate the development of pores and crack in final composite structure, see Figure 2 and Figure 3. Thorough structural analysis is the base for design of multiscale geometry model representing the studied composite specimen

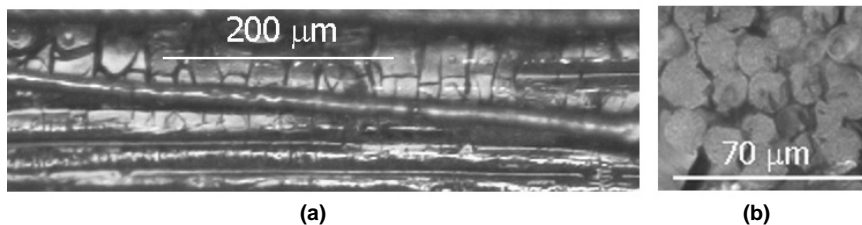


Figure 2. Basalt fiber reinforced silicon oxycarbide (optical microscope):
(a) surface view, **(b)** cross-section view

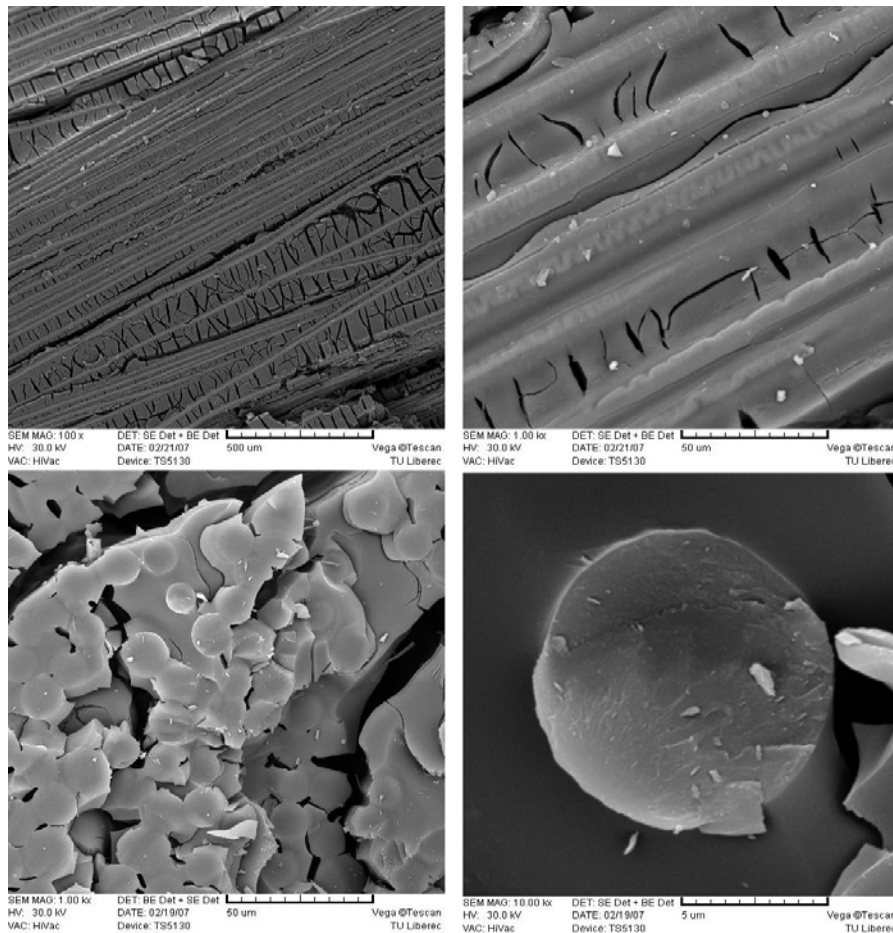


Figure 3. Surface and fracture area of basalt fiber reinforced silicon oxycarbide (scanning electron microscope)

■ Multiscale geometry model

For numerical simulation the multi-scale geometry model of specimen have been prepared with respect to structural information obtained from composite micrographs, see Figure 4. Thus have been determined three levels representing the geometry of specimen in particular level. The material parameters acquired from numerical simulation in one level are utilized as homogenized input parameters in higher levels. The parameters acquired from highest level of the model represent parameters of final composite plate.

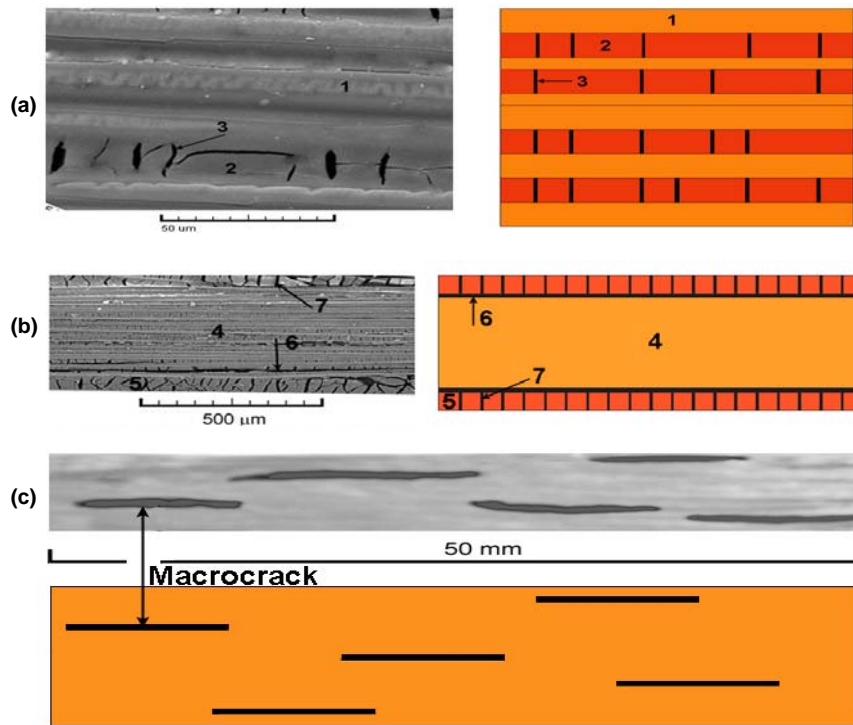


Figure 4. Multiscale geometry model of studied composite specimen: **(a)** microscale level, 1 - basalt fibre, 2 - SiOC matrix, 3 - microcracks **(b)** mesoscale level, 4 - part composed of microscale particles, 5 - SiOC matrix, 6 elamination cracks, 7 - transversal cracks **(c)** composite plate with macrocracks (macroscale level)

Parameters of basic structural components are uniquely determined, see Table 1. Conductivity of basalt fibres has been measured, obtained data are in good agreement with the ones mentioned in literature. Conductivities of SiOC and air have been estimated with respect to information presented in [4,5,6].

Table 2. Electrical conductivities of basic composite components, that are initial data for numerical simulation of composite conductivity [5,6].

Composite parts	Basalt fibres	SiOC matrix	Voids filled with air
Electrical conductivity [S.m ⁻¹]	$1,02 \cdot 10^{-13}$	10^{-1}	10^{-10}

■ Numerical simulation

Numerical simulation of electrical conductivity have been realized using Comsol Multiphysics software, the Electromagnetics Module that provides a unique environment for the simulation of electromagnetic wave and field propagation in conductive media. The problem of electromagnetic analysis is that of solving *Maxwell's equations* subject to certain boundary conditions. Maxwell's equations are a set of equations, written in differential or integral form, stating the relationships between the fundamental electromagnetic quantities. These quantities are [10]:

- *electric field intensity, \mathbf{E} , electric displacement or electric flux density, \mathbf{D} , magnetic field intensity, \mathbf{H} , magnetic flux density, \mathbf{B} , current density, \mathbf{J} , electric charge density, ρ*

You can formulate the equations in differential or integral form. The software uses differential form because it leads to differential equations that the finite element method can handle. COMSOL Multiphysics provides many tools for postprocessing and visualizing model quantities. You can also compute numerical integrals of model quantities as well as display and save postprocessing data. The software can postprocess expressions that combine user-defined variables, application mode variables, and standard variables.

2.3 Experimental measurement of composite resistance

The HP 4339B High Resistance Meter, which is designed for measuring very high resistances and related parameters of insulation materials, has been utilized to determine the resistivity of studied composite specimen, see Figure 5. Measurement features have been set as follows:

Test voltage	- 100 V
Air moisture	- 36 %
Mean current	- 0,8 mA

The surface resistivity [$\Omega \cdot m$] is calculated automatically and the result is displayed [3].

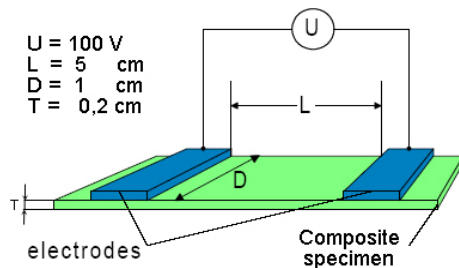


Figure 5. Scheme of specimen resistivity measurement

3. RESULTS

The computed electrical properties of composite specimen are final results obtained within the numerical simulation. The influence of studied composite structure on charge transport in electric field is shown in Figure 6. The numerical results have been verified with the aid of experimental measurement, the input parameters of SiOC ceramic matrix have been calibrated with respect to the experimental results. Acquired electrical properties are displayed in Table 3.

Table 3. Resultant electrical properties of examined composite specimen in directions parallel to composite plate. The values are valid for temperature 25°C.

Electrical properties	Computed	Measured
Electrical conductivity [S.m^{-1}]	$1,8 \cdot 10^{-11}$	$4,3 \cdot 10^{-11}$
Surface resistivity [$\Omega.\text{m}$]	$5,6 \cdot 10^{10}$	$2,3 \cdot 10^{10}$

The model calibration using experimental data serves for precision of input parameters representing the properties of individual composite compounds. This is mostly important in estimation of matrix properties, which is formed within the composite preparation, and it is hardly possible to measure its properties separately. The resultant values of pure matrix properties also indicates possible order of matrix structure. With respect to acquired results we may assume the resultant matrix is semiconductor with high fraction of free carbon with sp^2 - hybridization [5]. The proof of this assumption will be subject to further research.

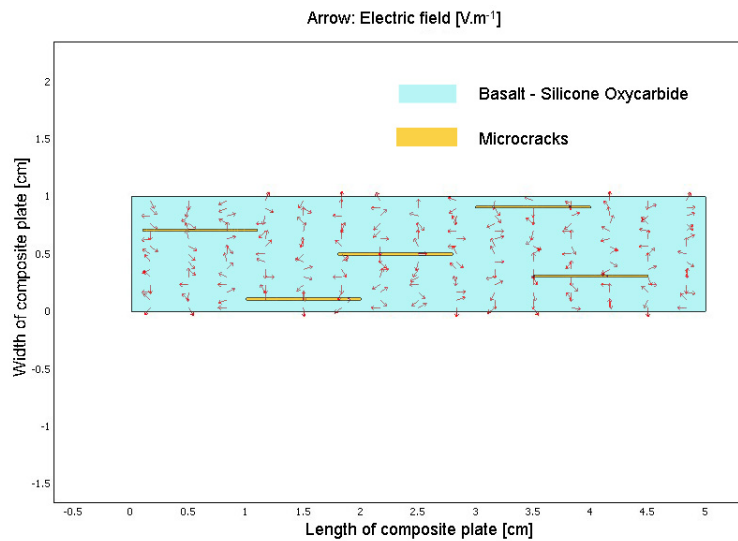


Figure 5. Behavior of electric field in composite plate

4. CONCLUSIONS

Development of new composite material in general, it is project combining the material design based on prediction of final material properties, design of technology, and practical preparation of composite specimen to verify the theoretical expectations. Thorough study of real specimen structure and properties is essential part of the research. As not all properties may be reliably measured, and not each of material response on certain type of load may be studied experimentally, the tests of new material properties are the combination of experimental measurement and numerical simulations. Numerical simulation requires the geometry description of area or volume representing studied specimen, and estimation of particular input parameters.

There is no universal geometry model for complex composite specimen. The models are prepared individually with respect to real structure of studied specimen, and properties of basic composite compounds. It is necessary to verify the reliability of suggested models using the comparison of particular numerical results with available experimental data. Such models may be used for prediction of other material properties.

In present paper the geometry model, representing the structure of newly developed basalt fiber reinforced SiOC composite, have been generated, and applied for prediction of electrical conductivity of studied specimen. The comparison of numerical results to the experimental ones enable us to specify conductivity of pure SiOC matrix, and estimate probable order of SiOC structure. Obtained results are comparable to data mostly mentioned in the literature [5,6], and give us new information how to evaluate the structure and properties of ceramic matrix itself, and within the scope of whole basalt fiber reinforced SiOC composite.

Good agreement between the computed values of electrical conductivity and the experimental ones indicates the geometry model of composite structure may be used for prediction of other material properties of studied composite. This will be objectives of future research.

ACKNOWLEDGEMENT

Authors are grateful for the financial support by the Czech Science Foudation in the frame of the Projects No. 106/05/0817, and 106/07/1244. Word of thanks also belongs to Ministry of Education, Youth and Sports in the frame the Projects Textile Research Centre 1M4674788501, and The Center of Quality and Reliability 1M06047C468.

REFERENCES

1. Brus, J. and others, J. of Non-Crystalline Solids 289, 2001, pp. 62-74.
2. Tomková, B., Doctoral Thesis, TU Liberec, 2006.
3. HP 4339B High Resistance Meter, Operation Manual, Hewlett-Packard, Japan, 1998. Haňka, L., Electromagnetic Field Theory, SNTL, Praha, 1982 (in Czech).

4. Cordelair, J., J. of the European Ceramic Society 20, 2000, pp. 1947-1957.
5. Chiang, Ch., J. of Electrochemical Society, 151, 9, 2004, pp. G612-G617.
6. Tomková, B. and others, Reinforced Plastics 2007, Karlovy Vary, 2007, pp. 175-180.
7. Bansal, N.P.: Handbook of Ceramic Composites, Kluwer A. P., New York, USA, 2005.
8. Černý, M. and others, Bulletin 1/04 Czech Carbon Society, ÚSMH AV, Praha, 2004

FILTRATION AND RESPIRATORY PROTECTION

D. TOPRAKKAYA KUT, K. ÇELEBİ

Department of Textile Engineering, University of Uludağ

ABSTRACT

Nowadays, as known filters have so many application areas from daily life to industrial utilization. The improvement of environmental consciousness and the necessity of clean air at food-health sectors and for computer systems; make filtration becomes fairly important. Nonwovens, thanks to their high performance such as collection efficiency are used instead of woven fabrics in so many areas.

The aim of this paper to present a literature compilation about filtration and respiratory protection masks.

Key Words: Filtration, nonwoven, spun-bond, melt-blown, electrospun, nanofiber, permeability, respiration resistance, EN 149.

1. INTRODUCTION

Filtration means disturb the material with making it pass through continuous phases. Material is become filtered by these phases. The place that the material passes is called filtration media. In theoretical gases and liquids pass through the filter pores with particles smaller than the pores. The particles larger than the pores are stopped by the membrane.

Filtration systems can be classified in two parts; superficial filtration systems and deeply filtration systems. In superficial systems, the sizes of the particles are the same as filter pores or larger than them. Using these filtration systems the contamination is trapped by the filters surface. In deeply filtration systems pores are larger than particles sizes. In such filters, big particles are caught by the surface and the smaller ones captured in through the filters.

Textile materials used for filtration can also be classified in like this:

- a. Nonwoven fabrics: 70 – 75 % (air filtration)
- b. Woven fabrics: 20 – 25 % (filter presses)
- c. Knitwear: 1 – 5 % (dust bags, food)

In filtration systems, to increase the collection efficiency some new applications have been improved. These applications which have been in use now are indicated below:

1. Fiber fineness (micro and nano fibers)
2. Coated and laminated filtering systems

3. Functionalised filtering systems:

3.1. Electrostatic charge

3.2. Conductive filter materials

3.3. Active filtering systems (catalysers, active carbon)

2. HISTORY OF FILTRATION

17th century – Bernardino Ramazzini – indication of the need for protection of the respiratory tracts against dusts of workers labouring in various professions.

1814 – Brise Fradin - first device, which provided durable protection of the respiratory tracts.

It was composed of a container filled with cotton fibres which was connected by a duct with the user's mouth.

19th century – the first filtration respiratory mask with the aim of protecting the users against diseases transmitted by the breathing system.

19th century – first masks specially designed for firemen.

Construction of such a 'mask' was primitive: a leather helmet was connected with a hose which supplied air from the ground level.

1868 – John Tyndall - a mask consisting of some layers of differentiated structure. A clay layer separated the first two layers of dry cotton fibers. Between the two next cotton fiber layers was inserted charcoal, and the last two cotton fiber layers were separated by a layer of wool fibers saturated with glycerine.

1914 –the development of filtration materials connected with absorbers of toxic substances manufactured with the use of charcoal and fibrous materials.

1930 – Hansen - a mixture of fibres and resin as filtration materials, electrostatic field created inside the material.

The action of electrostatic forces on dust particles significantly increased the filtration efficiency of the materials manufactured.

20th century –the first attempts of scientific description the filtration mechanism presented by Albrecht, Kaufman, Langmuir and by Brown.

➤ History of Meltblown Filtration Materials:

1950s - the first nonwovens using melted organic polymers, using a method similar to air-blowing the polymer melt.

Wente – development of melt-blown technique.

Buntin – introduce of the melt-blown technique into industry for processing.

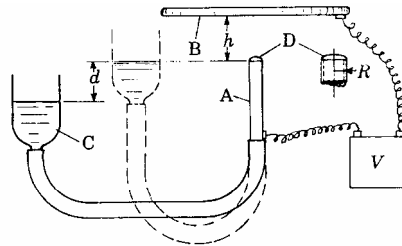
2005 - NonWoven Technologies Inc. from USA - melt blown PP nonwovens composed from nano-size fibres of diameter equal to 300nm.

➤ History of Electrospun Filtration Materials:

1600 - Gilbert - the first observation concerning the behaviour of electroconductive fluid under the electrical field.

1914 - Zeleny - the first investigations into the phenomena of interaction of an electric field with a fluid drop.

1934 - Formhals - the use of the apparatus for electrospinning designed by Zeleny for the spinning of thin polymer filaments.



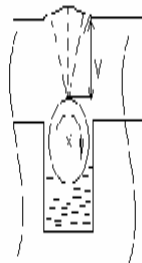
1964 - Taylor - theory: for a given type of fluid, a critical value of the applied voltage exists, at which the drop of fluid flowing from the capillary tube is transformed into a cone under the influence of the electric field and loss its stability.

1980 - Schmidt - demonstration of the possibility of the application of electrospun polycarbonate fibers to enhance the dust filtration efficiency.

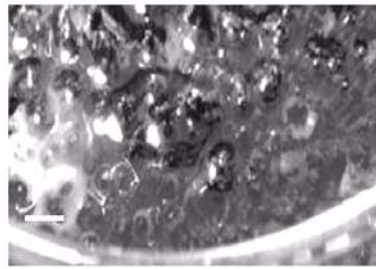
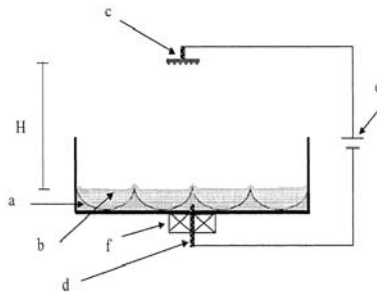
80s of the 20th century - Carl Freudenberg Company the first use of the electrospinning technology commercially.

2000 - Donaldson Inc. USA - dust filters with the thin layer of nanofibers.

2003 - Jirsak - development of the new electrospinning method - the spinning directly from the solution surface.



2004 - Yarin and Zussman - another system for the spinning directly from the solution surface.

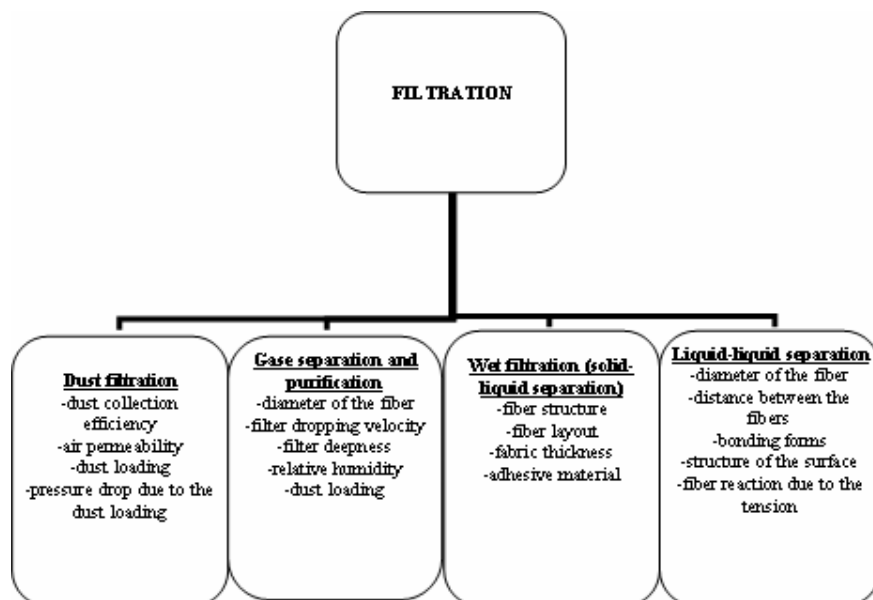


3. BASICS OF FILTRATION

The general purpose of filtration is, in any flow environment in order to prevent energy losings, to make the particles hit the filter and being intercepted. This provides a clear flowing.

In case, the amount of the pores in filters increases the pressure drop has to be reduced to a minimum. The pressure drop also increases with rising in the air flowing quantity. This is related to the system construction and do not have to be linear.

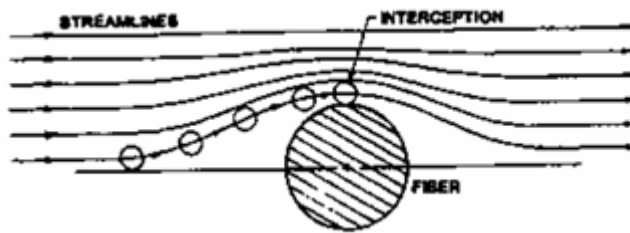
Filtration is classified in four groups as defined below:



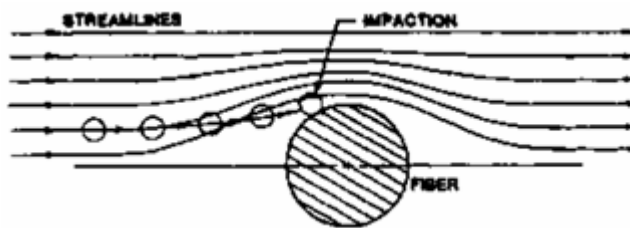
4. FILTRATION MECHANISMS

Particles can be intercepted and stopped by the filter in five different ways:

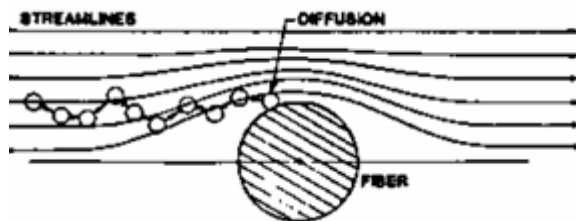
1. Particles contact fiber as air stream flows around fiber.



2. Particles with sufficient inertia cannot change direction sufficiently to avoid the fiber. It depends on particle size, density, speed, shape.



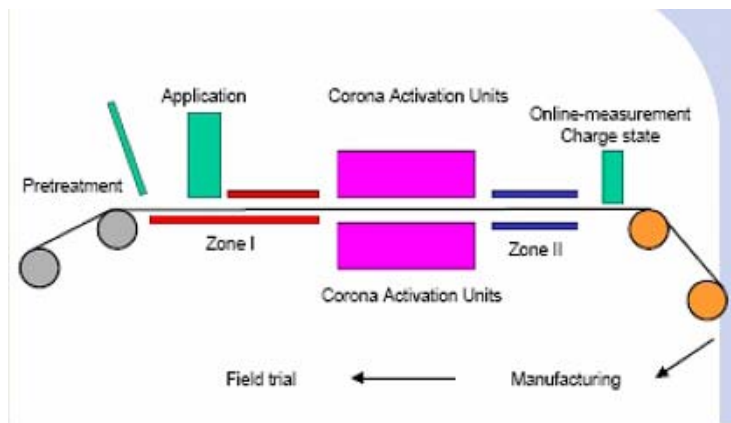
3. Brownian diffusion: Random motion in the smaller particles within the air stream. The smaller the particle and the warmer the air temperature the more random motion can occur and this increases diffusion capture. Lower flowrate also increases capture.



4. It is very difficult to intercept very small particles by mechanical ways. To pull these kind of particles towards to fiber surface electrically charged fibers are used. By this way filter efficiency also can be increased. The three basic mechanisms of electrical stimulation of particle deposition:

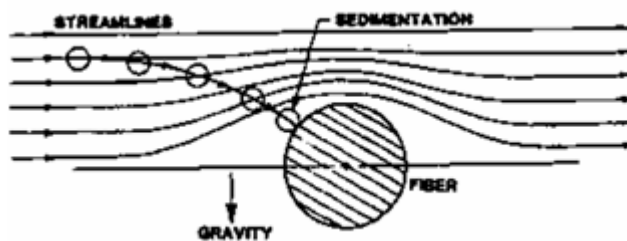
a. Materials in which the charge is generated by induction during spinning through an electrostatic field.

b. Materials in which the charge is generated by corona discharge after fibre or web formation.



c. Materials in which the charge is induced as the result of the triboelectric effect.

5. Gravity pulls larger particles from air stream. ($\geq 2 \mu\text{m}$) this works best with low flow-rate.



5. FIBERS USED IN FILTRATION

Choosing fibers for nonwoven filters; resistance to environment, structural benefits and appropriateness of effective surface area must be considered. Variation of hole sizes and fiber surface area in a unit weight or volume are used in filter design processes.

Some reasons wherefore fibers used in filters are indicated below:

1. Bonding force in nonwoven structure.
2. Quantity of the covering area when being spread out randomly.
3. Capability of filtering gases and concentrated liquids.

Using weak and soft fiber mixtures increase the efficiency in nonwoven filters. But in general there is always a basic supporting fiber. Thick fibers are for structural frame and fine fibers are for filtering. Sometimes a fiber in mixture is melted in order to be used as a binding agent. In manufacturing, using binding agents and mechanical bonding methods are preferred mostly.

Table1. Effects of Fiber Properties to Filtration

Properties of Fibers	Effects To Filtration
Broken Fibers, Twist, Loop-Pile	For a better filtration, projection area should be higher as far as possible. So these properties increase the filtration.
Section Area	To increase the projection area, it can be circular or sickle.
Mixture Of Fibers In Different Diameters	Used when particle collection efficiency and high storage are both required.
Mixture Of Fibers In Different Triboelectric Properties	Increase the particle collection efficiency.
Resistance	Prevent effects of chemical, thermal and environmental factors.

5.1. Properties of Fibers Used in Filtration

1. Properties that effect the manufacturing methods:
 - a. Weight in grams
 - b. Thickness
 - c. Hardness
 - d. Tearing resistance
 - e. Tension resistance
 - f. Structure of the surface
 - g. Porous surface (flow resistance)
2. Factors effect the filtration processes:
 - a. Chemical stability
 - b. Thermal resistance
 - c. Resistance to bacteria
 - d. Reliability and usage life-span
 - e. Ability of being purified and renovated

6. RESPIRATORY PROTECTION

6.1. Criteria of Respiratory Protection Standards (En 149)

- a. Permeability of the filter
- b. Breathing resistance
- c. Leakproofing at the parts that filter contacts to face
- d. Compatibility with other equipments
- e. Inflammability

6.2. Choosing the Dust Masks According to Media Concentration

Dust concentration in the media is determined and then the calculation below is made.

Maximum value : Utmost concentration that can be permitted.

Media dust concentration / maximum value = according to the results from this calculation choices of mask can be made.

Results	Dust Mask
<4	FFP1 – 4* max 78 % protection
4-10	FFP2 – 10* max 92 % protection
10-50	FFP3 – 50* max 98 % protection
>50	If the dust concentration is high than 50 times of maximum value, it must be decreased. Otherwise closed respiratory devices must be used.

6.3. Factors Effect the Usage Life-Span Of Masks

- a. Ratio of breathing and exhaling
- b. Concentration of contaminants
- c. Ratio of media humidity
- d. Type of the contaminant
- e. Capacity of absorption

REFERENCES

1. College Of Textiles North Carolina State Universtiy, Nonwovens Cooperative Research Center, Aerosol Filtration, Q. Wang, B. Mazé, H. Tafreshi, B. Pourdeyhimi
2. Department Of Fibre Physics And Textile Metrology Technical University Of Lodz, Poland, New Textile Materials For Environmental Protection, Izabella Krucińska, Eulalia Klata, Michał Chrzanowski
3. Ecotextiles/ Filtration, Bob Vander Beke, Centexbel Cost Action 628, 1 September 2005
4. Ege Üniversitesi Tekstil Mühendisliği Bölümü, Nonwoven Filtreler, Prof. Dr. Kerim Duran, Arş. Gör. Pinar Çelik
5. Elektrik Üretim Anonim Şirketi Eğitim Ve Bilgi İşlem Dairesi Başkanlığı, İş Güvenliği Malzemeleri Teknik Özellikleri/ Solunum Koruyucular, Veri Kayıt Opt. Orhan Kuru, Ankara, 2005
6. Experimental Evaluation Of The Protective Properties Of Some Nonwoven Materials For Respiratory Protection Means And Prospects Of Their Use, Gig Sanit, 2007 Jan-Feb;(1):31-4. Russian, Pmid: 17343048 [Pubmed - Indexed For Medline]
7. Filtration Properties Of Nonwovens, Int J Occup Saf Ergon, Gador W., Jankowska E., 1999;5(3):361-79. Pmid: 10602654 [Pubmed - Indexed For Medline]

FR TREATMENT ON LYOCELL BLENDS

E. Ç. BAYRAMOĞLU¹, M. AKALIN²

¹ Materials Institute, TUBITAK –Marmara Research Center,

²Marmara University, Technical Education Faculty, Dept. of Textile Education

ABSTRACT

In this work, the changes in flame retardancy and performance characteristics of lyocell and lyocell/cotton blended commercially produced fabrics are examined. Previous studies of lyocell flame retardancy were mainly on fibre form. The main aim in this research is to clarify how the flame retardancy characteristics (LOI value) are affected when the lyocell fibres are used alone or in blends with cotton in fabric form. From the LOI measurement results, it is understood that the flame retardancy of the samples tested increase with the increase in lyocell content. This appears in connection with the fibrillation characteristics of these fibres. However, the performance properties of the fabrics have also been examined and it is found that the most suitable mixture is 50/50% lyocell / Cotton, which, while giving rise to no unacceptable level changes in performance of lyocell/cotton blended fabrics, enable flame retardant finishing to be undertaken.

Keywords: Flame retardancy, Fibre Surface, Fibrillation, Limited Oxygen Index, lyocell/cotton blends.

1. INTRODUCTION

Polymeric textile fibers are highly combustible materials. Due to safety risks of this characteristic of textiles, different chemicals are used to flame retardancy [1–3]. Experimental researches of textile flame retardancy are mostly on reducing of cellulose's flammability. Because cellulose are not only sustains combustion but also it is self –accelerating [3–5].

According to properties of chemicals flame retardancy finishes can be durable, semi-durable or non-durable [6–8]. Phosphorus based durable finishes have preferred for cellulosic based materials. Among various phosphorus based finishes Pyrovatex has been widely used as flame retardant [3, 4, 9–11].

In this work, cellulosic lyocell and lyocell/cotton blended fabrics are treated with Pyrovatex CP and tested for flame retardancy to assess the burning behaviour and fabric performance.

Lyocell fibers are regenerated cellulosic fibers which known their high performance [12]. Even though little or no research has been carried out on flame retardancy of lyocell in fabric form some research has been done on lyocell in fibre form by Hall et al. These earlier results on lyocell have suggested that lower amounts of flame-retardants are used in lyocell in order to achieve same levels of flame retardancy of cotton with higher amounts of flame-retardants used [13-14].

The main aim in this research is to clarify how the flame retardancy characteristics (LOI value) are affected when the lyocell fibres are used alone or in blends with cotton in fabric form. From the LOI measurement results, it is understood that the flame retardancy of the samples tested increase with the increase in lyocell content.

However, the performance properties of the fabrics have also been examined and it is found that the most suitable mixture is 50/50% lyocell/cotton, which, while giving rise to no unacceptable level changes in performance of lyocell/cotton blended fabrics, enable flame retardant finishing to be undertaken.

2. MATERIALS AND METHODS

Properties of the fabrics used in this work are given in Table I. Blend ratios of the lyocell/cotton fabrics are determined by using the ASTM 629 method. All fabrics used were twill weave and were dyed commercial samples. Abbreviations used for lyocell is CLY and for cotton, C. The blend ratios of fabrics used were 40/60 %, 50/50 %, 67/33 % lyocell /cotton as well as 100 % cotton and 100% lyocell. Fabrics were conditioned under standard atmosphere in standard circumstances (20°C, 65% RH) before all tests.

Table 1. Basic Properties of Fabrics

Blend Ratio, CLY/C	Yarn Number, tex		Number of Threads per Unit Length, Threads /cm		Fabric Weight, g/m ²
	Warp	Weft	Warp	Weft	
100 (C)	33	33	44	24	207
40/60	31	31	44	25	206
50/50	56	24	52	23	234
67/33	63	25	48	21	250
100 (CLY)	36	33	44	25	208

Before the application of FR to the fabrics, fabrics were treated with preparatory define treatments, which include scouring to remove sizing or any other oils, left on the fabrics.

The standard formulation for application of Pyrovatex CP is given in Table II.

Table 2. Recipe of pad-bath liquor containing Pyrovatex CP

Chemicals	Ratio
Pyrovatex CP new	400 g/L
Lyofix CHN	80 g/L
Ultratex FSA New	40 g/L
Tinovetin June	2 g/L
Phosphoric acid, 85%	25 g/L

The flame retardant solution was applied at laboratory scale by a conventional padding application technique. Drying was carried out in curing oven at six rooms at 100°-110°-120°-130°-130°C and cured at 165°C for 90s. Flame retardancy characteristics of treated fabrics were investigated by the Limiting Oxygen Index method and these results are compared with general fabric performance characteristics, such as fabric tenacity and elongation. LOI (Limiting Oxygen Index) tests were carried out according to the ISO 4589-1984 standard with a CEAST OXYGEN INDEX P/N 6443,000 apparatus. The Kjedhal method (AOAC 920.105) was used to find fabric nitrogen contents. Phosphorus contents were determined by using an INCA Analytic System of a JEOL JSM-6335F Field Emission Scanning Electron Microscope. Fabric breaking load and elongations have been measured according to ISO 5081:1977 before and after flame retardancy applications. The JEOL JSM-6335F Field Emission Scanning Electron Microscope was also used to investigate of surface defects of fibre and fibrils in this research.

3. RESULTS AND DISCUSSION

3.1. Flammability Testing

Results in Table III show that all LOI values of FR treated fabrics are above 29 %. This suggests the reasonable flame retardancy is achieved with all fabrics. To the author knowledge, the LOI value of lyocell in fabric form has not previously been reported and in this work LOI values for untreated lyocell fabric was found to be 21.3%.

Higher ratio of sorbency of lyocell is reflected on the higher levels of LOI values. Phosphorus and nitrogen content in FRtreatedfabrics are given in Table III.

Table 3. LOI and Nitrogen/Phosphorus Content Results

<i>Blend Ratio, CLY/C</i>	LOI, %		Add-on, %, w/w	Nitrogen Content, %, w/w	Phosphorus Content, %, w/w
	Untreated	Treated			
100 (C)	20.2	30.2	14	1.30	2.20
40/60	21.3	30.3	10	1.31	1.78
50/50	21.2	32.3	17	1.36	2.26
67/33	21.4	32.6	12	1.56	2.66
100 (CLY)	21.3	32.2	19	1.52	2.32

LOI result of 100% cotton is slightly above the suggested values of the literature.

3.2. Fabric Performance Analysis

In Table IV the effect of flame retardant treatment on the performance characteristics of the fabrics is given in terms of tenacity and elongation both of which tend show to loses, expressed as percentages.

Table 4. Losses of Tenacity and Elongation in % Due to FR Application

Blend Ratio, CLY/C	Loss in Tenacity, %		Loss in Elongation, %	
	Weft	Warp	Weft	Warp
100 C	-8	-6	-31	-30
40/60	-14	-8	-24	-17
50/50	-20	-16	-27	-20
67/33	-20	-7	-31	-27
100 CLY	-35	-30	-40	-44

Loss of tenacity arises from phosphoric acid tendering of cellulose and cross-linking effects of the finish [1].

However, loss of tenacity was more in weft direction than the warp direction. This could be due to the effect of less twist on the weft yarn than the warp yarn, which will allow more flame retardants into yarn and then into fibre as a result more tenacity was lost weft direction.

3.3. Scanning Electron Microscopy of the Fibre Surface

Fibrillation, which is one of the characteristics of lyocell fibres, has been investigated before and after treatment [15]. Fibrils are seen adhere to the surface of the fibre after flame retardant application in all fabrics (Figure 1.). Scanning electron microscopy photographs show the absence of cracks and individual peeling of the fibrils along the fibre axis on FR treated lyocell fibres. Fibrils tend to stick together with the effect of FR and then adhered on to the fibres.

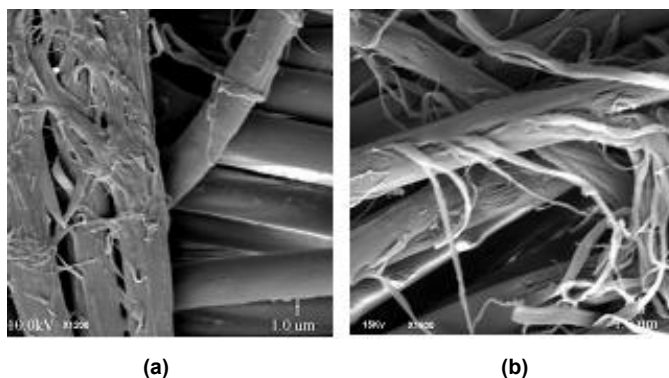


Figure 1. (a) Fibril Adhesion on the Fibre Surface of Lyocell FR-Treated Fabrics, (b) Fibrils of Untreated Lyocell Fibres

3. CONCLUSION

In this work, LOI value of untreated lyocell was found to be (%21) higher than any other untreated cellulose such as cotton or viscose suggested values in the literature. However, this still requires more investigation to confirm. LOI values of FR treated lyocell were also much higher than that of

FR treated cotton under same condition. This suggests that the better and even distribution of flame-retardants on lyocell than cotton.

SEM results show that the fibrils are stuck together and looks like the cracks on the fibre surfaces are filled by the flame retardant chemicals on the lyocell fibres. Fibrillation is thought to allow more flame retardants in lyocell fibre and also flame retardants absorbed by the fibrils which sticking the fibrils together and also back on the fibre surface with the flame retardant treatment creating like a second coat of FR.

In the cotton/lyocell blends presence of FR solid add-ons between 10-20 % increases the LOI values above 30%.

Fabric tenacity results show the most loss in 100 % lyocell when FR is applied. However, optimum blends in terms of better tenacity results and LOI values were observed in 50/50 % lyocell/cotton blends.

ACKNOWLEDGMENTS

Authors would like to express their thanks to Telateks Textile Corporation for the use of laboratory scale finishing equipments and Poliya Polyester Corporation for the use of LOI equipment.

REFERENCES

1. Horrocks Ar., Rev. Prog. Color, 1986; 16; 62.
2. Horrocks Ar., Polymer Degradation And Stability, 54 (1996) 143-154.
3. Yang Cq, Qui X., Fire And Materials, 2007, 31:67-81.
4. Yang Cq, Wu W., Polymer Degradation And Stability, 92 (2007) 363-369.
5. Batty J W, Textile Auxiliaries, (Pergamon Press, Oxford), 1974, 33.
6. Mark H, Woodings N, Atlas S M, Chemical After Treatment Of Textiles, (Wiley-Interscience, New York), 1973, 591.
7. Horacek H., Grabner R., Polymer Degradation And Stability, 54 (1996) 205-215.
8. Wu W., Yang Cq., Polymer Degradation And Stability 91, (2006), 2541-2548.
9. Weil Ed, I: Grayson M., Editor Kirk Othmer Encyclopedia Of Chemical Technology, 4th Ed. New York, Wiley, 1995, 976 P.
10. Weil Ed. In: Engel R. Editor, Handbook Of Organophosphorus Chemistry, New York , Marcel Decker 1992 683 P.
11. Guan, Jp, Author Guan Jin-Ping Guan, Jin-Ping , Chen, Gq, Et Al., Fire Mater 30 (6): 415-424 Nov-Dec 2006.
12. Albrecht W, Reintjes M, Wulforst B, Lyocell Fibres, Fibre Tables According To P. -A. Koch, (Institut Für Textiltechnik Der Rwth, Aachen), 1997, 1.
13. Hall M, Horrocks A R, Seddon H, Polym Degrad And Stabil, 64, (1999) 505.
14. Seddon H, Hall M, Horrocks A R , Polym Degrad And Stabil, 54, (1996), 401.
15. Rohrer C, Retzl S, Firgo H, Man-Made Fiber Year Book, (Cms Publishing, Uk), 2001, 26.

DESIGNING SPECIAL CLOTHING USING NEW TECHNOLOGIES ON PRODUCED TEXTILE SURFACES

F. ÖZTÜRK, Ş. EROL

Gazi University, Vocational Education Faculty, Clothing Industry and Fashion Designing Education Division

ABSTRACT

The upswing in textile and other sectors have affected ready-made apparel products and have added new functions to the main features of the apparel. According to marketing surveys, the demand for apparels which are used for special purposes such as business suits, protective suits and first-aid suits is increasing day by day. In parallel to the increasing interest in healthcare awareness, the needs for modern and comfortable clothing have been improving. In this study, it is aimed to be evaluated with fashion concepts of apparel purpose usage of textile surfaces produced by using new technologies and to be carried the problems determined, which have been met, to the new designs dimension. Making functional apparel designs that are able to be put by workers employed in especially first aid crew, have been taken into consideration in the direction of this aim. In accordance with this, the result of the joint working with the textile company ACL, a sample of special clothing, which may be put on by especially employees working in first aid crew, which the functionality and the form of the apparel design can be easily changed according to the its usage aim, has been come up.

Key Words: Nanotechnology, technical textiles, special purpose apparel, high performance fibers, comfort, performance.

1. INTRODUCTION

Mankind has been using textile products for ages almost all fields in the daily life. At the beginning, human beings used textile goods only for cover, shelter and decorations but in the last 50 years, revolutionary changes have happened.

Technological improvement and life standards gaining much more importance day by day, have caused its effects to perceive in every field of humans life and have led to the expectation to become higher. The upswing in technology and life standards has taken its place in human life and it is making it impact more and more every passing day. Because of this, in order to compete and to make a better place in the textile sector, not only to produce but also to make the most quality, the best and the highest performance textile surface possible have become required.

Especially in recent years, more scientific researches have been made related to the higher technological fibers made with new technologies and have produced very interesting fibers and cloth.

After the first production of the synthetic fibers in the year 1939, the use and production of the technical textiles has grown %7-15 in last 30 years and every passing year has made it a giant sector in the world. Nearly as old as the traditional textiles, these textiles can be used out of the textile sector which the traditional textiles cannot. These products have resistance to chemicals, weather conditions and micro-organisms; and the products are the products which show higher resistance, non-flammable, resistance to higher corrosion (11). The result of improved processes applied to the various fibers, now they can now be used in cleaning, construction technology, hygiene, medical services, decoration, furniture and geo textile fields (9).

2. CLOTHES USED IN SPECIAL PURPOSE APPAREL DESIGNS

The use of modern technology in textile production has represented the improving of the new point of view to the existing technologies. On one hand, this states an increase of performance in technical, economical and ecological parameters for products and processes known, on the other hand, it also states new products improved by advancement of using existing technologies and application fields of these products.

Technical textiles and new technologies used in high performance fibers have been preferred in order to improve the performance of the new textile goods. Textile products have become multifunctional with the assistance of the new technologies which have made them gain different properties. For example, by using the new technologies, textile apparels can make improve the performances of water repellent, anti-bacterial, heat isolation and can be used as sensors for the aim of camouflage.

According to the experts that have agreed that the smart-textiles are the group that have the highest add value among the technical textiles, in order to be able to produce especially comfortable and ergonomics apparels which are able to be put on with smart apparel, it is necessary to be carried out joint working with the fashion design division of the universities. As Dr.Gök Sadıkoğlu says:

“In these days, the importance of the fashion is unquestionable. If we could make the smart-clothing appropriate to fashion, we could make its value much more.”

By saying this, he tells us that we should get back our advantage against far eastern countries because Turkey has impressive utilities and infra structure about confection (5).

It has been known that lots of firms that have made up their R&D teams and proven themselves in the textile and ready wear clothing, have started to produce textile surfaced goods using new technologies. But in our country, there hasn't been a complete investigation and inventory about this subject; this makes it pretty hard to make an evaluation about the current state. İsmail Gölle, who is the president of İTHİB says that there has been a growth

in technical textile exports about % 18, and the new technology products which are based on completely information and know-how and cannot be copied, which gives these goods a lot of high added value to them.

In our country, the big groups such as Sabancı, Zorlu, YeşimTekstil have been making on technical textile investments and firms such as Damat,Yeşim, Abbate have been making apparels that are water proof and stain proof (5).

In this chapter, we will look at the cloths used in special purpose apparel designs.

2.1 Water Proof, Breathable Clothing Kinds

Methods used to produce cloths that have both water proof and breathable features can be divided into three groups (3).

- Dense texture cloth
- Membranes
- Covering

The designs used for the subject research are clothing with membranes.

Membranes are quite thin films made with polymeric materials which allow the water vapor to pass thru it but it show a high level degree resistance against fluid water penetration. Membranes are divided into 2 groups such as micro pore and hydrophilic.

2.1.1 Micro Pored Membranes

These are the thin film of polymers made with PTFE which have 1.4 million pores per square centimeter. Hydrophobic structure of polymer and tiny pore dimensions requires very big pressure for water penetration. It is believed that if materials such as body grease, bug spray, particular dust, sun lotions, salt used for cleaning interact with the membrane, then it will lower its water vapor permeability. For this reason, these micropored membranes have a hydrophilic polyurethane layer on them to lower the pollution of the membrane.

2.1.2 Hydrophilic membranes

Hydrophilic membranes are chemically modified which gives them the feature of having no pores on them and sometimes called no pored films.

Membranes should be infused with modern technology making its functions maximized but having no side affects such making its visual and the cloths quality worse (10). The method used in process and function is linked to the cost of the product. There are four basic ways to link membranes to the textile surfaces.

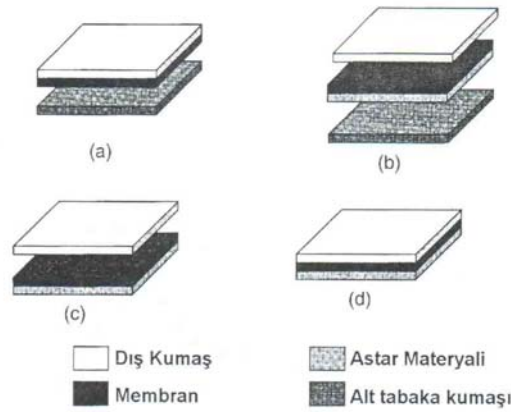


Figure 1. Membrane linking methods

First method is called the lamination of the membrane and the outer plate (Figure 1.a). For making a two plate system the membrane is pasted under the outer cloth. This method, like a rustling sound and similar to the paper, lowers the aesthetic attraction of the cloth but it gives the advantages such as water proof and wind breaking abilities to the cloth. They are used in protective clothing.

Second method which is called as lining or intermediate linkage process, is that the membrane is laminated to the light weaved or knitted cloth. The parts are cut to fit the materials shape and sewed together and the sewing lines are covered with a water proof material which makes it water proof. Later on this fabric is put between the outer cloth and the lining. The three parts (outer cloth, lamina and lining) are sewn together with a secret stitch (covered with waterproof stripe on it). If a high thermal isolation is needed then it is supported by hard cotton or cloth stuffing. This method has the advantage of soft attitude and drapery. It can also be modified for fashion needs.

Third way is called the lamination of either the membrane or the lining and the lamination process is done on the lining cloth. The functional covering is pasted to the clothing apart from the outer cloth. This method has its advantages because it can be modified for fashion purposes.

The forth way is called outer cloth, membrane and lining lamination. A three plated system is made but it is not that much used because it doesn't have the quality as the others.

The properties of the membrane cloth used in the research;

They have a PU membrane in the middle of 2 different clothing or one sided membrane with one layer of cloth. The cloths are micro fiber cloths, parachute cloths and polar. Due to the breathable, wind proof and the ability to sweat it out, those are appropriate for the sports wear and first aid dress,

like Montgomery/waistcoat designs carrying the features of comfort, functional and aesthetic components and they are shown as below.

They are durable against dry cleaning and washing.

Table 1. Technical features of the cloths used in apparel designed

WIDTH (cm)	WEIGHT (gr/m2)	COMPOSITION	TECHNICAL SPECIFICATIONS		
			STANDARD TEST METHOD RESULT		
145	300	%90 PES, %10 PU MEMBRANE (3 LAYERS)	WATER PROOF	10 000 mm WG	TS 257 EN 20811
			WATER REPELLENT	ISO 4	TS 259 EN 24920
			PHOSPHORUS COLOUR	SUITABLE	TS EN 471
			COLOUR AGAINST LIGHT	4	S 1008 EN ISO 105 B02
			BREATHABLE	FRONT: 0,401 N	TS EN ISO 13937-4
				BACK:0,175 N	
			TEAR RESISTANCE	WEFT: 138 N	TS EN ISO 13937-4
				WARP:148 N	
			SNAP RESISTANCE	WEFT:1043 N	TS EN ISO 13934-1
				WARP: 1547 N	
SEWING BAND APPLIED					
STANDARD TEST METHOD RESULT					
145	250	OUTER CLOTH %100 PES INNER CLOTH %50 PES,%50 COT (BY LAMINATION)	WATER PROOF	500 mm WG	TS 257 EN 20811
			WATER REPELLENT	ISO 4	TS 259 EN 24920
			PHOSPHORUS COLOUR	SUITABLE	TS EN 471
			COLOUR AGAINST LIGHT	4	S 1008 EN ISO 105 B02
			BREATHABLE	FRONT: 0,403 N	TS EN ISO 13937-4
				BACK: 0,154 N	
			TEAR RESISTANCE	WEFT: 68 N	TS EN ISO 13937-4
				WARP: 56 N	
			SNAP RESISTANCE	WEFT: 903 N	TS EN ISO 13934-1
				WARP: 1127 N	
SEWING BAND APPLIED					

3. APPAREL DESIGN FOR SPECIAL PURPOSE CLOTHING

Clothing designs is to comment the apparels as two or three dimensions according to the buyers' social and economical status with a serious research and development studies (4). At apparel design, in passing an idea

as an authentic style and gaining individual comment as a unique quality, taking into consideration the production processes, it is required for the components to be adopted, to be assimilated, to be transformed into concrete offers and to be evaluated. In clothing design for an idea to be translated as authentic thus including the production process they should be made into concrete proposals.

In present day, the process of clothing design shouldn't only be perceived as making an artistic guise but also a process prepared in every detail planned to the end. In the design of private ended clothing, all factors affecting the design have become on the scene in an effective way.

At the present day, in multi functional cloth design understanding, that the functionality of apparels designed according to the structural and environmental conditions are carried out completely, are overlapping with the evaluation of the cloth that have economical and aesthetic value. Cloth designing has brought a 3 dimensional view together, resistance and functionality that is used in cloth designing as well as its aesthetic. One of the many problems in the designing part is that the understanding of technical textiles constructive behavior. In this study the textile goods made with modern technology is used in fashion thus opening new ways for new designs.

For this aim, data about the vests and Montgomery used in first aid by the company ACL Textile have been evaluated while explicating the likes and dislikes of the product then a new production has been made and submitted to those concerned. In the study, the vest and Montgomery have been made as one and has aimed to get more functionality, the arm portions of the Montgomery have been made more portable and when required, it can be removed out and can be used as vest. Caption of the Montgomery, when required, is designed as portable. It has been designed as unisex and increased the functionality. There are two different clothing membranes used in this product.

Design (VEST) submitted to be used by ACL Textile (15)



Figure 2. Front view of clothing

Figure 3. Back view of clothing

Design (MONTGOMER) submitted to be used by ACL Textile (15)



Figure 4. Front view of clothing

Figure 5. Back view of clothing

4. CONCLUSIONS

Two main factors which determine the value of production in upcoming years in ready wear apparel sector, will gain importance. First one is the textile material and products manufactured for the aim of technical and performance features more than technological functions gained at the production stages of the product, aesthetic or decorative features; second one is the factors brought by the fashion design and creativeness.

In mass production, the goods that are produced in large numbers have a share of %70 of the global commerce but in assets it is %60. In the textile

sector, Turkey, has always been keeping the top brand place and as worlds' 6th exporter country, has been advancing on her way making a brand each passing day. Anyhow, Turkish firms have reached the position that can sell their own fashion products and designs by taking advantages of her market researches, observations and experiences. Also, they can produce the required goods with the required quality and price. Competence dominance in production and marketing fields has shown that she can maintain locomotive sector in ready wear field. At this stage, Turkey is giving speed to new technologies that require less labor. It has been realized that Turkish textile firms that would like to gain success with her products in the international competition which causes productivity to increase in reasonable degree, have been heading towards production of high performance cloth and have been offering smart cloth in a faster, reliable and effective course.

In this study, the work done jointly with the ACL Textile firm has come up with an apparel design that the functionality and the form according to the usage aim can be changed easily, that especially the first aid crew can put on, and a sample apparel designed for this aim, have been formed.

REFERENCES

1. Anonim (2006) "Öztek Tekstil" Hedef Dergisi, Şubat-Mart. Sayı:146 s. 48-50
2. Cireli, A., Sarıışık, M.,(2000) "Koruyucu Giysilerde Termal, Biyolojik, Fiziksel, Kimyasal Test Yöntemleri ve Değerlendirmeleri", Tekstil & Teknik Dergisi, Temmuz, s.120-128
3. Horrocks, A.R., Anand, S.C., (Editör), (2006) "Teknik Tekstiller El Kitabı", The Textile Institute, Türk Tekstil Vakfı, İstanbul
4. Kalıncara,V., (1992) " Giysi Tasarımında Ergonomi" Gazi Üniversitesi Sosyal Bilimler Enstitüsü, Yüksek Lisans Ders Notları, Ankara
5. Karataş, S., (2006) "Gelecek Teknik Tekstilde" Hedef Dergisi, 156. sayı, 15 Aralık 2006 - 15 Ocak 2007
6. Nomez G, (2001) "Applications And Markets Of Technical Textiles", Institute Français Du Textile-Habillement, Vicenza, Kasım
7. Qian, L., Hinestroza,J. P., (2004) "Application Of Nano Technology For High Performance Textiles" JTATM Volume 4, Issue 1, Summer
8. Tarakçıoğlu, I., ve Diğerleri, (2006) "Teknik Tekstiller ve Kullanım Alanları" www.tubitaktam.ege.edu.tr
9. Usta, İ., (2004) "Nonwoven ve Elyafar", TAD Dergisi
10. W. Mayer, U. Mohr And M. Schuierer,(1989), İnt. Textile Bull., No:2, 18
11. Yıldırım K., Aydın N., Çelikbilek A. Ve Güçer Ş., (2002) "Kaliteli Yaşam İçin Teknik Tekstiller Ve Kullanım Alanları", Kimya Teknolojileri Dergisi, Sayı 17, Mayıs
12. www.tekstilteknik.com/Referanslar/Tekniktekstiller.asp?Kimlik=1
13. www.oztektekstil.com.tr
14. www.abbate.com.tr
15. www.112acilkiyafet.com.

THE EFFECTS OF FABRIC CONSTRUCTION PROPERTIES ON THE ABRASION PERFORMANCES OF AUTOMATIVE UPHOLSTERY FABRICS

F. GÖKSEL, Ş. GÜÇER

TÜBİTAK Bursa Test ve Analyze Laboratory

ABSTRACT

Industrial Textiles are widely used in transportation vehicles and systems including cars interior, airplanes, trains, buses etc. Technical textile materials are used in cars for interior trim; as seating areas, headliners, carpets, side panels, belts, filters, air bags, etc.

Upholstery fabrics which are used in automotive industry to coat seating areas have to perform some special properties namely high tenacity, high abrasion resistance and flexibility. Thus sentetic fibers which have more tenacity and elasticity than natural fibers, are preferably used in order to get these properties mentioned above.

Performance tests have been performed to determine the properties of an automotive upholstery fabric by International and National standards. There are also company standards such as Renault, Fiat, Peugeot.

This study was performed to examine the effects of fabric structural properties on the abrasion performances of automotive upholstery fabrics. Two different abrasion test methods were compared to determine the abrasion performances.

Key words: Automotive upholstery fabrics, abrasion resistance, fabric properties, Taber method, Martindale method.

1. INTRODUCTION

Technical textiles play critical roles in areas requiring higher technology such as space and aeronautics, military and medical science; moreover, their informal use in daily life has become active in areas such as sports, sightseeing or outdoor sports, entertainment, home upholstery, furnishing and buildings and related equipment. Technical textiles are expected to be used much widely and indispensably in daily life in the near future [3].

The fast improvement in technical textiles is a result of their numerous design possibilities, disposability and spontaneous decomposability as well as their special properties such as flexibility, elasticity and high resistance.

These products are as old as conventional textiles; contrarily they have been used in areas other than textile industry, since they show higher resistance to chemicals, different air conditions and microorganisms and they have higher performance with their high endurance, fireproof characteristics and high abrasion resistance. Following the first use of synthetic fibers in 1939, the production and usage of technical textiles has become common. The

production of synthetic fibers with different characteristics has facilitated the production of technical textiles [1].

Industrial fabrics included in the “technical textile” category are widely used in cars, airplanes, trains and ships for interior trim; as seating areas, headliners, carpets, side panels, belts, filters, air bags, etc. Therefore, these fabrics have to show special performance characteristics.

This study aimed to investigate the effects of fabric structural properties on the abrasion performances of automotive upholstery fabrics. For this purpose, the parameters composing structural properties of patterned and plain fabrics were changed and fabric performance indices such as breakage endurance, pilling and surface fuzzing were tested as well as their abrasion resistance which was tested by two different methods.

2. MATERIAL–METHOD

In order to test the effects of fabric structural properties on the abrasion performances of polyester automotive upholstery fabrics, three patterned and three plain fabrics with similar structural properties which given in Table 1. and Table 2. were chosen. The parameters related to structural properties were altered and fabric performance indices namely breakage strength, pilling and surface fuzzing and abrasion resistance were tested.

Turkish standard coded TS EN ISO 13934-1 was used to evaluate breakage strength according to strip method, a universal testing machine with a constant elongation ratio was adjusted to 5 testing samples (test specimen) with weft and warp in the same direction having 200 mm jaw distance and 100 mm/min jaw speed; test sample dimensions were 50 x 200 mm. These conditions of the testing method match most company standards in automotive upholstery industry [5].

Pilling and surface fuzzing were determined using the Martindale method, internationally accepted and most commonly preferred method. The test was performed in the Martindale machine in accordance with the TS EN ISO 12945-2 standard. When compared to the other methods, Martindale method was defined as the most suitable method showing the pilling and surface fuzzing performance resulting from frictions on the outer surface of the fabric. At the end of the test, after testing samples run at 1000 and 5000 cycles on the Martindale device, under D-65 light in the testing cabinet were evaluated using the standard criteria in comparison with the standard photographs. In the same time, test specimen were evaluated using the grading scheme from 5 to 1 given below [6].

Fuzzing and/or Pilling Assesment were done to standard method below:

- 1: Dense surface fuzzing and/or severe pilling.
- 2: Distinct surface fuzzing and/or distinct pilling.
- 3: Moderate surface fuzzing and/or moderate pilling.

4: Slight surface fuzzing and/or partially formed pills.

5: No change [2, 6].



Figure 1. Martindale abrasion and pilling testing machine.

Abrasion resistance was determined using two different methods. First method was the Martindale method commonly preferred to evaluate the abrasion resistance of the conventional textile products. This test complied with the TS EN ISO 12947-2 standard. Briefly, the testing samples were rubbed with Lissajous movements to a standard wool abradant fabric inserted in the abrading table of the Martindale machine at 12 kPa load and specimen breakdown was controlled under microscope at particular cycles. The test was stopped when/if two thread breakage would be observed [2, 7].

Second method for the evaluation of abrasion resistance was the Taber method used commonly in automotive upholstery fabrics. Briefly, this test uses an abrasive trunk wheel rolling with a constant pressure over the testing sample surmounted on a rotary platform. The platform, as well as the wheel, is set to a constant speed, while the wheel pressure on the fabric is variable [4, 8]. The test piece was installed on the the test piece holder of the Taber-type abrasion tester with the front surface up, the trunk wheel was placed on the test piece and the test was performed under the conditions listed below. At the end of the test, surface of the test piece was checked for the degree of wear and compared with the standard test piece or graded using the reference criteria.

Test conditions were adjusted as follows; trunk wheel CS10 emery was used in the Taber machine, platform speed was 60 cycles/min, 1000 g load was performed, test cycles (revolutions of test piece holder) was 2000. Abrasion resistance result was determined under D-65 light in the viewing cabinet and evaluated with grey scale using the colour change in the fabric, and also evaluated degree of wear and compared with the standard test piece or graded using the reference criteria given below [8, 9].

Determination Criteria for Appearance Change (Degree of Damage):

- 1: Very serious.
- 2: Serious.
- 3: Definitely visible.
- 4: Slightly visible but not noticeable.
- 5: No damage is visible [8].

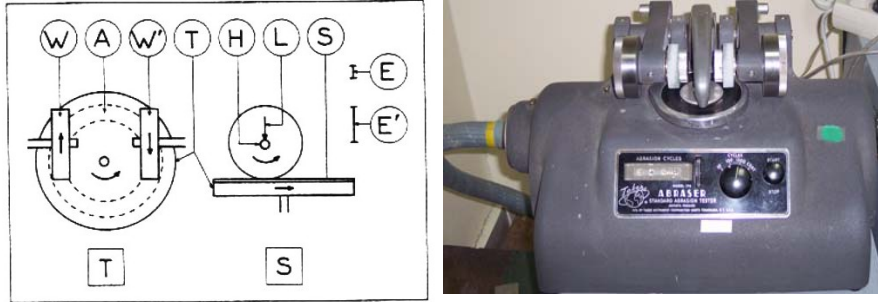


Figure 2. Taber Rotary Abraser

3. RESULTS AND DISCUSSION

Fabric structural properties and the performance values which used our study were shown in Table 1. and Table 2. respectively.

The evaluation of construction values and performance test results for coloured, plain fabrics in Table 1. was as follows:

a. Fabric samples number 1 and 2 which identified in Table 1. were weaved with yarns which had similar yarn lineer density. When the fabric structure was changed, fabric breaking strength, pilling and surface fuzzing, as well as abrasion resistance as determined by the Martindale method, remained unchanged; however Taber method showed that change in the fabric structure directly affected the abrasion resistance. Taber abrasion test revealed that fabric number 1 weaved with 3/1 twill had an half decrease in the colour change (grade 2-3), however the apperance change which showed the real abrasion value was graded as 2.

It has been suggested that this results from the increase in the surface coverage as a consequence of warp yarns having higher float in 3/1 twill weave compared to 2/2 twill weave. The high float of warp yarns weakens the connection points in the fabric structure resulting with the coverage of fabric surface with the warp yarns. According to the Taber abrasion principle, the trunk wheel induces a particular pressure on the fabric and as the rotary platform the fabric is mounted on rotates, the trunk wheel shaves and wears the fabric away by means of friction. Thus, the float warp yarns are exposed

Table 1. Fabric structure and performance values for plain fabrics

TESTS	PLAIN AUTO FABRIC SAMPLES		
	1	2	3
Yarn Linear Density (ISO 7211-5)			
Weft	946 denier	930 denier	939 denier
Warp	743 denier	755 denier	1198 denier
Fiber Content (Weft/Warp)	Polyester	Polyester	Polyester
Number of Threads per unit length (ISO 7211-2)			
Weft (Weft picks/cm)	14,6	14,4	12,5
Warp (Warp ends/cm)	18,1	18,3	13,6
Weight per Unit Area (ISO3801)	440 g/m ²	444 g/m ²	450 g/m ²
Weave Type (with microscope)	3/1 Twill	2/2 Twill	2/2 Twill
Tensile Strength (ISO 13934-1)			
Weft (Maximum Load)	1673 N	1655 N	1409 N
Warp (Maximum Load)	2129 N	2228 N	2189 N
Elongation (Strain at peak)			
Weft	36%	39%	37%
Warp	33%	35%	33%
Pilling and Appearance Change (ISO 12945-2)			
At Martindale			
1000 cycles	5	5	4 -5
2000 cycles	4 -5	4 -5	4 -5
Abrasion Resistance (ISO 12947-2)			
With Martindale ; At 12 kPa	Over 50.000 cycles	Over 50.000 cycles	Over 50.000 cycles
Abrasion Resistance			
At Taber; Trunk Wheel: CS 10			
Load: 1000 g, Test cycles: 2000			
Color Change	2 - 3	3	3
Appearance Change (Degree of Damage)	2	3 - 4	3 - 4

Assesment Grade: 1: The worst, 5: The best

to more abrasion. This results in the higher impact of the friction force on the warp yarns as confirmed by the abrasion test results.

b. When fabric samples 2 and 3 which identified in Table 1. are compared, it has been noticed that these two fabrics have similar structural properties

or weave type with similar weft yarn linear density; however the warp yarn linear density differs in order to save the similar weight in grams resulting in number of warp yarn difference. This small change causes a 10 % decrease in the breakage strength of the weft yarn of the product without any changes in the breakage strength in the warp direction. The pilling and surface fuzzing tests in the Martindale machine and the abrasion resistance test have revealed no difference between these two fabrics. Taber abrasion resistance test has shown that only the appearance of the fabric with the decreased weft breakage strength has a half-decreased grade.

The evaluation of construction values and performance test results for patterned fabrics in Table 2. was as follows:

a. Fabric samples 1 and 2 which identified in Table 2. have similar weave type with similar weft yarn linear density. The warp yarn linear density has been half decreased in fabric 2; however, the number of warp yarns per unit length has been doubled; the number of weft yarns has been slightly increased, as well as the weight per unit area. Evaluation of the performance values of such a fabric has indicated that when the weft yarn linear density is accepted as similar, any increase in number of weft yarns correlates with an increase in weft resistance. A half decrease in warp yarn linear density and the doubling of number of warp yarns (warp density) has failed to save the warp yarn breaking strength and a 15 % decrease in the warp breakage strength has been observed without any changes in the pilling and surface fuzzing of the fabrics. The appearance change in the Taber abrasion resistance test has shown a 1,5 degree increase in the abrasion resistance when the yarn density (Number of yarns) is increased even thin yarns are used; indicating that any increases in yarn density improve the abrasion resistance of the product.

b. When fabric samples 2 and 3 which identified in Table 2. were compared, it has been noticed that the fabrics have similar weave type and similar weft yarn linear density; however they differ in warp yarn linear density so that warp yarn linear density has been increased in fabric 2 to save the desired value for fabric weight per unit area. Thin yarn/high yarn density characteristics of the fabric caused an increase in the breakage strength. Martindale pilling and surface fuzzing test results have failed to display any significances in the abrasion resistance; this was confirmed by the appearance difference parameter of the Taber test which has shown that thin yarn/high yarn density feature of the fabric does not affect the abrasion resistance.

Table 2. Fabric structure and performance values for patterned fabrics

TESTS	PATTERNED AUTO UPHOLSTERY FABRIC SAMPLES		
	1	2	3
Yarn Linear Density (ISO 7211-5)			
Weft	964 denier	1037 denier	974 denier
Warp	1188 denier	593 denier	771 denier
Fiber Content (Weft/Warp)	Polyester	Polyester	Polyester
Number of Threads per unit length (ISO 7211-2)			
Weft (Weft picks/cm)	13,6	15,3	15,6
Warp (Warp ends/cm)	13,6	26,5	18,1
Weight per Unit Area (ISO3801)	476 g/m ²	496 g/m ²	460 g/m ²
Weave Type (with microscope)	3/1 Twill	3/1 Twill	3/1 Twill
Tensile Strength (ISO 13934-1)			
Weft (Maximum Load)	1547 N	1729 N	1731 N
Warp (Maximum Load)	2111 N	1789 N	2152 N
Elongation (Strain at peak)			
Weft	33%	37%	34%
Warp	50%	53%	37%
Pilling and Appearance Change (ISO 12945-2)			
At Martindale			
1000 cycles	4 - 5	4 - 5	4 - 5
2000 cycles	4	4	4 - 5
Abrasion Resistance (ISO 12947-2)			
With Martindale ; At 12 kPa	Over 50.000 cycles	Over 50.000 cycles	Over 50.000 cycles
Abrasion Resistance			
At Taber; Trunk Wheel: CS 10			
Load: 1000 g, Test cycles: 2000			
Color Change	3 - 4	3 - 4	3
Appearance Change			
(Degree of Damage)	2 - 3	4 - 5	1 - 2

Assesment Grade: 1: The worst, 5: The best

In the publication named "Abrasion of Textile Surfaces" section of the "Surface Characteristics of Fibers and Textiles" book that a fabric's resistance to abrasion depends on a number of factors specific to the fabric, including fiber content, fiber mechanical properties, fiber shape, yarn and fabric structure, yarn twist, yarn size, yarn ply, yarn crimp, fabric thickness, thread count, weave type, and finishes that parallel like our study [10].

In the other publication named "Change in Surface Properties of Fabrics During Wear" that polyester and its blends plain fabrics have higher strength than twill fabrics and assessment of abrasion resistance in two broken yarns in the sample (end-point assessment) displays that the number of turns to cause abrasion per unit areal density shows no significant difference between different fiber types (i.e. wool and wool blends, polyester and its blends) and weave structures (i.e. plain, 2/1 twill, 2/2 twill and fancy weaves). Comparing to this study, our current study shows correlation in the Martindale test data; beside, Taber abrasion test data have revealed that the fabric type affects abrasion parameters when serious abrasion conditions are performed on the fabric and the existence of high float type weaves in the fabric structure has negative effects on the Taber abrasion resistance test result [11].

In the publication named "Upholstery Fabric Performance: Actual Wear Versus Laboratory Abrasion" that Taber method ideally simulates the abrasion of upholstery fabrics during daily use. They have exposed the fabrics to abrasion with H18 emery with a speed of 70 cycles/min at 40 cycles and evaluated the breakage resistance of the abrasion surface at the warp yarn direction. The breakage resistance parameters of the upholstery fabric of a chair used for 2 years and the testing sample abraded at the Taber machine in the laboratory have been compared. It has been concluded that the breakage strength and breakage elongation of the laboratory-abraded fabric is slightly less than the upholstery fabric of the chair. Statistical evaluation using the least significant differences (LSD) method has shown no linear correlation between the breakage resistance parameters of the "real-time" upholstery fabrics and "laboratory simulation" fabrics in that study [12].

4. CONCLUSIONS

One of the important performance characteristics of an upholstery fabric in automotive industry during daily use is the abrasion resistance, as well as the high strength. High strength and abrasion resistance of the product depends directly on the use of high resistant fibers and the fabric structure on the textile surface.

This study has compared the abrasion resistance parameters of various automotive upholstery fabrics with different yarn thickness (linear density), yarn density (number of weft/warp yarns) and fabric type and evaluated the breakage strength, pilling and surface fuzzing of these fabrics, as well as the abrasion resistance using two different methods.

In conclusion, the current study has shown that the differences in the yarn thickness, density and weave type directly affects the abrasion properties of the fabric surface. The use of high resistant polyester fibers with thin linear density in the structure of an high-density fabric increases the abrasion resistance and the use of high float weave type at the outer surface of the

fabric results in the higher rubbing of the yarns with more cover on the surface and, therefore, decreases the abrasion resistance of the product.

To confirm the data obtained in the current study, further studies using fabrics with similar weave, but different fiber types are required to test the effect of physical performance characteristics of the product.

REFERENCES

1. Adanur, S., (1995), "Wellington Sears Handbook of Industrial Textiles", Technomic Publishing Co.Inc., Pennsylvania, USA.
2. GÖKSEL, F., KÖSTEM, M., YILDIRIM, K., GÜÇER, Ş., (Ocak 2002), 'Kumaş Kalitesi ile İlgili Performans Testleri Boncuklanma ve Yüzey Değişimi', Kimya Teknolojileri Dergisi, Sayı:13
3. Yıldırım, K., Çelikbilek, A. Aydın, N. Ve Güçer, Ş., (Mayıs 2002), "Kullanım Alanları Gün Geçtikçe Artan Tekstiller: Teknik Tekstiller", Kimya Teknolojileri Dergisi, sh. 46-54
4. Charrier, J. M., (1991), "Polymeric Materials and Processing", Hanser Publisher..
5. TS EN ISO 13934-1, (1999), "Maksimum Kuvvet ve Maksimum Kuvvetteki Uzamanın Şerit Metodu ile Tayini"
6. TS EN ISO 12945-2, (2002), "Boncuklanma ve Yüzey Tüylülüğüne Eğilim Tayini: Martindale Metodu"
7. TS EN ISO 12947-1/2, (1998), "Martindale Metodu ile Kumaşlardaki Aşınma Dayanımının Tayini: Numunedeki Kopmanın Belirlenmesi Metodu".
8. HES News, (2000/06/06), D6506-00 General Test Methods for Fabrics.
9. SAEJ 948, (1196), "Test Method for Determining Resistance to Abrasion of Automotive Body Cloth, Vinyl and Leather, and the Snagging of Automotive Bodycloth".
10. Galbraith, R.L., (1975), Abrasion of Textile Surfaces, in "Surface Characteristics Fibers and Textiles", M.J. Schick, Ed., Marcel Dekker, Inc., New York.
11. Amirbayat, J., ve Cooke, W.D., (1989), "Change in Surface Properties of Fabrics During Wear", Textile Research Journal, Volume 59, No.8, sh.469-477.
12. Warfield, Carol L. ve Slaten, B. Lewis, (1989), "Upholstery Fabric Performance: Actual Wear Versus Laboratory Abrasion", Textile Research Journal, Volume 59, No.4, sh. 201-207.

A RESEARCH ON NONWOVEN FILTERS USED IN TECHNICAL TEXTILE APPLICATIONS

H.K. KAYNAK, Z.DEĞİRMENCİ, P. ERDAL

Department of Textile Engineering, University of Gaziantep

ABSTRACT

Filtration can be defined as the separation of one material from another. Textile filters are usually used for solid-gas and liquid-gas separation. Among textile materials, especially woven and nonwoven fabrics are suitable for filtration applications, because of their complex structures and appropriate thickness. Nonwoven filters are used in medtech, mobiltech, protech, packtech and hometech application areas of technical textiles. The market for nonwoven fabrics for filtration media on a worldwide basis is approximately \$2 billion. For developing countries; producing safe drinking water and having a better indoor air quality are main objectives. At the same time; increasing investments in chemical and pharmaceutical industries in Asian countries, strengthening environmental legislation cause the importance and production rates of filtration materials to increase worldwide. In this study; types of nonwoven fabrics used for different filtration requirements, raw materials, the recent developments, uses of nonwoven filters in technical textile applications and marketplace are investigated.

Key-words: Nonwoven filters, filtration, nanofiltration

1. INTRODUCTION

Filtration can be defined as separation of one material from another. The main purpose of filtration is to improve the purity of the filtered material. Textile filter materials are generally used in solid-gas separation and solid-liquid separation. Depending on the process of separation, filtration is generally referred to as particle filtration, microfiltration, ultrafiltration, nanofiltration and reverse osmosis[1].

In filtration, nonwoven fabrics can be generally described as a random fibrous web, formed by either mechanical, wet or air laid means and having interconnecting open area throughout the cross-section and able to remove a percentage of particulate from liquid or gaseous fluids streams flowing through it[2].

Nonwoven filtration media has existed for hundreds of years in one form or another, including wool felt and cellulose formed by various means into a web. However, the modern advent of synthetic nonwoven filter media began with disposable diaper in the 1950's and 1960's[2].

2. NONWOVEN FILTERS

Textile materials especially woven and nonwoven fabrics are particularly suitable for filtration because of their complicated structures and considerable thickness. The advantages of nonwoven filter media over woven filter media include:

- High permeability
- Higher filtration efficiency
- Less binding tendency
- No yarn slippage as in the case of woven media
- Good gasketing characteristics [1]

Nonwoven fabrics have thicker cross-sections and bulk compared to membranes, wire cloth and monofilament fabrics. Thus, nonwoven fabrics are the material of choice when large quantities of particulate loading, long-life or where general clarification of a liquid or gas stream is required. Nonwoven fabrics are relatively inexpensive compared to most other media[2].

2.1. Types of Nonwoven Fabrics Used for Different Filtration Requirements

Wet-laid synthetics are preferred when a thinner web and consistent pore size is important. Spunbonded fabrics which are relatively strong with modest dirt holding capacity, lacks the consistent pore size distribution of wet-laid and meltblown webs. Spunbond fabrics serve in applications, which include coolant filtration media and pleat support and drain layers in membrane and melt blown fabric cartridges. Needlefelt fabrics are common when strength and durability are necessary such as in baghouse applications. Air-laid and air bonding are popular because of its high-loft, bulk and large dirt holding capability in air filtration, including prefilters capable of capturing larger particles. These fabrics typically have high void volumes. Melt blown nonwoven fabric continues to be the rising star with rapid penetration into many liquid and air filtration applications [2].

Melt blown nonwovens are relatively low cost and are used in prefiltration and as final filters in applications where high-performance in fine filtration is required. Resin bonded nonwovens are popular in air filtration and point-bonded fabrics provide an alternative to overall bonded fabrics which commonly are used to fibers consisting dissimilar melt or softening points [2].

2.2. Raw Materials for Nonwoven Filters

Needlepunched filter fabrics provide good dimensional stability, excellent particle retention and freedom from plugging. They are mostly made of polyester, homopolymer acrylic, nylon, polypropylene, Nomex®, Ryton®, P84® and PTFE.

Dupont developed a Teflon®-fiberglass blend nonwoven filter fabric called Tefaire®. Dust is collected on the Teflon® fiber; the glass fiber bundle appears cleaner. According to manufacturer, Teflon® fibers improve the filter bag lifewhile small amount of fine glass fibers increase the total available fiber surface area and reduce the porosity of the felt which results in improved dust collection efficiency.

Polypropylene is widely used in woven and nonwoven structures in liquid filtration to improve the filtration properties because of their resistance to chemical breakdown.

Rayon and polyester needled felts are used in micron rated vessel bags which are used as disposable filter elements. Nylon and polypropylene felts are also used for this purpose[1].

2.3. Recent Developments on Nonwoven Filters

Recent developments on filtration materials can be classified as follows:

- Fibre fineness (micro- and nano-fibres)
- Coated and laminated filtering systems
- Functionalised filtering systems
 - ✓ Electrostatic charge
 - ✓ Conductive filter materials
 - ✓ Active filtering systems (catalysers, active carbon)[3]

Among these aspects with no doubt nanospinning has the vast importance with respect to nonwoven filtration today. Nanofibres are an exciting new class of material used for several value added applications such as medical, filtration, barrier, wipes, personal care, composite, garments, insulation, and energy storage[4]. Nowadays it is possible that the filters, used in technical textile applications, can make sensitive and high performance filtration by using nanospin system.

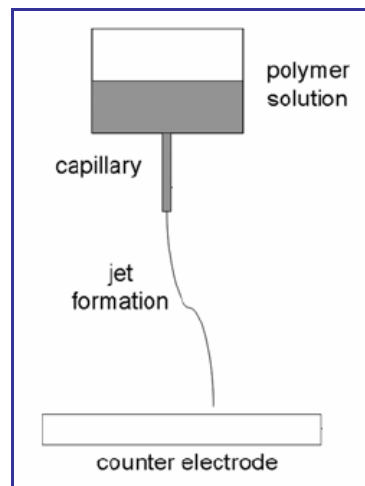


Figure 1. Principal setup for electrostatic spinning

Electro-spinning is an interesting technology to produce very fine fibers with sub-micrometer diameter. In the process, a strong inhomogeneous electric field acts on a polymer solution leading to the extraction of a polymer jet which solidifies and orientates through the evaporation of the solvent. Irregular webs made of these fibers have the potential to form highly efficient filters for micron and submicron particles but also bacteria or viruses [5].

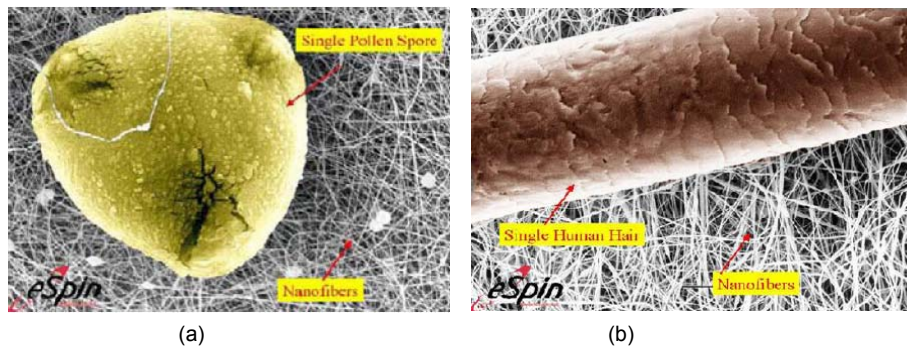


Figure 2. (a) Comparison between human hair and Nanofibre web (b) Entrapped pollen spore on Nanofibre web

Nanofibres exhibit special properties mainly due to extremely high surface area to weight ratio compared to conventional nonwovens. Low density, large surface area to mass, high pore volume, and tight pore size make the nanofibre nonwoven appropriate for a wide range of filtration applications. The simplest comparison between electro spun nanofibres, melt blown fibers and spun bonded fibres is fiber size. The difference in fiber size leads to vast differences in basic web properties such as fiber surface area, basis weights, thicknesses, permeability, and strength. In both static and self-cleaning filtration applications, nanofibre filter media has demonstrated longer filter life over several conventional filtering materials. Filter engineers are continually balancing the three major technical parameters of filter performance: filter efficiency, pressure drop, and filter life [4].

2.4. Uses of Nonwoven Filters in Technical Textile Applications

Nonwoven filters have many application areas such as;

- Hometech (vacuum cleaner filters, air filters)
- Medtech (face masks)
- Mobiltech (oil, air, pollen, fuel filters)
- Protech (nanomasks against Sars and H5N1 viruses)
- Packtech (coffee filters, tea bags)

2.5. Marketplace for Nonwoven Filtration

The market share of textile filters are; 70-75% for nonwoven fabrics (air), 20-25% for woven fabrics (filter presses), 1-5% for knits (dust bags, food) [3].

The market size for filtration and separation products was estimated to be over US\$20 billion in 2004. The forces driving this market growth are:

- the demands for improved clarity in water treatment (fresh or waste)
- better indoor air quality (domestic and industrial)
- a universal demand for finer degrees of separation – from hydraulic oils to semiconductor wash water

- the need for better hot exhaust gas filtration, including diesel exhausts
- the need for higher energy efficiencies in all separation operations
- strengthening environmental legislation.

The overall growth in the industry was forecast to exceed 34% from 2004 to 2009, with an annual average growth rate of 6%. On a more basic level of water purification, the objective is simply to produce safe drinking water for developing countries. The fastest growing geographical markets in this sector are China, India and South America[6].

The market for nonwoven fabrics for filtration media on a worldwide basis is approximately \$2 billion. The distribution is roughly in thirds across the major territories of North America, Europe and Asia. Of the largest volume uses, needlefelt fabrics for baghouse filtration represent the heaviest weight and most costly, whereas spunbonded fabrics, especially from polypropylene polymer for use in coolant filtration used in automotive and aircraft machining are the lowest weight and least expensive[2].

Filtration markets for nonwoven fabrics are especially broad. The largest single market for nonwovens is baghouse filtration with needlefelted fabrics being the media of choice. Needlefelted fabrics also serve as a base substrate for a microporous membrane or porous coating in this application. Similar needlefelted fabric constructions are found in liquid filter bags in paint, chemical and general industrial applications. Melt blown fabrics are increasingly popular in air filtration for use in vacuum cleaner bags to HVAC and other applications requiring high-efficiency. Meltblowns are also widely used in pleated liquid cartridges as prefilters or as final filters in many high-performance applications from pharmaceutical to the semiconductor industries. Membrane cartridge suppliers were the first to exploit the use of melt blown fabrics in the 1970's and early 1980's and the market continues to expand. Spunbonded fabrics are perhaps the most versatile, with filtration applications including coolant, cartridge pleat and membrane support, downstream layers to retard media migration for both air and liquid, tie-on bags, pool and spa filters and much more. These fabrics supply strength, reasonable dirt holding capacity and in certain cases stiffness and lateral flux[2].

Nonwoven fabrics continue to grow and in some cases, take market share from other media. However, filtration industry mega-trends provide many challenges for nonwoven fabrics. These mega-trends include (1) environmental consciousness (2) finer filtration and (3) specialized media (4) one-world business. Environmental consciousness suggests that nonwoven media should be reusable, have extended-life, chemical or vapor capture capabilities, compostability and/or be recyclable. Nonwoven fabrics will keep pace with the need for finer filtration and in some cases may even challenge microporous membranes in some applications as some companies are now beginning to claim efficiencies below one micron mean flow pore. Specialized filtration media is the key to nonwoven growth. As a result, the best years are

ahead for nonwoven fabrics as both suppliers and filter manufacturers continue to exploit untapped opportunities for specialized and performance nonwoven filtration media. Finally, filtration is a business where media, particularly specialized filtration media, often patented or from an unique process type is shipped worldwide [2].

Today in Turkey 6 nonwoven fabric producers are member of EDANA (European Disposables and Nonwovens Association). In 2004 the nonwoven fabric production of Turkey is estimated to be 110.000 tons and by the same year the nonwoven fabric import of Turkey is 41.000 tons and export is 18.000 tons. This means the total nonwoven fabric consumption of Turkey is 133.000 tons. In addition to this, in year of 2003, the share of Turkey's nonwoven fabric export among world nonwoven fabric export is 0.4% [7].

Table 1. Turkey's Nonwoven fabric export by years (2000-2004) [7]

Year	export
2000	US\$ 9mn
2001	US\$ 5mn
2002	US\$ 20mn
2003	US\$ 28mn
2004	US\$ 46mn

Table 2. Turkey's nonwoven fabric import by years (2000-2004) [7]

Year	import
2000	US\$ 55mn
2001	US\$ 52mn
2002	US\$ 77mn
2003	US\$ 107mn
2004	US\$ 143mn

3. CONCLUSIONS

The importance of filtration and requirements for filtered materials gaining an increasing importance in our daily life and in technical textile applications. This rapidly increasing importance causes more consumption of filtering materials. Due to this demand production quantities are increasing and by the same time production techniques are changing to achieve better performance, longer life for filtering materials. In this situation nonwoven fabrics come to the fore with reasonable price, high production rates and easily applicable techniques in comparison to other fabrication techniques. Because of these advantages the market share of nonwoven filters is seem to be increase in the future.

REFERENCES

1. Adanur S., (1995), "Wellington Sears Handbook of Industrial Textiles", Technomic Publishing, USA.
2. Gregor E.C., (2007), "Primer on Nonwoven Fabric Filtration Media". <http://www.egregor.com/whitepapers/NONWOVEN%20PRIMER.pdf>
3. Beke B.V., (2005), "Ecotextiles".
4. <http://www3.itv-denkendorf.de/itv2/downloads/d0005056/WG3TamBeke2.pdf>
5. Ariharasudhan S., Gopalakrishnan D., (2007), "Polymeric Nanofibre Web in Filtration".
6. <http://www.fibre2fashion.com/industry-article/technology-industry-article/polymeric-nanofibre-web-in-filtration/polymeric-nanofibre-web-in-filtration1.asp#>
7. Bahners T., (2007), "Electro-spun nanofibers – a way to improved wet filtration efficiency of textile filter media" <http://www.dtnw.de/Filter.pdf> Rideal G., (2005), "Filtration: The marketplace", Filtration+Separation, Pp:30-33
8. EMEK A. (2004) "Teknik Tekstiller Dünya Pazarı, Türkiye'nin Üretim ve İhraç İmkanları", Msc Thesis, Araştırma ve Geliştirme Başkanlığı Sanayi Dairesi, Ankara.

ANIMATION OF REAL WOVEN COMPOSITE STRUCTURE

J. SALACOVA

Department of Textile Material, University of Liberec

ABSTRACT

Woven composites are prepared by the use of prepreg technology under the joint impact of press and heat. It can be considered as the very complicated anisotropy system from the structural point of view. In order to visualization of real internal structure, it is necessary to precisely identify the yarn parts. This paper presents animation how the composite created is and how the ideal structure changed is after pressing to real one. Boolean operations, Bezier curves and tools of software Macromedia Flash have been use here. Short animation program was created for e-learning.

Key Words: animation, real structure, Macromedia Flash, woven fabrics, composite, reinforcement

1. INTRODUCTION

Woven composites are prepared by the use of prepreg technology under joint pressing and heat-treatment. From structural point of view we have two constituents of material – reinforcement and matrix. The prepreg (1 layer of reinforcement with resin) determines the particular elements of structure of reinforcement - longitudinal yarns and cross yarns. Voids and imperfections of reinforcement are formed during hot pressing. Fig. 1 represents structural hierarchy of woven composites with their structural elements.

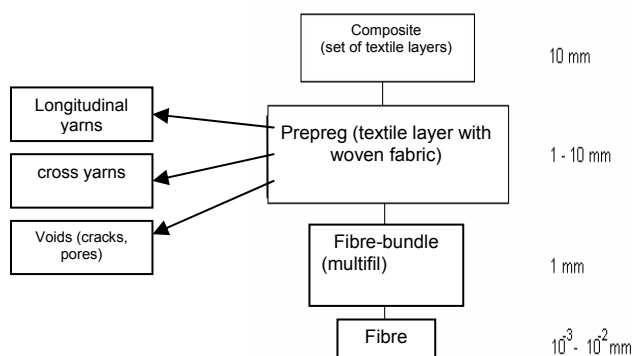


Figure 1. Structure hierarchy of woven composites

Imperfections and voids influence mechanical and thermal composite properties. Modelling of mechanical and thermal properties can be realized in macro-, meso- and micro-scale. Features obtained from microscopic point of view can be included to macro-scale modelling. There is possible to calculate macro-response of system from micro-response of system."

2. THEORETICAL BACKGROUND

2.1 Bézier Curves

Bézier curves can represent all different types of conic sections including circles, ellipses, parabolas and hyperbolas. The curve always interpolates the two points of control polygon. Simple and intuitive interaction between the control polygon, with its weights, and the curve makes Bézier curve representation so useful.

Bézier curve is defined by the parametrical equation, see the formula (2.1.1) and Fig. 2.

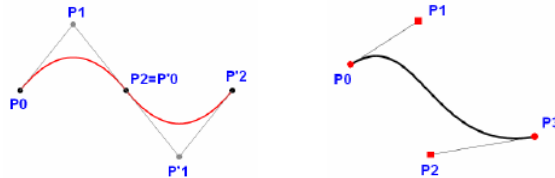


Figure 2. Bézier curves with their polygon

The Bézier curve of degree n can be generalized as follows. Given points P_0, P_1, \dots, P_n , the Bézier curve is

$$B(t) = \sum_{i=0}^n \binom{n}{i} P_i (1-t)^{n-i} t^i = P_0 (1-t)^n + \binom{n}{1} P_1 (1-t)^{n-1} t + \dots + P_n t^n, \quad t \in [0, 1]. \quad (2.1.1)$$

This formula can be expressed recursively as follows:

Let $B_{P_0 P_1 \dots P_n}$ denote the Bézier curve determined by the points P_0, P_1, \dots, P_n . then

$$B(t) = B_{P_0 P_1 \dots P_n}(t) = (1-t) B_{P_0 P_1 \dots P_{n-1}}(t) + t B_{P_1 P_2 \dots P_n}(t) \quad (2.1.2)$$

in words, the degree n Bézier curve is an interpolation between two degree $n-1$ Bézier curves.

Some terminology is associated with these parametric curves. We have

$$B(t) = \sum_{i=0}^n P_i b_{i,n}(t), \quad t \in [0, 1] \quad (2.1.3)$$

where the polynomials

$$b_{i,n}(t) = \binom{n}{i} t^i (1-t)^{n-i}, \quad i = 0, \dots, n \quad (2.1.4)$$

are known as Bernstein basis polynomials of degree n , defining $0^0 = 1$.

The points P_i are called *control points* for the Bézier curve. The polygon formed by connecting the Bézier points with lines, starting with P_0 and finishing with P_n , is called the *Bézier polygon* (or *control polygon*). The convex hull of the Bézier polygon contains the Bézier curve.

The $n + 1$ Bernstein basis polynomials of degree n are defined as

$$b_{\nu,n}(x) = \binom{n}{\nu} x^{\nu} (1 - x)^{n-\nu}, \quad \nu = 0, \dots, n. \quad (2.1.5)$$

where $\binom{n}{\nu}$ is a binomial coefficient.

The Bernstein basis polynomials of degree n form a basis for the vector space Π_n of polynomials of degree n .

A linear combination of Bernstein basis polynomials

$$B(x) = \sum_{\nu=0}^n \beta_{\nu} b_{\nu,n}(x) \quad (2.1.6)$$

is called a Bernstein polynomial or polynomial in Bernstein form of degree n . The coefficients β_{ν} are called Bernstein coefficients or Bézier coefficients.

The most important advantage of Bézier's curves is its ability to change the shape of the curve without the change of position of control polygons.

2.2 Boolean Operations

In abstract algebra, a Boolean algebra is an algebraic structure (a collection of elements and operations on them obeying defining axioms) that captures essential properties of both set operations and logic operations. Specifically, it deals with the set operations of intersection, union, complement; and the logic operations of AND, OR, NOT.

Boolean logic is a complete system for logical operations. In its simplest meaning in mathematics and logic, an operation is an action or procedure which produces a new value from one or more input values.

The general Boolean operations are union, intersection and difference. See Fig. 3.

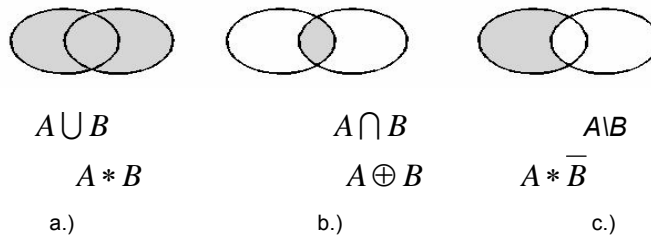


Figure 3. Boolean operation – a.) union, b.) intersection, c.) difference

The *union* of a collection of sets is the set that contains everything that belongs to any of the sets, but nothing else. If A and B are sets, then the union of A and B is the set that contains all elements of A and all elements of B , but no other elements. The union of A and B is usually written " $A \cup B$ ". Formally:

x is an element of $A \cup B$ if and only if

- x is an element of A or
- x is an element of B .

The *intersection* of two sets A and B is the set that contains all elements of A that also belong to B (or equivalently, all elements of B that also belong to A), but no other elements.

The intersection of A and B is written " $A \cap B$ ". Formally:

x is an element of $A \cap B$ if and only if

- x is an element of A and
- x is an element of B .

The *difference* is relative complement. If A and B are sets (in mathematic meaning), then the relative complement of A in B , also known as the set-theoretic difference of B and A , is the set of elements in B , but not in A and is usually written $B - A$ (also $B \setminus A$). Formally:

$$B - A = \{x \in B \mid x \notin A\}.$$

The principle of vector drawing was used in first way of solution. Boolean operations and Bezier curves were used here. These operations are suited for rapid generation of complex geometries. Only drawing of ideal structure shape is possible. See Fig. 3.

3. EXPERIMENT

Software Macromedia Flash[®] was used for animation of real woven composite structure. There was created program how composite is rising. At first images of ideal shape of reinforcement were created. Single structural elements were drawn, weave layers were putted together from structural elements and than all composite structure. Drawing of structural elements and weave layers is on the Fig. 3. Different colors represent different elements of vector drawing.

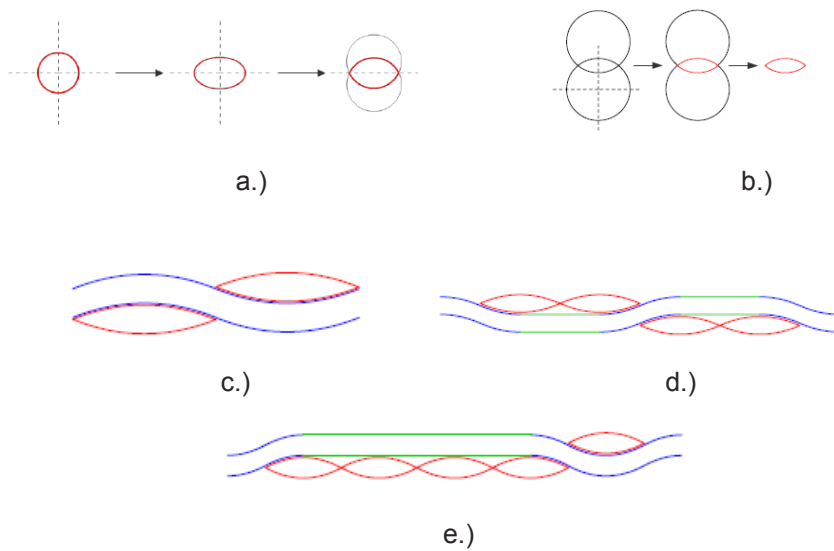


Figure3. Structural elements in vector drawing – a.) shape of cross fibres, b.) creating of shape of cross fibres, c.) basic unit of plain weave, d.) basic unit of twill weave, e.) basic unit of satin weave

Software scene and some results of weave reinforcements of woven composites are on the Fig. 4.

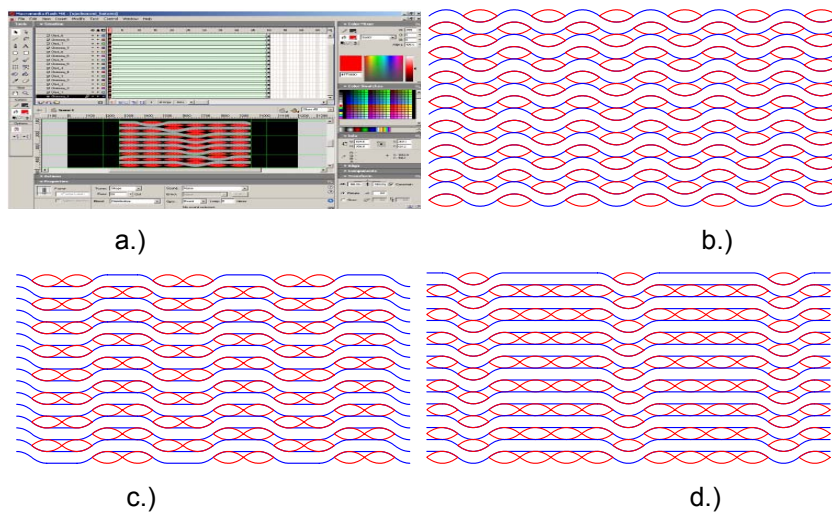


Figure 4. Ideal internal structure - a.) software scene, b.) weave plain, c.) weave twill, d.) weave satin

There have to create supported file for interactive editing of curves, program code see hereinafter.

//curve parameters

```
// dynamic input field initialization
amp.text=100;
per.text=0.05;
sY.text=0;
cara.text=2;
salfa.text=80;
sX.text=0;
barva=0x000000;
//function for curve generation
function generuj() {
    A = new Number (amp);
    t = new Number (per);
    c = new Number (cara);
    alfa = new Number (salfa);
    setX = new Number (sX);
    setY = new Number (sY);
    _root.createEmptyMovieClip ("sinuska", 1);
    with (_root.sinuska){
        setX=setX-22; //initial condition
        setY=-setY+300+A;
        lineStyle (c, barva, alfa);
        moveTo(setX,setY);
        for (i=1;i<1000;i++) {
            lineTo (setX, setY);
            setX=setX+1.1; //point displacement in axis X
            setY=setY-((A*t)*Math.sin(i*t)); //amplitude in axis Y
        }
    }
}
```

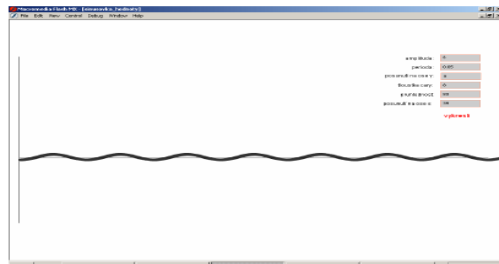


Figure 11. User's scene of file for interactive editing of curves

Vector images of real structure were obtained from raster images of hard cross section of internal structure. Some of results are on the Fig. 5 and Fig. 6.

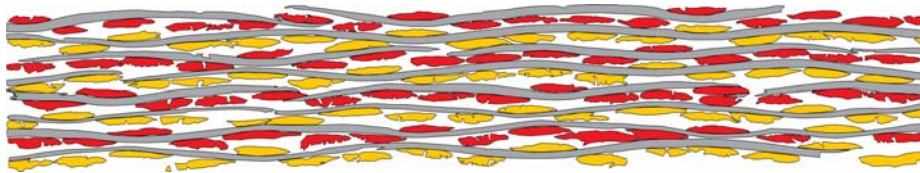


Figure 5. Vector image of real composite structure - weave satin, press 0,5 MPa, 8 composite layers

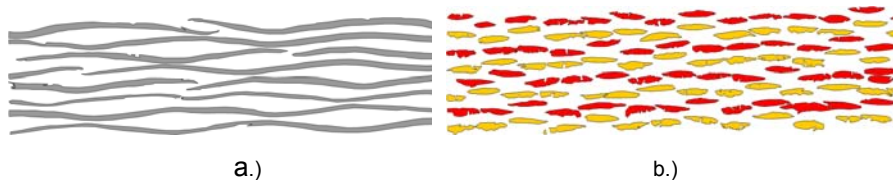


Figure 6. Vector image of real weave satin, press 0,5 MPa, 8 composite layers –a.) longitudinal yarns, b.) cross yarns

Underlining in time axe was the main problem of animation. We used the function “shape hints” for link guide points in time axis.

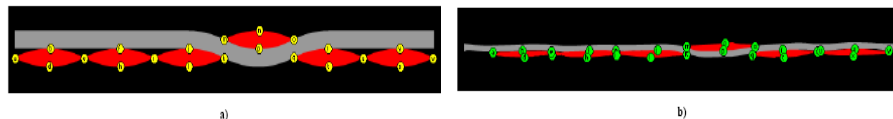


Figure 10. Using of function “shape hints” for interlining of time frames – a.) yellow guide points in started ideal structure, b.) green guide points in finish real structure

Work in user's scene of animation is in particular steps. At first weave pattern is chosen, the layers are stacked, height of compacting pressure is chosen after composing and the pressing is started. Ideal enter shape is changed to real one. All is on the move.

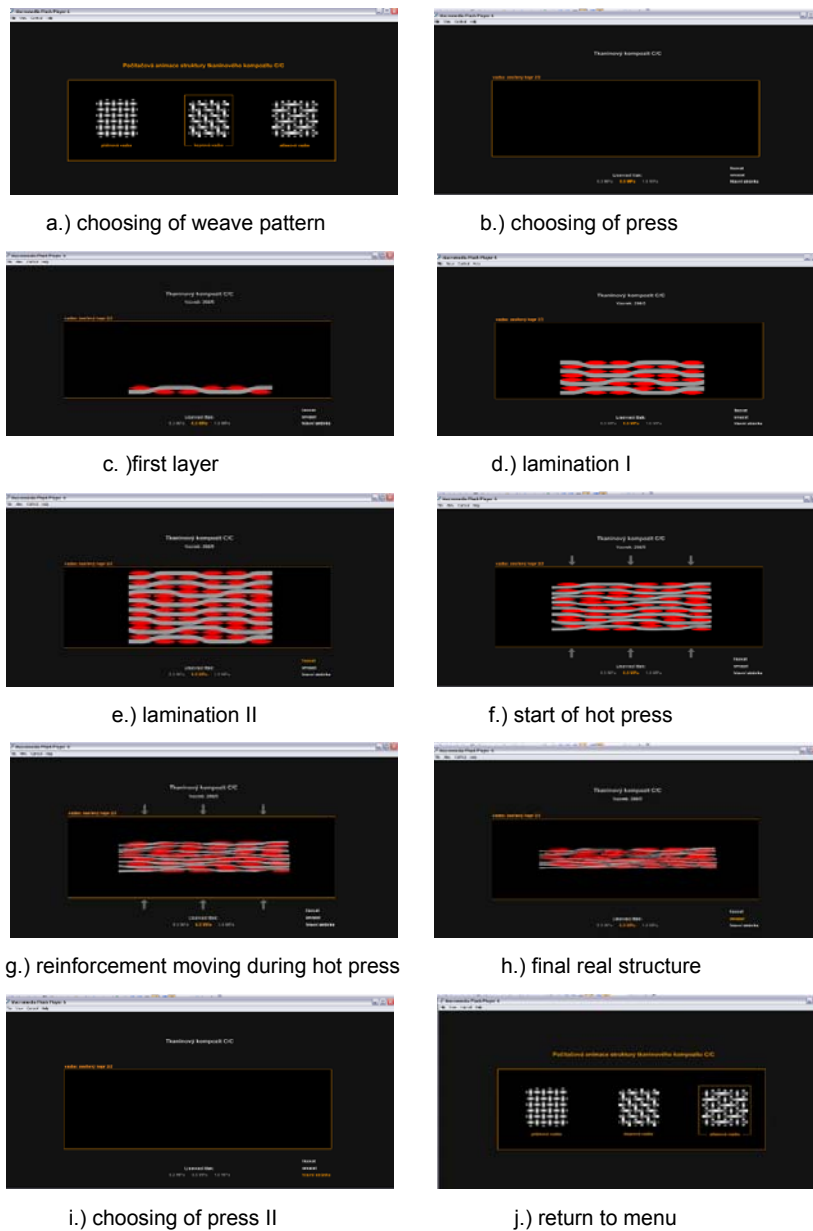


Figure 10. User's scene of animation in steps – a.) choosing of weave pattern, b.) choosing of press, c.) first layer, d.) lamination I., e.) lamination II., f.) start of hot press, g.) reinforcement moving during hot press, h.) final real structure, i.) choosing of press II, j.) return to menu

4. CONCLUSIONS

There was suggested a way for animation of internal structure of woven composites. Animation is the first step in artificial intelligence. Especially, this animation is usefull tool for e-learning and structure investigation.

Non-destructive tests and scanning on the confocal microscope are possibilities for improvement investigation in future.

ACKNOWLEDGEMENTS

This study was supported by the Czech Scientific Foundation within project No 106/03/H150 and by Ministry of Education, Youth and Physical Training VCT II – 1M4674788501.

REFERENCES

1. Hlaváč V.: Computer image processing <http://cmp.felk.cvut.cz>, FEL CVUT Praha, 2003
2. Salacova J.: GUI for voids segmentation, Technical computing Prague 2006, p. 87, ISBN 80-7080-616-8
3. Haškovec V., Mudrova M., Threshold Selection Methods in Edge Detection Applied to Biomedical Images, ISTCPC 2004, Kouty n. Desnou,
4. Salacova J.: Boolean operations and Bézier curves in woven composites, Bulgaria 2004
5. Salačová, J.: Digitalization of woven composite structures in software Femlab, ICCE 11, New Orleans, USA, 2004

MICROCLIMATE COOLING GARMENTS

Ö. KAYACAN, A. KURBAK

Dokuz Eylül University Engineering Faculty, Textile Engineering Department

ABSTRACT

Human beings are the creatures having stable core temperatures. Their metabolisms are capable of regulating their core temperatures in all environmental conditions. However when a person wears an insulation suit in a very hot environment such as in a cockpit, in a fire or when a person having a special illness like Multiple Sclerosis (MS), he/she needs to use a special garment to reduce the heat stress on his/her body. These garments are called microclimate cooling garments. In general, the principle of operations of these garments is to create a cool microclimate around the person, to facilitate to remove metabolic heat from the body and to block heat exchange between the wearer and the environment. There are basically three categories of these garments: Air cooling garments, liquid cooling garments and phase change cooling garments. All of these systems are effective in reducing heat strain.

In this study the types of microclimate cooling garments, their usage areas and their importance are discussed.

1. INTRODUCTION

Human beings are the creatures having stable core temperatures, which range from 36-38°C (37°C). They attempt to maintain their core temperatures efficiently between 35-40°C by the help of physiologic and behavioural mechanisms. Their bodies lose heat when the environmental temperatures are lower and gain heat when environmental temperatures are higher [1].

When the ambient temperature and the humidity are so high, the body stores excess heat, which rises the core temperature. The body loses this excess heat through conduction, convection, evaporation and radiation [1]. However when a person wears an insulation suit in a very hot environment such as in a cockpit, in a fire or when a person works in a very hot place like mines, his/her body must remove the heat stress, otherwise this heat stress can lead to heat related illnesses or death of the person. Also in some special illnesses like multiple sclerosis (MS) and hypohidrotic ectodermal dysplasia (HED) the heat stress causes the symptoms of diseases to increase [2, 3]. In order to remove this excess heat from the body, people have used special garments, called microclimate cooling garments. In general, the principle of operations of these garments is to create a cool microclimate around the person, to facilitate to remove metabolic heat from the body and to block heat exchange between the wearer and the environment. There are basically three categories of these garments: Air cooling garments, liquid cooling garments and phase change cooling garments.

All of these systems are effective in reducing heat strain. They reduce skin and core temperatures, heart rates and sweat rates of humans. By the help of the regulation of the physiologic characteristics of the body the duration or efficiency of the work increases, the hydration needs decreases, mental acuity and comfort improves [4].

In this study the types of microclimate cooling garments, their usage areas and their importance are discussed.

2. TYPES OF MICROCLIMATE COOLING GARMENTS

Cooling garments can be separated into passive and active systems. In passive system, ice or chemical based frozen packs and in active system air or water circulation devices are used in cooling garments (Figure 1) [5]. They can cool the trunk, head, neck and extremities of the body [6].

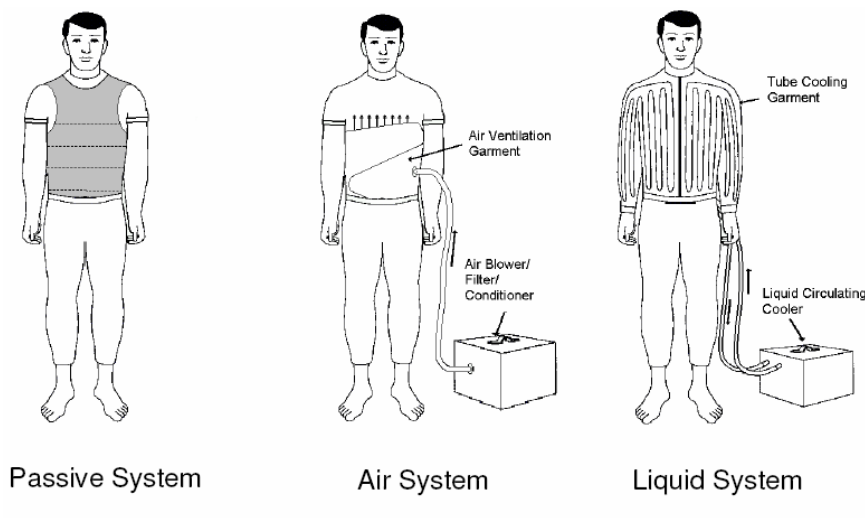


Figure 1. Types of cooling garments (trunk cooling) [7]

2.1 Active Systems

Active systems use an external heat sink to cool a fluid (air or water). The fluid is pumped through the clothing system to provide cooling of the body. The heat absorption of the cooling system may come from metabolism and from the environment. The heat sinks are based on different mechanisms. They can be portable or not [8].

2.1.1 Air Cooling Garments

Air cooling garments acts like an air conditioning system. A compressor forced the cool air to the suit and against the body through the small openings of the suit [6]. If circulating air systems have a good air flow and air distribution with low air temperatures, they should provide sufficient

protection. When the air temperature is lower, the convective cooling effect achieved the greater [9].

Air cooling is the most natural way of cooling, since heat is mainly extracted via natural sweat evaporation and enhanced convection. However, it is limited by dependence on amount of sweat production, low heat capacity of air and poorer control of the cooling rate [8].

These garments have got some advantages and disadvantages [6, 8, 9]:

1. Air cooling garments are lightweight clothes.
2. They are comfortable because of high evaporation and condensation.
3. They have low power consumption.
4. The hose connecting the system to the air source limits the area within which the worker can operate. Because, a compressor is connected to the garment, which restricts the wearer's movement.
5. The blower design is difficult.
6. It is difficult to cool the inlet air.
7. Pumping the air in a high velocity in hot environmental conditions can damage the skin surface of the wearer.
8. The air warms very quickly, when long air distribution hoses are used and cooling effect decreases.

2.1.2 Liquid Cooling Garments

Liquid cooling garments consists of a heat sink, a circulation pump and the suit with small tubings. The liquid is cooled in the heat sink automatically in the refrigeration system or by means of ice or dry ice (solid carbon dioxide). Then it is pumped through the tubings of the suit. The circulating fluid is usually water [9].

These garments are usually worn close to skin and heat is mainly removed by conduction and convection [8]. The cooling capacity of liquid cooling garments differs according to the environmental conditions, tubing length and type, liquid inlet temperature and flow rate, pattern flow etc. [10]. When the tubing length of the cooling garment increases, the liquid inlet temperature decreases or the flow rate of the garment increases, also the cooling capacity increases.

The advantages and disadvantages of these garments are given below [6, 8]:

1. They are sealed systems.
2. The water has high heat capacity then air. So they can cool the person effectively.
3. They are capable of cooling with high metabolic rates
4. They are heavy garments.
5. They have possibility to leak.

6. During the cooling, condensation could occur.
7. The garment limits the movements of the wearer.
8. They are expensive systems

2.1 Passive Systems

In passive systems ice, dry ice or other chemical based materials are used. When these material changes their phases, they absorb or generate heat energy. For example when ice changes its solid state to liquid state, it absorbs heat and produces cooling effect. When it goes back to the solid state, it generates heat and warming effect [11].

These garments are also called as phase change cooling garments and consist of large pockets. The frozen phase change material packs are inserted in these pockets [9]. When these materials melt, they cool the body of the wearer.

These garments need no energy. They are economic, but they provide short term of cooling [8]. When the phase changing material melts, the melted packs must replaced with the new frozen packs in order to continue cooling.

3. APPLICATION AREAS OF COOLING GARMENTS

The cooling garments are used especially in space, in military, in industry, in sports and medical field.

In space suits liquid cooling garments are used. These garments are used for the extravehicular activity, namely they are used outside the spaceship. These garments are long underwear like garments worn inside the space suit and can cool the body with liquid circulation (Figure 2).

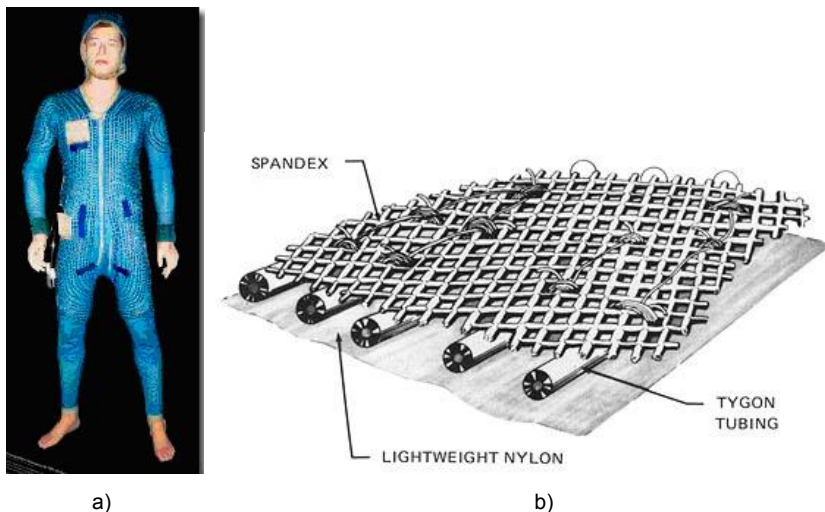


Figure 2. a) Liquid cooling garment, Russia 1985 [12] b) A liquid cooling garment construction for spacesuits [13]

In order to reduce the heat stress of soldiers the cooling garments are worn under armour materials, heavy chemical/biological protective suits and other protective clothing. [Figure 3 and Figure 4].



Figure 3. Liquid cooling vest for pilots (left), cooling garment connected to aircraft environmental system (right) [14]



Figure 4. Cooling with phase change cooling garments [15]

In industry, the cooling garments are used in mines, in protective clothes (for protection against hazardous materials, fire etc.) to increase the productivity of the wearer and to protect against the heat related illnesses and death (Figure 5 and Figure 6).



Figure 5. Ice cooling garments [9]



Figure 6. Cooling Cap [16]

In sports, the cooling garments are used for pre-cooling the athletes or used for cooling auto and motorcycle racers etc. Especially when the environment is very hot and humid, in order to enhance the performances of the athletes and to reduce the heat stress on their body, they use cooling garments prior to competition and during rest periods [6, 17].

Auto and motorcycle racers use these types of garments during the races in order to alleviate the heat stress on their body.

In medical field these cooling garments are used for doctors and for patients. Doctors use these cooling garments when they are working in warm environments. A patented air cooling system is used for cooling doctors (Figure 7) [18].

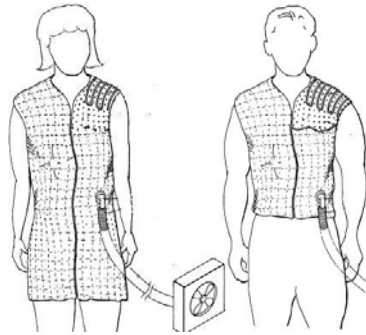


Figure 7. Air cooling garments for doctors [18]



Figure 8. "Mark I" surgical cooling system for medical staff [19]

The patients with MS and hypohidrotic ectodermal dysplasia also use cooling garments.

Multiple Sclerosis (MS) is the most commonly diagnosed neurological disorder. MS is characterized by a disruption of nerve impulses travelling from the brain or spinal cord to other parts of the body, along the nerves of the central nervous system (CNS). Damaged nerves are sensitive to changes in temperatures. A rise in temperature may cause a failure in the effective transmission of signals from the brain to the body and a reduction in temperature may allow more signals to be transmitted across the damaged nerve. In order to remove this heat from the body cooling garments can be used [20]. There are many kinds of commercially used cooling garments for MS patients.



Figure 9. “Mark VII” cooling system for patients (left) and an alternative cooling vest (right)[19]

Hypohidrotic ectodermal dysplasia (HED) occurs when the abnormal development of certain tissues derived from embryonic ectoderm (teeth, hair, nails and glands). The patients with HED have no sweat glands and low levels of perspiration. So they can suffer heat exhaustion, heatstroke, and even death by doing something as simple as going outside to work or for children play. People with this disorder must stay in a well-regulated environment [21, 22].

NASA and HED foundation designed a special protection suit for the children with HED in order to protect them against the UV rays (Figure 10). This cloth includes white jacket, pants, gloves, and headgear, including goggles. However this cloth provides full insulation to the patient and in this type of suit their body temperatures could increase much because they could not perspire. In order to avoid this, small phase change cooling garment is used underneath the suit. The cooling unit uses four gel packs in a vest-like garment, and supplies cooling for 2 to 4 hours before needing to be re-cooled in a refrigerator. This suit allows children with HED to go outside and play—something most children take for granted [21, 22].



Figure 10. Special protection suit for the children with HED

The cooling garments are also used in costumed characters. Phase change cooling systems are used in these costumes [15].



Figure 11. Cooltech cooling vests for costumed characters [15]

3. CONCLUSIONS

Thermal balance in body is very important for the people in all environmental conditions. In warm environments cooling garments are used for helping to regulate the thermal balance of the body. They play an important role in reducing heat stress of individuals by keeping their body temperature at safe levels. They are used by patients and by workers, who work in very hot conditions, such as fire-fighters, soldiers, astronauts, pesticide workers, etc.

REFERENCES

- 1 Keim, S.M., Guisto, J.A., Sullivan, J.B., Environmental Thermal Stress, Annals of Agricultural and Environmental Medicine (AAEM), 2002, 9, 1-15.
- 2 Roberts, A., Harper-Bennie, J.. MSAA Multiple sclerosis and cooling. 2004, www.msaa.com.
- 3 Nasa Explores, Suited up for Outdoors, 2002, www.NASAexplores.com

- 4 Gonzalez, R., Microclimate Cooling- A Hot Topic, DOJ / DHS Conference Technologies for Public Safety in Critical Incident Respons, 28. 10. 2004, www.nlectc.org/training/nij2004/gonzalez.pdf
- 5 Figura, S.Z., Cooling Off, Occupational Hazards, 1997, 5, 81-82.
- 6 Laing, R.M., Sleivert, G.G., Clothing, Textiles and Human Performance, Textile Progress, 2002, 32, 1-101.
- 7 Teal, W., Cadarette, B., Laprise, B., In-Theatre Cooling, The Science Behind the Warrior: Yesterday, Today and Tomorrow, 2007, chppm-www.apgea.army.mil/heat/MicroclimateCoolingOptions_May_2007.pdf.
- 8 Pu, Z., A Dynamic Model of the Human /Cooling System/Clothing/ Environment System, PhD Thesis, 2005, University of Central Florida.
- 9 Schutte, PC, de Klerk, C., Matesa J. (2002). Body Cooling Systems. CSIR Mining Technology Draft Final Report, Project No: 020702.
- 10 Nunneley, S.A., Water Cooled Garments: A Review. Space Life Sciences, 1970, 2, 335-360.
- 11 Shim, H., The Use of Phase Change Materials in Clothing, PhD Thesis, 1999, Kansas State University.
- 12 www.deutsches-museum.de/en/sammlungen/verkehr/astronautics/space-suits
- 13 history.nasa.gov/SP-368/s6ch6.htm
- 14 www.nasa.gov/centers/dryden/about/Organizations/LifeSupport/current1.html
- 15 www.deltathermal.com/products.htm
- 16 www.bodycooler.com/industry.htm
- 17 Webster, J., Holland, E.J., Sleivert, G., Laing, R.M., Niven, B.E., A Light-Weight Cooling Vest Enhances Performance of Athletes in The Heat, Ergonomics, Vol. 48, No. 7, 10 June 2005, 821 – 837
- 18 Weber, S., Air Cooling Garment for Medical Personnel, 1999, United States Patent No: 5,970,519.
- 19 New Help For MS Patients, NASA Spinoff, 1993, 52-56, <http://www.sti.nasa.gov/tto/>
- 20 Roberts, A., Harper-Bennie, J., Multiple Sclerosis and Cooling, Multiple Sclerosis Association of America (MSAA), 2004, www.msaa.com
- 21 9-12: Suited for Updoors (Student article), Nasa Explores, 2002, www.nasaexplores.com/show2_912a.php?id=02-064&gl=912
- 22 5-8: Suited for Updoors (Student article), Nasa Explores, 2002, www.nasaexplores.com/show2_5_8a.php?id=02-064&gl=58

DEVELOPMENT OF ZnO NANOPARTICLE DOPED COATINGS ON TEXTILES

Ö. ALTINTAŞ, C. DURUCAN

Department of Metallurgical and Materials Engineering, Middle East Technical University

ABSTRACT

In this study, preparation of UV-blocking coating for polyester-based fabrics has been described. The nanosized ZnO particles and binder were applied to fabrics via aqueous solution routes by dip coating. The microstructural and optical properties of the coated fabrics have been examined using SEM, XRD and UV-Vis measurements in order to relate UV absorption performance of the finished textile surface with microstructural and morphological modifications in ZnO containing coatings after successive detergent laundering steps.

Keywords: UV blocking, zinc oxide, protective clothing, technical textiles

1. INTRODUCTION

Zinc oxide (ZnO) has been widely used in many different technological areas such as varistor and gas sensor applications, as pigment and luminescent material industries as well as in pharmaceutical and cosmetics due to its unique electrical and optical properties [1]. Variety of synthesis methods including spray [2] and plasma [3] pyrolysis, chemical vapor deposition (CVD) [4], physical vapor deposition (PVD) [5], sol-gel [6], hydrothermal method [7], microemulsion [8,9] had been already employed in making various forms of ZnO from nanostructures to thin films and coating applications. Among these numerous possibilities microemulsion techniques are especially attractive as they do not require sophisticated equipment and rigorous experimental conditions, but still providing possibilities in controlling the size and morphology of the ZnO powders in a size scale approaching to nanometers.

Currently, we have been studying microemulsion systems to produce ZnO nanopowders in an effort parallel with the general context of our presented work, i.e. for UV-blocking textile applications. Results of microemulsion related work are not presented here. The growing of health and hygiene concerns in textile based consumer products brings in an increasing demand in development new materials for textile finishing with UV-blocking, antimicrobial and self-cleaning surface properties. Antimicrobial properties for example can be achieved by applying nano sized silver and self-cleaning and UV blocking properties are imparted by the use of TiO₂ nanostructures. ZnO nanoparticles have superior UV-blocking property in addition its antimicrobial and in some cases self-cleaning properties making a good candidate in technological textile industry comparable to above mentioned novel surface

finishes. [10-12]. In particular, nano-sized ZnO is more efficient at absorbing and scattering UV radiation than the conventional size due to increased surface area and intense absorption in the UV region. In the present study we have explored the potential use of previously synthesized ZnO nanoparticles in developing a durable UV-blocking coating on polyester-based fabrics.

2. EXPERIMENTAL PROCEDURES

2.1 Materials

ZnO nanoparticles with an average particle size of less than 100 nm, acetic acid (CH_3COOH , 99%) and ethanol were purchased from Merck. All reagents were used without further purification. The detergent used in laundering process was sodium bis(2-ethylhexyl) sulfosuccinate (Aerosol OT, $\text{C}_{20}\text{H}_{37}\text{NaO}_7\text{S}$, 96%, Merck).

2.2 Coating Process, Pre- and Post Treatments

The fabrics initially treated by immersing into ethanol for 10 minutes. Typically, 2x2 cm pieces were used. After ethanol treatment fabric samples were submerged into ethanol based coating solution containing ZnO (1 wt %) and 17.5 M acetic acid (1 wt %) as the acrylic binder for 20, 50 or 80 s. Afterwards coated fabrics were dried for 30 s at 60°C in a conventional oven and further cured for 3 min. at 140°C to polymerize the acetic acid. Additionally, some samples were exposed to subsequent coating steps for second and third times and multiple layer coatings were obtained according to same coating procedure. Simply, single layer and double layer coated samples were used as a starting substrate for double and triple layer coated fabrics, respectively. Coated samples were washed by two different ways. In one set, selected coated fabrics was washed at 50°C for 5 min. in 2.0 g/l of sodium bis(2-ethylhexyl) sulfosuccinate, an anionic detergent. Then the fabrics were rinsed using distilled water for 5 times to remove residual traces of detergent solution. The second set of fabrics was detergent washed for 15, 30 and 45 min. at 50°C. Some coated fabrics were not exposed to any washing process and kept in as-prepared condition. Additionally, all sets were reproduced using 160°C as new polymerization temperature.

3. CHARACTERIZATION

3.1 X-ray Diffraction (XRD)

X-ray diffraction analyses were performed using a RIGAKU D/Max-2000 PC diffractometer. The spectra were obtained using $\text{Cu-K}\alpha$ radiation ($\lambda=1.54 \text{ \AA}$). Diffraction measurements were performed in a 2θ of range $2\theta=10-80$. The scan rate was 2 degree/minute.

3.2 Scanning Electron Microscopy (SEM)

The general morphology of the ZnO coated fabrics were investigated by JEOL JSM-6400 model SEM. Prior to examination fabrics mounted on metal stubs were gold coated in a sputtering systems to avoid charging problem.

3.3 Energy Dispersive X-Ray Analysis (EDX)

In order to verify the chemical identity of the coated fabrics selected area EDX measurements were done on representative regions of the samples.

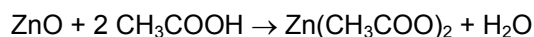
3.4 Optical Measurements

UV-absorption properties of the coated fabrics were evaluated by optical measurements. UV-vis spectra of the coated fabrics were obtained using a TOMOS UV1900 model spectrophotometer in transmittance mode in the region of 200-450 nm.

RESULTS AND DISCUSSION

The XRD pattern in Figure 1 shows the highly crystalline nature of the ZnO used in this study. The precursor ZnO was also phase pure and free of any impurities or contamination.

Figure 2 shows the XRD patterns of as-prepared and washed cotton fabrics with various number coating layer applications. Samples polymerized at 140°C and 160°C are both shown in Figure 2a and Figure 2b, respectively. All the patterns include broad and relatively low intensity peaks of the polyester fabric (in the 2θ range of 15-30 degrees) as well as the peaks from the crystalline ZnO embedded onto the fabrics. These diffraction peak positions are in very good agreement with the values of crystalline ZnO shown in Figure 1. Regardless of polymerization temperature the intensity of ZnO peaks increases with number of coatings applied. But as the retention of ZnO enhances with additional coatings, this also promotes formation of a new zinc-compound for the coated fabrics. Zinc acetate dihydrate forms regardless of the number of coatings for the samples polymerized at 140°C as well as 160°C. But, it should be noted that zinc acetate dehydrate formation according to:



was favored in multiple coatings due to prolonged interaction of ZnO precursor and acetic acid. Figure 2 also summarizes how laundering affects

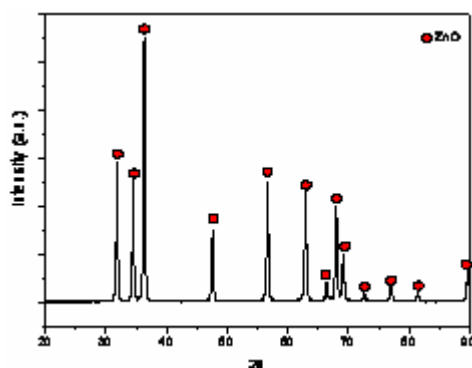


Figure 1. XRD pattern of the ZnO used in this study.

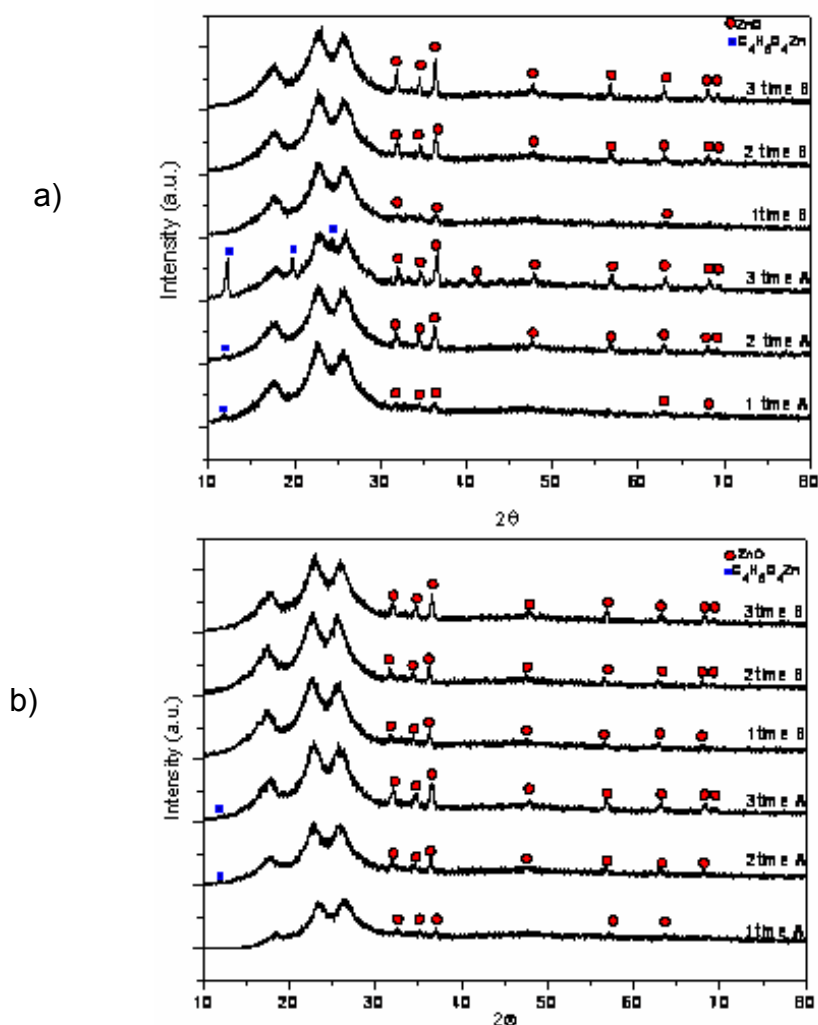


Figure 2. XRD patterns of single and multi layer ZnO coated fabrics after polymerization heat treatments at (a) 140°C and (b) 160°C. As-prepared samples are marked with "A" and detergent washed (5 min at 50°C) samples are marked with "B".

ZnO-doped coatings. First; detergent washing eliminates the zinc acetate dehydrate, as it is highly soluble in water. The second and more important point in regard to washing, as illustrated by these XRD results, is that laundering does not generate any adverse effect in terms of ZnO erosion from the coating at least after 5 min of washing at 50°C. These imply that ZnO powders firmly attach to fabrics with the use acrylic binder. In fact, the averaged amount of the Zn on the coated fabrics in as-prepared condition was at around 24-27 at% as determined by EDX analysis. After the

preliminary washing the amount of zinc decreased but not more than 1 at%, which is attributed to dissolution of zinc acetate dehydrate.

The formation of zinc acetate dehydrate in the coatings occurs due to kinetic reasons and formation in excess amount is induced when longer dip coating times are applied. As shown by the XRD patterns in Figure 3 a coatings period (i.e. immersion time in the coating solution) up to 80 s do not lead to additional ZnO deposition on the fabrics. The intensities of the characteristic ZnO peaks remain almost unchanged with increasing immersion time. Zinc acetate dehydrate precipitation on the other hand, occurs at a greater extent within the coating times studied. The strongest zinc acetate dehydrate peak at around $2\theta \approx 12^\circ$ is observable for the coatings obtained after 50 s of longer immersion times.

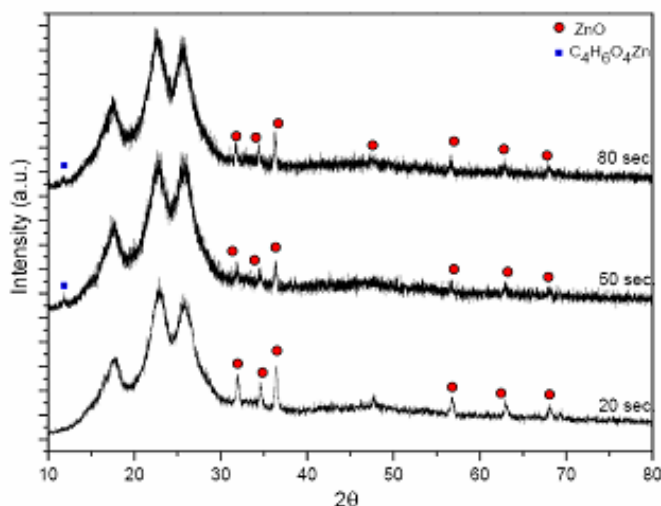


Figure 3. XRD patterns of single layer coated fabrics in as-prepared condition after immersing in ZnO coating solutions for 20, 50 and 80 seconds.

Acrylic agent in the coating formulation achieves binding of the ZnO to the fabrics to some degree and coating can still survive after a relatively mild washing process. But aggressive laundering for longer times removes ZnO from the surface as shown by the XRD data presented in Figure 4 as well as by SEM analyses shown in Figure 5. Figure 4 shows the XRD patterns of the coatings exposed to detergent washing at 50°C for different time periods: 5, 15, 30 and 45 minutes. These XRD data show that zinc acetate dihydrate completely dissolves within 5 min of washing and after 15 min ZnO also begins to leach out from the coating. After 45 min. of washing only a limited amount of the ZnO remains on the fabric. SEM micrographs and EDX results shown in Figure 5 are in agreement with these XRD results and also point out on how washing treatment changes the coating properties. Figure 5 shows the SEM micrographs and related EDX spectra of bare (in a), and a

three-time coated fabric before (in b) and after (in c) washing for 5 min. at 50°C in detergent, respectively. Figure 5 a represents pristine fiber surface. Figure 5b shows that the ZnO coating covers the fabric fibers in a uniform manner. In as-prepared condition coated fibers are enlarged in cross section by a couple microns and ZnO (and most probably zinc acetate dehydrate) crystals appearing are randomly embedded on the fibers. At some locations bridging of certain fibers with ZnO-acrylic coating material can be observed. The washed coated fabrics of Figure 5c exhibit remarkable differences in coating morphology and coverage with their partially degraded appearance indicating erosion of coating, which is accompanied with ZnO leach out. Same is also implied by the EDX spectra indicating relative decrease in the Zn radiations at approximately 1.1 keV and 8.7 keV after washing.

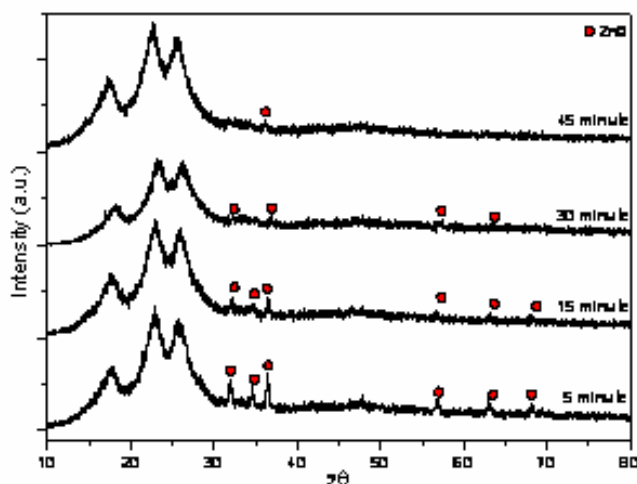


Figure 4. XRD patterns of ZnO coated fabrics after detergent washing at 50°C for various durations.

The effects of multiple coating applications and laundering on UV blocking efficiencies of the coated fabrics can be related to optical measurements shown in Figure 6. Figure 6a shows the UV absorption spectra of ZnO coated fabrics in as-prepared condition (polymerized at 140°C), where the overall absorption by the specimen increases with the multiple application of the coating. The effect of washing time on UV absorption can be seen in Figure 6b where longer washing leads to an absolute decrease in absorption.

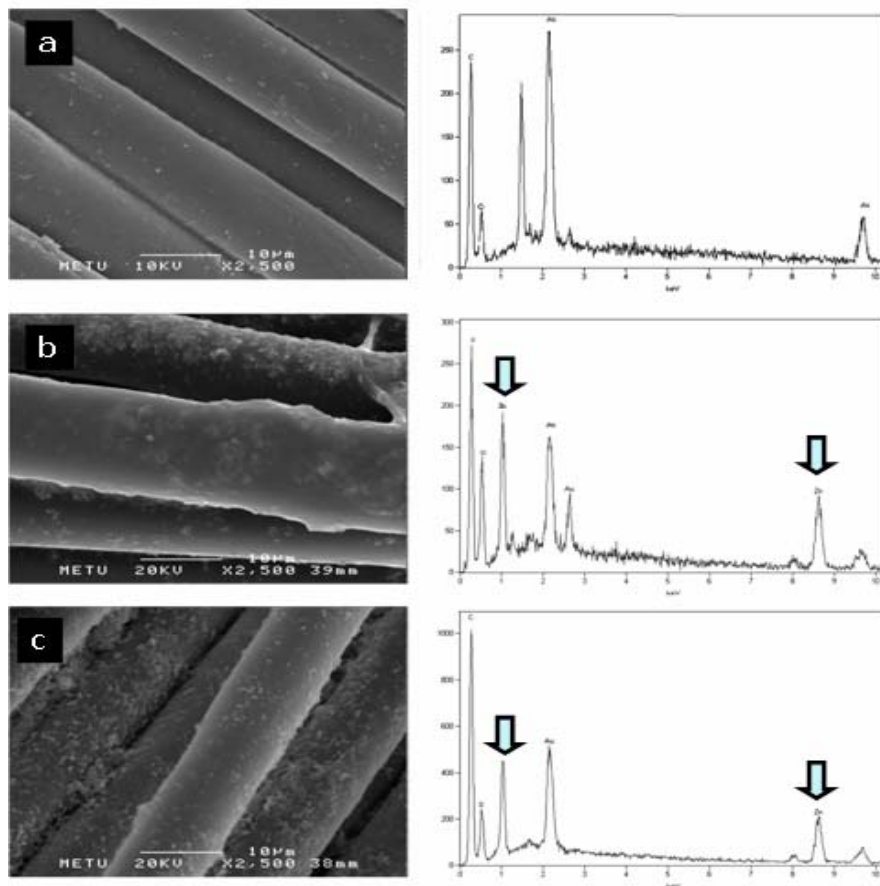


Figure 5. SEM micrographs and related EDX spectra for (a) bare fabric (uncoated) and three-time coated fabric (b) before and (c) after 5 min. detergent washes at 50°C. Arrows indicate the change in the relative intensity change for zinc radiation.

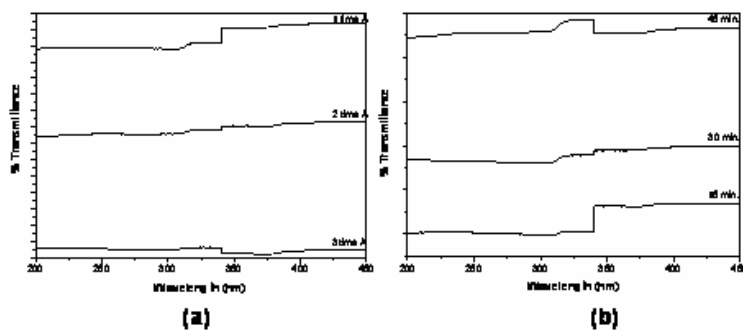


Figure 6. UV-visible transmission spectra of coated fabrics polymerized at 140°C (a) effect of subsequent coating applications, (b) effect of washing time for single layer coated fabrics.

4. CONCLUSIONS

A simple procedure has been developed to prepare ZnO nanoparticle embedded coatings on polyester based fabrics using a dip coating method. It was confirmed that ZnO coated textiles possess the UV blocking property strengthening when multiple coating is applied. But there are limiting factors for applying subsequent coatings as well as in the coating formulation. The coating formulation contains acetic acid as the binding agent. This binder actually works well and the nature of attachment is not just physical adsorption as ZnO does not come off from the fabric during mild washings. Additionally, multiple coatings and prolonged immersion results in an increase in the amount of ZnO in the coating but these also promote formation of water soluble zinc binding compound-zinc acetate dehydrate. This eventually reduces the effective Zn incorporation to the fabrics in the form of ZnO. Similar results should be expected by increasing the binder content in the initial formulation to improve the coating attachment, as this would also promote more formation of water soluble zinc compound. Therefore there is not much freedom in adjusting the coating formulation by increasing the binder amount. Formation of zinc-acetate dehydrate can be more effectively avoided in single layer coatings or by shortening the immersion time.

ACKNOWLEDGEMENTS

The authors acknowledge the financial support through ODTU-OYP Program.

REFERENCES

1. M. Jitianu, Dan V. Goia, J. Colloid Interface Sci. (2007) 309.
2. J. De Merchant, M. Cocivera, Chem. Mater. 7 (1995) 1742.
3. X.H. Zhang, S.Y. Xie, Z.Y. Jiang, X. Zhang, Z.Q. Tian, Z.X. Xie, R.B. Huang, L.S. Zheng, J. Phys. Chem. 107 (2003) 10114.
4. A.P. Roth, D.F. Williams, J. Appl. Phys. 52 (1981) 6685.
5. H. Kim, W. Sigmund, J. Nanosci. Nanotechnol. 4 (2004) 275.
6. H. Van der Rul, D. Mondelaers, M.K. Van Bael, J. Mullens, J. Sol-Gel Sci. Technol. 39 (2006) 41.
7. C.H. Lu, C.H. Yeh, Ceram. Int. 26 (2000) 351.
8. R. Moleski, E. Leontidis, F. Krumeich, J. Colloid Interface Sci. (2006)246.
9. M. Singbal, V. Cbbabra, P. Kang and D.O. Shah, Pergamon, (1996) 239.
10. A. Tokeer, S. Vaidya, N. Sarkar, S. Ghosh, A.K.Ganguli, Nanotechnology (2006) 17.
11. N. Vigneshwaran, S. Kumar, A A Kathe, P V Varadarajan, V. Prasad, Nanotechnology 17 (2006).
12. M.H. Zohdy, H. Abdel Kareem, A. M .El-Naggar,M. S. Hassan, J. Appl. Polym. Sci.89 2604 (2003)

ANTIBACTERIAL PROTECTION FOR POLYPROPYLENE

R.DASTJERDI, A.M.SHOSHTARI, M.R.M.MOJTAHEDI, A.KHOSROSHAHI

Textile Engineering Department, Amirkabir University of Technology

ABSTRACT

In this research, investigating the possibility of producing, processing and also characterization of bioactive polypropylene fiber has been presented. For this purpose PP powder and inorganic nanocomposite filler were mixed, modified granule was prepared and continuous filament yarns were produced by a pilot plant melt spinning machine. Samples were drawn, textured and finally weft knitted. Physical and structural properties (e.g. linear density, tenacity, breaking elongation, initial modulus, rupture work, density based crystallinity) of as-spun yarns were investigated. Finally antibacterial efficiency of weft knitted samples was evaluated according to AATCC100.

Key Words: Antibacterial, Melt spinning, Silver/TiO₂, Organic/Inorganic, Nanocomposite

1. INTRODUCTION

A wide class of micro-organisms coexists in a natural equilibrium with human body and living environments, but a rapid and uncontrolled multiplication of microbes can seriously lead to three unpleasant effects. The first is the degradation phenomena as coloring, discoloration and deterioration of fibers. The second one is producing of unpleasant odor and the third, which is the most important effect, is increasing of potential health risks [1, 2].

The conventional fibers and polymers not only do not show any resistance against micro-organisms and resulting effects of their metabolism but also they are most common materials for accumulation and proliferation of micro-organisms into the surrounding environments. In fact, several factors such as suitable temperature and humidity, presence of dust, soil, spilled food and drinks stains, the skin dead cells, sweat and oil secretions of skin gland, also finishing materials on the textile surfaces can make textile as an optimal enrichment culture for a rapid multiplication of micro-organisms [2].

Polypropylene fiber is one of the most widely used synthetic fibers in textile industry specifically for its various application fields. In fact, some advantages of this fiber type including cheapness, lightness, high chemical strength and high absorbency has made it suitable for many demands, such as carpets, automotive interior trim, films, packaging, cover stock, cables, napkins, wipes and so on. In particular, it is used for sanitary applications such as surgical masks, diapers, filters, hygienic bands, etc which need to display antibacterial effects [3].

Silver is one of the safer antibacterial agents in comparison with some possible organic antibacterial agents that have been avoided because of the risk of their harmful effects to the human body. Silver has been described as being 'oligodynamic' because of its ability to exert a bactericidal effect on products containing silver, principally due to its antimicrobial activities and low toxicity to human cells [4, 5]. Its therapeutic property has been proven against a broad range of micro-organisms (over 650 disease-causing organisms in the body) even at low concentrations [6, 7]. Silver nanoparticles are a non-toxic and non-tolerant disinfectant [8]. Using silver nanoparticles leads to increasing the number of particles per unit area and thus antibacterial effects can be maximized [3].

TiO_2 nanoparticles have unique properties (e.g. stable, long lasting, safe and broad-spectrum antibiosis). TiO_2 nanoparticles containing Ag^+ can be widely used as filler in the manufacture of antibacterial plastics, coatings, functional fibers, dishware and medical facilities, because Ag^+ has a strong antibacterial activity against many kinds of bacterial [6].

In this research, possibility of producing and processing nanocomposite polypropylene filament yarns has been investigated [9]. In fact, this research has been started from the modification of polymer powder as a by-product of petrochemical companies. Then the ability of accepting process have been investigated till the production stage of the fabric. Finally, some physical properties of as-spun yarns and the microbiological efficiency of the produced fabric have been further studied.

2. EXPERIMENTAL

2.1 Materials

Isotactic polypropylene powder, supplied by Navidzarchimie petrochemical company, Iran, was used as a polymer matrix.

The filler, Nanocid P101, kindly provided by Pars Nano Nasb Research departman of Iran Nasb Niroo co, Iran, is a nanocomposite of anatase TiO_2 as the career core coated with 1 wt% of Nano-Silver particles.

2.2 Method

The bacteriostatic filament yarn has been realized in two stages:

- In the first stage, Polypropylene (iPP) powder and the silver nanocomposite were premixed and melt blended in a co-rotating-screw extruder (Brabender, Germany). Pure PP granule and nanocomposite granules were prepared. The melt flow indexes (MFI)s of the pure and modified granules have been recorded in table 1.

Table 1. MFI of the pure and modified granules.

Sample	Melt flow index(gr/10min)
prepared granule of pure pp	24.80
Prepared modified granule	22.10

In the second stage pure pp fiber and the composite fiber containing nano-filler were prepared by an Automatik pilot plant spinning machine(Germany). This machine has an extruder with two spinning nozzles. Two 36 holes spinnerets of 0.25mm hole diameter were used for spinning partially oriented filament yarns at the take up speeds of 2000 m.min⁻¹. Then as-spun samples were drawn (to gain the constant breaking elongation of 50% for having a suitable further texturing process), textured by means of a Scragg-Shirley minibulk false-twist texturing machine and finally weft knitted.

2.3 Test Methods

- Density-based crystallinity (structural analysis)

Density of nanocomposite yarns (ρ_t) has been measured according to ASTM D792 using mixture of distilled water and ethanol.

First, the density of matrix ρ_{pp} was calculated from equation 1 [10].

$$1/\rho_t = w_f / \rho_f + w_{pp} / \rho_{pp} \quad (1)$$

Where ρ_f is the density of nanocomposite filler, w_f and w_{pp} are weight fractions of nanocomposite filler and PP, respectively.

$\rho_f = 3.86 \text{ gr/m}^3$ was obtained from substituting $\rho_{silver} = 10.5 \text{ gr/m}^3$ and $\rho_{tio_2} = 3.84 \text{ gr/m}^3$ in equation 2 [11].

$$1/\rho_f = w_{silver} / \rho_{silver} + w_{tio_2} / \rho_{tio_2} \quad (2)$$

Finally density-based crystallinity (x_c) was calculated from equation (3).

$$X_c = \left(\frac{\rho_{pp} - \rho_a}{\rho_c - \rho_a} \right) \frac{\rho_c}{\rho_{pp}} \quad (3)$$

Where $\rho_a = 0.8576 \text{ gr/m}^3$ and $\rho_c = 0.9363 \text{ gr/m}^3$ are the density of amorphous and crystalline areas respectively [12].

- Rheological measurements

Melt-flow index was recorded as the mass (grams) of molten polymer passing through a fixed capillary under the constant pressure (2.16 kg) at 230°C for 10 min (according to ASTM D1238).

- Linear density

The linear density of yarns was determined as an average of 5 measurements of the weight of 100 m of yarns.

- Evaluation of Antibacterial efficiency

Antibacterial efficiency was expressed according to AATCC 100 that is formulated as:

$$\text{Antibacterial efficiency} = A-B/A * 100 \quad (4)$$

Where A is the number of bacteria recovered from the inoculated test specimen swatches in the jar after 24 hours incubation with unmodified fiber and B is the number of bacteria according to "A" conditions, but with antibacterial modified fiber.

-Tensile properties

Tensile properties were evaluated by an EMT 3050 tensile tester (Iran). The conditions of measurements were as follows: gage length of 100 mm for as-spun yarns, and 300 mm for drawn yarns, and deformation rate of 500 mm.min⁻¹ (according to ASTM (D3822-95a)). Average values obtained from measurements of 10 samples.

3. Results and Discussion

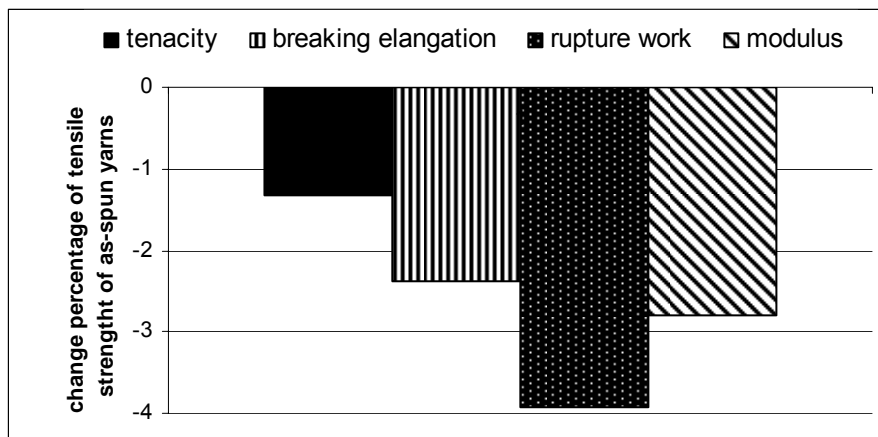
Crystallinity of fibers is noted in table 2. As shown, adding the antimicrobial agent resulted in the reduction of crystallinity(3%). The reduction of crystallinity is caused by the silver nanocomposites interfering with crystallization process of polypropylene. In fact, there are several factors that affect the crystallinity, some of them decreased crystallinity, while others can increase and compensate the change in crystallinity. First, silver nano particles have a high thermal conductivity comparing to polypropylene as a non-polar polymeric matrix. Therefore, these particles can accelerate quenching rate of nanocomposite fiber. This acceleration results in the fast passing of the temperature in which maximum velocity of crystallization growth can take place. Consequently, the polymeric matrix opportunity for PP crystal growth is limited.

Table 2. Crystallinity, shrinkage and linear density of samples

sample type property	pure	modified
Crystallinity(%)	48.96	45.96
shrinkage	2.95	3.28
linear density (Tex)	14.38	13.91

Second, the silver may sometimes be a function of nuclear agent (because nanoparticles acts as a type of impurities in the PP matrix) which can cause a higher temperature for maximum velocity of crystallization growth. Fast passing this point can reduces crystallization growth. These effects could cause such the reduction of crystallinity. On the other hand, nucleation effect during the crystallization process of PP accelerates crystallization of PP matrix. Due to these contradictory effects or because of low concentration of active filler, the crystallinity of as-spun PP fibers including nanoparticles had a slight decrease with increasing silver content.

The reduction of mechanical properties of as-spun fibers was not substantial (see figure 1).

**Figure 1.** The change percentage of tensile strength of samples compared to the pure PP.

The antibacterial activity of silver/TiO₂ composite in fabric was evaluated after the specified contact time and calculated by reduction percent of *Staphylococcus aureus* ATCC25923. The *Staphylococcus aureus* is a pathogenic microorganism that causes many diseases (e.g. toxic shock, purulence, abscess, fibrin coagulation, endocarditis). Moreover it is resistance

to common antimicrobial agents [1,13]. Almost all tests for evaluation of textile antibacterial effectiveness have proposed testing this bacterium. Also it has been deduced that antibacterial efficiency of silver composite against *Kleb.pneum* and *Escherichia coli* is higher than *Staphylococcus aureus* [14]. Thus the *Staphylococcus aureus* was selected for evaluation of antibacterial efficiency in this research. Table 3 confirms that the modified fabrics showed a high percentage of biostatic efficiency (more than 99%).

Table 3. Antibacterial efficiency of produced fabric

Sample type	number of bacteria in 1ml $\times 10^{-3}$	percentage of biostatic efficiency
pure	11200	0
modified	4.89	99.97
pure	11200	0
modified	4.89	99.97

-Number of bacteria at the beginning in 1ml of solution recovered from the inoculated fabric was estimated 1980.

4. CONCLUSIONS

This research has been started from the modification of polymer powder as a common by-product of petrochemical companies. The processability of these starting materials samples (fiber to fabric) has been investigated. Finally, some Physical properties of as-spun yarns and the microbiological efficiency of the produced fabric have been further studied.

The experimental results revealed that pure and modified PP samples showed good spinnability at the take-up speed of 2000 m/min by a pilot plant melt spinning process. It was observed that the biostatic efficacy of nanocomposite fibers was excellent. However any bactericide efficiency was not observed.

The crystallinity of fiber containing silver was slightly decreased compared to the pure PP fiber. The tensile properties changes of modified yarns compared to the pure PP yarns were not significant.

ACKNOWLEDGMENTS

The authors would like to thank to Dr. Goudarzi and Moayyed at the Shaheed Beheshti University of Medical Sciences & Health Services (Microbiological group), the Iran Nasb Niroo co and the Iranian Nanotechnology Initiative.

REFERENCES

1. J.V.Edwards and T.Vigo (2001), .Bioactive fibers & polymers. American Chemical Society, Washington DC.

2. http://www.montefiber.it/en/polyester/pdf/sani_conoo.pdf(G.salvio, A new polyester fiber with antimicrobial activity).
3. S. Y. Yeo, S. H. Jeong and S. H. Jeong (2003), "preparation of nanocomposite fibers for Permanent antibacterial effect "Journal of Materials Science, 83, P2143-2147.
4. S.L.Percival, P.g.Bowler and D.Russell (2005), "Bacterial resistance to silver in wound care" Journal of Hospital Infection, 60, P1-7.
5. T.Wright (2002), "AlphaSan :a thermally stable silver-based inorganic, antimicrobial technology" Chemical Fiber International, 25(2) P125.
6. Q.Cheng, C.Li.Pavlinek, P. Saha, H. wang (2005), "Surface-modified antibacterial tio2/Ag nanoparticles : preparation and properties," Applied Surface Science, APSUSC-12989, P7.
7. S.H.Jeong, S.Y.Yeo, S.C.Yi (2005), The effect of filler particle size on the antibacterial properties of compounded polymer/silver fibers," J. of Materials Science 40, P5407-5411.
8. S.H.Jeong, Y.H.Hwang, S.C.Yi (2005), "Antibacterial properties of padded PP/PE nonwovens incorporating nano-sized silver colloids," J. of Materials Science 40, P5413-5418.
9. R.Dastjerdi (2006), "Investigating the production and some properties of antimicrobial polypropylene filament yarn," a thesis submitted for the degree of master of science, Amirkabir University of Technology, Textile Engineering Department.
10. .B.Gupta and Y.C.Bhuvanesh (1996), " Processability and properties of yarns made from polypropylene contaning small amounts of polystyrene," Journal of Applied Polymer Science, 60, P1951-1963.
11. 11. CRC Handbook of chemistry and physics 52nd, Edtion, P:1971-1972 PB-134 and B149.
12. L. Mandelkem and R. G. Alamo (1996), "Physical properties of polymers ", Air press, Woodbury, New York.
13. M.Montazer, M. G. Afjeh, (2007) "Simultaneous X-Linking and antimicrobial finishing of cotton fabric" Journal of Applied Polymer Science, Vol. 103, P178–185
14. A.Marcincin, A.Ujhelyiova, J.Legen, V.Kabatova and P.Jambrich" (1997) "Bioactive polypropylene fibres" Vlakana-a-textil. 4(2), P38-43

ANALYZING THE AFFECTED FORCES ON FIBER DISPERSION FOR PRODUCING WET-LAID NONWOVENS

S. FATHI¹, Z. MANSOORI², M. LATIFI¹

¹Department of Textile Engineering, Amir Kabir University of Technology

²Energy Research Faculty, Amir Kabir University of Technology

ABSTRACT

Dispersion and separation of fiber bundles requires exposing them to a shear stress field to overcome interfiber frictional forces. To this end, fiber-mixing tanks are used to enhance shear and agitation in the water to help disperse the fiber bundles. The time and agitation required to separate and disperse the fibers depends on the fibers being used. It is well known, however, that excessive agitation will give rise to the formation of rope defects in the output because of the high-energy vortices that form. Optimizing the break up time important in the wet-lay process. In this study the affected forces on fiber dispersion in water were analyzed by using a one-way modelling of fiber behaviours in mixing stirred tank. The reciprocal effects between fibers and fluid were neglected.

Keywords: Wet-laid nonwoven, mixing tank, fluid drag force

1. INTRODUCTION

The wet-lay process involves the suspension of fibers in water. A wet-laid nonwoven is formed by depositing this solution onto a forming surface and subsequently bonding the fibers to form a fabric [2]. Most fibers are in the form of separable clumps (fig.1) and need to be separated into individual fibers in the mixing tank through the shear exerted on them by the flow field. To yield a uniform web and a satisfactory fabric, the fibers must be well dispersed in water. If they are not separated sufficiently, they may stay attached and appear as thick spots, referred to as log defects. Logs (or sticks) are bundles of fibers that have failed to disperse in the mixing tank; in most cases, the cut ends remain aligned. Logs usually appear in the fabric because of under-agitation during the initial dispersion [3]. An analytical study accompanied by experimental observation by Shiffler [1] showed that the break-up rate of logs increases with increasing shear rate (speed of the stirrer). On the other hand, the interaction of vortices with individualized (dispersed) fibers may wrap them around one another and form a new twisted bundle, referred to as a rope[5].

Ropes are fiber assemblies twisted over and around one another with unaligned ends. They form when fibers encounter a vortex that is about the size of the fiber [1]. Under such conditions, fibers are twisted into a string. Rope formation is a major concern, especially when fibers with varying degrees of stiffness are mixed. In this case, the more flexible fibers will twist and wrap around the stiffer fibers. Shiffler observed rope formation in a pilot mixing tank with a central vortex about ten times stronger than that in a nonvortex regime [4].

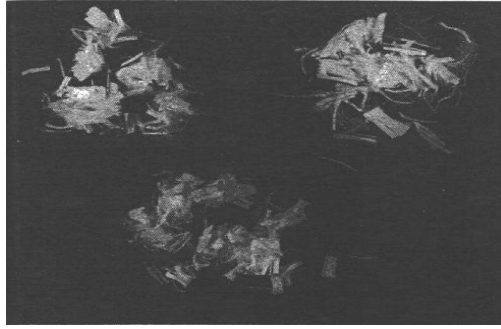


Figure 1. Initial appearance of water-dispersible fibers [1]

As mentioned above, because a normal consequence of synthetic fiber manufacture, the individual fibers come in separable clumps or logs, which are the vestigial remains of the original spinning cell. It is the task of dispersion system to separate each fiber from the parent bundle, or log, using only the fluid shear field. This shear force is resisted by surface tension, friction, and fiber fusion forces (fig. 2) [1].

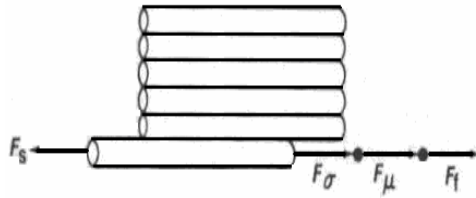


Figure 2. Force balance for a fiber in the shear field[1].

For dispersion to occur, the following inequality must be satisfied:

$$\mathbf{F}_s > \mathbf{F}_\sigma + \mathbf{F}_\mu + \mathbf{F}_f \quad (1)$$

Where

F_s = shear force

F_{σ} = surface tension force

F_{μ} = friction force

F_f = force from polymer fusion or incipient fusion.

This means bundles that do not satisfy this inequality can never be dispersed in the shear field specified by F_s . Thus it might be expected any defect count to have one component that is mixing time dependent and one that is not. The energy required to disperse the fibers depicted in Fig. 2 can be approximated by the work against surface tension and friction forces. Shiffler ignored fusion force in his study because the fusion forces are either

irrelevant because they are greater than shear force and the fibers never disperse, or they are include in the coefficient of friction. Shiffler calculated the dispersing energy as follow:

$$\Delta E_f = \pi \sigma D L + \sigma \mu L^2 \quad (2)$$

Where

Delta Ef = energy to disperse a single fiber, joules/fiber

D = fiber diameter, mm

Sigma = surface tension, dynes/mm

L = cut length, mm

Mu = coefficient of friction.

In this study we trend to analyze and determine the amount of each force effect on fiber dispersion. Therefore the dispersion energy was analyzed properly. For this a two phase solid-liquid flow in a stirred mixing tank simulated with one way modeling. In this model the inter action between solid and liquid particles were ignored. Fiber trajectories were calculated by integrating the fiber motion equation and the trajectory equation. The fiber motion equation is as below:

$$\begin{aligned} \frac{du_{p,i}}{dt} = \frac{18\mu}{\rho_p d_p^2} \frac{C_D Re_p}{24} (u_i - u_{p,i}) - \frac{1}{\rho} \frac{\partial p}{\partial x} + \\ C_{am} \frac{\rho}{\rho_p} \frac{d}{dt} (u_i - u_{p,i}) + \left(1 - \frac{\rho}{\rho_p} \right) g + F_t \end{aligned} \quad (3)$$

Where

u_i, μ, ρ, p Are fluid velocity, viscosity, density and pressure and $u_{p,i}, d_p, \rho_p$ fiber velocity, diameter and density respectively. C_D, C_{am} Are drag coefficient and virtual mass force coefficient. F_t Is the complex of surface tension, friction and fusion forces. According to using a two dimensional modeling the virtual mass, buoyant and lift force were neglected.

2. RESULT AND DISCUSSION

For studying the effects of affected forces on fiber dispersion in a stirred mixing tank, two spheres in contact each other were simulated as two adjacent fibers in a fiber clumps. The position of simulated fibers was in the $r/R=0.5$ in the stirred mixing tank. According to Mayan tyagi study [6], radial velocity of fluid in this position with the tank geometry mentioned before is 0.06, tangential velocity of fluid is 0.54 m/s and axial velocity will be equal to -0.15 m/s. these data were used as initial data in model. Other data used in this

model were diameter, density and length of polyester and polypropylene fibers. At first the effect of drag force, surface tension and friction force on separation of polyester fibers in form of individual fibers from fiber clumps analyzed.

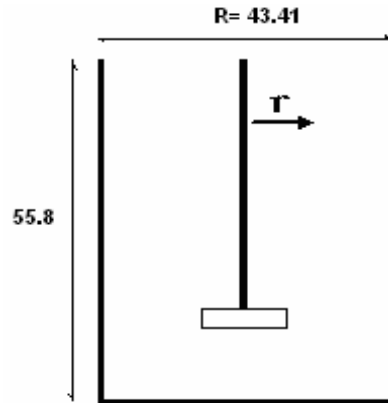


Figure 3. Schematic diagram of stirred mixing tank used in model

Displacement of fibers in a determined time was investigated. This time was determined base on the longest time observed in real dispersing time that was done before. This time for polyester fibers increased with increasing fiber diameter. The diagrams of fiber diameter- displacement curvatures of polyester fibers (tangential and radial displacement) in different cases are shown in figures 4 and 5. the cases comprising that when the force act on fiber bundles was or were just drag force, drag and friction force, drag, friction and surface tension forces. As shown in figures, with increasing in fiber diameter, the amount of fiber displacement in mixing fluid decreased. And also the effect of surface tension force that withstand to the shear force of fiber break up is greater than friction force. Figures 4 and 5 imply on the low effect of friction force comparing to drag force.

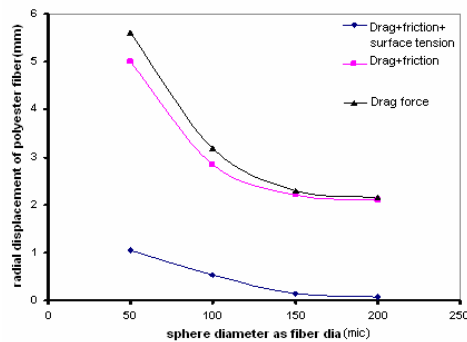


Figure 4. the effect forces on fiber radial displacement

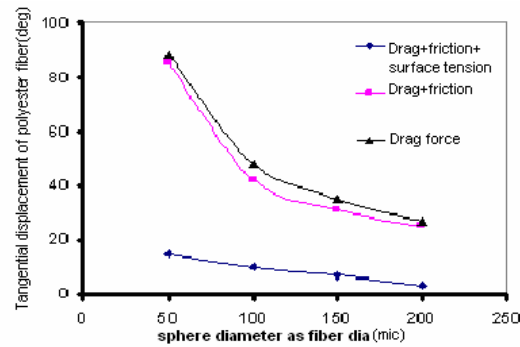


Figure 5. the effect forces on fiber tangential displacement

In second stage polyester fibers replaced with polypropylene fibers. Similar to polyester fibers by using the initial data and solving the equation 3, fiber diameter-fiber displacement diagrams for different diameter of polypropylene fibers were drawn in figures 6 and 7.

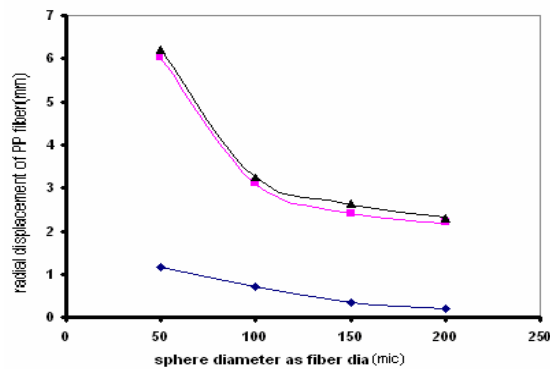


Figure 6. the effect forces on PP fiber radial displacement

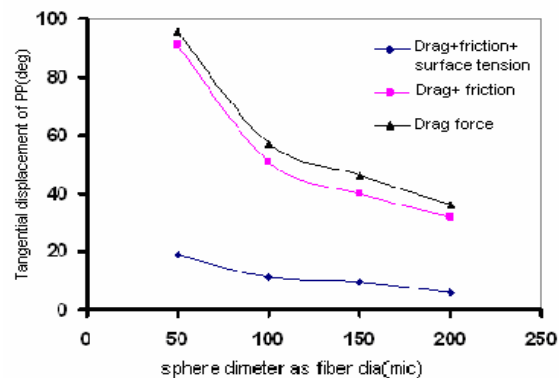


Figure. 7. Figure 6 the effect forces on PP fiber displacement

In spite of the fact that poly propylene fiber bundles break up in shorter time, their behaviour in fiber dispersing process is completely similar to polyester fibers. For analyzing the type of fibers on dispersing time of the fiber clumps, the equation 3 were solved according to polyester and polypropylene types with different type. The results are shown in figure 8. It evident that with increasing in fiber diameter the breaking up time increased and the time required to separate fibers from each other in polyester fibers is less than polypropylene fibers.

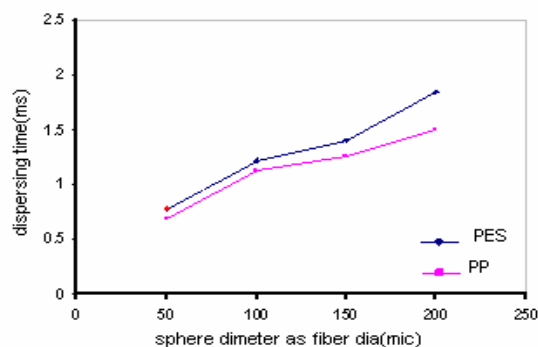


Figure 8. Effect fiber types on dispersing time

3. CONCLUSION

The theoretical studies have done on fiber dispersing time show that with increasing in fiber diameter, the time requiring for break up of fiber bundles and clumps are increased. Thus in dispersing stage of a wet-laid nonwoven, the role of fiber diameter and size of fibers are essential. This is completely obvious from the shiffler's studies [1]. In this study the effect of fiber type on the amount of fiber break up and dispersing time also analyzed. As shown in figures type of fiber have a great effect on fiber dispersion and with increasing fiber density.

REFERENCES

1. D.A. Shiffler, "Characterizing the Dispersion Kinetics of Synthetic Fibers in Water", TAPPI Journal, p88-91, Aug.1985
2. Jayachandran, "Fundamentals of Fiber Dispersion in Water", Msc thesis, NCSU, Aug.2001
3. J. M. Nouri and J. H. Whitelaw, "Particle Velocity Characteristics of Dilute to Moderately Dense Suspension Flows in Stirred Reactors", Int. J. Multiphase Flow, vol.18, No.1, pp. 21-33, 1992
4. H. Vahedi Tafreshi and B. Pourdeyhimi, "Role of Baffles on Flow Field Inside Wet-Lay Mixing Tanks and Potential Influence on Fiber Dispersion", Textile Research Journal, vol.73, no.7, pp. 575-582, July. 2003
5. Joonee Henrasakti, "A Study of Micro Fiber Dispersion using Digital Image Analysis", PhD Thesis, Texas A&M University, Aug.2003
6. Mayank Tyagi, Somanth Roy, "Simulation of laminar and turbulent impeller stirred tanks using immersed boundary method", chemical engineering science, vol.62, pp.1351-1363, 2007

PERFORMANCE OF DIFFERENT ANTIMICROBIAL FINISHING ADDITIVES ON 100% COTTON FABRICS

S. PALAMUTÇU¹, M.ŞENGÜL², N.DEVRENT¹, R.KESKİN¹,
B.HASÇELİK¹, Y.İKİZ¹

¹Textile Engineering Department of Pamukkale University

² Microbiology Department of Medical College, Pamukkale University,

ABSTRACT

In this work silver, triclosan, dichloro phenol, quarternary amonyum and chitosan based six different antimicrobial additives have been used for the antimicrobial treatment of 100% cotton woven fabric. Antimicrobial bioactivity of the treated and washed fabric specimens in vitro was tested for different groups of bacteria and a fungus (Staphylococcus aureus, Escherichia coli, and Candida albicans). The results of the experiment showed that the antimicrobial-treated woven fabric expressed a wide range of antimicrobial activity versus the three different microorganisms. The influence of the antimicrobial treatments on the tensile and tear strengths, tensile and tear elongations, wrinkle recovery angle, color change and sweat fastness of the specimens are examined. Fabric performance properties of the specimens are found to be affected at various levels by the antimicrobial treatments and washing cycles. It has seen that efficiency of each antimicrobial agent differs from each other and changes depending on the number of washing cycles.

Key Words: Antimicrobial textiles, cotton fabric, chitosan

1. INTRODUCTION

Cellulose fibers are most abundantly used as textile fibers, and their share of the textile market is almost 50%. As result of technological improvements, consumer demands, medical requirements and increased hygiene awareness of the population, antimicrobial textile product demand has been increased. Humid and warm environment still aggravate the problem. Infestation by microbes cause cross infection by pathogens and development odor where the fabric is worn next to skin. In addition, the staining and loss of the performance properties of textile substrates are the results of microbial attack. Basically, with a view to protect the wearer and the textile substrate itself antimicrobial finish is applied to textile materials. [1] Textiles for medical and hygienic use have become important areas in the textile industry. In general, antimicrobial properties can be imparted to textile materials by chemically or physically incorporating functional agents onto fibers or fabrics. The antimicrobial properties of such textile materials can be grouped into two categories, temporarily or durably functional fabrics. Temporary biocide properties of fabrics are easy to achieve in finishing, but easy to lose in laundering. There are many trade names in the antimicrobial

textile market which are developed for cellulose materials to provide antibacterial properties. [2]

Use of antimicrobial finishing to the textile products replies the following objectives:

- Avoidance of cross infection by pathogenic micro organisms;
- Controlling the infestation by microbes;
- Arresting metabolism in microbes in order to reduce the formation odor;
- Safeguarding the textile products from staining, discoloration and quality deterioration.

The objective of this project was to explore and compare the effect of six different antimicrobial treatments on antimicrobial efficiency and some performance properties of the woven cotton fabric.

2. EXPERIMENTAL

2.1 Materials

2.1.1 Fabric

The experiment was conducted with commercially produced plain cotton woven fabric, appropriate for use of sheet fabric. Density of 100% cotton plain woven fabric is measured as 153g/m². Fabric is scoured and bleached white fabric and optical whiteners finish or any other finishing process is not applied to the fabric.

2.1.2 Antimicrobial Finishing Materials

Antimicrobial finishing materials are maintained from the different textile chemical companies^{1 2 3 4 5}, , , , ,

For the antimicrobial finish of fabric samples advised recipe of the related antimicrobial has been used. In the Table 1, contents of antimicrobial additives, recipe of the treatment and measured pick-up rates of the sample fabrics has been summarized.

2.2. Methods

2.2.1 Antimicrobial finishing process

Antimicrobial finishing processes have been completed in the industrial type finishing machinery of a textile company⁶ using pad dry method according to

¹ Cognis Türkiye,

² Gernsan,

³ Rudolf Kimya

⁴ Setaş Kimya,

⁵ Seafresh –Thailand.

⁶ Kiraz Tekstil A.Ş.

advised application recipe of the commercial antimicrobial additives. Textile performance tests of treated specimens are completed in two different place, textile laboratory of a textile company⁷ and textile quality control and research laboratories of Pamukkale University. Microbiological evaluation tests are also completed in the microbiology laboratory of Pamukkale University.

Antimicrobial finishing procedure of each additive has been completed as it is mentioned by the related companies. (Table 1)

Table 1 Antimicrobial additives and recipe of application procedure

Antimicrobial additive	Recipe	Calculated pick up rate, %
1 (Triclosan, Sec. alkyl poly glycol ether C11-15 with EO)	7gr/lt. additive, 1 gr/lt wetting agent, pH=5-6 (acetic acid) pre drying →fixation (130°C, 3 min)	60-70
2 (Triclosan, Quaternary ammonium compounds..)	15 gr/lt additive 1 gr/lt wetting agent pH=5-6 (acetic acid) pre drying →fixation (130°C, 3 min)	60-70
3 (dichloro phenol)	30 gr/lt additive 1 gr/lt wetting agent pH=7, pre drying →fixation (130°C, 3 min)	60-70
4 (Silver)	3 gr/lt additive 1 gr/lt wetting agent pH=7, pre drying →fixation (130°C, 3 min)	60-70
5 (quaternary ammonium salt)	30gr/lt additive 1 gr/lt wetting agent pH=7, pre drying →fixation (130°C, 3 min)	60-70
6 Chitosan	%5 acetic acid concentration %1 chitosan pre drying →fixation (150°C, 3min.)	60-70

⁷ Gökhan Tekstil A.Ş.

Note: Different antimicrobial treated specimens are coded with the numbers, changing from the 1 to 6, as it is mentioned in the first column of the Table 1.

2.2.2 Applied tests to antimicrobial fabric samples

After proper antimicrobial finishing procedure of the each six antimicrobial additives, fabric samples are cut into appropriate sizes for the fabric performance tests and antimicrobial evaluation tests. Table 2 shows the test list, applied to the prepared fabric samples.

At the microbiological testing stage of the study the *S.aureus*, *E.coli* and *C. albicans* were incorporated to test the antimicrobial activity of both the formulation of the antimicrobial additives and treated fabric samples. The antimicrobial activity of formulation as well as the treated and untreated samples was evaluated according to AATCC 100 and AATCC 147 test methods.

Table 2 Fabric sample evaluation tests

Test type	Name of the test	test standard
Physical fabric test	Fabric tensile strength test	TS EN ISO 13934-1
	Fabric tear strength test	TS EN ISO 13937-1
	Crease recovery angle test	ISO 9867
	Color change test (whiteness)	TS 12552
Chemical fabric test (fastness test)	Sweat fastness test	TS EN ISO 105-E04
Microbiological tests	Antibacterial finishes on textile materials	AATCC 100
	Antibacterial assessment of textile materials: Parallel streak methods	AATCC 147

Laundering durability of the samples is tested after the 1st, 5th, 10th, and 20th washing of the samples according to TS 5720 EN ISO 6330. Samples are also tested to evaluate their fabric performances of tensile strength (TS EN ISO 13934-2), tear strength (TS EN ISO 13937-1), crease recovery angle (EN 22313), color change of whiteness (TS 12552) and sweat fastness (TS EN ISO 105-D01) changes. [3, 4, 5, 6, 7, 8, 9, 10]

3. RESULTS

3.1. Fabric Performance Test Results

3.1.1 Fabric Strength Tests

To establish the influence of the antimicrobial treatments on the strength properties of the 100% cotton woven fabric, tensile and tear strength – elongation of the specimens were examined according to TS EN ISO 13934-1 and TS EN ISO 13937-1 respectively. Tensile strength results of the washed and unwashed specimens are shown in the Figure 1 (weft) and Figure 2 (warp).

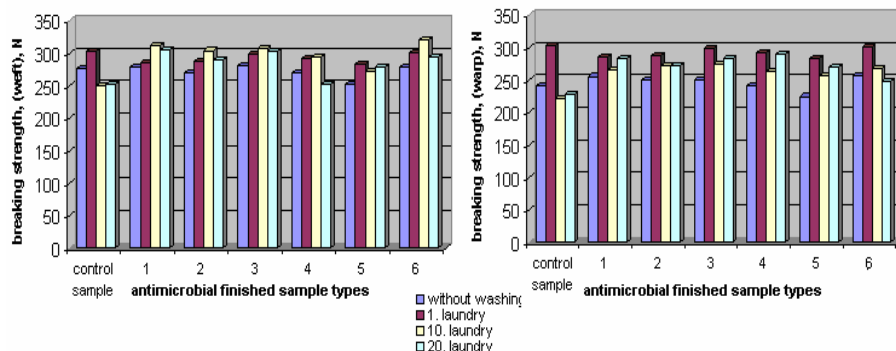


Figure 1 Tensile strength changes of fabric samples –weft direction

Figure 2 Tensile strength changes of fabric samples –warp direction

The results given in Figure 1 and Figure 2 testify to the increase in the tensile strength both weft and warp direction in the investigated material after treatment with five of the antimicrobial agents, except 5th specimen. Number of washing cycles are also found influencing tensile and tear strength of both weft and warp direction of the specimens. Washing of up to ten cycles, causes some increase on the tensile and tear strength of specimens. Similar results are also found in the work of Balcı and Mihailovic for the tensile strength of the specimens. [11, 12]

3.1.2 Fabric Crease Recovery Angle Test

To evaluate the influence of the antimicrobial treatments on the crease recovery angle of the 100% cotton woven fabric, ISO 9867 crease recovery test has been applied to the specimen. Crease recovery angle results of the washed and unwashed specimens are shown in the Figure 3 (weft) and Figure 4 (warp).

The results given in Figure 3 and 4 testify to the increase in the crease recovery angle on both weft and warp direction in the investigated material after treatment with five of the antimicrobial agents, except 5th specimen. Number of washing cycles is also found influencing crease recovery angle of both weft and warp direction of the specimens. Washing of up to ten cycles causes increase on the crease recovery angle of antimicrobial treated specimens. Increase in the crease recovery angle of the specimens with the increasing number of washing cycles might be explained with the calcareous of the washing water. Increased number of washing cycle might rise with the amount of residual calcareous on the surface of specimens. However after 20 cycle of washing, crease recovery angle of specimens has decreased dramatically. It may be explained as result of fabric wear of. Similar results are also found in the work of Balcı.[11]

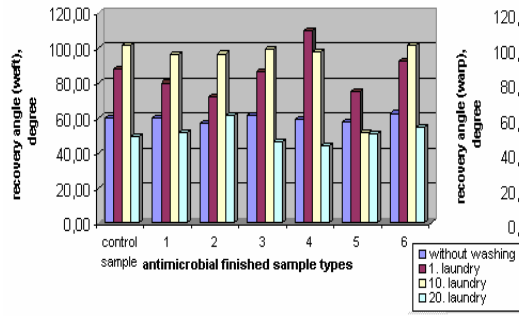


Figure 3 Crease recovery angle changes of specimens –weft direction

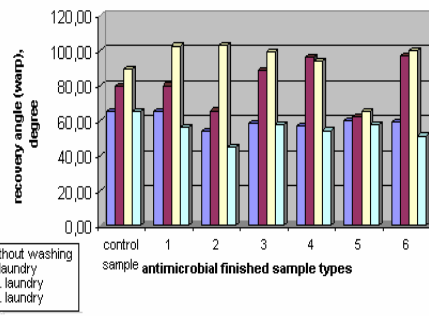


Figure 4 Crease recovery angle changes of specimens –warp direction

3.1.3 Fabric Color Change and Color Fastness against Sweat

Influence of the antimicrobial treatments on the color change and color fastness against the sweat of the 100% cotton woven fabric has been examined using TS 12552 and TS EN ISO 105-E04 respectively. Color change of the treated specimens are measured using Berger whiteness, results are given in the Table 3.

Tablo 3. Color change results, Berger whiteness

Sample code	Unwashed	5. washing	10. washing	20. washing
Control sample	147.10	149.72	149.74	151.75
1	140.82	149.01	148.78	150.17
2	144.03	148.97	148.18	151.07
3	145.54	151.58	151.79	153.73
4	143.81	145.91	148.00	150.70
5	142.38	150.04	150.73	150.85
6	129.80	144.37	144.81	146.45

It has been noted that different antimicrobial treatments influences the color of the specimens. Sample number six has been found the most affected sample among other six specimens. It can also be mentioned that number of washing cycles is an influencing parameter on the Berger whiteness of the specimens. Color of specimens becomes whiter while the number of washing increases.

Table 4 Sweat fastness, (ac: acidic sweatfastness test; al: alkali sweatfastness test; sweatfastness value is changed between 1 (worse) and 5 (best))

Sample code	number of laundry	Sweat fastness values													
		fading		staining											
				wool		acrylic		polyester		polyamid		cotton		diacetat	
		ac	al	ac	al	ac	al	ac	al	ac	al	ac	al	ac	al
control sample	0	5	5	4/5	4/5	5	4/5	5	5	5	5	5	5	5	5
	1	5	5	4/5	4/5	5	4/5	5	5	5	5	5	5	5	5
	10	5	5	4/5	4/5	5	4/5	5	5	5	5	5	5	5	5
	20	5	5	4/5	4/5	5	4/5	5	5	5	5	5	5	5	5
1	0	5	5	4/5	4/5	5	4/5	5	4/5	5	5	5	5	5	5
	1	5	5	4/5	4/5	4/5	4/5	5	4/5	5	5	5	5	5	5
	10	5	5	4/5	4/5	5	5	5	5	5	5	5	5	5	5
	20	5	5	4/5	4/5	5	5	5	5	5	5	5	5	5	5
2	0	5	5	4/5	4/5	5	4/5	5	4/5	5	5	5	5	5	5
	1	5	5	4/5	4/5	5	4/5	5	4/5	5	5	5	5	5	5
	10	5	5	4/5	4/5	5	5	5	5	5	5	5	5	5	5
	20	5	5	4/5	4/5	5	5	5	5	5	5	5	5	5	5
3	0	5	5	4/5	4/5	4/5	5	5	5	5	5	5	5	5	5
	1	5	5	4/5	4/5	4/5	5	5	5	5	5	5	5	5	5
	10	5	5	4/5	4/5	4/5	5	5	5	5	5	5	5	5	5
	20	5	5	4/5	4/5	4/5	5	5	5	5	5	5	5	5	5
4	0	5	5	4/5	4/5	4/5	5	5	5	5	5	4/5	5	5	5
	1	5	5	4/5	4/5	4/5	5	5	5	5	5	5	5	5	5
	10	5	5	4/5	4/5	4/5	5	5	5	5	5	5	5	5	5
	20	5	5	4/5	4/5	4/5	5	5	5	5	5	5	5	5	5
5	0	5	5	4/5	4/5	4/5	5	5	5	5	5	4/5	5	4/5	5
	1	5	5	4/5	4/5	4/5	5	5	5	5	5	4/5	5	4/5	5
	10	5	5	4/5	4/5	4/5	5	5	5	5	5	4/5	5	4/5	5
	20	5	5	4/5	4/5	4/5	5	5	5	5	5	4/5	5	4/5	5
6	0	4/5	4/5	4/5	4/5	4/5	4/5	5	5	5	5	4/5	5	4/5	5
	1	4/5	4/5	4/5	4/5	4/5	4/5	5	5	5	5	4/5	5	4/5	5
	10	5	5	4/5	4/5	4/5	4/5	5	5	5	5	4/5	5	4/5	5
	20	5	5	4/5	4/5	4/5	4/5	5	5	5	5	4/5	5	4/5	5

Sweat fastness measurement results of acid and alkali are shown in the Table 4. The results testify that fading properties of specimen 6 has been influenced both by acidic and alkali tests of sweat fastness, other specimens are not influenced by the different antimicrobial additives.

Staining properties of antimicrobial fabric specimens are found at the level of 4/5 or 5 for both acidic and alkali sweat fastness tests. Results show that different antimicrobial additives do not have great influence on the sweat fastness properties of 100 % cotton, white woven fabric specimens. [11] Washing of up to twenty cycles also does not influence sweat fastness value of the specimens.

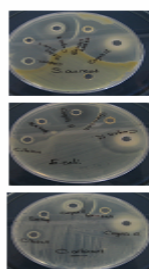
3.2. Antimicrobial Efficiency Test Results

Antimicrobial efficiency of the antimicrobial textile finishing additives and treated fabric samples are evaluated using three different methods, agar gel diffusion method; standard tests AATCC 100, and AATCC 147.

3.2.1 Agar Gel Diffusion Method

Table 5 Agar Gel Diffusion Test Results

code of additive material	Micro organisms	Control	
		alignment control of organisms	efficiency control of the additives
		Control SF+Org	1/1 Positive control Well 6. mm
1	<i>E.coli</i>	+	(-)32mm
	<i>S.aureus</i>	+	(-)42mm
	<i>C.albicans</i>	+	(-)8mm
2	<i>E.coli</i>	+	(-)30mm
	<i>S.aureus</i>	+	(-)40mm
	<i>C.albicans</i>	+	(-)28mm
3	<i>E.coli</i>	+	(-)34mm
	<i>S.aureus</i>	+	(-)42mm
	<i>C.albicans</i>	+	(-)8mm
4	test has not been performed for this additive		
5	<i>E.coli</i>	+	(-)12mm
	<i>S.aureus</i>	+	(-)24mm
	<i>C.albicans</i>	+	(-)28mm
6	<i>E.coli</i>	+	(-)10mm
	<i>S.aureus</i>	+	(-)18mm
	<i>C.albicans</i>	+	(-)14mm



Antimicrobial finishing additives are microbiologically tested to understand their efficiency against *S.aureus*, *E.coli* and *C. albicans* using agar gel diffusion method. In Table 5 inhibition zone of the five antimicrobial additives against three different organisms have been seen visually and numerically. (Antimicrobial additive number 4 is not included in this evaluation study.)

3.2.2 AATCC 100

AATCC 100 test method provides a quantitative procedure for the evaluation of the degree of antibacterial activity. Percent reduction of bacteria by the specimen treatments is calculated using the following formula:

$$R(\%) = 100 (B-A)/B, \text{ where}$$

R = rate reduction,

B = the number of bacteria colonies recovered from the inoculated treated test specimen swatches in the jar incubated over the desired contact period

A = the number of bacteria colonies recovered from the inoculated treated test specimen swatches in the jar immediately after inoculation.(at "0" contact time)

It has been seen from the Table 6 that all six specimens of the antimicrobial treated fabrics are effected against *S.aureus* and *E.coli*, but not *C.albicans* right after the treatment and also after 10 washing cycle.

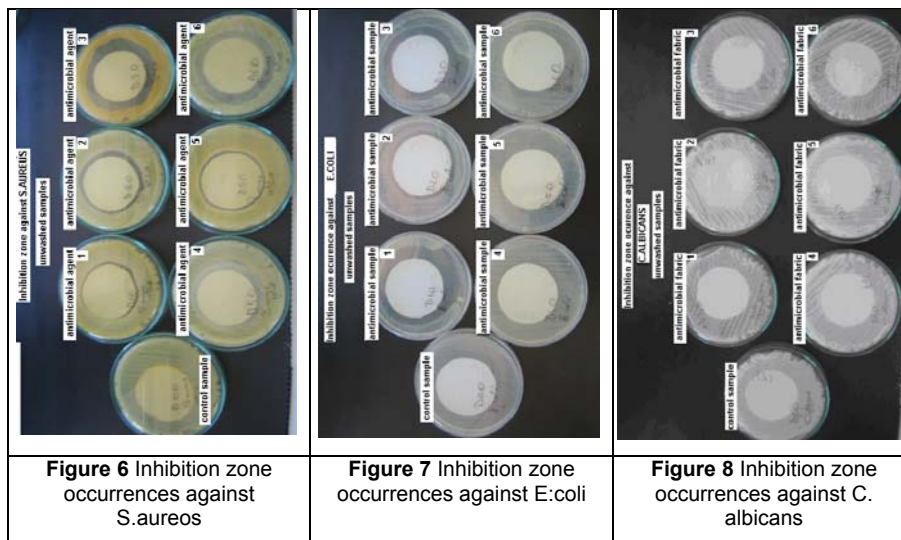
Table 6 Reduction rate of antimicrobial fabric samples against *S. aureus*, *E.coli*, and *C.albicans* (after 1 hour and 24 hours incubation)

		Without washing		After 5 washing cycle		After 10 washing cycle	
		1 hour	24 hours	1 hour	24 hours	1 hour	24 hours
<i>S. aureus</i>	1	99,99	99,99	99,97	99,99	20,00	99,55
	2	99,99	99,99	99,95	99,99	80,00	99,55
	3	99,00	99,99	99,75	99,16	-100,00	-199,00
	4	0	99,66	99,75	99,99	20,00	50,00
	5	30,00	99,96	99,00	99,96	-100,00	99,99
	6	30,00	99,06	99,75	99,99	-100,00	80,00
<i>E.coli</i>	1	95,55	99,99	99,98	99,00	97,00	93,33
	2	99,99	99,99	93,33	98,57	-60,00	98,33
	3	94,44	99,99	97,16	57,14	99,00	99,00
	4	91,11	99,96	83,33	91,42	92,00	93,33
	5	92,22	90,00	95,00	14,28	94,00	98,66
	6	22,22	70,00	83,33	-471,42	99,00	0
<i>C.albicans</i>	1	86,66	0	0	-4900,00	-100,00	
	2	97,00	99,88	-400,00	-150,00	0	
	3	66,66	80,00	-100,00	-1650,00	-100,00	
	4	96,66	91,00	0	50,00	-300,00	
	5	73,33	99,00	-200,00	-2400,00	0	
	6	0	80,00	-300,00	-400,00	-300,00	

(negative values indicates increased number of living organisms)

3.2.3 AATCC 147

AATCC 147 parallel streak method of antibacterial activity assessment is quick and easily executable qualitative test method. Fabric specimens are cut into 50 mm diameter circles and examined in the incubated plates for interruption of growth along the tracks of inoculum beneath the specimen and for a clear zone of inhibition beyond its edge.



Inhibition zone of the unwashed specimen fabrics can be seen in Figure 6, 7 and 8. It can be seen from the figures that antimicrobial treated fabric samples have inhibition zone against the *S. aureus* and *E. coli* but not against the *C. albicans*.

4. CONCLUSION

-As result of three antimicrobial test methods, it can be concluded that antimicrobial efficiency of each antimicrobial agent differ from each other and their efficiency is affected by the number of washing cycle.

-It has been seen efficiency of fabric performance parameters are affected at different levels by the different antimicrobial additives and number of washing cycle of the sample fabrics.

-On the basis of the results of the experiments, it is possible to conclude that 100% cotton woven fabric as used in this investigation, shows a wide range of antimicrobial and antifungal activity for all the groups of examined microorganisms: *S. aureus*, *E. coli*, and *C. albicans*.

-It can also be concluded that the application of the antimicrobial treatments changes the tensile strength of the woven fabric. These treatments lead to a

positive change in the tensile strength and crease recovery of angle of (weft direction) the treated fabrics.

-In the case of sweat fastness properties of the specimens, antimicrobial treatments does not have great influences on the sweat fastness properties of the 100% cotton white woven fabric.

-The investigated woven fabric specimens have satisfied the requirements of suitability for antimicrobial efficiency up to 10washing cycles, except *C.albicans*.

-Antimicrobial treatment effects the Berger whiteness of the fabric, whiteness get better with the increasing number of washing cycles.

This investigation was carried out within a Project 106M338, supported by the TUBITAK Turkish Scientific and Technological Research Council of Turkey.

REFERENCES

1. Ramachandran T., Rajendrakumar K., Rajendran R., ((2004) Antimicrobial Textiles . an Overview, IE (I) Journal.TX, Vol 84,
2. Lee, S., Cho, J., and Cho, G., (1999 "Antimicrobial and Blood Repellent Finishes for Cotton and Nonwoven Fabrics Based on Chitosan and Fluoropolymers, *Textile Res. J.* 69, 104-112
3. TS 5720 EN ISO 6330, Textiles- Domestic washing and drying procedures for textile testing
4. TS EN ISO 13934- 1, Textiles - Tensile properties of fabrics – Part I:
5. EN 22313 Wrinkle Recovery Angle
6. TS EN ISO 105-E04, Colour fastness to perspiration
7. AATCC 147 Antibacterial finishes on textile materials
8. AATCC 100 Antibacterial assessment of textile materialsTS EN ISO 13937- 1, Tear strength change of fabrics
9. TS 12552, Color change measurement of textile fabrics
10. Mihailovic, T., Asanovic, K., Simovic, L., Skundric P., (2007), Influence of an Antimicrobial Treatment on the Strength Properties of Polyamide/Elastane Weft-Knitted Fabric, *Journal of Applied Polymer Science*, Vol. 103, 4012–4019
11. Balcı, H., Babaarslan O., (2005) Antibakteriyel bitim işleminin % 100 pamuklu kumaş özelliklerine etkisi, TMMOB Tekstil Teknolojileri ve Tekstil Makineleri Kongresi, 11- 12 Kasım Gaziantep, Türkiye

A STUDY ON ABRASION AND WASHING OF SEWING YARNS USED ON THE ARAMIDE BASED FIRE FIGHTERS FABRICS

S. CANOĞLU¹, S.M. YÜKSELOĞLU¹, S.İ. MISTIK¹

¹Marmara University, Faculty of Technical Education, Department of Textile Education

ABSTRACT

During the sewing process, the sewing yarns are subjected to abrasion on the various parts of the sewing machine and are affected by different forces and hence can be abraded. This abrasion may lead to an increase after being washed and may result decrease in use ability period. This is very important for the aramide based fire fighters' fabrics. In this research, aramide yarns which are used on the aramide based fire fighters' fabric were tested on the yarn abrasion tester and damages were analysed after conventional washing and sewing strengths were tested regarding to the sewing needle count. Sewing yarn damages were then observed and discussed on the scanning electron microscope (SEM) photographs.

Keywords: aramide, fire fighters fabric, sewing yarn, conventional washing, abrasion

1. INTRODUCTION

One of the most important states during the usage of the clothing, which are produced for various aims and designs, is sewing strength and elongation. Sewings must be strong enough to resist the different tension during the usage regarding to the body movement and also preferred to break rather than the fabric itself, as it is much cheaper than the fabric. Additionally due to the sewing thread, washing method of the cloths affects both the sewing strength and fabric properties (fabric strength-elongation, abrasion and pilling, tearing strength etc.)

Regarding to the reasons mentioned above, previous works were studied carefully; mostly flame retardancy of the aramide based fire fighters' fabrics were studied, on the other hand, there is no research on sewing yarn strength, abrasion and performance on sewing strength according to the washing methods.

Hence, in this current work, aramide based sewn fabrics were studied regarding to their sewing strengths and yarn abrasions before and after conventional washings.

2. HISTORICAL PROGRESS OF THE HIGH PERFORMANCE FIBRES

2.1 Arise of New Fibres

Up to date, mainly two types of fibres have been used for the man-kind: natural fibres which are almost exist 4000 years and synthetic fibres which were first introduced a century ago. So far, it was only a man-kind dream that Chardonnet first discovered the man-made silk almost a hundred years ago. Dr. Carothers, for the first time in 1935 had produced the nylon which is claimed to be thinner than the "spider thread, stronger than the steel and more elegant than the silk". Today, synthetic fibres are not only be an alternative to natural fibres but also have an important role for the advance technologies that presents high functionality and skills to the new materials. Nowadays, these new materials can be designed and produced for their using properties. In the Figure 1, fibre development from 1950's up to the near future has been given. Also, it must be remembered that nano-fibres are produced and used in recently.

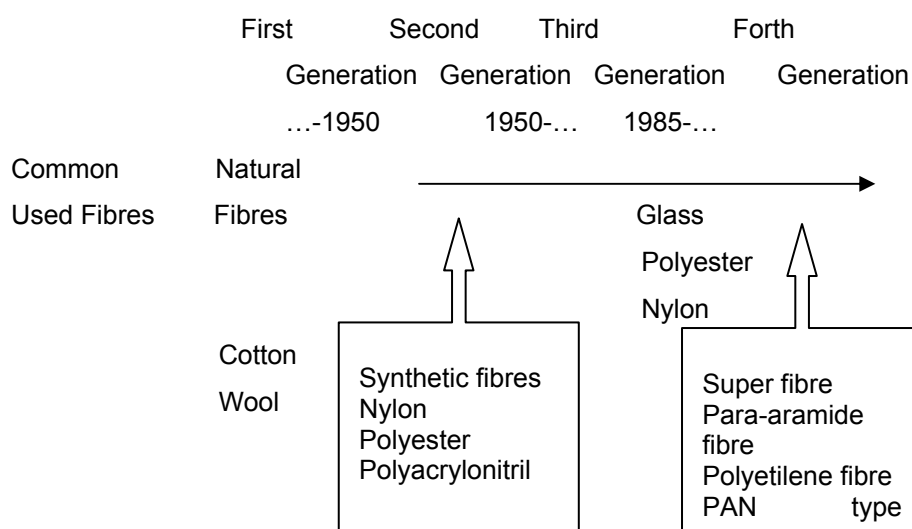


Figure 1. Fibre development [1]

New developed fibres have shown higher strengths and modules than the metals and are used in aircraft wings and other body parts of the space shuttles to strengthen the alloy materials.

Many other fibres have been developed with various achievements and functionality. Even though these fibres are named as "high performance fibres" this given name was first discovered in 1980's as can be seen in Figure 2. Before the 1980's, the fibres were shown as either general

purposed fibres or special purposed fibres. For example, carbon and aramide fibres were classified as special purposed fibres. In this way, during 1980-1984's high quality fibres were clearly identified such as fine denier polyester fibres, carbon and aramide fibres an action was appeared to be able to identify high performance fibres from the high value added fibres. Later, high quality high functional fibres have been described as high-tech fibres [1].

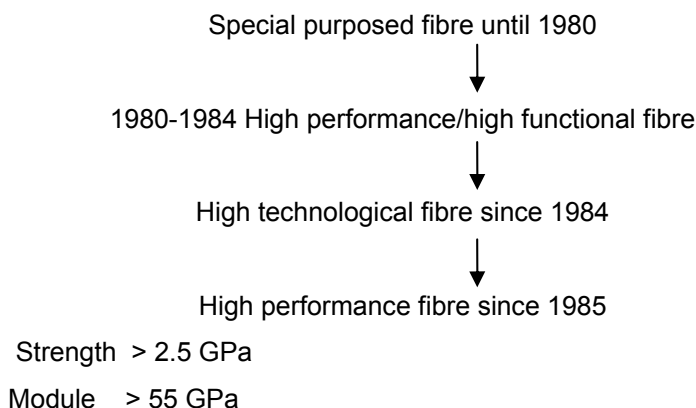


Figure 2. Historical progress of the high performance fibres [1]

3. ARAMIDE FIBRES

Aromatic polyamides, which have different properties than the classic aliphatic polyamides, have named "aramides" in 1974 by the U.S. of Commerce Commission. The first aramide fibre was introduced in 1965 by the Dupont; this is well known Nomex® which is meta-aramide (Metaphenyleneisophthalamide). There are two types of commercially successful aramide and both are categorised as man-made fibres. One of them is highly resistant to the high temperature and belongs to meta-aramide group. It has a regular strength and a low module. It is being used in high temperature areas and flame-retardant applications (Figures 3,4). These aramides can be damage at 600-800 C°. Nomex has been developed by Dupont and Conex has been introduced by Teijen as meta-aramides. In the beginning of 1970's Dupont has introduced Kevlar which is known as para-aramide fibre. There are many types of these p-phenylene terephthalamides such as Kevlar®29, Kevlar®49, Kevlar®149 and Kevlar®981 [2]. Kevlar®29 and Kevlar®49 are the most used ones [3]. One of the similar types of para-aramide is known as Twaron® which Akzo, one of the largest producers, has been introduced. Also, Teijen in Japan, has been developed a new fibre known as Thecnora®, is a co-polymer based aramide. This is a poly-p-phenyleneterephthalamide and poly3-4-oxydiphenylene terephthalamide copolymer. In the recent years Hoechst has

been produced a new type of p-aramide fibre which has a similar chemical structure to Thecnora® and has high mechanical performance. The commercial fibres mentioned above have a common property that is a phenylene molecular structured of a para state [2].

General properties of M-aramide fibre:

Strength (g/d) : 3.8-7.2

Elasticity (%) : 25-40

LOI : 30 and Chemical resistance : Sufficiently good

General properties of P-aramide fibre:

Strength (g/d) : 22-26

Module (g/d) : 460-1100

Elasticity (%) : 2.4-4.4

LOI : 25-28 and Chemical resistance : Sufficiently good [4]



Figure 3. A view of a flame- retardant Nomex fabric's flammability test [5]



Figure 4. Fire fighters clothing produced from Nomex HP fibre [5]

4. TYPE OF ARAMIDE FIBRES

4.1 Kevlar®

Kevlar® of aramide fibre was produced in 1972 by the Dupont. Dupont Researchers have described the fibre as made from the para-oriented symmetrical polymer molecule and is a very high moduled fibre with has a super resist molecular chain.

Chains that exist on the aromatic rings of the Kevlar®49 fibre increase the rigidity of the fibre with a great amount. This provides a high module, a better chemical and thermal stability to the fibre. During the production, rigid polymer molecules are oriented parallel to the fibre axis. This orientation helps to obtain a high module. As the Kevlar® fibres have an extremely high in strength/weight proportion may lead to wider application areas. Today in aviation industry, production of high performance belt and ropes, pipes that resist to high pressure and high performance radial wheels are widely produced from this fibre [6].

Saunders Thread also produces various sewing threads both with continue multifilament and spun Kevlar. Continue multifilament Kevlar can be either in single or in doubled form. But it is only finding in natural yellow colour. On the other hand, spun Kevlar can be in a wide range of colour and can be polished at the final stage [7].

4.2 Nomex®

Nomex was developed by the Dupont in 1965. It is a meta-aramide and resistant to high temperature. It has low modules and has high damage degrees (600-800 C°). Nomex yarns known as flame retardant properties and are widely used for protective clothing. Other application areas are filtration and wire cables. Advantages of Nomex yarns are:

- flame retardancy,
- good chemical resistance,
- good abrasion properties.

Nomex is better than nylon and polyester when compared with twist and stretch properties. Nomex industrial products have shown superior abrasion resistance than the cotton, wool and acrylic. Nomex, does not melt and has very low ignition properties. Depending on the source of temperature density it becomes brittle and turns into coal above the 371 C° and fibre damages. If any type of flame during the oxidation will be removed from the fibre, the fibre will be extinguished by oneself. Nomex is resistant to many of the chemicals and most of the hydrocarbons and highly resistant to many most of the organic solvents. Also, it shows good resistant to the alcalises in room temperature; however it damages with strong alkalises at the higher temperatures. Additionally, does not affected from the fluorine compounds

which can be found at gases in mines and rocks where formatted. Nomex can be damaged by the ultraviolet waves of the natural and synthetic lights. Hence, it is recommended that precautions are necessary where strength is critical value if ultraviolet lights are directly applied. On the other hand, Nomex has an extraordinary strength to the radiation [8].

5 MATERIALS AND METHOD

In this study, 198 g/m² weight of 75% Nomex/ 23 % Kevlar / 5% P140 Antistatic fibre blend of aramide based fire fighters fabric were used with two different thickness and form type of sewing needles. Plain seam were applied at 4 stitch/cm in warp and weft directions. Later, the seam strengths of un-washed and conventionally washed sewn fabrics were both studied according to the needle thickness. Also, yarn abrasion photographs were taken on the SEM and sewn yarns taken from the washed fabrics were analysed according to these photographs of the abraded yarns. Yarns and fabrics were conditioned 48 hours at the standard atmosphere (20 ± 2 C° and $65 \% \pm 2$ RH) for the tests.

6 INSTRUMENTS AND PROCESS

6.1 Instron 4411 Strength Tester

This instrument was used for the yarns and fabric's tensile tenacity (Figure 5). Yarns were carried out according to the TS 245 (ISO 2062), warp and weft seam strengths were tested with the ASTM D 1684-96 standard.



Figure 5. Instron 4411 strength tester

6.2 James H.Heal Yarn Twister

Yarn twists were determined by un-twisting and re-twisting technique. Testing lengths were 500 mm and 30 tests were carried out regarding to TS 247 standard.



Figure 6. Nu-Martindale fabric abrasion and pilling tester

6.3 SDL Atlas Yarn Abrasion Tester

Earlier studies show that coefficient of friction affects the seam strength and this coefficient does not a diagnostic for the single type yarn. For this reason, sewing yarns abrasion tests were carried out at the SDL Atlas yarn abrasion tester and the results are given in Table 3.

This instrument is about 24 kg and 410x510x600 mm in dimension; it measures abrasion values of the woven and knitted fabrics and seam yarns. The instrument identifies the abrasion values of the 10 different yarns where they are set until breaks on the two steel bar; the values obtain after the yarns break by the microprocessor. The abrasion results are given by the RS 232 spreadsheet output data. Figure 7 shows the SDL Atlas yarn abrasion tester where the sewing yarns were tested in this study.

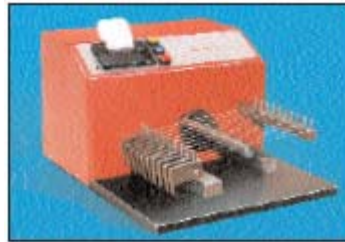


Figure 7. SDL Atlas yarn abrasion tester

7 CONVENTIONAL WASHING

Sewn fabrics were washed on the Arçelik washing machine (Model 4050) without a pre-wash; the B Programme was used. The following conditions were applied:

Amount of the detergent: 200 g

Washing time: 60 min.

Washing temperature: 60 C°

Squeezing and drying: 15-20 min.

8 SEWING YARNS AND PROPERTIES

Sewing yarns were conditioned under the standard atmosphere for 48 hours and later were tested for their linear density, twist, strength and elongation; the results are given in Table 3.

Table 3. Sewing yarn properties (un-washed)

Yarn type, linear density (theoretical) (Nm)	Yarn linear density (measured) (Nm)	Twist (T/m)		Strength (g)	Elongation (%)	Yarn friction strength (rev)
		Single	Final			
Kevlar 50/2	49.6/2	553	500	4900	3.9	33
Kevlar 50/3	46.6/3	586	378	7200	3.7	50
Kevlar 50/4	51.1/3	537	358	11500	4.2	312

Table 4. Seam strengths of un-washed and washed samples

Fabric	Needle no.	Yarn linear density (Nm)	Seam strength (kg)	
			Warp direction	Weft direction
Raw (un-washed)	12	50/2	65.2	63.9
	12	50/3	91	86.4
	16	50/2	70.1	66.2
	16	50/3	101.5	99.5
Conventionally washed	12	50/2	71.9	64.5
	12	50/3	89.5	96.5
	16	50/2	63.4	70.1
	16	50/3	99.8	98.4

9 OBSERVATION ON THE ELECTRON MICROSCOPE (SEM)

In the literature, a general result of the abrasion test shows that yarns may little or more abraded after the testing [9]. For this reason, it is thought that it would be useful to observe damaged yarns (Nm50/2 and Nm50/3) on the JEOL-JSM 5910LV model electron microscope; the photographs of these samples are given in Figures 8-17.

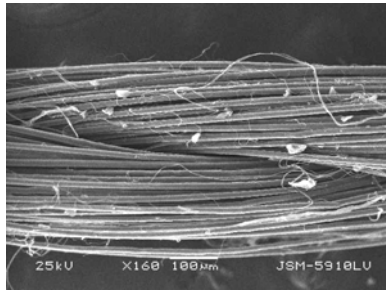


Figure 8. Nm 50/2 Raw yarn (un-used)

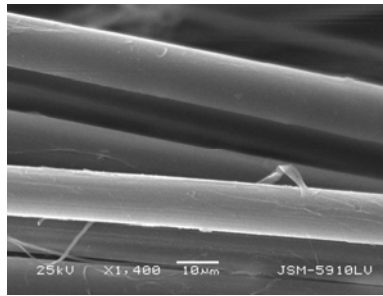


Figure 9. Nm 50/2 Raw yarn
(Single fibre)

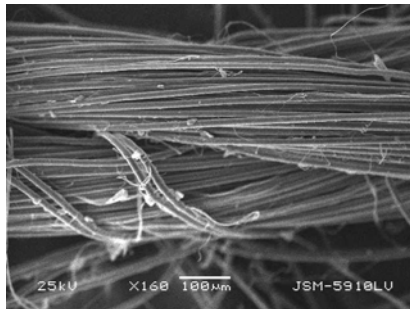


Figure 10. Nm 50/3 Raw yarn (un-used)

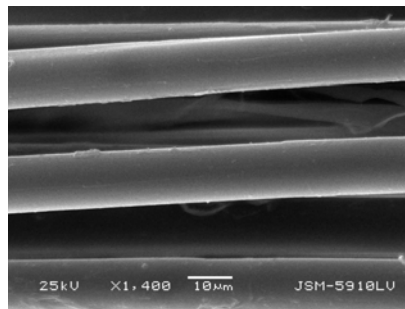


Figure 11. Nm 50/3 Raw yarn (Single fibre)

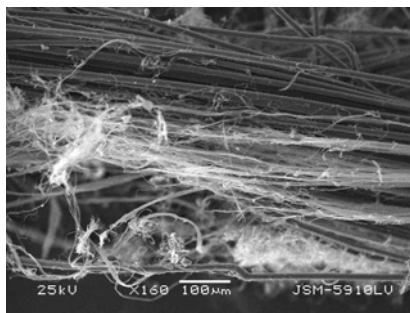


Figure 12. Nm 50/2 Yarn taken after
the 35 rev. from the SDL ATLAS
Yarn Abrasion Tester

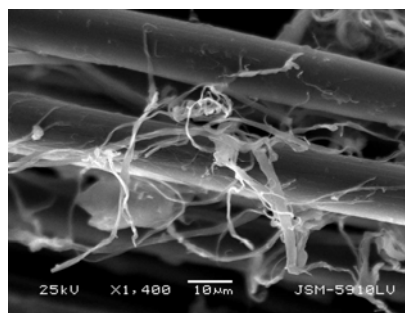


Figure 13.Single fibre (from
(Nm 50/2 Yarn) taken after the
35 rev. from the SDL ATLAS Yarn
Abrasion Tester

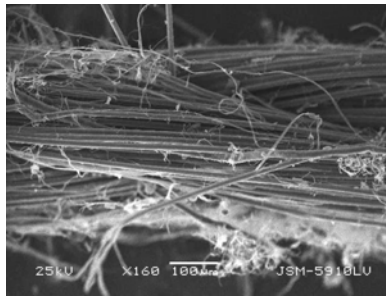


Figure 14. Nm 50/3 Yarn taken after the 35 rev. from the SDL ATLAS Yarn Abrasion Tester

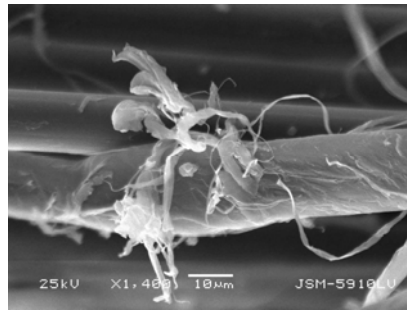


Figure 15. Single fibre (from (Nm 50/3 Yarn) taken after the 35 rev. from the SDL ATLAS Yarn Abrasion Tester

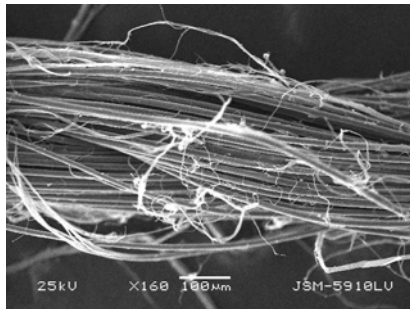


Figure 16. Nm 50/2 Yarn taken from the conventionally washed fabric (Needle number 12)

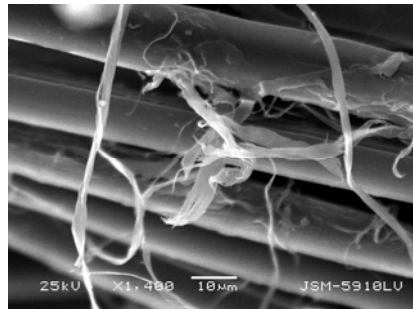


Figure 17. Single fibre (from (Nm 50/2 Yarn) taken from the conventionally washed fabric (Needle number 12)

10 RESULTS

1. Depending on the yarn coefficient as the yarn becomes coarser the yarn strength increases.
2. As the yarn becomes finer its elongation increases.
3. Depending on the yarn coefficient as the yarn becomes coarser the yarn abrasion increases.
4. As yarn strength increases, generally both un-washed and conventionally washed fabrics have presented increase in seam strengths in warp directions.
5. Similar results, as in item 4, were obtained on the seam strengths of the weft directions of the fabrics.

6. If SEM photographs were analysed due to the abrasion, fibres on the yarn surface and fibrillation were seen and hence some breaks were occurred. Also, it was observed that if the deformation was considered, as the yarn layer increases (Nm50/3) the resistance of the yarn may lessen the deformation.
7. If the SEM photographs were compared, regarding to the washing procedure the fibres on the yarn surface and fibrillation were partly increased.

ACKNOWLEDGEMENT

The authors are thankful to the Research Center of Marmara Univeristy for supplying the SDL Atlas yarn abrasion tester.

REFERENCES

1. Tatsuya,H.; Phillips,G.O.; "New Fibers", Ellis Harwood Ltd.,(1990) 1-23, 28, 30-33, 44-48.
2. Joyse,M.A.;CText ATI, BSc Tech, AMCT, M.ı.Mgt,MCIM; "High Performance Fibers" (1993) 5-12, 56-70.
3. Arana,A.; "Elyaf Takviyeli Karma Malzemeler", İ.T.Ü. Fen Bilimleri Enstitüsü, M.K.-575 Ders Notları, İstanbul, Türkiye (1990).
4. www.intexa.com. (reached date: May 2004).
5. http://www2.dupont.com/Personal_Protection/en_US/tech_info/nomex_industrial_thermaltesting.html
6. (Erişim tarihi: Kasım 2005)
7. Karahan,M.; "Kompozit Malzemeler İçin Yüksek Performanslı Spectra Liflerinde Arabirim Kuvvetinin Çeşitli Kimyasallar Etkisinde İncelenmesi", Yüksek Lisans Tezi, Uludağ Üniversitesi, Fen Bilimleri Enstitüsü, Bursa. Türkiye,(1994) 9-17.
8. www.saunders-thread.com. (reached date: April 2004.)
9. <http://www.offshore-technology.com>. (reached date: February 2004.)

SOME INTERESTING EXAMPLES OR PROJECTS ABOUT THE SOLUTIONS OF THE GEOTECHNICAL PROBLEMS USING GEOSYNTETICS

H. R. YILMAZ, T. ESKİŞAR

Department of Civil Engineering, Ege University

ABSTRACT

Geosynthetics are an established family of geomaterials used in a wide variety of civil engineering applications. Many polymers (plastics) common to everyday life are found in geosynthetics. The most common are polyolefins and polyesters although rubber, fibreglass, and natural materials are sometimes used to function as a separator, filter, planar drain, reinforcement, cushion/protection, and/or as a liquid and gas barrier. The various types of geosynthetics available, along with their specific applications in some interesting projects will be presented below in subsequent chapters.

The American Society for Testing and Materials (ASTM) has defined geosynthetics in D4439 terminology as follows:

“Geosynthetic: n.- a planar product manufactured from polymeric material used with soil, rock, earth or other geotechnical engineering related material as an integral part of a man-made project, structure or system.”

The use of geosynthetics has basically two aims which will be easily seen from the examples: to do the job better and to do the job more economically (either through lower initial cost or through greater durability and longer life, thus reducing maintenance costs).

The specific families of geosynthetics are as follows: geotextiles, geogrids, geonets, geomembranes, geosynthetic clay liners, geopipes, geocomposites, and geoothers.

Key Words: Geosynthetics, geotextiles, geogrids, geomaterials

1. INTRODUCTION

In the past, when dealing with difficult sites for construction purposes, the conventional practice was limited to either replacing the unsuitable soils or by-passing them with costly deep foundations. Additionally, the age-old problem of land scarcity and the need to rebuild aging infrastructure in urban areas, increased realization of seismic hazards, and regulations mandated for various environmental problems have been the impetus for the evolution of a number of ground improvement techniques during the past 25 years.

Innovative ground modification approaches are routinely used now to solve unique soil related problems and often are considered to be the most economical means to improve an undesirable site condition.

Geosynthetics have proven to be among the most versatile and cost-effective ground modification materials. Their use has expanded rapidly into

nearly all areas of civil, geotechnical, environmental, coastal, and hydraulic engineering (GMA, 2002).

2. GEOSYNTHETIC ADVANTAGES

Geosynthetics, including geotextiles, geomembranes, geonets, geogrids, geocomposites, and geosynthetic clay liners often used in combination with conventional materials offer the following general advantages over traditional materials. The advantages are space savings, material quality control, construction quality control, cost savings, technical superiority, construction timing, material deployment, material availability, and environmental sensitivity (GMA, 2002).

For example, sheet-like geosynthetics take up less space in a landfill than do comparable soil and aggregate layers. Soils and aggregates are heterogeneous materials but geosynthetics are produced in controlled conditions in factories. That is why more accurate designs can be made with minimal variations.

Geosynthetic materials are generally less costly to purchase, transport and install than soils and aggregates. Geosynthetics can be installed quickly and geosynthetic systems reduce the use of natural resources and the environmental damage.

Stabilization of geotextiles substantially reduce construction costs for paved and unpaved roads. For example, unpaved road aggregate thickness can be reduced by as much as 30% to 50% when stabilization textile is used (Amoco, 2002).

In retaining wall applications geotextiles and geogrids make retaining walls financially feasible. In fact, a geotextile retaining wall can be built for less than half the cost of a conventional wall.

In drainage applications, geotextiles have replaced graded soil filters for drainage of virtually all structures, including groundwater intercept systems, pavements, building foundations and dams.

Compared to conventional soil filters geotextiles offer advantages by providing a consistent and continuous filter, reduced excavation, reduced environmental impact, simplified higher quality construction and a substantial reduction in material costs.

In railroad stabilization, geotextiles perform multiple functions in railroad applications. Nonwoven fabrics are used to stabilize both new and rehabilitated tracks. They prevent contamination of new ballast layer with underlying fine grained soils and provide a mechanism for lateral water drainage.

In sediment control problems, temporary silt fences perform a vital function for the construction industry. Silt fences provide very economical environmental protection.

In waste containment projects, both geomembranes and the geotextiles are necessarily used together to prevent the destruction of geomembrane.

The chosen, interesting examples and projects from world wide applications are summarized below in subsequent chapters.

3. A FEW GEOSYNTHETIC INSTALLATION PROJECTS FROM WORLD WIDE

3.1 İzmir Melez Delta Project in Turkey

In this application, after forming a new streambed in the delta formed by Melez Stream, which is one of the longest streams of İzmir, conservation is aimed by covering the mud, which remained out of the bed by using geotextile (Figure 1). Thus, the obstruction of malodorous hydrogen sulphide spreading from the water of the delta was planned (İBB, 2001).

After completing the main fill, the mud area approximately 100.000 m² which is in the east of the embankment parallel to the main fill was covered by a 50 kN tensile strength double woven geotextile. The purpose of covering the mud by a geotextile is to prevent the scent and to obtain a reliable platform by covering the mud, and to prevent the bad appearance. Also, by the membrane action of the 20 cm crushed stone on the geotextile layer the soil will consolidate in time and will increase its bearing capacity additionally. Imported geotextile was in the form of big rolls, which are 5 meters in width and 100 meters in length. If the geotextile is stiff enough to bear the stresses of the people walking on it; first it was sewn in the shape of a sheet covering an area of 3000 – 5000 m² (Yılmaz and Eskişar, 2003).

After completing the work made by special sewing machines and PE filaments the ropes were tied at the end of the geotextile and the mud was covered with the geotextile by the withstand force formed by the workers. If the mud is too soft to walk on and the workers are sinking into the mud during the period of application, single sheets of 5.30 m and 5.50 m width are placed over the mud and with the help of bearing capacity of the geotextile sewing is complicated on the mud.

The cohesion intercept of this type of soil can be estimated as $c_u = 10 \text{ kN/m}^2$. As it is not possible even to walk on such an area there is an obligation (which is wholly formed by very soft mud) to cover of it to prevent the malodorous scent. The geotextiles to be used on such an area should have the protection and separation properties at first. That is why after examining the similar projects and evaluation of their results, woven type of geotextile was arranged for usage (Yılmaz et.al, 2005).



Figure 1. Application of geotextile and lay out of crushed stone in Melez Delta and the final view (İBB, 2001, Yılmaz et al., 2003)

3.2 An Embankment Stabilization Project on Soft Ground In Japan

Geosynthetics of many types such as non-woven geotextiles and geogrids have been widely used as reinforcements for embankments. In this project, one of these materials, a geosynthetic based on a high strength web material, was installed to stabilize an embankment until the soft ground to get sufficient strength due to consolidation. It was used in order to reduce the cost of construction of an expressway. In road constructions, the initial construction cost of an embankment is cheaper than that of a bridge or a viaduct, etc. Recently, it was important to use local excess soils effectively and a huge embankment has been constructed with these soils (Hashizume et al., 2004; Yilmaz et.al., 2005).

In this project, a high strength web shaped geosynthetic was used to stabilize an embankment of 13.2 m heights on soft ground, which was the main problem. The area was composed partly of highland skirt and flat land to the south of Butsuzou tectonic line. This land is alluvium and its bottom base is approximately 15m deep. The embankment of a 13.2 m height and the subgrade layers consisted of clay and peat, which were expected to consolidate by the load of the embankment. The shear strength of the soft ground after 300 days completion of the embankment was regarded as a sufficient support for the embankment. The width of the one web of geosynthetic reinforcement was 91 mm. One sheet of this reinforcement material is made from 25 pieces of this web. The separation of web is 18 cm and total width of one sheet is 4.5m. The web is covered with polypropylene. The polyethylene is resistant to corrosion, chemicals and impact load. From the results of calculations, the design standard tensile strength of the reinforcement material is estimated as 700 kN/m and the tensile strength of one web is 126 kN.

As a result, using the high strength web-shaped geosynthetics as reinforcements in an embankment on soft ground only by rolling of the material, the stability was increased and the settlement was decreased. The total geosynthetic of 9000 m² was installed completely in four days (Figure 2). According to the observations, the embankment on the soft ground was stable during construction. The observed tension of the geosynthetic was less than the calculated value that was based on the circular slip method. Therefore this behavior might be explained by the additional effect of the geosynthetic (Hashizume et al., 2004; Yilmaz et.al., 2005).

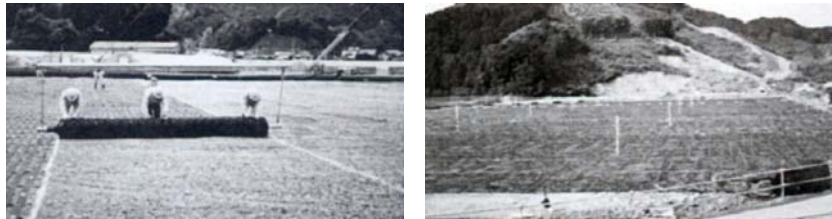


Figure 2. Ribbed Installation work of geosynthetic and installed situation (Hashizume et al., 2004).

3.3 The Construction of a Green Faced Retaining Structure near Foix/France

Project details could be briefly given as:

Slope geometry (MS3/MS5), total height: 12/16 m, height of reinforced structure: 8/12 m, slope inclination: 70°, geosynthetics used - tensile strength 95 to 230 kN/m vertical distance 50 cm anchor length up to 10 m, total quantity 50.000 m², erosion protection mat woven from green HDPE and biologically degradable yarns, construction time: 1999 – 2000 (Polyfelt, 2002)

A geotextile-reinforced earth structure up to 12 m high was perfectly adapted to the surrounding landscape due to its special structure incorporating high strength composites, an erosion protection woven fabric, and finally hydro-seeding. The Foix bypass section of the RN 20 in southern France crosses many zones of unstable soil. Experience gained in the construction of a 25 m high wall reinforced with geosynthetic in 1994 (the highest in Europe) encouraged the owner to engage the same construction method. In the first wall, pre-cast concrete facing panels were used, but here special requirements in terms of stringent environmental protection had to be met. The structure was to be integrated into extended woodland, which underlined the need for a green facing. The reinforcement was provided by a geosynthetic with tensile strength up to 230 kN/m, in horizontal layers 50 cm thick, with anchor lengths up to 10 m from the face of the structure (Figure 3). At the face, a temporary erosion protection composite was installed, filled with approximately 25 cm of a humous/topsoil mix. The erosion protection composite, consisting of a knitted UV-stabilised HDPE fabric interspersed with natural fibers which protect the humus from erosion, was folded back at the front of the slope and anchored within the fill material. Finally, the slope was hydro-seeded by a specialist firm of contractors (Figure 4).

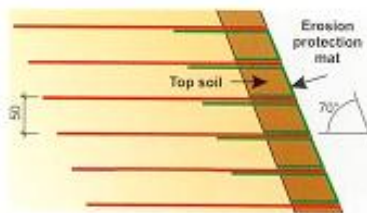


Figure 3. Schematic cross section of the reinforced slope (Polyfelt, 2002).



Figure 4. The greened retaining wall is perfectly integrated into the surrounding woodlands (Polyfelt, 2002).

3.4 Landslide Repair near Samobor/Croatia

Project details could be briefly given as:

Year of construction: 1998, vertical distance of the geotextiles: 50cm, total slope height: 12m, slope inclination: 1:1.5 (Polyfelt, 2002)

A landslide near Samobor in Croatia was successfully and economically repaired by reinforcing the slope with high strength composite geotextiles.

In 1997, a landslide occurred on the road between Hamor and Greguric Breg in Croatia. The slope with an inclination of 1:1.5 failed over an area of approximately 25 x 30 m, between the upper and lower road of a switchback section. In the upper part, below an old concrete retaining wall, the road sagged over an area of 2 m width and 16 m length. The on-site material was water-saturated and had a tendency to flow. At relatively low depth, weathered rock with an adequate bearing capacity was found (Figure 5).

By order of the municipal authorities of Samobor, a repair strategy was devised achieving long term slope stabilization at minimum cost.

The lower part of the slope, where the rock was found very close to the surface was secured by means of a simple small gabion wall. For the upper section which was 12 m high with a 1:1.5 slope inclination, a combination of gabion wall and geotextile reinforced soil structure was constructed. The 3 m high gabion wall was founded in the rock subgrade. During the works, the slope was covered with plastic sheeting to prevent further landslides caused by rainfall. The slope above the gabion wall was reinforced with 16 layers of geotextiles. The geotextiles were installed in 500 mm lifts (Figure 6). The installation of the soil mass including 24 reinforcing layers took only ten working days. Finally, a vegetation mat and top soil were applied to the surface allowing for vegetation and assuring UV protection of the geotextiles (Figure 7).

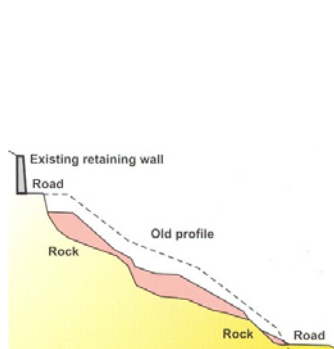


Figure 5. Landslip between upper and lower road (Polyfelt, 2002)

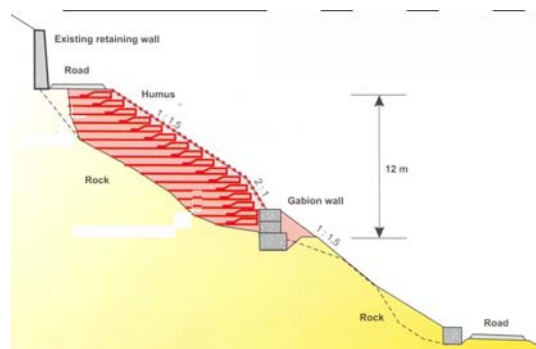


Figure 6. Schematic cross section of the repair concept carried out (Polyfelt, 2002)



Figure 7. Construction of the reinforced soil structure (Polyfelt, 2002)

3.5 Prominent Examples from Turkey

Additional to Melez Delta Project in İzmir - Turkey, a few prominent examples from Turkey are listed below with very little detail.

1. Baltalimanı – TEM Highway Reinforced Retaining Wall Application in İstanbul
2. Karadeniz Coast Highway Project (Polymer strip reinforced retaining walls)
3. Ovacık Goldmine Waste Deposit Projects (Geomembrane-geotextile application) in İzmir
4. Antalya- Manavgat Solid Waste Destroy Facility (Geomembrane-geotextile application)
5. İzmir – Çiğli Waste Water Treatment Plant (Wick Drain Applications)
6. Konya Hotel's Foundation Improvement Project on a Geotextile Reinforced Fill Application
7. Zümrütevler Junction Polymer Strip Reinforced Earth Abutment Application in İstanbul

4. CONCLUSIONS

As it is easily seen from the examples and the imported projects or based on review of many case histories, the success and need of geosynthetics can be explained by three reasons:

- i. There is a need for two dimensional materials in geotechnical engineering.
- ii. Geosynthetics are the only available materials that meet the requirements for two dimensional materials in geoengineering
- iii. Many geosynthetics are two dimensional materials made with one dimensional element which is a very efficient use of matter.

In conclusion, when used as a reinforcement, drainage or liners, geosynthetics are respectively, the muscles, the veins and the skin of the

earth. Never before have construction materials displayed such versatility and performed such fundamental functions.

REFERENCES

1. AMOCO Fabrics and Fibers Co.(2002), "Geotextile Capabilities – Helping You Design with Confidence", Austell, GA.
2. İBB, (2001), "Arap, Manda, Melez Dereleri Islah Projesi", 45pg, İzmir
3. Geosynthetics Materials Assoc. (2002), Handbook of Geosynthetics, 60pg, (also available at www.gmanow.com), Roseville, MN.
4. Hashizume, H., Konami, T., Kawahara, H., Nagao, K., and Imayoshi, H., (2004), "The Effect of High Strength Geosynthetics to Stabilize an Embankment on Soft Grounds", Geosynthetics 2004, September 5-8, Schloss Pillnitz, Dresden, Germany.
5. Polyfelt Products Brochure, (2002), 11 Chapters, Linz, Austria.
6. Yılmaz H.R., Aklik P., and Eskişar T. (2005) "A Few Examples on the Alteration and Remediation Techniques of Problematic Soils Using Geosynthetics in Geotechnical Engineering Applications", Proceedings of the Int. Conf. on Problematic soils, GEOPROB 2005, Eastern Mediterranean University, Famagusta, pp. 801-808, 25-27 May.
7. Yılmaz H. R., and Eskişar T. (2003), "Cost Considerations on the Economy of Using Geotextiles and an Improvement Application from İzmir – Melez Delta", Journal of Nonwoven Technical Textiles Technology, pp.28-33, June.
8. H. Recep Yılmaz, Associate Professor, Ege University, Department of Civil Engineering, 35100 İzmir, Turkey, E-Mail: yilmazrecep@yahoo.com; Phone: +90 232 388 60 26, FAX: +90 232 342 56.
9. Tuğba Eskişar, Research Assistant, Ege University, Department of Civil Engineering, 35100 İzmir, Turkey, E-Mail: tugba.eskisar@ege.edu.tr; Phone: +90 232 388 60 26, FAX: +90 232 342 56.

ENHANCEMENT OF INTERFACIAL STRENGTH IN CARBON FIBER/THERMOPLASTIC MATRIX' COMPOSITES

S. ERDEN, H. YILDIZ

Ege University, Mechanical Engineering Department

INTRODUCTION

In general, the microstructure of fiber reinforced composite materials is composed of the reinforcing fiber, the surrounding matrix as the binder, and the interphase region as illustrated in Figure 1. The interphase, which is thought to involve the interface areas as its boundaries between the constituents of the composite material, is mostly pronounced as "interface" in the literature [67].

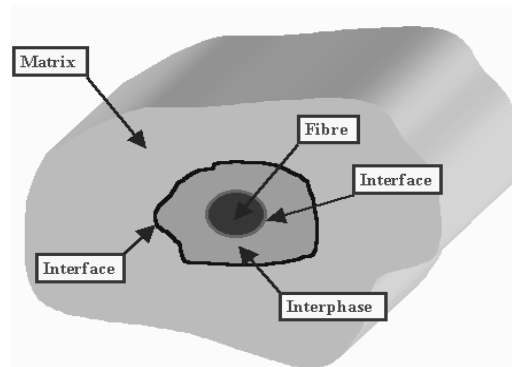


Figure 1. Schematic illustration of the microstructure of composite materials [70].

Interface (or interphase) is the region of significantly changed chemical composition that constitutes the bond between the matrix and reinforcement (Fig 2). Microstructure-property relationship at the interface region is an essential key to the successful design and proper use of composite materials. Properties of an interface are governed largely by the chemical/morphological nature and physical/thermodynamic compatibility between the two constituents and most often limit the overall performance of the bulk composite.

Controlling the interface properly to provide the composite with improved mechanical performance and structural integrity, requires understanding the mechanisms of adhesion which are specific to each fiber/matrix system, and the physico-chemical characterization of the interface with regard to the origin of adhesion. Adhesion can be attributed to mechanisms including adsorption and wetting, electrostatic attraction, chemical bonding, reaction bonding, and exchange reaction bonding, schematically shown in Figure 3. In addition to the major mechanisms, hydrogen bonding, van der Waals forces and other low energy forces may also be involved [67].

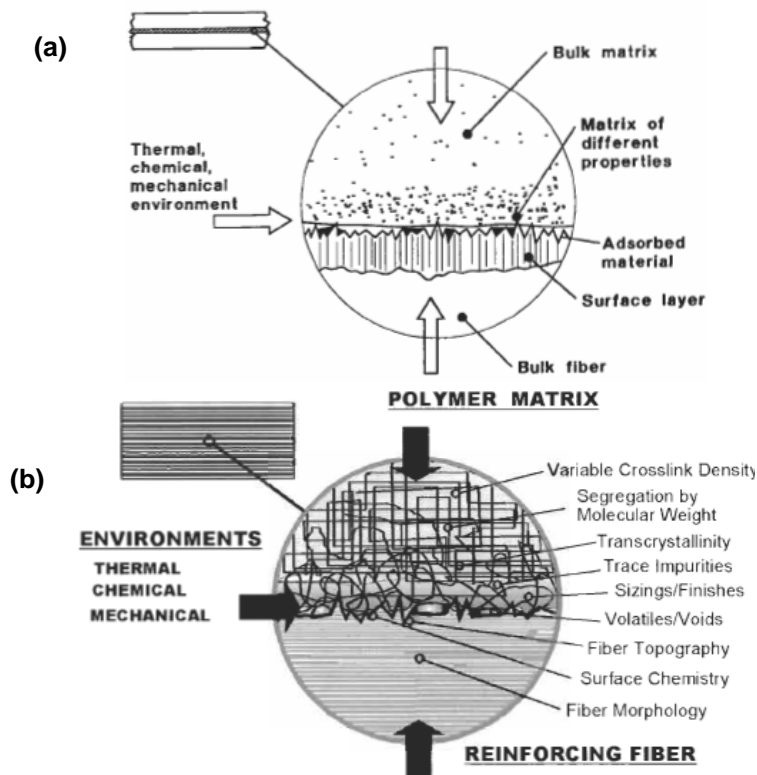


Figure 2. Schematic illustration of the components of the three-dimensional interphase between fiber and matrix by a) Drzal et al [67] and b) Drzal and Herrera-Franco [68].

Interfacial adhesion phenomenon in composite materials, recently considered with respect to wettability in most cases, leads us to the surface free energy aspect as an important criterion. Consequently, this is followed by studies aiming at modification of the interface either by fiber surface treatments or matrix modification in order to achieve improved interfacial bonding between the fiber and the matrix.

This study reviews the studies carried out in particular utilising carbon fibers and thermoplastic matrices owing to their properties mentioned below. Moreover, its objective is to group different techniques used to improve interfacial adhesion and therefore macro-mechanical properties of carbon fiber reinforced thermoplastic composites (CFTC).

TREATMENT METHODS IN CFTCs

Carbon fiber reinforced polymer matrix composites have been utilized especially in the last two decades for the design and manufacture of lightweight structures owing to their high load-bearing capacity and low density. Although thermosets have been preferred mostly as matrix material in high-performance composites,

widespread demand on thermoplastics have also started to increase recently due to their properties such as low water absorption, good chemical resistance at elevated temperatures, high impact strength, good formability, dimensional stability, recyclability, and being non-toxic and non-corrosive. On the other hand, as thermoplastics have low solubility and high melt viscosity, and as they lack reactive groups, it is harder to establish the required adhesion at the fiber/matrix interface when compared to the thermosets. For this reason, interface properties have to be enhanced via different methods including fiber surface treatments and/or matrix modification.

The studies reviewed here are classified under the category names coating, plasma, sizing, surface treatment, and matrix modification. Also, a classification named nano has been added to overview further and most recent studies in fiber/matrix interface enhancement.

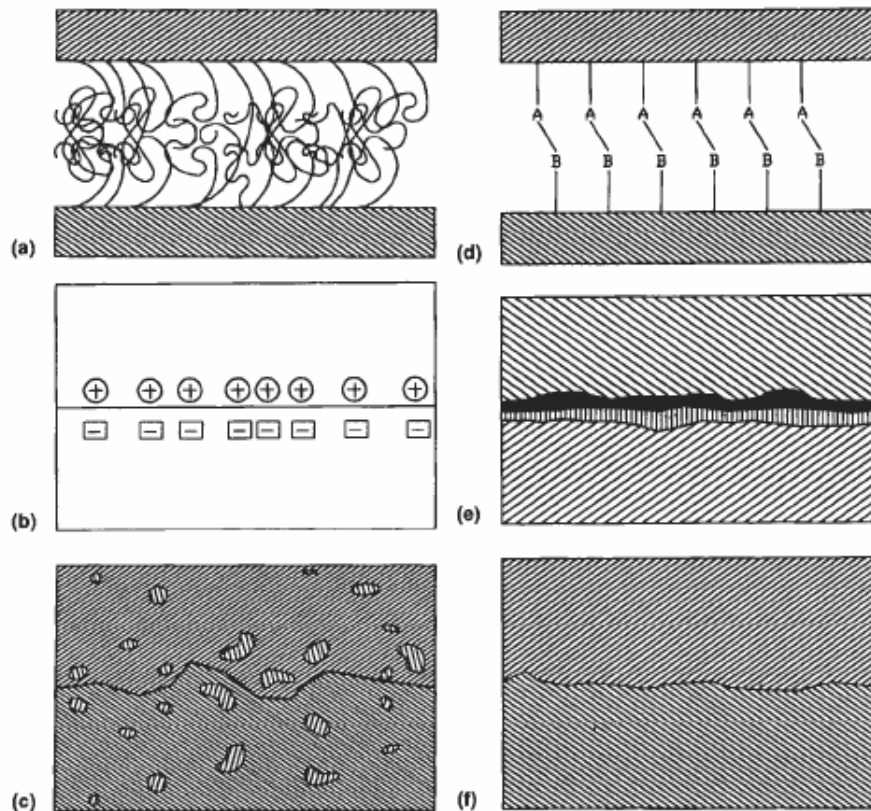


Figure 3. Major mechanisms of interfacial adhesion: a) molecular entanglement, b) electrostatic attraction, c) elemental interdiffusion, d) chemical reaction between functional groups, e) chemical reaction after formation of new compounds (in metal matrix composites), f) mechanical interlocking [67].

FIBER SURFACE TREATMENTS

These can be grouped as oxidative and non-oxidative treatments, each of which can be sub-grouped as seen in Chart 1. In our study, fiber surface treatments are classified in categories named coating, plasma, sizing, and surface treatment.

Category coating includes studies involving the coating of carbon fiber surfaces with a thin layer of polymer to improve the compatibility with the matrix. This is achieved utilizing the methods namely electrocoating (or electropolymerization, or electrodeposition), polymer grafting, and in situ polymerization. Plasma studies mostly involve oxygen treatment while some include nitrogen, argon, and ammonia treatments as well. Plasma polymerization was also realized in a study. Surface treatments involve thermal, chemical, and electrochemical oxidation at most. Besides are ozone (O_3), cryogenic treatments, the use of oxidizing agents, and electric charge application. Sizing is the common classification name given to those studies that involve the inclusion of a sizing material compatible with the matrix prior to composite fabrication. This will be considered under the group surface treatment in this study.

Coating

Iroh et al, electropolymerized copolymers of a wide range of N-substituted maleimides and styrene directly on the surface of AS4 unsized graphite fibers, which they used as the working electrode. They recorded a variation in the rate of electrocopolymerization with the electrocopolymerization parameters, such as the comonomer concentration, current density, supporting electrolyte concentration, electropolymerization time, nature of the solvent, solvent/dilute sulfuric acid ratio and the structure of the maleimide. Then, a process was carried out for the manufacture of unidirectional composite laminates of graphite fiber/poly(maleimide-co-styrene) which showed excellent physical and mechanical properties [1].

Iroh went on his studies with different coworkers using the electropolymerization method again, but to coat this time pyrrole onto unsized Thorne T650 graphite fibers, where they investigated the effect of reaction conditions on the rate of electropolymerization. These involved parameters such as initial monomer and supporting electrolyte concentration, and applied voltage. They found that the rate of electropolymerization increased with the initial monomer concentration and the applied voltage up to the peak oxidation potential of pyrrole, beyond which a significant decrease in the rate occurred. Slight increase in electrolyte concentration had little impact on the rate of electropolymerization, while a sharp increase was recorded in the rate when the electrolyte concentration was raised in large amount. The morphology of the electropolymerized pyrrole was found to be highly porous and grainy. They observed that the individual single graphite fibre filament was completely covered with polypyrrole after about 30 seconds of electropolymerization [2].

In another study, it was found that the order of aqueous electropolymerization with respect to the monomer concentration and applied voltage varied slightly with the concentration and type of electrolyte used. The pH of the reaction medium decreased with increased reaction time. Correspondingly, the amount of polypyrrole coatings formed into Thorne T650/35 graphite fibers increased with decreased pH and increased reaction time. In fact, a sharp rise in the amount of polypyrrole coatings was observed at an approximate pH value of 3. Elemental analysis and infrared spectroscopy were used to show that supporting electrolyte was embedded in the coatings [4]. Another study involving aqueous electropolymerization of pyrrole on polyacrylonitrile(PAN)-based Zoltek untreated carbon fibers claims that coating process is reaction-limited and thus, weight gain increases linearly with time. However, it was found that the increase in reaction time caused the weight gain to become proportional to the square root of time. This led to the idea that diffusion of the monomer onto the reactive sites of the growing aggregates becomes the controlling mechanism. By the motivation from these observations, the study proposes the mechanism of electrocoating with a multiscale modelling approach [6].

Iroh and Yuan, also studied the surface property changes of unsized Thorne T650/35 and T300 carbon fibers resulting from the electrodeposition of polyamic acid. Scanning electron microscopy (SEM) analysis showed smooth, continuous and thick polyamic acid coatings. Electrodeposition of polyamic acid on graphite fibres did not result in a self-limiting film growth. Fourier transform infrared spectroscopy (FTIR) confirmed that the electrodeposited coatings possessed the same chemical structure and functionality as the bulk polymer, indicating that electrodeposition did not result in alteration of the polymer structure. Dynamic contact angle analysis (DCA) and thermogravimetric analysis (TGA) were also realized for the surface property change analyses. The surface energy of the coated T650/35 and T-300 fibres was found to be about 15% and 20% respectively, lower than that of the uncoated fibres [3].

Introduction of an interphase was achieved again by electrodeposition to improve the weak bonding strength between carbon fiber and polypropylene (PP) matrix. By evaluation of interlaminar shear strength and impact strength of the composites, it was found that composites with introduced composites showed higher mechanical properties than those of composites without interphase. Reactive polymers which have either anhydride or free acid functional group were used as interphase materials. It was stated that these polymers also behave as charge carrier in aqueous solution during the electrodeposition process. Weight gain on the carbon fibers was evaluated by changing process parameters such as concentration of solution, current density, and electrodeposition time [5].

Bismarck et al also used the electropolymerization technique to create coatings of poly methylmethacrylate (PMMA) and copolymer of methylmethacrylate and

carbazole [poly(MMA-co-Cz)] on PAN based untreated and unsized high tensile strength Tenax HTA 5000 carbon fibres. Photoelectron spectroscopy (XPS) was helpful in the investigation of surface chemical composition of the electrocoated fibers. Practical adhesion before and after coating of fibers was determined using the single fiber pull-out test, which confirmed improved adhesion strengths after electrodeposition [7].

Li et al made an effort to analyze the interface surface structure in carbon fiber reinforced polyetheretherketone (PEEK) composites. In order to analyze the surface functional groups forming on the unsized AS4 fiber, the fiber coated with PEEK, and the coated fiber that had experienced heat treatment at 400 °C, they used the interfacial FT-Raman spectra and were able to prove that the electron interaction at the boundary of graphite crystallites of a carbon fiber contributed much to the composite interfacial structure. PEEK coatings on carbon fibers were obtained by immersion in a chlorophenol solution of PEEK and de-gassing in a vacuum oven [8].

Drzal and Raghavendran showed that the adhesion can be improved in a range of 25-100 % by forming covalent linkages between the fiber and the matrix via grafting a polymer of appropriate compatibility, molecular weight (MW), and sufficient density onto the surface of the fiber. They grafted either low MW bisphenol-a polycarbonate (BPA-PC) or high MW PMMA onto the surface of oxidized IM7 carbon fiber tows. Microindentation tests were helpful in determining the interfacial shear strength (IFSS) values. Passivating the oxidized fiber surfaces via hydrogenation at elevated temperature, in order to decouple the effects of surface roughness and surface oxides on the interfacial adhesion, helped increasing IFSS values to a limited extent. It was also observed that the level of improvement in adhesion appeared to be independent of the MW of the grafted polymer. Examination of the fracture surfaces and failure mechanisms of the composites using transverse tensile tests revealed that the failure was cohesive in the matrix for the polymer grafted fiber composites, while it was adhesive for the ungrafted ones. Furthermore, it was seen that the failure mechanism changed after grafting, which indicates that the strain energy released from the grafted fiber composite during failure is higher than that of the ungrafted ones and that it is sufficient to rupture the polymer backing [9, 10].

Another work aimed at hypothesizing that carbon/nylon thermoplastic composites would have enhanced mechanical properties considering that the procedure of applying a thin coating of polyamide (PA) monomer to be in situ polymerized onto the surface of chopped carbon fibers would induce good fiber/matrix wetting [11].

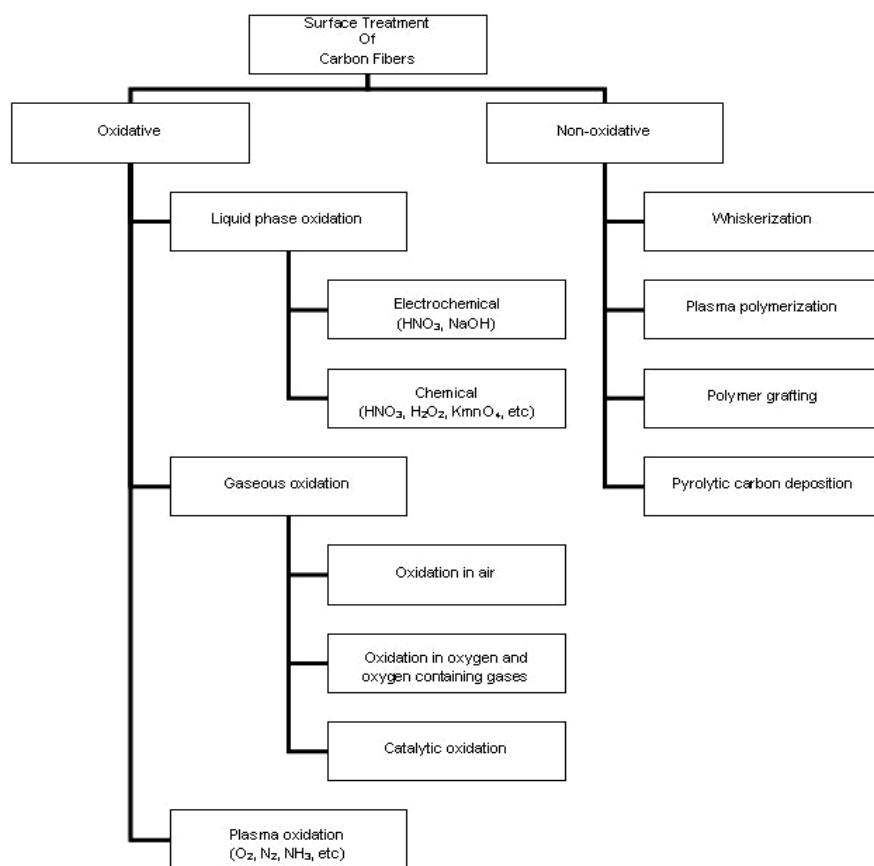


Chart 1. Treatment methods for carbon fibers [69].

Plasma

Jang demonstrated the effectiveness of cold plasmas of oxygen, nitrogen, argon, ammonia, and propylene in improving the interfacial adhesion between carbon fibers and matrix resins. A two-component bismaleimide, an epoxy, and a model thermoplastic resin PP were used as the matrices for composites. Oxygen and argon plasmas were found to promote mechanical keying by increasing the level of fiber surface roughness and porosity. The wettability of carbon fiber surface by the matrix resin was also enhanced by oxygen plasmas and to a lesser extent by argon plasmas, as evidenced by the increased total surface energies and their polar components. These surface energy increases were considered to be mainly due to the various oxygen-containing functional groups observed on the oxygen plasma-treated surface. For the cases of ammonia and combined ammonia/argon plasma treatments, possible chemical bonding between bismaleimide and the plasma-deposited amine groups was thought to be one important promoter

of interfacial bonding. In these cases increased wettability was also observed. Ammonia and ammonia/argon plasmas appeared to be more appropriate treatments for carbon-fiber/thermoset resin composites considering that they generally did not induce any appreciable reduction in fiber strength. In contrast, it was stated that excessively prolonged exposure of carbon fibers to oxygen, nitrogen or argon plasma could lead to a significant reduction in fiber strength. It was also seen that the plasma-polymerized PP deposited on the fiber surface was capable of improving the compatibility and adhesion between the fiber and the PP matrix [12].

Another study involving plasma oxidation treatment was via radio frequency (RF) glow discharge oxygen plasma in order to modify the surfaces of PAN-based and mesophase pitch-based carbon fibers. Surface chemical changes to the fibers were monitored by XPS and by fiber wetting studies evaluated in terms of dispersive-polar components of surface energy and acid-base contribution to the work of adhesion. Also, physical changes to the fibers were monitored using SEM. Stress transferability of the fibers was evaluated by the embedded single fiber test in PMMA, poly(ethyl methacrylate) (PEMA), poly(methacrylonitrile) (PMAN) and poly(vinyl chloride) (PVC) as these matrices offered varying degrees of dispersive-polar and acid-base character. Experimentally determined critical aspect ratios were compared to the theoretical work of adhesion determined by dispersive-polar interactions and with the Lewis acid-base nature of the matrices [13]. The effects of oxygen plasma treatment by using microwave (MW) plasma reactor on the surface properties of virgin (untreated and unsized) ultra-high modulus pitch-based and high strength PAN-based carbon fibers and the interfacial properties of their composites with polycarbonate (PC) were studied by Montes-Moran et al. Single fiber tensile test results revealed no substantial change in the fiber strength after oxidation. Single fiber fragmentation tests showed significant increase in interfacial shear strength after plasma treatment. A direct relation between the increase in interfacial strength and the increment of surface functional groups was established after surface characterization of the fibers by inverse gas chromatography (IGC), which was concluded to be the main reason for the improvement of the interfacial adhesion [14]. In their continuing study, they concluded that although appearing to be little selective, oxygen plasma can be efficient for improving the interaction with polymer matrices which do not exhibit either neat acidic or basic surface properties. They attributed the improvement in interfacial adhesion of amphoteric matrices such as PC to the creation of surface functionalities with various acid-base strength [15]. They continued their efforts selecting PC and polyamide 6 (PA 6) as matrices treating the carbon fibers using plasma oxidation. Characterizing the fiber surfaces by XPS and STM, and conducting fragmentation tests for mechanical properties, they decided working further with PC while they thought mechanical property improvement in PA 6 composite was much limited. Surface roughness was concluded to be the main responsible for the level of fiber/matrix adhesion in CF/PC composites [16].

Surface treatment

Besides coating and plasma treatments, compatible sizings have been applied widely onto carbon fibers for interfacial adhesion improvement. Matrices in these studies include thermoplastics such as PP and polysulfone (PSU) [17], liquid crystal polymer (LCP) [18], acrylic [19], polyethersulfone (PES) [20], J2 [21]. Short-beam shear (SBS), transverse flexural (TF) and transverse tensile tests were helpful for the determination of mechanical property improvement in composites after application of sizing [18]. To improve adhesion in carbon/acrylic composites, isocyanate urethane methacrylate and isocyanate urethane styrenic compounds have been synthesized and used as sizing agents on carbon fibres with the concept of difunctional chemical coupling agent. Interlaminar shear strength (ILSS) values were evaluated using SBS tests and pull-out tests were also used to evaluate the fibre/matrix adhesion. This study led to the conclusion that polymerization processing by electron beam irradiation can be further developed [19]. The role of sizing resin in carbon fibre/PES composites was obviously positive as determined by single fiber fragmentation tests. Analysis by time-of-flight secondary ion mass spectrometry suggested that this arises from a strong interaction between sizing resin, the fibre and the matrix [20]. Application of epoxy sizing on electrochemically treated PAN-based carbon fibers to form composites with J2, was investigated using the meso-indentation technique to quantify the interfacial quality. The transverse and shear strength values increased and the examination of fracture surfaces indicated a change to cohesive failure from adhesive [21]. Poly(vinyl pyrrolidone) (PVP) was introduced as sizing to high modulus sized AS4 carbon fibers from Grafil to form composites with Nylon 66, after removal of the commercial sizing. Transcrystallinity of the resulting morphology was studied using polarized hot-stage optical microscopy. Microdebond tests showed that transcrystallinity caused an increase in IFSS values [22]. Rosso et al investigated the interfacial effects on differently treated PAN-based high tenacity Tenax, Zoltek and Sigrafil carbon fibers and a new in-situ polymerized semicrystalline polyamide 12 (PA 12) matrix system. Fibers had the standard oxidative treatment, standard oxidative treatment with PA 12 compatible sizing, surface treatment with epoxy sizing from the companies and one set formed of virgin fibers. The failure mechanisms of the compounds were evaluated by examination of fracture surfaces using SEM after tensile and Charpy impact loading at room and cryogenic temperatures. The sizings were found to decrease the fiber surface tension and adhesion level to the matrix while oxidized fibers adhered better to PA 12 [24]. Thielmann et al calculated the thermodynamic work of adhesion values between untreated, oxidized, and oxidized and epoxy-sized carbon fibers and PC, PSU, and PEI matrices by measuring the dispersive and specific surface energetics of the individual components using IGC. The practical adhesion measurements were performed by conducting mechanical tests, i.e. IFSS values were determined by single fiber pull-out testing. The IGC surface energy experiments revealed a much higher dispersive surface energy for the oxidized fiber compared to the untreated sample, indicating that oxidation

creates a more active surface. The sized sample had the lowest dispersive surface energy due to the passivation of the surface from the epoxy-based sizing agent. Specific interactions showed a decrease in the basicity from the untreated to oxidized samples, while the acidity increased. The calculated works of adhesion correlated well with the IFSS values. For all three polymers, increase in both the work of adhesion and shear strength values was recorded after fiber oxidation. The sizing material did not significantly increase the shear strength despite a higher work of adhesion value, which was attributed to the incompatibility between the polymers and epoxy-based sizing agent [25]. With an effort to indicate the potential for clinical use in dental prostheses, mechanical properties and the quality of fiber/matrix adhesion in composites of PAN-based T300 carbon fiber tubes and PMMA were examined with the application of a developed sizing resin, which contained PMMA, butanediol dimethacrylate (BDMA) and MMA. Three-point bending tests were performed for flexural strength and modulus values, thermophysical analysis for linear coefficient of thermal expansion (LCTE) using thermo-mechanical analyzer (TMA) and examination of fracture surfaces after mechanical tests were done by SEM. The composites exhibited higher flexural strength with use of the developed matrix and sizing systems. The improved mechanical properties were attributed to the pre-polymerized PMMA content in the sizing [26]. Some works concentrated on the friction and wear properties of composites also involved fiber/matrix adhesion enhancement. Polytetrafluoroethylene (PTFE) composites filled with differently surface treated PAN-based carbon fibers, sliding against GCr15 steel under oil lubrication, were investigated on a reciprocating ball-on-disk UMT-2MT tribometer. Fibers were surface treated with air-oxidation, air-oxidation followed by rare earths (RE) treatment and RE (LaCl₃) treatment. The worn surfaces of the PTFE composites were examined using SEM. Experimental results revealed that surface treatment of carbon fibers reduced the wear of CF-reinforced PTFE composites. Among all the treatments to carbon fibers, RE treatment was the most effective and lowest friction and wear rate of CF-reinforced PTFE composite was exhibited, owing to the effective improvement of the interfacial adhesion between the carbon fibers and PTFE matrix [27, 28]. Another study focussed on Mode-I and Mode-II fracture toughness of the composites of unsized Toho G30-500 carbon fibers and newly developed phenylethynylphthalic anhydride terminated poly(etherimide) (PEI) oligomer, which were investigated by means of double cantilever beam (DCB) and end-notch flexure (ENF) tests. Towpregs were manufactured for the mechanical tests by a minimal dry powder prepregging system [23].

A systematic study of oxidative surface treatment of carbon fibers by wet, dry and anodic oxidation showed that in cases where thermosetting resins are used as the matrix, improvement of adhesion between fiber and matrix is caused by chemical interaction. The reactive surface oxides were identified by titration, desorption analysis and selective blocking treatment. The additional effect of sizing on adhesion between fiber and matrix was also shown by reinforcement of thermoplastics such as PP and PSU [17]. Interfacial adhesion

in unidirectional composites of UKN-01 braided carbon fiber fillers and PA 12 was investigated by Rashkovan and Korabel'nikov using the three-point bending method after electrochemical and O_3 treatments applied to reinforcements. Fiber and composite strengths were found to increase, but more with electrochemical treatment when compared to the initial state, which was explained by surface modification of fibers. They used an acoustic-emission apparatus to determine the scale relationships of fibers and shear strength on the phase interface [29]. Tibbetts and McHugh discussed the mechanical properties of vapor-grown carbon fiber(VGCF)/nylon and VGCF/PP composites. They increased infiltration of fibers by polymers via ball milling, and also recognized that fiber surface treatments such as air-etching and coverings with low concentrations of aromatics caused improvement in properties [30]. Raghavendran et al investigated the effect of surface chemistry and rugosity on the interfacial adhesion between BPA-PC and a PAN based intermediate modulus IM7 carbon fiber surface subjected to surface treatment to add surface oxygen groups. The oxidative surface treatment also caused an increase in surface roughness by creating pores and fissures in the surface by removing carbon from the regions between the graphite crystallites. The results of interfacial adhesion via microindentation tests indicated that an increase in the oxygen content of the fiber does not increase the interfacial adhesion significantly. Comparing adhesion results between oxidized and hydrogen passivated fibers showed that the effect of the surface roughness on the interfacial adhesion is also insignificant. Overall, dispersive interactions alone appeared to be the primary factor in adhesion of carbon fibers to thermoplastic matrices in composites [31]. Other oxidative treatment studies involved the use of PC, PSU, PEI, and PTFE as thermoplastic matrices [25, 27, 28]. Ibarra et al studied the mechanical and dynamic properties of oxidized PAN based carbon fiber and butadiene-styrene thermoplastic elastomer (SBS) composites as a function of the level of fiber oxidation in comparison with the untreated commercial carbon fiber. They concluded that an optimisation is required to achieve interfacial adhesion improvement [32].

Meretz et al studied the influence of morphology and especially transcrystallinity on the fiber/matrix adhesion in composites of high-modulus (HM) and high-strength (HS) carbon fibers subjected to different thermal treatments and poly(phenylene sulphide) (PPS) matrix. Conclusion involved that transcrystallinity led to brittle fracture behaviour and higher apparent shear strength values [33]. Other thermal oxidation studies involved knitted and sized T300 CF/PEMA composites [34], and PEEK and PES as matrices. IFSS was observed to increase while fiber surface free energy was found to decrease [35]. CF/PA 12 composites with different fiber thermal treatments to obtain acidic and basic surfaces were examined by Bismarck et al via contact angle and zeta-potential measurements, and single fiber tensile and fragmentation tests [36]. Ramanathan et al worked on heat treated HM and HS CFs and PPS as matrix

using ESCA and single-fiber pull-out tests [37], and compared epoxy and PPS as matrices using microindentation technique [38].

Electrochemical fiber treatment studies include the use of PP, PSU, copolymers of ethylene and methacrylic acid (E-MAA), J2, PA 12, etc as thermoplastic matrices [17, 39, 40, 21, 41]. Bismarck et al studied the effect of anodic oxidation of HS CFs on the adhesion properties to PC by SEM, XPS, and EDX analyses, contact angle and zeta-potential measurements, and single-fiber tensile and microdroplet pull-off tests. They detected oxygen containing surface functional groups and slightly smoother CF surfaces as a result of oxidation. Although a decrease in water contact angle appears after oxidation, remaining of direct wetting contact angle of PC melt-droplets and thermodynamic work of adhesion almost unchanged pointed out that no evident relation could be found between the anodically oxidation time and IFSS of fibers [42]. Lee and Drzal also examined the effect of electrochemical oxidation on the adhesion of CFs to PC utilizing XPS, STM, and single fiber fragmentation test [43]. Rashkovan and Korabel'nikov studied the effect of electrochemical, O₃, and cryogenic treatments on scale dependence of the strength of high-tenacity UKN-01 carbon fiber and its adhesion to matrices EDT-10 epoxy and PA 12 [41].

Chemical treatment of CFs were realized for use with matrices PP, PSU, E-MAA, polyethernitrile (PENI), and tetraethylenepentamine (TEPA) [17, 39, 40, 44, 45]. Use of nitric acid and hydrogen peroxide solutions as oxidizing agent resulted in improvements in both ILSS and transverse flexural strength (TFS) while longitudinal flexural strength of CF/PENI remained the same [44].

A copolymer of trioxane-1,3,5 with dioxolan-1,3 (TDC) was used as thermoplastic matrix to be reinforced with hydrated cellulose based CFs to study the effect of fiber treatment with organosilicon finishes (polyalkyloxysilanes) via solution impregnating. Increase in composite tensile strength, elastic modulus, and notch toughness and improvement in its tribological characteristics were recorded [46]. A special treatment applied to CFs promoted adhesion to PC allowing for use in injection molding manufacturing technique [47]. PC and PES were used as matrices with commercial, oxygen and O₃ treated CFs where composites with PES showed considerable increase in ILSS and processing temperature was found to be an important factor [48, 49]. Effect of different treatments applied to PAN-based high tenacity CFs on the adhesion quality with PA 12 was also evaluated [24]. Another study by Zhandarov et al concentrated on the effect of electric fields and charges on the UKN-P CF/PE and CF/PC adhesion resulted in indicating its significant effect on bonding between monofilament and matrix [50].

MATRIX MODIFICATION

Matrix modification studies are grouped under this topic. They include mostly the effects of different MWs, the use of matrix modifiers and compatibilizers. Some of the matrix studies investigate the effects of crystallinity as well.

Venderbosch et al studied the application of poly(2,6-dimethyl-1,4-phenylene ether) (PPE), which is an amorphous thermoplastic exhibiting a high glass transition temperature (T_g) (220 °C) and outstanding mechanical properties (toughness), as a matrix material for continuous carbon fibre reinforced composites. However, due to the limited thermal stability at temperatures above T_g , PPE can be regarded as an intractable polymer, thus its introduction in a composite structure via a melt impregnation route is not feasible. Therefore, in their investigation they developed a solution impregnation route using epoxy resin as a reactive solvent. It was stated that formation of epoxy 'interlayer' at the fibre surface as a result of initiation of phase separation upon curing, can provide a high level of interfacial adhesion. A preliminary investigation of the resulting composite materials revealed outstanding mechanical properties (mode-II interlaminar toughness and strength) [51-53].

Adhesion of BPA-PC to CF was studied by Raghavendran et al by varying properties such as MW, processing conditions, and test temperature. It was seen that processing methods and conditions had significant effect on adhesion as measured by the IFSS. Commercial grade Lexan 141 solvent was deposited onto carbon fibers, which had to be optimised for processing between glass transition temperature and a limiting higher temperature. Melt consolidated pure PC specimens showed increases in adhesion both with increasing processing temperature and with time. Pure PC had to be above a critical MW, where exhibited a higher adhesion at different processing conditions [54]. Dányádi et al treated anodically oxidized carbon fibers with four different coupling agents containing epoxy, anhydride, and isocyanate functionality. The bonding of the coupling agents to the fiber surface was determined by dissolution experiments, while the chemical composition of the surface was studied by diffuse reflectance infrared spectroscopy (DRIFT). The effect of surface coverage, processing temperature and molecular weight on IFSS was determined by fragmentation. They stated that the organofunctional group of the coupling agents reacts with the chain-end hydroxyl groups of PC, and it is limited, significantly lower than the concentration of reactive groups available on the surface of the coated fiber. Consequently, it was decided that interfacial interaction can be improved only to a limited extent in PC/CF composites, and that it is similar in IFSS with the three coupling agents reacting with the polymer. The agent containing anhydride functionality did not enter into coupling reactions with PC. Interfacial adhesion increased with processing temperature, which could be explained by the increased rate of reaction. The effect of MW on interfacial adhesion was not clear in the study [55]. Nogueira et al aimed at evaluating the fiber/matrix interface of CF reinforced PP-based matrices after tensile and impact tests. CF reinforcements were in the form of plain weave fabric and four different PP matrices were used; PP, polypropylene-polyethylene copolymer (PP-PE), PP-PE with an interfacial compatibilizer (AM1), and PP-PE containing an elastomeric modifier (AM2). CF/PP-PE-

AM1 composites had the lowest impact strength and the highest tensile strength values, while CF/PP-PE-AM2 specimens showed a lower tensile strength and higher impact strength values compared to the prior. CF/PP-PE and CF/PP presented the lowest impact strength values [56].

Tohgo et al investigated the influence of matrix resin on tensile strength properties and splitting fracture toughness in unidirectional carbon fiber-reinforced plastic laminates. Tensile tests and splitting fracture toughness tests were carried out on two kinds of thermoplastic composites; 3KCF/Nylon 6 and 3KCF/modified Nylon. The modified Nylon was developed to improve the adhesion on the basis of Nylon 6. The performance of the present composites was discussed in comparison with that of AS4/3501-6 carbon/epoxy system. On all the unidirectional composites, the splitting fracture toughness under pure mode II was higher than that under pure mode I and the splitting was controlled by the tensile stress intensity in the wide range from pure mode I to mixed-mode loading. The fracture toughness for splitting in the specimens was drastically increased by changing matrix resin from epoxy to Nylon 6, and furthermore by modified Nylon [57].

Studies on the effects of polymer MW went on with the use of PEEK, BPA-PC, and PC as thermoplastic matrices [58, 59, 60, 54, 55]. Hine et al examined the effects of the polymer MW, the strength of the fibre/matrix bond and the volume fraction of the fibre on the fracture behaviour of unidirectional CF/PEEK composites. DCB testing geometry was used throughout the fracture study and cracks were mainly propagated parallel to the individual laminates (interlaminar fracture). Varying the MW reinforced the link between matrix ductility and fracture behaviour, established in their previous work, with the highest toughness for the CF/PEEK system measured for the composite with the high MW matrix. The composite treated to obtain low fibre/matrix adhesion showed a reduction in toughness by limiting the energy absorption of the matrix phase. However the increase in damage and appearance of fibre/matrix debonding may account for the good crack stability seen in the material, even at low temperatures. Finally results were presented for the effect of fibre volume fraction, and it was shown that the change in behaviour is directly related to the amount of matrix material available [58]. Raghavendran et al focussed on investigation of the effect of processing conditions (processing temperature, residence time at melt temperature and cooling rate) and the MW of an amorphous thermoplastic resin on the interfacial adhesion between BPA-PC and CF. The study was conducted using the fragmentation test on single fiber specimens. The results showed a significant influence of consolidation time and temperature on interfacial adhesion, with improvement resulting from increasing both. Increases of 16% to 35% in IFSS were seen for different MW ranges. Slowly cooled matrix specimens showed evidence of shear band formation in both polarized and unpolarized light microscope observations. Rapidly cooled specimens appeared to fail by stick-slip interfacial cracking accompanied by some matrix deformations. Interfacial adhesion studies with pure PC in

different MW ranges were also conducted. The results showed that the interfacial adhesion is dependent upon the matrix properties and there is an increase in IFSS with increase in MW of the matrix [59, 60, 54].

Effect of transcrystallinity in CF/PEEK composites was investigated by Zhang et al. They prepared composites with and without transcrystalline interphase under different conditions and examined its effect on the tensile behaviour of semicrystalline composites. As a result, it was found to improve tensile stiffness, strength, and toughness, and therefore enhance the fiber/matrix adhesion, reduce stress concentration and cavitation at fiber ends. It was observed that deformation mechanism of the composites changed from cavitation to shearing process, and significant local plastic deformation that absorbs more energy occurred, resulting in cohesive failure of the composite instead of adhesive that took place in the composite without transcrystalline interphase [61]. Ramanathan et al evaluated the energy release rate (ERR) of the fiber/matrix interface in composites of pitch-based HM-HS and HM CF, and PAN-based HM and HS CF with amorphous PC, semicrystalline PP and PPS by interfacial crack propagation arising in the single-fiber pull-out test, and discussed the crack propagation at the fiber/matrix interface with different matrix morphology using the photo-elastic pattern observed utilizing polarization microscope. Effect of crystalline phase in the polymer affected the crack propagation and the photo-elastic patterns at the crack propagation as follows: Blunt crack tip was observed in the semicrystalline polymer, which makes it unable to measure the crack length and subsequently the ERR. In amorphous polymer, PC was provided with a good and visible crack propagation, the measurement of crack length and ERR. The evaluated ERR was independent of crack length with CF/PC systems. The initial increment in ERR as a function of crack length may have been caused by the inhomogeneous stress distribution in the fiber-matrix interphase due to the meniscus. The crack was initiated at the entrance of the fiber in the matrix and propagated towards the fiber ends inside the matrix [62].

NANOSCALE STUDIES

Nanoscale studies focussing on fiber/matrix adhesion mainly involved grafting and other different treatments such as thermal and oxidative treatments.

Finegan et al used PP as thermoplastic matrix and Pyrograph carbon nanofibers (CnF) to which they applied heat treatment at high temperatures (to obtain more graphitic nanofibers), wet treatments of DH (diamine salt of carboxylic acid, high), DL (diamine salt of carboxylic acid, low), EH (epoxy, high), and EL (epoxy, low) and oxidation treatments by air-etching and CO₂. Mini-tensile test specimens were manufactured by injection molding. Data obtained for tensile strength and modulus of composites revealed that more graphitic fibers adhered poorly to PP, that air or CO₂ oxidation may improve interfacial adhesion to some extent as a result of increase in surface area and free energy of nanofibers, and that the two chemically active coatings did not increase tensile stiffness while somewhat decreased the strength [63].

Another study attempted on developing composites of polycarbonate urethane (PCU) and multiwalled carbon fibers with four different diameter in the range of 60-200 nm were manufactured into discs via uniaxial pressing for cytocompatibility studies to be used in neural prostheses. Results provided the first evidence of decreased adhesion of astrocytes (glial scar tissue-forming cells) with increasing weight percents of the high surface energy carbon nanofibers in the polymer composite; this further demonstrated that formulations containing carbon fibers in the nanometer regime could limit astrocyte functions leading to decreased glial scar tissue formation. Positive interactions with neurons, and, at the same time, limited astrocyte functions leading to decreased gliotic scar tissue formation were found to be essential for increased neuronal implant efficacy [64].

Oh et al grafted amorphous and semicrystalline polyetherketones (PEK) to the surface of either an as-received multi-walled carbon nanotube (MWNT) or a vapor-grown carbon nanofiber (VGCNF) in polyphosphoric acid (PPA) via direct covalent attachment with optimized phosphorous pentoxide (P_2O_5) content. Soxhlet extraction experiment, the spectra from FT-IR spectroscopy and the clear images from high-resolution transmission electron microscopy showed that the covalent attachment was effective in uniformly coating the PEK grafts on the surfaces of both MWNT and VGCNF. Additionally, a drastic increase in solution viscosity due to the formation of giant molecules was monitored during polymerization. As such, the resulting nanocomposites were easily fabricated via a simple compression molding technique. The alignment possibility of MWNT and VGCNF grafted with semicrystalline PEK in these thermoplastic nanocomposites via solution fiber spinning was also demonstrated [65].

McIntosh et al stated that in creating nanocomposite fiber systems, the issues of dispersion and nanotube-matrix interaction and adhesion become of utmost importance when improved mechanical properties are anticipated. In addressing these issues, it was found that sidewall chemical functionalization can be an effective tool for improving both the dispersion and interaction between the nanotube and the matrix. Their work evaluated the effect of sidewall functional groups on fluorinated single-walled carbon nanotubes (F-SWNTs) as a precursor for improved interfacial adhesion in PP via partial defluorination of the F-SWNTs. The partial removal of functional groups from the F-SWNTs during melt processing with PP by shear mixing provided the opportunity for in situ direct covalent bonding between the nanotubes and the matrix during melt processing which ultimately resulted in better mechanical reinforcement of the composite. The study demonstrated that in comparison with PP composites filled with purified nanotubes (P-SWNTs), improved dispersion, interfacial adhesion, and mechanical properties are achieved for F-SWNT-loaded matrices due to chemical functionalization [66].

CONCLUSION

Review of the literature including efforts for the improvement of fiber/matrix interfacial adhesion point out that this study field will continue being an important area with the ongoing developments in the composite materials. Our study seems to have a property of reviewing only the literature related with the interaction between carbon fibers and thermoplastic matrices when compared to other reviews summarizing interfacial adhesion studies. It covers studies involving the methods used for the enhancement of carbon fiber/thermoplastic matrix interfacial adhesion and consequently for the improvement of the properties of their composites. This gives the opportunity to figure out which improvement technique was used with which thermoplastic matrix material for enhancing the compatibility with carbon fibers.

REFERENCES

- 1 Iroh J.O, Bell J.P, Scola D.A, Wesson J.P. Electrochemical process for preparing continuous graphite fibre-thermoplastic composites. *Polymer* 1994; 35 (6): 1306-11.
- 2 Grunden B, Iroh J.O. Formation of graphite fibre-polypyrrole coatings by aqueous electrochemical polymerization. *Polymer* 1995; 36 (3): 559-63.
- 3 Iroh J.O, Yuan W. Surface properties of carbon fibres modified by electrodeposition of polyamic acid. *Polymer* 1996; 37 (18): 4197-4203.
- 4 Iroh J.O, Wood G.A. Effect of electrolytes on the kinetics and mechanism of the electropolymerization of pyrrole on to carbon fibers. *Eur Polym J* 1997; 33 (1): 107-114.
- 5 Kim M, Kim J, Kim W, Choi Y, Hwang B. Fabrication of PP/carbon fiber composites by introducing reactive interphase and its properties. *Polymer (Korea)* 2000; 24 (4): 556-63.
- 6 Lin B, Surehkumar R, Kardos J.L. Electropolymerization of pyrrole on PAN-based carbon fibers: Experimental observations and a multiscale modeling approach. *Chemical Engineering Science* 2001; 56: 6563-75.
- 7 Bismarck A, Lee A.F, Saraç A.Z, Schulz E, Wilson K. Electrocoating of carbon fibres: A route for interface control in carbon fibre reinforced poly methylmethacrylate? *Composites Science and Technology* 2005; 65: 1564-73.
- 8 Li T.Q, Zhang M.Q, Zeng H.M. Strong interaction at interface of carbon fiber reinforced aromatic semicrystalline thermoplastics. *Polymer* 1999; 40: 4307-13.
- 9 Raghavendran V.K, Drzal L.T. Fiber-Matrix Interfacial Adhesion Improvement in Carbon Fiber-Bisphenol-A Polycarbonate Composites by Polymer Grafting. *The Journal of Adhesion* 2002; 78: 895-922.
- 10 Drzal L.T, Raghavendran V.K. Adhesion of thermoplastic matrices to carbon fibers: Effect of polymer molecular weight and fiber surface chemistry. *Journal of Thermoplastic Composite Materials* 2003; 16: 21-30.
- 11 O'Connor J.E, Lewis A.F. On the enhancement of carbon fiber/nylon matrix adhesion via in situ polymerized coatings. *Am Chem Soc Div Org Coat Plast Chem Prepr* 1977; 37 (1): 751-7.
- 12 Jang B.Z. Control of interfacial adhesion in continuous carbon and kevlar fiber reinforced polymer composites. *Composites Science and Technology* 1992; 44 (4): 333-49.
- 13 Bourgeois P, Davidson T. Plasma modifications to the interface in carbon-fiber-reinforced thermoplastic matrices. *The Journal of Adhesion* 1994; 45: 73-88.
- 14 Montes-Morán M.A, Matínez-Alonso A, Tascón J.M.D, Paiva M.C, Bernardo C.A. Effects of plasma oxidation on the surface and interfacial properties of carbon fibres/polycarbonate composites. *Carbon* 2001; 39: 1057-68.
- 15 Montes-Morán M.A, Matínez-Alonso A, Tascón J.M.D. Adsorption of polar probe molecules on plasma-oxidised high-strength carbon fibres. *Fuel Processing Technology* 2002; 77-78: 359-64.

- 16 Montes-Morán M.A, van Hattum F.W.J, Nunes J.P, Matínez-Alonso A, Tascón J.M.D, Bernardo C.A. A study of the effect of plasma treatment on the interfacial properties of carbon fibre–thermoplastic composites. *Carbon* 2005; 43: 1778-1814.
- 17 Fitzer E, Weiss R. Effect of surface treatment and sizing of C-fibres on the mechanical properties of CFR thermosetting and thermoplastic polymers. *Carbon* 1987; 25 (4): 455-67.
- 18 Blackketter D.M, Upadhyaya D, King T.R, King J.A. Evaluation of fiber surfaces treatment and sizing on the shear and transverse tensile strengths of carbon fiber-reinforced thermoset and thermoplastic matrix composites. *Polymer Composites* 2004; 14 (5): 430-6.
- 19 Thomas Y, Parisi J.P, Boutevin B, Beziers D, Chataignier E, Désarmot G. Improvement of fibre/matrix bonding in carbon-fibre/acrylic composites by electron-irradiation: Concept of difunctional chemical coupling agent. *Composites Science and Technology* 1994; 52 (3): 299-307.
- 20 Yumitori S, Wang D, Jones F.R. The role of sizing resins in carbon fibre-reinforced polyethersulfone (PES). *Composites* 1994; 25 (7): 698-705.
- 21 Chang Y.S, Lesko J.J, Case S.W, Dillard D.A, Reifsnider K.L. The effect of fiber-matrix interphase properties on the quasi-static performance of thermoplastic composites. *Journal of Thermoplastic Composite Materials* 1994; 7 (4): 311-24.
- 22 Clark Jr R.L, Kander R.G, Sauer B.B. Nylon 66/poly(vinyl pyrrolidone) reinforced composites: 1. Interphase microstructure and evaluation of fiber–matrix adhesion. *Composites: Part A* 1999; 30: 27-36.
- 23 Bullions T.A, Mehta R.A, Tan B, McGrath J.E, Kranbuehl D, Loos A.C. Mode I and Mode II fracture toughness of high-performance 3000 g mole⁻¹ reactive poly(etherimide)/carbon fiber composites. *Composites: Part A* 1999; 30: 153-62.
- 24 Rosso P, Friedrich K, Wolny A. Evaluation of the adhesion quality between differently treated carbon fibers and an in-situ polymerized polyamide 12 system. *Journal of Macromolecular Science: Part B – Physics* 2002; B41: 745-59.
- 25 Thielmann F, Burnett D, Bismarck A. Measuring adhesion phenomena between carbon fibers and model polymer matrices. *International SAMPE Symposium and Exhibition (Proceedings)* 2005; 50: 1551-8.
- 26 Segerström S, Ruyter I.E. Mechanical and physical properties of carbon–graphite fiber-reinforced polymers intended for implant suprastructures. *Dental Materials* 2007; 23 (9): 1150-6.
- 27 Qian-qian S, Xian-hua C. On the friction and wear behavior of PTFE composite filled with rare earths treated carbon fibers under oil-lubricated condition. *Wear* 2006; 260: 1243-7.
- 28 Bao D, Cheng X, Evaluation of Tribological Performance of PTFE Composite Filled with Rare Earths Treated Carbon Fibers under Water-Lubricated Condition. *Journal of Rare Earths* 2006; 24 (5): 564-8.
- 29 Rashkovan I.A, Korabel'nikov Y.G. Realization of properties of the fibrous reinforcement in unidirectional thermoplastic composites. *Mekhanika Kompozitnykh Materialov* 1993; 29 (1): 61-5.
- 30 Tibbetts G.G, McHugh J.J. Mechanical properties of vapor-grown carbon fiber composites with thermoplastic matrices. *Journal of Materials Research* 1999; 14 (7): 2871-80.
- 31 Raghavendran V.K, Drzal L.T, Askeland P. Effect of surface oxygen content and roughness on interfacial adhesion in carbon fiber-polycarbonate composites. *J. Adhesion Sci. Technol.* 2002; 16 (10): 1283-1306.
- 32 Ibarra L, Macías A, Palma E. Mechanical and viscoelastic properties of butadiene-styrene thermoplastic and oxidized carbon fibre composites. *Polymer International* 1996; 40: 169-78.
- 33 Meretz S, Auerch W, Marotzke C, Schulz E, Hampe A. Investigation of morphology-dependent fracture behaviour with the single-fibre pull-out test. *Composites Science and Technology* 1993; 48: 285-90.
- 34 Mayer J, Giorgetta S, Koch B, Wintermantel E, Patscheider J, Spescha G. Characterization of thermally oxidized carbon fibre surfaces by ESCA, wetting techniques and scanning probe microscopy, and the interaction with polyethylmethacrylate. Development of a biocompatible composite material. *Composites* 1994; 25 (7): 763-9.

- 35 Wu G. Effects of carbon fiber treatment on interfacial properties of advanced thermoplastic composites. *Polymer Journal* 1997; 29 (9): 705-7.
- 36 Bismarck A, Richter D, Wuertz C, Springer J. Basic and acidic surface oxides on carbon fiber and their influence on the expected adhesion to polyamide. *Colloids and Surfaces A: Physicochemical and Engineering Aspects* 1999; 159: 341-50.
- 37 Ramanathan T, Bismarck A, Schulz E, Subramanian K. The use of a single-fibre pull-out test to investigate the influence of acidic and basic surface groups on carbon fibres on the adhesion to poly(phenylene sulfide) and matrix-morphology-dependent fracture behaviour. *Composites Science and Technology* 2001; 61: 1703-10.
- 38 Ramanathan T, Bismarck A, Schulz E, Subramanian K. Investigation of the influence of surface-activated carbon fibres on debonding energy and frictional stress in polymer-matrix composites by the micro-indentation technique. *Composites Science and Technology* 2001; 61: 2511-8.
- 39 Shah R.J, Belfiore L.A. Interfacial adhesion between ionomers and carbon fibres. *Polymeric Materials Science and Engineering, Proceedings of the ACS Division of Polymeric Material* 1987; 56: 68-72.
- 40 Belfiore L.A, Shah R.J, Cheng C. Interfacial adhesion between ionic copolymers and high-modulus surface-treated carbon fibers. *Polymer Composites* 1989; 10 (2): 122-33.
- 41 Rashkovan I.A, Korabel'nikov Y.G. The effect of fiber surface treatment on its strength and adhesion to the matrix. *Composites Science and Technology* 1997; 57: 1017-22.
- 42 Bismarck A, Kumru M.E, Song B, Springer J, Moos E, Karger-Kocsis J. Study on surface and mechanical fiber characteristics and their effect on the adhesion properties to a polycarbonate matrix tuned by anodic carbon fiber oxidation. *Composites: Part A* 1999; 30: 1351-66.
- 43 Lee J, Drzal L.T. Surface characterization and adhesion of carbon fibers to epoxy and polycarbonate. *International Journal of Adhesion & Adhesives* 2005; 25: 389-94.
- 44 Itoi M, Yamada Y, Pipes R.B. Effect of surface treatment of pitch-based carbon fiber on mechanical properties of polyethernitrile composites. *Polymer Composites* 1992; 13 (1): 15-29.
- 45 Pittmann Jr C.U, He G.R, Wu B, Gardner S.D. Chemical modification of carbon fiber surfaces by nitric acid oxidation followed by reaction with tetraethylenepentamine. *Carbon* 1997; 35 (3): 317-31.
- 46 Bashtannik P.I, Kabak A.I, Chervakov O.V. Study of the effect of the dressing of carbon fibers on the properties of carbon-fiber-reinforced plastics based on polyacetals. *Mechanics of Composite Materials* 1997; 33 (1): 64-9.
- 47 Kompalik D, Schmid B. Injection molding of carbon-fiber-reinforced polycarbonate. *IPE. Industrial & production engineering* 1988; 12 (3): 26-9.
- 48 Krekel G, Hüttinger K.J, Hoffman W.P. The relevance of the surface structure and surface chemistry of carbon fibres in their adhesion to high temperature thermoplastics. Part II. Surface chemistry. *Journal of Materials Science* 1994; 29: 3461-8.
- 49 Krekel G, Zielke U.J, Hüttinger K.J, Hoffman W.P. The relevance of the surface structure and surface chemistry of carbon fibres in their adhesion to high temperature thermoplastics. Part III. Interface adhesion and reinforcement effects. *Journal of Materials Science* 1994; 29: 3984-92.
- 50 Zhandarov S.F, Dovgyalo V.A, Pisanova E.V, Mironov V.S. Effect of electric fields and charges on the adhesion interaction between components of polymer fibrous composites. *Mekhanika Kompozitnykh Materialov* 1993; 2: 267-73.
- 51 Venderbosch R.W, Nelissen J.G.L, Peijs A.A.J.M, Lemstra P.J. Polymer blends based on epoxy resin and polyphenylene ether as a matrix material for high-performance composites. *Proceedings of the International Conference on Advanced Composite Materials* 1993; 837-42.
- 52 Venderbosch R.W, Meijer H.E.H, Lemstra P.J. Processing of intractable polymers using reactive solvents: 2. Poly (2,6-dimethyl-1,4-phenylene ether) as a matrix material for high performance composites. *Polymer* 1995; 36(6): 1167-78.

- 53 Venderbosch R.W, Peijs T, Meijer H.E.H, Lemstra P.L. Fibre-reinforced composites with tailored interphases using PPE/epoxy blends as a matrix system. *Composites: Part A* 1996; 27A: 895-905.
- 54 Raghavendran V.K, Waterbury M.C, Rao V, Drzal L.T. Influence of matrix molecular weight and processing conditions on the interfacial adhesion in bisphenol-A polycarbonate/carbon fiber composites. *Journal of Adhesion Science and Technology* 1997; 11 (12): 1501-12.
- 55 Dányádi L, Gulyás J, Pukánszky B. Coupling of carbon fibers to polycarbonate: Surface chemistry and adhesion. *Composite Interfaces* 2003; 10 (1): 61-76.
- 56 Nogueira C.L, de Paiva J.M.F, Rezende M.C. Effect of the interfacial adhesion on the tensile and impact properties of carbon fiber reinforced polypropylene matrices. *Materials Research* 2005; 8 (1): 81-9.
- 57 Tohgo K, Hirako Y, Ishii H. Influence of resin on splitting fracture toughness in unidirectional CFRP. *Nippon Kikai Gakkai Ronbunshu, A Hen/Transactions of the Japan Society of Mechanical Engineers, Part A* 1995; 61 (585): 959-64.
- 58 Hine P.J, Brew B, Duckett R.A, Ward I.M. Failure mechanisms in carbon fibre reinforced poly(ether ether ketone). II: Material variables. *Composites Science and Technology* 1990; 40 (1): 47-67.
- 59 Raghavendran V.K, Waterbury M.C, Drzal L.T. Effects of processing conditions and molecular weight of the resin on the interfacial adhesion in polycarbonate/carbon fiber composites. *Proceedings of the American Society for Composites* 1994; 12-9.
- 60 Drzal L.T, Raghavendran V.K. Adhesion of carbon fibers to polycarbonate matrices-interphase composition and structure. *Annual Technical Conference - ANTEC, Conference Proceedings* 1995; 2: 2877-81.
- 61 Zhang M, Xu J, Zhang Z, Zeng H, Xiong X. Effect of transcrystallinity on tensile behaviour of discontinuous carbon fibre reinforced semicrystalline thermoplastic composites. *Polymer* 1996; 37 (23): 5151-8.
- 62 Ramanathan T, Schulz E, Subramanian K. Determination of Energy Release Rate in Carbon Fiber-Thermoplastic Composites and Comparison of Crack Propagation in Amorphous and Crystalline Interface By Single Fiber Pullout Test. *Journal of Reinforced Plastics and Composites* 2004; 23 (15): 1639-50.
- 63 Finegan I.C, Tibbetts G.G, Glasgow D.G, Ting J.M, Lake M.L. Surface treatments for improving the mechanical properties of carbon nanofiber/thermoplastic composites. *Journal of Materials Science* 2003; 38: 3485-90.
- 64 McKenzie J.L, Waid M.C, Shi R, Webster T.J. Decreased functions of astrocytes on carbon nanofiber materials. *Biomaterials* 2004; 25: 1309-17.
- 65 Oh S, Lee H, Keum D, Lee S, Wang D.H, Park S, Tan L, Baek J. Multiwalled carbon nanotubes and nanofibers grafted with polyetherketones in mild and viscous polymeric acid. *Polymer* 2006; 47: 1132-40.
- 66 McIntosh D, Khabashesku V.N, Barrera E.V. Nanocomposite fiber systems processed from fluorinated single-walled carbon nanotubes and a polypropylene matrix. *Chem. Mater.* 2006; 18: 4561-9.
- 67 J. Kim, Y. Mai. *Engineered Interfaces in Fiber Reinforced Composites*, Elsevier, 1998.
- 68 Drzal L.T and Herrera-Franco P.J. *Measurement Methods for Fiber-Matrix Adhesion in Composite Materials in Adhesion Science And Engineering – I: The Mechanics of Adhesion*, Dillard D.A and Pocius A.V, Elsevier, 2002.
- 69 Tang L, Kardos J.L. A Review of Methods for Improving the Interfacial Adhesion Between Carbon Fiber and Polymer Matrix. *Polymer Composites*, 1997; 18 (1): 100-13.
- 70 Yıldız H, Baltacı A, Erden S, Sarıkanat M, Karbon Fiberlerin Elektrokaplanması, Ebiltem Proje Pazarı, 2005.

THE INFLUENCE OF CLOTHES WEAR FACTORS ON THE BENDING RIGIDITY OF LAMINATES

V. MASTEIKAITE^{1,2}, V. SACEVIČIENE¹

¹Kaunas University of Technology

²Siauliai University

ABSTRACT

Fabric stiffness is one of the most important parameter estimating textile materials wear and comfort properties. For laminates bending rigidity evaluation we have used compressed loop method and three different wear factors: specimens' dry cleaning, fatigue with tension, bending and tearing, and fatigue with shearing. The results indicate that coated fabrics and laminates bending properties depends on wearing conditions and their structural features, such as textile layer structure, film and textile layers thickness and type of layers bonding. Most of laminates showed large differences of anisotropy in various cutting direction and when they were bend on the film and the base fabric side. Also it was observed the breaking areas of film layer during fatigue of some laminates.

Keywords: laminates, fatigue, tension, shearing, dry cleaning, bending rigidity

1. INTRODUCTION

Laminated or coated fabrics are technical textile products and are defined as materials composed of two or more layers, at least one of which is a textile fabric and one or more polymer film layers. The presence of film layer changes all fabric's properties and behavior during its deformation. A principal requirement for all garments is comfort in all its interpretations. Protective clothes are used to protect the human body from various factors. Also they must be flexible without restricting body movements. After mechanical and chemical treatments which took place during clothes wearing laminates deformation properties may be changed. Review of literature indicated that selection of the laminates for the clothes is often based on their strength, tensile, tear, surface and permeability properties [1, 2, 3, 4]. There is a lack of works devoted to the stiffness investigation of clothing laminates. A high stiffness could be a disadvantage to the comfort. The bending rigidity of laminate is very important in some parts of the clothes, especially where additionally seams are used: behind trousers legs, under arm. Also the laminates rigidity is important in such parts of clothes, as below the hip line in bodies' front, back of knee and others. During some wearer movements the shape of clothes deformations may be similar to wave: the laminate is bending on both sides simultaneously (Figure 1).

Taking into account the increased applying of laminates for the protective clothes the researches investigate not only initial laminates rigidity, but also the influence of various treatments to their rigidity change [6].

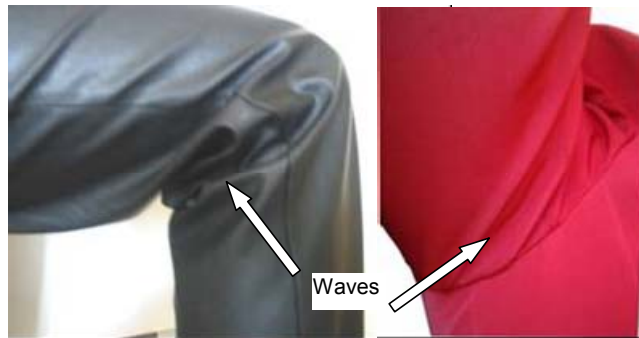


Figure 1. Deformation of Garments Parts in Wear Process (Photo of Authors)

For determining the laminates' bending rigidity more often is used the cantilever test [4, 5, 6].

The goal of this research was to choose new method for laminates stiffness evaluation and to investigate the influence of laminates dry cleaning and dynamic fatigue to their bending rigidity.

2. EXPERIMENTAL

For this work were used three commercial textile laminates of different structures – woven or knitted substrate with one film layer. These laminates we received from apparel enterprises. Table 1 provides basic information about tested materials.

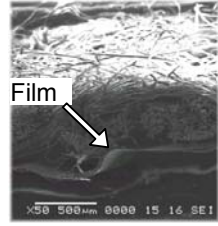
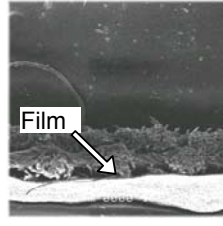
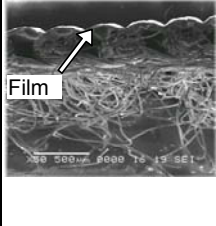
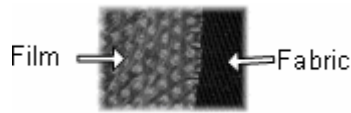
Table 1. The main characteristics of investigated laminates

Fabric	Density, dm^{-1}		Thickness, mm		Weight, g/m^2
	Length wise	Cross wise	Fabric	Film	
L2	300	480	1,0	0,02	320
L5	610	270	0,43	0,02	191
L8	120	120	0,71	0,1	234

For this experiment we have chose laminates which are different from the point of view of their layers thickness and bonding characteristics (Table 2). Laminates thickness was measured at pressure of 0.196 MPa.

On purpose to simulate wearing conditions, were chosen two types of specimens' fatigue.

Table 2. Structural Characteristics of Investigated Laminates

Laminates	L2	L5	L8
The cross section			
Polymer film	PU	PU	PU
Base fabric: fibre content structure	rayon, cotton twill weave, napped	cotton twill weave	PES weft knitted, napped
Layers joining	Laminated, pointed bond 		Coated

Fatigue 1. The test of specimen's cyclical extension, bending and surface abrasion was carried out using an original instrument ARRIV [8], which schematic diagram is shown in Figure 2 a. The working sequence of this device is described in work [9]. For laminates we have used these conditions of dynamic fatigue: the film surface of the specimen was "scraped" by the rolls with the velocity $v=1,8 \text{ m/s}$, the degree of relative deformation of specimens $\varepsilon=2.7 \%$, time of fatigue $t=60 \text{ min}$. For these test rectangular specimens of 60 mm wide and 200 mm high cut in three directions: length wise (0°), bias (45°) and cross wise (90°) were used.

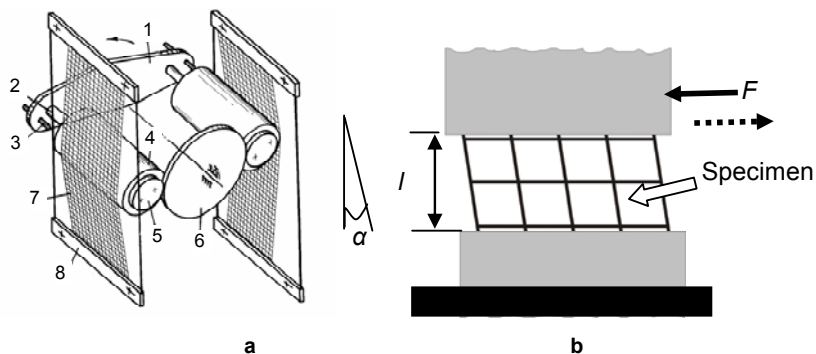


Figure 2. Schematic diagrams of the instrument ARRIV: 1 – rotor, 2 – axle, 3 – fastening bolts, 4 – polished steel rolls, 5, 6 – tooth-wheels, 7 – specimen, 8 – frame (a) and method of laminates shearing (b)

Fatigue 2. For the cyclical shearing of laminates was choused another original device [10, 11] often used for leather softening (Figure 2, b). The distance between clamps l was 20 mm, shearing angles $\alpha_1 = 8^\circ$ (fatigue 2a) and $\alpha_2 = 16^\circ$ (fatigue 2b), number of shearing cycles – 10, shearing speed – 0.01 m/s specimens width – 80 mm. Specimens were clamped in length wise direction. Also during this type of fatigue the shear force F was determined.

The laminates dry cleaning was carried out in industry environment with perchloroethylene according standard [12].

Laminates were investigated by bending them on fabric (+) and on film (-) sides (Figure 3, a). For the laminates bending rigidity determination were used specimens which were cut in three different directions: length wise (0°), cross wise (90°) and for some test in bias (45°) direction.

It was determined that for bending properties evaluation of stiffer fabrics is suitable loop shape specimen [13]. In case of laminates investigation such type of specimen eliminates their twist and curl which often take place during cantilever tests. In earlier our investigation [7] we have used pear shape loop and laminate's stiffness represented loop's measurements. However our experiment indicated that pear shape loop method is less sensitive due to smallest differences between results of some specimens. Therefore in this work we have used the specimen's loop with a little transformed shape (Figure 3, b). Choosing such type of loop shape allowed us to give the experiment closer to the behaviour of laminates in clothes during the wearer movements (Figure 1) and possibility to compress loop in direction of its high. The stiffness B of laminates was determined by the force P_F which needs to compress the specimen's loop in some degree a . For this purpose we have used loop compressing devise [14] which allows compress specimen's loop in desirable degree. The compression degree b was measured on the devise scale (0-n).

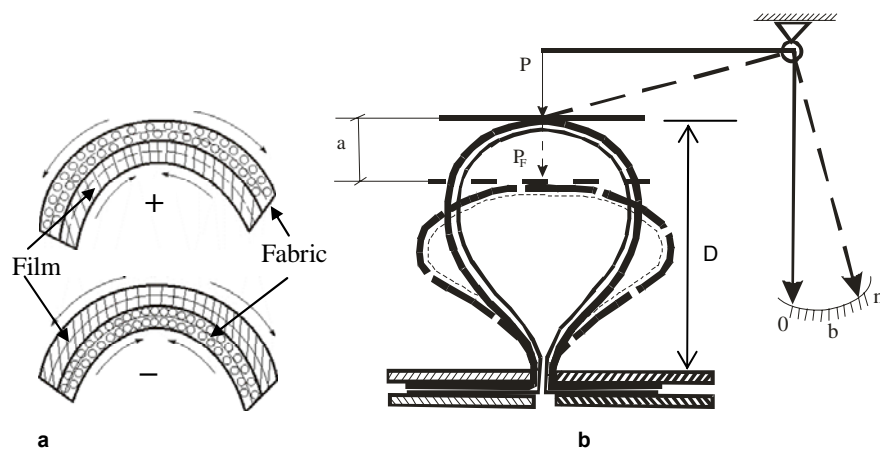


Figure 3. Two layers laminate bending on fabric (+) and on film (-) sides (a); the scheme of specimen loop's compressing (b)

From 3 to 9 measurements for every type of specimen were carried out and the averages calculated. The maximum coefficient of data variation achieved 15 %.

Before testing all materials were conditioned in a standard atmosphere of 65% RH and 20°C.

3. RESULTS AND DISCUSSIONS

It is known that fabrics rigidity depends on their deformation degree. In order to choose this parameter first of all we analyzed the laminates rigidity changing due to their compression degree. The specimen's loop was compressed from 1/12 to 2/3 of its high D (value b from 2.5 till 20 mm of device scale in 2.5 mm steps). It was found (Figure 4) that relationship between laminates compression degree and their rigidity may be linear (specimens L2 and L5) or exponential (specimen L8). Such results indicate that for coated fabric with more compact structure L8 the larger deformation cause the higher degree of its resistance to compressing forces. The initial part of laminates L8 curve may be qualified as linear, so for further investigations we have chose the compression degree $b=10$ mm which corresponds with the initial loop change of 1/3 D .

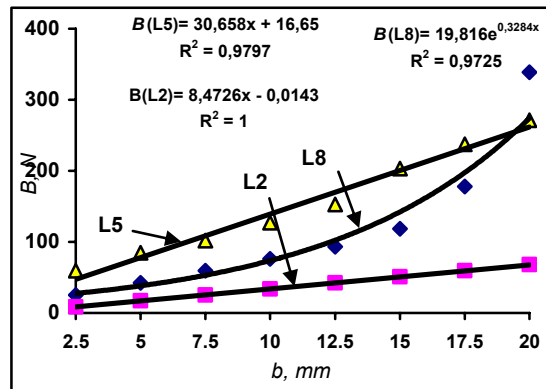


Figure 4. Dependence of loop compression degree to laminates bending rigidity (bent on the film side in crosswise direction)

It is known [15] that bending rigidity of fabrics as non-homogeneous materials depends on their flexibility and also on direction of their bending. The experiment have shown that rigidity of some control untreated specimens differ when they were bent on the fabric (+) or on the film (-) side. According to the results, presented in Figure 5 the significant differences of rigidity (about 18-20%) have shown laminates L5 and L8 in length wise and bias directions. Meanwhile in crosswise direction the bending side has no influence to the rigidity of these laminates.

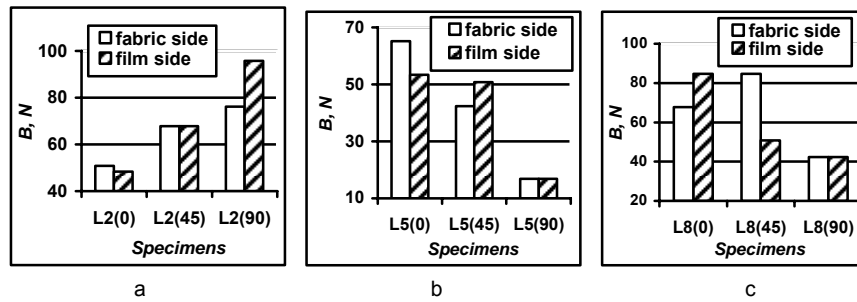


Figure 5. Influence of dry cleaning, cutting direction (0, 45, 90), bending side (+ or -) on the rigidity of laminates L2 (a), L5 (b) and L8 (c)

On the contrary the laminate L2 is more rigid in cross wise direction. Also in this direction we received that rigidity of laminate L2 is higher about 20.3% when specimen was bent on the film side. Taking into account that film layers of tested laminates are isotropic, we can confirm that the main reason of laminates unequal rigidity in three main cutting directions (0° , 45° , 90°) is fabric's layer structure. It should be noted that film layer changes the bending behaviour of the fabrics and the possibility of relatively movements between fibers and between yarns [16]. Therefore the stiffness of laminate L8 containing more flexible knitted fabric layer but thicker film layer is similar to other laminates stiffness. It can also be seen that more differences between laminates rigidity bent on fabric and on film side were determined for specimens with higher rigidity values: L2 in cross wise direction, L5 and L8 in length wise and bias directions.

The results of dry cleaning and fatigue have shown that these treatments have changed the rigidity of tested laminates markedly (Figure 6).

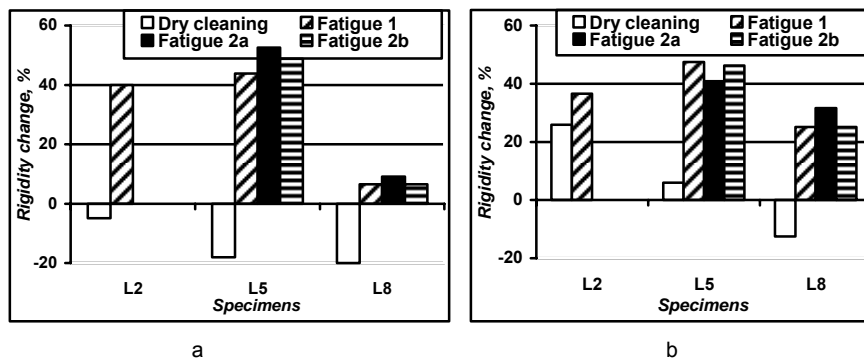


Figure 6. The influence of dry cleaning and mechanical fatigue to the change of laminates rigidity in length wise direction, when specimen was bent on fabric (a) and film (b) sides

It can be seen that after dry cleaning the rigidity of tested specimens in most cases decreases. Only for laminates L2 and L5 in case of film side deformation the rigidity was increased. The reason of higher degree of these

specimens rigidity may be the thin polyurethane film, which after dry cleaning losses part of its elasticity.

Though some authors [6] have received that mechanical treatment reduces the bending rigidity of coated fabrics, we have received another results. It can be seen from Figure 6 that type of choused fatigues increased the bending rigidity till 40-50% for laminate L5 and till 9-32% for laminate L8. According to the results less degree of rigidity increase was received for laminate L8. This laminate differs from others two of its structural characteristics. Maybe its knitted fabric layer is more elastic and coated film layer is better bond with fabric structure. In this regard during mechanical fatigue the laminates L8 two layers are deforming as one. The specimens L5 and L8 are laminated with thin polyurethane film which may delaminate partly during fatigue.

The laminates fatigue with their shearing have shown that when we used the shearing angle $\alpha = 8^\circ$, the shear force which also showed shear stiffness of specimens was similar for both laminates L5 and L8 (Figure 7). In case when shear degree was increased till $\alpha = 16^\circ$ the shear stiffness of laminate L8 was found about 25 % higher then laminate L5. It is important to note that with increasing shearing cycles till 10 the shearing force F of laminate L8 decreases about 7-8% and of laminate L5 about 13-14%. These results have shown that coated fabric is more rigid and has higher resistance to various external forces, as bending and shearing than laminated.

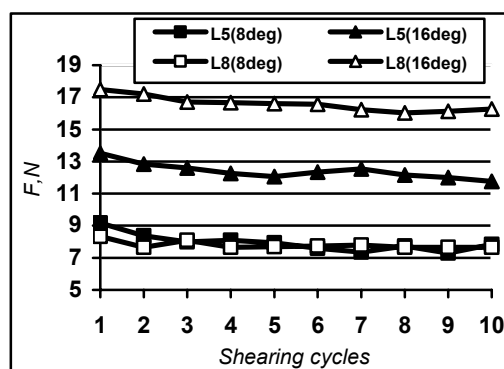


Figure 7. Influence of shearing cycles on the shear stiffness F of laminates

On purpose to explain the increased bending rigidity of laminates after their various treatments their thickness were measured, too. It was found that laminates thickness after dry cleaning and fatigue increases (Figure 8). So it may be the major factor of their increased stiffness. The results showed that laminates thickness after dry cleaning increased about 7.1 – 9.3%, after Fatigue 1 – 2.3-6.7% and after Fatigue 2 – 1.5-13.4%. Most significant influence on the specimens' thickness changes was determined for laminate's L8 after its cyclical shearing (Fatigue 2).

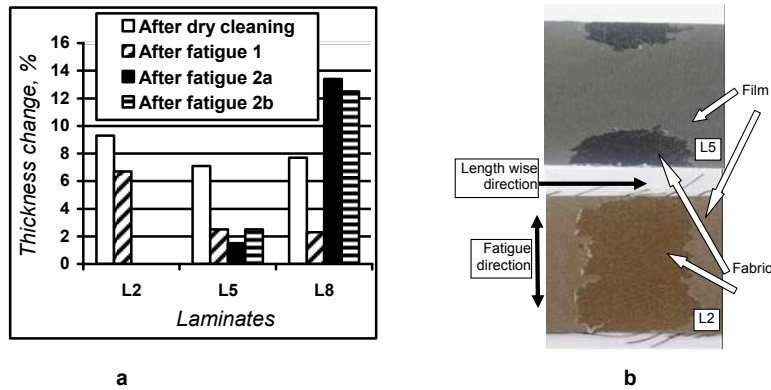


Figure 8. Influence of laminates dry cleaning and fatigue to their thickness change (a); photographs of laminates film distortion after Fatigue 1 (b)

The examinations of specimens' surface after their various treatments have shown that some of them were damaged especially after fatigue with surface tearing (Fatigue 1). The film layer of some laminates (Figure 8, b) especially those which contain thin films bonded to fabric layer only in points was scratched.

4. CONCLUSIONS

After study of laminates' bending rigidity the following conclusions were obtained:

- Choosing the loop shape of specimens allowed us to give the experiment closer to the behaviour of laminates in clothes during the wearer movements.
- The test have shown that values of bending rigidity when laminates are bending in film and in fabric sides differs more markedly for cutting directions of higher bending rigidity.
- Compressed loop method have shown that laminates bending rigidity depends on the loop compression degree. It was received two types of curves: linear for specimens in which film layer is laminated with base fabric by pointed bond and exponential – for coated fabric.
- After dry cleaning the bending rigidity of laminates in most cases decreases.
- A fatigue with extension, bending and surface abrasion or with shearing increase laminates bending rigidity markedly. The main reason may be their thickness enlargement.

- The results of shearing test have shown that due to increasing of shearing cycle the laminates shearing stiffness decreases more for fabrics with laminated layer and less with coated layer.
- The laminates with thin point bonded film have been damaged using fatigue method which contains surface abrasion.

REFERENCES

1. Cybulska M., Snycerski M. Qualitative Evaluation of Protective fabrics. *Autex Research Journal*, 2002, Vol.2, No2, June, p.69 - 77.
2. Masao Enomoto, Kazuaki Suehiro, Yoichiro Muraoka, Kiyohiro Inoue, Masao Sumita. Physical Properties of Polyurethane Blend Dope0Coated Fabrics. *Textile Research Journal*, 1997, Vol.67, No.8, p.601 - 608.
3. Milašius R., Milašienė D., Jankauskaitė V. Investigation of Stress Relaxation of Breathable-Coated Fabric for Clothing and Footwear. *FIBRES&TEXTILES in Eastern Europe*, April/June 2003, Vol.11, No2, p.52 - 54.
4. Gregor-Svetec D., Bezek R. Mechanical Properties and Permeability of Laminated Fabrics. *Proceedings of 5th World Textile Conference AUTEX 2005*, 27-29 June, p.379 - 383.
5. BS 3356. Testing of plastics films and textile fabrics (excluding nonwovens, coated or not coated fabrics – Determination off stiffness in bending – Method according to Cantilever (2003).
6. Chen Y., Lloyd D.W., Harlock S.C.: Mechanical Characteristics of Coated Fabrics, *Journal of Textile Institute* 1995, Vol.86, No.4, p.690 – 700.
7. Sacevičiene V., Masteikaitė V. Proučavanje krutosti savijanja laminata (A study of the bending stiffness of laminates), *Tekstil* 2006, Vol.55, No.9, p. 458 – 466 (in Croatian).
8. Patent of USSR No 1104386, M.Gutauskas. Ustroystvo dlya Tsiklicheskovo Nagruzhnya Ispytuyemovo obratztsa (The Apparatus for Cyclic Loading of Test Specimen), Int.Cl. G01N 3/34; G01N 3/56, 1983. (in Russian).
9. Gutauskas M., Masteikaite V. Mechanical Stability of fused Textile Systems. *International Journal of Clothing Science and Technology*. 1997, Vol. 9, No4/5, p.360 - 366.
10. Patent of Lithuania No 5092, Tričys V., Kazanavičius K. Odų minkštinimo būdas (Method for Leather Softening), Int.Cl. C14B 1/00. 2004 01, (in Lithuanian).
11. Kazanavičius K., Tričys V. Leather Softening by shearing. *Materials Science (Medžiagotyra)*, 2004, Vol.10, No1, p. 40 - 44. <http://internet.ktu.lt/en/index3.html>
12. ISO 3175-2:1998. Textiles. Dry-cleaning and finishing. Part 2: Procedures for perchlorethilene (tetrachloroethene) 1998:8p.
13. Naiyue Zhou, Tushar K. Ghost. On-line Measurement of Fabric-Bending Behaviour: Background, Need and Potential Solutions, *International Journal of clothing Science and technology*. 1998, Vol.10, No2, p.143 - 156.
14. GOCT 8977 – 74 Koza i iskustvennaja i plionocznyje materialy. Metody opredelenija zestkosti i uprugosti (Leather, synthetic leather, Woven Fabrics. *Textile Research Journal*, 2000, 70(3), p.247-255.

THE PROCEDURE FOR DESIGNING, PRODUCING AND TESTING OF COMPRESSION STOCKINGS.

N. ÖZBAYRAK¹, Y. KAVUŞTURAN²

¹ University of Uludag, Institute of Natural and Applied Sciences, Dept. of Textile Engineering

² University of Uludag, Faculty of Engineering&Architecture, Department of Textile Engineering

ABSTRACT

The superficial venous system is most often affected by varicose veins. Compression stockings are a recognized effective nonsurgical option to prevent and treat lower limb varicose veins. Stocking supports have represented, for more than two millennia, the most efficient way to treat the venous diseases and lymphatic disorders. Compression stockings apply maximum pressure at ankle level, progressively decreasing toward the top of the affected leg. They reduce the vein diameter and increase blood flow. There are many styles of compression hosiery, ranging from socks to pantyhose. The style and level of compression prescribed for patients with lymphoedema and venous leg ulcers is dependent on many factors including the site, extent and severity of the swelling, the patient's ability to manage and tolerate compression, and patient choice.. Several instruments are available for measuring the "in vivo"-pressure on the individual leg. This paper will give an introduction to compression stockings. The presentation will outline the procedure for designing, producing and testing compression stockings.

Key Words: Compression stockings, varicose veins, compression therapy, knitted fabrics

1. INTRODUCTION

The main function of arteries consists in bringing blood from the heart to the extremities while veins, which have one-way valves, channel the blood back into the heart[1]. When the walls of the veins are weak, they lose their normal elasticity, like an overstretched rubber band. This makes them longer and wider and causes the flaps of the valves to separate[2]. Damaged valves in the deep veins mean that blood is not pumped upwards, and this can be particularly harmful if the veins at knee level are affected. Failure of valves in the perforating veins allows blood to be pushed out under high pressure into the superficial veins, which can lead to varicose veins[3]. (Figure 1) These incidents in varicose veins can lead to deep vein thromboses, or more lethal injuries such as embolies if the clot reaches vital organs (kidneys, lungs, heart, brain) [1].

So far, and for ages, the most efficient treatment used against this deficiency has been the compression treatment which consists in exerting an external pressure on limbs through compressive bandages or compression stockings[1]. Unlike compression bandaging with its high working pressure, compression hosiery exerts a resting pressure. The daily build-up of pressure is controlled by the limited ability of the hosiery to stretch, so incompetent venous valves are approximated, venous return is accelerated, the fibrinolytic activity of the venous wall is increased and the risk of thrombosis reduced[4]. The great advantage of the treatment of venous leg ulcers by means of medical compression stockings is the fact that it is comfortable and easy to carry out at home. Furthermore, the costs of

compression therapy with medical compression stockings are only a fraction of those of conventional therapy by means of compressive non-elastic bandages. Once or twice weekly visits of the patient to the hospital are not necessary and less specialized dermatological nurses are needed[5].

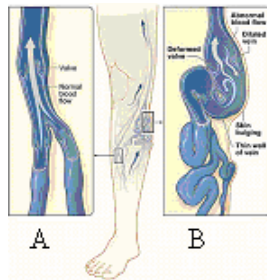


Figure 1. (A) Normal vein with (B) Varicose vein[2].

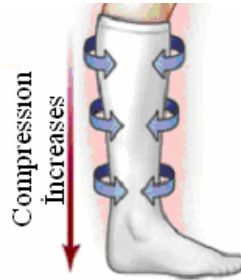


Figure 2. Level of compression in medical compression hosiery[6]

2. THE DESIGN AND PRODUCTION OF COMPRESSION STOCKINGS.

Compression stockings have been used to treat varicose veins and their complications for over 150 years[7]. Depending on the various needs of the patients there are many types and styles of compression hosiery, ranging from socks to pantyhose in a wide range of colours. Compression stockings may be fully footed or have open heels or toes. It is possible to wear compression stockings that look as beautiful as any stocking that can be bought in the hosiery department of fine stores. Dress, athletic and casual socks in a variety of styles and colors are also available. They offer support, comfort and help reduce fatigue[8,9] It is always possible to find a pair to suit even the most difficult cases. Most graduated compression stockings are mass-produced and are affordable. However, special cases require custom-made stockings, and they are more expensive[7].

Wearing medical compression hosiery provides support for the veins and muscles of the legs. They also can help heal skin sores and prevent them from returning[3,4]. Compression stockings are currently classified according to the pressure they exert at the ankle at the point of its minimum girth (B level) [10]. In most of Europe stockings are divided into four classes of compression. Compression is graduated, strongest at the ankle (minimum of 14 mmHg) with decreasing compression up the leg. This design compresses dilated veins to help move blood up the legs and back to the heart[4,11]. (Figure 2) Furthermore, there is no agreement as to the most effective stocking design to achieve the above effects. Thigh-length compression stockings, which are probably employed in most medical studies, have intended pressures of 18 mmHg at the ankle, 14 mmHg at the calf, 8 mmHg at the knee, 10 mmHg above the knee, and 8 mmHg at the thigh. It is not known whether these pressures are optimal. Moreover, some authors estimate calf-length stockings to be more effective than thigh-length and some prefer non-graduated ones. Stocking design is not always

specified in the study protocols and, particularly in some of the newer studies, it is not clear whether or not stockings were used at all. Even those stockings believed to be ideally designed may not achieve the warranted effects. A study measuring pressure gradients in patients wearing prophylaxis stockings showed that 98% of the stockings failed to produce the ideal pressure gradient of 18–14–8 from the ankle to the knee; 54% even produced an inversed gradient[12] .

Severe varicosities require a greater degree of compression than mild varicosities. The choice of the appropriate graduated compression garment depends on the indication, the area affected, and whether the patient is male or female. The doctor may order the garment in terms of the degree of compression required (mild, moderate or strong) or by the compression class. In all cases, the usefulness of the hosiery product is entirely dependent on the accuracy of the limb measurements and the correct selection of garments based on those measurements[9] High-compression stockings over 40 mmHg are often difficult or even impossible to apply. A specific technique is frequently used to overcome this problem: a high-compression stocking is replaced by two or even three lower compression stockings that are applied on top of each other, thereby reducing the effort of application. [13]

For both compression hosiery and bandages, the level of compression achieved is dependent upon a complex interaction of the physical properties and construction of the bandage or hosiery, the size and shape of limb to which it is applied, and the activity of the wearer. As a broad principle, the level of compression is directly proportional to the tension with which the compression device is applied and is inversely related to the size of the limb – this general rule is known as Laplace's Law. In compression hosiery, tension is largely determined by the materials and construction method used[14].

2.1. Yarn Construction

Compression hosiery uses two yarn systems knitted together to produce the fabric of the garment. The body (ground) yarn delivers the thickness and stiffness of the knitted fabric; the inlay yarn produces the compression. The circumferential (hoop) stiffness is directly given by the inlaid yarn. Inlay and body yarns are produced by wrapping polyamide or cotton around a stretchable core such as latex or elastane (Lycra). Polyamide fibres are used to cover the yarns so that the uncomfortable lycra touch feeling is improved[1, 14]. To reduce potential allergies all fibres are coated with cotton. Where a patient is shown to be allergic to one of the fibres use of a cotton tubular bandage under the stocking could prevent irritation[15].

The wrapping can be adjusted to vary the stretchability and power of the yarn, and the thickness, texture and appearance of the knitted fabric. Higher garment compression is mainly achieved by increasing the thickness of the elastic core of the inlay yarn, although the body yarn may also be adjusted[14].

2.2. Hosiery Construction

The knitted elastomeric fabrics used to treat the venous disorders may be of two types: inlaid knitted structure or floated structure. (Figure 3) The inlaid knitted fabrics are ensured sufficiently high level of confidence regarding the range of pressures delivered, unlike floated structures[1].

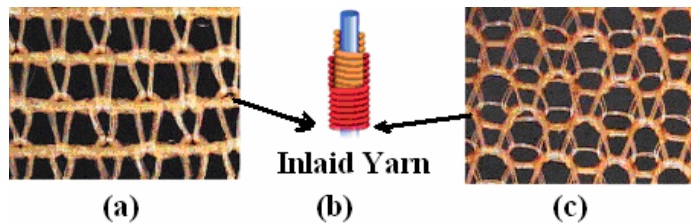


Figure 3. Knitted structure of medical compression stockings: (a) inlaid knitted structure, (b) Inlaid yarn construction (c) floated structure[1,14].

2.3. Knitting Techniques

The two main knitting techniques used to produce compression hosiery are flat knit and circular knit. Flat knit technology results in a flat piece of fabric, which needs to be stitched to produce the final garment. Circular knit technology produces a tube that requires comparatively little finishing to produce the final garment. Both flat and circular knit techniques are used to produce custom made and ready to wear hosiery. However, custom made garments are most often flat knit because this method of manufacture can better accommodate shape distortion. (Figure 4) The type of hosiery used for the treatment of varicose veins varies across Europe; in Germany and the Netherlands, most patients are treated with flat knit hosiery, but in the UK both circular and flat knit are used[14].

In flat knit technology, the total number of needles in use can be increased or decreased during the knitting of an individual garment to produce variations in the width and shape of the knitted piece used to construct the final garment. The inlay yarn is fed in with almost no tension and does not influence the shape of the final product[14]. Products made on flat knitting machines represent relatively heavy qualities. The “standart for this type of stocking is knitted on machine of gauges E14 and E16[16]. In circular knit technology, the number of needles in use during production of a particular garment is fixed, reducing the range of shape distortion that can be accommodated. However, some shape variation can be produced during knitting by altering the tension of the inlay yarn and, to a lesser extent, by varying stitch height. The “standart for this type of stocking is knitted on machine of gauges E24 and E32[14].

In general, flat knit fabric is coarser than circular knit because it uses thicker yarn and consequently fewer needles per inch during knitting. The thicker yarn produces stiffer and thicker material that is better at bridging skin folds and is less likely to cut in or cause a tourniquet effect. The finer finish of circular knit

hosiery may make it more cosmetically acceptable, but more likely to cut into the limb, particularly if worn for extended periods[14]. Flat-bed knit stockings are more flexible than circular knit stockings, making them easier to get on and off[17]. The quality which is made on circular knitting machines mostly covers classes 1 to 3, whereas the stockings produced on a flat knitting machine reach from class 2 up to class 4 (class 1 applying the lowest rate of compression). Products made on flat knitting machines are knitted in anatomical shapes. Stockings of class 3 and 4 are individually made to the patient's leg measurements. [16]. Wegen-Franken demonstrated that the pressures exerted by flat-knitted custom-made compression stockings were higher than those exerted by the ready-made round-knitted ones. [10]

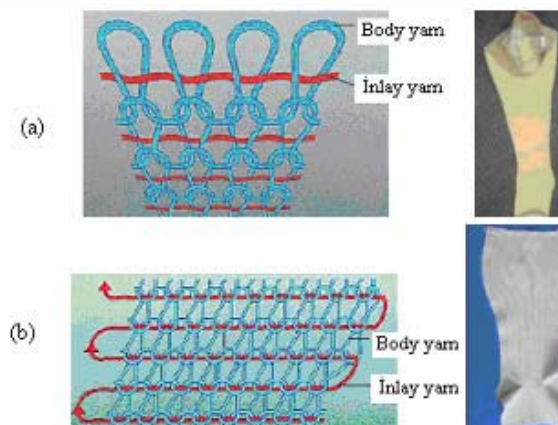


Figure 4. Schematic arrangement of inlay and body yarn in (a) circular knit (b) flat knit (before sewing) [14].

3. THE STANDARDS AND TEST METHODS FOR COMPRESSION STOCKINGS.

3.1. Standards

A British Standard (BS 6612) for graduated compression hosiery was introduced in July 1985. Its introduction was made possible by the development of a suitable testing device, the Hosiery and Allied Trades Association (HATRA) hose pressure tester [9]. There are few European national standards for compression hosiery (Table 1). The standards describe methods used to characterise the graduated compression applied to the lower leg by compression hosiery, and focus on *in vitro* measurement of the pressures likely to be applied at various points on the limb [14].

Attempts were made to produce a European Standard (draft standard: ENV 12718), but consensus could not be achieved and the standard was cancelled in 2005[14]. In the European Committee for Standardization prENorm (CEN ENV 12718-2001), medical compression hosiery are classified in compression

classes according to the pressure exerted on the leg (the so-called “B pressure”). To date this is the only way for distinguishing one medical compression hosiery from another. Nevertheless, in daily practice it is well known that the behavior of a compression class II medical compression hosiery can significantly differ from another compression class II medical compression hosiery for instance in the prevention of edema[18]

Table 1. Comparison of hosiery classification in standards (mmHg)[14].

Standards	British BS6612:1985	French ASQUAL	German RALGZ387:2000	CEN 12178
Testing Method	HATRA	IFTH	HOSY	CEN
Class I	14 – 17	10 – 15	18 – 21	15-21
Class II	18 – 24	15 – 20	23 – 32	23-32
Class III	25 – 35	20 – 36	34 – 46	34-46
Class IV	-	> 36	> 49	> 49

The efficacy of compression therapy depends mainly on the exerted pressure and on the stiffness of the material[19]. Despite the pressure classification, there are considerable differences between compression stockings belonging to the same compression class from the same manufacturers and between different manufacturers. This makes it difficult for the clinician to choose the most suitable compression stockings for the patient. The stiffness may be used to distinguish between compression stockings of different brands. [10]. Pressure is not the only parameter that differentiates one stocking from another. Another important parameter is so-called stiffness factor, the elasticity or slope value of the stocking. The slope value is defined as “the increase in pressure (mmHg) of the stocking, when the circumference of the stocking increases by 1 cm, expressed as kPa/cm². This slope value can be determined in the laboratory. Not only the compression class and the knitting technique, but also the slope value of medical elastic compression stockings is important to consider when prescribing stockings to patients[20]

3.2. Test Methods

The pressure values given by the producers of medical compression stockings are measured by different methods. There are some testing methods for compression stockings:

-Principle of stocking pressure measurement with SIGaT: The pressure sensor is a plastic pocket which is placed between the leg and the medical compression stockings. (Figure 5) The measurement itself consists in filling this sensor with air under constant flow. The variations of pressure reflect its dynamic behaviour during the pocket inflation. During this operation the first variation of the pressure curve versus time represents the separation of the walls of the sensor and at this moment the inflation pressure is exactly equal to the pressure generated by the medical compression stockings on the leg. When the pressure reaches the value of the compression, and exceeds it

slightly, the sensor starts to inflate and the pressure keeps increasing but with a new slope. Before beginning measurements on the leg, the sensors are calibrated by immersing them in a water container at a known depth[1].

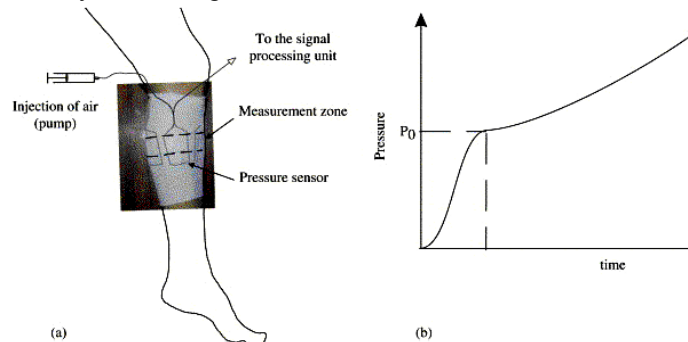


Figure 5. Principle of stocking pressure measurement with SIGaT: (a) schematic of the placement of the sensors on the leg, (b) typical response of the sensor as a function of time[1].

-Principle of stocking pressure measurement with Presstest device:

The pressure tests are carried out with the use of a measuring stand in the form of a flat model of the leg; the stand is linked to a computer. (Figure 6-a) The measurements are performed by stretching the product from the inner side, without any clamps or grips. During the five stretching and relaxation runs of the product, the circumference forces at the standardised points are measured by 10 tensometric gauges placed on the upper measuring board. Next, the values of pressure from the relaxation curves for the fifth hysteresis loop are automatically determined as a function of the circumferences of the body part. [21]

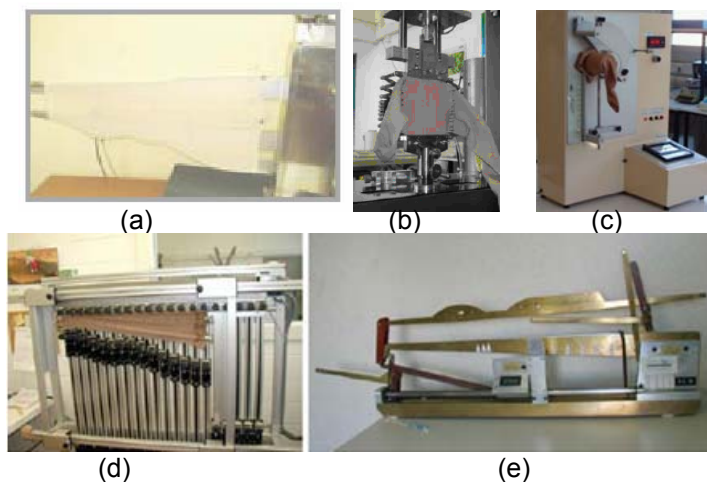


Figure 6. a)Presstest (b) CEN (c) Pressure sensor (d)Hosy (e) Hatra testing device

- Principle of CEN Medical Compression hosiery test method:

Measurement of the force exerted by hosiery across its width when it is stretched simultaneously both sideways and lengthways according to its size specifications. The measurement force is transformed into pressure using the Laplace formula. This method is intended for determining the mechanical properties of hosiery (Figure 6-b) [22]

-Pressure sensor: Another measuring device is based on a pressure sensor (Thuasne Research and Development Department), composed of a metal cylinder with an aperture at its superior part and an air circuit supplied by a small electric motor (Figure 6-c). The cylinder, with a constant circumference of 24 cm, is taken as an anatomical model of the ankle on which the smallest circumference stocking is placed. The aperture is connected to the air circuit and a manometer. The maximum pressure measured by this manometer is 60 mmHg[13].

- Principle of HOSY Compression test method: Measured in the force exerted by hosiery in circumferential direction, when stretched in longitudinal direction to the specified length and subsequently in transverse direction according to its size (Figure 6-d) [23].

-Principle of Hatra device: Individual stocking pressure at the ankle level is measured for each stocking fitted to each individual using the Hosiery Trade Research Association (HATRA) instrument. (Figure 6-e) The HATRA system is a mechanical testing model to measure the pressure profiles of stockings[24].

4. CONCLUSIONS

Up to 20% of the population may suffer from varicosities to different degrees, with women being five times as likely as men to develop symptoms. [9]. An appreciation of how the construction of hosiery, especially knitting technique, relates to performance can assist practitioners in selecting the most appropriate hosiery for their patients. Compression hosiery is made from a number of different fibres including nylon, cotton yarn and elastane. Off-the-shelf stockings include circular knit stockings and flat-bed knit stockings. Flat-bed knit stockings are more flexible than circular knit stockings, making them easier to get on and off. Current national standards were developed to guide manufacturers and to classify garments according to compression produced. Inconsistency remains across Europe in the classification of hosiery. [17]. Medical compression stockings are one of the most widely used mechanical compression approaches as a result of their convenience, ease of use, and sustained, ambulant therapeutic function. [25]

REFERENCES

1. Gaied, I; Drapier, S. and Lun, B. (2005), Experimental Assessment And Analytical 2D Predictions of The Stocking Pressures Induced On A Model Leg By Medical Compressive Stockings, Science Direct, France.

2. www.nhlbi.nih.gov/health
3. www.familydoctor.co.uk/htdocs/varicose/varicose_specimen.html
4. Lawrence D, Kakkar VV. (1980), Graduated, Static, External Compression Of The Lower Limb: A Physiological Assessment. *Br J Surg*; 67(2): 119-21.
5. Geest, A.J., Veraart, J.C.J.M., Nelesmans, P., Neumann, H.A.M., (2000), The Effect of Medical Elastic Compression Stockings with Different Slope Values on Edema, *Dermatol Surg.*, 26, 244-247.
6. http://www.vascularweb.org/_CONTRIBUTION_PAGES/
7. Evans, D. and Read, K. (2001), Graduated Compression Stockings For The Prevention Of Post-Operative Venous Thromboembolism, *Best Practice*, Volume 5, issue 2.
8. Drs. Young & Wouters, Calgary Vein And Laser.
9. Whitley, L., 2002, Patient Care in Community Practice - A handbook of non-medical health care, Edited by Robin J Harman, Pharmaceutical Pr 10. Wegen-Franken, K. , Roest W., Tank B., Neumann M., (2006), Calculating the Pressure and the Stiffness in Three Different Categories of Class II Medical Elastic Compression Stockings, *Dermatol. Surgery*, 32 (2), 216-223
11. www.sigvaris.com
12. Schulz SL, Stechemesser B, Seeberger U, Meyer D, Kesselring C. Graduated compression stockings for the prevention of venous thromboembolism in surgical patients in the age of low molecular weight heparins. *J Thromb Haemost* 2005; 3: 2363-5.
13. Cornu-Thenard, A., Boivin P., Carpentier P., Courtet F., Ngo P., (2007) Superimposed Elastic Stockings: Pressure Measurements, *Dermatol. Surgery* 33 (3), 269-275.
14. Clark, M. and Kimmel, G. (2006), Lymphoedema And The Construction And Classification Of Compression Hosiery, London, UK.
15. Johnson, S. (2002), Compression hosiery in the prevention and treatment of venous leg ulcers; the Journal of Tissue Viability, S Yorks.
16. Legner, M., (2005), II. International Technical Textiles Congress, 13-July İstanbul
17. Ngan, V. (2006), www.DermNet.org
18. Stolk, R. At all (2004) A method for measuring the dynamic behaviour of medical compression hosiery during walking, *Dermatol Surg.*, 30, 729-736
19. Hugo P., (2005) The Static Stiffness Index: A Simple Method to Assess the Elastic Property of Compression Material In Vivo *Dermatol. Surgery* 31 (6), 625-630.
20. Geest A., Dooren-Greebe R., Go I., Neumann H., (2000) An impressive therapeutic result of class III compression stockings in a patient with longstanding, extensive, combined leg ulcers *Journal of the European Academy of Dermatology and Venereology* 14 (1), 15-17.
21. Maklewska, E.; Nawrocki, A.; Ledwoń, J. and Kowalski, K. (2006), Modelling and Designing of Knitted Products Used in Compressive Therapy, *FIBRES & TEXTILES in Eastern Europe*.
22. European Committee for Standardization (CEN). 2001, Non-active Medical Devices. Working Group 2 ENV 12718: European Prestandard 'Medical Compression Hosiery.' CEN TC 205. Brussels: CEN,
23. RAL Deutsches Institut für Gütesicherung und Kennzeichnung e. V., 2000, Medical Compression Hosiery Quality Assurance RAL-GZ 387
24. Partsch, H.; Winiger, J. and Lun, B. (2004), Compression Stockings Reduce Occupational Leg Swelling, France.
25. Rong Liu, MSc, Yi Lin Kwok (2007), Skin pressure profiles and variations with body postural changes beneath medical elastic compression stockings, *Dermatologic surgery*, the Institute of Textiles and Clothing, Hong Kong Polytechnic University.

DETERMINATION OF TEXTILE-MECHANICAL PROPERTIES USING IMAGE PROCESSING AND SIMULATION

M. HALASZ¹ – L.SZABO¹ - P. TAMAS²

¹Department of Polymer Engineering, Budapest University of Technology and Economics

²Department of Information Engineering, Budapest University of Technology and Economics

ABSTRACT

We are presenting a new equipment for measuring the draping characteristics of static cloth. In contrast with Kawabata Evaluation System 3D geometrical data of the sample are captured from photo images. There is a mathematical reconstruction of geometry, so drape coefficients and mechanical parameters are evaluated upon the geometrical model. The computer controlled equipment moves a round table, positioned in the centre providing the natural pleating of fabric for the measuring. The core part of the equipment is a computer moved frame. There are laser-beams lighting the sample. Lasers light the cross section curves of the sample on different levels. There are four cameras on the frame taking the pictures of cross section curves in different levels. 3D geometry is reconstructed upon the pictures.

A mass, spring and damping element system is the basis of our cloth simulator. Springs are assumed to be linear, while damps are proportional to the velocity. The simulator calculates vertex positions at a time t based on interaction forces with neighbouring vertices, including stretch, bend, and shear forces. Collision of the cloth model with the model of the underlying object is performed and handled in each time step.

In order to evaluate the influence of the individual parameters, a series of simulations are performed. For the real cloth samples, a range of cross-section curves is captured, digitalized and interpolated by Fourier series. The same Fourier coefficients are determined for the cloth model as a function of simulation parameters.

The actual simulation parameters are defined by the minimum of the difference between the modelled and the measured geometry.

Key Words: draping characteristics, 3D test piece modelling, 3D measuring, garment trade

1. INTRODUCTION

The objectives of modelling cloth and cloth structures for needs of textile industry and for computer graphics use are very different. If you come to your – real or virtual – tailor, choose a fabric and – before making any decision – would like to see how a ready suit or skirt would fit your body, you will not have to wait long before the precisely modelled dress appears on the screen at least in terms of mechanical engineering. In case of such applications we want to create the simplest possible model that will produce realistic or acceptable results to the average observer.

Producing physically accurate and predictive models plays the least (if any) role; the main objective is to make computer-generated images and animations to “look right”. Nevertheless, your tailor should be able not only to

measure your body and create your personal virtual mannequin, but also to measure some parameters of real cloths needed for 3D visualisation.

Although the Kawabata Evaluation System (KES) can provide accurate measurements, your tailor will hardly possess it: It is expensive and not really meant for the special purpose. The measurements made by the KES are also problematic for computer graphics cloth simulation because it does not guarantee a direct and simple mapping between the parameters for a particular cloth model and the Kawabata parameters.

In many cases it would be more convenient to determine parameters for simulation system using conventional equipment such as photo/video capture devices. In our case we will fit parameters of a particle-based cloth model geometry of real cloth in a static rest configuration, draped over a round table (Drapemeter), estimating parameters from photo images of the cloth. We have developed an integrated robot-scanner to achieve a more accurate definition of geometry of test pieces. This presentation is about the background of the measuring process.

2. STRUCTURE OF THE EQUIPMENT

The computer controlled equipment (Fig. 1.) is mounted in a black box. The computer moves the round table positioned in the centre providing the natural pleating of fabric for the measuring.

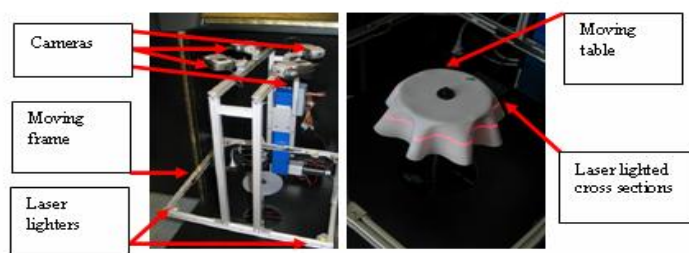


Figure 1. The 3D drape scanner

The core part of the equipment is a computer moved frame. There are laser-beams lighting the sample through mirrors. Lasers light the cross section curves of the sample on different levels. There are four cameras on the frame taking the pictures of cross section curves in different levels. The frame is programmed on serial a port. We have developed controlling programs by Borland Delphi [1], Alkenius' Cam Remote components [2] are used to program the Canon firmware [3].

3. MEASURING BY THE EQUIPMENT

As we want to achieve necessary accuracy for garment trade, we have to calibrate photos of parallel cameras, in order to develop measuring methods as well as to analyze errors.

3.1 Calibration Process

Laser beams light a planar curve in every position of the frame. Curve points are defined by processing four pictures. For 3D scanning the plane to plane perspective transformation is bijection. Perspective transformation by homogenous coordinates is a linear transformation [4] that projects quadrangles to quadrangles. The matrix of transformation (1) has eight independent coordinates.

$$\underline{\underline{P}} = \begin{bmatrix} p_0 & p_1 & p_2 \\ p_3 & p_4 & p_5 \\ p_6 & p_7 & 1 \end{bmatrix} \quad (1)$$

Corners of a rectangular calibration element are appropriate to define matrix coordinates (Fig. 2).

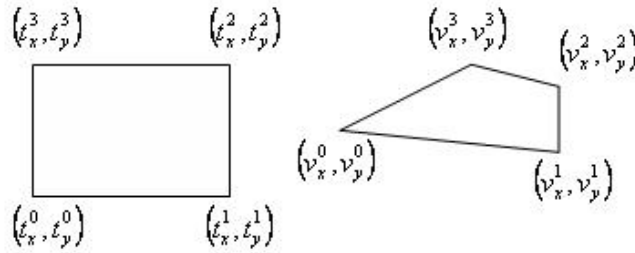


Figure 2. Planar perspective projection

Corners of calibration equipment are (t_x^i, t_y^i) , and corners of its picture are (v_x^i, v_y^i) ($i = 0, 1, 2, 3$) then the transformation is shown in (2)

$$\begin{bmatrix} v_x^i \\ v_y^i \\ 1 \end{bmatrix} = \begin{bmatrix} p_0 & p_1 & p_2 \\ p_3 & p_4 & p_5 \\ p_6 & p_7 & 1 \end{bmatrix} \cdot \begin{bmatrix} t_x^i \\ t_y^i \\ 1 \end{bmatrix} \quad (2)$$

There are eight unknown coordinates and eight equations there (3).

$$\begin{aligned} v_x^i &= \frac{p_0 \cdot t_x^i + p_1 \cdot t_y^i + p_2}{p_6 \cdot t_x^i + p_7 \cdot t_y^i + 1} \\ v_y^i &= \frac{p_3 \cdot t_x^i + p_4 \cdot t_y^i + p_5}{p_6 \cdot t_x^i + p_7 \cdot t_y^i + 1} \end{aligned} \quad i = 0, 1, 2, 3 \quad (3)$$

The determination of corner coordinates starts at the corner closest to the actual camera. If we define the point of the edge image in the coordinate

system connected to the left-bottom corner of the photo then regression lines can be defined for every x_s on section $x < x_s$ and $x > x_s$. Let the error of the regression H be a function of x_s ! In other words $H(x_s)$ is the sum of the differences of y_i point coordinates and the $a \cdot x_i + b$ lines [5] with unknown parameters (4).

$$H(x_s) = \sum_{x_i < x_s} (y_i - (a_{x < x_s} \cdot x_i + b_{x < x_s}))^2 + \sum_{x_i > x_s} (y_i - (a_{x > x_s} \cdot x_i + b_{x > x_s}))^2 \quad (4)$$

The minimum of $H(x_s)$ will be at the real position of the corner at x^* . Substituted back on $x < x_s$, or $x > x_s$ section y^* will be identifiable (Fig 3.).

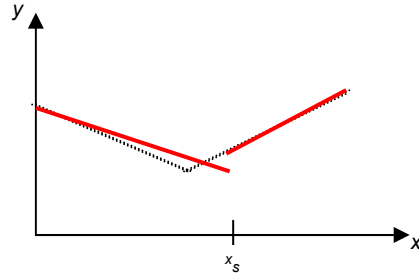


Figure 3. Corner point definition

The farthest away coordinates from the camera can be counted similarly. The only difference is that regression lines come to the edges of the square. Corner points on the left and right sides are derived as intersections of the defined regression lines. Fig 4. shows the defined regression lines and corners on calibrating square.

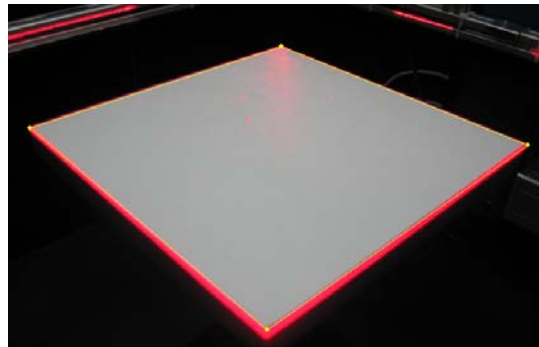


Figure 4. Calibration quadrangle

3.2 Determination of Laser Lit Cross Section Point Positions

Four pictures are stored by the newly developed software (left side on Fig. 5.). Points of the cross-section curves are defined by picture processing

methods. Considering the distortion and rotation cross-section points are placed in one picture

Cross-section curves are approached by a slice of Fourier series [5] in the polar coordinate system (5). Size of the slice (n) can be defined by the software.

$$R(\varphi) = \frac{1}{2} a_0 + \sum_{i=1}^n a_i \cos(i\varphi) + \sum_{i=1}^n b_i \sin(i\varphi) \quad (5)$$

Fourier coefficients are defined by least square method. If the N measured cross-section points of the actual level are (R_k, φ_k) then the a_i, b_i coefficients are defined by the minimum of a function (6).

$$\sum_{k=1}^N \left\{ R_k - \left[\frac{1}{2} a_0 + \sum_{i=1}^n a_i \cos(i\varphi_k) + \sum_{i=1}^n b_i \sin(i\varphi_k) \right] \right\}^2 = \text{minimum} \quad (6)$$

The point cloud and the approaching curve of an actual level are shown on right side of Fig. 5.

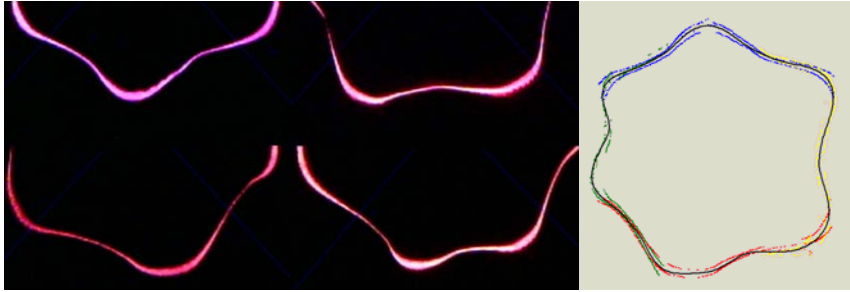


Figure 5. Four pictures of a cross section curves and the reconstructed cross section

3.3 3D Reconstruction

Geometry of the sample is modelled by Bezier surface patches. Shape of the patches is defined by $P_{i,j}$ vertices.

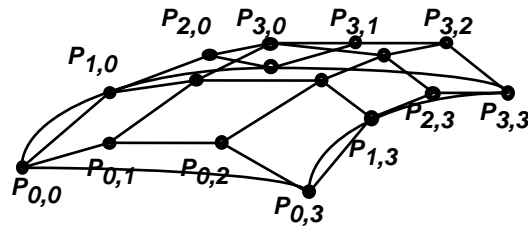


Figure 6. Bezier patch

Patches are connected to one another continuously in first order by the Catmull-Romm model. Edge slopes are defined by the vertices of the actual element, too [6].

Vertices of the 3D geometry are defined by approximating curves (5) on different levels (Fig. 7.).

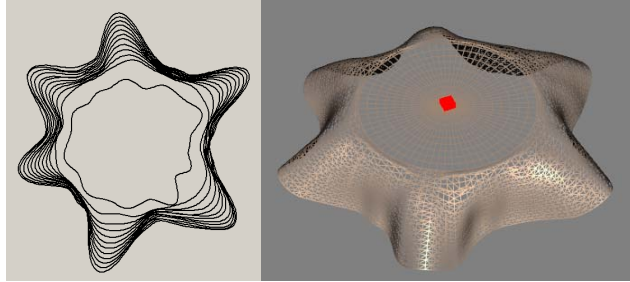


Figure 7. The reconstructed geometry

4. MEASURING MATERIAL PARAMETER BY SIMULATION

The basic measuring idea is simulating material behaviour as a function of properties. If the right set of properties is chosen we get the measured geometry.

4.1 The Mechanical Model

The fabric is modelled by the mass and spring system, where mass particles, arranged in a rectilinear grid are connected to the three types of springs [7] shown in Fig. 8.

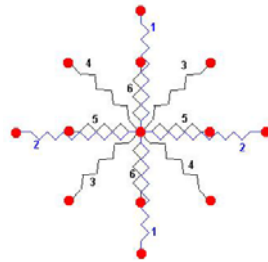


Figure 8. Springs and Mass Points for fabric model

The basic mathematical model is based on the Lagrangian equation (7):

$$\underline{\underline{M}}\ddot{\underline{q}} + \underline{\underline{K}}\dot{\underline{q}} + \underline{\underline{S}}\underline{q} = \underline{F}(t) \quad (7)$$

4.2 Parameter Estimation

Let us define the difference of the measured shape and the simulated shape (D) as a function of material properties (p) (8). The minimum position of the function defines the actual properties. [9, 10]

$$D(\underline{p}) = \text{minimum} \quad (8)$$

It is better to define the difference between shapes as the difference between the Fourier coefficients in a defined level then as the difference between the drape coefficients. In equation (5) the a_i^M and b_i^M indicates the Fourier coefficients of the measured shape and $a_i^S(p)$ and $b_i^S(p)$ indicates the Fourier coefficients of the simulated shape as functions of the mechanical properties.

$$D(p) = \left[\frac{1}{2} a_0^M - \frac{1}{2} a_0^S(p) \right]^2 + \sum_{i=1}^n \left[a_i^M - a_i^S(p) \right]^2 + \sum_{i=1}^n \left[b_i^M - b_i^S(p) \right]^2 \quad (9)$$

The optimum place emerges from an iterative simulation process.

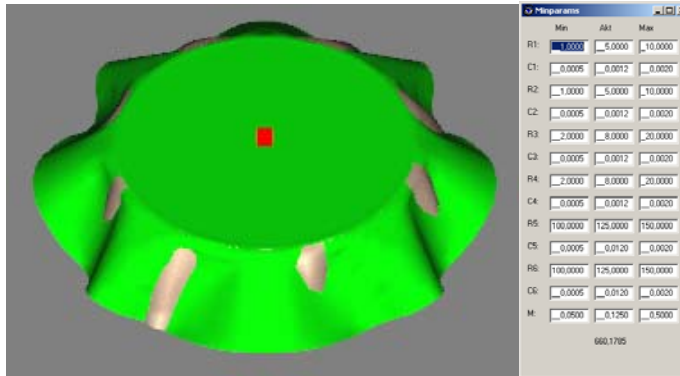


Figure 9. The iterative simulation process

4. CONCLUSIONS

The presented equipment and methods are appropriate to measure draping parameters of clothes as well as virtual fitting on [8] (Fig 10).

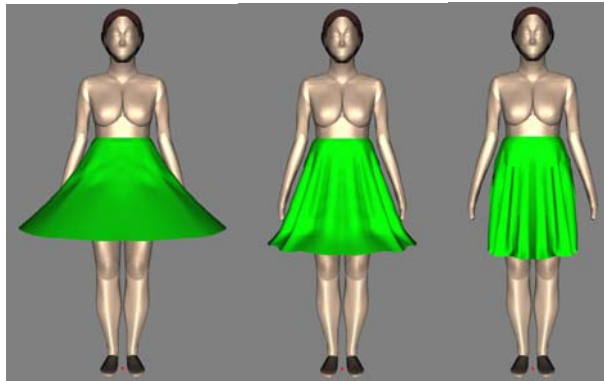


Figure 10. Virtual Fitting On

ACKNOWLEDGEMENTS

This work has been supported by the Hungarian Government, the National Office for Research and Technology and the Agency for Research Fund Management and Research Exploitation.

REFERENCES

1. J. Kuzmina, P. Tamás, B. Tóth: (2003), "Let Program in Delphi 7 System"; Computer Books Budapest.
2. CamRemote Component - <http://alkenius.no-ip.org/tcamremote>
3. Canon Imaging Developer Program - <http://www.didp.canon-europa.com>
4. D.K. Kim, B.T. Jang, C.J. Hwang (2002): "A Planar Perspective Image Matching using Point Correspondences and Rectangle-to-Quadrilateral Mapping" Fifth IEEE Southwest Symposium on Image Analysis and Interpretation
5. Stoyan Gisbert, Takó Galina (2002): "Numerical methods" Typotex, Budapest
6. Szirmay-Kalos László, Antal György, Csonka Ferenc (2003): "Computer Graphics" Computer Books Budapest.
7. Donald H. House, David E. Breen (2000): "Cloth Modeling and Animation" AK Peters Ltd. Massachusetts
8. Tamás, P., Halász, M., Gräff, J (2005): "3D Dress Design" AUTEX World Textile Conference, Portorož, Slovenia. pp 436-440
9. J. Kuzmina; P. Tamás, M. Halász, Gy. Gróf (2005): "Image-based cloth capture and cloth simulation used for estimation cloth draping parameters", AUTEX 2005, 5th World Textile Conference, Portorož, Slovenia, P 904-909
10. P. Tamás; J. Geršak; M. Halász: "Sylvie® 3D Drape Tester – New System for Measuring Fabric Drape" Tekstil, Zagreb, 2006/10, P 497-502, (IF=0,15)